VEHICLE POWERTRAIN SYSTEMS

Behrooz Mashadi | David Crolla

VEHICLE POWERTRAIN SYSTEMS

VEHICLE POWERTRAIN SYSTEMS

Behrooz Mashadi
Iran University of Science and Technology

David Crolla
University of Sunderland, UK

This book is dedicated to Professor David Crolla
who passed away unexpectedly while the book was in production. David led
an unusually full and productive life both in work and play, achieving great
success and popularity. David was a leading researcher, an inspiring
teacher, an excellent supervisor of research postgraduates and a friend to
many. David's energy, enthusiasm and irrepressible humour made a lasting
impression on me and everyone who knew him. He is sorely missed
and his essential contribution to the publication of this book will
always be remembered.

Contents

About the Authors

Behrooz Mashadi is an Associate Professor in the Department of Automotive Engineering, Iran University of Science and Technology (IUST), Tehran, Iran. He received his BSc and MSc in Mechanical Engineering from Isfahan University of Technology (IUT), Isfahan, Iran, and his PhD degree in Vehicle Dynamics Engineering from the University of Leeds, in 1996 under the supervision of Professor D. A. Crolla. He was then engaged in several R&D projects in the automotive engineering industry and joined the academic staff at IUST in 2002.

He has developed and taught a wide range of courses for undergraduate and postgraduate students in the field of Automotive Engineering. He served as Deputy for Education in the Department of Automotive Engineering and is currently Deputy of the Automotive Research Centre at IUST, which is the leading centre for automotive R&D in Iran.

His current research interests include vehicle powertrain systems, hybrid propulsion systems, vehicle dynamics, vehicle modelling, simulation and control. He has presented and published over 100 papers in journals and conferences. He also serves on the editorial board of several international journals.

David Crolla, FREng, was a Visiting Professor of Automotive Engineering at the Universities of Leeds, Sunderland and Cranfield. After graduating from Loughborough University, he first worked as a research engineer in off-road vehicle design, and then joined the University of Leeds (1979–2001) becoming head of the Mechanical Engineering Department. His research interests included vehicle dynamics, chassis control systems, powertrain systems, suspensions and terramechanics, and he had published and presented over 250 papers in journals and conferences.

His activities included research in low carbon vehicles, industrial short courses in vehicle dynamics and chassis control, and engineering consultancy, for example, the BLOODHOUND SSC 1000mph land speed record attempt.

He was Editor-in-Chief of the world's first *Encyclopedia of Automotive Engineering* to be published in 2013.

Preface

In writing this book, we have aimed it at the needs of both students and practising engineers in the automotive industry. For engineering students, we hope we have provided a sound explanation of the principles behind the design of vehicle powertrain systems. For practising engineers, we have tried to provide a comprehensive introduction to the subject area, which will set the scene for more specialized texts on, for example, engines, transmissions or hybrid electric components.

The book has arisen from our combined teaching experiences at a range of institutions including the Iran University of Science and Technology (IUST), Tehran, and the Universities of Leeds, Sunderland and Cranfield. We have attempted to incorporate two important themes which distinguish our book from other texts:

1. The inclusion of numerous worked examples and the provision of a MATLAB$^{®}$ code for many of the problems.
2. A systems approach to powertrain design – focusing on the integration and interactions of all the components, e.g. engine, transmission final drive, wheels and tyres – in analyzing the overall vehicle performance.

Our experience of teaching engineering students suggests that one of the most useful ways of learning engineering principles is through actually doing problems oneself. Hence, we have tried to provide a wide range of examples together with worked solutions, often with an accompanying MATLAB code. We hope that readers will run these short programmes themselves and modify them to examine other performance issues.

The term 'systems approach' is widely used in engineering but is not always clarified in the particular context. Here, we simply mean that in order to understand vehicle performance, it is necessary to analyze all the powertrain components together and examine how they interact, and how the designer tries to integrate them in a coordinated way. Our experience suggests that there are relatively few texts which deal comprehensively with this critical aspect of integration.

At the time of writing, there is considerable pressure on the automotive industry to minimize energy consumption and reduce global emissions. This has led to a huge upsurge in interest in alternative powertrain systems – and the development of a range of electric and hybrid electric vehicles. However, consumers do not appear to be willing to compromise some of the traditional aspects of vehicle performance, e.g. acceleration, speed, etc. in the interests of overall energy consumption. Drivability remains a key commercial issue and there is a demand for vehicles which are 'fun-to-drive'. Hence, the design challenge continues to involve a compromise between vehicle performance and energy usage. We have tried in this book to provide a comprehensive coverage of both these – often conflicting – aspects of vehicle behaviour.

Vehicle Powertrain Systems is accompanied by a website (www.wiley.com/go/mashadi) housing a solution manual with detailed explanations for the solution methods of more than a hundred exercises in

this book. The solutions of the majority of the problems are carried out in MATLAB environment and the program listings are also provided. In addition to the worked examples of the book itself, the website offers invaluable guidance and understanding to students.

Finally, we would like to thank all our colleagues and friends over the years who have contributed in some way or influenced us in writing this text.

Abbreviations

2WD	2-wheel drive
4WD	4-wheel drive
AC	alternating current
AFR	air-fuel ratio
Ah	amp-hour
AMT	automated manual transmission
AT	automatic transmission
BAS	belted alternator starter
BD	block diagram
BDC	bottom dead centre
BLDC	brushless DC
BMEP	brake mean effective pressure
BMS	battery management system
BSFC	brake specific fuel consumption
CAFE	corporate average fuel economy
CI	compression ignition
CO_2	carbon dioxide
COP	conformity of production
CPP	constant power performance
CSM	charge sustaining mode
CTP	constant torque performance
CVT	continuously variable transmission
DC	direct current
DCT	dual clutch transmission
deg.	degree
DOF	degree of freedom
DOH	degree of hybridization
EC	eddy current
ECU	engine control unit
EFCC	Efficient Fuel Consumption Curve
EGR	exhaust gas recirculation
EM	electric motor
EMS	engine management system
EOP	engine operating point
EPA	Environmental Protection Agency
EREV	extended range electric vehicle
EUDC	extra-urban European driving cycle
EV	electric vehicle

FBD	free body diagram
FC	fuel consumption
FCVs	fuel cell vehicles
FEAD	front engine accessory drive
FEM	finite elements methods
FTP	Federal Test Procedure
FTP	fixed throttle performance
FWD	front wheel drive
GDI	gasoline direct injection
HC	hydrocarbons
HCCI	homogeneous charge compression ignition
HEV	hybrid electric vehicle
IC	internal combustion
ICE	internal combustion engine
IMEP	indicated mean effective pressure
I/O	input/output
ISG	integrated starter-generator
ISO	International Standard Organization
IVT	infinitely variable transmission
kg/J	kilogram per joule
kWh	kW-hour
l	litre
LCV	low carbon vehicle
LS	low speed
MAP	manifold absolute pressure
MC	motor controller
MCU	motor control unit
MG	motor/generator
MPa	mega Pascal
MPD	mechanical power distribution
MPI	multi-point (port) injection
MT	Magic Torque (formula)
MT	manual transmission
NEDC	New European Driving Cycle
NOx	oxides of nitrogen
NRF	no-resistive-force
NVH	noise, vibration and harshness
OOL	optimal operating line
PCP	pedal cycle performance
PGS	planetary gear set
PHEV	plug-in hybrid electric vehicle
PID	proportional integral derivative
PSD	power split device
RMS	root mean square
rpm	revs per minute
RWD	rear wheel drive
SCU	supervisory control unit
SFG	single flow graph
SI	spark-ignition
SOC	state of charge

SPH	series-parallel hybrid
TA	type approval
TAD	torque amplification device
TBI	throttle body injection
TC	torque converter
TDC	top dead centre
THS	Toyota Hybrid System
TPS	throttle position sensor
VVT	variable valve timing
Wh	Watt-hour
WOT	wide-open throttle

1

Vehicle Powertrain Concepts

1.1 Powertrain Systems

Over the past 100 years, vehicles have changed our lives; they have provided mobility which we exploit in all our commercial activities around the globe and they have also provided millions of us with new opportunities afforded by personal transportation. At the very heart of vehicle design is the powertrain system; it is the engineering of the powertrain system which provides the driving force behind the mobility.

The output from the power source – to date, dominated by the internal combustion (IC) engine – is controlled by a transmission system and driveline to deliver tractive effort to the wheels. And all these components, collectively referred to as the powertrain system, are controlled by the driver. Drivers, who are also viewed as discerning customers by the vehicle manufacturers, have a range of performance criteria: acceleration, top speed, fuel economy, gradeability, and towing capacity are some of the more obvious quantitative features. But subjective judgements such as driveability, fun to drive, refinement and driving pleasure play a huge part in the commercial success of vehicles. On the other hand, society imposes different performance demands – with a huge recent emphasis on emissions and CO_2 usage of vehicles. And governments have gone as far as imposing overall emissions control targets on manufacturers' fleets of vehicles.

In order to meet all these conflicting demands, engineers must master the complete powertrain system. If there is one underlying theme to this book, it is that in order to understand vehicle mobility, one must analyze the entire system together – driver, engine, transmission, driving cycles, etc. The aim of this chapter is to provide the background to this theme.

1.1.1 Systems Approach

The key issue at the heart of this textbook is to adopt a systems approach to vehicle powertrain design. In simple terms, this means collecting all the individual components in the powertrain – or drivetrain as it is sometimes called – and analyzing how they combine and interact. The ultimate aim is, of course, to predict the overall vehicle behaviour in terms of speed, acceleration, gradeability, fuel economy, etc.

First, the behaviour of the powertrain components is analyzed – and then these components are put together as a complete system to capture the overall vehicle driveline from the prime mover, traditionally, an IC engine, through the transmission – clutch, gears, differential, etc. – to the final drive at the wheels. The important theme is that it is only by taking a system-level view of the powertrain that the vehicle designer can achieve the desired goals of vehicle performance. In a systems approach to any problem, it is important at the outset to define the system boundaries. So, for example, if we wish to study the overall use

(a) Well-to-Tank

(b) Tank-to-Wheels
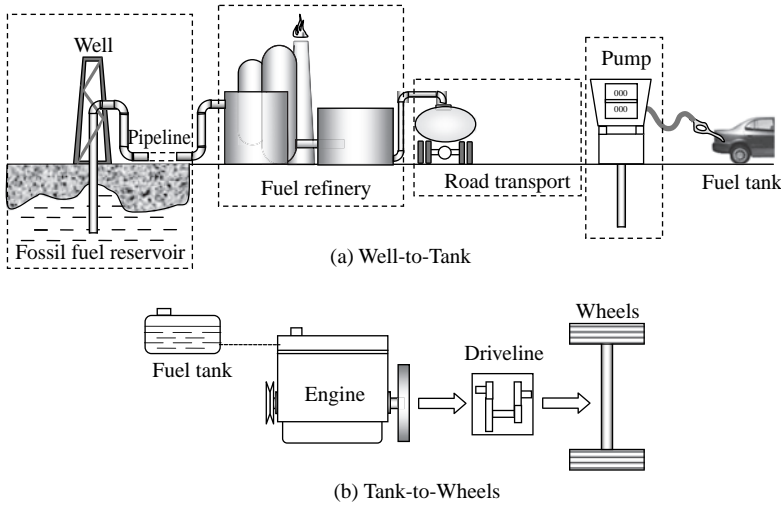
Figure 1.1   Overall energy conversion process in vehicle transportation – the Well-to-Wheels idea

of energy in passenger car transportation, the system would look like that shown in Figure 1.1 – in which the energy is tracked from its original source through to its final usage in propelling a vehicle. This overview is important in the context of powertrain system design, and is now commonly referred to as the Well-to-Wheels analysis of energy consumption.

1.1.2   History

There are lots of fascinating books describing the historical development of the automobile. It is not our intention in this book to dwell upon the history of automotive engineering; however, there are some interesting observations which set the scene for our analysis of powertrain systems.

In 1997, the SAE published an informative book [1] on the history of the automobile to celebrate its centenary. Each chapter was written by an invited US expert and all the powertrain components – powerplant (engine), transmissions, tyres, etc. – were covered. From the viewpoint of engineering innovation, it is very clear that there was plethora of innovative designs published in the late 1800s to early 1900s – but their practical exploitation was only realized decades later when material properties and mass manufacturing techniques had improved. For example, there were plenty of designs for what we consider fairly complex engineering components – automatic transmissions and continuously variable transmissions – patented in this period, but they had to wait several decades before they could be exploited commercially. The historical development of manufacturing, mass production and the economic context of automobile engineering is given in an excellent textbook by Eckerman [2].

In relation to powertrain systems, the two major components – the IC engine and the transmission have been reviewed from a historical perspective. The title of Daniels' book *Driving Force* [3] summarizes the role of the IC engine as the dominant power source for vehicles during the twentieth century. He presents a comprehensive overview of the detailed engineering development of engine design from its crude beginnings in 1876 as the stationary Otto engine to its current state of the art, characterized as much by sophisticated control systems as by mechanical design.

Some engineers would argue that developments in transmission design were equally important over the twentieth century. Taking the systems viewpoint, one would have to agree with this argument – since the IC engine power is only available over a limited speed range, and hence the transmission is crucial in
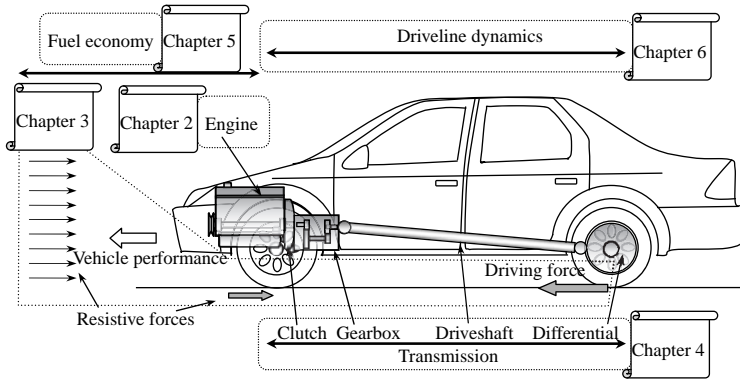
Figure 1.2 Overview of vehicle powertrain system and related book chapters

transforming it into usable power at the wheels. Gott [4] traces the history of engineering developments in transmissions – albeit with a bias towards the US preference for automatic transmissions. This review does, however, reinforce the systems approach since the control of the transmission must be totally integrated with the engine management control.

This holistic approach, in which all the interacting parts of the powertrain are considered together, leads to the idea of system optimization. For example, while it is clearly important to optimize the design of individual components, such as the engine and transmission, the overall aim must be that they are matched together as an integrated system.

1.1.3   Conventional Powertrains

This book concentrates mainly on what are commonly referred to as conventional powertrains – in which an IC engine drives the vehicle wheels through a transmission, incorporating a gearbox and final drive unit. A typical structure for a front-engined, rear wheel drive (RWD) car is shown in Figure 1.2, with a notation of how the chapters in this book are mapped on to the powertrain system. The most common layout for small passenger cars is front-engined, front wheel drive (FWD) but the principles associated with powertrain analysis are exactly the same.

The world's total population of cars and light trucks was estimated in 2009 at around 900 million, with a production of new cars and light trucks of about 61 million in the same year. The vast majority of these – more than 99% – employ conventional powertrains as described above. Hence, despite the enormous interest from 2000 onwards in alternative powertrains, described under the general heading of Low Carbon Vehicles (LCVs), it is clear that the principles of analysing and understanding conventional powertrain systems as described in this textbook will certainly be of interest for several more decades.

1.1.4   Hybrid Powertrains

During the late 1800s and early 1900s when engineers became fascinated with the opportunities for personal transportation provided by the motor car, there were three competing technologies for the powerplant – steam, electric and petrol. Each of these had their own merits and disadvantages, and it was not at all clear at the time which was likely to dominate in the longer term. In fact, a 1900 census in the eastern US states [5] showed that each of these technologies shared about a third each of the emerging market – however, horse-drawn carriages still dominated in terms of total vehicles!

Steam had a longer history of development and there was no problem installing sufficient power to give good performance. But fuel economy was poor, the boiler needed firing up prior to a journey and both water storage and usage were problems. Electric vehicles looked extremely promising – they were quiet, clean and remarkably easy to operate. Range was the major problem limited by the available energy storage in the battery – a problem which remains to this day! Gasoline cars in that period were less well developed and appeared extremely troublesome – they were difficult to start and when running they were noisy, dirty and pretty unreliable. But their fundamental advantage – which of course is obvious now – was the energy density of gasoline which was about 300 times better than a lead-acid battery. This meant it was worthwhile investing in the engineering refinement of the gasoline-based powertrain – and this approach of relentless development and refinement has continued to the present day.

Given these discussions at the time about the best way forward for the automobile powerplant, it is not surprising that several forward-thinking engineers have suggested combining two powerplants in order to extract the benefits of each – and hence, the notion of a hybrid vehicle was born around the turn of the nineteenth century. They were not called 'hybrid' at the time, but it is nevertheless remarkable that, for example, the 1902 Woods gas-electric car [5] did realize the potential of what we now know as a series-electric hybrid layout. The vehicle was driven by a motor which doubled as a generator, it could run on battery power alone at low speeds, the downsized gasoline engine could be used to charge the battery, and it featured regenerative braking.

Although there are a substantial number of different powertrain architectures for hybrid vehicles, at the time of writing this book in 2011, three are of particular interest, all linked to commercially available vehicle models. These three types are summarized in Figure 1.3 and are:

(a) Plug-in electric vehicle

(b) Electric vehicle with range extender and plug-in facility

(c) Hybrid electric vehicle – tractive power provided by engine, motor
or a combination of both
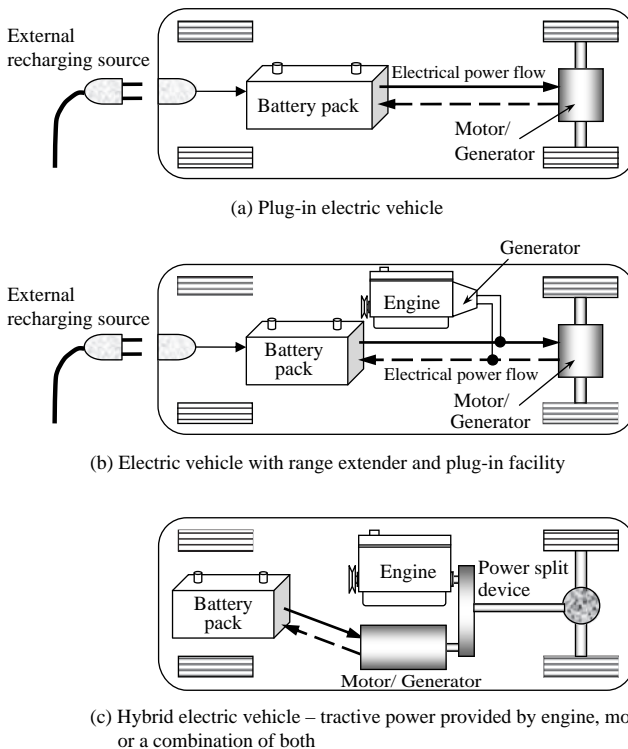
Figure 1.3   Three types of typical hybrid/electric vehicle architectures available in 2011

(a) plug-in electric vehicle (EV), e.g. Nissan Leaf;
(b) EV with range extender, e.g. Chevrolet Volt;
(c) hybrid electric vehicle (HEV), e.g. Toyota Prius

Chapter 7 in this book introduces the highly topical subject of hybrid vehicle powertrains. It is not intended to provide a comprehensive treatment of the rapidly changing subject of hybrid vehicle technology – many excellent texts have already been written on this topic and they are referenced at the end of Chapter 7. Rather, the chapter is intended to show how the same principles of powertrain systems analysis, which are the core of this textbook, can be applied to different technologies. The aim is to show how the systems approach to the analysis of so-called conventional powertrain components can readily be applied to powertrains built up of different components such as batteries, motor-generators, fuel cells, super-capacitors, etc.

1.2   Powertrain Components

The components in the powertrain are described in detail in each of the following chapters in the book – and references for further reading of the best books are also provided. Needless to say, all these components are subject to relentless efforts to improve their performance – efficiency, emissions control, refinement – as well as their overall cost effectiveness. The most recent trends in powertrain component engineering are summarized below.

1.2.1   Engine

- Stratified charge combustion
- Lean burn combustion
- HCCI (homogeneous charge compression ignition) combustion
- Variable valve timing
- Supercharging or twin-charging (when coupled with a downsized engine)
- Turbocharged direct injection diesel engines
- Gasoline direct injection petrol engines
- Common rail diesel engines
- Variable geometry turbocharging.

1.2.2   Transmission

- Lower-friction lubricants (engine oil, transmission fluid, axle fluid)
- Locking torque converters in automatic transmissions to reduce slip and power losses in the converter
- Continuously variable transmission (CVT)
- Automated manual gearbox
- Dual clutch gearbox
- Increase in the number of gearbox ratios in manual or automatic gearboxes.

1.2.3   Vehicle Structure

- Reducing vehicle weight by using materials such as aluminium, fibreglass, plastic, high-strength steel and carbon fibre instead of mild steel and iron.
- Using lighter materials for moving parts such as pistons, crankshaft, gears and alloy wheels.
- Replacing tyres with low rolling resistance models.

1.2.4   Systems Operation

- Automatically shutting off engine when vehicle is stopped.
- Recapturing wasted energy while braking (regenerative braking).
- Augmenting a downsized engine with an electric drive system and battery (mild hybrid vehicles).
- Improved control of water-based cooling systems so that engines reach their efficient operating temperature sooner.

1.3   Vehicle Performance

Ever since the first usable road vehicles appeared on the roads – built by, for example, Daimler, Benz, Peugeot and Panhard & Levassor in the 1890s and 1900s – people have quoted performance figures as a means of comparing vehicles. In the first instance, these were usually top speed and range; then came other performance measures as more powerful engines were installed – acceleration, gradeability and towing performance. Performance could be predicted based on very simple models using Newton's Second Law of Motion. For example, in Kerr Thomas' 1932 book [6], a chapter on the 'Mechanics of a Moving Vehicle' shows how to calculate speeds and accelerations based on knowledge of the engine torque and speed characteristics, gearbox ratios and estimates of the rolling resistance and aerodynamic drag terms.

According to a review paper in 1936 by the pioneering automobile engineer, Olley [7], the typical American car of that period weighed around 2 tons (2000 kg) and had an engine power of around 100 horsepower (75 kW), resulting in a typical acceleration of about $10\,\text{ft/s}^2$ ($\sim 3\,\text{m/s}^2$), a gradeability of about 11% and a top speed around 85 m.p.h. (38 m/s $\sim$ 140 km/h). The accuracy of these performance predictions gradually improved from the 1930s onwards as measurement techniques for engine performance [8], tyre rolling resistance characteristics [9] and aerodynamic drag effects [10] improved. An example to illustrate approximately where all the energy is used in vehicle longitudinal performance is shown in Figure 1.4 for typical urban and highway conditions.

In the 1970s, there was a massive shift in interest in vehicle performance to focus on fuel economy calculations. In the USA, this was prompted by the Corporate Average Fuel Economy (CAFE) regulations first enacted by Congress in 1975; these were federal regulations intended to improve the average fuel economy of cars and light trucks sold in the USA in the wake of the 1973 oil crisis. Basically, it was the sales-weighted average fuel economy of a manufacturer's range of passenger cars or light trucks, manufactured for sale in the United States. This signalled the start of a huge amount of interest around the world in both fuel economy and the linked topic of emissions – and governments became very active in legislating for the measurement and control of both these aspects of vehicle performance.

In recent decades, the highly competitive commercial environment for selling cars has meant that consumers require data and performance figures to compare different manufacturers' models. Longitudinal performance – maximum speeds, acceleration, hill climbing, towing abilities, etc. – are straightforward to measure and fairly non-controversial. In contrast, however, comparative data on fuel economy, and hence emissions – have proved extremely controversial.

The established method of quantifying a vehicle's fuel economy is to subject the vehicle, mounted on an instrumented dynamometer, to a standard drive cycle. The drive cycle simply consists of a set of data points which specify a speed vs distance travelled profile. Different drive cycles have been developed to simulate different types of vehicle operation, for example, extra-urban, urban, highway, and combined urban-highway.

Although this approach is internationally accepted, substantial detailed differences have emerged in different countries and different regions of the world. Thus, global comparisons of the fuel economy of vehicles are fraught with difficulties! Broadly speaking, the current range of standard drive cycles has emerged from the world's big three automotive markets – Europe, the USA and Asia – and the differences to some extent reflect different driving patterns in those regions. An excellent overview of the comparative
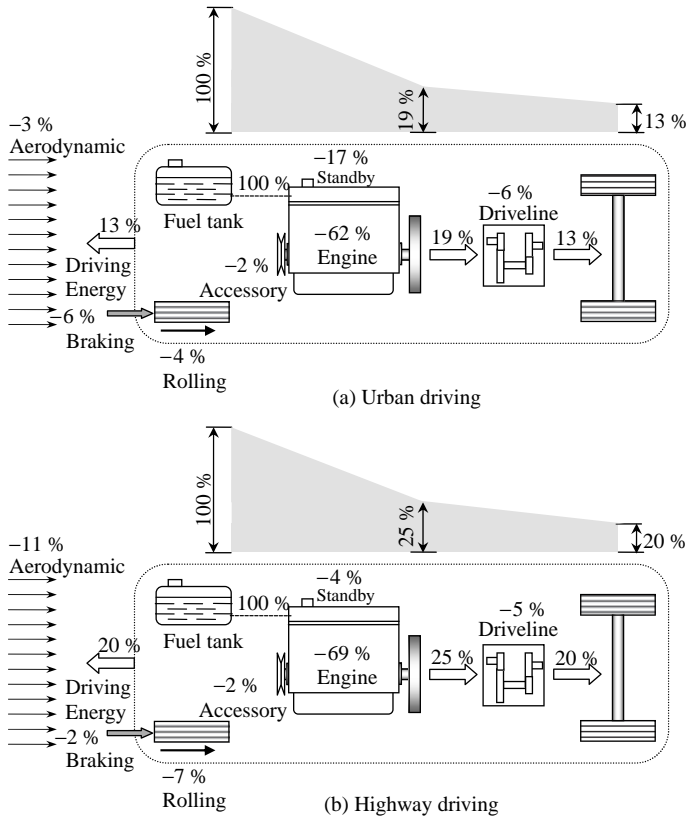
Figure 1.4 Example of typical energy flows during urban (a) and highway (b) driving

driving cycles is reported in [11]. The situation is further complicated by the fact that different countries or regions have developed different targets for fuel economy and emissions – which of course, makes life difficult for global manufacturers in meeting different standards for different markets.

Because of these regional differences, drive cycle testing has been a source of considerable controversy in the industry. But it has also proved extremely controversial from the consumer's point of view, because in real-world driving it has proved virtually impossible to achieve the ideal figures obtained under the standard test conditions. To the engineering community, this is an expected outcome – the tests and measurements are carried out in laboratory conditions over a repeatable drive cycle which can only be 'typical' of millions of real driving conditions. The key advantage is, of course, that vehicles are at least compared under fair and repeatable conditions. Nevertheless, consumer organizations and popular car publications continue to argue that the quoted figures – which now usually have to be displayed in the vehicle windscreen while on sale – should reasonably be achievable in practice.

In the European Union, the fuel economy of passenger vehicles is commonly tested using two drive cycles, referred to as 'urban' and 'extra-urban'. The urban test cycle (ECE-15) was introduced in 1999 and simulates a 4 km journey at an average speed of 18.7 km/h and a maximum speed of 50 km/h. The extra-urban cycle (EUDC) simulates a mixture of urban and highway running; it lasts 400 seconds with an average speed of 62.6 km/h and a top speed of 120 km/h. In the USA, the testing procedures are administered by the Environmental Protection Agency (EPA) and were updated in 2008 to include five

separate tests – which are then weighted together to give an EPA City and Highway figure that must be quoted in car sales information. It is claimed – with some justification – that these figures are a better reflection of real-world fuel economy performance than the EU figures.

Just to add to the confusion, fuel economy continues to be quoted in different units around the world. For example, both the USA and the UK use miles per gallon (mpg) – although even these are not comparable since the US gallon is 0.83 of an imperial gallon! In Europe and Asia, fuel consumption is quoted in units of l/100km. Note that both lower (l) and upper case (L) can be used for litres. This is effectively an inverse of the mpg approach and a large mpg is comparable to a small l/100km – so, for example, 30 mpg = 9.4 l/100km and 50 mpg = 5.6 l/100km.

However, most vehicle analysts agree that overall, the drive cycles are all less aggressive than typical real-world driving; in practice, this means that they include lower values of acceleration and deceleration than typically used in normal driving situations. With the upsurge of interest in hybrid powertrains over the first two decades of 2000, there has inevitably been an enormous focus on promoting their potential fuel economy relative to conventional powertrains. This has generated an on-going debate about whether the drive cycles tend to favour HEV powertrains over conventional ICE-based powertrains. The underlying principle is that HEVs offer the biggest scope for improvement under stop-start driving conditions in heavy city traffic, for example; hence, it is argued that since most drive cycles have their bias towards urban operation and inclusion of idle periods, they can distort the potential benefits available from hybrid powertrains – but again, there are a wide range of views!

In relation to emissions, there are two aspects; both of them are commonly referred to as 'tailpipe emissions' for the rather obvious reason that they emerge from the exhaust pipe as products of the combustion process. The first issue is the pollutant emissions – these include carbon monoxide (CO), unburnt hydrocarbons (HC) and oxides of nitrogen (NOx). In Europe, engine emission standards were introduced in the early 1990s to reduce all these pollutants from vehicles. It led to significant improvements in harmful emissions from passenger cars. Euro 5 is due to come into effect for passenger cars in 2011 and a further tightening of the regulations, Euro 6, is planned after that for both commercial vehicles and cars.

The second issue is the carbon dioxide (CO_2) emission levels of vehicles. These have assumed increasing attention during the early part of the twenty-first century due to global concerns about the environment – and they form part of the carbon footprint calculations which have now become embedded in all aspects of life. In the UK from 2001, the vehicle tax was linked to the CO_2 emissions of new vehicle, so that vehicle emitting less than 100g/km were actually free of road tax. And in 2008, an ambitious piece of legislation was passed which committed European car manufacturers to cut average CO_2 emissions from new cars to 130g/km by 2015.

1.4   Driver Behaviour

Although the focus of this textbook is entirely on the vehicle and the engineering of its powertrain system, it is important to recognize that whenever a vehicle is used on the road, the complete system actually involves both the vehicle and its driver. The complete system is shown in Figure 1.5, in which the driver effectively acts as a feedback controller – monitoring the performance of the vehicle and feeding back this information to compare with his demand signals to the accelerator, brake, gear selection, etc. Thus, from a dynamics point of view, we are in practice dealing with a control system. In designing the vehicle engineering system, therefore, we must be aware of the driver preferences as a controller.

In subjective terms, drivers tend to prefer systems which are:

- responsive
- controllable
- repeatable
- stable
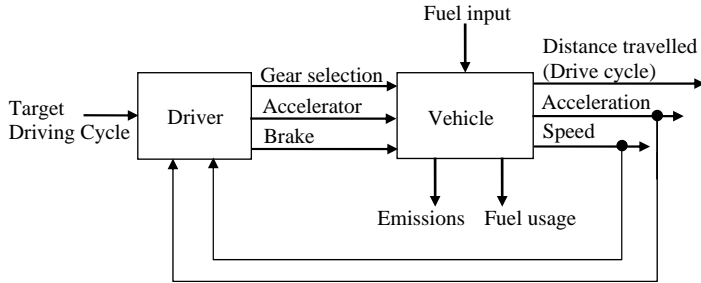
Figure 1.5 Overview of the driver–vehicle system governing vehicle longitudinal performance

- involving minimum time lags
- linear
- free from jerks or sudden changes.

The study of drivers' assessments of the longitudinal control of the vehicle is called 'driveability' and it is emerging as a crucial feature of vehicle refinement to assess the customer acceptance of new powertrain components. For example, it has been used in the industry from 2000 onwards to assess the smoothness of gear changes in new transmissions developments such as dual clutch gearboxes and continuously variable transmissions (CVTs). Indeed, procedures for the assessment of the highly subjective perception of the driver have been incorporated into specialized vehicle software packages such as AVL-DRIVE [12]. The idea is to generate an objective measure which is based on subjective judgements made by drivers using a range of vocabulary such as – jerk, tip-in, tip-out, kick, response delay, oscillations, ripple, backlash, etc. – some of which have more obvious interpretations than others.

There are occasions in vehicle performance calculations and simulations in which it is necessary to include a mathematical model of the driver in the complete system, as shown in Figure 1.5. In the so-called 'forward-facing' simulation, discussed in the next section, it is necessary to have a driver model which attempts to follow the specified driving cycle by applying appropriate signals to the accelerator and brake inputs. The approach used in this case is often a simple PID (Proportional Integral Derivative) model. This is good for tracking the speed profile, but is not necessarily representative of actual driver behaviour which is likely, for example, to include some element of look-ahead preview.

1.5 The Role of Modelling

The whole ethos of this book is based on a modelling approach to analyzing and understanding powertrain system design. The underlying aim is to explain how components function and then represent their behaviour through mathematical models based on the physics of their operation. Then, the components can be combined together as a complete powertrain system – and the resulting model should provide an important tool to contribute to vehicle design. Thus, although an analytical approach is used in order to understand the fundamental behaviour, the results are always aimed at being of practical value to vehicle engineers.

The models used throughout the text are relatively simple – and examples are provided in which the models are expressed and solved in the MATLAB®/SIMULINK environment. Thus, it should be easy to follow the complete process from the derivation of the governing equations, through to their coding in MATLAB/SIMULINK to their solution and presentation of results. Since the book is based on fundamental issues, it is felt to be important that the reader – whether a student or a practising engineer – can follow this whole procedure and try it out for themselves.

In calculations of vehicle performance over a specified driving cycle, there are two fundamentally different approaches – which are often not well understood by newcomers to the subject area. The most common simulation is called a 'backwards-facing' calculation. This means that at each point on the speed vs distance profile, the current values of both the vehicle speed and acceleration are known and using these it is possible to work backwards through the powertrain to calculate the speeds, accelerations, torques and powers of all the components. This process is simply repeated for all the points on the driving cycle and the results summed together at the end. This is the simplest and most commonly used method of predicting vehicle performance over a drive cycle.

The other approach is called a 'forward-facing' simulation; this requires a driver model in addition to the vehicle model. The drive cycle is a target trajectory which the driver tries to track via inputs to the vehicle system. The simulation is performed then as a conventional time history simulation, involving integration of the dynamic equations. This approach is required when developing control systems for the powertrain elements in order to simulate how the controller would actually behave in real time in the vehicle.

For more detailed analyses of powertrain components and systems, several commercial packages are available. These are used extensively in vehicle design offices around the world, and while they undoubtedly offer increased fidelity in their representation of the engineering systems involved, they are less informative of the underlying mechanics. Examples of such packages include;

- *ADVISOR* – (ADvanced VehIcle SimulatOR) was created by the U.S. Department of Energy's National Renewable Energy Laboratory's (NREL) Center for Transportation Technologies and Systems in 1994. It was a flexible modelling tool that rapidly assesses the performance and fuel economy of conventional, electric, hybrid, and fuel cell vehicles. It was acquired by AVL in 2003 [12].
- *AVL CRUISE* – Vehicle and driveline system analysis for conventional and future vehicle concepts [12].
- *AVL-DRIVE* – Assessment of driveability [12].
- *CarSim* – Vehicle performance in response to braking, steering and accelerating inputs [13].
- *IPG CarMaker* – Vehicle performance in response to braking, steering and accelerating inputs [14].
- *Dymola* – A multibody systems dynamics packages with automotive as well as other industrial applications [15].
- *WAVE* – 1D engine and gas dynamics simulation; also includes a drivetrain model to allow full vehicle simulation [16].
- *SimDriveline* – Blocks to characterize driveline components to include in a Simulink environment [17].
- *Easy5* – Multi-domain modelling and simulation of dynamic physical systems [18].

1.6   Aim of the Book

The overall aim of this book is to provide a comprehensive and integrated overview of the analysis and design of vehicle powertrain systems. This has the following objectives:

- to present a summary of the systems approach to vehicle powertrain design;
- to provide information on the analysis and design of powertrain components, in particular:
  - o internal combustion engine
  - o transmissions
  - o driveline components
- to analyze the longitudinal dynamics of the vehicle in order to predict performance;
- to analyze and discuss the fuel economy performance of vehicles;
- to analyze the torsional dynamics behaviour of the driveline system;
- to describe the fundamentals of hybrid electric components and the architecture of their usage in a hybrid vehicle powertrain;
- to present examples – some with worked solutions – throughout the text;
- to present case studies of powertrain performance using MATLAB as an analysis tool.

Further Reading

The books listed as references [1–5] all provide excellent background information on the history of automotive engineering, IC engine, transmissions and hybrid vehicle developments. They are all worth reading to set the scene for powertrain systems analysis.

References

[1] SAE (1997) *The Automobile: A Century of Progress*. SAE, ISBN 0-7680-0015-7.

[2] Eckermann, E. (2001) *World History of the Automobile*. SAE, ISBN 0-7680-0800-X.

[3] Daniels, J. (2003) *Driving Force: The Evolution of the Car Engine*. Haynes Manuals, 2nd edn, ISBN 978-1859608777.

[4] Gott, P.G. (1991) *Changing Gears; The Development of the Automatic Transmission*. SAE, ISBN 1-56091-099-2.

[5] Fuhs, A.E. (2009) *Hybrid Vehicles and the Future of Personal Transportation*. CRC Press, ISBN 978-1-4200-7534-2.

[6] Kerr Thomas, H. (1932) *Automobile Engineering*, Vol. 1. Sir Isaac Pitman & Sons.

[7] Olley, M. (1936) National Influences on American Passenger Car Design. *Proc. Institution of Automobile Engineers*, Vol. XXXII, pp. 509–541.

[8] Plint, M.J. (2007) *Engine Testing*, 3rd edn. SAE International, ISBN: 978-0-7680-1850-9.

[9] Clark, S.K. (ed.) (1981) *Mechanics of Pneumatic Tyres*. DOT HS 805 952, U.S. Dept of Transportation.

[10] Hucho, W-H. (ed.) (1998) *Aerodynamics of Road Vehicles*, 4th edn. SAE International, ISBN 0-7680-0029-7.

[11] Samuel, S., Austin, L. and Morrey, D. (2002) Automotive Test Drive Cycles for Emission Measurement and Real-World Emission Levels: A Review. *Proceedings of the Institution of Mechanical Engineers*, Part D: *Journal of Automobile Engineering*, 216 (7): 555–564.

[12] www.avl.com (last accessed March 2011).

[13] www.carsim.com (last accessed March 2011).

[14] www.ipg.de (last accessed March 2011).

[15] www.dymola.com (last accessed March 2011).

[16] www.ricardo.com (last accessed March 2011).

[17] www.mathworks.com (last accessed March 2011).

[18] www.mscsoftware.com (last accessed March 2011).

2

Power Generation Characteristics of Internal Combustion Engines

2.1 Introduction

The engine plays a dominant role in overall vehicle performance and it is essential to learn about its behaviour prior to performing vehicle studies. The internal combustion engine is a complicated system and its thorough analysis requires a multi-disciplinary knowledge of physics, chemistry, thermodynamics, fluid dynamics, mechanics, electrics, electronics and control. Electronics and control are becoming crucial parts of all modern engines and engine control units (ECUs) manage the engine operating parameters to try to achieve a good compromise between drivability, fuel consumption and emissions control.

Traditionally, in the literature on internal combustion engine design, the material discussed included: working fluids, thermodynamics, gas dynamics, combustion processes and chamber design, heat transfer, engine efficiency, friction, emissions and pollution. Also, the dynamics of engine moving parts and loads acting on the engine bearings and components are traditionally discussed in books on mechanism design or the dynamics of machinery. On the other hand, in areas related to the vehicle powertrain designs, the engine properties are needed as inputs to the system. Such vital information suitable for powertrain analysis cannot be found in the aforementioned books. Students have always seemed to have difficulties relating the engine design materials to powertrain design requirements. Moreover, it has been found that the engine performance characteristics described by full throttle engine maps usually given in the engine design books are misleading and confuse students, due to the fact that they try to explain the vehicle motion without sufficient information.

In this chapter, a review of internal combustion engine behaviour over a full range of operations is provided. This includes torque generation principles and characteristics as well as engine modelling for both petrol and diesel engines. This chapter is not intended to explain those materials generally covered by books written on the topics of internal combustion engines; instead, the torque generation principles of engines that are required in powertrain analysis will be the focus of this chapter.

2.2 Engine Power Generation Principles

In vehicle powertrain studies, the power generation properties of engines are of vital importance as the torque produced by the engine drives the vehicle in different and diverse driving situations. Internal combustion engines convert chemical energy contained in the fuel into mechanical power that is usually made available at a rotating output shaft. The fuel includes chemical energy that is converted to thermal energy by means of combustion or oxidation with air inside the engine. The pressure of the gases within

the engine builds up because of the combustion process that is generating heat. The high pressure gas then expands and pushes the surfaces inside the engine. This expansion force moves the mechanical linkages of the engine and eventually rotates a crankshaft. The output shaft of an internal combustion engine is usually coupled to a gear box, as in the case of transport vehicles.

Most internal combustion engines are of the reciprocating type, having pistons that move back and forth inside cylinders fixed to the engine blocks. Reciprocating engines range from single cylinder engines up to several cylinders arranged in many different geometric configurations. Internal combustion engines can be classified in different ways but the classifying method according to ignition type is most common. Two major ignition types are spark-ignition (SI) and compression-ignition (CI) types. Details of the combustion processes in SI and CI engines depend entirely on the characteristics of the fuel used in each type. Since the combustion process is quite different between SI and CI engines, the types and quantities of the various exhaust emission materials that are formed vary as a result.

2.2.1 *Engine Operating Modes*

The slider-crank mechanism is a basic linkage to convert the reciprocating motion of the piston into the rotating motion of a crankshaft in reciprocating engines. The piston acts as the slider and moves inside the cylinder and with the provision of the valves and manifolds, an engine with the ability to compress and expand gases results. Figure 2.1 shows the schematic of a typical slider-crank mechanism used in a single cylinder engine. At zero crank angle θ, the piston is at the position known as top dead centre (TDC), because the piston speed reaches zero at this point. Rotation of the crank arm through 180° displaces the piston from TDC to the other bottom extreme, again with zero piston speed, called bottom dead centre (BDC). The total distance that the piston travels during this 180° rotation of the crank is called one stroke that is twice the radius of the crank. Returning from BDC to TDC will take another 180° rotation of the crank and the piston behaviour is reverse of that between zero and 180°.

Reciprocating engines, both spark ignition and compression ignition, need four basic phases, namely intake (or induction), compression, combustion (or power) and exhaust to complete a combustion cycle.

2.2.1.1 **Four-Stroke Engines**

Some engines are designed to have four distinctive strokes for the piston in a complete working cycle and are called four stroke engines. In a four-stroke engine, the piston has to go through four strokes in order to
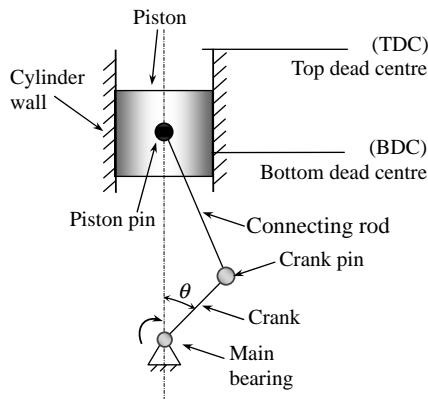
Figure 2.1 Schematic of engine slider-crank mechanism
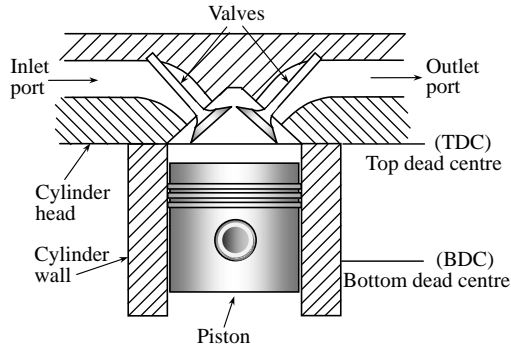
Figure 2.2 A classic four-stroke engine components

complete the cyclic thermodynamic processes. The crankshaft must perform two full turns in order that the piston completes four strokes. Figure 2.2 illustrates the basic parts of a four-stroke engine including the cylinder, the piston, the cylinder head, ports and valves.

Starting from TDC at the beginning of intake stroke, the inlet valve opens and the outlet valve closes. With the piston motion towards the BDC, fresh air (or mixture) flows into the cylinder. At BDC, the first stroke is complete and the inlet valve closes and the piston moves towards the TDC, compressing the gases inside the cylinder. At the TDC, the compression stroke ends and while both valves are closed, the power stroke starts with combustion and the resulting gases expand, pushing the piston down to the BDC at which the fourth and last stroke starts by opening the outlet valve to let the pressurized combustion products leave the cylinder. The motion of the piston to TDC helps the exhaust process by pushing the gases out. Table 2.1 summarizes these four strokes.

Note that the valve opening/closing crank angles given in Table 2.1 are only theoretical values and will be different in practice. For example, when the next intake process starts, it is better to leave the outlet valve open for a while in order that the burned gases leaving the combustion chamber continue their flow due to their momentum (also the fresh air can push them out). This will provide more room for fresh air and increase the combustion efficiency. Similarly when the piston is starting to move towards the TDC at the beginning of compression stroke, it is better to leave the inlet valve open for a while, so that the incoming air continues to flow into the cylinder due to its momentum.

2.2.1.2 Two-Stroke Engines

A two-stroke engine performs the four basic phases of a combustion cycle only in two piston strokes. In the two-stroke engine, the inlet and exhaust valves are eliminated and the ports for the entrance and exit of the gases are built on the cylinder walls and crankcase instead. The piston covers and uncovers the ports when it moves back and forth inside the cylinder (see Figure 2.3).

Table 2.1 The four strokes of a reciprocating engine

Order	Name of stroke	Piston position		Inlet valve	Exhaust valve	Crank angle (degrees)
		Start of cycle	End of cycle			
1	Intake (induction)	TDC	BDC	Open	Close	0–180
2	Compression	BDC	TDC	Close	Close	180–360
3	Combustion (power)	TDC	BDC	Close	Close	360–540
4	Exhaust	BDC	TDC	Close	Open	540–720
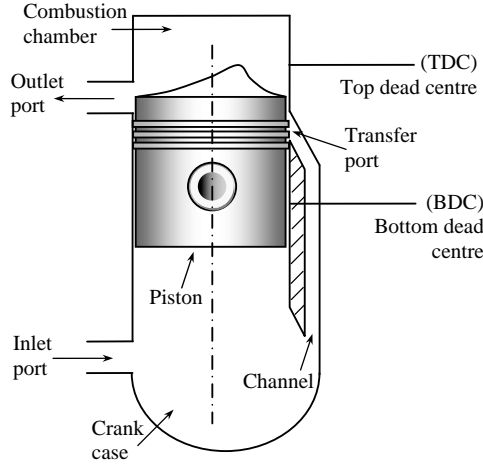
Figure 2.3   Schematic of a classic two-stroke engine

Let us start the cycle with the combustion stroke. The mixture in the combustion chamber is ignited in the same way as in the four-stroke engine at the top of the stroke. The piston moves downwards and uncovers the outlet port, allowing the pressurized burned gases to flow out of the cylinder. The downward movement of the piston at the same time compresses the gases in the crankcase. Further down, the piston uncovers the transfer port and the compressed gases in the crankcase flow through the channel into the combustion chamber and push the combustion products out through the outlet port. So, in a single stroke of the piston both combustion and exhaust cycles are accomplished. The upward movement of the piston compresses the gases in the combustion chamber and simultaneously depressurizes the crankcase to allow the pressure of the atmosphere to fill the crankcase with fresh air. Further up, the compression stroke will end and a new cycle will start by the combustion process. Again in a single upward piston stroke, both induction and compression cycles are accomplished.

It appears that two-stroke engines are more advantageous since they perform the power cycle faster than four-stroke engines and do not need the valves and valve trains either. But, in practice, two-stroke engines are not as efficient as four-stroke cycle engines, especially at high speeds. Two-stroke engines are generally used in small SI engines for motorcycles and in large CI engines for locomotives and marine applications that work in lower speeds. At large CI engine sizes, the two-stroke cycle is competitive with the four-stroke cycle, because in the CI cycle, only air is lost in the cylinder (see Section 2.2.2).

In the rest of this chapter it will be assumed that the engine works only on the four-stroke basis.

2.2.2   Engine Combustion Review

It is common to refer to engines as either petrol (gasoline in the USA) or diesel, according to the nature of the ignition and combustion, however, the terms 'spark ignition' (SI) and 'compression ignition' (CI) are also used. In SI engines the air and fuel are usually premixed before the initiation of combustion by sparking. In CI engines the fuel burns as it is injected into hot compressed air and produces a combustible mixture.

In order to have ideal combustion, the amount of fuel must be related exactly to the amount of intake air. In fact, according to the burning chemistry, for a specific amount of air molecules, there must be specific number of fuel molecules for perfect burning of the fuel. This fuel/air ratio is called the *stoichiometric* ratio and the objective in engine combustion is to produce fuel/air ratios as close to the stoichiometric as possible. More details will be discussed in the following sections.

2.2.2.1 SI Engine Combustion

In SI engines, the fuel is mixed with the air in the intake system prior to entry to the cylinder. In the past, carburettors were used for the homogenized mixing of the air and fuel. The basis of a carburettor operation was a pressure drop when air passed through a venturi and an appropriate amount of fuel (at higher pressure) surged into the air flow at the venturi throat from the float chamber. The throttle opening controlled the air flow inside the venturi and as a result the amount of fuel entering the engine was adjusted accordingly. This type of fuel metering was very sensitive to atmospheric changes and could not maintain accurate fuel to air ratios and resulted in poor engine performance and high levels of pollution.

In newer generations of engines, fuel injection systems that replace the carburettors inject the fuel in more accurate amounts. Injection systems are electronically controlled systems – the air flow rate must be measured and the desired amount of fuel per cylinder that is required for a proper combustion must be calculated and injected accordingly.

Currently there are two different fuel injection systems, namely, throttle body injection (TBI) and multi-port injection (MPI). TBI systems are something like a carburettor which contains one or more injectors. When fuel is injected, it will be mixed with the air and the mixture will move in the inlet manifold exactly like in the case of carburettor. In MPI systems, instead of having a throttle body for all cylinders, air is moved directly to the inlet port of each cylinder without mixing. The fuel is injected just at the entrance to each cylinder and is mixed with the air. In MPI systems, therefore, the number of injectors is equal to the number of cylinders. MPI systems are more efficient than TBI systems; first, because the fuel is more precisely metered for each cylinder in MPI systems and, second, the fuel is completely moved into the cylinder, whereas in TBI some part of the fuel in contact with the surface of intake manifold will stick and remain.

The newer generation of injection systems for SI engines includes the gasoline direct injection (GDI) systems that use the injection concept in CI engines (see Section 2.2.2.2) in which the fuel is injected into the combustion chamber inside the cylinder. These systems allow the achievement of both the fuel efficiency of a diesel engine and the high output of a conventional petrol engine.

Regardless of the injection type, the SI engine cycle can be described as follows. During the intake process the inlet valve is open and the air and fuel mixture is inducted in the cylinder. After the inlet valve closes, the cylinder contents are compressed by the piston movement upwards. Before the piston gets to the TDC, a high voltage electric discharge across the spark plug starts the combustion process. Burning the fuel during the combustion process increases the temperature in the cylinder to a very high peak value. This, in turn, raises the pressure in the cylinder to a very high peak value. This pressure forces the piston down and a torque about the crank axis is developed. The expansion stroke causes the pressure and the temperature to drop in the cylinder. For a given mass of fuel and air inside the cylinder, an optimum spark timing produces the maximum torque.

Before the end of the expansion stroke, the exhaust valve starts to open and the burned gases find a way through the valve into the exhaust port and into the manifold. Pressure in the cylinder is still high relative to the exhaust manifold and this pressure differential causes much of the hot products to be blown out of the cylinder before the piston starts its upward motion. The piston motion during the exhaust stroke transfers the remaining combustion products into the exhaust manifold. The timing for the exhaust valve opening is important since an early opening will reduce the work on the piston (less output torque) and a late opening will need external work delivered to the piston during the exhaust phase (see Section 2.2.3.1).

The intake valve opens before TDC and the exhaust valve closes some time after in order to help the combustion products trapped in the clearance volume when the piston reaches TDC to leave and to replace them with a fresh mixture. This period when both the inlet and exhaust valves are open is called valve overlap. The combustion process of SI engines is divided into four phases, namely ignition, flame development, flame propagation and flame termination [1]. Flame development is sometimes taken as part of the first phase and a total of three phases is considered [2]. The flame development interval is between the spark discharge and the time when a fraction of the fuel-air mixture has burned. This fraction is defined

differently such as 1, 5 or 10%. During this period, although ignition occurs and the combustion process starts, very little pressure rise and useful work is achieved.

In the interval between the end of the flame development stage and the end of the flame propagation process, usually the bulk of the fuel and air mass is burned and an energy release of about 90% is achieved. During this period, the pressure in the cylinder is greatly increased and thus the useful work of an engine cycle is the result of the flame propagation period. The remaining 5–10% of the fuel-air mass burning takes place in the flame termination phase. During this time, the pressure quickly decreases and combustion stops. The combined duration of the flame development and propagation phases is typically between 30° and 90° of the crank angle.

2.2.2.2   CI Engine Combustion

The operation of a typical four-stroke CI engine during the intake stroke is the same as for the intake stroke in an SI engine in terms of valve openings. The only difference is that air alone is inducted into the cylinder in this stroke. The compression ratio is higher for CI engines and during the compression stroke, air is compressed to higher pressures and temperatures than SI engines. The fuel is injected directly into the cylinder in the combustion stroke where it mixes with the very hot air, causing the fuel to evaporate and self-ignite and combustion to start. The power stroke continues as combustion ends and the piston travels towards BDC. The exhaust stroke is also the same as for SI engines.

In a CI engine at a given engine speed, the air flow is unchanged and the output power is controlled by only adjusting the amount of fuel injected. The nature of the fuel-air mixture in compression ignition engines is essentially different from SI engines. In SI engines, a homogeneous mixture is available and during the combustion process a flame moves through the mixture. In CI engines, however, the liquid fuel that is injected at high velocities through small nozzles in the injector tip, atomizes into small drops and penetrates into the hot compressed air inside combustion chamber. As a result, the nature of combustion is an unsteady process occurring simultaneously at many spots in a very non-homogeneous fuel-air mixture.

The process involved in the combustion of fuel after injection can be divided in four phases. The first phase is 'atomization' in which the fuel drops break into very small droplets. In the second phase called 'vaporization', due to the hot air temperatures resulting from the high compression, the droplets of fuel evaporate very quickly. After vaporization, because of the high fuel injection velocity and the swirl and turbulence of the air, in the 'fuel-air mixing phase' the fuel vapour will mix with the air to form a combustible mixture. Since the air temperature and air pressure are above the fuel's ignition point, spontaneous ignition of portions of the already-mixed fuel and air occurs in the 'combustion phase'. The cylinder pressure increases as combustion of the fuel-air mixture occurs. It also reduces the evaporation time of the remaining liquid fuel. The injection of liquid fuel into the cylinder will continue after the first fuel injected is already burning. After the start of combustion when all the fuel-air mixture that is in a combustible state is quickly consumed, the rest of the combustion process is controlled by the rate at which the fuel can be injected. Since only air is compressed in the cylinder during the compression stroke, much higher compression ratios are used in CI engines compared to those of SI engines. Compression ratios of modern CI engines range from a minimum of 14 up to 24.

Engine types include naturally aspirated engines where atmospheric air is inducted directly, turbocharged engines where the inlet air is compressed by an exhaust-driven turbine-compressor combination, and supercharged engines where the air is compressed by a mechanically driven pump or blower. Both charging systems enhance engine output power by increasing the air mass flow per unit displaced volume, thereby allowing more fuel combustion energy.

2.2.3   Engine Thermodynamics Review

During real engine cycles (intake, compression, combustion and exhaust), the composition of the substances inside the process is changing. The variable state of gases makes the analysis difficult and

to make the analysis manageable, real cycles are approximated with ideal air-standard cycles. This involves the following assumptions:

- The gas mixture in the cylinder is treated as an ideal gas with constant specific heats for the entire cycle.
- The real open cycle, in which the fresh air enters and combustion products leave it, is changed into a closed cycle by assuming that the exhaust gases are fed back into the intake system.
- Since air alone as the ideal gas cannot combust, the combustion process is replaced with a heat addition phase of equal energy value.
- The exhaust process is replaced with a closed system heat rejection process of equal energy value.

The processes are also idealized as reversible with the following properties:

- The intake and exhaust strokes are both assumed to be at constant pressure.
- Compression and expansion strokes are approximated by isentropic processes, and in spite of having small friction work and heat transfer within a cycle, these strokes are assumed to be reversible and adiabatic.
- The combustion process is idealized by a constant-volume process for SI engine and a constant-pressure process for CI engine.
- Exhaust blow-down is approximated by a constant-volume process.

Air standard cycles are the basis of determining the engine thermal efficiency and performance. These cycles are plotted in the pressure-displacement plane as the processes involved contain constant pressure, constant volume or isentropic processes, as explained above. On the other hand, the work carried out by pressure forces acting on the piston can be evaluated by $\oint p\,dV$ integral. Therefore, the work done during a single engine cycle is the area enclosed by the cycle process curves on the pressure-volume diagram. Plots of pressure versus volume for reciprocating engines are called indicator diagrams since they are the basis for the estimation of the engine performance.

2.2.3.1 Spark Ignition Engines

The Otto cycle shown in Figure 2.4 is the theoretical cycle commonly used to represent the processes of the spark ignition engines. As described earlier, a fixed mass of air as working fluid is assumed to be used
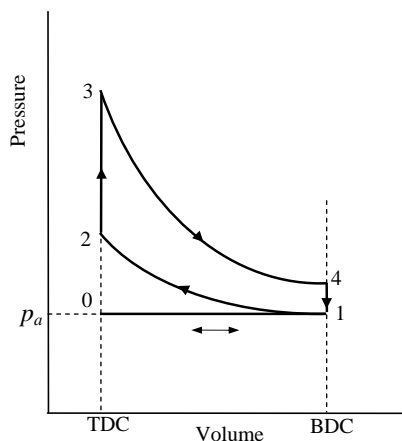
Figure 2.4   Standard Otto air cycle for SI engines

in the cycle and the piston moves from BDC to TDC and back again. The intake stroke of the Otto cycle starts with the piston at TDC (point 0) in a constant inlet pressure. The intake process of a real throttled engine will differ due to pressure losses in the air flow, therefore, Figure 2.4 represents an open throttle condition only. The compression stroke is an isentropic process from BDC to TDC (from point 1 to point 2). In a real engine, the intake valve is not fully closed at the beginning of the stroke and the spark plug is activated before TDC and thus the cycle is affected by these events. The heat input process from point 2 to point 3 represents the combustion process which in real engines occurs at close to constant-volume conditions. During this process an amount of energy is added to the air that raises the temperature to the peak cycle temperature at point 3. This increase of temperature during a constant-volume process also results in a large pressure at point 3. The expansion stroke (from point 3 to point 4) that follows combustion is approximated by an isentropic process in the Otto cycle. This is an acceptable approximation, as long as the stroke is frictionless and adiabatic.

The Otto cycle represents the exhaust blow-down process with a constant-volume pressure reduction process from point 4 back to point 1. The exhaust stroke occurs as the piston travels from BDC to TDC. The process from point 1 to point 0 is the exhaust stroke that occurs at a constant pressure of one atmosphere. At this point after two crank revolutions, the piston is at TDC and a new cycle begins.

Note that the processes from point 0 to point 1 and from point 1 to point 0 in the Otto cycle are thermodynamically opposite and cancel each other out during one complete cycle. Thus in cycle analysis the bottom line will no longer be needed.

A summary of the thermodynamic analysis will be presented for the cycle by considering the property of each stroke. Useful relationships for ideal gas are given in Table 2.2.

The thermal efficiency η_T of the Otto cycle is defined by the ratio of net specific output work w_{net} (work per unit mass) to the net input specific energy q_{in} (energy per unit mass):

$$\eta_T(Otto) = \frac{|w_{net}|}{|q_{in}|} \qquad (2.1)$$

The specific output work is obtained by subtracting the outgoing energy q_{out} in the exhaust stroke (4–1) from the input energy during the combustion stroke (2–3):

$$w_{net} = q_{in} - q_{out} = q_{2-3} - q_{4-1} \qquad (2.2)$$

in which from basic equations at constant volume (Table 2.2):

$$q_{2-3} = c_v(T_3 - T_2) \qquad (2.3)$$

$$q_{4-1} = c_v(T_1 - T_4) \qquad (2.4)$$

where c_v is the specific heat at constant volume and T is temperature. Substituting in Equation 2.1 gives:

$$\eta_T(Otto) = 1 - \frac{|q_{4-1}|}{|q_{2-3}|} = 1 - \frac{T_4 - T_1}{T_3 - T_2} \qquad (2.5)$$

Table 2.2   Ideal gas formulae

1	Basic relationship	$pV = mRT$
2	In terms of specific volume	$pv = RT$
3	In terms of specific mass	$p = \rho RT$
4	Isentropic (adiabatic-reversible) process	$pv^k = cte$
5	Isentropic process	$Tv^{k-1} = cte$
6	Constant volume process	$q = c_v \Delta T$
7	Constant pressure process	$q = c_p \Delta T$

The thermal efficiency can be simplified in the following simple form by using existing relations between the temperatures in isentropic compression and expansion strokes:

$$\eta_T(Otto) = 1 - \frac{T_1}{T_2} \tag{2.6}$$

For an isentropic compression cycle (1–2), one can write:

$$\frac{T_2}{T_1} = \left(\frac{v_1}{v_2}\right)^{k-1} \tag{2.7}$$

in which v is specific volume and $k = \frac{c_p}{c_v}$ is the ratio of specific heats at constant pressure and constant volume. Defining the compression ratio r_C as the ratio of maximum to minimum absolute air volumes:

$$r_C = \frac{V_1}{V_2} = \frac{v_1}{v_2} \tag{2.8}$$

and combining Equations 2.6–2.8 will result in:

$$\eta_T(Otto) = 1 - \left(\frac{1}{r_C}\right)^{k-1} \tag{2.9}$$

Equation 2.9 is very useful since if one knows only the compression ratio, the thermal efficiency can be determined. It also shows that the compression ratio is a fundamental parameter of the engines and that increasing compression ratio increases the cycle thermal efficiency. Figure 2.5 illustrates this relation graphically.
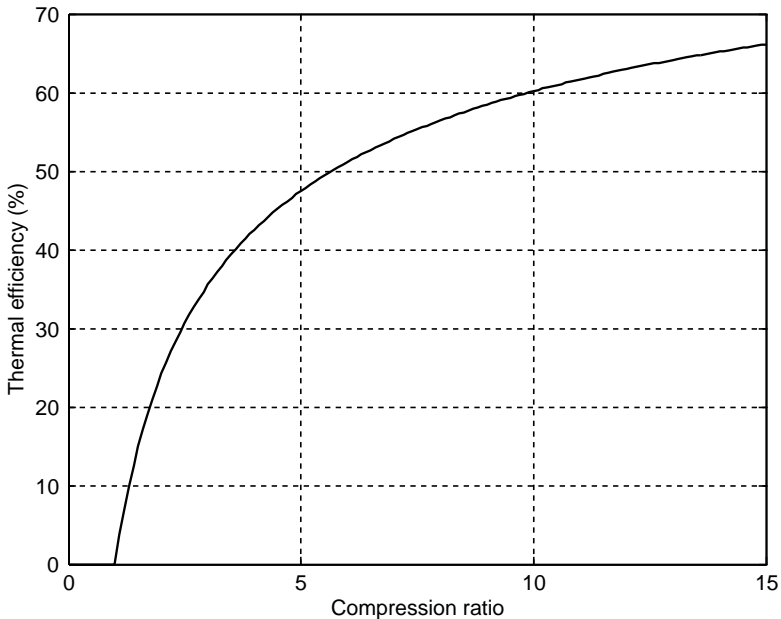
Figure 2.5 The variation of thermal efficiency of an Otto cycle with the compression ratio

In practice, the compression ratio of SI engines is limited by the condition that the fuel-air mixture should not spontaneously start burning due to the high temperature reached after the compression phase. This will in turn depend on the fuel octane number. Higher octane numbers allow higher compression ratios. Due to this limitation, commercial SI engines are normally designed with compression ratios less than 10.

Additional equations for the Otto cycle can be obtained as follows.

The total combustion energy (heat) in one cycle is:

$$Q_{2-3} = m_m c_v (T_3 - T_2) = m_f \eta_c Q_{HV} \tag{2.10}$$

where m_m and m_f are the mixture and fuel masses, and η_c and Q_{HV} are the combustion efficiency and fuel heating value respectively. From Equation 2.10 the net temperature increase can be found:

$$\Delta T_{2-3} = T_3 - T_2 = \frac{\eta_c Q_{HV}}{c_v (AF + 1)} \left(1 - \frac{m_r}{m_m} \right) \tag{2.11}$$

in which AF is the air to fuel mass ratio and m_r is the exhaust residual mass of a cycle. By using Equations 2.1, 2.3 and 2.9, the net specific work is found:

$$w_{net} = \eta_T q_{2-3} = \eta_T \eta_c \frac{Q_{HV}}{AF + 1} \left(1 - \frac{m_r}{m_m} \right) \tag{2.12}$$

The net work of the cycle is then:

$$W_{net} = m_m w_{net} = m_m \eta_T \eta_c \frac{Q_{HV}}{AF + 1} \left(1 - \frac{m_r}{m_m} \right) \tag{2.13}$$

Indicated mean effective pressure is defined as:

$$p_{ime} = \frac{W_{net}}{V_1 - V_2} = \frac{W_{net}}{V_d} \tag{2.14}$$

Indicated power P_i at a specific revolution speed n (rpm) is (in a four-stroke engine):

$$P_i = \frac{n W_{net}}{120} \tag{2.15}$$

If mechanical efficiency η_m is known, the brake power (that is output mechanical power) and brake mean effective pressure are obtained as:

$$P_b = \eta_m P_i \tag{2.16}$$

$$p_{bme} = \eta_m p_{ime} \tag{2.17}$$

Engine output (brake) torque is:

$$T_b = \frac{30 P_b}{\pi n} \tag{2.18}$$

The brake specific fuel consumption (BSFC) is defined as the ratio of fuel mass rate $\dot{m}_f$ to the brake power:

$$BSFC = \frac{\dot{m}_f}{P_b} \tag{2.19}$$

The engine volumetric efficiency is defined as the ratio of air mass inducted into the cylinder m_a to the total air mass displaced by the piston (at the ambient air conditions):

$$\eta_v = \frac{m_a}{\rho_a V_d} \tag{2.20}$$

in which ρ_a is the density of ambient air and V_d is the swept volume by the piston.

Example 2.2.1

Air at sea level and 30°C enters a 2.0 litre, four-cylinder, four-stroke SI (Otto) engine with a compression ratio of 8. The temperature of the fuel-air mixture entering the cylinder is 50°C. Use the information given in Table 2.3 and determine:

(a) the bore, stroke and clearance volume of each cylinder;
(b) the masses of mixture, air, fuel and exhaust in one cycle per cylinder;
(c) the maximum cycle temperature and pressure;
(d) the indicated thermal efficiency and the net indicated work of a cycle per cylinder;
(e) the indicated and brake effective pressures;
(f) the engine indicated power, brake power and torque at 3000 rpm;
(g) the brake-specific fuel consumption and volumetric efficiency of the engine.

Table 2.3 Engine information of Example 2.2.1

1	Air-fuel mass ratio	15
2	Combustion efficiency	95%
3	Mechanical efficiency	85%
4	Stroke/bore ratio	1.1
5	Fuel heating value	44 MJ/kg
6	Exhaust residual in a cycle	5%
7	k	1.35
8	c_v	0.821 kJ/kg °K

Solution

(a) For a single cylinder the displacement is:

$$V_d = 2.0/4 = 0.5 \ litre \ (5.0 \times 10^{-4} \ m^3)$$

The bore and stroke are:

$$B = \left(\frac{4V_d}{1.1\pi}\right)^{\frac{1}{3}} = 8.33 \ cm, \quad S = 1.1 \times B = 9.17 \ cm$$

The clearance volume V_c is equal to V_2 and since V_1 is the total volume (including V_2), the compression ratio can also be written as:

$$r_C = \frac{V_1}{V_2} = \frac{V_d + V_c}{V_c}$$

from which V_c is obtained:

$$V_c = \frac{V_d}{r_C - 1} = 71.43 \, cm^3$$

(b) From the basic ideal gas formula (Table 2.2) written for phase 1 of the Otto cycle:

$$p_1 V_1 = m_m R T_1$$

p_1 is the atmospheric pressure (101,330 Pa), R is the universal gas constant (287 J/kg.°K) and T_1 is the inlet temperature (in °K). Thus, the mixture mass is:

$$m_m = \frac{p_1(V_d + V_c)}{R T_1} = 0.6243 \, g$$

The total mixture mass is equal to:

$$m_m = m_a + m_f + m_r$$

where the residual mass is 5% of the total mass and the air-fuel mass ratio is given in Table 2.3, so the masses simply are:

$$m_f = \frac{0.95 \times m_m}{AF + 1} = 0.0371 \, g, \quad m_a = 15 m_f = 0.556 \, g \quad \text{and} \quad m_r = 0.0312 \, g$$

(c) The maximum cycle temperature and pressure occur at point 3 of Otto cycle. In order to find the quantities at point 3, those at point 2 are needed first. Thus, for the isentropic process 1–2 we can write:

$$p_2 = \left(\frac{v_1}{v_2}\right)^k p_1 = r_C^k p_1 = 8^{0.35} \times 1.0133 = 1.68 \, MPa$$

$$T_2 = \left(\frac{v_1}{v_2}\right)^{k-1} T_1 = r_C^{k-1} T_1 = 8^{0.35} \times 323.16 = 669.1°K \, (396°C)$$

From Equation 2.10:

$$T_3 = T_2 + \frac{m_f \eta_c Q_{HV}}{m_m c_v} = 669.1 + \frac{0.0371 \times 0.95 \times 44 \times 10^6}{0.6243 \times 0.821 \times 10^3} = 3692°K \, (3419°C)$$

For constant volume process 2–3 we have:

$$p_3 = p_2 \frac{T_3}{T_2} = 1.68 \times \frac{3692}{669.1} = 9.26 \, MPa$$

(d) Indicated thermal efficiency from Equation 2.9 simply is:

$$\eta_T = 1 - \left(\frac{1}{r_C}\right)^{k-1} = 0.517$$

The net indicated work can be calculated directly from Equation 2.13:

$$W_{net} = 0.6243 \times 0.517 \times 0.95 \times \frac{44 \times 10^6}{15 + 1} \times 0.95 = 801.12 \, J$$

(e) Indicative and brake effective pressures are obtained from Equations 2.14 and 2.17 respectively:

$$p_{ime} = \frac{W_{net}}{V_d} = \frac{801.12}{5 \times 10^{-4}} = 1.602 \times 10^6 \, Pa$$

$$p_{bme} = \eta_m p_{ime} = 0.85 \times 1.602 = 1.36 \, MPa$$

(f) The indicated power and brake power can be determined directly from Equations 2.15 and 2.16. So for four cylinders at 3000 rpm, we have:

$$P_i = 4 \times \frac{nW_{net}}{120} = 80.1 \, kW$$

$$P_b = \eta_m P_i = 0.85 \times 80.1 = 68.1 \, kW$$

The engine torque from Equation 2.18 is:

$$T_b = \frac{30 \times 68.1 \times 10^3}{\pi \times 3000} = 217 \, Nm$$

(g) For brake specific fuel consumption, the fuel mass rate is needed. The fuel mass in one cycle per cylinder was obtained earlier in (b). The total fuel mass flow rate and BSFC then are:

$$\dot{m}_f = 4 \times \frac{nm_f}{120} = 0.0037 \, kg/s \, (13345 \, g/h)$$

$$BSFC = \frac{13345}{68.1} = 196 \, g/kWh$$

The volumetric efficiency of the engine needs the density of air in intake that can be obtained from the state equation at an input temperature of 30 °C. Thus:

$$\eta_v = \frac{m_a}{\rho_a V_d} = \frac{0.556 \times 10^{-3}}{1.165 \times 5 \times 10^{-4}} = 0.955 \, (95.5\%)$$

2.2.3.2 Compression Ignition Engines

In an ideal air standard diesel cycle shown in Figure 2.6, combustion takes place at a constant pressure rather than at the constant volume of the Otto cycle. The justification is that by controlling the fuel injection rate and thus the rate of chemical energy release during the expansion of the combustion gases, a constant pressure process could be achieved.

The thermodynamic analysis of the CI cycle is similar to that of the Otto cycle. However, in addition to the volumes V_1 and V_2 of the Otto cycle, in this case, a third volume V_3 also plays a role. Therefore, a
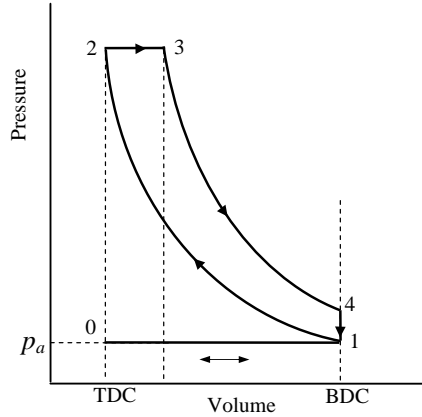
Figure 2.6   Standard air cycle for CI engines

'cut-off ratio' is defined to relate this value to V_2 as:

$$r_{Co} = \frac{V_3}{V_2} = \frac{T_3}{T_2} \tag{2.21}$$

The right-hand side equality holds owing to the constant pressure process. Starting with Equation 2.1 for the thermal efficiency of the cycle, the net specific output work is similar to Equation 2.2 but differs in that the input energy is given at a constant pressure rather than at a constant volume. Thus:

$$q_{2-3} = c_p(T_3 - T_2) \tag{2.22}$$

Substituting Equations 2.22 and 2.2 into Equation 2.1 results:

$$\eta_T(Diesel) = 1 - \frac{|q_{4-1}|}{|q_{2-3}|} = 1 - \frac{c_v(T_4 - T_1)}{c_p(T_3 - T_2)} = 1 - \frac{T_4 - T_1}{k(T_3 - T_2)} \tag{2.23}$$

This equation cannot be simplified as in the case of SI engine. The simplest form of the equation reads:

$$\eta_T(Diesel) = 1 - \frac{1}{kr_C^{k-1}} \cdot \frac{r_{Co}^k - 1}{r_{Co} - 1} \tag{2.24}$$

that is, a function of both the compression and cut-off ratios. Other useful relations for the diesel cycle are obtained below.

The total combustion energy (input heat) in one cycle is (constant pressure process):

$$Q_{2-3} = m_m c_p(T_3 - T_2) = m_f \eta_c Q_{HV} \tag{2.25}$$

Equation 2.11 of the Otto cycle will have a minor change (c_p replaces c_v):

$$\Delta T_{2-3} = T_3 - T_2 = \frac{\eta_c Q_{HV}}{c_p(AF + 1)}\left(1 - \frac{m_r}{m_m}\right) \tag{2.26}$$

The rest of the relations are similar for the diesel cycle and those obtained for SI engines (Equations 2.12–2.20) can be used also in this case.

Example 2.2.2

For compression ratios ranging from 5 to 20, compare the thermal efficiencies of air standard SI and CI engines with similar specifications. Compare the results for different cut-off ratios ranging from 2 to 6.

Solution

A simple MATLAB® program with two inner and outer loops for r_C and r_{Co} can be used to find the result. The output is shown in Figure 2.7. It can be seen that the efficiency of the SI engine is always higher than that of the CI engine. Nevertheless, due to the low compression ratios in the SI engine, the air standard thermal efficiency is limited to around 60%. In CI engines, on the other hand, higher compression ratios allow similar or even higher thermal efficiencies. For instance, a compression ratio of 15 and a cut-off ratio of 2 results in a similar 60% thermal efficiency. The effect of the cut-off ratio on the thermal efficiency of the CI engine is also clear from the three curves of 2, 4 and 6 cut-off ratios. Smaller cut-off ratios produce larger thermal efficiencies. It is a straightforward task to use the MATLAB program and show that as r_{Co} approaches unity, the efficiency curve of the CI engine will be identical to that of the SI engine.
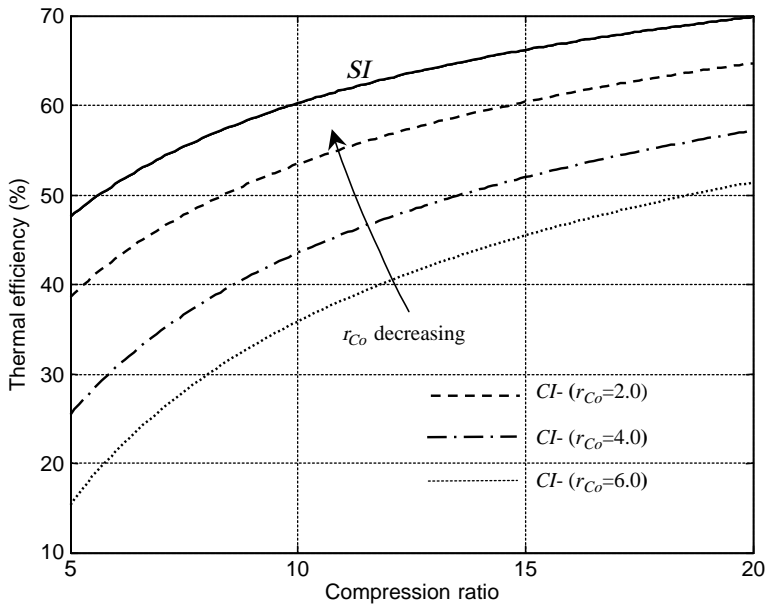
Figure 2.7   Comparison between the standard thermal efficiencies of SI and CI engines

Example 2.2.3

Consider a four-cylinder, four-stroke and 2.0 litre CI (diesel) engine with a compression ratio of 16. The ambient air is at sea level and 30°C. The temperature of the fuel-air mixture entering into the cylinder is 50°C. Use the information given in Table 2.4 and determine:

(a) the bore, stroke and clearance volume of each cylinder;
(b) the masses of mixture, air, fuel and exhaust in one cycle per cylinder;
(c) the maximum cycle temperature and pressure;
(d) the indicated thermal efficiency and the net indicated work of a cycle per cylinder;
(e) indicative and brake effective pressures;
(f) engine indicated power, brake power and torque at 3000 rpm;
(g) brake specific fuel consumption and volumetric efficiency of the engine.

Table 2.4   Engine information of Example 2.2.3

1	Air/fuel mass ratio	18
2	Combustion efficiency	95%
3	Mechanical efficiency	85%
4	Stroke/Bore ratio	1.3
5	Fuel heating value	43 MJ/kg
6	Exhaust residual in a cycle	5%
7	k	1.35
8	c_p	1.11 kJ/kg°K

Solution

The procedure to solve this problem is similar to that of Example 2.2.1.

(a) The displacement for a single cylinder is $V_d = 0.5\, litre\, (5.0 \times 10^{-4}\, m^3)$. The bore and stroke are:

$$B = \left(\frac{4V_d}{1.3\pi}\right)^{\frac{1}{3}} = 7.88\, cm, \quad S = 1.3 \times B = 10.25\, cm$$

V_c is:

$$V_c = \frac{V_d}{r_C - 1} = 33.33\, cm^3$$

(b) The mixture mass is:

$$m_m = \frac{p_1(V_d + V_c)}{RT_1} = 0.5827\, g$$

As can be seen, less mass is inducted compared to the SI case (Example 2.2.1) owing to the smaller clearance volume. The mass composition is:

$$m_f = \frac{0.95 \times m_m}{AF + 1} = 0.0291\, g, \quad m_a = 18m_f = 0.524\, g \quad \text{and} \quad m_r = 0.0291\, g$$

(c) The maximum cycle pressure occurs at points 2 and 3 of the cycle. The maximum temperature will be at point 3. For the isentropic process 1–2:

$$p_2 = r_C^k p_1 = 16^{0.35} \times 1.0133 = 4.28 \, MPa$$

$$T_2 = r_C^{k-1} T_1 = 16^{0.35} \times 323.16 = 852.8°K \, (580°C)$$

From Equation 2.10:

$$T_3 = T_2 + \frac{m_f \eta_c Q_{HV}}{m_m c_p} = 852.8 + \frac{0.0291 \times 0.95 \times 43 \times 10^6}{0.5827 \times 1.11 \times 10^3} = 2693°K \, (2420°C)$$

$$\eta_T (Diesel) = 1 - \frac{1}{1.35 \times 3.16^{0.35}} \cdot \frac{3.16^{1.35} - 1}{3.16 - 1} = 0.516 \, (51.6\%)$$

For constant pressure process 2–3:

$$p_3 = p_2 = 4.28 \, MPa$$

which is very low compared to that for the SI engine of Example 2.2.1. The cut-off ratio is:

$$r_{Co} = \frac{T_3}{T_2} = \frac{2693}{852.8} = 3.16$$

(d) Indicated thermal efficiency from Equation 2.24. The net indicated work can be calculated directly from Equation 2.13:

$$W_{net} = 0.5827 \times 0.516 \times 0.95 \times \frac{43 \times 10^6}{18 + 1} \times 0.95 = 613.85 \, J$$

(e) Indicative and brake effective pressures are obtained from Equations 2.14 and 2.17 respectively:

$$p_{ime} = \frac{W_{net}}{V_d} = \frac{613.85}{5 \times 10^{-4}} = 1.228 \times 10^6 \, Pa$$

$$p_{bme} = \eta_m p_{ime} = 0.85 \times 1.228 = 1.044 \, MPa$$

(f) The indicated power and brake power are determined for four cylinders at 3000 rpm:

$$P_i = 4 \times \frac{n W_{net}}{120} = 61.4 \, kW$$

$$P_b = \eta_m P_i = 0.85 \times 61.4 = 52.2 \, kW$$

The engine torque from Equation 2.18 is:

$$T_b = \frac{30 \times 52.2 \times 10^3}{\pi \times 3000} = 166 \, Nm$$

(g) The total fuel mass flow rate and BSFC are:

$$\dot{m}_f = 4 \times \frac{nm_f}{120} = 0.0029 \, kg/s \, (10488 \, g/h)$$

$$BSFC = \frac{10488}{52.2} = 201 \, g/kWh$$

The volumetric efficiency is:

$$\eta_v = \frac{m_a}{\rho_a V_d} = \frac{0.524 \times 10^{-3}}{1.165 \times 5 \times 10^{-4}} = 0.900 \, (90.0\%)$$

2.2.3.3   Comparison of Standard SI and CI Cycles

The standard cycles for SI and CI engines may be compared for an equal displacement, as Figure 2.8 shows. For this case, the input condition is also similar and the difference in process 1–2 is due to the different compression ratios. It is clear that the SI cycle has a larger peak pressure and the surface under the closed cycle 1–2–3–4–1 of the SI engine is greater than that of 1–2$_D$–3$_D$–4–1 of the CI engine. Thus, the indicated specific work of the SI cycle is greater than the work of the CI engine with a similar displacement.

It is also clear from Figure 2.8 that the maximum pressure of the SI cycle is considerably higher than that of the CI engine. However, CI engines with higher compression ratios can have pressures as high as those of SI engines since in the engine design this would be the mechanical limitation. A different comparison, therefore, can be made by having both engines with equal high pressures as depicted in Figure 2.9. In this case, the area enclosed by the cycle 1–2$_D$–3–4–1 of the CI cycle is apparently greater than that of SI cycle 1–2–3–4–1 and thus the indicated specific work of the CI cycle would be greater than the work of the SI cycle when the maximum pressures are identical.

2.2.3.4   Real Engine Cycles

Typical real indicator cycles of SI and CI engines are given in Figures 2.10 and 2.11. In the SI case, the cycle differs in the constant volume exhaust blow-down process with the ideal Otto cycle. A greater difference can be seen in CI cycle. In addition to the same phenomenon of exhaust blow-down, a constant volume segment exists in the real cycle that is absent in the ideal cycle. This segment is due to an early fuel
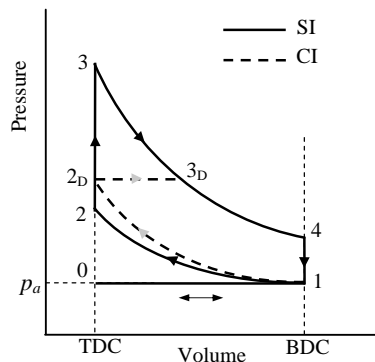
Figure 2.8   Comparison of standard air cycles for SI and CI engines with equal displacements
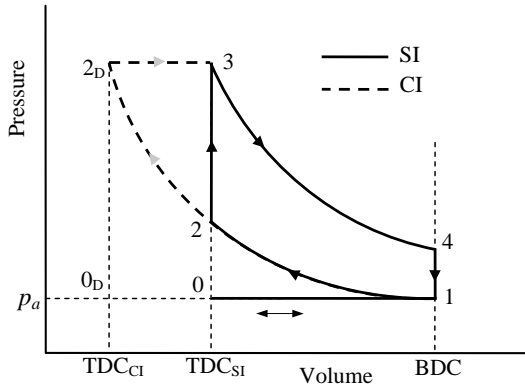
Figure 2.9 Comparison of standard air cycles for SI and CI engines with equal high pressures
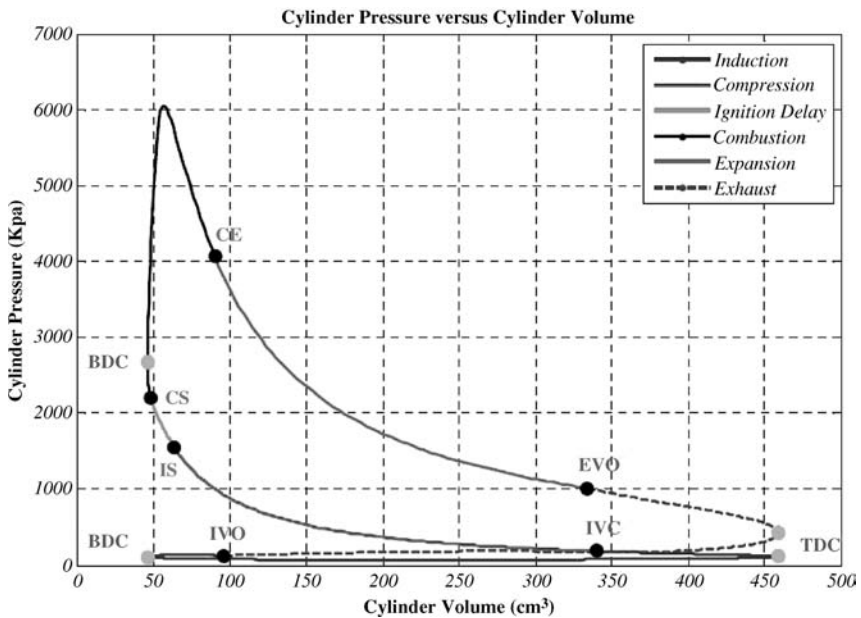
Figure 2.10 A real cycle for a four-stroke SI engine

injection (before TDC) in real engines which builds up the pressure in the cylinder when the piston is close to TDC (constant volume). A dual cycle approximation (Figure 2.11b) is sometimes used to model the cycle more accurately.

2.2.3.5 Part Throttle SI Engine Cycle

So far it has been assumed that the intake air was unthrottled (wide open throttle, WOT) and that the inlet air in the intake manifold was at atmospheric pressure. At part throttle, the valve is partially open and restricts the flow, resulting in a lower than atmospheric inlet pressure. This will in turn cause a lower air
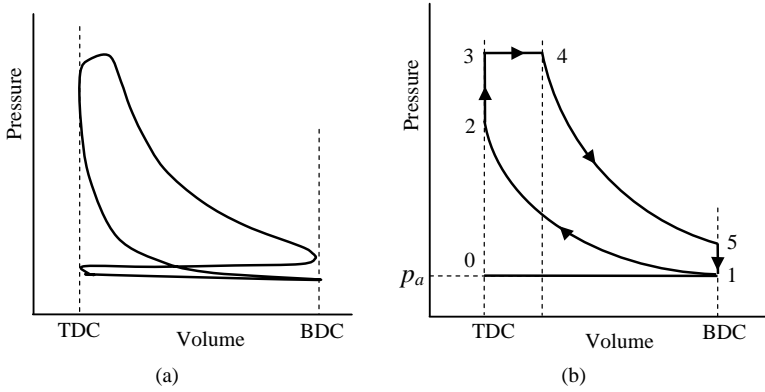
Figure 2.11 Indicator cycles of a four-stroke diesel engine: (a) real engine; (b) a dual cycle approximation

mass to fill the cylinder and the required amount of fuel will also be lower, resulting in less thermal energy from combustion and less resulting work.

The typical air cycle for the part throttle engine is shown in Figure 2.12. According to Figure 2.12, the net work is less than that of the standard Otto cycle, since the upper loop of the cycle represents positive work output (power cycle), while the lower loop is negative work absorbed by the engine (pumping cycle).

2.2.3.6   Effect of a Turbocharger

Turbochargers or superchargers use the exhaust pressure or a mechanical power respectively to drive a compressor to pump the inlet air and increase the intake pressure to higher than atmospheric values. This increases the inlet air in the combustion chamber during the cycle and, clearly, the more mixture mass there is in the cycle, the more chemical energy is released and the resulting net indicated work is therefore increased. The effect of turbocharging or supercharging on the air standard cycles would be to increase the intake pressure at point 1 to higher values. For example, in the Otto cycle, the result would be similar to
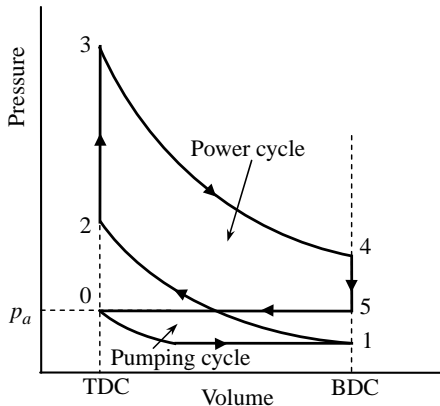
Figure 2.12   Part throttle SI air cycle
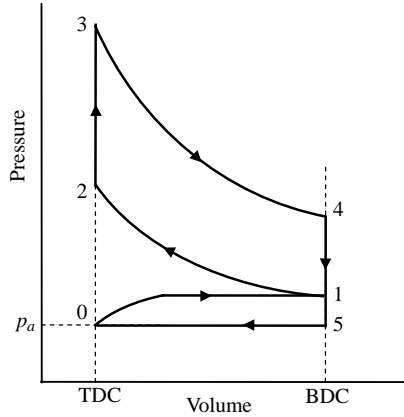
Figure 2.13   Effect of turbocharging on the SI air cycle

that shown in Figure 2.13. Again, the increase in the positive areas under the cycle loops is an indication of the increased net indicated work of the cycle.

2.2.4   Engine Output Characteristics

In the foregoing discussion it was observed that the standard cycles were able to generate the engine indicated outputs at WOT and desired working speeds (see Examples 2.2.1 and 2.2.3). Nevertheless, the net indicated work of the cycle was found to be independent of speed (Equation 2.13). In practice, however, an engine works at diverse conditions of output speeds and powers. An important question is how the engine performance is related to the speed. The variation of engine output power and torque versus speed can be obtained from Equations 2.16 and 2.18 respectively. These equations can be rearranged in the following forms:

$$P_b = \frac{\eta_m W_{net}}{120} n \equiv k_P n \tag{2.27}$$

$$T_b = \frac{30 P_b}{\pi n} = T^* = cte \tag{2.28}$$

So according to the air standard cycles, the WOT engine output torque and power in the entire range of operation will be similar to that shown in Figure 2.14. This is true for both SI and CI engines and only the constant values T^* and k_P will be different.

The characteristics of real engines are in general similar to the characteristics of ideal cycles but differ at low and high speeds. The reason is that the overall engine efficiency η_e is not constant and varies with the engine speed. To see this, let us combine Equations 2.13, 2.14 and 2.17 (assume no residual mass in the cycle) to obtain:

$$p_{bme} = \frac{m_m}{V_d} \eta_m \eta_T \eta_c \frac{Q_{HV}}{AF+1} \tag{2.29}$$

Recalling $m_a = \frac{AF}{AF+1} m_m$ and substituting in Equation 2.20 gives:

$$\frac{m_m}{V_d} = \rho_a \eta_v \frac{AF+1}{AF} \tag{2.30}$$
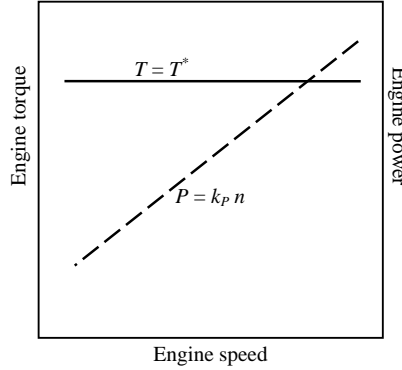
Figure 2.14 Ideal engine torque and power outputs

which eventually leads to the following equations for p_{bme}, torque and power (four-stroke engines):

$$p_{bme} = \eta_v \eta_m \eta_T \eta_c \frac{\rho_a Q_{HV}}{AF} \tag{2.31}$$

$$T_b = \eta_v \eta_m \eta_T \eta_c \frac{\rho_a V_d Q_{HV}}{4\pi AF} = \eta_e k_T^* \tag{2.32}$$

$$P_b = \eta_v \eta_m \eta_T \eta_c \frac{\rho_a V_d Q_{HV}}{120AF} n = \eta_e k_P^* n \tag{2.33}$$

As mentioned earlier, the overall efficiency of engine η_e is not a constant and is dependent on several factors, including engine load and speed. The relation of η_e to engine working parameters is very complex and is not well documented in the literature. For real engines, even the factors k_T^* and k_P^* are not constant and change with changing atmospheric conditions and engine speed.

Among the different factors influencing the overall engine efficiency, the one with substantial importance is the volumetric efficiency, since it governs how much air gets into the cylinder during each cycle. More inlet air means more fuel can be burned and more energy can be converted to output power. However, because of the limited cycle time available, the pressure losses across the air cleaner, the intake manifold, the intake valve(s), the reduction of mixture density due to hot cylinder walls and the gas inertia effects, less than the ideal amount of air enters the cylinder and reduces the volumetric efficiency. The variation of volumetric efficiency with engine speed is shown in Figure 2.15 for a typical spark ignition engine.

Torque and power characteristics of a real engine, therefore, will be affected especially at low and high engine speeds. The result will be a lowering of engine torque at low and high speeds. The maximum engine power will not occur at its maximum speed but at a lower speed. Typical WOT engine performance curves for an SI engine are shown in Figure 2.16.

2.2.5 Cylinder Pressure Variations

The piston is controlled by the cylinder pressure and its motion to produce the engine speed and output torque. The instantaneous pressure variation, therefore, controls the output characteristics of
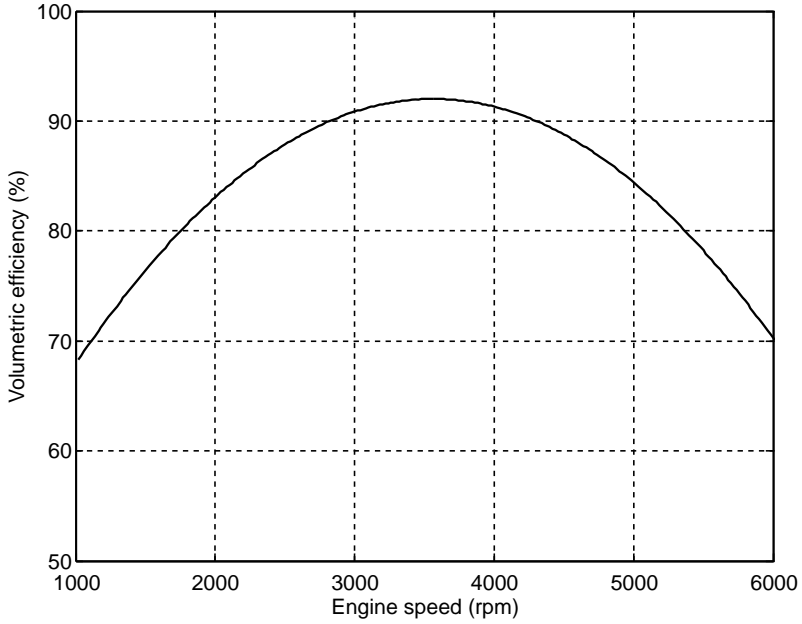
Figure 2.15   Typical volumetric efficiency of SI engines
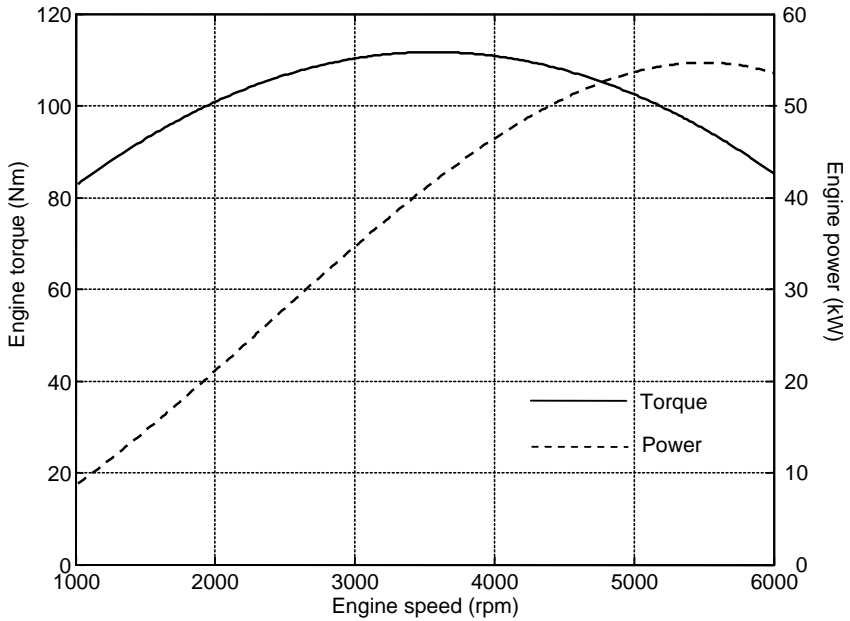
Figure 2.16   WOT torque and power-speed curves of a real SI engine

the engine. A suitable variable against which to express the engine pressure variations is the crank angle. As a result, the plot of pressure versus crank angle is commonly used. These curves, in addition, provide further understanding of the effect of engine torque variation with a spark or injection timing.

The values for the pressure of the cylinder were determined for air standard SI and CI cycles in Section 2.2.3, for the end points of each stroke. In order to plot the pressure variation, the pressures in the mid-region are also necessary. For this reason the cylinder volume must be related to the crank angle θ. It can be written as:

$$V(\theta) = V_1 - yA_P \tag{2.34}$$

in which A_P is the piston area and (see Section 2.3.1):

$$y = R\cos\theta + l\cos\beta \tag{2.35}$$

$$\beta = \sin^{-1}\left(\frac{R}{l} \cdot \sin\theta\right) \tag{2.36}$$

Note that at $\theta = 0$ the piston is at TDC and at $\theta = 180$ degree it is at BDC. Also $S = R + l$ is the stroke. The cylinder pressure variations will be examined in Example.2.2.4.

Example 2.2.4

Consider Example 2.2.1 and find the variation of pressure versus the crank angle during one complete cycle. The radius of the crankshaft is 40 mm.

Solution

During the intake stroke the pressure is constant at atmospheric pressure p_a (see Figure 2.4). This stroke starts from TDC to BDC. During the compression stroke the pressure at angle θ is determined from the following equation for crank angles from 180 degrees to 360 degrees:

$$p(\theta) = \left(\frac{V_1}{V(\theta)}\right)^k p_1$$

At 360 degrees (end of compression process), at a constant volume the pressure builds up abruptly to $p_3 = 9.26\,MPa$. Then from 360 to 540 degrees (the expansion stroke), the pressure at angle θ is determined from similar equations for the compression phase. Again at a constant volume the pressure drops to the atmospheric pressure $p_4 = 101\,kPa$. The exhaust stroke takes place at a constant atmospheric pressure.

A MATLAB program to solve this example is listed in Figure 2.17 and the output plot is given in Figure 2.18.

```
% Example 2.2.4
% Atmospheric data
T0=273.16+30;
p0=101330;  % Atmospheric condition
R=287;
T1=273.16+50; % Inlet temperature

% Engine data:
Dis=2.0;    % Litre
N=4;           % Number of cylinders
AF=15;       % Air/fuel ratio
ce=0.95;     % Combustion efficiency
me=0.85;    % Mechanical efficiency
SB=1.1;      % Stroke/bore ratio
QHV=44e6;  % Fuel heating value
er=0.05;      % Exhaust residual percent
rC=8;          % Combustion ratio
k=1.35;       % cp/cv
cv=0.821e3; % J/kg.K
Rc=40/1000; % Crank radius

% Pre-calculations
Vd=Dis/4/1000;
B=(4*Vd/pi/1.1)^(1/3);
S=1.1*B;
Vc=Vd/(rC-1);
l=S-Rc;
V1=Vd+Vc;
Ap=pi*B^2/4;
mm=p0*(Vd+Vc)/R/T1;
mf=(1-er)*mm/(AF+1);

% Intake stroke:
p=ones(1,181)*p0;
crak_ang=0: 1: 180;
plot(crak_ang, p/10^6)

% Compression stroke:
for i=1: 181
    ang=(i+179)*pi/180;
    theta(i)=i+179;
    beta=asin(Rc*sin(ang)/l);
    y=Rc*cos(ang)+l*cos(beta);
    Vt=V1-y*Ap;
    rv=V1/Vt;
    p2(i)=p0*rv^k;
end
T2=T1*rC^(k-1);
T3=T2+mf*QHV*ce/mm/cv;
p3=p2(181)*T3/T2;
p2(181)=p3;
hold on
plot(theta, p2/10^6)
```

Figure 2.17 MATLAB listing for Example 2.2.4

```
% Expansion stroke:
for i=1: 181
    ang=(i+359)*pi/180;
    theta(i)=i+359;
    beta=asin(Rc*sin(ang)/l);
    y=Rc*cos(ang)+l*cos(beta);
    Vt=V1-y*Ap;          rv=Vc/Vt;
   p4(i)=p3*rv^k;
end
T4=T3*(1/rC)^(k-1);
T5=T1;          p5=p4(181)*T5/T4;
p4(181)=p5;
plot(theta, p4/10^6)

% Exhaust stroke:
p=ones(1,181)*p0;
crank_ang=540: 1: 720;
plot(crank_ang, p/10^6)
xlabel('Crank angle (degrees)')
ylabel('Pressure in cylinder (MPa)')
```

Figure 2.17   (*Continued*)
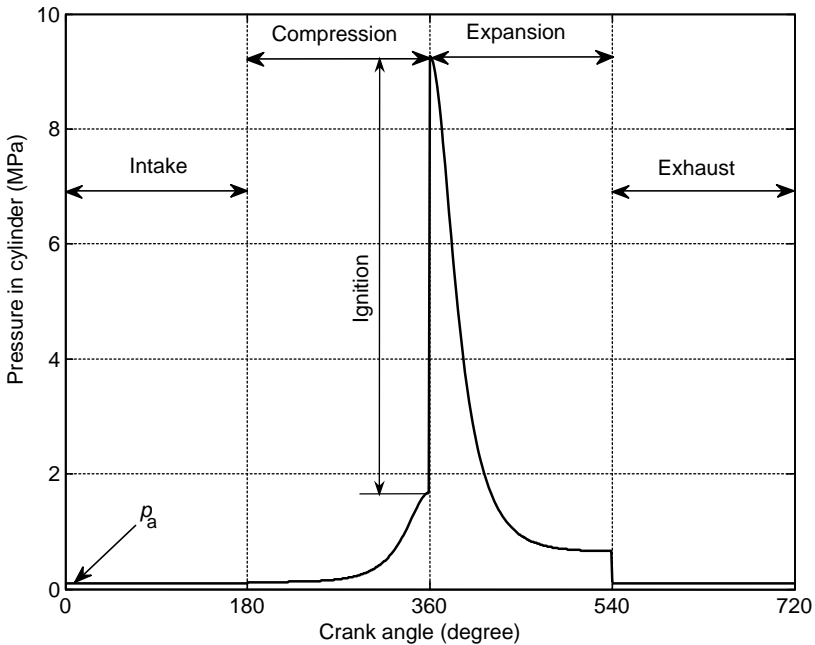
Figure 2.18   The pressure variation in a single cycle (Example 2.2.4)

The cylinder pressure can also be obtained from laboratory tests. A pressure sensor can detect the variation in cylinder pressure and produce an electric (or digital) signal proportional to it. With simultaneous recording of the crank rotation angles, test results for the pressure variation versus crank angle can be obtained. Tests are usually performed at specific constant engine speed. At different engine
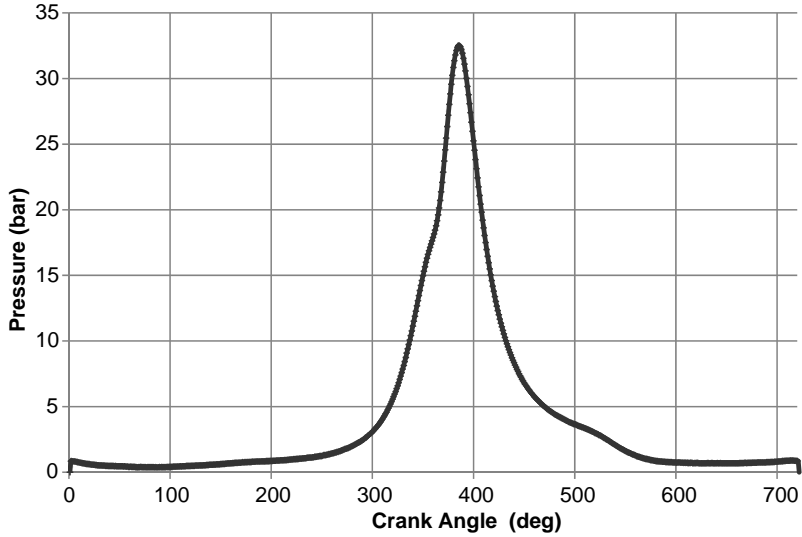
Figure 2.19 Cylinder pressure variations versus crank angle for a real SI engine

speeds, the pressure curve will be different and as a result the engine performance will also be different. A typical cylinder pressure versus crank angle variation of a real SI engine is given in Figure 2.19. The overall trend is seen to be quite similar to that of Figure 2.18 for the ideal engine.

2.3 Engine Modelling

In the preceding section, the principles of engine power generation based on the combustion of fuel inside the engine and the related energy release were discussed. The output power and torque obtained from such an analysis, however, are average and indicative. In order to find instantaneous outputs of an engine, two different approaches, illustrated in Figure 2.20, are available. Process modelling is a more elaborate method of what was discussed in Section 2.2, in which the details of fluid flow to the engine, valve timing, combustion process, thermodynamics, heat transfer and fluid flow out of the engine are all modelled.
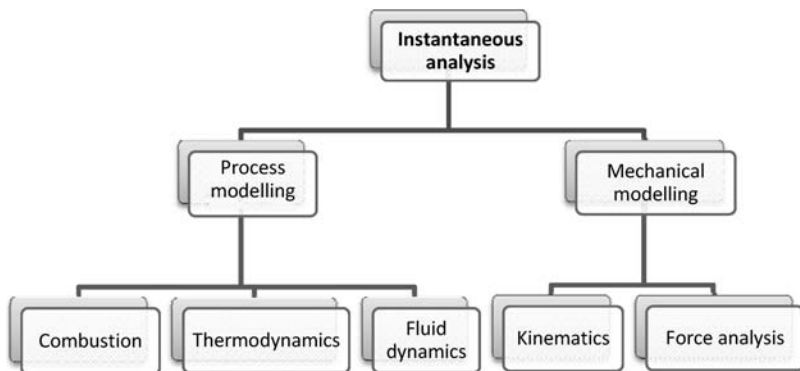
Figure 2.20 Methods of analyzing instantaneous engine outputs

The accuracy of such modelling depends on how correct its subsystems are. This approach uses sophisticated software with a large number of inputs. The second approach is a mechanical analysis method which is rather simple and accurate, provided that accurate combustion pressure data are available.

In this section, we will use the second approach to develop relations for the engine's instantaneous torque by analyzing the engine kinematics and force balance. We will start with single cylinder engines and the outputs of multi-cylinder engines will be discussed later. The justification is that a single cylinder internal combustion engine is a building block for the multi-cylinder engines. Since all cylinders are similar in an engine, once a model is built for a single cylinder, it can easily be extended to the other cylinders.

2.3.1 Engine Kinematics

The kinematics of a single cylinder engine is that of a slider-crank mechanism. Figure 2.21 illustrates the terminology of the parts of a single cylinder engine and a simplified slider-crank mechanism. The piston travels up to the top dead centre (TDC) while the crank rotates. The displacement of the piston relative to the TDC is denoted by variable x. Revolution of the crank is considered positive clockwise and denoted by angle θ (crank angle). The crank radius is R and the length of the connecting rod between points A (wrist pin or gudgeon pin) and B (connecting rod journal bearing) is l.

The total distance travelled between TDC and bottom dead centre (BDC) is denoted by L and can be written as:

$$L = R + l \tag{2.37}$$

According to Figure 2.21, the displacement x can be expressed as:

$$x = L - R\cos\theta - l\cos\beta \tag{2.38}$$

The piston speed and acceleration are the first and second time derivatives of the displacement x:

$$v_P = \frac{dx}{dt} \tag{2.39}$$

$$a_P = \frac{d^2x}{dt^2} \tag{2.40}$$
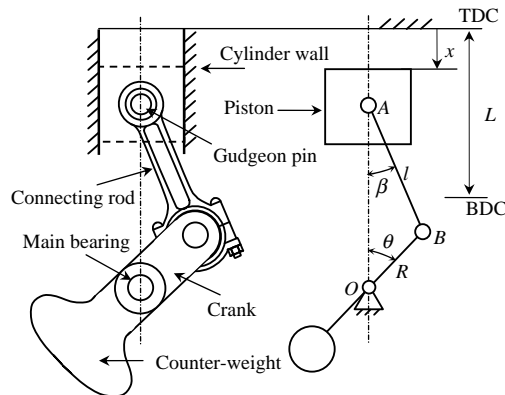
Figure 2.21   A single cylinder engine terminology

Differentiation of Equation 2.38 with respect to time will lead to equations for the speed and acceleration of piston in following forms:

$$v_P = k_v R \omega_e \tag{2.41}$$

$$a_P = k_v R \alpha_e + k_a R \omega_e^2 \tag{2.42}$$

in which ω_e and α_e are angular speed and acceleration of the engine respectively, defined as:

$$\omega_e = \frac{d\theta}{dt} \tag{2.43}$$

$$\alpha_e = \frac{d\omega_e}{dt} = \frac{d^2\theta}{dt^2} \tag{2.44}$$

k_v and k_a can be obtained from the equations below:

$$k_v = \sin\theta + \frac{R}{2l} \cdot \frac{\sin 2\theta}{\cos\beta} \tag{2.45}$$

$$k_a = \cos\theta + \frac{R}{l} \cdot \frac{\cos 2\theta}{\cos\beta} + \left(\frac{R}{l}\right)^3 \cdot \frac{\sin^2 2\theta}{4\cos^3\beta} \tag{2.46}$$

In deriving Equations 2.45 and 2.46, the trigonometric relation between the two angles θ and β is used:

$$R\sin\theta = l\sin\beta \tag{2.47}$$

Also, to determine $\cos\beta$ term in the above equations, β can be obtained from Equation 2.47:

$$\beta = \sin^{-1}\left(\frac{R}{l} \cdot \sin\theta\right) \tag{2.48}$$

Equations 2.45 and 2.46 can be simplified to approximate equations with good accuracy. The results are of the following forms [3]:

$$k_v = \sin\theta + \frac{R}{2l}\sin 2\theta \tag{2.49}$$

$$k_a = \cos\theta + \frac{R}{l}\cos 2\theta \tag{2.50}$$

In Equation 2.42, the engine acceleration term also exists (first term) but vanishes for constant engine speeds. Nonetheless, this term is usually very small and negligible compared to the term resulting from the engine speed squared, especially at top speeds. In order to obtain an impression of the relative magnitudes of the piston acceleration terms related to tangential acceleration $R\alpha_e$ and centripetal acceleration $R\omega_e^2$, consider an extreme case in which an engine is accelerating from 1000 rpm to 6000 rpm in just 1 second. During this phase rotational acceleration is constant and equal to 523.6 rad/s^2 and rotational speed is increasing. At very low engine speeds the ratio of ω_e^2 over α_e is one order of magnitude, around 2000 rpm it becomes 2 orders of magnitude and at around 6000 rpm it gets close to three orders of magnitude. This will be further examined in the next example. It is, therefore, reasonable to always use only the second term in Equation 2.42 for the piston acceleration even when the engine is accelerating. Hence:

$$a_P = k_a R \omega_e^2 \tag{2.51}$$

Example 2.3.1

The radius of the crankshaft and the connecting rod length in an engine are 50 mm and 200 mm respectively:

(a) For engine speeds of 1000, 2000 and 3000 rpm, plot the variations of piston speed and acceleration with the variation of crank angle in one full revolution of the crankshaft.
(b) Suppose an engine is accelerating from 1000 rpm to 6000 rpm in 1 second and plot the variations of both terms of Equation 2.42 at a speed of 1000 rpm.

Solution

(a) A simple use of Equations 2.41 and 2.42 together with Equations 2.45, 2.46 and 2.48 can produce the required results. A MATLAB program with two loops for engine speed (outer loop) and crank angle (inner loop) is suitable for this solution (see Figure 2.22).

```
% Example 2.3.1 (Piston speed and acceleration)

clear all, close all, clc

% Data
R=50/1000;
l=200/1000;
Rl=R/l; % define

for j=1:3
    omega(j)=1000*j;  % Engine speed (rpm)
    omeg=omega(j)*pi/30;  % (rad/s)

for i=1: 360
    theta(i)=i;    % Crank angle (deg)
    ang=i*pi/180;        % (rad)
    beta=asin(Rl*sin(ang));
    kv=sin(ang)+Rl*sin(2*ang)/cos(beta)/2;
    ka=cos(ang)+Rl*cos(2*ang)/cos(beta)+Rl^3*(sin(2*ang))^2/cos(beta)/4;
    v(i)=R*kv*omeg;
    a(i)=R*ka*omeg^2;
end
    figure(1),  plot(theta, v),  hold on
    figure(2),  plot(theta, a),   hold on
end

figure(1), grid
xlabel('Crank angle (deg)')
ylabel('Piston speed (m/s)')

figure(2), grid
xlabel('Crank angle (deg)')
ylabel('Piston acceleration (m/s2)')
```

Figure 2.22   MATLAB program listing for Example 2.3.1
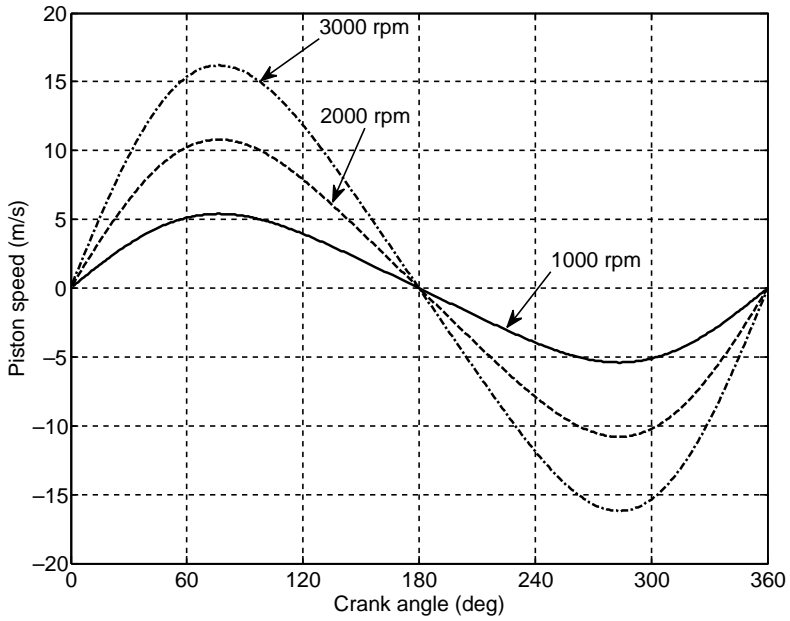
Figure 2.23   Piston speed versus crank angle for Example 2.3.1
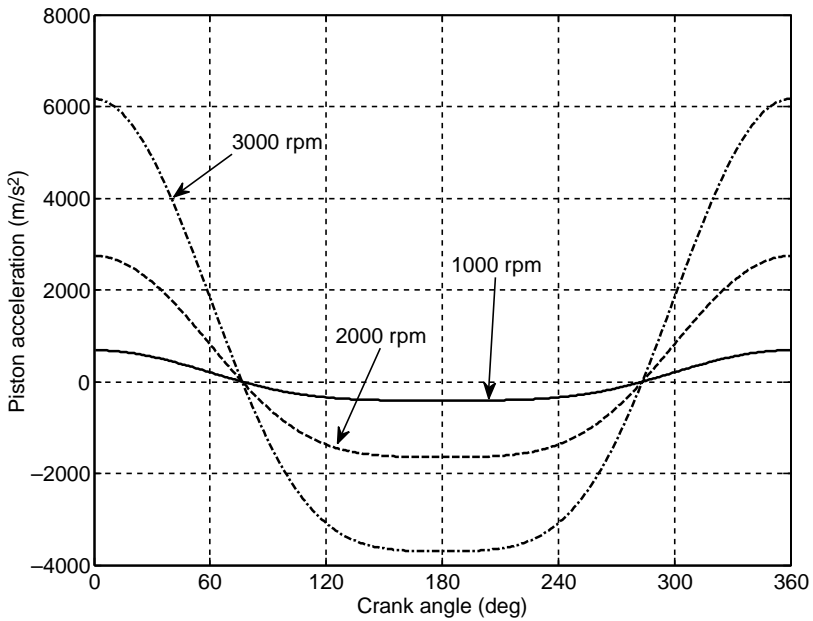
Figure 2.24   Piston acceleration versus crank angle for Example 2.3.1

Results for the piston speed and acceleration are plotted in Figures 2.23 and 2.24. Positive values refer to the downward direction and negative values to the upward direction. It is interesting to note the very large values of piston acceleration at TDC which increase with crank speed. At 3000 rpm, an acceleration higher than 600 g results and for 5000 rpm the corresponding value is more than 1700 g.

(b) It was previously mentioned that the engine acceleration is 523.6 rad/s^2. The variations of the two terms of Equation 2.42 ($k_v R \alpha_e$ and $k_a R \omega_e^2$) while the crank angle is varied from zero to 360 degrees have been calculated by the MATLAB program and the results are shown in Figures 2.23 and 2.24. It is clear from Figure 2.25 that the $k_v R \alpha_e$ term is very small compared to the centripetal acceleration term, even at very low engine speeds and its influence is to shift the whole curve a bit to the right.
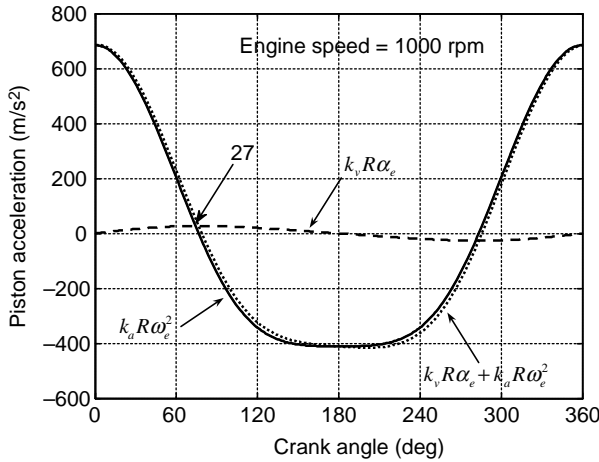
Figure 2.25 Piston acceleration terms of Equation 2.42 for Example 2.3.1

Once the piston kinematics are known, equations for the connecting rod kinematics including its rotational speeds and acceleration, and the speed and acceleration of its centre of gravity can be developed. Starting with velocity and acceleration vectors of point B, one can write according to classical dynamics:

$$V_B = \omega_e \times R \tag{2.52}$$

$$a_B = \alpha_e \times R + \omega_e \times (\omega_e \times R) \tag{2.53}$$

In which radius vector R is shown in Figure 2.26 and:

$$\omega_e = -\omega_e \hat{k} \tag{2.54}$$

$$\alpha_e = -\alpha_e \hat{k} \tag{2.55}$$

$\hat{i}, \hat{j}$ and $\hat{k}$ are a set of mutually perpendicular unit vectors fixed to the cylinder block. $\hat{i}$ and $\hat{j}$ as shown in Figure 2.26 are in horizontal and vertical directions and $\hat{k}$ makes the third direction. The solutions of
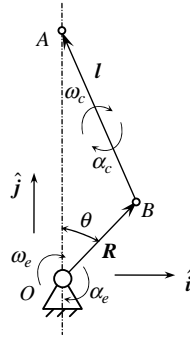
Figure 2.26 Terminology of connecting rod rotational kinematics

Equations 2.52 and 2.53 are:

$$V_B = R\omega_e(\cos\theta\hat{i} - \sin\theta\hat{j}) \tag{2.56}$$

$$a_B = R(\alpha_e\cos\theta - \omega_e^2\sin\theta)\hat{i} - R(\alpha_e\sin\theta + \omega_e^2\cos\theta)\hat{j} \tag{2.57}$$

Angular velocity and acceleration of the connecting rod can be obtained by relating the velocity and acceleration of the two ends of the connecting rod:

$$V_B = V_A + \omega_c \times l \tag{2.58}$$

$$a_B = a_A + \alpha_c \times l + \omega_c \times (\omega_c \times l) \tag{2.59}$$

In which:

$$\omega_c = -\omega_c\hat{k} \tag{2.60}$$

$$\alpha_c = -\alpha_c\hat{k} \tag{2.61}$$

and vector l is shown in Figure 2.26. Substituting for $V_A = -v_P\hat{j}$ and $a_A = -a_P\hat{j}$ in Equations 2.58 and 2.59 and making use of Equations 2.56 and 2.57, ω_c and α_c are found after some manipulations to be:

$$\omega_c = -\frac{R}{l} \cdot \frac{\cos\theta}{\cos\beta}\omega_e \tag{2.62}$$

$$\alpha_c = -\frac{R}{l} \cdot \frac{\cos\theta}{\cos\beta}\alpha_e + \frac{R}{l} \cdot \frac{\sin\theta}{\cos\beta}\omega_e^2 \tag{2.63}$$

In the derivation of Equation 2.63, a third term is also found but it is negligible. Moreover, the first term of Equation 2.63 is very small compared to the second term and can be ignored. It means that the connecting rod rotational acceleration mainly results from engine speed squared and not from engine acceleration.

With reference to Figure 2.27, the velocity and acceleration of connecting rod centre of mass G are:

$$V_G = V_A + \omega_c \times l_A \tag{2.64}$$

$$a_G = a_A + \alpha_c \times l_A + \omega_c \times (\omega_c \times l_A) \tag{2.65}$$

The right-hand sides of both Equations 2.64 and 2.65 are all known quantities and after some operations the solutions are of the final forms:

$$V_G = R\omega_e(k_1\hat{i} + k_2\hat{j}) \tag{2.66}$$
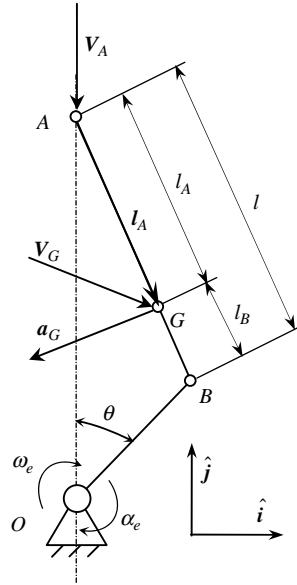
Figure 2.27   Connecting rod centre of mass kinematics

$$\boldsymbol{a}_G = R\alpha_e(k_1\hat{\boldsymbol{i}} + k_2\hat{\boldsymbol{j}}) - R\omega_e^2(k_3\hat{\boldsymbol{i}} + k_4\hat{\boldsymbol{j}}) \tag{2.67}$$

With:

$$k_1 = \frac{l_A}{l}\cos\theta \tag{2.68}$$

$$k_2 = -\left(1 + \frac{R}{l} \cdot \frac{\cos\theta}{\cos\beta} \cdot \frac{l_B}{l}\right)\sin\theta \tag{2.69}$$

$$k_3 = \frac{l_A}{l}\sin\theta \tag{2.70}$$

$$k_4 = \cos\theta + \frac{R}{l} \cdot \frac{\cos2\theta}{\cos\beta} \cdot \frac{l_B}{l} \tag{2.71}$$

In Equation 2.67, a negligible term has been excluded. l_A and l_B in Equations 2.68–2.71 as illustrated in Figure 2.27 are the distances from the CG of the connecting rod to points A and B respectively.

Example 2.3.2

The connecting rod of engine in Example 2.3.1 has a length l_A of 140 mm. Determine:

(a) the connecting rod angular speed and angular acceleration versus the crank angle for the constant engine speeds of 1000, 3000 and 5000 rpm;
(b) velocity and acceleration of connecting rod centre of mass (horizontal components, vertical components and resultant values) at engine speed of 3000 rpm.

Solution

(a) From Equations 2.62 and 2.63 the connecting rod rotational speed and acceleration can readily be obtained. The MATLAB program of Figure 2.22 can still be used by including the necessary equations for this example. The results are given in subplot format depicted in Figure 2.28. Note the huge values of angular accelerations resulting for the connecting rod especially at high speeds. These will lead to large inertia torques around the centre of gravity of the connecting rod.

(b) After evaluating the coefficients k_1 to k_4, the CG speed and acceleration can be determined from Equations 2.66 and 2.67. Results are plotted in Figures 2.29 and 2.30. The resultant speed and acceleration are obtained by taking the square root of the x and y components. Again the high values of the CG acceleration are notable. These values multiplied by the connecting rod mass will produce large inertia forces acting at the CG point.
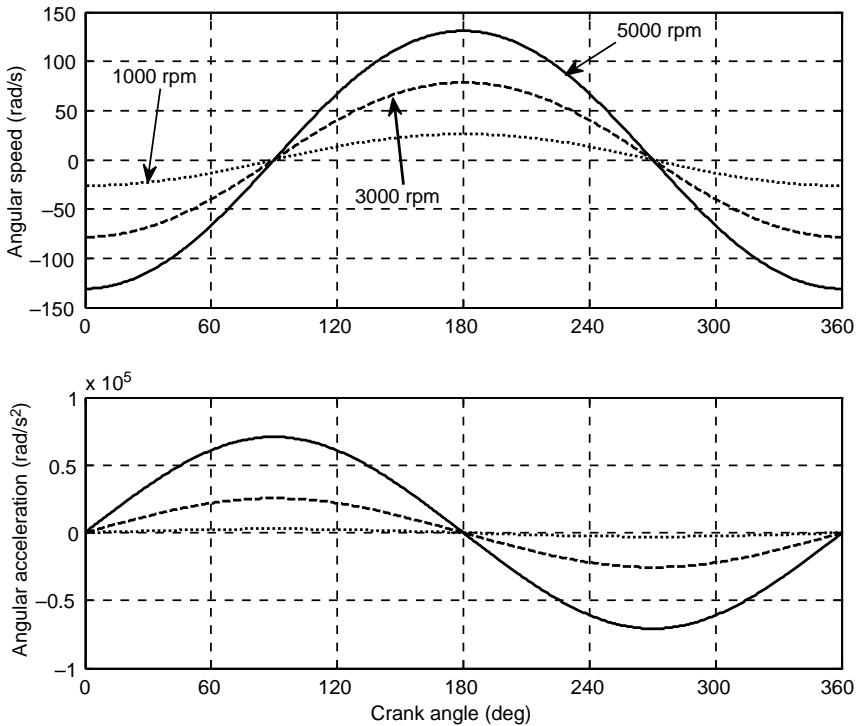
Figure 2.28 Connecting rod angular speed (top) and angular acceleration (bottom)
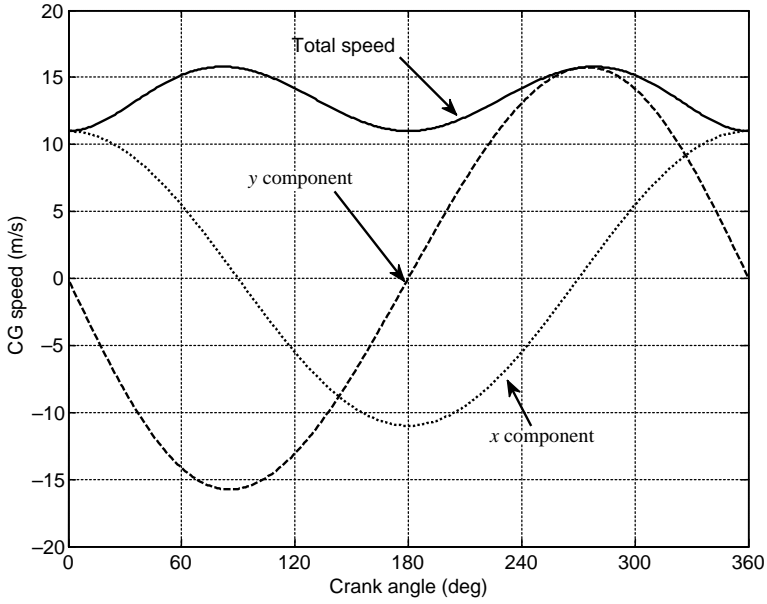
Figure 2.29   Centre of mass speed of connecting rod
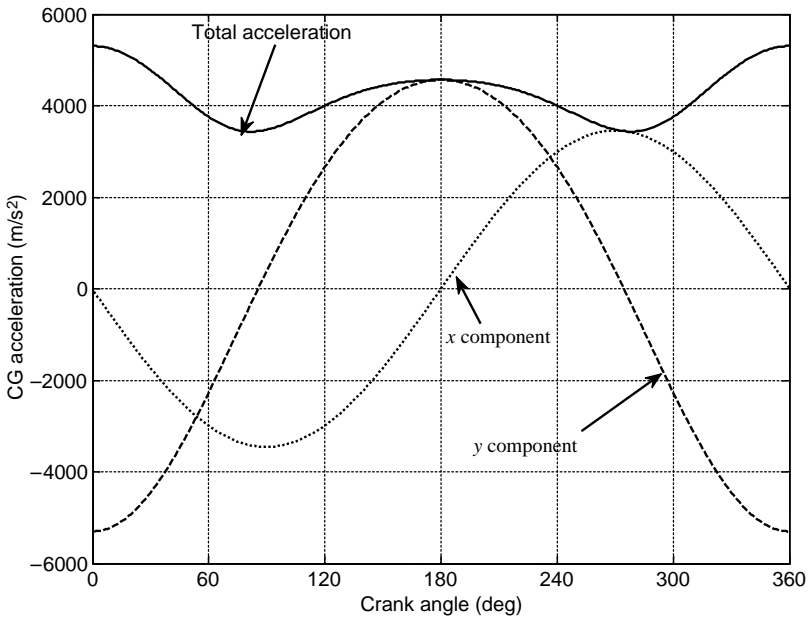
Figure 2.30   Centre of mass acceleration of connecting rod

2.3.2   Engine Torque

The pressure developed in the combustion chamber of an engine (Section 2.2.5) exerts a force on the piston top surface which pushes it down and in turn the connecting rod forces the crank to produce the engine torque T_e. Although this phenomenon looks simple, nonetheless the engine torque has no simple relation with the piston force as the line of action of this force, according to Figure 2.31, actually passes through point O, the axis of rotation of crankshaft. The complexity arises, on one hand, from the trigonometric relations and, on the other, from the inertia forces and torques acting on the connecting rod. These will be explained in this section.

In the following analyses, D'Alembert's principle will be applied in order to deal with a static problem instead of a dynamic one. To this end it suffices to include inertia forces and moments on the free-body diagrams of members under the study. The inertia force F_I and the inertia torque T_I acting on a body B are defined as:

$$F_I = -m_B a_B \tag{2.72a}$$

$$T_I = -I_B \alpha_B \tag{2.72b}$$

in which m_B is the mass of body, I_B is the mass moment of inertia of the body around its centre of mass, a_B is the centre of mass acceleration vector and α_B is the angular acceleration vector of the body in planar motion. In spatial motions, the inertia torque has a more complex form [4].

The piston force F_P is generated due to the pressure build-up in the combustion chamber. Denoting this pressure by p and the piston area by A_P, the piston force simply is:

$$F_P = pA_P \tag{2.73}$$

with units of Pascal and square metre for pressure and area, the piston force is in Newtons. If pressure is expressed in MPa (mega Pascal), obviously the force could still be in Newtons, provided the area is expressed in square millimetres.
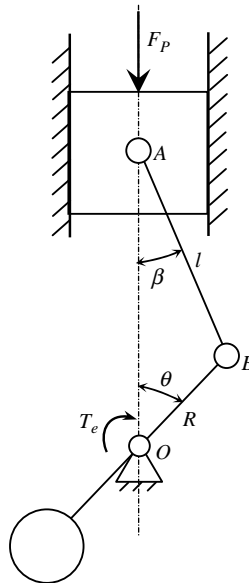
Figure 2.31   Piston force and resulting engine torque
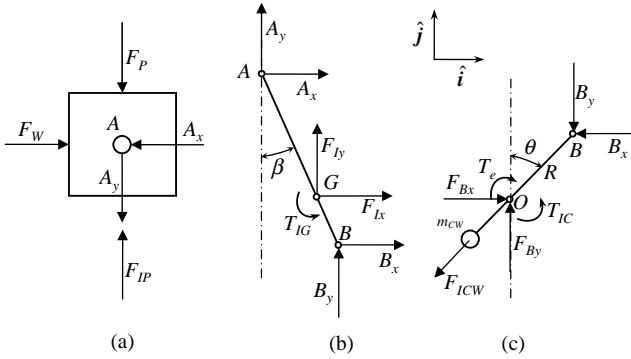
Figure 2.32 Free body diagrams of engine components

Forces acting on the piston, illustrated in Figure 2.32a, include four components apart from the pressure force F_P. Forces A_x and A_y are horizontal and vertical components of the internal bearing force acting from connecting rod side on the piston. F_W is the normal contact force exerted by the cylinder wall to the piston. In practice, the contact force also has a component along the direction of motion resulting from friction. This component has been ignored by assuming frictionless motion between the piston and cylinder. The last force acting on the piston is the inertia force F_{IP} with magnitude:

$$F_{IP} = m_P a_P \tag{2.74}$$

where m_P is the mass of piston and all attached elements (pin and keys), and a_P is the piston acceleration (Equation 2.42). Note that the direction of piston acceleration was considered to be positive downwards, thus the positive inertia force is shown upwards. Note also that the gravitational force has been disregarded due to its very small magnitude relative to the large forces involved. In addition, it has been assumed that the piston has only reciprocating motion with no rotation. In reality, however, the piston also rotates due to the backlash. This rotation, apart from producing an inertia torque, causes the contact forces to be present at both sides of the piston simultaneously. Moreover, it has been assumed that the line of action of the wall force passes directly through point A, in order to constrain the rotational balance of the piston.

The free body diagram (FBD) of the connecting rod is shown in Figure 2.32b. Two of the forces acting on the connecting rod are the reaction forces A_x and A_y (obviously in opposite directions to the piston forces). Similar bearing forces acting at point B are B_x and B_y respectively. The two other remaining forces are components of inertia force $\boldsymbol{F}_{IG}$ acting at the centre of gravity of the connecting rod G. The two components have the following magnitudes:

$$F_{Ix} = m_C a_{Gx} \tag{2.75}$$

$$F_{Iy} = m_C a_{Gy} \tag{2.76}$$

in which m_C is the mass of connecting rod, and a_{Gx} and a_{Gy} are the horizontal and vertical components of $\boldsymbol{a}_G$ in Equation 2.67. It should be noted that the both acceleration components are negative (ignoring angular acceleration components) so that the directions of the inertia forces have been taken as positive in Figure 2.32b. T_{IG} is the inertia torque acting on the connecting rod resulting from its rotational acceleration. The magnitude of this torque is:

$$T_{IG} = I_G \alpha_C \tag{2.77}$$

where I_G is the mass moment of inertia of connecting rod around its principal axis passing through its centre of gravity and α_C is the angular acceleration of connecting rod (Equation 2.63). Note that the acceleration of the connecting rod was taken to be positive clockwise, thus the direction of inertia torque is shown as counter-clockwise.

Figure 2.32c shows the free body diagram of the crankshaft. Apart from the reaction bearing forces B_x and B_y, the components of the main bearing force F_B (i.e. F_{Bx} and F_{By}) act at point O. Due to the crankshaft rotational acceleration, an inertia torque T_{IC} is present around O with magnitude:

$$T_{IC} = I_C \alpha_e \tag{2.78}$$

in which I_C is the crankshaft mass moment of inertia around its rotation axis and α_e is the engine angular acceleration. It should be noted that the centre of mass of the crankshaft and its counter-weight combined is assumed to be at point O. This is achieved by choosing an appropriate counter-weight. It is also assumed that the axis of rotation of the crankshaft is its principal inertia axis. It is worth mentioning that all bearings have been considered frictionless, otherwise the discussion would become more complicated.

The engine torque according to Figure 2.32c can be obtained by taking a moment sum around O:

$$T_e = R(B_y \sin\theta - B_x \cos\theta) - T_{IC} \tag{2.79}$$

B_x and B_y have to be obtained from the free body diagram of Figure 2.32b by writing equilibrium equations consisting of two force equations and one moment equation shown below:

$$B_x + A_x + F_{Ix} = 0 \tag{2.80}$$

$$B_y + A_y + F_{Iy} = 0 \tag{2.81}$$

$$B_x l\cos\beta + B_y l\sin\beta + T_{IG} + F_{Ix} l_A \cos\beta + F_{Iy} l_A \sin\beta = 0 \tag{2.82}$$

There are four unknowns in the three equations above, thus we will need to write one equilibrium equation for Figure 2.32a as well. For the vertical direction we have:

$$F_{IP} - A_y - F_P = 0 \tag{2.83}$$

From Equations 2.81–2.83, the two required unknowns B_x and B_y are found as:

$$B_x = \left(F_{IP} - F_P + \frac{l_B}{l} F_{Iy} \right)\tan\beta - \frac{l_A}{l}F_{Ix} - \frac{T_{IG}}{l\cos\beta} \tag{2.84}$$

$$B_y = F_P - F_{IP} - F_{Iy} \tag{2.85}$$

The engine torque (Equation 2.79) can be evaluated by making use of Equations 2.84 and 2.85. In this process, the other equations for the piston force and all inertia forces and torques will also be required. It is clear now that in calculating the engine torque from the piston force F_P, several other unknowns are necessary and the resulting equation for the engine torque is highly non-linear. Recalling that the pressure in combustion chamber is itself a function of several engine working parameters adds to the complexity of engine torque determination. Additional information regarding the external loads can also be determined from the foregoing analysis. The wall force F_W can be obtained by making use of Equation 2.80 together with an additional horizontal equation for Figure 2.32b. The result is:

$$F_W = -F_{Ix} - B_x \tag{2.86}$$
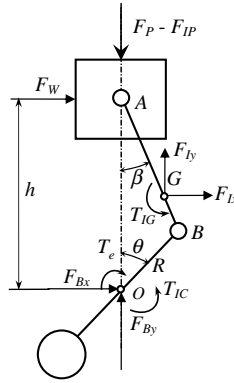
Figure 2.33   Engine torque results from the external forces

The main bearing forces are determined from the force equilibrium of Figure 2.32a as:

$$F_{Bx} = B_x + F_{ICW}\sin\theta \tag{2.87}$$
$$F_{By} = B_y + F_{ICW}\cos\theta \tag{2.88}$$

in which F_{ICW} is the inertia force resulting from centripetal acceleration of the counter-weight with mass m_{CW} at a radius R_{CW} from the crank axis:

$$F_{ICW} = m_{CW}R_{CW}\omega_e^2 \tag{2.89}$$

An alternative way to determine the engine torque is to consider the whole engine assembly under the action of external forces and moments shown in Figure 2.33. The main advantage of this approach is that the internal forces will not be present. Note that the inertia forces and torques are taken into account. Taking moments around the crankshaft axis of rotation results in the following relation for the engine torque:

$$T_e = F_W h + F_{Ix}(h - l_A\cos\beta) - F_{Iy}l_A\sin\beta - T_{IG} - T_{IC} \tag{2.90}$$

in which:

$$h = R\cos\theta + l\cos\beta \tag{2.91}$$

Example 2.3.3

Specifications of a single cylinder, four-stroke engine are available in Table 2.5. The variation of pressure in the combustion chamber with crank angle at engine speed of 3000 rpm is given in Table 2.6. Determine and plot the variation of following parameters with the variation of crank angle in one engine cycle:

(a) piston pressure force, inertia force and their resultant force in one single figure;
(b) connecting rod inertia forces;
(c) connecting rod inertia torque;
(d) crank-pin bearing forces;
(e) engine torque.

Table 2.5   Engine information of Example 2.3.3

1	Piston mass	430 g
2	Connecting rod mass	440 g
3	Connecting rod pin-pin length l	140 mm
4	Connecting rod pin B-CG length l_B	37 mm
5	Crank radius	49 mm
6	Piston area	5800 mm^2
7	Connecting rod inertia	0.0015 kgm^2

Table 2.6   Combustion chamber pressure for Example 2.3.3

θ (deg)	0	20	23	26	50	60	70	80	100	110	150
P (bar)	18	32	32.5	32	20	15	10	8	6	5	3
θ (deg)	190	200	220	540	600	630	660	690	710	720	
P (bar)	1.2	0.6	0	0	1.0	2.0	4	9	15	18	

Solution

A MATLAB program provided in Figure 2.34 is suitable to solve this problem. Since the engine is four-stroke, one complete cycle takes two revolutions or 720 degrees. Data given for pressure is not

```
% Example 2.3.3 - Single cylinder, 4 stroke-engine torque

clc, clear all, close all

% Inputs:
mP=430/1000;    % Piston mass  kg
mC=440/1000;    % Connecting rod mass  kg
l=140/1000;     % Connecting rod pin-pin length    m
lB=37/1000;     % Connecting rod pin B-CG length lB    m
R=49/1000;      % Crank radius    m
Ap=5800;        % Piston area    mm2
IC=0.0015;      % Connecting rod inertia   kg.m2

% Pressure in combustion chamber
pr=[18 32 32.5 32 20 15 10 8 6 5 3 1.2 0.6 0 0 1.0 2.0 4 9 15 18];
% Corresponding crank angles (deg)
ca=[0 20 23 26 50 60 70 80 100 110 150 190 200 220 540 600
630 660 690 710 720];

% Generate an evenly distributed data for pressure
theta=0: 2: 720; % Crank angle for two complete revolutions
p=interp1(ca, pr, theta);
```

Figure 2.34   MATLAB program for Example 2.3.3 (First part)

```
% Piston pressure force
Fp=p*Ap/10;

omega=3000;  %Engine speed (rpm)
omeg=omega*pi/30;
Rl=R/l;        % define ratio R over l
lA=l-lB

% Loop to solve engine kinematics
for i=1: 361
    ang=2*(i-1)*pi/180;
    sa=sin(ang); ca=cos(ang); s2a=sin(2*ang); c2a=cos(2*ang);  % define
    beta=asin(Rl*sin(ang));
    ka=ca+Rl*c2a/cos(beta)+Rl^3*s2a^2/cos(beta)^3/4;
    aP(i)=R*ka*omeg^2;                % Piston acceleration
    alpha_c(i)=Rl*omeg^2*sa/cos(beta);  % Connecting rod angular acceleration
    k3=lA*sa/l;
    k4=ca+Rl*c2a*lB/cos(beta)/l;
    agx(i)=-R*omeg^2*k3;              % x component
    agy(i)=-R*omeg^2*k4;              % y component
    ag(i)=sqrt(agx(i)^2+agy(i)^2);    % Resultant acceleration
end

% Piston inertia force
FIP=-mP*aP;
FPt=Fp+FIP;  % Resultant piston force
plot (theta, Fp, '--')
hold on
plot (theta, FIP, '-.', theta, FPt)
xlabel('Crank angle (deg)')
ylabel('Forces on the piston (N)')
grid
% Connecting rod inertia forces
FIx=-mC*agx; FIy=-mC*agy;
figure
plot (theta, FIx)
hold on
plot (theta, FIy, '--')
xlabel('Crank angle (deg)')
ylabel('Connecting rod inertia forces (N)')
grid
% Connecting rod inertia torque
TIG=IC*alpha_c;
figure
plot (theta, TIG)
xlabel('Crank angle (deg)')
ylabel('Connecting rod inertia torque (Nm)')
grid
% Crank-pin bearing forces
for i=1: 361
    beta=asin(Rl*sin(theta(i)*pi/180));
    Bx(i)=(-FIP(i)-Fp(i)+lB*FIy(i)/l)*tan(beta)-lA*FIx(i)/l-TIG(i)/l/cos(beta);
end
```

Figure 2.34   (*Continued*)

```
                      By=Fp+FIP-FIy;
                 figure
                 plot (theta, Bx)
                 hold on
                 plot (theta, By, '--')
                 xlabel('Crank angle (deg)')
                 ylabel('Crank-pin bearing forces (N)')
                 grid
                 % Engine torque
                 for i=1: 361
                    thetai=theta(i)*pi/180;    beta=asin(Rl*sin(thetai));
                    Te(i)=R*(By(i)*sin(thetai)-Bx(i)*cos(thetai));
                 end
                 Teav=mean(Te)*ones(1,361); % Average torque
                 figure
                 plot (theta, Te)
                 hold on
                 plot(theta, Teav)
                 grid
                 xlabel('Crank angle (deg)')
                 ylabel('Engine torque (Nm)')
```

Figure 2.34   (*Continued*)

distributed evenly and thus is not suitable to be used in a program. A small loop is included to convert the pressure data to evenly distributed points throughout 720 degrees of crank angle, 2 degrees apart. Comments are included in the program to make it self-explanatory. The results obtained from the program are depicted in Figures 2.35 to 2.39. It should be emphasized that the
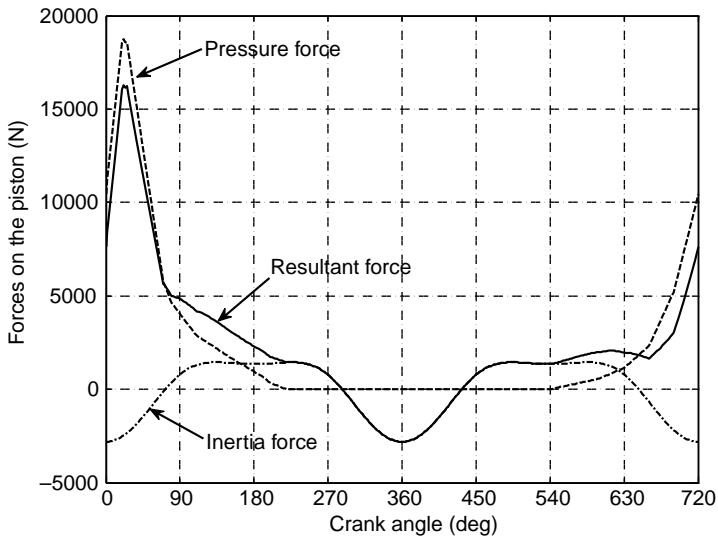
Figure 2.35   Piston forces of Example 2.3.3, part (a)
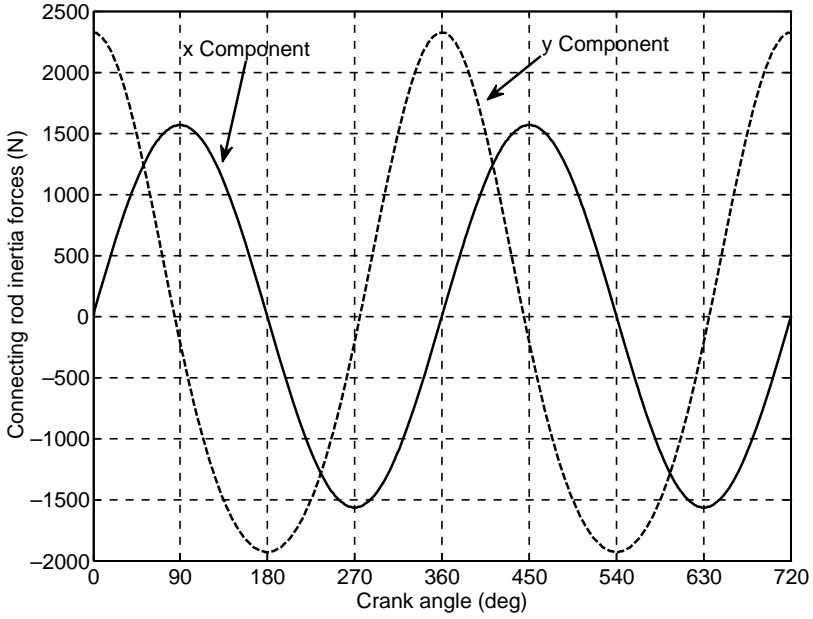
Figure 2.36 Connecting rod inertia forces of Example 2.3.3, part (b)
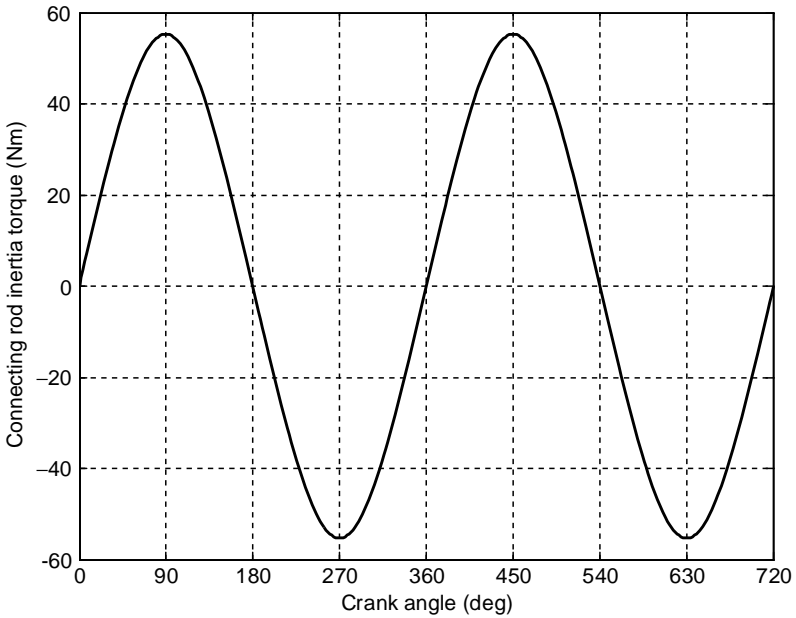
Figure 2.37 Connecting rod inertia torque of Example 2.3.3, part (c)
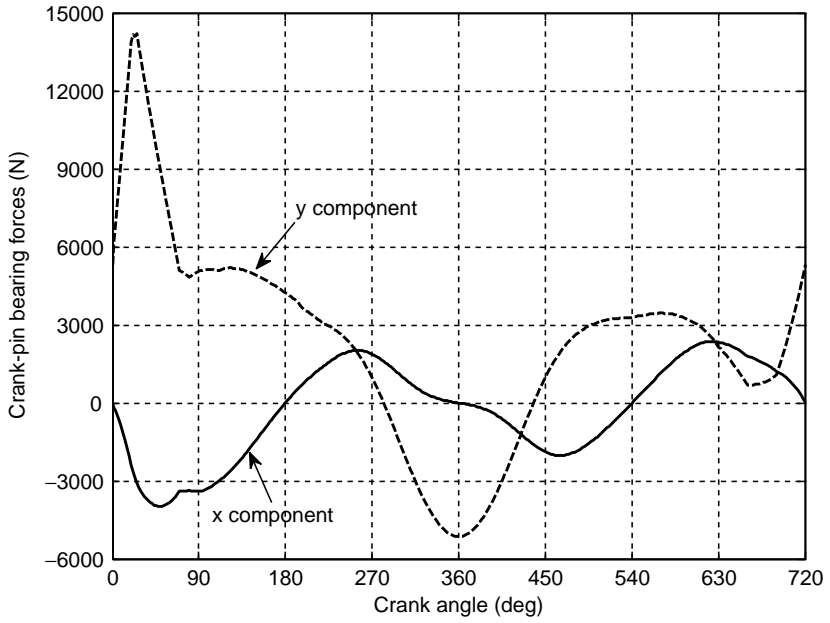
Figure 2.38 Crank-pin bearing forces of Example 2.3.3, part (d)
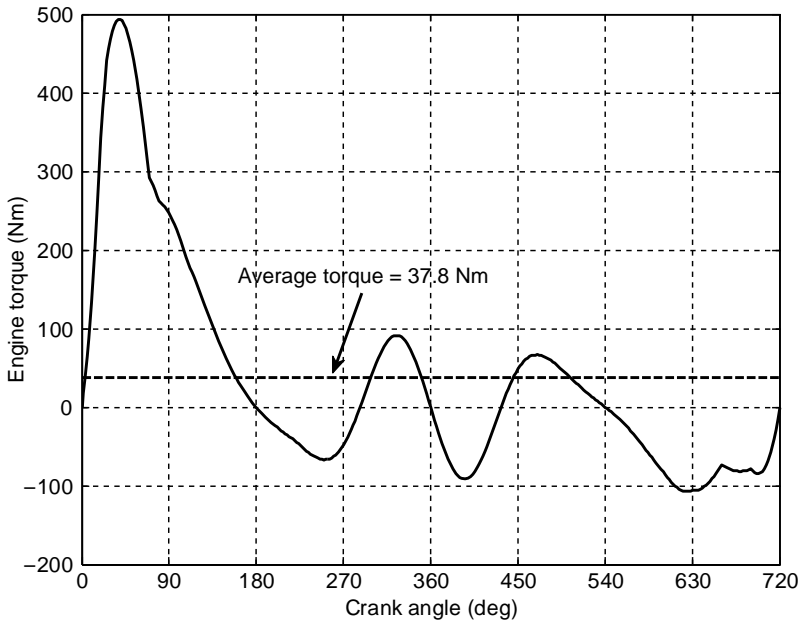
Figure 2.39 Engine torque of Example 2.3.3, part (e)

results obtained from this solution belong to the specific set of data used here and only general conclusions can be made.

   Figure 2.35 shows that the net piston force resulting from pressure and inertia is downwards (positive) most of the time and becomes upwards (negative) for only around 20% of a cycle. Figure 2.36 shows that the connecting rod inertia force is larger in the vertical direction. The inertia torque of the connecting rod in Figure 2.37 has zero average but it has large values compared to the engine output torque. Figure 2.38 indicates that the crank pin vertical force is larger than its horizontal component. This vertical force produces the main part of the engine torque. The engine torque is shown in Figure 2.39. Although the instantaneous values of engine torque are at some points very large, nevertheless the average value of the output torque is less than 10% of its maximum value. It is worth noting that the whole engine torque shown in Figure 2.39 belongs to only one average speed of 3000 rpm. The question may arise of how an engine acquires a constant speed (say, 3000 rpm) when the torque output is varying. This issue will be discussed in more detail in Section 2.3.4.

2.3.3   A Simplified Model

The concept of excluding the internal forces from the analysis was used in Figure 2.33 and to derive Equation 2.90. Nonetheless, the evaluation of Equation 2.90 is still dependent on the availability of components that were obtained from the full separation method presented earlier. As a result the concept is not really useful unless all components can be obtained within the method itself.

   Consider Figure 2.33 once again to analyse the problem for a stand-alone determination of all unknown loads in the engine assembly. This system involves four unknowns F_{Bx}, F_{By}, F_W and T_e, and is statically indeterminate. One additional equation, therefore, is necessary in order that the four unknowns can be determined. An approximate solution can be found by replacing the connecting rod with a two-force member. As such, in addition to providing an additional relation between the unknown external forces, the connecting rod inertia forces and moment will be removed from the model. To see how the additional relationship is formed, consider the engine model with a two-force connecting rod member shown in Figure 2.40. The connecting rod element will carry the force F along its direction. Resolving the forces along the direction γ perpendicular to the direction of F, will lead to the equilibrium of upper part:

$$F_W = (F_P - F_{IP})\tan\beta \tag{2.92}$$

This will serve as the additional equation.

   However, the question remains of what justification can one use to replace the actual connecting rod with a two-force, mass-less member? Obviously by doing so, the dynamic properties of the system will change unless the replacement member keeps the dynamic properties of the original connecting rod.

   The original connecting rod shown in Figure 2.41a has mass m, length l, moment of inertia I_C and its CG is located a distance l_A from point A (wrist pin) and a distance l_B to point B (crank pin). Let us examine the possibility of replacing this connecting rod with a mass-less link L of Figure 2.41b with two point masses m_A and m_B attached to it at endpoints A and B respectively. In order that the dynamical properties for the proposed system remain identical to the original connecting rod, the following conditions must be satisfied:

$$m_A + m_B = m \tag{2.93}$$
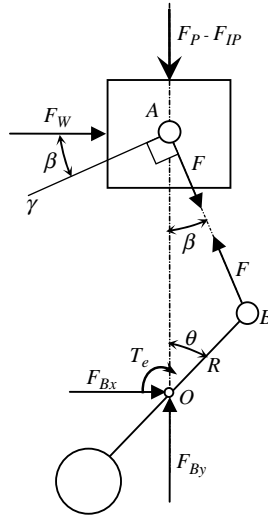
Figure 2.40 Engine model with two-force connecting rod

$$m_A l_A = m_B l_B \tag{2.94}$$

$$m_A l_A^2 + m_B l_B^2 = I_C \tag{2.95}$$

Equations 2.93–2.95 stand for the equality of mass, CG location and moment of inertia of the two systems. Since the locations of two point masses are chosen to coincide with points A and B, only two equations out of three are adequate to determine the two masses m_A and m_B. However, as long as the third equation is not satisfied, there is no guarantee that the two systems are dynamically equivalent. For instance, from
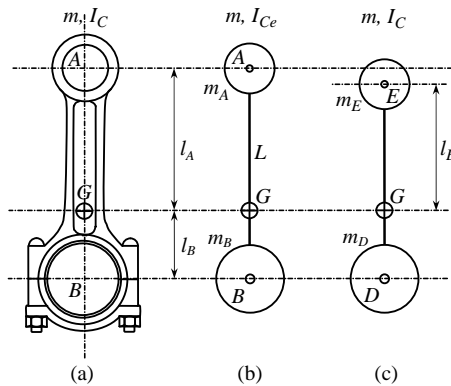
Figure 2.41 Connecting rod equivalent masses

Equation 2.93 and 2.94, the two masses are obtained as:

$$m_A = \frac{l_B}{l}m \qquad (2.96)$$

$$m_B = \frac{l_A}{l}m \qquad (2.97)$$

Substituting into Equation 2.95 results:

$$ml_A l_B = I_C \qquad (2.98)$$

In practice for a real connecting rod, usually $I_C < ml_A l_B$, which means if the two masses are fixed at A and B, the resulting moment of inertia from Equation 2.98 would be greater than the actual value. In other words, if an exact dynamic equivalence is to be used, then only one of the masses, say, m_B, can be fixed and the location of the other one together with the values of the two masses should be obtained from Equations 2.93–2.95. Calling the first mass in this case m_D and the other m_E, equations to calculate the unknowns l_E, m_D and m_E are:

$$l_E = \frac{I_C}{ml_B} \qquad (2.99)$$

$$m_D = \frac{l_E}{l_B + l_E}m \qquad (2.100)$$

$$m_E = \frac{l_B}{l_B + l_E}m \qquad (2.101)$$

Since $I_C < ml_A l_B$, l_E is less than l_A and the mass m_E will be positioned below point A as indicated in Figure 2.41c.

The foregoing discussion indicated that in order to substitute a dynamically equivalent mass system for the connecting rod, one of the end masses will be located out of the rotation points A or B. This system, therefore, is not kinematically compatible with the engine motions and hence despite its accuracy it is not workable. On the other hand, placing the two masses over the required joints A and B, makes the mass system kinematically compatible, but dynamically different with the original system to some degree, mainly due to the change in the moment of inertia of the connecting rod. The resulting error for the increase of the connecting rod inertia may vary for different engines but is limited to around 30%. This difference will not make major deviations to the system outputs and hence this simplified mass system is generally used for the engine torque generation analysis.

With this substitution the simplified engine model will look like that of Figure 2.42 in which two point masses m_A and m_B are placed at wrist-pin and crank-pin points and the connecting rod is replaced by a rigid link L. According to the preceding discussions, the crank angular acceleration is not influential in the inertia force and torques of the components, therefore, inertia forces for the masses rotating with crank angular acceleration are considered only in radial directions. These include the inertia forces, F_{IB} belonging to mass m_B and F_{ICW} belonging to mass m_{CW}. The mass of the counter-weight can be selected properly to balance the inertia force F_{IB} and thus free the main bearing from the related loads. On the other side, m_A will move with piston and can be regarded as part of the piston mass. Therefore, the inertia force F_{IP} has the magnitude:

$$F_{IP} = (m_P + m_A)a_P \qquad (2.102)$$

Now according to this simplified engine model all external forces will pass through point O, except F_W, the force acting on the cylinder wall. Therefore, the engine torque simply is:

$$T_e = F_W h \qquad (2.103)$$
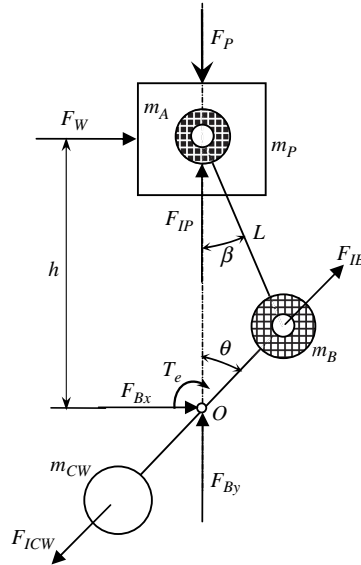
Figure 2.42 Simplified engine model

in which h and F_W are obtained from Equations 2.91 and 2.92 respectively. Finding the main bearing forces for the simplified model is then straightforward and the results are:

$$F_{Bx} = -F_W \tag{2.104}$$

$$F_{By} = F_P - F_{IP} \tag{2.105}$$

Example 2.3.4

Use the information given in Example 2.3.3 for the connecting rod:

(a) Calculate the exact dynamic equivalent system.
(b) Calculate masses m_A and m_B located at A and B and corresponding inertia I. As a percentage how much larger is I than the actual value?

Solution

(a) The solution to this part can be obtained by using Equations 2.98–2.100. The results are:

$$l_E = \frac{0.0015}{0.440 \times 0.037} = 0.0921 \ m \ (92.1 \ \text{mm})$$

$$m_D = \frac{92.1}{37 + 92.1} \times 440 = 313.9 \ g$$

$$m_E = \frac{37}{37 + 92.1} \times 440 = 126.1\,g$$

(b) To find the answers for this part, Equations 2.95–2.97 must be used. The results for m_A, m_B and I are:

$$m_A = \frac{37}{140} \times 440 = 116.3\,g,$$

$$m_B = 440 - 116.3 = 323.7\,g$$

$$I = ml_A l_B = 0.44 \times 0.103 \times 0.037 = 0.0017\,kgm^2$$

The percentage that I is larger than I_C is:

$$\frac{I - I_C}{I_C} \times 100 = \frac{17 - 15}{15} \times 100 = 13.3\%$$

Example 2.3.5

Use the engine data of Example 2.3.3 together with a simplified engine model and plot the variation of the following parameters with the crank angle variations during one full cycle:

(a) the forces acting on the piston;
(b) the engine torque compared with that of the exact model.

Solution

The MATLAB program of Example 2.3.3 can be modified in order to obtain the results of this example. The changes are provided in Figure 2.43. The results of running this program will look like those presented in Figures 2.44 and 2.45.

```
% Example 2.3.5 – Single cylinder engine torque (simplified model)

% Inputs: See Example 2.3.3
% Generate an evenly distributed data for pressure: See Example 2.3.3
% Piston pressure force: See Example 2.3.3

% Connecting rod point masses
mA=lB*mC/l;
mB=mC-mA;
lA=l-lB;
IC=mC*lA*lB;

% Kinematics: See Example 2.3.3

% Piston and mA inertia force
FIP=-(mP+mA)*aP;
```

Figure 2.43   MATLAB program modifications for Example 2.3.5

```
% Plot piston forces: See Example 2.3.3

% Engine torque
for i=1: 361
    thetai=theta(i)*pi/180;
    beta=asin(Rl*sin(thetai));
    h=R*cos(thetai)+l*cos(beta);
    FW(i)=FPt(i)*tan(beta);
    Te(i)=h*FW(i);
end
% Plot engine torque: See Example 2.3.3
```

Figure 2.43   (*Continued*)

The inertia force acting on the piston shown in Figure 2.44 has larger magnitudes compared to those of Example 2.3.3 obviously due to addition of m_A to the piston mass. The resultant force, therefore, has lower amplitudes for this model.

The variation of engine torque in Figure 2.45 shows that the output of simplified model is close to that of the exact model. It is worth noting that the engine average torque remains unchanged.
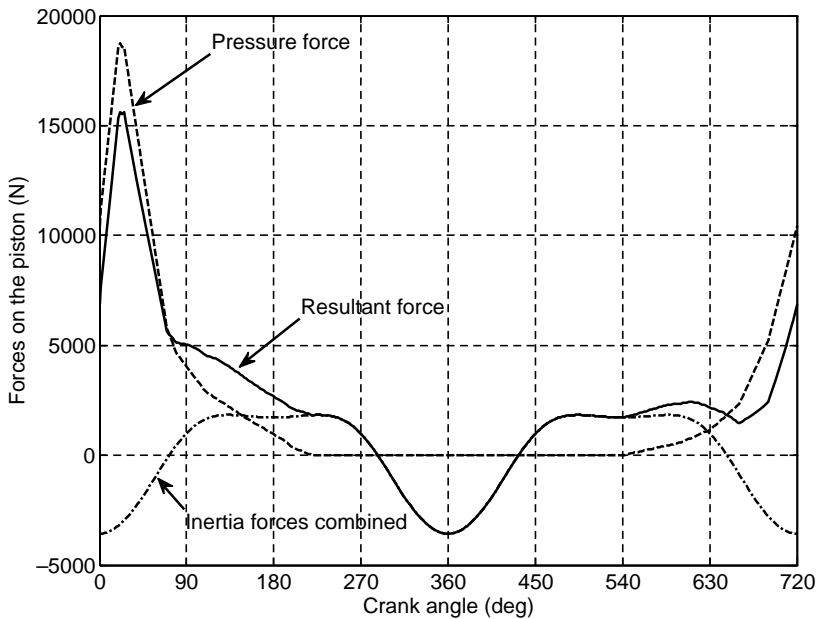
Figure 2.44   Forces acting on the piston for Example 2.3.5
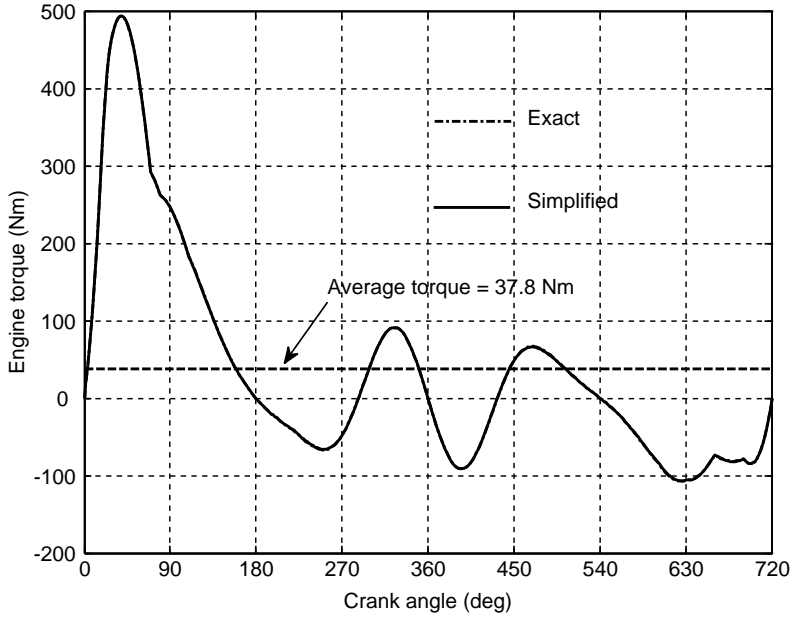
Figure 2.45   Engine torque of Example 2.3.5 compared to results of Example 2.3.3

Example 2.3.6

Use $F_{ICW} = F_{IB}$ of the simplified model to determine the main bearing force of the exact model and compare the wall force F_W and main bearing force F_B of the two models for the engine data of Example 2.3.3.

Solution

In Equations 2.87 and 2.88, F_{ICW} is needed in order that the components of F_B can be determined. F_{IB} is the inertia force of the equivalent mass at point B or $F_{IB} = m_B R \omega_e^2$. In the program written for the exact model, the calculation of F_{IB} should be included and used to determine the main bearing force components. The cylinder wall force F_W was already determined in the program for the simple model and can be included in the last loop of Figure 2.43 for the exact model. The results obtained in this way are plotted in Figures 2.46 and 2.47.

It can be seen that the differences in the wall forces are small but those of the main bearing forces are considerable for the simplified and exact models. The average value of F_W is exactly equal for the two cases, but the average of main bearing force is different as indicated in Figure 2.47.
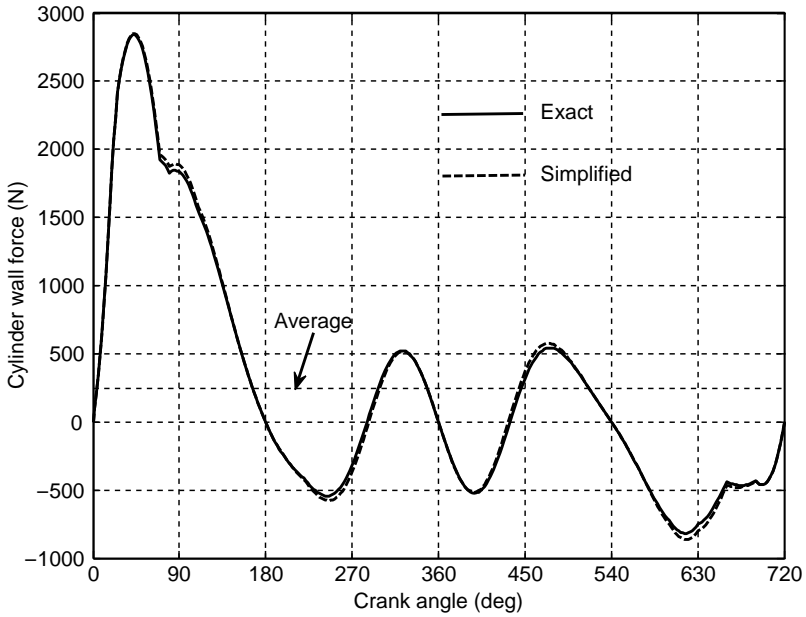
Figure 2.46   Comparison of cylinder wall force for exact and simplified models
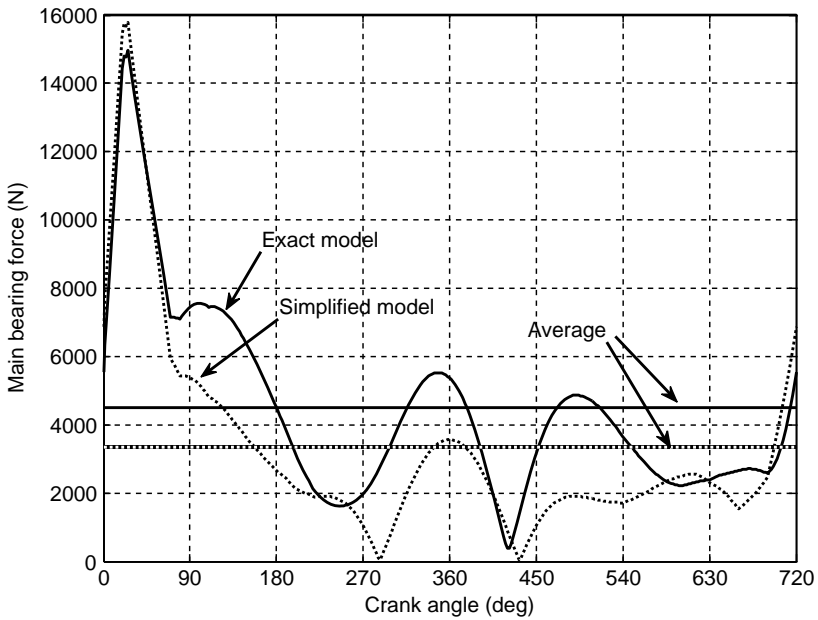
Figure 2.47   Comparison of main bearing force for exact and simplified models

2.3.4   The Flywheel

Since the pressure variation in the combustion chamber is speed dependent, each engine torque diagram is obtained for a specific engine speed. The variation of engine torque with the crank angle was studied in the previous section and typical diagrams were presented. On the other hand when the engine torque varies, it will also cause the engine speed also to vary. This is contradictory to the first assumption that the torque variation belongs to a specific (constant) engine speed. In this section, the objective is to clarify how a flywheel can resolve this conflict.

Consider an engine output shaft that is attached to a flywheel with inertia I_e (including inertia of crankshaft and other related masses) and drives a load L (Figure 2.48). According to Newton's Second Law of Motion in rotation, the net torque on the rotating mass with speed ω_e causes it to accelerate with acceleration α_e:

$$T_e(t) - T_L = I_e \alpha_e = I_e \frac{d\omega}{dt} \qquad (2.106)$$

Assuming a constant load torque T_L, then in order to obtain a constant engine rotational speed, the instantaneous engine torque $T_e(t)$ must be equal to the load torque. This means that the engine must produce a net torque that is not time-variant, contrary to what we found earlier that the engine torque was varying with the crank angle. Therefore, according to Equation 2.106, the speed fluctuations will be inevitable and the best one could do is to require an average engine speed with small fluctuations. The first step is to put the average engine torque T_{av} equal to the load torque:

$$T_{av} = T_L \qquad (2.107)$$

By using the chain rule in differentiation, Equation 2.106 can be written in terms of the crank angle variations:

$$T_e - T_{av} = I_e \omega \frac{d\omega}{d\theta} \qquad (2.108)$$

and can be integrated between two arbitrary points 1 and 2:

$$\int_1^2 (T_e - T_{av}) d\theta = \frac{1}{2} I_e (\omega_2^2 - \omega_1^2) \qquad (2.109)$$
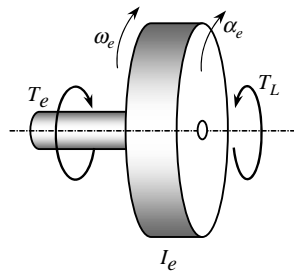
Figure 2.48   Engine output shaft attached to a flywheel

The right-hand side is the net kinetic energy of rotating inertia when its speed changes from ω_1 to ω_2. The left-hand side of the equation is the work done by the net external torque on the rotating mass from angle θ_1 to angle θ_2. The speeds ω_1 and ω_2 correspond to the crank angles θ_1 and θ_2. In other words the speed ω_i occurs when the crank angle is θ_i.

From Equation 2.109, it is clear that when the net work from point 1 to point 2 is positive, the speed ω_2 will be larger than speed ω_1 and vice versa. Of course it makes sense that the kinetic energy will increase when the work done by the external torques is positive. This work according to Equation 2.109 is the area under the $T(\theta)$ curve relative to T_{av}. Graphically in the torque diagram of Figure 2.49, the shaded areas above and below the average torque illustrate the positive and negative areas. On the left side of the positive shaded area, the crank angle and speed are θ_0 and ω_0 and at the right side θ_1 and ω_1 respectively. Thus $\omega_1 > \omega_0$ since from θ_0 to θ_1 the area under the torque-angle diagram is positive. A similar explanation results in $\omega_2 < \omega_1$, $\omega_3 > \omega_2$, etc.

Among all individual speeds ω_i, one will be the largest ω_{Max} and one the smallest ω_{min}. It is desirable to keep these two extreme speeds of the engine as close to each other as possible in order that the speed fluctuations remain small. The ideal situation is to have ω_{Max} equal to ω_{min} and both equal to the average engine speed ω_{av}. A fluctuation index i_F can be defined to quantify the speed fluctuations of an engine:

$$i_F = \frac{\omega_{Max} - \omega_{min}}{\omega_{av}} \quad (2.110)$$

in which:

$$\omega_{av} = \frac{\omega_{Max} + \omega_{min}}{2} \quad (2.111)$$
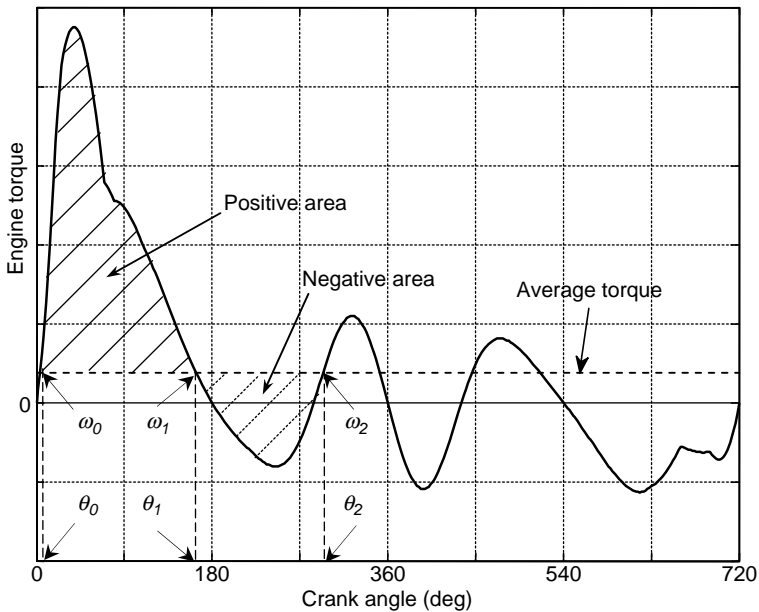
Figure 2.49 Positive and negative areas in a typical engine torque diagram

Table 2.7   Areas under the engine torque curve

	1	2	3	4	$\cdots$	$\cdots$	k
A_i	A_1	A_2	A_3	$\cdots$	$\cdots$	$\cdots$	A_k
ΣA	A_1	$A_1 + A_2$	$A_1 + A_2 + A_3$	$\cdots$	$\cdots$	$\cdots$	$\cdots$
$min\ \Sigma A$		A_{min}					
$Max\ \Sigma A$					A_{Max}		

A desirable design goal is to have small values for the dimensionless factor i_F in order to ensure small speed fluctuations relative to the average engine speed. If ω_1 and ω_2 in Equation 2.109 are replaced by ω_{min} and ω_{Max} respectively, the right-hand side of equation will convert to:

$$\frac{1}{2} I_e(\omega_{Max}^2 - \omega_{min}^2) = i_F I_e \omega_{av}^2 \tag{2.112}$$

The left-hand side of Equation 2.109 by this substitution is the net area under the engine torque curve between crank angles θ_{min} and θ_{Max} corresponding to speeds ω_{min} and ω_{Max}. Designating this net area by A^* and using Equation 2.112, one simply finds:

$$I_e = \frac{A^*}{i_F \omega_{av}^2} \tag{2.113}$$

which is an equation to estimate the flywheel inertia, provided that the area A^* and the fluctuation index i_F are available. The latter should be chosen by experience and the former can be evaluated from the engine torque diagram.

Suppose there are k individual areas under the engine torque-θ curve. In order to determine the net area A^*, first the crank angles θ_{min} and θ_{Max} should be found. Let us construct a table like Table 2.7 in which the individual areas are recorded in the second row. In the third row cumulative sum of areas up to that point is recorded. Since some of the areas are positive and some negative, one of the cells in ΣA row will have the minimum value and one the maximum value.

The cells with the minimum and maximum cumulative areas A_{min} and A_{Max} have θ_{min} and θ_{Max} points respectively. The net area under the curve between the minimum and maximum speed points simply is:

$$A^* = A_{Max} - A_{min} \tag{2.114}$$

It is important to note that when the engine is connected to the vehicle driveline, the inertia resulting from the rotating masses and vehicle mass itself (see Section 3.9) is greater than that needed to keep the engine speed regular. In fact, the flywheel is a device that consumes energy to accelerate together with the engine and this energy is wasted in many circumstances, especially when the vehicle stops. Therefore, the best solution is to keep the flywheel as small as possible.

Example 2.3.7

An engine has a torque-θ diagram shown in Figure 2.50 at 3000 rpm. Design a flywheel in order that the maximum fluctuation in engine speed is 2% of its average speed.
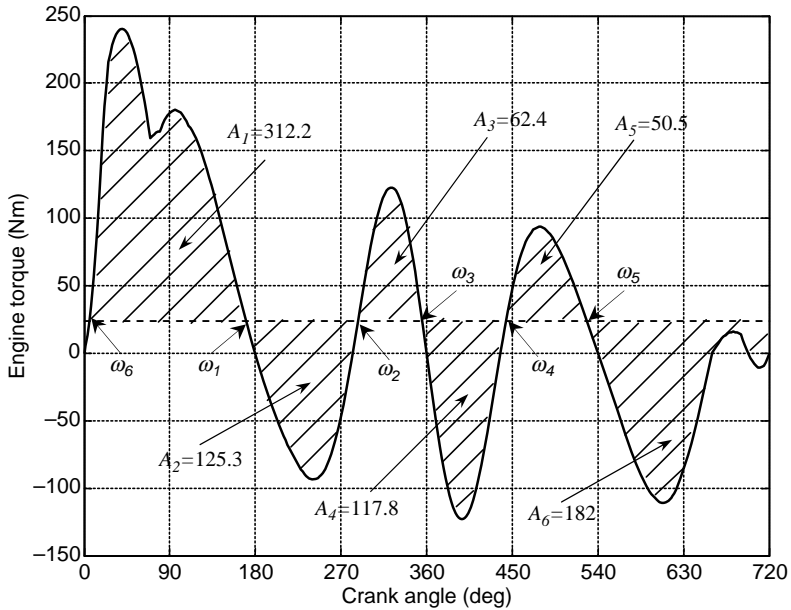
Figure 2.50   Engine torque curve of Example 2.3.7

Solution

Data from Figure 2.50 is inserted in Table 2.7 and the results are summarized in Table 2.8. According to the ΣA values, ω_1 is the maximum speed and ω_6 is the minimum speed. A^* can therefore be calculated from Equation 2.114 and the result is $A^* = 312.2$. From the given information, the maximum fluctuation in speed is 2% relative to the average speed. Thus the fluctuation index is 0.02 and from Equation 2.113, the flywheel inertia can be calculated:

$$ I_e = \frac{312.2}{0.02 \times (3000 \times \pi/30)^2} = 0.158 \, kg \, m^2 $$

Table 2.8   Areas under the engine torque curve of Example 2.3.7

Item	1	2	3	4	5	6
A_i (Joule)	312.2	−125.3	62.4	−117.8	50.5	−182
ΣA (Joule)	312.2	186.9	249.3	131.5	182	0
$min \, \Sigma A$						A_{min}
$Max \, \Sigma A$	A_{Max}					

2.4 Multi-cylinder Engines

In practice, almost all automotive applications use multi-cylinder engines; single cylinder engines are extremely rare but may still be found in low duty earthmoving vehicles. A multi-cylinder engine is a combination of several single cylinder engines that share a single crankshaft. Different crank arrangements and firing orders are possible for multi-cylinder engines and these have important effects on the overall smoothness of power delivery.

2.4.1 Firing Order

In a multi-cylinder engine there must be a sequence in which the power stroke of each cylinder takes place, one after another. The power stroke always follows the compression stroke and thus the layout of crankshaft plays an important role in designating the power or firing order in an engine. Firing order also depends on the number of cylinders and by increasing this number, the choices for the firing order also increase.

In order to determine the firing order in an engine, it is necessary to first specify the crank layout and define the state of each cylinder relative to the state of cylinder 1. It is convenient to assume the first cylinder is in the combustion stroke and from the relative crank angles of the multiple cylinders, the state of each cylinder can be specified. When the cylinder 1 advances to the next stroke (exhaust), one of the cylinders that was in its compression stroke previously must fire at this stage. This sequence will continue until the first cylinder's turn starts over again.

This process can be illustrated graphically by specifying the foregoing information for a four-cylinder, four-stroke in-line engine in a chart format as shown in Figure 2.51. First the crankshaft layout is drawn vertically on the left side with the number of cylinders shown next to each crank. In front of each crank, four boxes are drawn on the right side indicating the successive strokes of each cylinder. For instance, cylinder 1 starts with power stroke and follows by exhaust, intake and compression strokes. Moving to cylinder 2, one must decide whether it is in exhaust or in compression stroke, since both cylinders 2 and 3 are in the same state and thus either can be in exhaust or compression. Selecting the exhaust for cylinder 2 will stipulate the states of the other cylinders as indicated in Figure 2.51. In fact, inside each row the stroke order for each cylinder is specified and in each column the relative state of all cylinders is denoted. Once the first left column is specified, the contents of each row are known by the permutation of strokes in each
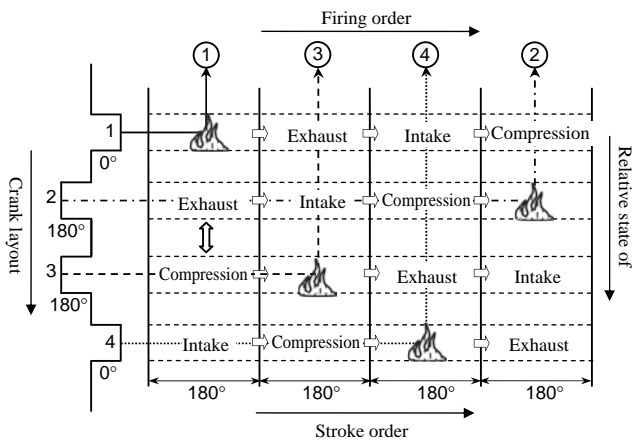
Figure 2.51   Chart for determination of firing order
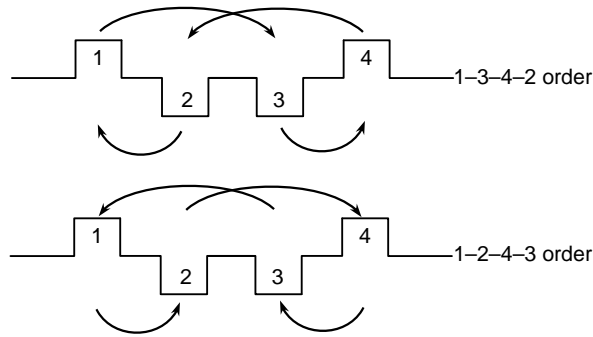
Figure 2.52   Symmetry of power strokes for both firing orders

cylinder. On construction of the chart, the firing order can then be specified by taking the number of cylinders in each column that are in power stroke (from left to right). For instance, the engine of Figure 2.51 has a firing order of 1–3–4–2.

It was possible to select the compression stroke for the 2nd cylinder after cylinder 1. In that case the second and third rows would be swapped over and the firing order would become 1–2–4–3. The choice between these two options must be made according to other criteria since, as far as the engine operation is concerned, both choices are acceptable.

Other factors in choosing the firing orders are torsional loads on the crankshaft and uniform charge and discharge of intake and exhaust gases insides manifolds. For a four-cylinder inline engine, these factors are similar for both choices of firing order. Figure 2.52 illustrates how the two cases have symmetrical circulation of power strokes among the cylinders.

Example 2.4.1

Consider a two-cylinder, four-stroke engine with a crankshaft arrangement shown in Figure 2.53. Analyze the firing order of the engine by constructing the chart of Figure 2.51.
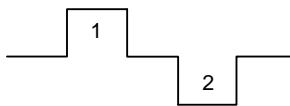
Figure 2.53   Crankshaft layout of two-cylinder engine

Solution

According to the chart of Figure 2.51, the firing order of the two-cylinder engine can simply be considered as the two upper rows as shown in Figure 2.54a. Thus the firing of cylinder 2 will take place after one and half complete revolutions (540 degrees) of the crankshaft behind the cylinder 1. Alternatively, one could assume that cylinder 2 is at the compression stage rather than the exhaust state when cylinder 1 is at ignition. This situation is illustrated in Figure 2.54b.

(a) Cylinder 2 starting from exhaust stage

(b) Cylinder 2 starting from compression stage
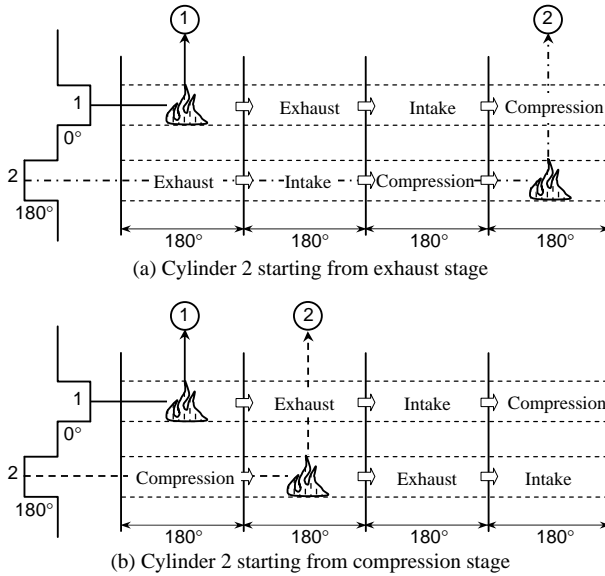
Figure 2.54 Firing order charts of a two-cylinder engine

In the previous examples, the crank angles were all multiples of 180 degrees, however, in several types of engines the crank angles are different. For example, a six-cylinder inline engine has crank angles for different cylinders as multiples of 120 degrees. In such a case, the procedure for developing the firing order is similar to that explained earlier; nevertheless care must be taken in the construction of the crank layout and stroke shifts. Crank angles can be specified in the chart for each individual cylinder. We did this previously by writing the crank angle below each crank. The stroke shifts were all 180 degrees for flat crankshafts; for other types such as inline six-cylinder crankshaft the stroke shifts are multiples of 120 degrees. Let us construct the firing order chart for this six-cylinder engine. The crank layout is 0-240-120-120-240-0 and in order to make the layout clearer in the chart, a side view of crankshaft will be useful. Figure 2.55 shows this type of presentation. Starting from cylinder 1 as usual, the top row can easily be constructed. For cylinder 2, we note that according to the crank layout it has a 120 degree lag relative to cylinder 1, so the stroke order for this cylinder must be shifted accordingly. The stroke order can begin either from intake or from combustion, thus leaving two possibilities for the firing order (in Figure 2.55, the intake stroke is chosen). Cylinder 3 has a 240 degree lag relative to cylinder 1 and to construct the stroke order for this case, the excess over 180 degree (i.e. 60 degrees) is taken for the starting stroke. The stroke order can begin either from combustion or exhaust; here the former is considered. The processes for remaining cylinders are similar to those explained for cylinders 2 and 3.

As Figure 2.55 illustrates, the firing order for this engine is 1–5–3–6–2–4. However, if other choices for the stroke orders of cylinders 2 and 3 were considered, alternative firing orders could also be achieved. Other possibilities are: 1–6–5–4–3–2, 1–2–3–4–5–6, 1–4–2–5–3–6 and 1–4–5–2–3–6.

2.4.2 Engine Torque

Successive firings cause a continuous torque delivery to the crankshaft output. Since the torque generated by every individual cylinder is dependent on the crank angle, the resultant engine torque is a combination
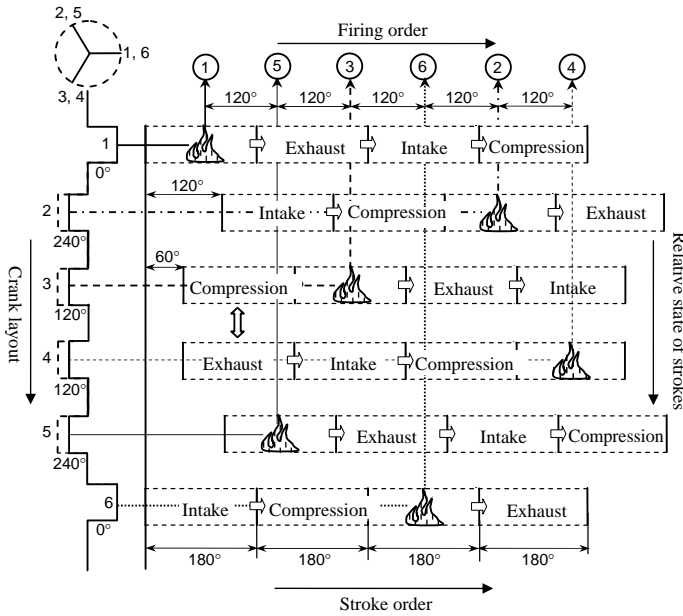
Figure 2.55 Firing order chart for a six-cylinder inline engine

of all individual torques from all cylinders. In order to evaluate the net engine torque, information on the firing order must be available.

Let us assume all cylinders have identical pressure-crank angle profiles, otherwise the engine torque for each cylinder would be different. The torque variation of a single cylinder was obtained for its own crank angle variations. In order to add up the torques of all cylinders, they must be represented relative to a single reference. It is common to take the crank angle of the first cylinder as a reference for all cylinders. Therefore, the crank angle of each cylinder can be written in terms of the crank angle of first cylinder θ_1:

$$\theta_i = \theta_1 - \Delta_{Ci} \tag{2.115}$$

where Δ_{Ci} is the crank angle of ith cylinder relative to the crank of cylinder 1. In order to write the torque of each individual cylinder in a form that can be added to the other torques, it is also necessary to express the cylinder pressure according to the correct state of that cylinder. If the pressure of cylinder 1 is denoted by $P(\theta_1)$ then pressure for other cylinders can be written in the form:

$$P_i = P(\theta_1 + \Delta_{Si}) \tag{2.116}$$

in which the state angle Δ_{Si} is the angle of rotation of the crankshaft for the current state of the ith cylinder. Or simply for the states of combustion, exhaust, intake or compression, Δ_{Si} will be $0°$, $180°$, $360°$ and $540°$ respectively.

Once the correction angles Δ_{Ci} and Δ_{Si} for all cylinders are obtained, the engine torque can be determined simply by adding up all individual torques of n cylinders in the following form:

$$T_e = \sum_{i=1}^{n} T_i(\theta_1, \Delta_{Ci}, \Delta_{Si}) \tag{2.117}$$

In an alternative approach, 'shift-sum' processes can be used to add up the torques of individual cylinders to obtain the overall torque variation of a multi-cylinder engine. A torque diagram for a single cylinder
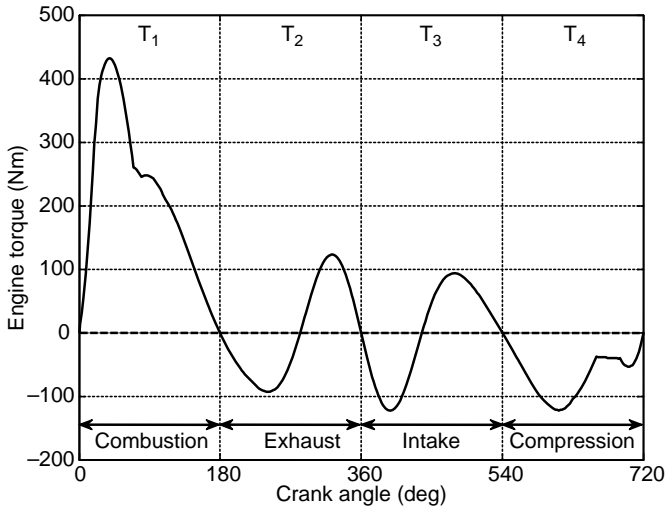
Figure 2.56 Torque variations in different strokes

engine can be divided into four sections according to the engine strokes (see Figure 2.56). The torque variation for cylinder 1 of a multi-cylinder engine is taken as the basis for all engine cylinders. Thus the permutation of torque segments for this cylinder according to Figure 2.56 simply is $T_1 + T_2 + T_3 + T_4$. The torque variation of other cylinders can be obtained according to their state angle. In order to construct the torque variation of another cylinder with state angle of Δ_{Si}, the base torque diagram should be shifted backwards by the amount of Δ_{Si}. Whatever falls off on the left end moves to the right end of the resulting diagram. For instance, if cylinder i has $\Delta_{Si} = \pi$, the torque permutation for this cylinder will be $T_2 + T_3 + T_4 + T_1$. Once the torque variation of each cylinder is obtained, the summation of all torques will result in the total engine torque.

Example 2.4.2

Consider the two-cylinder engine of Example 2.4.1 and assume that the pressure distribution given in Example 2.3.3 is also applicable to this engine. The engine dimensions are considered to be identical to those of Example 2.3.3 except the piston area which has to be determined assuming equal displacements for both engines. Use the firing order of Figure 2.54b.

(a) Calculate the correction angles Δ_{Ci} and Δ_{Si} for cylinder 2.
(b) Write a MATLAB program to obtain the overall engine torque according to simplified engine model and plot the variation of engine torque at 3000 rpm.
(c) Plot the variation of forces acting on the pistons.

Solution

(a) According to crankshaft layout of Figure 2.53, Δ_{Ci} is 180° (or π). Δ_{Si} from an analysis of Figure 2.54b is 3×180° (or 3π) since cylinder 2 starts from compression.

(b) For the simplified engine model the overall engine torque for a two-cylinder engine can be written as:

$$T_e = \sum_{i=1}^{2} F_{W_i} h_i$$

in which:

$$F_{W_i} = (F_{P_i} - F_{IP_i})\tan\beta_i$$

$$h_i = R\cos\theta_i + l\cos\beta_i$$

Since the engine displacement is meant to be equal to previous single cylinder engine of Example 2.3.5, the piston area should be halved.

A MATLAB program implementing above procedure is listed in Figure 2.57. Engine torque output is depicted in Figure 2.58. It is seen that the torques of both cylinders are similar but with a shift.

```
% Example 2.4.2 - Two cylinder engine torque (simplified model)

% Multicylinder information
N=2;            % Number of cylinders
DC=[0 pi];           % Crank angles of cylinders
DF=[0 3*pi];       % State angle of cylinders
Tet=zeros(1,361);      % Overall engine torque vector

% Inputs: (See Example 2.3.3)
Ap=5800/N;      % Piston area      mm2

% Connecting rod point masses (See Example 2.3.5)

omega=3000;          %Engine speed (rpm)
omeg=omega*pi/30;
Rl=R/l;

for j=1:N
for i=1: 361
   ang=(2*(i-1)*pi/180+DC(j));      % Crank angle
   sa=sin(ang); ca=cos(ang);          % define
   s2a=sin(2*ang); c2a=cos(2*ang); % define
   beta=asin(Rl*sa);
   ka=ca+Rl*c2a/cos(beta)+Rl^3*s2a^2/cos(beta)^3/4;
   aP(i)=R*ka*omeg^2;      % Piston acceleration
   % Piston pressure force
   n=i+DF(j)*360/4/pi;          % n: Variable to shift pressure
   if n>=361 n=n-360; end
   Fp(j,i)=p(n)*Ap/10;          % Shift pressure
   FIP(j,i)=-(mP+mA)*aP(i); % Piston and mA inertia force
   FPt(j,i)=Fp(j,i)+FIP(j,i);   % Resultant force
   % Engine torque
   h=R*ca+l*cos(beta);
   FW(j,i)=FPt(j,i)*tan(beta);
   Te(j,i)=h*FW(j,i);
end
Tet=Tet+Te(j,:);      % Torque sum
end
Teav=mean(Tet)*ones(1,361);      % Average torque
% Plot outputs:
```

Figure 2.57 MATLAB program listing for Example 2.4.2
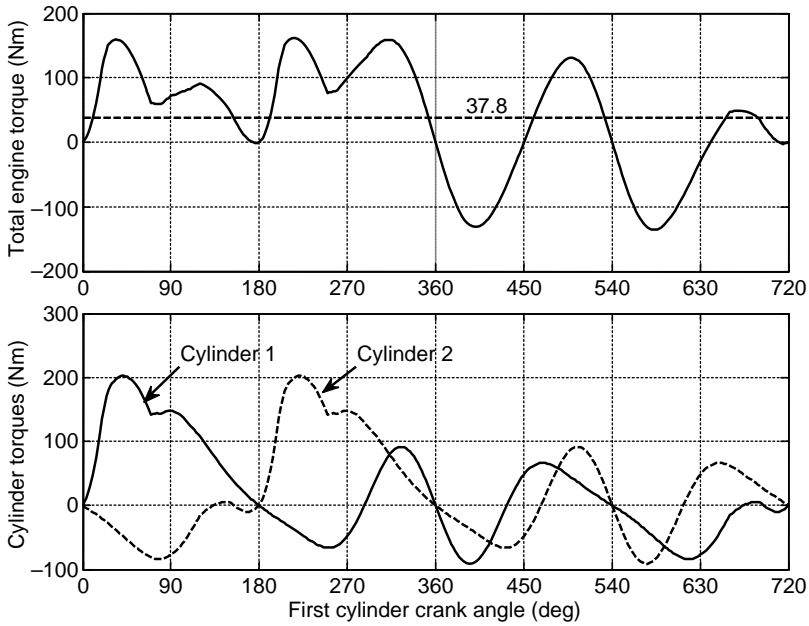
Figure 2.58 Engine torques of Example 2.4.2
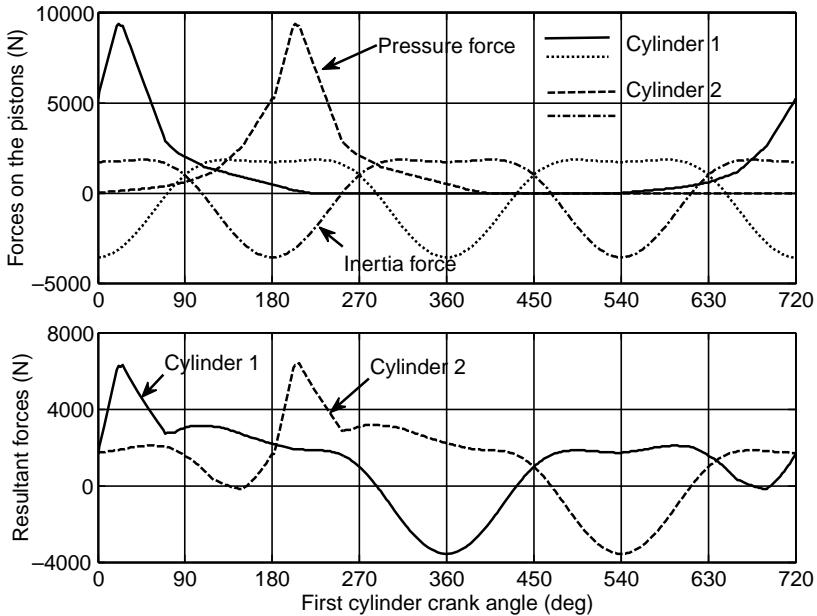
Figure 2.59 Piston forces of Example 2.4.2

(c) The variation of piston forces of both cylinders is plotted in Figure 2.59. Piston forces are also similar for both cylinders and are generated according to the firing order of each cylinder.

Example 2.4.3

For a four-cylinder engine with 1–3–4–2 firing order, use the information of Example 2.4.2 and assume the same engine displacement:

(a) Plot the variation of engine torque versus the angle of rotation of first crank at 3000 rpm.
(b) Estimate the flywheel inertia for the engine for a 2% fluctuation.

Solution

(a) According to the firing chart of a four-cylinder engine with 1–3–4-2 firing order (Figure 2.51), the states of all cylinders are 'fire', 'exhaust', 'compression' and 'intake' respectively. Thus the state angles of cylinders are 0°, 180°, 540° and 360°. A sample MATLAB program given in Figure 2.60 solves the problem by 'shift and sum' method. The output is shown in Figure 2.61.

(b) The torque variation of (a) consists of 8 total loops, 4 positive and 4 negative. Since all the positive loops are identical and all the negative loops are also equal, this means that one positive loop

```
% Example 2.4.3 – Four cylinder engine torque (simplified model),
% "shift-sum" method

% Multicylider information
N=4;                          % Number of cylinders
DF=[0 pi 3*pi 2*pi];                       % State angle of cylinders
Tet=zeros(1,361);             % Overall engine torque vector

% Inputs: (See Example 2.3.3)
Ap=5800/N;                                 % Piston area       mm2
% Connecting rod point masses (See Example 2.3.5)

omega=3000;  %Engine speed (rpm)
omeg=omega*pi/30;
Rl=R/l;
% Single cylinder engine base torque
for i=1: 361
    ang=2*(i-1)*pi/180;     % Crank angle
    sa=sin(ang); ca=cos(ang);       % define
    s2a=sin(2*ang); c2a=cos(2*ang); % define
    beta=asin(Rl*sa);
    ka=ca+Rl*c2a/cos(beta)+Rl^3*s2a^2/cos(beta)^3/4;
    aP(i)=R*ka*omeg^2;      % Piston acceleration
    Fp(i)=p(i)*Ap/10;                % Piston pressure force
    FIP(i)=-(mP+mA)*aP(i); % Piston and mA inertia force
    FPt(i)=Fp(i)+FIP(i);                   % Resultant force
    % Engine torque
    h=R*ca+l*cos(beta);
    FW(i)=FPt(i)*tan(beta);
    Te(i)=h*FW(i);
end
```

Figure 2.60 MATLAB program listing for Example 2.4.3

```
for j=1:N                              % Torque summation loop
   for i=1: 361                        % Shifting loop
   n=i+(DF(j)*360/4/pi);
   if n>=361 n=n-360; end
   Tei(i)=Te(n);
   end
Tet=Tet+Tei;
end
Teav=mean(Tet)*ones(1,361);                        % Average torque
plot (theta, Tet)
hold on
plot(theta, Teav)
grid
xlabel('First cylinder crank angle (deg)')
ylabel('Total engine torque (Nm)')
```

Figure 2.60   (*Continued*)
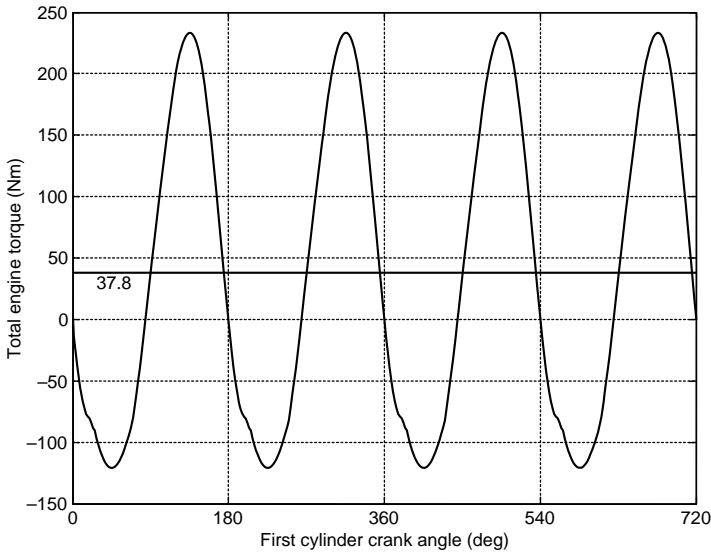
Figure 2.61   The torque output of four-cylinder engine of Example 2.4.3

area equals to one negative loop area. Therefore each one of the areas in the torque diagram is equal to A^* of Equation 2.113. An approximate value for each area is 160 Nm, so:

$$I_e = \frac{A^*}{i_F \omega_{av}^2} = \frac{160}{0.02 \times (3000 \times \pi/30)^2} = 0.08 \, kg \, m^2$$

Comparing this value with that found for the single cylinder engine, it is observed that for an identical average engine torque, a smaller flywheel is necessary as the engine torque becomes more regular.

2.4.3   Quasi-Steady Engine Torque

The average engine torque is the mean value of the torque fluctuations during one complete engine cycle that can be considered at any arbitrary steady engine speed. It was, however, seen that the engine speed also had an unsteady nature and fluctuated around an average value. In practice, the average speed of the engine is treated as its steady speed. Strictly speaking, however, it can be considered as a quasi-steady speed. Hence, the average engine torque associated with its quasi-steady speed will be its quasi-steady torque.

The mean value of the engine torque at a specified speed was evaluated in the foregoing examples simply by averaging the values of torque at different crank angles. That process required the availability of the pressure variations of the cylinder(s) with the crank angle at the specified speed, as well as the dynamic properties of the engine elements. If only the quasi-steady engine torque is required, instead of using the pressure distribution at a specified speed, an alternative way is to work with the brake mean effective pressure p_{bme} (or $bemp$) which is similar to the indicative mean effective pressure p_{ime} defined in Section 2.2.3. In fact p_{bme} is related to the real (measured) engine output work whereas p_{ime} is related to the indicated work calculated from the standard engine cycles.

The work done by the pressure force in the ith cylinder of an engine during one revolution of the crankshaft is:

$$W_i = \frac{2}{s} p_{bme} A_P L \tag{2.118}$$

in which A_P and L are the piston area and stroke length respectively, and s is the number of strokes in the full cycle of engine operation (for a two-stroke engine, s is 2 and for a four-stroke engine, it is 4). At the engine speed of n (rpm), the engine power (work per second) for the ith cylinder is:

$$P_i = p_{bme} A_P L \cdot \frac{n}{30s} \tag{2.119}$$

For an N cylinder engine, the engine power simply is:

$$P_e = p_{bme} A_P L \cdot \frac{nN}{30s} \tag{2.120}$$

Engine displacement V_e is defined as the total volume swept by all pistons:

$$V_e = N A_P L \tag{2.121}$$

The engine power, therefore, can be written as:

$$P_e = p_{bme} V_e \cdot \frac{n}{30s} \tag{2.122}$$

The engine power at the same time can be expressed in terms of the average engine torque T_{av}:

$$P_e = \frac{\pi}{30} T_{av} \cdot n \tag{2.123}$$

Combining Equations 2.122 and 2.123 leads to:

$$T_{av} = \frac{V_e}{\pi s} p_{bme} \tag{2.124}$$

This equation indicates a direct relationship between the engine average torque and mean effective pressure at a given engine speed.

Example 2.4.4

For the engine of Example 2.3.3, determine the mean effective pressure and compare it with the average of pressure values during a cycle.

Solution

The stroke length and engine volume are:

$$L = R + l = 189 \, mm$$

$$V_e = A_P L = 5800 \times 10^{-6} \times 189 \times 10^{-3} = 0.0011 \, m^3$$

The engine is four-stroke and from Example 2.3.3 the average torque was 37.8, using Equation 87 the p_{bme} is:

$$p_{bme} = \frac{\pi s}{V_e} T_{av} = \frac{4\pi}{0.0011} \times 37.8 = 431,826 \, Pa$$

The average pressure distribution during a cycle is found by command 'mean(p)' and the result is 4.10 MPa which is almost ten times larger than p_{bme} calculated above.

2.5 Engine Torque Maps

The foregoing discussions in Sections 2.3 and 2.4 were all focused on determination of the engine torque at certain speeds for single cylinder and multi-cylinder engines. In practice, engines work at an infinite number of different conditions depending on the input and output parameters. Each working condition of an engine corresponds to a torque and a speed (and hence power).

In the vehicle powertrain analysis process, the engine characteristics contain critical input information and hence inaccurate information for engine performance will result in unrealistic vehicle behaviour outputs. Hence, for a complete vehicle performance analysis, a full range of engine working conditions is necessary. Such information must be collected either from analytical engine models that solve the mathematical equations related to the engine fluid flow, combustion and dynamics, or from experiments. Due to the complexity of the full engine operation modelling, and the lack of fully developed technical software, the main trend so far has been to conduct experimental data collection for the engine performance using dynamometers.

2.5.1 Engine Dynamometers

A dynamometer, in general, is a device for measuring the power of a rotating source by simultaneously measuring its output torque and rotational speed. Dynamometers are of two general types, namely absorption (or passive) and driving (or active) dynamometers. The first category of dynamometers is used as loading devices for power generating machines such as engines. The second types of dynamometers are used to rotate machines such as pumps. A dynamometer can be designed to either drive a machine or to absorb power from a machine and is called a universal dynamometer.
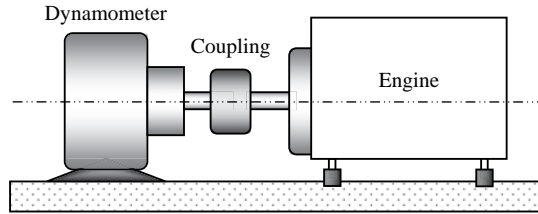
Figure 2.62 Schematic of an engine dynamometer set-up

A dynamometer applies variable braking loads on the engine and measures its ability to change or hold the speed accordingly. The main role of a dynamometer is to collect speed and torque measurements, but they can also be used in engine development activities such as combustion behaviour analysis, engine calibrations and simulated road loadings. Apart from engine dynamometers that are used for testing the engine and its components, the full vehicle powertrain can also be tested by using a chassis dynamometer that applies road loads to the driving wheels.

An engine dynamometer acts as a variable load that must be driven by the engine and it must be able to operate at any speed and any level of torque that engine can produce. The main task of a dynamometer is to absorb the power developed by the engine in the form of heat and dissipate it to the atmosphere or possibly convert the power to electrical energy. An engine dynamometer set-up is schematically shown in Figure 2.62.

A laboratory dynamometer requires measuring devices for the operating torque and speed. Dynamometers also need control systems in order to maintain a steady operating condition suitable for measurements. They can be controlled based on load speed or load torque. Dynamometers having torque regulators operate at a set torque and the engine operates at the full range of speeds it can attain while developing that specified torque. Conversely dynamometers with speed regulators develop a full range of load torques and force the engine to operate at the regulated speed. In addition, engine tests require standard or regulated atmospheric conditions. For this purpose dynamometers are equipped with peripheral air quality control systems.

Load torques can be produced by different means of energy absorption systems and this concept is the basis for the development of different types of dynamometers. Some dynamometers have absorber/driver units that can produce both load and driving torques. Figure 2.63 lists several types of dynamometers.

Eddy current (EC) dynamometers are currently the most popular type used in modern dynamometers. The EC absorbers provide quick load change rates for rapid load settling. Eddy current dynamometers use vehicle brake type cast-iron discs and use variable electromagnets to change the strength of the magnetic field to control the amount of braking torque. EC systems also allow controlled acceleration rates in addition to steady state conditions.

The power calculation from a dynamometer must be carried out indirectly from torque and angular velocity measurements. Measurement of the load torque can be achieved in several mechanical or electrical ways. In a purely mechanical way, the dynamometer housing is restrained by a torque arm that prevents it from rotating. The internal reaction torque exerted on the housing is borne by the torque arm and this torque can be determined by measuring the force exerted by the housing on the arm and multiplying it by the arm length from the centreline of the dynamometer. A load cell transducer can provide an electrical signal scaled in such a way that it is directly proportional to the load torque. Alternatively a torque-sensing coupling or torque transducer producing an electrical signal proportional to the load torque can be used.

Speed measurement is a simpler task and a wide selection of tachometer equipment with an electrical signal output proportional to speed is available for this purpose. Once the load torque and rotational speed signals have been obtained and transmitted to the data acquisition system of the dynamometer, the engine output power can simply be determined by multiplying the two quantities (in proper units).
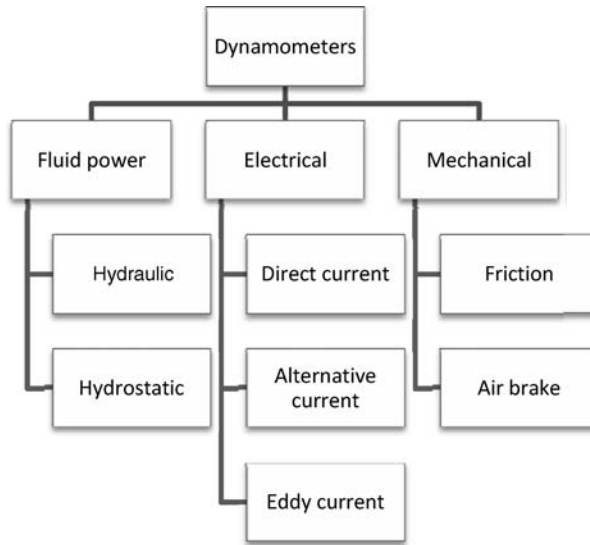
Figure 2.63 Different types of dynamometers

In steady state tests, the engine is held at a specified rotational speed (within an allowed tolerance) by the application of variable brake loading and the necessary applied torque is measured. The engine is generally tested from idle to its maximum achievable speed and the output is the engine torque-speed graph. If the rated power of engine is required, then correction factors also have to be calculated and multiplied by the measured power (see Section 2.5.3). Sweep tests are performed by the application of a certain load torque while the engine is allowed to speed up continuously. The rate of engine acceleration is an indication of the engine power output during the test under the applied load and attached inertia. A modern engine dynamometer facility is shown in Figure 2.64 and a typical engine test report looks like that shown in Table 2.9.

2.5.2 Chassis Dynamometers

An engine dynamometer measures speed and torque directly from the engine's crankshaft or flywheel on a test bed. The power losses in the drivetrain from the gearbox to the wheels are not accounted for in such tests. A chassis dynamometer is a device that measures power delivered to the driving wheels through the vehicle driveline and thus the effective vehicle power is measured. The vehicle is positioned on the dynamometer and the driving wheels are positioned on the surface of drive roller(s) which apply resistive loads on the vehicle driving tyres. In order to eliminate the potential wheel slippage on the drive rollers, some types of chassis dynamometers are attached directly to the wheel hub and apply the load torque directly.

Owing to frictional and mechanical losses of the drivetrain components, the measured wheel brake horsepower in general is considerably lower than the brake horsepower measured at the crankshaft or flywheel on an engine dynamometer. Typical figures for the overall driveline efficiency – including gearbox, differential gears and driveline friction losses – may be around 87–91% for manual transmissions and as low as 80% for automatic transmissions. However, these figures must be treated only as guidelines, since the actual efficiencies in practice depend on the driving cycle. For example, the losses in the torque converter of an automatic transmission are rather high for stop-start driving, but they reduce dramatically when the torque converter is locked for highway cruising.
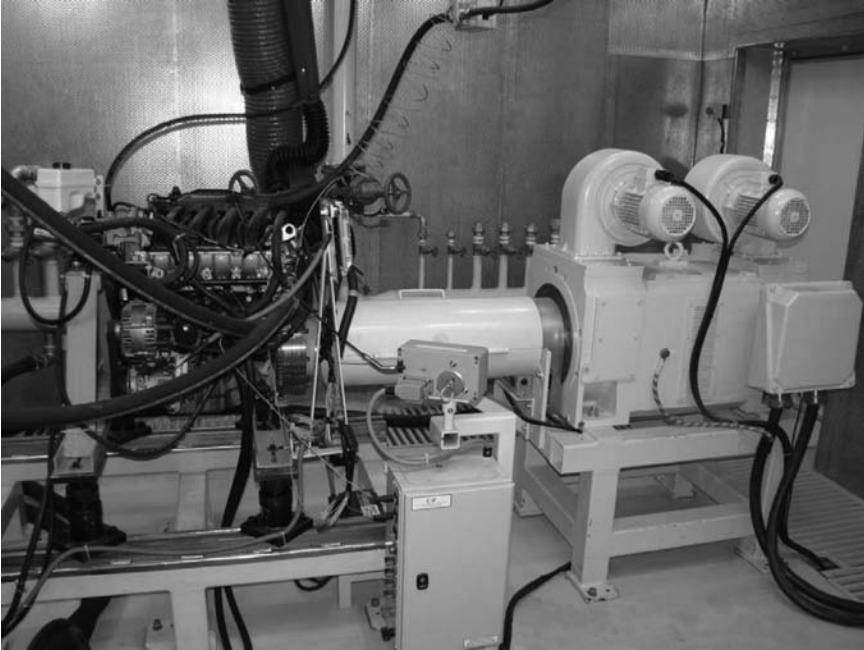
Figure 2.64   Engine dynamometer at Automotive Research Centre of IUST

However, the test conditions are very important and environmental changes can also have a great influence on the results. In addition to the driveline losses, other resistive loads such as rolling resistance, aerodynamic and slope (see Chapter 3) are also present during the vehicle motion on the road. One of the important uses of the chassis dynamometers in addition to measuring speed, torque and vehicle's effective power, is to determine vehicle fuel consumption (see Chapter 5) and emissions. To this end, dynamometers have to simulate and apply the associated road loads to the driving wheels. Dynamometers are also used to measure and compare the power flow at different points on a vehicle driveline. This is used is for the development and modification of the vehicle driveline components, usually at vehicle research centres.

2.5.3   Engine Torque-Speed Characteristics

From the point of view of overall powertrain analysis, the actions and interactions inside the engine are not essential. The important issue is how the engine produces shaft output power to be used for vehicle motion. Engine torque-speed characteristics demonstrate the output performance suitable for powertrain analysis use. Full throttle engine torque-speed maps provide some useful information regarding engine performance, but the part-throttle maps are necessary for the full performance analysis of vehicle motion.

2.5.3.1   Full Throttle Maps

Full throttle or full load or wide-open-throttle (WOT) maps are indications of the engine's peak power performance. Maximum engine torque and power can be obtained in this type of maps. A typical full

Table 2.9 Typical engine dynamometer test report

Measured quantities									Corrections			Reference values	
Engine rpm	Torque (Nm)	Power (kW)	Oil pres. (bar)	Oil temp. (°C)	Exhaust temp. (°C)	Intake air temp. (°C)	Intake air pres. (bar)		Correction factor	Corrected power	Corrected torque	Torque range	Power range
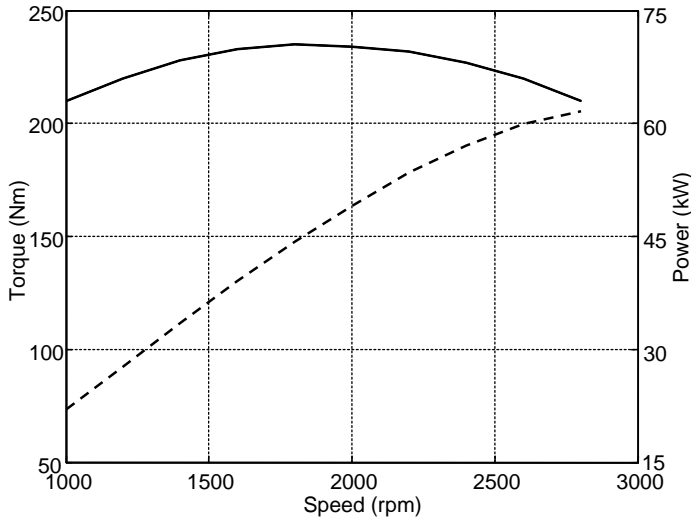
Figure 2.65 Typical full load map for a naturally aspired CI engine

throttle map for a spark ignition engine was already shown in Figure 2.15. A similar map for a compression ignition engine can be seen in Figure 2.65.

Important points on the typical full load engine performance map are specified in Figure 2.66. These are defined as:
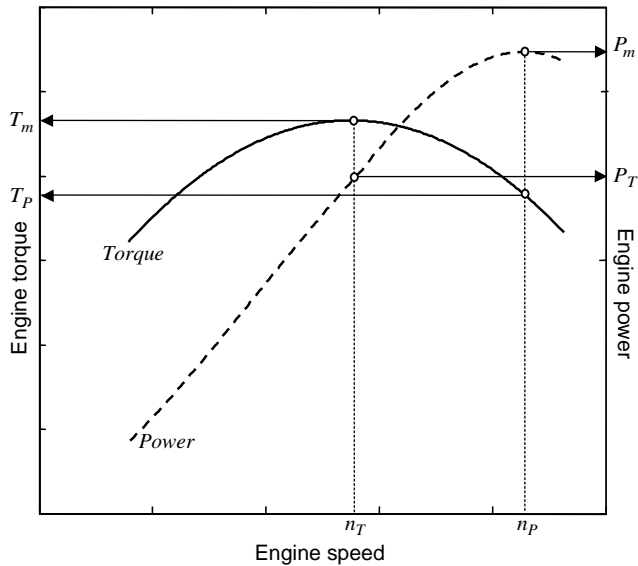
Figure 2.66 Important points on the typical full load map

P_m Maximum engine power.
P_T Power at point of engine maximum torque.
T_m Maximum engine torque.
T_P Torque at point of engine maximum power.
n_P Engine speed at engine maximum power.
n_T Engine speed at engine maximum torque.

Engine torque flexibility F_T and speed flexibility F_n are defined by:

$$F_T = \frac{T_m}{T_P} \tag{2.125}$$

$$F_n = \frac{n_P}{n_T} \tag{2.126}$$

The engine flexibility F_e is defined as the product of the two terms above:

$$F_e = F_T F_n = \frac{T_m n_P}{T_P n_T} \tag{2.127}$$

Good flexibility means that maximum torque occurs at lower speeds. In general, diesel engines work at lower speeds compared to petrol engines at similar powers. It means that they produce higher torques at lower speeds. The naturally aspired diesel engines have the characteristics that can be interpreted as high engine flexibility. It is argued that higher engine flexibility will result in less frequent shifting [5].

The following example is designed in such a way that a better understanding is obtained regarding engine flexibility.

Example 2.5.1

Three engines have been designed with equal maximum torque of 150 Nm. The general torque speed relations of all engines are of the basic form:

$$T_e = 120 + a(\omega_e - 1000) - b(\omega_e - 1000)^2$$

in which engine speed ω_e is in *rpm* and coefficients a and b are two constants given in Table 2.10. The maximum working speed of all engines is 6000 rpm.

Table 2.10   Coefficient a and b for Example 2.5.1

Engine	1	2	3
a	0.030	0.020	0.015
b	7.50×10^{-6}	3.333×10^{-6}	1.875×10^{-6}

(a) Plot the variation of engine torque and power versus speed from 1000 to the top speed.
(b) Obtain engine flexibilities and compare the results in a tabular format.

Solution

(a) The variation of the engines' torque and power with speed can easily be obtained. The results are plotted in Figure 2.67. It can be seen that the maximum torques for the engines occur at 3000, 4000 and 5000 rpm respectively.
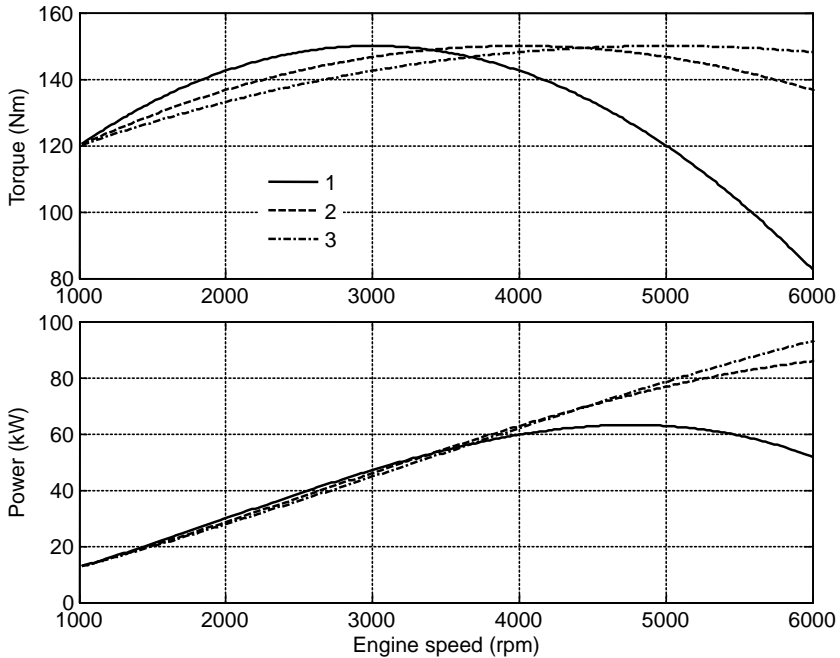
Figure 2.67   Engine performances for Example 2.5.1

(b) All the required quantities can be read from Figure 2.67 and the results are summarized in Table 2.11.

Table 2.11   Flexibility parameters for Example 2.5.1

Engine	T_m	T_P	n_T	n_P	F_T	F_n	F_e
1	150	127	3000	4760	1.183	1.59	1.88
2	150	137	4000	6000	1.095	1.50	1.64
3	150	144	5000	6000	1.042	1.20	1.25

The results simply indicate that engine 1 has higher flexibility. From Figure 2.67, too, it is clear that engine 1 has larger torques at lower speeds compared to the two other engines. On the other hand, the output powers for all engines have no significant differences at these low speeds. Therefore, engine 1 can produce higher tractive forces at similar outputs and is preferred at low speeds.

However, engine 1 has lower power compared to the two other engines at higher speeds and will produce lower top speeds for the vehicle.

In this example, only the issue of engine flexibility is studied. Later, the effect of gear ratios on the overall vehicle working condition will be included in other chapters.

2.5.3.2 Part Throttle Maps

Full throttle operation is only a small part of the engine operation during normal vehicle motions. In other words, the full throttle maps are only the upper boundary of the engine performance area. Therefore, the full throttle information has only limited value in powertrain analysis. Throttling has different meanings in spark ignition and compression ignition engines. In SI engines there is a butterfly valve-type restriction in the air inlet of the engine (see Figure 2.68) that controls the amount of air input into the manifold. Diesel engines do not have such restrictions and the throttling effect is done by controlling the injection of fuel according to the demands of the driver when the accelerator pedal is depressed.

The definition of throttle opening is not clear and is sometimes misleading. The reason is explained by differentiating between the accelerator pedal displacement, the throttle butterfly valve rotation and the ratio of opening area to full area of the inlet pipe. When the accelerator pedal is depressed, usually a cable (wire) is pulled and the throttle valve is turned (Figure 2.69). When the pedal is released, the spring force returns the throttle to the closed position.

According to the schematic illustration of Figure 2.69, the quantities 'pedal rotation angle' θ_P, 'throttle valve rotation angle' θ, and 'throttle opening ratio' r_A (the ratio of opening area to the full bore cross-sectional area) are related as follows:

$$\theta = k_T \theta_P \tag{2.128}$$

$$r_A \approx 1 - \frac{\cos\theta}{\cos\theta_0} \tag{2.129}$$
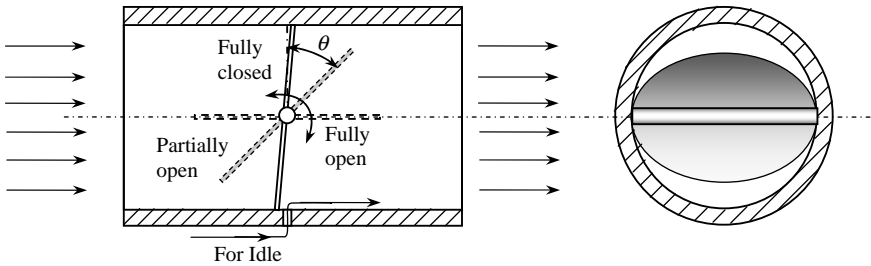
Figure 2.68   SI engine throttling
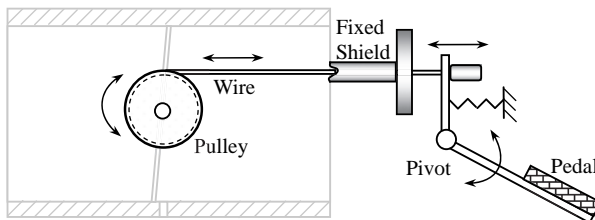
Figure 2.69   From pedal displacement to throttle rotation
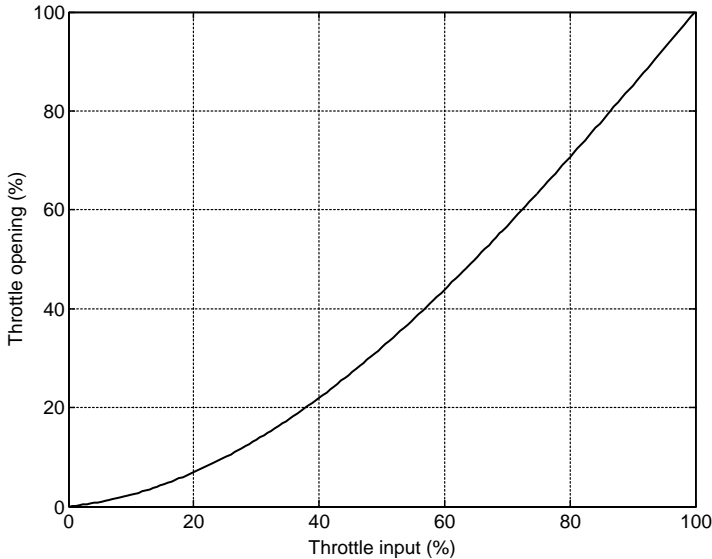
Figure 2.70   Throttle opening versus throttle input

where k_T is a constant and θ_0 is the initial value of the throttle angle at closed position. The approximation sign of Equation 2.129 is for the effect on the throttle shaft diameter at large throttle angles. Equation 2.128 indicates that the throttle angle is proportional to the accelerator pedal angle (unless the mechanism used was non-linear). Therefore the driver's feeling of depressing the pedal is effectively transferred to the engine throttle. The throttle opening of Equation 2.129, however, shows a non-linear relation with the throttle angle (or pedal angle). As seen in Figure 2.70 for a 5-degree θ_0, the variation of throttle opening is highly non-linear at low pedal inputs. In order to have a similar definition for SI and CI engines when discussing part throttle curves, it is better to use the accelerator pedal displacement (or rotation) since no throttle valve is available for CI engines (the throttle is always fully open).

In SI engines the variation of engine torque with speed at different throttles is different due to different mass flow rates into the engine. In CI engines the mass of fuel injected is proportional to the pedal input which varies with the resulting engine torque. The part load performances of engines are measured on engine dynamometers during special procedures. The result is sometimes illustrated by a three-dimensional map with axes being engine torque, speed and throttle respectively. A typical map of this type is shown in Figure 2.71 based on engine dynamometer test results.

A more useful representation of the part throttle engine map, however, is in two dimensions. If a left view of the 3D picture is taken, in the torque-rpm plane a series of curves for different throttle values will be present. Such a plot is depicted in Figure 2.72 for the same engine.

At idle speed (0% throttle) only one operating point will exist on the map. With increasing throttle, the operating points will increase across the speed and torque axes. Part throttle maps are shown at specific throttle values. For working points in between, interpolation of two adjacent points can be used. For interpolation purposes it is often easier to use look-up tables instead of maps.
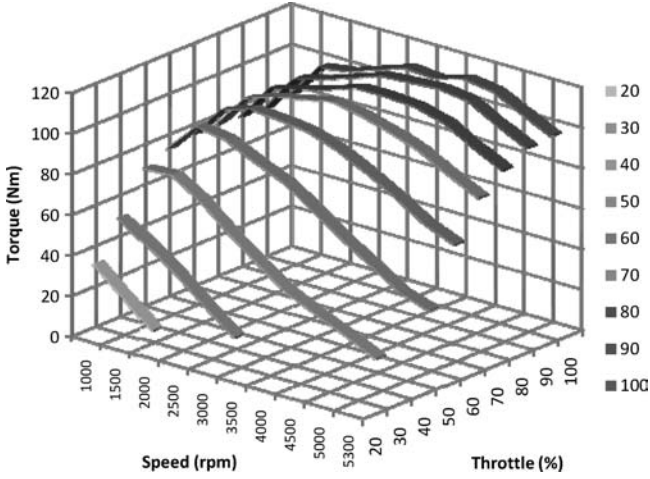
Figure 2.71   Engine 3D part throttle map

Figure 2.72   2-D part throttle plot of engine

Example 2.5.2

For the engine with the part throttle plot of Figure 2.72, calculate the torque at 57% throttle and 4200 rpm.

Solution

From Figure 2.72 the values given in Table 2.12 can be read. Now by three linear inter-polations the torque can be calculated. At 4000 and 57% the torque is 77.6. At 5000 and 57% it is 60.3. At 4200 rpm and 57% throttle, the interpolation result between 77.6 and 60.3 is 74.14 Nm.
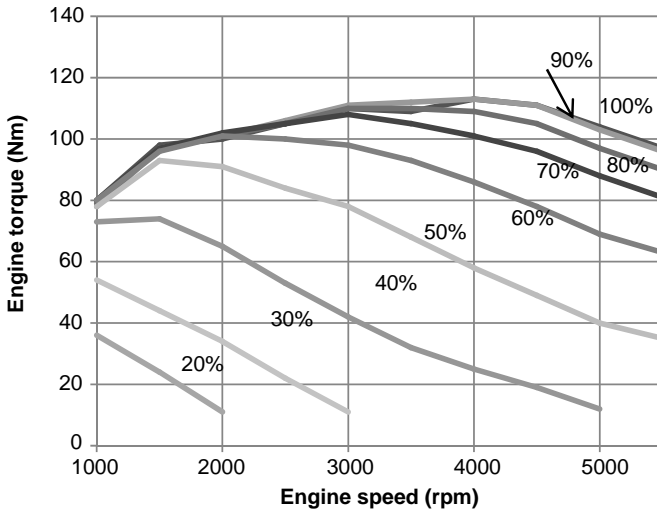
Table 2.12   Engine torques (Nm)

speed (rpm)	throttle (%)	50	60
4000		58	86
5000		40	69

2.6   Magic Torque (MT) Formula for Engine Torque

As discussed earlier, the torque-speed characteristics of an engine over the full range of operation are usually expressed with part throttle look-up tables or maps and are used in powertrain analysis work to obtain the full range of engine operation outputs. The midpoints between available data in look-up tables are obtained by linear interpolations.

   The availability of a universal formula for engine torque-speed-throttle dependency could provide several benefits for researchers by simplifying the processes as well as providing a mathematical relationship that can be utilized in many ways in the analyses. Research work was carried out at the Department of Automotive Engineering, IUST in Tehran, in order to discover the part throttle behaviour of SI engines. Three engines were fully tested on engine dynamometers and part throttle data were recorded. The data were then analyzed in order to determine whether a similar torque-speed property could be obtained for the tested engines. This work led to a universal mathematical relationship for the torque-speed characteristics of SI engines which was verified by the available test results.

2.6.1   Converting Part Throttle Curves

As may be seen from Figures 2.71 and 2.72, the part throttle curves do not follow a single rule. Part throttle plots of other engines also showed a similar trend. In order to explore the inherent characteristics of the torque-speed data, different representations were examined. The plot of a two-dimensional part throttle look-up table can be prepared in three different ways: (1) the torque-speed variations at different throttles, which is a popular form frequently used; (2) torque-throttle variation at different speeds; and (3) throttle-speed variations at different torques. When the latter plots were generated for all engines, although a better correlation was observed among the curves, it was not possible to identify a uniform trend. The variation of torque-throttle at different speeds, however, showed a good uniform trend for all engines. The result for one of the engines is given in Figure 2.73.

   This result of course is explicable in that the torque increases with increasing the throttle at a specified speed, because increasing the throttle opening will increase the fuel-air mixture input rate and in turn the resulting torque. The consistent behaviour of the engines in the torque-throttle map allows the examination of different functions for the description of this relationship. Regression methods were applied to the problem and a universal equation for the SI engines named the MT (Magic Torque) formula was developed. (It also stands for Mashadi-Tajalli because of their contribution.)
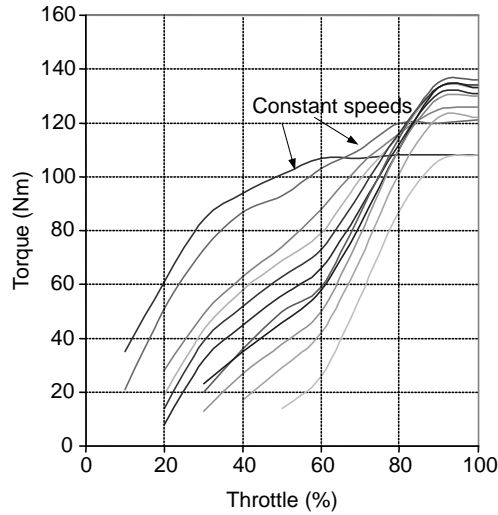
Figure 2.73 Part throttle plot at different speeds

2.6.2 The MT Formula

The MT formula has the following basic form:

$$T(\omega, \theta) = \frac{T_{F.L}(\omega)}{\left[1 + \exp(A - B\theta)\right]^{C\omega^D}} \tag{2.130}$$

in which $T_{F.L}(\omega)$ is the full load or wide-open-throttle (WOT) engine torque-speed curve and coefficients A, B, C and D are four constants for a specific engine and can be determined from part load tests. Coefficients can be obtained in such a way that the torque, speed and throttle are in Nm, rpm and % respectively.

Example 2.6.1

For a V8 engine the coefficients of the MT formula are given in Table 2.13 and the full load torque versus speed data is given in Table 2.14 for intervals of 250 rpm.

Table 2.13 Coefficients of MT formula for an eight-cylinder engine

Coefficient	A	B	C	D
Value	−10.07	0.1348	2.083	1.363

Table 2.14 Engine full throttle data

Speed (rpm)	Torque (Nm)									
750–3250	115	128	140	145	149	152	154	158	163	167	170
3500–6000	172	173	175	181	188	190	188	188	186	183	178

(a) Plot the variation of torque versus speed at throttles of 20, 30, 40, 60 and 100%.
(b) Plot the variation of torque versus throttle at speeds of 2000 to 6000.

Solution

A MATLAB program may be written to generate the two plots. Results are shown in Figure 2.74.
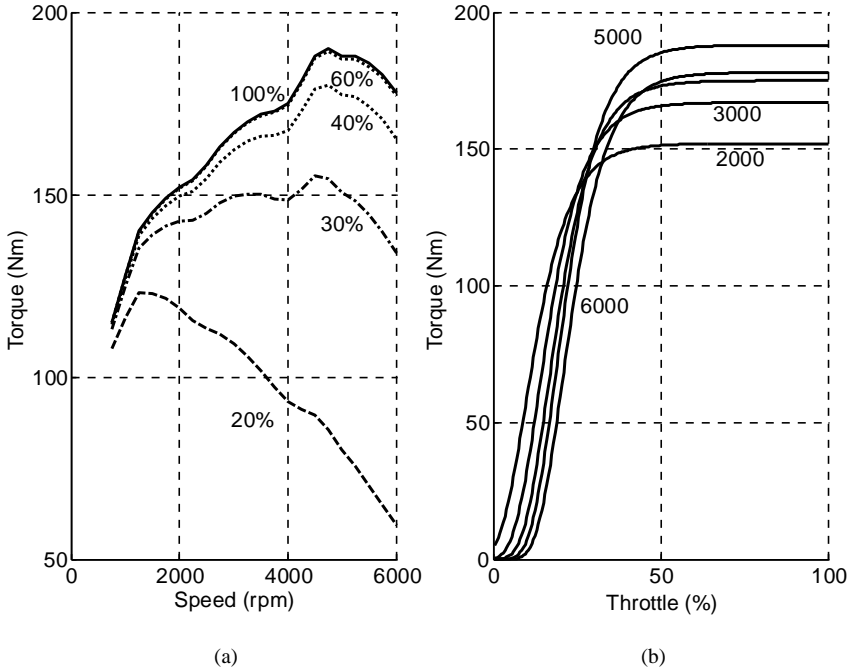
Figure 2.74   Part throttle plots at different throttles (a); and speeds (b)

2.6.3   Interpretation

Each of the coefficients A, B, C and D in the MT formula has an influence on the output torque variation of the formula. In this section a brief explanation will be presented for the role of the coefficients. The first point to note is that the MT formula can be written as:

$$T(\omega, \theta) = k(\omega, \theta) \cdot T_{F.L}(\omega) \tag{2.131}$$

in which $k(\omega, \theta)$ is a correction factor that is always smaller than unity and $T_{F.L}(\omega)$ is the WOT curve of the engine. In other words, the part throttle values in an engine are shaped from its full throttle curve. Approaching full throttle curve at large throttle inputs can be examined in Equation 2.130

by observing:

$$\lim_{\theta \to 100} \exp(A - B\theta) \approx 0 \tag{2.132}$$

Therefore all of the coefficients are influential only at part throttle, and at full throttle the MT formula will generate the WOT curve. The influence of each factor in the MT formula is explained below:

- *Factor A*: Coefficient A is called the *magnitude factor* since it controls the value of torque at a specified point. Reducing the magnitude of A decreases the torque magnitudes of a part throttle curve. The changes in magnitudes are different at different throttles and speeds.
- *Factor B*: This coefficient is called the *throttle interval factor* since it controls the interval between every two part throttle curves. In fact, reducing coefficient B displaces the part throttle curves further from one another and distributes the part throttle curves more evenly.
- *Factor C*: Coefficient C is called the *low speed magnitude factor* since it controls the torque values especially at low speed points. Reducing the magnitude of C increases the torque magnitudes of a part throttle curve especially in the low speed regions.
- *Factor D*: Coefficient D is called the *high speed magnitude factor* since it controls the torque values especially at high speed points. Increasing the magnitude of C decreases the torque magnitudes of a part throttle curve especially in the high speed regions.

2.7   Engine Management System

In the past, the engine functions such as fuel-air mixture and ignition control were achieved by mechanical devices like carburettors and advancing mechanisms (e.g. centrifugal advance units). An engine control unit, or ECU for short, is an electronic control system for engines that is responsible for monitoring and managing the engine functions that once were performed mechanically. Over the past three decades, the control of a few parameters for engine ignition has developed into the management of several variables that govern the performance of an engine. For this reason, the term 'Engine Management System' (EMS) is becoming increasingly popular. EMS is responsible for monitoring and controlling additional parameters such as exhaust-gas recirculation (EGR) and fuel evaporative emissions to ensure better fuel economy, much lower pollution, more power, easier cold start, smoother idling, and consistently good performance under all circumstances. Electronic engine management has also made possible sophisticated engine monitoring functions and provides diagnostics and warning information.

Modern engine management systems incorporate information from other vehicle systems by receiving inputs from other sources to control the engine performance. Examples are control of variable valve timing systems, communication with transmission control units and traction control systems. For engine maintenance and repair purposes, the ECU stores diagnostic codes based on sensor information. In conditions where the engine faces a problem, the ECU displays warning lights for the attention of the driver.

2.7.1   Construction

The engine management system in general includes an ECU that receives information from several sensors to control the ignition process of the engine. A fuel delivery system is responsible for working with the ECU and supplying sufficient fuel to the engine. The ignition system receives commands from the ECU for accurate control of the combustion. The sensors provide feedback to the ECU to indicate the way engine is running so that the ECU can make the necessary adjustments to the operation of the fuel delivery and/or ignition system for emission control, fuel economy and good driveability. Figure 2.75 illustrates the main components of an EMS (see also [6, 7]).

The ECU uses a microprocessor which can process the inputs from the engine sensors in real time and compute the necessary instructions. The hardware consists of electronic components based on a microcontroller chip (CPU). Memory is also needed in order to store the reference information and
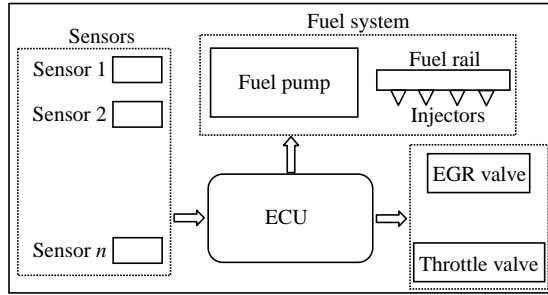
Figure 2.75   Basic components of an EMS

ECU software. The input information from sensors is conditioned to remove noise and digitizing (if necessary). The low energy command signals of ECU must be amplified by the output drivers before they are used to drive the actuators. Figure 2.76 schematically illustrates the basic parts of an engine electronic control unit.

2.7.2   Sensors

A sensor is a device that measures a physical quantity and outputs an electronic signal in proportion to the measured quantity. Engine sensors are responsible for measuring and reporting several important quantities to the ECU. These sensors include throttle position sensor, mass airflow sensor, temperature sensor, manifold pressure sensor, crank angle sensor, oxygen sensor and knock sensor. A brief explanation follows for each of these sensors (see also [8, 9]).

- *Throttle position sensor (TPS)*: As the name implies, a throttle position sensor provides the ECU with information on the throttle rotation. This information produces the angle of throttle rotation as well as the driver's intention to accelerate the vehicle from the rate of changing the angle. The ECU will use this information to control the fuel delivery and ignition timing. Three examples are idle, heavy throttle input and braking. In idle conditions, the throttle is closed for a time period, so that the ECU will notice it is idle. In a sudden acceleration the accelerator pedal will be depressed rapidly. The ECU receives two signals: throttle angle and rate of change of throttle angle. Therefore, it determines the situation is
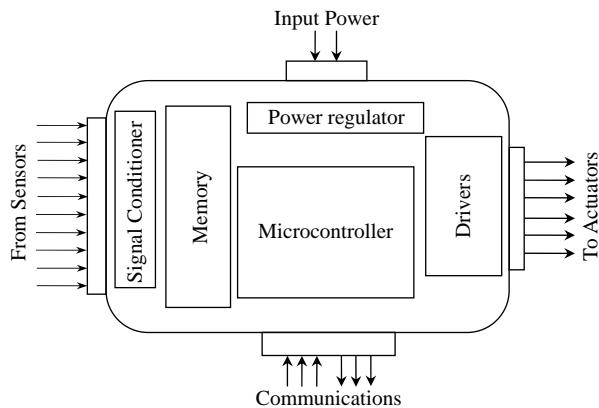
Figure 2.76   Basic parts of an ECU

acceleration and the combustion timing will usually be advanced more than under a light throttle input. In braking circumstances, the accelerator pedal is released suddenly and the signal will be to close the throttle and thus, the ECU will issue an injection cut-off command.

- *Mass air flow sensor*: The amount of fuel needed for a perfect combustion is proportional to the amount of air entering the engine. The measurement of the mass flow rate of air into the engine, therefore, is necessary to try and optimize the operation of an engine. There are different ways of measuring the amount of air entering the intake manifold. Hot wire sensors use electric current variations to keep the temperature of wire constant. Other methods include the vane system and the heated film method.

- *Temperature sensors*: The optimum spark advance depends on intake manifold temperature. The air temperature sensor measures the temperature of the air and the ECU modifies the fuel flow to suit the ambient air temperature. In some engines, the air temperature information is combined with information from the pressure sensor to calculate the intake air mass flow rate. The coolant temperature sensor is used to report to the ECU the operating temperature of the engine, allowing it to modify the fuel flow as the engine temperature changes, and to assist with warm-up and for maximum fuel economy at normal engine operating temperatures.

- *Manifold pressure sensor*: The pressure drop in intake manifold is an indication of air flow rate. The pressure drop is higher at lower throttle openings. This information is useful for the ECU to tailor fuel delivery and combustion timing for different operating conditions. The manifold absolute pressure (MAP) sensor (also called a vacuum sensor) measures the degree of vacuum in the engine's intake manifold. This type of sensor is used with some types of fuel injection systems.

- *Angle/speed sensors*: These sensors provide information to the ECU regarding the crankshaft turning position and speed respectively. The camshaft rotation may also be measured to obtain ignition timing. This information is used by the ECU to control fuel flow and ignition.

- *Oxygen sensor*: An oxygen sensor (also called a Lambda sensor) is placed in the exhaust system to measure the amount of oxygen leaving the engine together with combustion products. This quantity is used in a feedback loop to allow the ECU to control the fuel delivery system to provide a proper fuel-air ratio. With this information the ECU will continually correct itself in small time steps.

- *Knock sensor*: The knock sensor detects knocking and sends a signal to ECU to gradually retard ignition timing or to enrich the air-fuel mixture.

2.7.3 Maps and Look-up Tables

When controlling slow systems with few influencing parameters, the microprocessor can be provided with a mathematical control function to evaluate the best conditions for each set of input data and to generate an appropriate actuator drive signal. For complex, high-speed systems like engines, however, this method does not work since the control of an engine requires the high speed evaluation of several complicated non-linear equations, each with a large number of variables.

The solution to this problem is to use engine maps that are sets of pre-calculated results that cover all of the engine's possible operating conditions. During the engine operation the ECU receives sensor signals, calculates the preferred output values and passes them to the output driver circuits. Two basic examples are engine ignition and injection maps with typical shapes illustrated in Figures 2.77 and 2.78. The map of Figure 2.77 relates the ignition timing to engine speed and load and it is controlled by selecting the advance value determined from the data stored in the memory. The map of Figure 2.78 also relates the injection timing to the same two parameters.

The process of obtaining engine map data is called mapping and involves operating a fully instrumented test engine on a dynamometer throughout its entire speed and load range. While quantities such as the fuel-air ratio and the spark control are varied in a systematic manner, the fuelling and timing for maximum power and lowest emissions are obtained. Once the preliminary map data have been obtained, the engine is run in a test vehicle to calibrate the map for higher efficiency and performance in various working conditions.
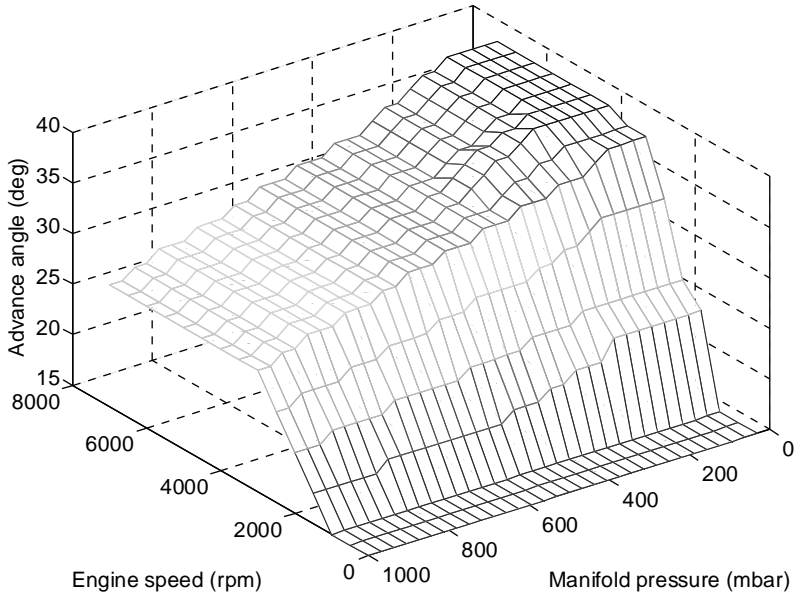
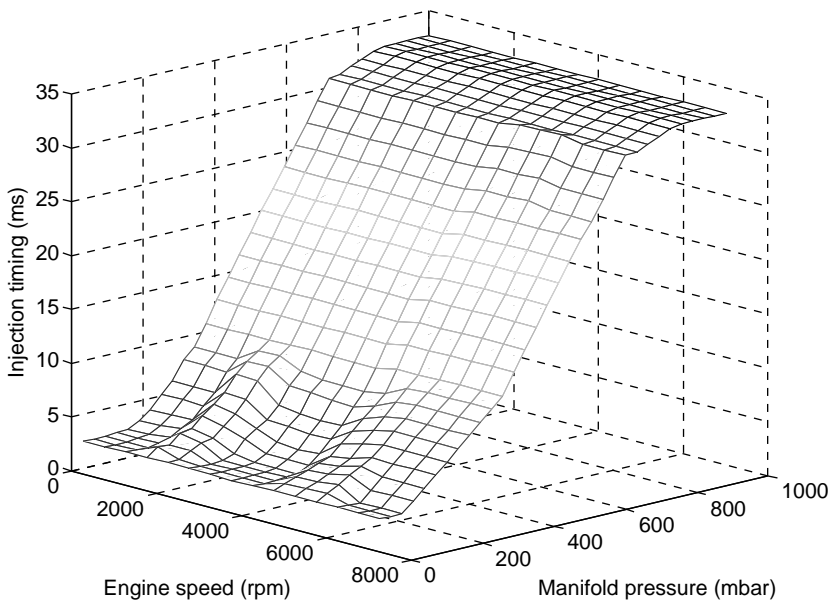**Figure 2.77** A typical ignition map

Figure 2.78 A typical injection map

The maps are then programmed into memories that are installed in production ECUs. In order to make very fast calculations possible, mapping results are stored in the form of look-up tables. The ECU microprocessor executes simple instructions in order to evaluate the output commands. Modern ECUs are able to hold numerous detailed maps relating each output variable to several input variables (sensor outputs).

2.7.4 Calibration

During the engine development phase, ECU maps are obtained by using engine dynamometers in laboratory conditions. At this stage the overall relations between the inputs and outputs are determined in the forms of typical functions. When an engine is fitted on a vehicle, the working conditions will be different from those tested during the dynamometer tests. By changing the working conditions such as different climatic conditions and altitudes, the data stored in the ECU memory must be adjusted.

With tougher legislations on emissions and rising customer expectations for increasing fuel economy, the ECU algorithms are growing in complexity, and the volume of software and data is increasing rapidly. This is why the EMS has progressed from a simple fuel metering device to a multi-functional control system with diagnosis and fault management capabilities. The calibration parameters on ECUs have also increased with increasing software complexity.

The calibration of an ECU involves multi-disciplinary knowledge of electrical, electronics, computer and mechanical engineering along with control and combustion theory.

2.8 Net Output Power

An engine is a device that converts chemical energy to mechanical energy. Inevitably, in this process a large portion of the energy is wasted and only a small part of it reaches the output shaft. The chemical (fuel) energy is not fully released during the combustion and some unburned fuel leaves the system together with the combustion products that also take out some energy with them. The released energy from the burned fuel turns into heat and fluid energy which then partly turns into mechanical energy. Engine internal components such as the oil pump and the camshaft consume power from the available shaft power. Friction between the contacting surfaces generates resistive forces against the engine rotation. In addition, in order to suck the air into the engine and pump the burned gases out, energy is needed. The vehicle accessories such as the air conditioning compressor and a power steering pump also use power from the shaft at the engine front end. The remaining power at the engine flywheel is left to provide tractive forces for vehicle motion. Figure 2.79 illustrates the energy flow inside the engine. Typical values for the energy balances are available in [10].

The input energy to an engine varies by the amount of fuel-air mixture in the engine combustion chamber. This is controlled either by throttling in SI engines or by fuel injection control in CI engines. The atmospheric conditions, too, have important effects on changing the amount of engine air input and resulting fuel energy release.

It is common to work with only three descriptions of power, namely indicated power P_i, brake power P_b and friction power P_F. The indicated power is the total mechanical power produced by engine and can be estimated from Equation 2.133 (see Section 2.2.4):

$$P_i = \eta_v \eta_T \eta_c \frac{\rho_a V_d Q_{HV}}{120AF} n \qquad (2.133)$$

The total indicated power is divided into two parts; the useful mechanical power at the output shaft (brake power) and the friction power (lost power):

$$P_i = P_b + P_F \qquad (2.134)$$
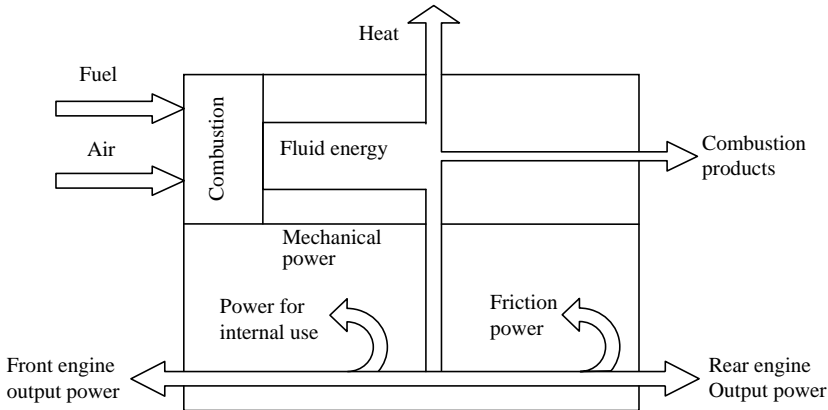
Figure 2.79   Power flow in an engine

With this definition the friction power also includes all negative power such as pumping power as well as power used for internal uses.

2.8.1   Engine Mechanical Efficiency

Mechanical losses in an engine are described by the friction power of the engine and have several sources including:

- pumping losses that are due to the energy required to pump the air into the cylinders and also to pump the combustion products out of cylinders;
- frictional losses are due to friction of piston skirt and rings, bearing frictions and valve frictions;
- power losses of oil pump for engine lubrication;
- valve train power losses.

The ratio of the brake or useful mechanical power to the total indicated power is called the mechanical efficiency η_m:

$$\eta_m = \frac{P_b}{P_i} = 1 - \frac{P_F}{P_i} \tag{2.135}$$

The friction power can be divided into three main parts: frictional power by friction forces between moving surfaces (cylinder-piston, bearings, valves), power for internal uses (oil pump, camshaft, etc.); and the power required to pump air into the engine and burned gases out of the engine. The first two are dependent on the engine speed and the third is throttle dependent. Indicated power also is dependent on both throttle (volumetric efficiency) and speed (Equation 2.133). Therefore, the mechanical efficiency depends on the throttle position as well as engine speed.

2.8.2   Accessory Drives

Engine mechanical power to accelerate the vehicle must be delivered to the crankshaft end or to the flywheel. The net engine output power is not fully available at the output shaft since there are different accessories that are receiving power from the crankshaft. Major accessories are the alternator, air conditioning compressor and power steering pump that are usually driven by belt drives. The water pump is also usually driven by an accessory drive belt. In automobiles these belt drives are typically placed in front of engine and for this reason they are called Front Engine Accessory Drive or FEAD in short. A typical single belt FEAD system is shown in Figure 2.80.
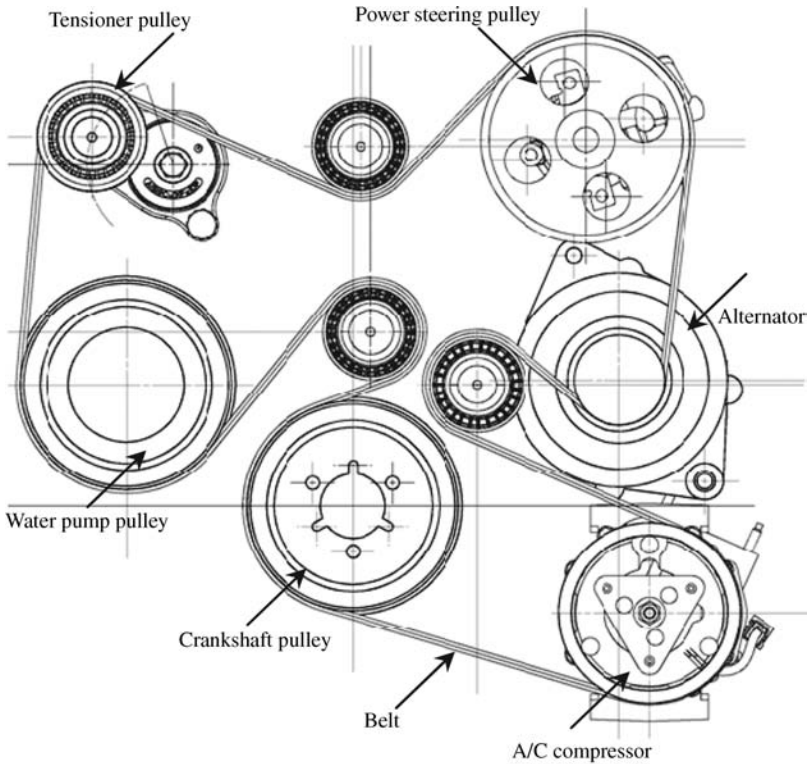
Figure 2.80   A typical FEAD system

Each accessory consumes power from the engine and the net power available to be used for vehicle motion, therefore, is reduced. Figure 2.81 shows typical torque and power demands of different accessories.

2.8.3   Environmental Effects

The engine performance is highly dependent on the ambient air conditions, especially air pressure and temperature. These atmospheric effects can be viewed from two different perspectives. In the first point of view, the main concern is the differences between the performances of different engines in similar working conditions. In other words, different engine designs are being compared with each other in terms of overall performance when they work in similar conditions. The second point of view compares the performances of one particular engine when it works at different climatic conditions. Examples are the performance variations of a specific vehicle during different seasons and in different geographical areas. In order to provide a more accurate basis for comparisons between performances of different engines, it is necessary to carry out tests under equal standard conditions. Engine tests performed in such standard ambient conditions are comparable, otherwise obviously an engine performs differently in different atmospheric conditions.

For both perspectives the idea of introducing correction factors has proved useful. In the first approach, correction factors can make the comparisons more reliable. Correction factors for the second approach can indicate how differently an engine is expected to perform in atmospheric conditions other than the ideal standard condition.
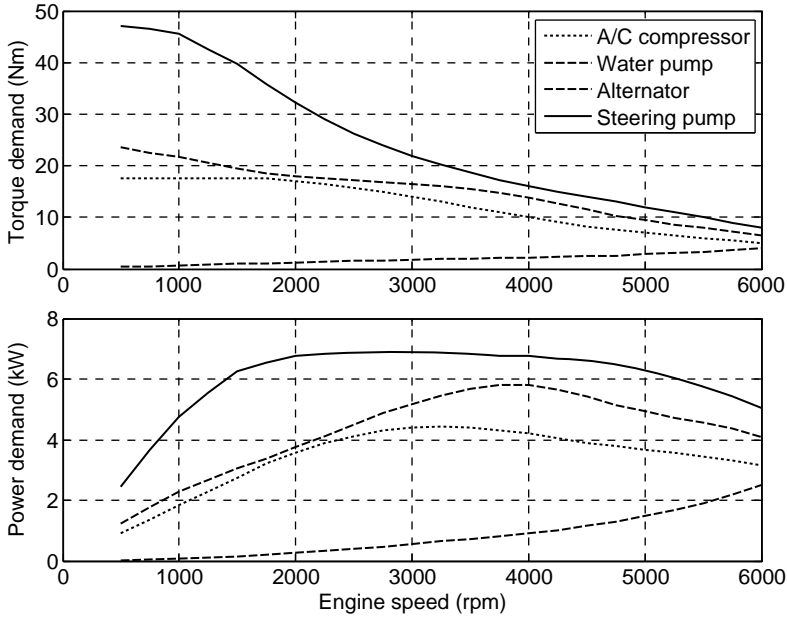
Figure 2.81 Typical accessory loads

2.8.3.1 Atmospheric Properties

Air properties in the atmosphere depend on the ambient temperature, pressure and humidity. Atmospheric air properties change not only by seasons, but also by altitude. Basic relations for estimating air properties can be developed by using ideal gas formulas. Typical equations are [11]:

$$\frac{T}{T_0} = \left(1 - 9.21 \times 10^{-5} H\right)^{0.286} \tag{2.136}$$

$$\frac{p}{p_0} = 1 - 9.21 \times 10^{-5} H \tag{2.137}$$

$$\frac{\rho}{\rho_0} = \left(1 - 9.21 \times 10^{-5} H\right)^{0.714} \tag{2.138}$$

In the above equations, T is air temperature (Kelvin), p is air pressure (kPa), ρ is air density (kg/m^3) and H is altitude (m). Subscript $_0$ indicates the values at sea level ($H = 0$). Standard or reference values for the three parameters are defined differently. One reference point is given as $T_0 = 25°C$ and $P_0 = 100\,kPa$. The variations of the three parameters with altitude up to 3000 metres are shown in Figure 2.82.

2.8.3.2 Engine Test Standards

Engine manufacturers perform standard tests on their products to measure the performances of engines for type approval (TA) tests or conformity of production (COP) tests. Type approval is the confirmation that production samples of a design will meet specified performance standards. Conformity of Production (COP) is a means of evidencing the ability to produce a series of products that exactly match the
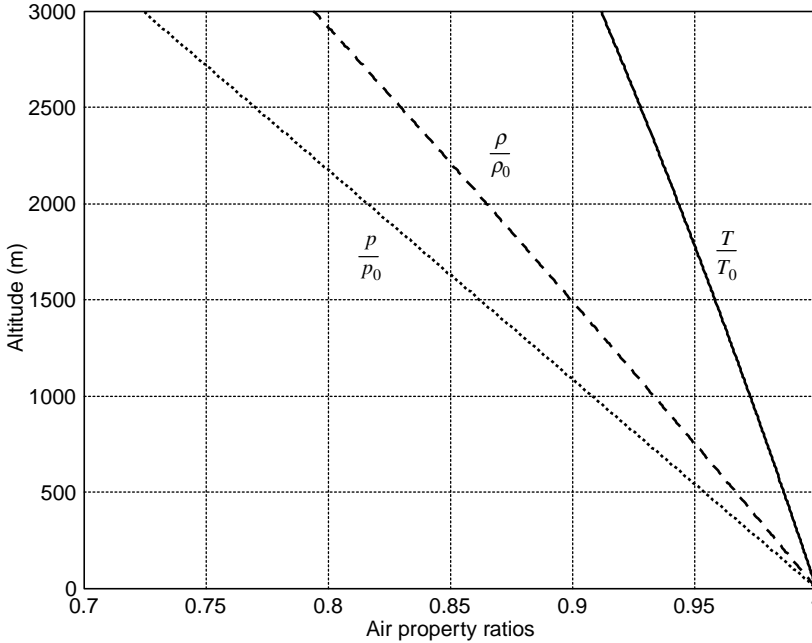
Figure 2.82   The variation of standard air properties with altitude

specification, performance and marking requirements outlined in the type approval documentation. Standard conditions are defined by standardization organizations such as the ISO, SAE, JIS, DIN and others. Typical standard atmospheric conditions for engine tests are given in Table 2.15. The exact provision of standard conditions for an engine test is a difficult and costly task. The level of control may include only input air temperature or at the same time humidity and pressure. In case of any deviations from the standard atmospheric conditions, within a limited range allowed by the standard, corrections are needed to adjust the measured engine power values. Application of such correction factors to the measured powers on engine dynamometers will establish a reference engine power comparable with other standard values.

Test procedures for obtaining and correcting engine powers are defined in detail by different standard organizations and tests must be carried out in accordance with the guidelines set out in each standard. Test procedures define which auxiliary equipment must be fitted and which must be removed from the engine. They also define setting conditions for the engine and tests, fuel specifications, cooling of engine and tolerances, and reference atmospheric conditions. According to different standards, the correction formula for the engine power is of the basic form:

$$P_S = C_F P_m \tag{2.139}$$

Table 2.15   Standard or reference atmospheric conditions for engine tests

Item	SAE	ISO	EEC	DIN
Dry air supply pressure	99 kPa	99 kPa	990 mbar	993 mbar
Air supply temperature ($^\circ$K)	298	298	298	293

Table 2.16 Coefficients for correction factors

Coefficient	SAE	ISO	EEC
α	1	1.2	1
β	0.5	0.6	0.5

In the above equation, P_S is the corrected engine power for the standard atmospheric conditions and P_m is the laboratory test result before correction. C_F is the power correction factor and for SI engines, it can be written in the following general form:

$$C_F = \left(\frac{99}{p_m}\right)^{\alpha} \left(\frac{T_m}{298}\right)^{\beta}$$ (2.140)

in which T_m (Kelvin) and p_m (kPa) are the standard air temperature and dry air pressure observed in actual test conditions. The values 99 and 298 are the standard values for the pressure and temperature and could differ according to different standards (see Table 2.15). The powers α and β are two constants defined by the standardization bodies (see Table 2.16 for different values according to different standards).

The power definitions used in the correction equations are different for different standards, some use brake powers and some indicated powers. Theoretically speaking, the general form of the correction factor C_F (Equation 2.139) is based on the one-dimensional steady compressible air flow through a restriction. For this reason it should be applied to the indicated power of an engine. However, the values of α and β may be used to adjust the formula differently.

The total brake power P_b of engine is the subtraction of friction power P_F from the 'indicated power' P_i (Equation 2.135):

$$P_b = P_i - P_F$$ (2.141)

Assuming Equation 2.139 is written for indicated powers and substituting from Equation 2.141, it will give:

$$P_{Sb} = C_F P_{mb} + (C_F - 1)P_F$$ (2.142)

in which subscripts Sb and mb denote standard corrected and measured brake powers respectively. It is assumed that the friction power of engine is independent of small climatic differences (that are present during the test with respect to the reference values) and is taken to be identical for the test and standard conditions. Defining k_p as the ratio of friction power to the brake power:

$$k_p = \frac{P_F}{P_{mb}}$$ (2.143a)

Then Equation 2.142 can be written in the following form:

$$\frac{P_{Sb}}{P_{mb}} = (1 + k_p)C_F - k_p = C_{Fb}$$ (2.143b)

which is an alternative form for correcting the measured power. This time by calculating and applying the correction factor C_{Fb}, the brake power will be corrected directly. In this form of the correction, it is assumed that the friction power will also be measured during the engine test. If the engine friction power is not measured, with an assumption of 85% mechanical efficiency for the engine [12], the correcting

formula reads:

$$C_{Fb} = 1.177C_F - 0.177 \tag{2.144}$$

The dry air pressure p_m used in the calculations is the total barometric pressure p_b minus the water vapour pressure p_v:

$$p_m = p_b - p_v = p_b - \Phi p_{vs} \tag{2.145}$$

in which Φ and p_{vs} are the humidity and saturation vapour pressure respectively. Φ is used in percentage and p_{vs} can be calculated from the following approximate equation (in mbar):

$$p_{vs} = 6.11 \times 10^m \tag{2.146}$$

in which for T in Kelvin:

$$m = \frac{7.5T - 2049}{T - 35.85} \tag{2.147}$$

and for T in °C:

$$m = \frac{7.5T}{T + 237.3} \tag{2.148}$$

Different standards propose different correction formulas for diesel engines. The EEC formula for the naturally aspirated diesel engines is similar to Equation 2.140 for SI engines but with $\beta = 0.7$. The SAE also introduces an engine factor which makes the correction formula different and more complicated. It should be noted that the correction formulas can only be used when the correction factor resulting from this procedure remains very close to unity by a margin specified by the standard (typically around $\pm 5\%$). In other words, if the correction factor calculated for an engine test remains outside the allowed bounds, the test is not valid and must be repeated.

Example 2.8.1

An SI engine was tested on a stand and at 2500 rpm the output torque in a steady condition was recorded 140 Nm. Test conditions were according to data given in Table 2.17. Determine the standard brake power of the engine at 2500 rpm:

(a) Compare the results of Equations 2.140 and 2.144 for $\alpha = 1$ and $\beta = 0.5$.
(b) Compare the previous results with those obtained for $\alpha = 1.2$ and $\beta = 0.6$.

Table 2.17   Test conditions of Example 2.8.1

1	Inlet air temperature	30°C
2	Room pressure	740mm-Hg
3	Relative humidity	60%

Solution

The conversion factor from mm-Hg to kPa is 133.32, thus the room pressure is $740 \times 133.32 = 98657$ Pa or 98.657 kPa. The saturation vapour pressure p_{vs} can be calculated by using Equation 2.146. The result is 42.33 mbar. The dry air pressure is:

$$p_m = p_b - \Phi p_{vs} = 98.657 - 60 \times 42.33/1000 = 96.119 \, kPa$$

The measured power is:

$$P_{mb} = 140 \times 2500 \times \pi/30 = 36,652W \, (49.131 \, hp)$$

(a) From Equation 2.140:

$$C_F = \left(\frac{99}{96.119}\right)\left(\frac{30+273.16}{298}\right)^{0.5} = 1.0389$$

The corrected standard power, therefore, is:

$$P_S = 1.0389 \times 36652 = 38,076W \, (51.04 \, hp)$$

and from Equation 2.144:

$$C_{Fb} = 1.177 \times 1.0389 - 0.177 = 1.0458$$

and the corrected standard power is:

$$P_{Sb} = 1.0458 \times 36652 = 38,330W \, (51.38 \, hp)$$

The difference between the two results is 254 W which is 0.67% of the power.

(b) Correcting factor from Equation 2.140 for $\alpha = 1.2$ and $\beta = 0.6$ is:

$$C_F = \left(\frac{99}{96.119}\right)^{1.2}\left(\frac{30+273.16}{298}\right)^{0.6} = 1.0468$$

The corrected standard power for this case is:

$$P_S = 1.0468 \times 36652 = 38,367W \, (51.43 \, hp)$$

The largest difference between the results is 291W (0.4 hp) and the smallest is 37 W (0.05 hp). Therefore, the results obtained from SAE and ISO formulations are almost identical although the formulae are apparently different.

2.8.3.3   Engine Power under Normal Conditions

Usually, the rated powers of engines are provided by the manufacturers defined as the standard corrected brake power of engine obtained according to standard dynamometer tests. The actual engine power will differ from the rated power since the intake air density is a function of atmospheric temperature and pressure and hence in warm or cold weather, and at low or high altitudes the air density will differ and will affect the engine performance. Thus, if the engine test results for the standard condition were available, corrections must be applied when using the engine information for vehicle performance analyses under normal conditions. These corrections are not identical to those explained earlier for engine test correction factors since those factors were designed for small deviations in standard test conditions. For normal driving conditions, however, the climatic conditions may differ enormously from those of the standard test conditions.

Owing to the analytical complexity of engine power dependency on the environmental conditions, an accurate model has not yet been developed for this purpose. From simplified models for the one-dimensional steady compressible air flow through a restriction, however, equations for the air mass flow rate have been derived. Such equations are also based on the assumption that air is an ideal gas with constant properties. Application of this technique for engine air mass flow at full throttle, assuming that the mass flow rate of air entering the engine is almost proportional to its indicated power, provides a correction factor for the engine indicated power P_i in the following form [2]:

$$P_S = C_F P_i - P_F \tag{2.149}$$

in which P_S is the standard brake power, P_F is the friction power (assumed independent of environmental changes) and the correction factor C_F is given below:

$$C_F = \left(\frac{p_s}{p_m}\right)\left(\frac{T_m}{T_s}\right)^{\frac{1}{2}} \tag{2.150}$$

where s and m stand for the 'standard' and 'measured' values. It should be noted that pressure terms in the above equation must be for the dry air (absolute barometric pressure p_b minus the water vapour pressure p_v) and temperatures are in degrees Kelvin.

Equation 2.149 can be written in a more useful form of:

$$\frac{P_b}{P_{Sb}} = \frac{1 + k_p(C_F - 1)}{C_F} \tag{2.151}$$

in which P_b and P_{Sb} are the actual and standard brake powers of the engine and k_p is the ratio of friction power to the brake power. The term $k_p(C_F - 1)$ is usually very small compared to unity and may be ignored. The simplified form of Equation 2.151, therefore, is:

$$\frac{P_b}{P_{Sb}} = \left(\frac{p_m}{p_s}\right)\left(\frac{T_s}{T_m}\right)^{\frac{1}{2}} \tag{2.152}$$

Note that the temperature values must be used in Kelvin and pressure terms are the dry air pressures (though the water vapour pressure is usually very small). Equation 2.152 simply indicates that pressure drop reduces the engine power and overheated air entering the cylinders has the same effect on engine power as a drop in atmospheric pressure. At a certain altitude the daily and seasonal temperature variations change the engine power. At a certain temperature, an increase in altitude will reduce the air pressure and consequently reduce the engine power.

Example 2.8.2

In order to include the effects of altitude and temperature on engine power, in practice, rule of thumb formulae are proposed. Two examples are:

(a) A 2.5% engine output power is said to be lost for every 1,000-ft increase in elevation above sea level.
(b) A reduction of 1% is also suggested for each 10°F rise in the intake air temperature above the 'normal' temperature of 70°F.

Compare these rules with those discussed in this section to see how accurate they are.

(c) Suggest similar SI version rules for power reduction by altitude and temperature.

Solution

(a) Using the atmospheric properties presented earlier (Equations 2.136–2.138), the variation of temperature and pressure with altitude can be obtained. Then Equation 2.152 represents the power loss of engine at that particular altitude. A MATLAB program shown in Figure 2.83 can facilitate this process for different altitudes. The result is illustrated in Figure 2.84. It can be seen that the

```
% Example 2.8.2- part (a)

close all, clear all
% Atmospheric reference conditions
t0=21;          % Reference temperature (Centigrade)
T0=273.16+t0;
P0=1.0133;     % Reference pressure (bar)

% Variation of temperature and pressure with altitude
for i=1: 300
    H=10*i;    h(i)=H;
    slope=1-92.1e-6*H;
    Tm(i)=T0*slope^0.286;          % Local temperature
    Pm(i)=P0*slope;            % Local pressure
    Cf(i)=(slope)*(T0/Tm(i))^0.5;     % Power ratio
    pl(i)=100-Cf(i)*100;            % Power loss (%)
end
plot(pl, h*3.2808)
grid
xlabel('Power loss (%)')
ylabel('Altitude (ft)')
```

Figure 2.83   MATLAB program listing for Example 2.8.2
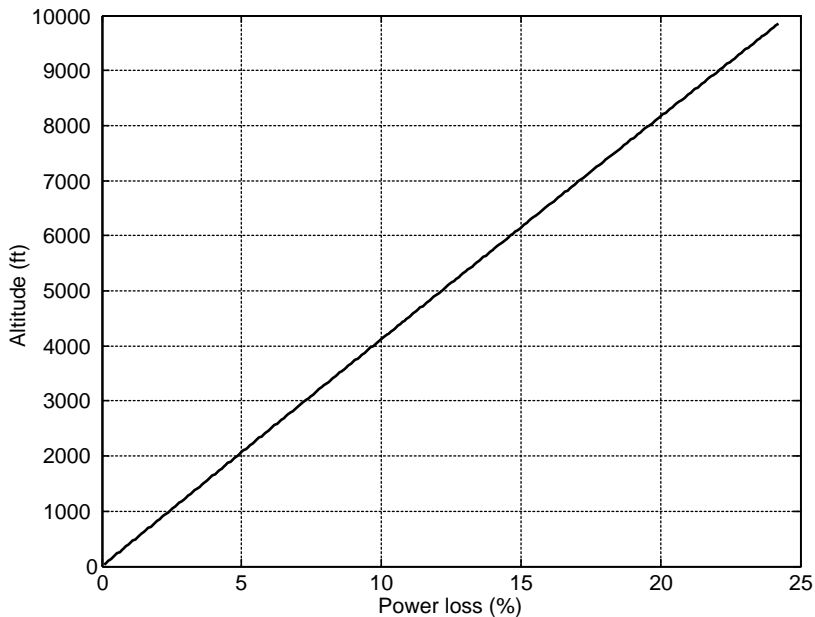
Figure 2.84   Variation of engine power loss with altitude

simple rule of thumb formula is very accurate. It should be noted that the reference temperature is taken to be 21 °C (70 °F) at sea level.

(b) Assuming no change in the atmospheric pressure due to temperature changes at sea level, the power ratio equation simplifies to a temperature ratio only. A simple loop in which the temperature varies will generate the result depicted in Figure 2.85. The reduction in power for each 10°F rise in the intake air temperature is slightly less than 1%.
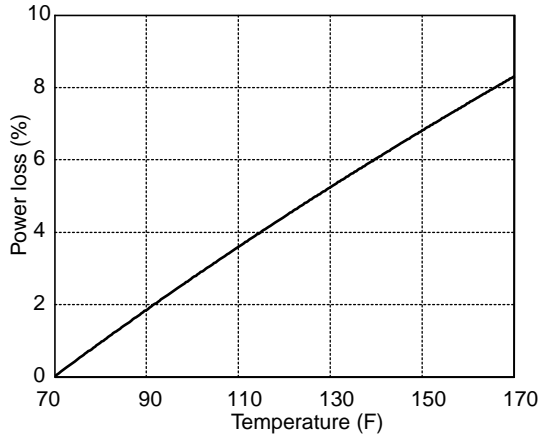
Figure 2.85   Engine power loss variation due to temperature increase

(c) From the results obtained in (a) and (b), similar rules for SI units are:
  (i) A 4% engine output power is lost for every 500 m increase in elevation above sea level.
  (ii) A reduction of 1.5% in engine power will occur for each 10°C rise in the intake air temperature above the 'normal' temperature of 20°C.

Example 2.8.3

An engine with 120 hp rated power is installed in a vehicle. What would be the real engine power in a mountainous town at 1000 m altitude above sea level in two temperature cases of a summer day at 40°C and a winter day at 0°C?

Solution

The variation of pressure with altitude is available from Equation 2.137. Ignoring the deviations of the base conditions from standard values, at a given altitude we have:

$$p = 1 - 9.21 \times 10^{-5} \times 1000 = 0.9079 \; bar$$

At a temperature of 40°C:

$$P = \left(\frac{0.9079}{1}\right)\left(\frac{298}{273+40}\right)^{\frac{1}{2}} \times 120 = 106.3 \, hp$$

Similarly, at 0°C, the power is 113.8 hp.

2.9   Conclusion

The power generation process in an internal combustion engine involves the flow of working fluids in and out of the engine, together with combustion and thermodynamics processes. Understanding engine behaviour in various working conditions, therefore, needs a thorough knowledge of several areas such as fuel and reaction chemistry, physics, thermodynamics, fluid dynamics and machine dynamics. Modern engines are controlled by electronic management systems that are very influential on the overall behaviour of the engine and make the understanding even more complex.

The objective in this chapter was to familiarize the students with the power generation principles of the internal combustion engines. Therefore, the intention was to simplify the working principles of an engine and explain them in manageable sections. The subjects covered in this chapter should be treated in context. For example, Section 2.2 and especially subsections 2.2.2 and 2.2.3 only review the basic rules of engine theory and must not, therefore, be considered as design methods since the results differ from those of real engines. The method of torque estimation presented in Sections 2.3 and 2.4 are accurate as long as the input information, especially the pressure distribution versus crank angle, is accurate.

The new engine MT formula presented in Section 2.6 is very helpful for powertrain analyses since it estimates a continuous output for all working conditions. Hence, it is a useful mathematical representation of an engine map that is valuable for whole vehicle performance calculations. Section 2.8 is very important in that it emphasizes the engine dynamometer test results must be corrected for accessory drive power consumption and weather conditions before using them in vehicle powertrain analyses.

2.10   Review Questions

2.1 Explain the main differences of four-stroke and two-stroke engines in terms of working phases, construction and performance
2.2 The valve opening angles of Table 2.1 are theoretical and different angles are used in practice. Describe the reason.
2.3 What is the main difference between TBI and MPI systems in SI engines?
2.4 Describe the function of GDI systems and their main benefits.
2.5 Explain the reason for higher compression ratios of CI engines.
2.6 Compare the theoretical thermal efficiencies of SI and CI engines.
2.7 Which of the SI or CI standard cycles more accurately describes the real engine cycle?
2.8 Describe how the volumetric efficiency influences the engine output torque and power.
2.9 Explain the concept of connecting rod dynamic equivalent and how it simplifies the engine modelling.
2.10 Describe how a flywheel reduces the engine speed fluctuations.
2.11 What is the process of designing a flywheel?
2.12 Describe the engine flexibility properties.
2.13 Name the engine control sensors and explain their functions.
2.14 Explain why an ECU needs calibration.
2.15 Describe the process of correcting the engine power for environmental differences.

2.11   Problems

Problem 2.1

Use the MATLAB program of Example 2.3.3 to study the effects of changing engine parameters on its torque generation performance:

(a) Find the effect of a 10% reduction of piston and connecting rod masses on the engine torque.
(b) Find the effect of reducing the connecting rod length by 10%.
(c) Find the effect of reducing the connecting rod inertia by 10%.

Problem 2.2

Use the data of Problem 2.1 to study the effects of changing the engine parameters on the engine bearing loads.

Problem 2.3

Derive expressions for the gudgeon-pin and crank-pin bearing forces A and B of the simplified model according to the directions of Figure 2.32.

Results:

$$A_x = -A_y \tan \beta, \ A_y = -F_P - (m_P + m_A)a_P, \ B_x = -A_x \text{ and } B_y = -A_y.$$

Problem 2.4

For the engine of Example 2.3.3 compare the gudgeon-pin and crank-pin resultant forces of the exact and simplified engine models at 3000 rpm.

   Hint: To find the gudgeon-pin forces of the exact model, use Equations 2.80, 2.81, 2.84 and 2.85.

Problem 2.5

Show that for the exact engine model the average of term T_e-$F_W h$ during one complete cycle vanishes.

Problem 2.6

Construct the firing map for a three-cylinder in-line engine with cranks at 0-120-240 degrees.

Problem 2.7

Construct the firing map for a four-cylinder 60° V engine with cranks at 0-0-60-60 degrees.

Problem 2.8

Construct the firing map for a six-cylinder in-line engine with cranks at 0-240-120-0-240-120 degrees.

Problem 2.9

For an in-line, four-cylinder engine the firing order is 1-4-3-2:

(a) Construct the firing map for the engine.
(b) Determine the crank angle and state angle for each cylinder.

Problem 2.10

Compare the torque outputs of an in-line four-cylinder, four-stroke engine at two firing orders of 1-3-4-2 and 1-2-4-3- using the information in Example 2.4.3.

Problem 2.11

Use the information in Example 2.4.3 to plot the variation of the torque of the three-cylinder engine of Problem 2.6 and calculate the flywheel inertia.

Problem 2.12

Compare the variation of the torque of the four-cylinder V engine of Problem 2.7 with an in-line layout. Use the information in Example 2.3.3.

Problem 2.13

Plot the variations of engine power losses with altitude and temperature changes for Example 2.8.2 in SI units.

Problem 2.14

The variation of gas pressure of a single cylinder four-stroke engine during two complete revolutions at a speed of 2000 rpm is simplified to the form shown in Figure P2.14. Other engine parameters are given in Table P2.14.
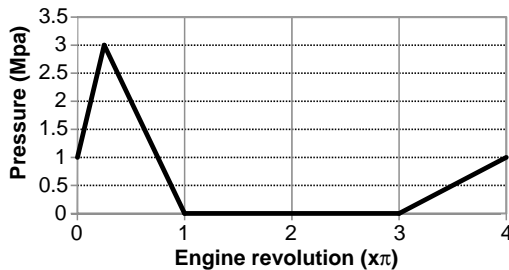
Figure P2.14   Cylinder pressure

Table P2.14   Engine parameters

Parameter	Value
Cylinder diameter	10 cm
Crank radius	10 cm
Connecting rod cent-cent	25 cm
Con rod CG to crank axis	7 cm
Con rod mass	1.0 kg
Piston mass	1.0 kg

Use the simplified engine model:

(a) Find the equivalent mass m_A for the connecting rod.
(b) Calculate the inertia force F_{IP} in terms of crank angle and engine speed.
(c) Write an equation for the total vertical force F_{BY} acting at point A.
(d) Plot the variation of F_{BY} and F_W versus crank angle.
(e) Plot the variation of torque versus crank angle.
(f) Find the average engine torque and compare it with the quasi-steady torque resulting from average pressure during the combustion phase.
(g) Determine the mean effective pressure for the engine.

Problem 2.15

The torque-angle relation for a four cylinder engine at an idle speed of 1000 rpm is of the form:

$$T = T_0 + T_a \cos 2(\theta + \theta_0)$$

(a) Find the area A^* of torque fluctuations relative to the average engine torque.
(b) Show that the value of necessary flywheel inertia can be written as $I = kT_a$.
(c) For a value of 2% permissible speed fluctuations, evaluate k.

Results:

(a) T_a,
(c) 0.0046.

Further Reading

Of all the topics in automotive engineering, engines have dominated when it comes to textbooks. Because of its role as the fundamental power source, the internal combustion engine (ICE) has been seen as the heart of the vehicle. But although its importance is undisputed, it nevertheless seems to have attracted more than its fair share of textbooks. Only a small selection of these is referenced here, but these will provide the interested reader with plenty of excellent background material on engine design.

The classic book on the fundamentals of thermodynamics of engine is by Heywood [2] and this has been used throughout the world as a university teaching text. It starts with the fundamentals of thermochemistry and then uses this to analyze the combustion processes of both spark ignition (SI) and compression ignition (CI) engines. All aspects of the thermodynamic design are covered – including engine cycle analysis, gas flows and heat transfer. Stone's book [13] has also been extensively used as a teaching reference text. As well as covering the thermodynamics aspects of the combustion processes within engines, the book also contains some introductory material on the modelling, mechanical design and experimental testing of engines. This material is brought together in the final chapter which looks at three practical case studies of different engine designs.

For more detailed information on the mechanical design of engines, the definitive reference is by Hoag [14]. He concentrates on the design of all the engine components – block, cylinder head, pistons, bearings, camshafts, etc. – and discusses how they are all brought together in an integrated engine design. He also discusses operational issues such as balancing, durability and the overall development process.

Of particular interest to powertrain system design is the question of how to represent the behaviour of an ICE – in other words, how to characterize its properties without necessarily representing all the details of the thermodynamic processes. For example, the simplest method is to use empirical data – measured on a dynamometer – to obtain an engine map. This is often referred to as an empirical model and can then simply be used as a look-up table to obtain the engine performance properties under different operating conditions. Although modelling of engines has received a huge amount of attention, much of the information only exists in journal and conference papers. However, a recent book by Guzzella and

Onder [15] has brought together some of the available information in a useful textbook. In particular, the authors explain in some detail, two types of engine models – the Mean Value and Discrete Event approaches. The book then goes on to explain how engine control systems operate and provide an excellent overview of engine management systems.

References

[1] Pulkrabek, W.W. (2004) *Engineering Fundamentals of the Internal Combustion Engine*. Prentice Hall, ISBN 0131405705.

[2] Heywood, J.B. (1989) *Internal Combustion Engine Fundamentals*. McGraw-Hill Higher Education, ISBN 978-0070286375.

[3] Mabie, H.H. and Ocvirk, F.W. (1978) *Mechanisms and Dynamics of Machinery*, 3rd edn. John Wiley & Sons, Inc., ISBN 0-471-02380-9.

[4] Kane, T.R. and Levinson, D.A. (1985) *Dynamics: Theory and Applications*. McGraw-Hill, ISBN 0-07-037846-0.

[5] Lechner, G. and Naunheimer, H. (1999) *Automotive Transmissions: Fundamentals, Selection, Design and Application*. Springer, ISBN 3-540-65903-X.

[6] Chowanietz, E. (1995) *Automobile Electronics*. SAE, ISBN 1-56091-739-3.

[7] Ribbens, W.B. (2003) *Understanding Automotive Electronics*, 6th edn. Elsevier Science, ISBN 0-7506-7599-3.

[8] Denton, T. (2004) *Automobile Electrical and Electronic Systems*, 3rd edn. Butterworth-Heinemann, ISBN 0-7506-62190.

[9] Bonnick, A.W.M. (2001) *Automotive Computer Controlled Systems: Diagnostic Tools and Techniques*. Butterworth-Heinemann, ISBN 0-7506-5089-3.

[10] Martyr, A.J. and Plint, M.A. (2007) *Engine Testing: Theory and Practice*, 3rd edn. Butterworth-Heinemann, ISBN-13: 978-0-7506-8439-2.

[11] Rakosh Das Begamudre (2000) Energy Conversion Systems, in *New Age International*, section 5.2, ISBN 81-224-1266-1.

[12] SAE J1349, Engine Power Test Code, REV.AUG. 2004.

[13] Stone, R. (1999) *Introduction to Internal Combustion Engines*, 3rd edn. SAE International, ISBN 978-0-7680-0495-3.

[14] Hoag, K.L. (2005) *Vehicular Engine Design*. SAE International, ISBN 978-0-7680-1661-1.

[15] Guzzella, L. and Onder, C. (2009) *Introduction to Modelling and Control of Internal Combustion Engine Systems*, 2nd edn. Springer, ISBN-13: 978-3642107740.

3

Vehicle Longitudinal Dynamics

3.1 Introduction

The longitudinal motions of a vehicle include accelerating, cruising, uphill and downhill motions. The performance and the driveability of a vehicle including accelerations at various loadings and driving conditions are the main topics of this chapter. Vehicle engineers have long realized the importance of driveability in the commercial success of vehicles. Vehicle longitudinal dynamics involves the study of several issues including engine behaviour, tyre tractive force generation, resistive forces acting on the vehicle and the drivers' gearshifting habits.

In this chapter first, simple vehicle models are developed which are useful for the initial estimation of vehicle longitudinal performance. For more detailed analyses and reliable design, however, more elaborate models including the engine characteristics, tyre slips, shifting delays, rotating masses and driveline losses have to be used. Such models with increasing details are being developed and many examples using typical vehicle data are included throughout and MATLAB® codes for vehicle performance calculations are provided in this chapter.

3.2 Torque Generators

The vehicle is accelerated by a tractive force at the driving wheels which in turn depends on the torque applied at these wheels. In the vehicle longitudinal performance analysis, therefore, the power source which delivers the torque – usually an internal combustion engine (ICE) – plays an important role. Different power sources have different torque generation characteristics. In vehicle performance studies, however, the power source can be regarded as delivering a quasi-steady source of torque (see Section 2.4.3) with predefined characteristics.

Traditionally, IC engines have dominated as power sources in vehicles. However, in spite of all the years of experience using IC engines in vehicles, their torque characteristics and related effects on the vehicle performance still remain an area of discussion. A detailed discussion of the torque generation properties of IC engines was presented in Chapter 2. Electric motors are the main counterparts for engines in hybrid electric vehicles (HEVs) and they have significantly different torque-generating characteristics from engines. In a later section a short review of the performance of electric motors used in vehicle applications will be provided.

3.2.1 Internal Combustion Engines

The torque-speed characteristics of IC engines were discussed in detail in Chapter 2 so only the key features for its application in the current chapter are covered here. The quasi-steady or stationary torque of an ICE is dependent on the speed of rotation ω_e and the amount of throttle opening, θ, i.e.:

$$T_e = f(\omega_e, \theta) \tag{3.1}$$

A typical part throttle engine performance curve representing Equation 3.1 for an SI engine is shown in Figure 3.1. This plot is generated based on engine dynamometer tests.

Using the MT engine formula (see Section 2.6) the performance curves can be represented mathematically by a formula of the form:

$$T(\theta, \omega) = \frac{T_{F.L}(\omega)}{[1 + \exp(A - B\theta)]^{C\omega^D}} \tag{3.2}$$

in which $T_{F.L}(\omega)$ is the engine full load or wide-open-throttle (WOT) curve and coefficients A, B, C and D are four constants for a specific engine and can be determined from part load tests. For an engine with coefficients given in Table 3.1 and full throttle data of Table 3.2, the part throttle curves are shown in Figure 3.2. In order to produce smooth curves, polynomial curve fitting is applied to the WOT data.
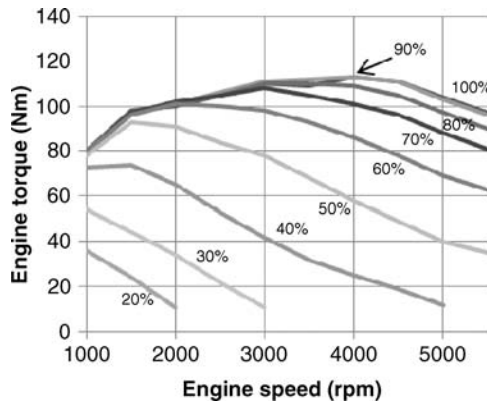

Figure 3.1   Typical SI engine part-throttle chart

Table 3.1   Coefficients of MT formula for a specific engine

Item	A	B	C	D
Value	−11.12	0.0888	1.003	1.824

Table 3.2   Engine full throttle data

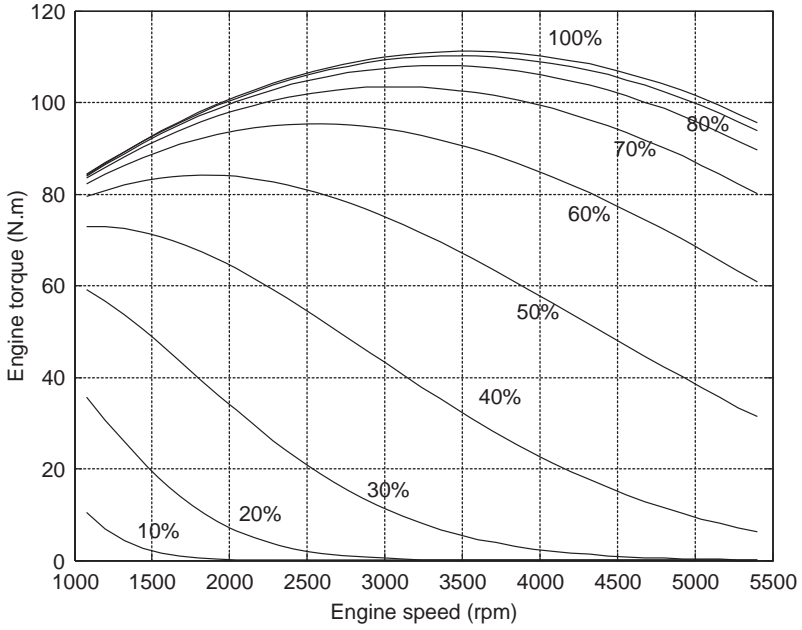| Speed (rpm)	1000	1500	2000	2500	3000	3500	4000	4500	5000	5300
Torque (Nm)	80	98	100	105	110	109	113	111	104	97

Figure 3.2 Engine part-throttle chart generated by the MT formula

Engines are different in terms of their full load and part load torque-speed characteristics. Diesel engines typically work at larger torques and lower speeds. For diesel engines with common rail fuel injection systems, the WOT torque typically has a flat area of constant torque. Figure 3.3 shows the performance curve of a diesel engine with a common rail system.
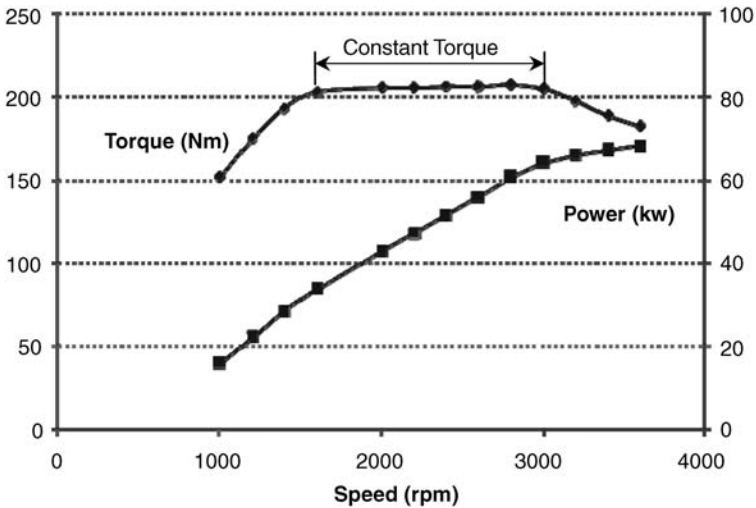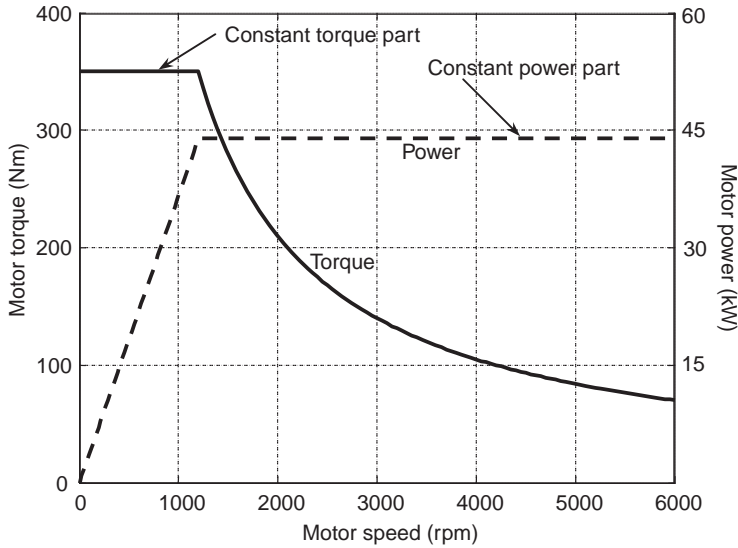

**Figure 3.3** Performance curves of a diesel engine with a common rail system

Figure 3.4 Typical performance curves of electric motors used in hybrid vehicles

3.2.2 *Electric Motors*

Electric motors play a crucial role in hybrid vehicle powertrain systems (see Chapter 7). Their potential to work as a motor or generator provides opportunities to use them for generation of both traction or braking forces whichever required. There are several types of electric motors suitable for use in hybrid vehicles. Separately excited DC motors are good at speed control and they need relatively simple control electronics. Their brushes need to be changed from time to time and they have high maintenance requirements. Alternating current (AC) motor types include permanent magnet synchronous, induction motors and switched reluctance motors. AC motors are in general less expensive, but require more sophisticated control electronics. Nonetheless, they have higher power density and higher efficiency and in the majority of vehicle applications AC motors are used. The induction AC motors are generally characterized by higher specific powers than permanent magnet motors. One of the inherent properties of electric motors is the production of torque at zero speed. This gives them advantages over IC engines in moving the vehicle from rest without needing a clutch. Power electronics provide the necessary tools for controlling the torque-speed characteristics of the electric motors to suit automotive applications. A constant high torque at low speeds and the retention of maximum power afterwards can be achieved by proper control of the motor voltage, field, flux or frequency depending on the type of the motor. A typical performance curve of an electric motor used in hybrid vehicles is shown in Figure 3.4.

3.3 Tractive Force

The vehicle accelerates through the application of tractive forces. The tractive force of a vehicle is produced at the tyre–road interface and it is therefore a function of both tyre and road properties. Different tyres produce different traction forces on a particular road surface, and a particular tyre produces different traction forces over different road surfaces. The tractive force originates from the torque applied on the axle from the torque source. Thus the tractive force is dependent on both the torque source properties as well as the tyre–road properties.
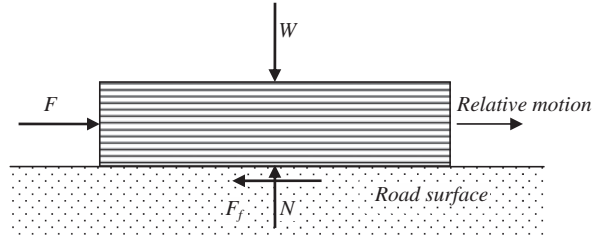
Figure 3.5   A tyre segment on the road surface

3.3.1   Tyre Force Generation

The tyre produces a tractive force due to the existence of friction at the road interface. The friction force generation by the tyre, however, is quite complicated owing to its rolling motion. In order to examine the difference between a simple sliding friction and that of a rolling tyre, consider a tyre segment cut out from the tyre contact patch as shown in Figure 3.5. A load W equal to a wheel load is considered to act vertically on the tyre segment. When a force F is applied to the segment in order to move it along the road surface, three cases may exist:

(a) F is small and no relative motion is produced. In this case, the friction force F_f is simply:

$$F_f = F \tag{3.3}$$

(b) F is large enough to bring the segment to the verge of slip. The friction force in this case is:

$$F_f = \mu_S N = \mu_S W \tag{3.4}$$

where μ_S is the static coefficient of friction.

(c) The segment skids over the surface. In this case all particles on the contact surface will theoretically slide with a similar relative speed to the ground. The friction force can be expressed as:

$$F_f = \mu_k N = \mu_k W \tag{3.5}$$

where μ_k is the dynamic (or kinematic) coefficient of friction and is usually smaller than μ_S. For F larger than F_f, the segment will accelerate. In practice, the friction force varies by increasing the force F in the following range:

$$0 \leq F_f \leq \mu_S N \tag{3.6}$$

Now consider a tyre with the same axle load W standing on the road surface as shown in Figure 3.6. As long as the tyre does not rotate, the friction force F_f will be similar to that of the segment discussed earlier.

Now if instead of force F, a torque T is applied at the wheel axis as illustrated in Figure 3.7, the direction of friction force at the contact surface will be reversed because the slip direction at the contact surface changes. With the wheel initially at rest, when the torque is applied, the wheel tends to rotate around its axis. This is possible only if the contact patch of the tyre is allowed to slip in reverse direction to the forward motion. The relative motion in the presence of friction at the contact area will result in a friction force opposite to the slip direction. This force will act at the direction of motion of the wheel centre and is called tractive force F_T.
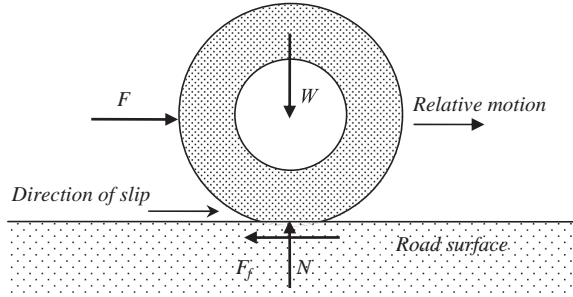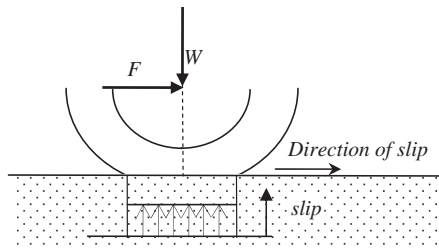
Figure 3.6   Skid of a non-rolling tyre
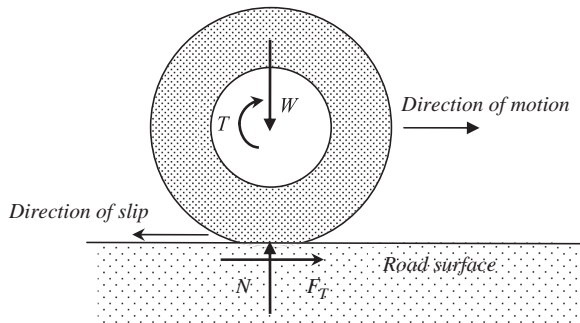
Figure 3.7   The tractive force as a result of applying a torque at the wheel axis

One major difference between the simple slip of the tyre segment or the similar case for a non-rolling tyre with the case of a rolling tyre is the slip phenomenon in the contact patch. In the two former cases, the whole contact area slides relative to the ground surface. All contact points, therefore, will experience similar situations. Each point in contact region will generate a share of the total force proportional to the pressure distribution. In the case of the tyre segment, the pressure distribution will be uniform, so any point will have an equal share. For the non-rotating tyre case, the pressure distribution in the contact area is not uniform, but the slip will be uniform, as illustrated in Figure 3.8.

When the torque is applied at the wheel axis, those elements of the tyre entering the contact region will be forced to stay in contact with the ground and gradually move forward in the direction of the slip. Those close to the leading edge cannot move as fast as those close to the trailing edge. This results in zero slip at

Figure 3.8   Slip distribution for a non-rolling tyre
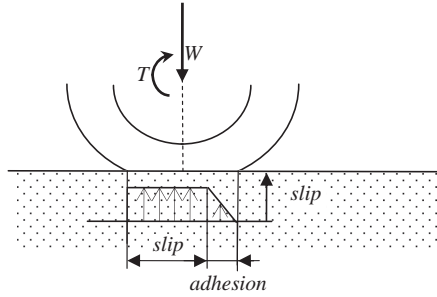
Figure 3.9 Slip distribution for a rolling tyre

leading edge and full slip at the trailing edge. The distribution of slip along the contact length does not have a simple form and an approximation for the slip is illustrated in Figure 3.9. According to this model, a linear slip will exist at the leading region called the 'adhesion area' and a uniform slip will exist at the trailing region called the 'slip area'.

Even this simplified model is difficult to work with, since it needs information regarding the relative width of adhesion and slip lengths, which is dependent on many factors and difficult to determine. In practice, however, a uniform slip is considered in the contact patch of a tyre which means the contact points all have a uniform speed V_s opposite to the direction of wheel travel. If the velocity of wheel centre is denoted by V_w, then the velocity vector, according to Figure 3.10, can be written as:

$$V_W = V_S + \boldsymbol{\omega} \times r_W \tag{3.7}$$
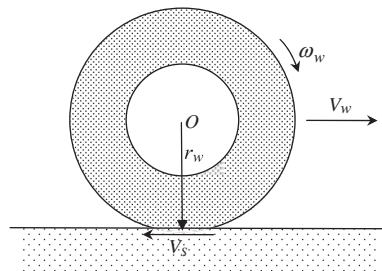
or in an algebraic form:

$$V_W = r_W \omega_W - V_S \tag{3.8}$$

in which r_W is the effective radius of the tyre. In a pure rolling case, the wheel centre velocity equals $r_W \omega_W$, that means no slip condition with $V_S = 0$. For the slipping case:

$$V_S = r_W \omega_W - V_W \tag{3.9}$$

Longitudinal slip S_x of tyre is defined by dividing the slip speed by the rolling speed $r_W \omega_W$:

$$S_x = \frac{V_S}{r_W \omega_W} \tag{3.10}$$
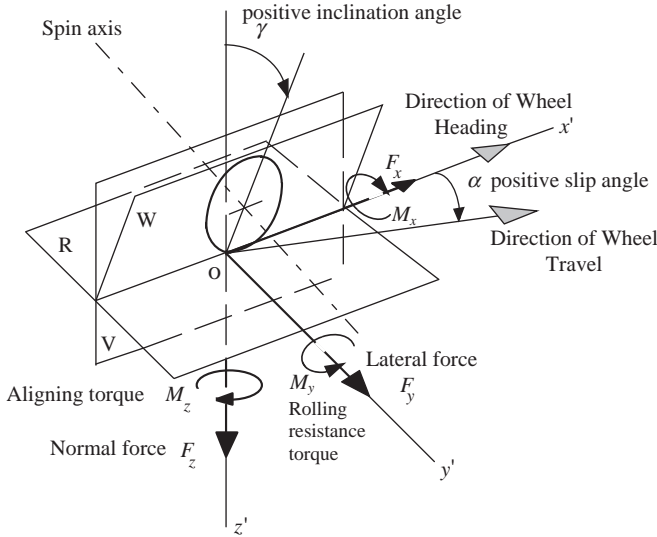

Figure 3.10 Wheel kinematics during slip

Figure 3.11   SAE tyre co-ordinate system [1]

From Equation 3.9:

$$S_x = 1 - \frac{V_W}{r_W \omega_W} \tag{3.11}$$

S_x is sometimes expressed as a percentage. The tractive force of the tyre is dependent on the slip within the contact area. However, there are other factors that control the tractive force, e.g. the normal load F_Z on the tyre and tyre pressure p. Thus, the tractive force of the tyre can be expressed as a function f of the influencing variables:

$$F_T = f(S_x, F_Z, p, \ldots) \tag{3.12}$$

At a certain tyre pressure, the tractive force will be dependent mainly on the longitudinal slip and normal load.

What has been considered so far is the pure slip of the tyre in the longitudinal direction. In practice, the tyre is subjected to slips with components in both the longitudinal and lateral directions. In these combined slip conditions, the slip in the contact region has a complicated nature, since the contact patch is distorted under the application of loads in different directions. For this reason the tyre will produce a force that is acting somewhere other than on the centre of contact patch and in addition to the forces in three directions, moments are also generated.

The tyre force system can be defined in different ways. According to the SAE definition [1], the origin O of the axis system (see Figure 3.11), is taken on the centre of tyre contact (the intersection of wheel plane W and the projection of spin axis onto the road plane R). The x' axis is the intersection of the wheel and the road planes. The z' axis lies in vertical plane V and is perpendicular to the road plane and pointing downward. The y' axis is therefore in the road plane with positive direction to the right. Only F_x (tractive/brake force) and M_y (rolling resistance torque) will be needed in this chapter and they are discussed in more detail in the next sections.

3.3.2   Mathematical Relations for Tractive Force

A large volume of work is available in the literature dealing with the modelling and prediction of the force generating properties of the tyres. In general, tyre modelling is performed in two basic ways: physical and

experimental. In physical modelling a simplified model is assumed for the tyre that accounts for the main physical properties affecting the force generation mechanism. By the application of mechanical laws governing the deformation of tyre elements and friction effects at the contact region, mathematical equations are developed. The accuracy of such models depends on the quality of the assumptions made for the physical model. The advantages of these types of models are their simple nature and that the predicted tyre forces do not necessarily require difficult measurements.

There are also software-based physical models involving considerable complexity. These models usually use Finite Elements methods (FEM). Although these sophisticated models are claimed to generate more accurate results than those of simple physical models, they are unnecessarily complicated for vehicle longitudinal performance predictions. Another approach is based on experimental work to measure the force generation properties of the tyres. Experimental results can also help to explain the physics of tyre behaviour when different loading conditions are tested, and hence influence the further developments of tyre models. The normal approach is to fit curves to the measured tyre data.

Finding a general mathematical relationship applicable to all tyres has been a challenge to the automotive industry. The 'Magic Formula' tyre model is the result of work carried out at Delft University. The attraction of this approach is its accuracy in fitting the lateral tyre force and aligning moment data in addition to the longitudinal force data of the tyre. The equations of this tyre model are of basic form [2]:

$$Y(X) = D\sin[C\,Arctan(B\Phi)] + S_v \tag{3.13}$$

where:

$$B\Phi = G(1-E) + E\,Arctan(G) \tag{3.14}$$

$$G = B(X + S_h) \tag{3.15}$$

X stands for either longitudinal slip S_x or sideslip angle α (see Figure 3.11). Y stands for either longitudinal force F_x, side force F_y or self-aligning moment M_z. The coefficients B, C, D, E and the horizontal and vertical shifts S_h and S_v are non-linear functions of the vertical tyre load F_z (and camber angle γ for F_y and M_z). For each tyre, a set of tests must be carried out in order that the dependency of the coefficients on the variables (e.g. F_z) is calculated. Typical relations for longitudinal force of a specific tyre are [2]:

$$\begin{aligned}
C_x &= 1.65 \\
D_x &= a_1 F_z^2 + a_2 F_z \\
bcd_x &= (a_3 F_z^2 + a_4 F_z)e^{-a_5 F_z} \\
B_x &= \frac{bcd_x}{C_x \times D_x} \\
E_x &= a_6 F_z^2 + a_7 F_z + a_8 \\
S_h &= a_9 F_z + a_{10} \\
S_v &= 0
\end{aligned} \tag{3.16}$$

The numerical values for the coefficients a_1 to a_{10} of the same tyre are given in Table 3.3. F_z is in units of N for these values.

The advantage of the Magic Formula representation is that once the tyre parameters are available, it will be valid for all loading cases with a large range of parameter variations.

Table 3.3 Magic Formula coefficients for a specific tyre [2]

Coefficient	a_1	a_2	a_3	a_4	a_5	a_6	a_7	a_8	a_9	a_{10}
Value	−2.13e-5	1.144	4.96e-5	0.226	6.9e-5	−6.0e-9	5.6e-5	0.486	0	0

Example 3.3.1

Use the Magic Formula with the information in Table 3.3 and plot the variation of tyre longitudinal force for a full range of tyre slips at normal loads of $F_z = 1000$ to $3500\,\text{N}$.

Solution

The full range of tyre slip is between 0% and 100%. With a simple MATLAB program the plot can be obtained. The MATLAB program is written in two 'main' and 'function' parts as shown in Figure 3.12. The output result is given in Figure 3.13.

```
% MATLAB program to plot tyre longitudinal force
% the longitudinal slip is varied from 0 to 100%

for fz=1000: 500: 3500;    % Normal load in N
for i=1:200
   sx(i)=(i-1)/2;
   Fx(i)=fx(fz,sx(i));
end
plot(sx, Fx)     % Fx in N
hold on
end
grid
xlabel('Longitudin al slip (%)')
ylabel('Longitudinal force (N)')
```

```
% MATLAB function called in the main program

function  f = fx (fz,sx)
%
c=1.65;
d=-21.3e-6*fz*fz+1144.e-3*fz;
e=-.006e-6*fz*fz+.056e-3*fz+0.486;
bcd=(49.6e-6*fz*fz+226.e-3*fz)*exp(-.069e-3*fz);
b=bcd/c/d;
phai=(1.0-e)*sx+e*atan(b*sx)/b;
%
f=d*sin(c*atan(b*phai));
```

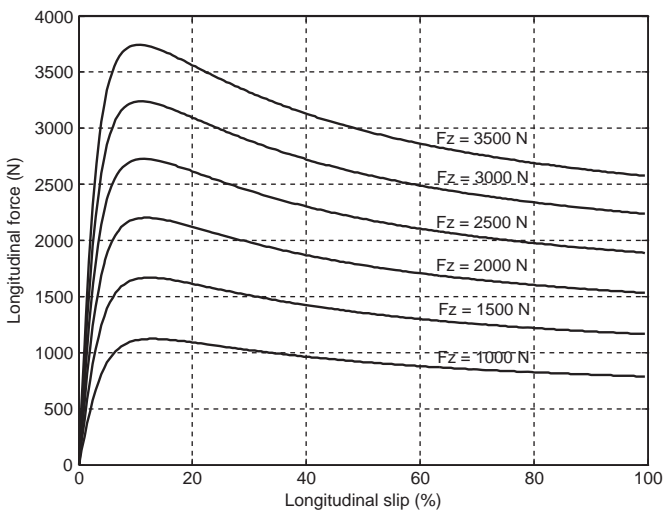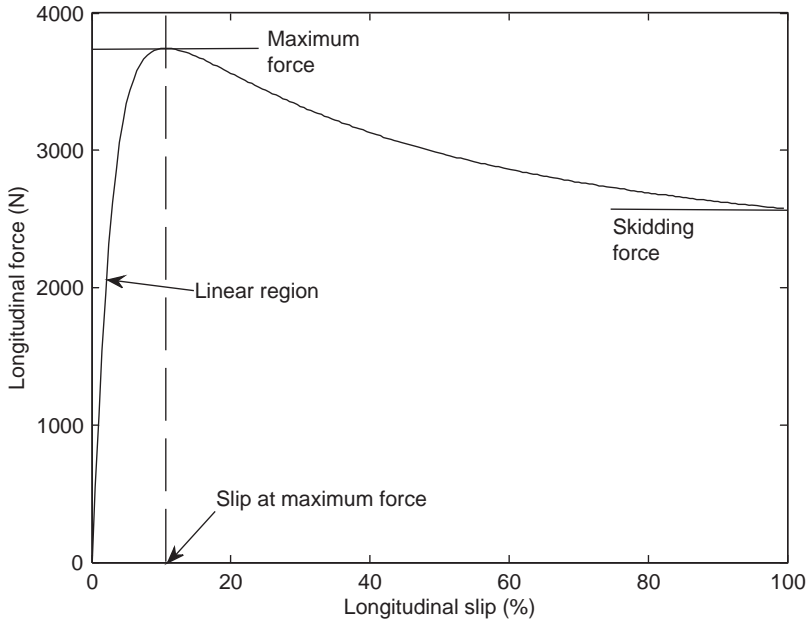**Figure 3.12**   MATLAB programs of Example 3.3.1

Figure 3.13   Plot of longitudinal tyre force versus slip at different normal loads

Figure 3.14   The properties of tyre force

From the results of Example 3.3.1, it can be seen that the overall variation of the tyre longitudinal force with slip can be considered in two linear and non-linear regions as shown in Figure 3.14. The linear region begins from zero slip up to a certain value of 5–10% and the maximum tyre force is developed at slip values around 10–20%. At the full slip (100%) the tyre force is considerably lower than the maximum force. This phenomenon is a typical property of the rolling tyres and if the concept of dry friction is employed, the longitudinal force can be related to the normal load by the coefficient of adhesion:

$$F_x = \mu F_z \tag{3.17}$$

At a specific normal load, F_z^*, the coefficient of adhesion μ is a function only of F_x which is already a function of slip S_x i.e.:

$$\mu = \mu(S_x) \tag{3.18}$$

In fact, by dividing the values of F_x by the normal load F_z^*, the trend of variation of μ against the slip will be similar to the variation of F_x with S_x.

Example 3.3.2

Use the information in Example 3.3.1 and plot the variation of tyre adhesion coefficient versus tyre slip at different normal loads.

Solution

The results shown in Figure 3.15 are obtained by dividing the F_x values by the normal load in the outer loop of Example 3.3.1. Since the curves lie close to each other, only two for $= 1000$ and 4000 N are presented. It is observed that the dependency of adhesion coefficient on the normal load is very small and in an inverse order.
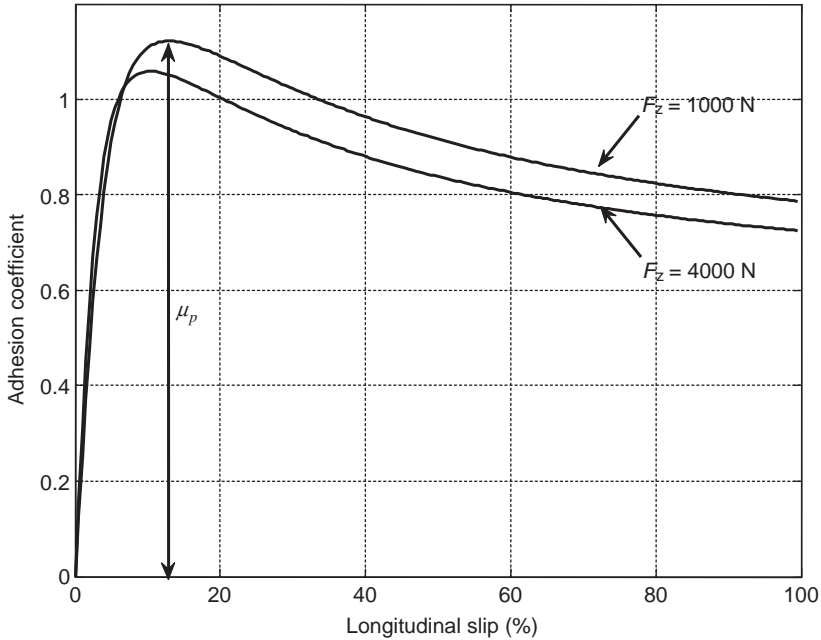

Figure 3.15   Coefficient of adhesion (Example 3.3.2)

From the variation of the coefficient of adhesion, two other issues can be noticed. First, the peak of adhesion coefficient μ_p (Figure 3.15) can become even greater than unity at relatively low slips of below 20%. Second, at 100% slip, the value of sliding adhesion coefficient is the lowest value in the non-linear region – in the example tyre in Figure 3.14 it was some 30% lower than μ_p. Thus, the behaviour of coefficient of adhesion in rolling tyres is quite different from the coefficient of friction between the two surfaces. Hence, the following conclusions can be drawn:

1. In order that a tractive force is generated by the rolling tyre, a slip must occur in the contact area, otherwise no force will be developed.
2. To obtain the largest tractive force, the tyre slip should be regulated around a specific value, depending on the tyre and road surface. Larger slips will cause the tractive force to reduce considerably.

It should be noted that the adhesion coefficient depends not only on the tyre but on the type of road surface as well. On wet surfaces, the values of μ_p will be reduced. Other factors such as tyre treads (shape and depth) will also be influential on the adhesion coefficient. It is worth mentioning that the braking behaviour of the tyre is very similar to its tractive behaviour. Again, to generate braking force at the
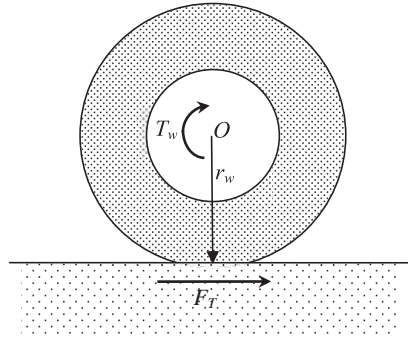
Figure 3.16 The tractive force in a quasi-steady condition

contact area, slip should take place. This time the rotational speed of tyre is lower than the corresponding straight line speed of the wheel, therefore, the slip will be negative. The braking force can also be determined with the Magic Formula by simply using negative slips. The overall shape of the braking force, therefore, will be similar to that of the tractive force but mirrored relative to the origin.

3.3.3   Traction Diagrams

The tractive force is produced at the tyre–road interface provided that two conditions are fulfilled:

1. A torque T_w is applied at the wheel axis.
2. Slip is produced in the contact area.

In a quasi-steady condition, with reference to Figure 3.16:

$$F_T = \frac{T_w}{r_w} \tag{3.19}$$

There is, however, a force limitation in the contact area of the tyre depending on the road conditions. Equation 3.19 is valid up to the limit of tractive force:

$$F_T \leq F_{\max} \tag{3.20}$$

As long as the wheel torque is lower than $r_w F_{\max}$, a limited amount of slip will build up, otherwise if a larger torque is applied, the wheel will spin.

Example 3.3.3

A torque of 500 Nm is applied at a wheel axis with effective radius of 35 cm. The weight on the wheel is 360 kg. Use the MF tyre with information given in Table 3.3 and determine:

(a) the tractive force available;
(b) the maximum possible tractive force and corresponding wheel torque;
(c) the value of longitudinal slip (in percentage).

Solution

The load on the wheel in Newton is: $F_z = 360 \times 9.81 = 3531.6\,\text{N}$.

(a) From Equation 16: $F_T = \dfrac{500}{0.35} = 1428.6\,(\text{N})$.

(b) The maximum tractive force must be determined by using the MF tyre at a normal load of 3531.6 N. A relation for the maximum force is not available, so we can use the program in Example 3.3.1 to find the whole force-slip data (no plot is necessary). Then in MATLAB command window we type: 'Fmax = max(Fx)' and 'Enter'. The result is: Fmax = 3774.4 N.

In order that this force is developed at the contact area a torque of $T_{\max} = 3774.4 \times 0.35 = 1321\,(Nm)$ must be applied at wheel axis.

(c) Finding a closed form solution for the slip at a specified force is not possible. One way is to plot the variation of the tyre force versus slip and at a specified tyre force, read the slip value. A trial and error solution can also be followed by choosing a value for slip and evaluating the tyre force for it. The slip value must be changed in such a way that the force approximates to the specified value. MATLAB function 'fsolve' is also suitable for this work. Issue the following command in MATLAB:

$$sx = \text{fsolve(inline('1428.6-fx(3531.6, x)'), 5, optimset('Display', 'off'))}$$

in which the 'inline' function defines our equation to be solved, i.e. $F_T - F_x(S_x,\ F_z) = 0$ with given values of $F_T = 1428.6\,(\text{N})$ and $F_z = 3531.6\,(\text{N})$. 'fx' in the command line is our earlier defined MF tyre function in Example 3.3.1. The value '5' is our initial guess for the S_x. The answer will appear as:

$$sx = 1.36\,(\%)$$

This means the required tractive force is developed at a very small slip.

Assuming the wheel torque is below the limit, Equation 3.19 means the tractive force is also dependent on the nature of the torque of the wheel. The wheel torque in general is an amplification of the torque of vehicle torque generator (see Section 3.2). Denoting the amplification factor by n (i.e. the overall gear ratio between the torque generator and the wheel):

$$T_w = n\,T_g \le r_w F_{\max} \tag{3.21}$$

and from 3.19:

$$F_T = \frac{nT_g}{r_w} \tag{3.22}$$

Thus, the traction force will resemble the torque characteristics of the torque generator (T_g) multiplied by an amplification factor.
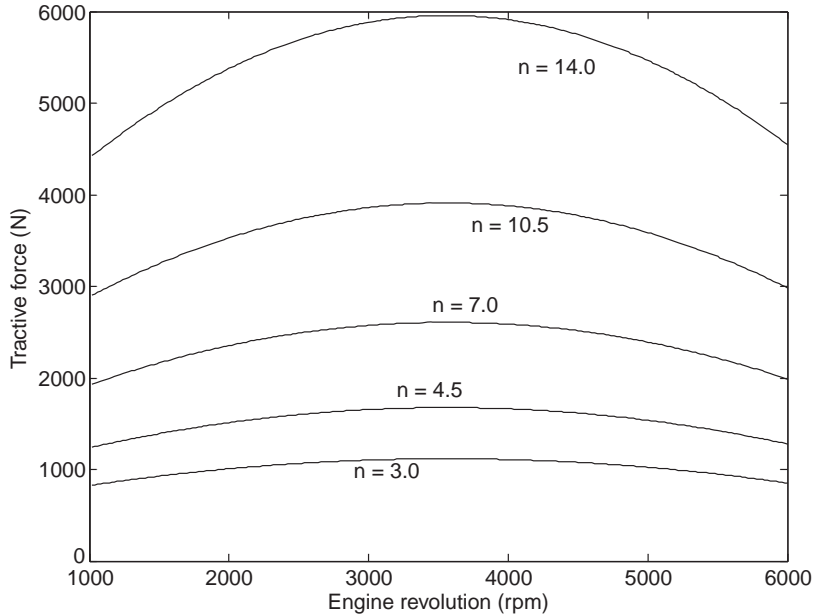
Example 3.3.4

An engine torque at wide open throttle (WOT) is approximated by the following equation:

$$T_e = -4.46 \times 10^{-6}\omega_e^2 + 3.17 \times 10^{-2}\omega_e + 55.24, \quad 1000 \le \omega_e \le 6000\,rpm$$

Plot the variation of the tractive force versus engine rpm for the overall gear ratios of 16.0, 10.5, 7.0, 4.5 and 3.0 respectively, all in a single figure. The wheel effective radius is 30 cm.

Solution

Using Equation 3.22, a simple MATLAB program can be written to plot the required figures. The result is shown in Figure 3.17.

Figure 3.17   Tractive force versus engine rpm of Example 3.3.4

3.4   Resistive Forces

There are resistive forces opposing the motion of the vehicle; some exist from the start of motion and others build up with speed. Resistive forces consume some part of engine power and reduce the speed and acceleration of the vehicle. In order to analyze the straight line performance of the vehicle, it is necessary to characterize the resistive forces acting on the vehicle during the motion. The resistive forces can be categorized into three types: frictional, air resistance and gravitational. The frictional forces are commonly called 'rolling resistance' force. Air resistance forces are known as 'aerodynamic force' and the gravitational force is called 'grade force'.

3.4.1   Rolling Resistance

As the name implies, the resistance to motion of rotating parts is summed up together and builds a total resistive force to slow down the vehicle. The rotating parts work under two conditions: with and without the transmission of torque. The former can be excluded from the current discussion since it deals with the driveline power loss during torque transmission and will be treated separately in Section 3.13. The rolling resistance term, therefore, deals only with those resistive torques during vehicle motion with the driveline freely rolling. This includes all the rotating parts in the driveline components. The driving

wheels are constantly connected to the driveline and their connection to the engine is controlled by the clutch. Therefore, even when the gearbox is disengaged and left in the neutral position, the driving wheels will rotate the driveline components except for gears inside the gearbox. The total resistive torques of the free rotating parts can be divided into two main categories: due to friction and tyre deformation resistance.

3.4.1.1 Frictional Torques

The frictional torques in the vehicle driveline consist of three parts:

1. *bearing torques*: the bearing friction terms are usually small compared with other resistive factors and typically increase with load on the bearings.
2. *gear teeth friction*: friction forces at gear teeth contact points create resistive torques. These are load dependent and thus are relatively small when no load is carried.
3. *brake pads*: torque resulting from the contact of brake pads with wheel disks or drums is also a resistive factor. Even with no brake activation, there is often a small rubbing effect between the pads and discs that results in a resistive torque. The values of such torques depend on many detailed factors in the design of the brake.

3.4.1.2 Tyre Deformations

For a non-rolling tyre, the load W will cause a symmetrical pressure distribution around the centre of contact area. The resultant reaction load N will act at the centre of contact region as illustrated in Figure 3.18.

For a rolling tyre, the tyre elements entering the contact region will experience a compression whereas the trailing materials exiting the contact area will tend to stretch. The pressure on the materials in the contact zone, therefore will tend to increase at the leading edge and decrease at the trailing edge. The pressure distribution will be something similar to that shown in Figure 3.19. The resultant reaction force at the ground will act off-centre closer to the leading edge.

With the resultant reaction force moving forward, it is equivalent to an opposing torque acting around the wheel axis. This torque shown in Figure 3.20a is called rolling resistance torque (T_{RR}). Since the action of the rolling resistance torque is to slow down the wheel (or vehicle), in practice, it is assumed that a resistive force is acting at the ground level with the same effect (see Figure 3.20b). This force is called rolling resistance force (F_{RR}).
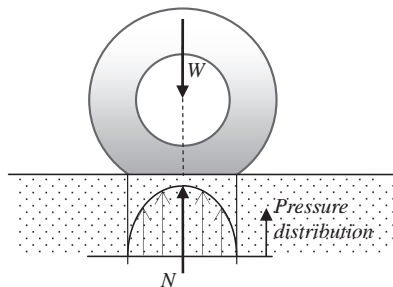
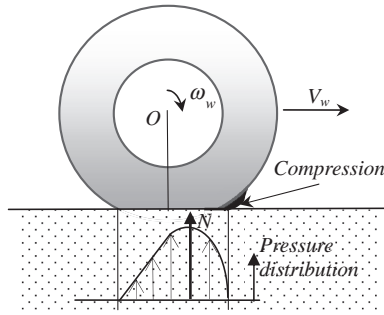**Figure 3.18**   Pressure distribution for a non-rolling tyre

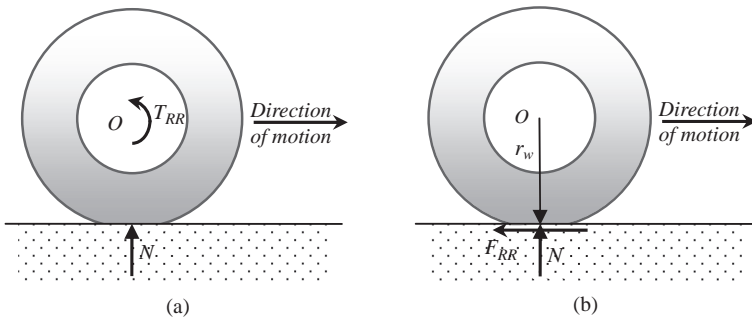**Figure 3.19**   Pressure distribution for a rolling tyre

Figure 3.20   Rolling resistance (a) torque and (b) force

From an energy point of view, the rolling resistance is caused by the deformations of the tyre. The tyre elements require energy to deform when they enter the contact region. Owing to the visco-elastic properties of rubber, the tyre elements are unable to fully restore this energy when they leave the contact region. This phenomenon is called a hysteresis effect. Therefore a net amount of energy is lost to heat during tyre rolling and is equivalent to the work done by the rolling resistance torque or the work done by the rolling resistance force.

3.4.1.3   Other Factors

There are also other factors besides the rolling frictions and tyre deformation that have small influences on the total resistive force:

- *Tyre–road friction loss* – due to slipping of the tread compound on the ground surface, heat will be generated.
- *Aerodynamic resistance due to wheel spin*. The aerodynamic resistance for the whole vehicle usually includes the resistive force for a non-spinning wheel. However, to spin a wheel in the presence of air requires a small amount of energy which will add to the other sources of energy loss.
- *Propeller effect of wheel rim during spin*. Air passing through the spinning wheel rim also adds a small term to the energy losses.

3.4.1.4 Influencing Parameters

Several parameters influence the rolling resistance force. The main parameters are those which affect the tyre or the contact surface including:

- tyre construction:
  - type of tyre (radial or bias ply)
  - tyre materials
  - tread design
  - tyre diameter

- tyre operating conditions:
  - tyre pressure
  - tyre speed
  - tyre temperature
  - vertical load
  - tyre lateral slip
  - tyre age

- road surface: it is worth noting that the deformations of the road surface, e.g. on soft deformable ground requires energy and such energy losses are also considered as rolling resistance loss. Some influencing items are:
  - road texture
  - rigidity
  - dryness.

The extent to which the named parameters influence the rolling resistance has been discussed in specialist references (e.g. [3]). An overview of the influence of various parameters qualitatively is shown in Tables 3.4 and 3.5.

3.4.1.5 Mathematical Representation

A mathematical formula for the rolling resistance force will help in the analysis of vehicle motion. To this end, one can write the rolling resistance force as a function of influencing parameters p_1, p_2, etc., that is:

$$F_{RR} = f(p_1, p_2, p_3, \ldots) \tag{3.23}$$

Table 3.4 Effect of increasing tyre parameter values on the rolling resistance force

Parameter	Diameter	Pressure	Speed	Temperature	Load
Effect	↓	↓	↑	↓	↑

Table 3.5 Effect of tyre and road types on the rolling resistance force

Parameter	Radial	Bias ply	Soft road	Smooth road
Effect	↓	↑	↑	↓

Finding the unknown function f, however, is not a simple task. Of the parameters mentioned earlier, some such as diameter and construction are fixed for an existing tyre, some have little importance such as temperature and some have fixed values, such as pressure. The remaining parameters are speed, load and road type. The type and quality of roads are hard to formulate, thus, for each road type a different formulation is necessary. The dependency of the rolling resistance force on the wheel load is of a linear nature, thus, the ratio of rolling resistance force to the wheel load, f_R is called the rolling resistance coefficient and is independent of load:

$$f_R = \frac{F_{RR}}{W} \tag{3.24}$$

The rolling resistance coefficient in general is a function of all the above-mentioned parameters, but according to the justification presented, the only important parameter is the forward speed of the wheel centre, i.e. the vehicle speed:

$$f_R = f(v) \tag{3.25}$$

The variation of rolling resistance coefficient with speed is reported somewhat differently in various references. The general trend nonetheless shows an increase in the rolling resistance coefficient with speed. From an energy point of view this is acceptable since if a particular amount of energy is lost for one revolution of the tyre, then increasing the revolutions in a time interval will increase the lost energy. The variation of rolling resistance coefficient with speed in general can be approximated in the form of a second order polynomial:

$$f_R = f_0 + f_1 v + f_2 v^2 \tag{3.26}$$

where the coefficients f_0, f_1 and f_2 are three constants. The quadratic term, however, can be removed since a similar dependency on speed is available through aerodynamic resistance (see Section 3.4.2). In fact, by eliminating this term we are not disregarding this effect, but leaving it included in the aerodynamic force term. With this justification, the rolling resistance coefficient can be simplified to a first order form:

$$f_R = f_0 + f_1 v \tag{3.27}$$

Often, the dependency of the rolling resistance on speed is also ignored (i.e. $f_1 = 0$) and only a constant coefficient f_0 is considered for the rolling resistance coefficient. Typical ranges for the coefficient of rolling resistance f_0 can be found in Table 3.6 (additional information may be obtained from [3]).

Table 3.6   Ranges for the rolling resistance coefficient f_0 at low speeds

Type of vehicle	Asphalt/concrete	Earth road	
		Hard-medium	Soft
Car	0.010–0.015	0.05–0.15	0.15–0.3
Truck	0.005–0.010	–	–
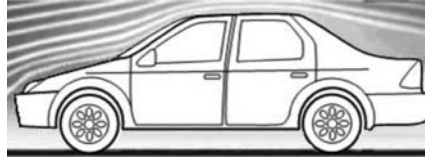
Figure 3.21   Streamlines around the body

3.4.2   *Vehicle Aerodynamics*

The motion of a vehicle is taking place in the air and the forces exerted by air on the vehicle will influence the motion. Aerodynamics is the study of the vehicle motion in air and the effects include:

- *internal flows*: air flows through the front grills for the purpose of ventilation and cooling. Air flow through windows and sunroof are other examples.
- *ground clearance*: in ground vehicles, the ground clearance is very low and causes ground effects.
- *streamlining*: the design of the exterior in accordance with the streamlines of air flow around the body is of great importance in order to reduce the air resistance. For ground vehicles, however, the exterior shape of body is dependent on several factors and streamlining is only one of them (Figure 3.21).

3.4.2.1   Aerodynamic Resistance

Aerodynamic resistance forces result from three basic effects:

1. *Form resistance*: The basis for this resistance force is the pressure difference in front and behind the vehicle due to the separation of the air flow and the vortex creation behind the vehicle. The pressure in front will be higher and a net force opposite to the direction of the air speed will be exerted on the vehicle. The cross-sectional area of vehicle in front of the air flow, therefore, plays an important role in this respect.
2. *Skin friction*: Air coming into contact with the vehicle surface with a relative speed will apply frictional forces opposite to the direction of motion. The surface roughness of vehicle body is an important factor in this part of the aerodynamic force.
3. *Internal flow*: Air entering the internal parts of vehicle is slowed down by taking energy from the vehicle and will cause additional resistive force on the vehicle.

The form resistance is responsible for the main part of the aerodynamic force, around 80%, whereas the two others share the remainder at around 10% each.

3.4.2.2   Aerodynamic Forces and Moments

The aerodynamic resistance forces are not in reality discrete forces acting at specific locations, but are actually a summation of infinitesimal forces acting at all points on the vehicle body. The result is a single force R_A acting at a point called the centre of aerodynamic force, or centre of pressure C_P. In general, the aerodynamic forces are described by a three-dimensional force system with three resolved components at the vehicle body axes. The centre of pressure is also different from the vehicle centre of mass C_G and thus the aerodynamic force will have moments around the vehicle axes. Figure 3.22 illustrates the aerodynamic forces and moments.

In aircraft aerodynamics, it is a common practice to define other axes systems such as wind axes, separate from the body axes. Aerodynamic forces – drag, lift and sideforce – are defined as components of
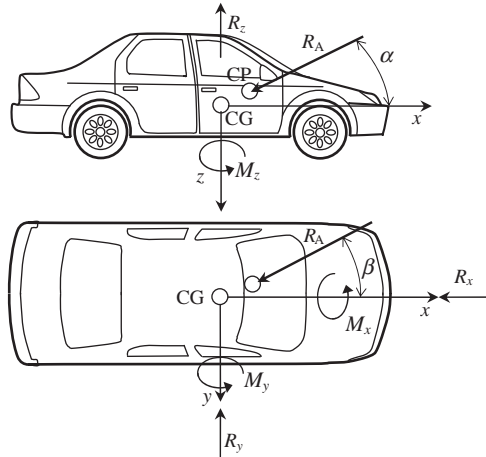
Figure 3.22 Aerodynamic forces and moments acting on the vehicle

the aerodynamic force on the wind axes. In ground vehicle applications, due to small aerodynamic angles (in the absence of side wind), the two axes systems are often taken to be coincident. With this assumption, therefore, the components of force in the negative directions of x, y, and z axes are drag, sideforce and lift respectively. As far as the longitudinal motion of the vehicle is concerned, the most important aerodynamic force is the drag force opposing the motion. The lift component can alter the normal loads of the tyres and will therefore also be indirectly influential.

3.4.2.3 Mathematical Representation

It is common practice to express the aerodynamic forces and moments in terms of dimensionless coefficients. In general, any aerodynamic force is written in the basic form:

$$F_A = qC_F A^* \tag{3.28}$$

where C_F is aerodynamic force coefficient and stands for drag C_D, sideforce C_S and lift C_L coefficients respectively. A^* is the characteristic area for the vehicle and it is taken as the frontal area A_F (also called the projected area). q is called dynamic pressure and is:

$$q = \frac{1}{2}\rho_A v_A^2 \tag{3.29}$$

in which ρ_A is the air density that is dependent on the ambient conditions. Under the standard conditions of 1 atmosphere (1.013 bar, 10132.5 Pa) at sea level and a temperature of 15 °C (288.15°K), the air density is 1.225 kg/m^3. The air density can be approximately calculated from:

$$\rho_A = 0.0348\frac{p}{T} \tag{3.30}$$

with p in Pascal and T in Kelvin (273.15 + °C).

The velocity v_A in Equation 3.29 is called the air speed and is the magnitude of speed of air relative to the vehicle body. In order to calculate the air speed, information on the wind velocity is also necessary.
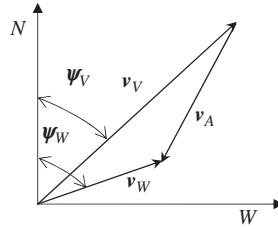
Figure 3.23 Definition of air velocity vector v_A

Let us assume a wind speed v_W is acting at angle ψ_W relative to the geographical north (see Figure 3.23). A vehicle is travelling at a speed of v_V in the direction of ψ_V. Vector v_A is the air velocity and can be determined as:

$$v_A = v_W - v_V \tag{3.31}$$

v_A can also be obtained graphically as shown in Figure 3.23.

The aerodynamic moments are expressed as:

$$M_A = qlC_M A^* \tag{3.32}$$

where l is the characteristic length and for the vehicle usually the wheelbase is considered. C_M is the moment coefficient and represents C_l, C_m and C_n for roll, pitch and yaw moments respectively.

Example 3.4.1

A vehicle is travelling with a constant speed of 100 km/h. Determine the air speed for a wind speed of 30 km/h, for: (a) a head wind; and (b) a tail wind.

Solution

It can be assumed that the vehicle velocity vector has a zero angle ($\psi_V = 0$), thus for case (a) the head wind, $\psi_W = 180$ and from Equation 3.31:

$$v_A = -30 - 100 = -130 \text{ km/h (opposite to the direction of motion)}$$

For the tail wind of case (b) $\psi_W = 0$ and similarly:

$$v_A = 30 - 100 = -70 \text{ km/h (opposite to the direction of motion)}$$

Graphical representations are also shown in Figure 3.24.
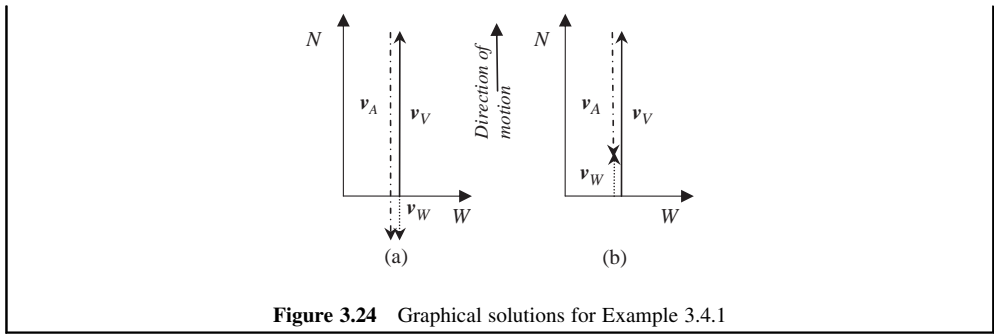
Figure 3.24 Graphical solutions for Example 3.4.1

Aerodynamic forces are dependent on several parameters, such as the body geometry, ambient conditions and airstream properties. The geometry of the vehicle body includes its shape and dimensions. The latter was already considered as the characteristic area, and the vehicle wheelbase was considered as the characteristic length for the aerodynamic moments. The main influential ambient parameter is the air temperature that influences the air density and directly alters the aerodynamic forces.

The airstream properties include air speed and its direction relative to the body coordinates. When the airstream is at an angle to the vehicle forward axis, this angle is called the angle of attack. This angle also has an influence on the magnitude of the aerodynamic force. In order to account for these influential parameters, the dimensionless parameters Reynolds number (Re) and Mach number (M) are used. In general, the force (or moment) coefficients C_F (C_M) are a function of these parameters as well as angle of attack α and sideslip β (see Figure 3.22), i.e.:

$$C_F = f(\text{Re}, M, \alpha, \beta) \tag{3.33}$$

In vehicle motion the Mach number is always of a small range of less than 0.2, and the variation of the Reynolds number is also very small. In the case of longitudinal horizontal wind, both angles α and β are small and under these circumstances, the force coefficient is virtually a constant. It is, therefore, practical to consider constant force or moment coefficients for the vehicle.
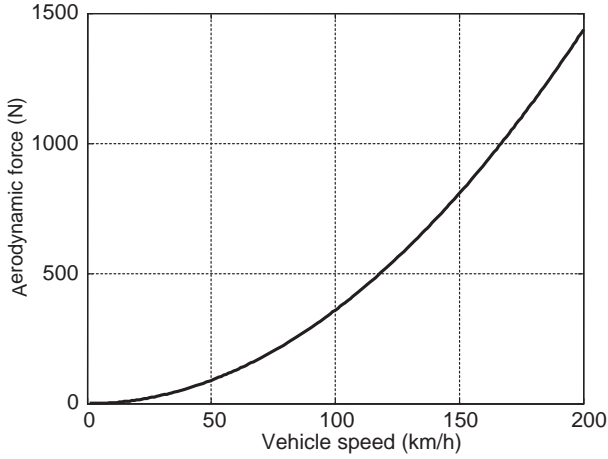
Example 3.4.2

A vehicle with frontal area of 2.0 square metres has drag coefficient of 0.38. Plot the variation of aerodynamic drag force at the standard ambient condition and in still air up to a speed of 200 km/h.

Solution

The air density at the standard condition is 1.225 kg/m^3 and the aerodynamic force is:

$$F_A = 0.5 \times 1.225 \times 0.38 \times 2.0 \times v^2 = 0.4655 v^2$$

The variation of this force with speed can be plotted easily in MATLAB. The result is given in Figure 3.25.

Figure 3.25   Variation of aerodynamic force for vehicle of Example 3.4.2

Example 3.4.3

For the vehicle in Example 3.4.2, calculate the aerodynamic force at a speed of 100 km/h and examine the changes in the drag force for head and tail winds of 20, 30 and 40 km/h.

Solution

From the equation for the drag force found in the previous example, the force at 100 km/h is 359.2 N.

For the head and tail winds the drag forces simply are $0.4655 \times (100/3.6 + v_W)^2$ and $0.4655 \times (100/3.6 - v_W)^2$. The results are compared in Table 3.7.

Table 3.7   Air drag forces (N) for Example 3.4.3

Wind speed (km/h)	0	20	30	40
Head wind	359.2	517.2	607.0	704.0
Increase (%)	0	44	69	96
Tail wind	359.2	229.9	176.0	129.3
Decrease (%)	0	36	51	64

3.4.3   Slopes

The gravitational force on a slope will act in opposite directions for uphill and downhill motion of the vehicle. With reference to Figure 3.26 for a slope of angle θ relative to horizontal, the gravitational force simply is:

$$F_G = \pm W \sin\theta \tag{3.34}$$
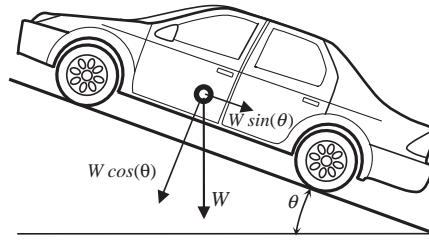
Figure 3.26   Gravitational force

The positive and negative signs are for the downhill and uphill motions respectively. The gravitational force is a constant force as long as the slope is constant.

The slope is often expressed as a percentage rather than an angle. It is the tangent of the angle of the slope multiplied by 100:

$$slope\ (\%) = 100 \times \tan\theta \tag{3.35}$$

It should be noted that in vehicle motion on a slope, the normal reaction force will also change and the rolling resistance force will be altered accordingly:

$$F_{RR} = f_R\ W\ \cos\theta \tag{3.36}$$

3.4.4   Resistance Force Diagrams

The total resistive force is the summation of the rolling resistance, aerodynamic and gravity forces:

$$F_R = F_{RR} + F_A + F_G \tag{3.37}$$

Of these forces, the gravity force is constant and the two others are speed-dependent.

Example 3.4.4

Use the information in Example 3.4.2 and for a vehicle of mass 1200 kg, consider a constant rolling resistance coefficient of 0.02.

(a) Plot the total resistive force for speeds up to 200 km/h at slope of 10% and specify each component.
(b) Plot the total resistive force for slopes of 0, 10, 20, 30, 40 and 50% all in a single figure.

Solution

The results are obtained by making simple use of Equations 3.28, 3.34, 3.36 and 3.37. Plots for (a) and (b) are shown in Figures 3.27 and 3.28.
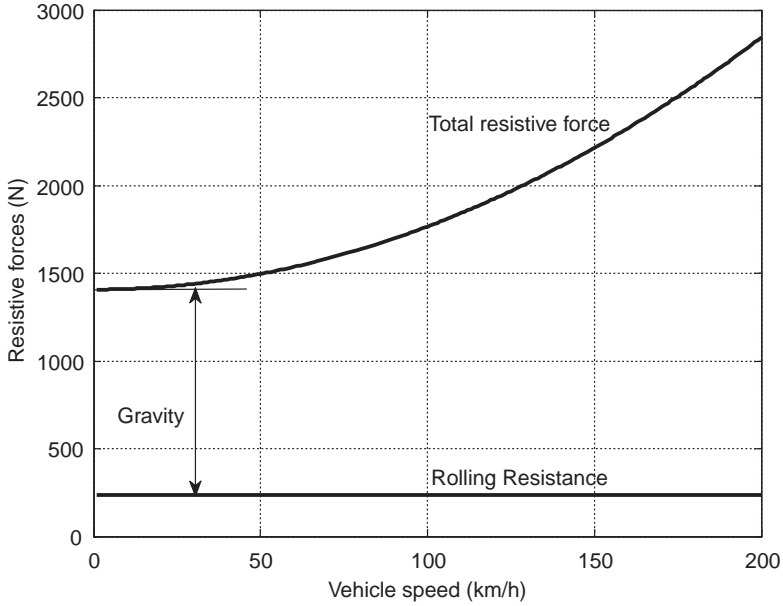
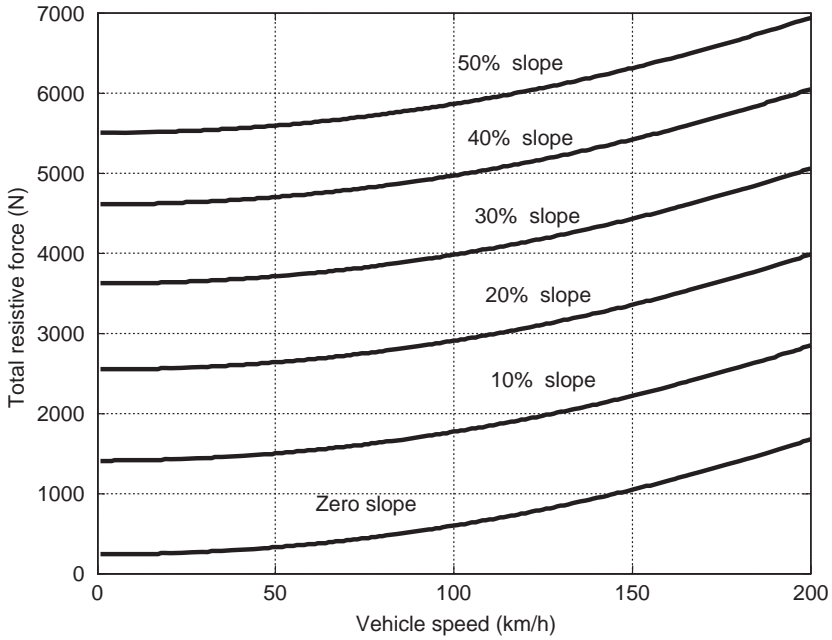**Figure 3.27**   Resistive forces at level road

Figure 3.28   Total resistive force at different slopes

3.4.5   Coast Down Test

A vehicle coast down test is designed to experimentally measure the resistive forces including the rolling resistance (see Section 3.4.1) and aerodynamic drag. In a coast down experiment the vehicle is accelerated up to a high speed and then with the drivetrain disengaged, it is allowed to slow down under the action of the resistive forces. In general, the resistive forces depend on environmental and road conditions (e.g. temperature, wind, road surface and type). Therefore, under standard conditions, usually in still air and on a level road of sufficient length, useful information of vehicle speed variation with elapsed time can be obtained. This information then can be processed in order to estimate the rolling resistance and air resistance forces. Simple methods for the estimation of the resistive forces from speed-time data are discussed in Section 3.12.

3.5   Vehicle Constant Power Performance (CPP)

Modelling the longitudinal performance of a vehicle in general driving conditions is quite complicated when the engine throttle and gearbox ratios vary during motion. Simple models are used in the first instance to facilitate the analysis and understanding of the vehicle performance. One useful approach is to assume that the vehicle uses constant power to accelerate up to its maximum speed, corresponding in practice to full throttle acceleration. Later on it will be revealed that such acceleration is not a constant power motion, nonetheless, the assumption of constant power simplifies the equations of motion initially and provides a simple workable model for rough calculations.

3.5.1   Maximum Power Delivery

There have been arguments about how a power source can deliver maximum power as a function of its rotational speed. We shall examine this by the following mathematical procedure.

Consider a power source with output speed ω that is a function of time t. As shown in Figure 3.29, the output torque T is a function of speed. Therefore:
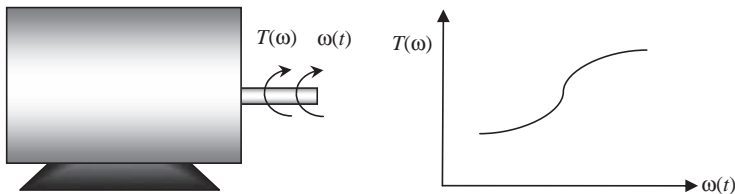
$$P(\omega) = \omega T(\omega) \tag{3.38}$$

In order to obtain maximum power output, we are interested to find a speed at which the power is at maximum. To this end, Equation 3.38 can simply be differentiated with respect to speed ω:

$$\frac{dP}{d\omega} = T(\omega) + \omega \frac{dT}{d\omega} = 0 \tag{3.39}$$

or:

$$\frac{dT}{T(\omega)} = -\frac{d\omega}{\omega} \tag{3.40}$$

Figure 3.29   A power source with output torque characteristics

This is a differential equation that relates the output torque to the speed. Integration of Equation 3.40 results in:

$$\ln T = C - \ln \omega \tag{3.41}$$

where C is the constant of integration. If $C = \ln P_0$ is assumed, then Equation 3.41 can be rewritten as:

$$\ln T = \ln \frac{P_0}{\omega} \tag{3.42}$$

or,

$$P_0 = \omega T(\omega) = P(\omega) \tag{3.43}$$

Equation 3.43 apparently implies that to deliver a maximum power from a source, it must be a constant power P_0. This statement by itself is false, since the power P_0 does not have to be the maximum power and can have different values. So what is wrong with the mathematical approach for the analysis? One must recall that the differentiation as performed in Equation 3.39 was only a necessary condition to obtain the maximum, and to ensure the existence of the maximum, there is also a sufficient condition, namely:

$$\frac{d^2 P}{d\omega^2} < 0 \tag{3.44}$$

In the case of our problem, one can simply show by using Equations 3.39 and 3.40 that:

$$\frac{d^2 P}{d\omega^2} = 0 \tag{3.45}$$

which means this point is not a maximum, nor a minimum, but a critical point. Thus this analytical approach does not lead to any workable conclusion on the way a power source can deliver maximum power. The discussion of this section is aimed at demonstrating that the idea of a constant power delivery does not relate to the maximum power delivery of a power source as is sometimes claimed. The constant power that is considered in the following sections can be any desired value of power.

3.5.2 Continuous Gear-Ratio Assumption

A geared transmission with clutch shifts causes discontinuous torque flow to the wheels and, in turn, delivers discontinuous tractive forces, and hence acceleration. Figure 3.30 shows a typical acceleration time history of a vehicle equipped with a manual transmission. When first gear is engaged, the vehicle accelerates up to a speed at which the engine rotation speed is too high and a gearshift is necessary. During the gearshift from first to second gear, the clutch is first disengaged, gearshifted, and the clutch re-engaged. This process will take some time during which there will be no tractive force available but the resistive forces are still acting on the vehicle. This situation will result in a temporary negative acceleration, as can be seen from Figure 3.30. During other gearshifts the same phenomena will result in discontinuous vehicle accelerations.

We will eventually obtain vehicle performance curves similar to Figure 3.30, but first it is more effective to start with simpler models. The main complexity involved in the general case arises from the gearshift process. One simple and useful assumption is to consider a transmission with continuous gear changing property; in other words, infinite gear ratios and continuous gear ratio changing. This assumption will lead to having a continuous torque flow and corresponding uninterrupted vehicle acceleration.
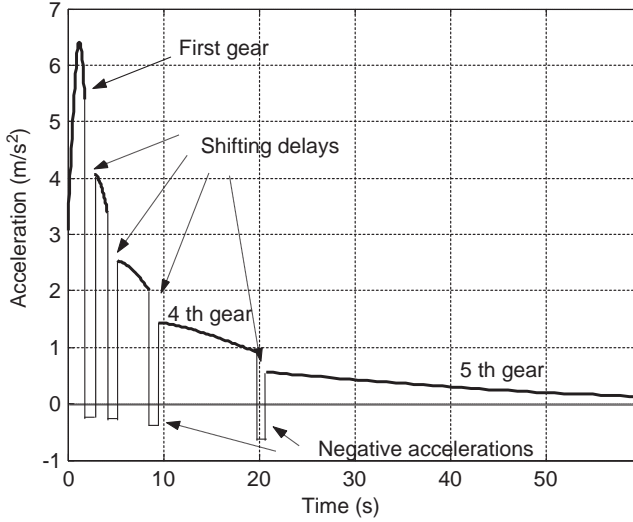
Figure 3.30   Typical time history of vehicle acceleration

The constant power assumption may be considered as a single torque-speed point for the engine. In fact, when the power is unchanged, the optimum operating point for the engine can be chosen at this specific power. This means the engine works at a particular torque and speed values denoted by ω^* and T_e^*. At such a point the engine power P_e is:

$$P_e = T_e \omega_e = T_e^* \omega^* = P^* = cte \tag{3.46}$$

in which T_e^* is engine torque in Nm, and P_e and ω^* are in Watt and rad/s respectively.

At this engine speed, the vehicle moves ahead with an infinitely variable gear ratio and no shift delays. From a simple kinematic relation one can relate the wheel rotational speed ω_w to the engine rotational speed $\omega_e = \omega^*$ by:

$$\omega_w = \frac{\omega^*}{n} \tag{3.47}$$

in which n is the overall vehicle gear ratio, that is the gearbox gear ratio n_g times the differential (final drive) gear ratio n_f, i.e. (see Figure 3.31):

$$n = n_g n_f \tag{3.48}$$

Now if it is further assumed that there is no slip for the driving wheels when they roll on the road surface, with reference to Figure 3.32 it is clear that the vehicle speed can be written as:

$$v = \omega_w r_w = \frac{\omega^* r_w}{n_g n_f} \tag{3.49}$$

where r_w is the effective rolling radius of tyres. Equation 3.49 simply shows that the vehicle speed is inversely proportional to the transmission gear ratio.
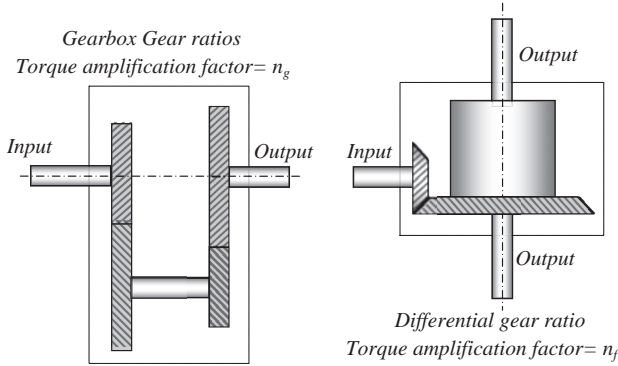
Figure 3.31   Vehicle transmission and final drive gear ratios
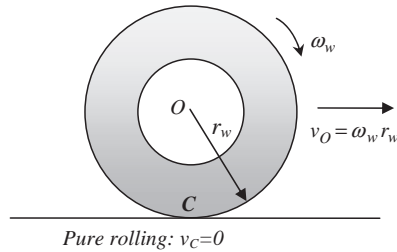
Figure 3.32   The pure rolling of a wheel

It should be noted that the assumption of no slip for the tyre is strictly in conflict with its force-generating mechanism which depends on slip (see Section 3.3.1). Nevertheless, including slip in the analysis will cause difficulties we would like to avoid at this stage.

3.5.3   Governing Equations

The mathematical representation of vehicle motion involves the application of Newton's laws of motion to the vehicle. For our case, the motion of interest involves the longitudinal motion properties including the acceleration, speed and distance travelled. Newton's second law of motion is suitable for this problem of a unidirectional motion of the vehicle centre of mass. In Sections 3.3 and 3.4 the tractive and resistive forces acting on the vehicle were explained. The vehicle motion will be the result of interaction between these forces. The longitudinal vehicle motion involves a multitude of situations with different driving and resistive forces. For a moving vehicle the tractive forces are generated at tyre contact patches. The total tractive force F_T is the sum of individual driven tyre forces. The total power consumed due to the forward motion of vehicle with speed v is:

$$P_v = F_T v \tag{3.50}$$

The power available at the driving wheels is:

$$P_w = T_w \omega_w \tag{3.51}$$

Due to driveline losses we must have:

$$P_v < P_w < P_e = P^*$$ (3.52)

in which P_e is the engine power and it was assumed to remain a constant value P^*. Equation 3.52 indicates that the power generated by the engine is not fully utilized and some part is lost due to friction in the vehicle driveline system. To include this effect we must consider the driveline efficiencies in our equations. In order to simplify the equations of motion, we will ignore this effect for the time being and it will be included later on in Section 3.13. For an ideal driveline with 100% efficiency, all three power values are equal:

$$P_v = P_w = P_e = P^*$$ (3.53)

Therefore P^* is the constant power delivered to the driving wheels and from Equation 3.50:

$$F_T = \frac{P^*}{v} = f(v)$$ (3.54)

This equation shows that the traction force depends only on the forward speed in an inversely proportional fashion. The variation of F_T versus speed in Equation 3.54 at different power outputs is depicted in Figure 3.33.

Note that Equation 3.54 implies that at low vehicle speeds, the tractive force mathematically becomes infinite. In practice, however, the tyre force is dependent on the tyre–road friction coefficient and slip ratio
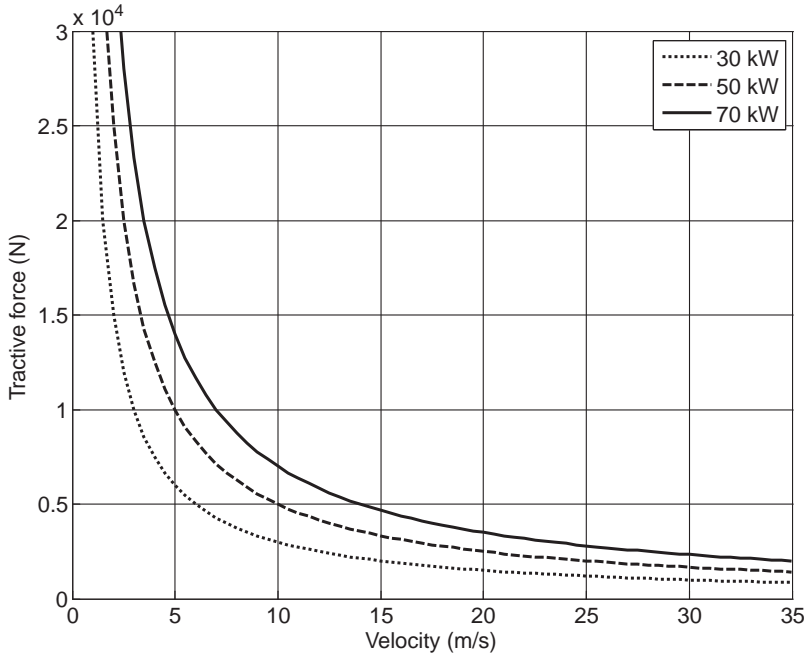
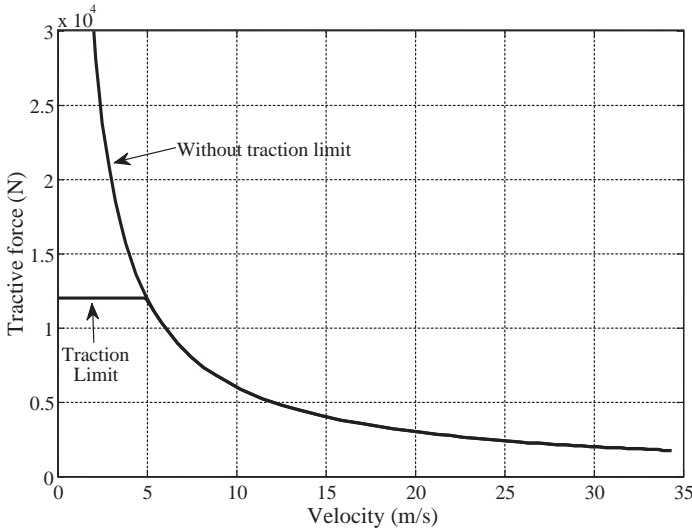**Figure 3.33**   The variation of total tractive force with vehicle speed

Figure 3.34   Tractive force versus speed including tyre traction limit

and there will be a maximum tractive force available for the tyre. If this limit is imposed, the total tractive force-speed diagram will be similar to Figure 3.34.

With this constraint in force, the tractive force will no longer remain uniform and it must be divided into two regions of limit adhesion and constant power. For the sake of simplicity this constraint will also be ignored for the time being and the amount of error induced with this assumption will be examined later in this chapter.

Now Newton's Second Law is applied to the longitudinal motion of vehicle with reference to the free body diagram of the vehicle shown in Figure 3.35. The longitudinal equation of motion simply is:
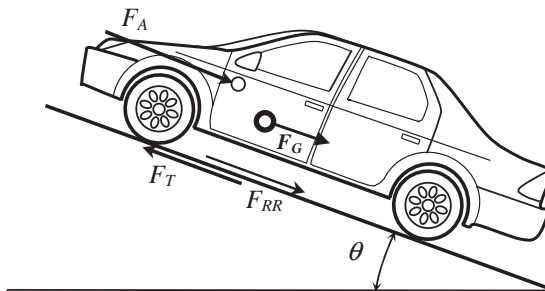
$$F_T - F_R = m\frac{dv}{dt} \tag{3.55}$$

Figure 3.35   Free body diagram of a vehicle

Table 3.8 Assumptions involved in derivation of Equation 3.58

There is a constant power demand from the engine during entire motion
The vehicle gearbox has infinite gear ratios, changing continuously during vehicle motion
The driving wheels roll and there is no slip at road surface
There is no power loss in the vehicle driveline
Tyres can produce very large tractive forces
Rolling resistance force is a constant in all speeds
There is no wind during vehicle motion

with:

$$F_R = F_{RR} + F_A + F_G \tag{3.56}$$

Substituting for the resistive forces F_{RR} (Section 3.4.1), F_A (Section 3.4.2) and F_G (Section 3.4.3), will lead to:

$$F_T - W(f_R \cos \theta + \sin \theta) - 0.5 \rho_A C_D A_F v_A^2 = m \frac{dv}{dt} \tag{3.57}$$

In most elementary performance analyses, a constant rolling resistance coefficient is considered and with this assumption and using Equation 3.54, the final form of the longitudinal equation of motion of the vehicle will be:

$$m \frac{dv}{dt} = \frac{P^*}{v} - F_0 - cv^2 \tag{3.58}$$

where c and F_0 are two constants defined below:

$$c = 0.5 \rho_A C_D A_F \tag{3.59}$$

$$F_0 = W(f_R \cos \theta + \sin \theta) \tag{3.60}$$

It should be noted that in Equation 3.58 the air speed v_A is replaced with the vehicle speed v for conditions of still air with no wind.

Equation 3.58 is an ordinary differential equation in terms of the forward speed v of the vehicle. The time history of vehicle velocity will result from the integration of this equation.

It should be noted that Equation 3.58 was obtained under certain assumptions summarized in Table 3.8.

3.5.4 Closed Form Solution

Equation 3.58 can be rearranged as:

$$dt = \frac{m dv}{\frac{P^*}{v} - F_0 - cv^2} \tag{3.61}$$

Then, integration by separation of variables leads to:

$$t = \int \frac{m dv}{\frac{P^*}{v} - F_0 - cv^2} \tag{3.62}$$

It can be shown that the governing equation of longitudinal vehicle motion will be of the form:

$$t = k_1 \ln \frac{v_m - v}{\sqrt{v^2 + vv_m + a}} + k_2 Arc \tan \frac{2v + v_m}{\sqrt{4a - v_m^2}} + C_t \tag{3.63}$$

in which v_m is the real root of the third order polynomial:

$$cv^3 + F_0 v - P^* = 0 \tag{3.64}$$

C_t in Equation 3.63 is the constant of integration and must be calculated by introducing an initial condition (e.g. at $t = 0$, $v = 0$), and the three constants a, k_1 and k_2 are given below:

$$a = \frac{P^*}{cv_m} \tag{3.65}$$

$$k_1 = -\frac{m}{c} \cdot \frac{v_m}{2v_m^2 + a} \tag{3.66}$$

$$k_2 = -\frac{m}{c\sqrt{4a - v_m^2}} \cdot \frac{2a + v_m^2}{2v_m^2 + a} \tag{3.67}$$

Although Equation 3.63 provides a mathematical solution to the vehicle longitudinal motion, it is in the unusual form of $t = f(v)$ instead of the more useful $v = f(t)$ form. In order to solve for speed vs time, therefore, this non-linear equation must be solved by iteration techniques.

Example 3.5.1

For a vehicle of mass 1000 kg, the rolling resistance coefficient, overall aero-drag coefficient (Equation 3.59) and engine power are 0.02, 0.4 and 60 kW respectively. On a level road, determine the time history of vehicle speed starting at standstill.

Solution

With the given initial condition of starting from rest, the constant of integration is determined. In order to avoid iteration, instead of evaluating speed for a given value of time, with increasing the speed from zero to the maximum speed, the corresponding times can be calculated. The maximum speed is v_m and should be determined by solving Equation 3.64. A MATLAB program is prepared

for this example with listing given in Figure 3.36 and several comments included to make it explanatory. The result is depicted in Figure 3.37.

```
% Example 3.5.1
% Analytical solution of vehicle longitudinal motion

clc              % Clears working space
close all        % Closes previously opened (figure) windows
clear all        % Clears all memories for variables

% Vehicle information:
m=1000;          % Vehicle mass (kg)
c=0.4;           % Aerodynamics overall coefficient
fr=0.02;         % Rolling resistance coefficient
Ps=60000;        % Input power (watts)
theta=0;         % Angle of slope (rad)

% Determine the total constant resistive force:
F0=(fr*cos(theta)+sin(theta))*m*9.81;

% Solution of 3rd order polynomial c*v^3+F0*v-p=0 (Eq. 3.64)
r=Ps/c/2;
q=F0/c/3;
d=sqrt(q^3+r^2);
s1=(r+d)^(1/3);
t1=sign(r-d)*abs(r-d)^(1/3);
vm=s1+t1;        % vm is the real root

% Pre-calculations:
c1=c/m;
a=Ps/c/vm;       % Also a=s1^2+t1^2-s1*t1
c2=vm/(2*vm^2+a);
c3=sqrt(4*a-vm^2);
c4=(vm+2*a/vm)/c3;
k1=-c2/c1;       k2=k1*c4;        % Coefficients of Equation 3.63

% Set initial condition:   @t=0, v=0
t0=0; v0=0;

% Determine the constant of integration:
C=t0-k1*log((vm-v0)/sqrt(v0^2+vm*v0+a))-k2*atan((2*v0+vm)/c3);

for i=1: 200
    v(i)=vm*i/200;
    sq1=sqrt(v(i)^2+vm*v(i)+a);
    t(i)=k1*log((vm-v(i))/sq1)+k2*atan((2*v(i)+vm)/c3)+C;
end

% Plot the variation of speed versus time
plot(t,v)
xlabel('Time (s)')           % Label for time (Horizontal axis)
ylabel('Velocity (m/s)')     % Label for velocity (Vertical axis)
grid                         % Horizontal and vertical grids
```
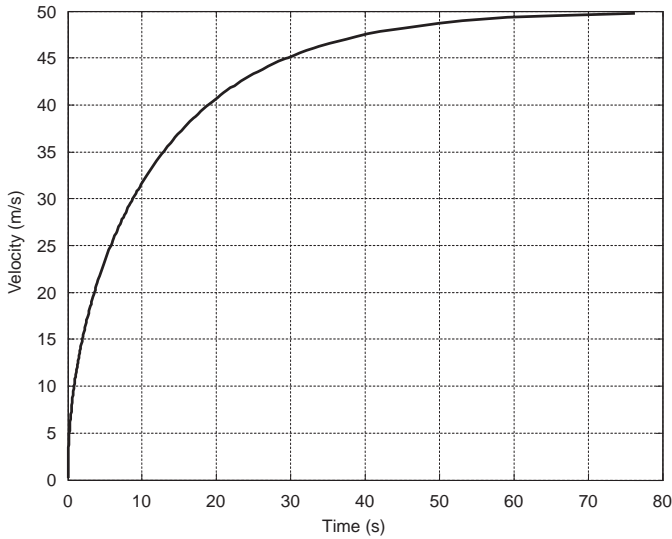
Figure 3.36 MATLAB program listing for Example 3.5.1

Figure 3.37   Variation of speed versus time for Example 3.5.1
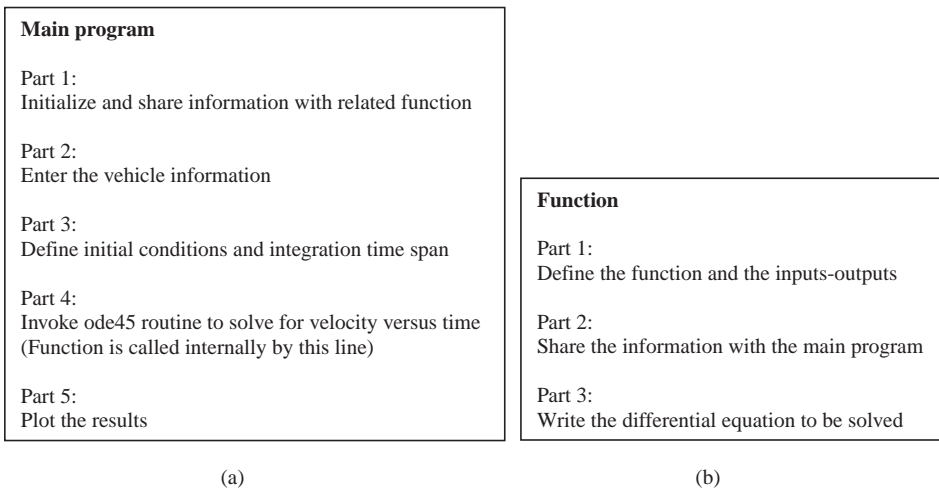
3.5.5   Numerical Solutions

In spite of the availability of a closed form solution for the problem, numerical solutions are often advantageous. Nowadays with the widespread availability of computer software, it is not difficult to set up a program and solve the problem numerically. Equation 3.58 for the vehicle acceleration can be written in the form:
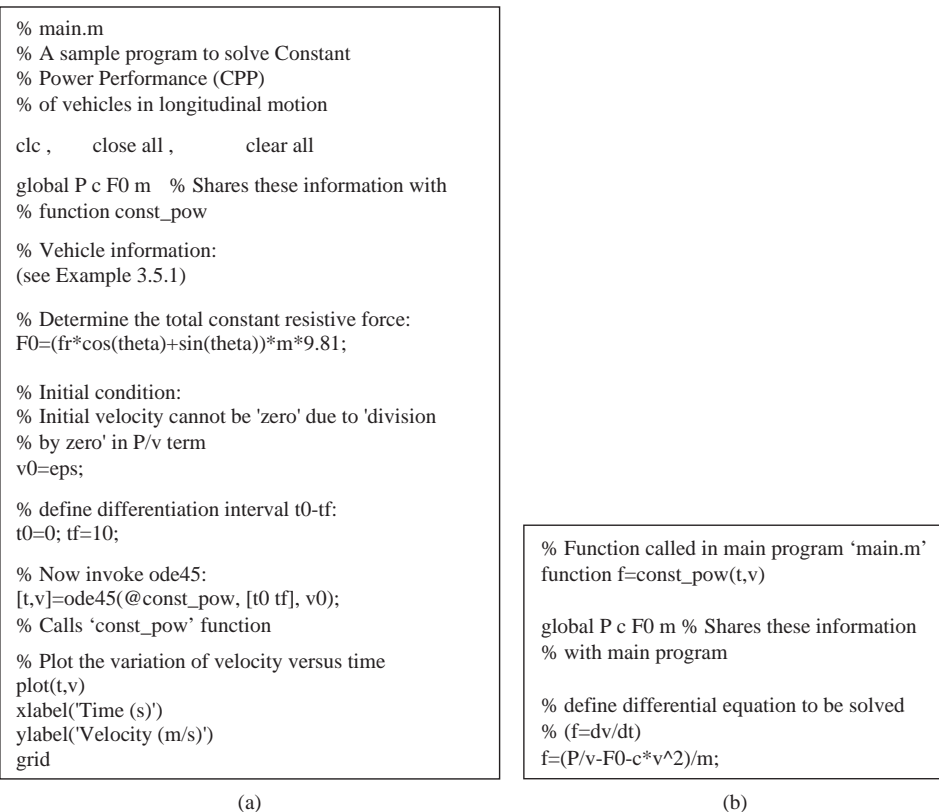
$$\frac{dv}{dt} = \frac{1}{m}\left(\frac{P^*}{v} - F_0 - cv^2\right) \tag{3.68}$$

which is an ordinary first order differential equation for the velocity v and can be integrated numerically by using well established numerical methods such as the Runge-Kutta method. Different software packages provide this routine for programmers and MATLAB is a good example which has a family of functions called 'ode' (standing for Ordinary Differential Equations). One of these functions called '*ode45*' is a medium order method suitable for solving non-stiff differential equations. Using this routine is quite straightforward and will suffice for our case. In order to become familiar with using this function, Figure 3.38 shows two '*m*' files, one as the main program and the other as a function to be called within the main program. As shown in Figure 3.38, the main program consists of five parts, whereas the function consists of three parts. The main program introduces values for the main parameters and sets the initial values (e.g. at time t = 0) for the main variables. MATLAB starts integrating the differential equation given in the separate '*function*', starting from time 't0' and ending at time 'tf'. An internal MATLAB function '*ode*' with input arguments will call the differential equation available in '*function*' and once the integration process is complete, it will return the result. In other words, the user does not have access to the intermediate steps of the integration process.

A detailed program listing for the solution of the differential Equation 3.68 is presented in Figure 3.39. It is worth noting that the values for the parameters are also needed in the '*function*', so one way is to provide the vehicle information inside the '*function*' itself. Another way is to give the information in the main program and then share them with the '*function*' by using '*global*' statement. One more point is to note that the value of dv/dt approaches infinity at v = 0, due to division by zero in p/v term. To avoid this, we can set the initial value of velocity to a very small value close to zero. MATLAB uses a variable called '*eps*' for this purpose (eps = 2.2204e-016).

```
Main program

Part 1:
Initialize and share information with related function

Part 2:
Enter the vehicle information

Part 3:
Define initial conditions and integration time span

Part 4:
Invoke ode45 routine to solve for velocity versus time
(Function is called internally by this line)

Part 5:
Plot the results
```

```
Function

Part 1:
Define the function and the inputs-outputs

Part 2:
Share the information with the main program

Part 3:
Write the differential equation to be solved
```

(a)   (b)

Figure 3.38 Structure of programming for numerical integration by MATLAB: (a) main program and (b) function

```
% main.m
% A sample program to solve Constant
% Power Performance (CPP)
% of vehicles in longitudinal motion

clc ,      close all ,        clear all

global P c F0 m   % Shares these information with
% function const_pow

% Vehicle information:
(see Example 3.5.1)

% Determine the total constant resistive force:
F0=(fr*cos(theta)+sin(theta))*m*9.81;

% Initial condition:
% Initial velocity cannot be 'zero' due to 'division
% by zero' in P/v term
v0=eps;

% define differentiation interval t0-tf:
t0=0; tf=10;

% Now invoke ode45:
[t,v]=ode45(@const_pow, [t0 tf], v0);
% Calls 'const_pow' function

% Plot the variation of velocity versus time
plot(t,v)
xlabel('Time (s)')
ylabel('Velocity (m/s)')
grid
```

```
% Function called in main program 'main.m'
function f=const_pow(t,v)

global P c F0 m % Shares these information
% with main program

% define differential equation to be solved
% (f=dv/dt)
f=(P/v-F0-c*v^2)/m;
```

(a)   (b)

Figure 3.39 MATLAB programs (a) Main program 'main.m' and (b) Function 'const_pow.m'

Example 3.5.2

For the vehicle of Example 3.5.1, use the program of Figure 3.39 and find the variation of vehicle velocity for the first 80 seconds.

Solution

The solution is found by entering the vehicle data into the MATLAB program. The variation of velocity versus time resulting from this program is shown in Figure 3.40. It can be seen the result is similar to that obtained by the closed form solution given in Figure 3.37.
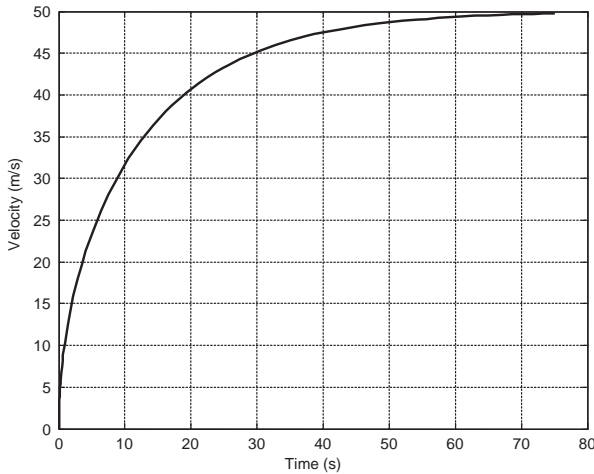
Figure 3.40   The result of numerical solution to Example 3.5.2 using MATLAB

3.5.6   *Power Requirements*

The value of the engine power is one of the first requirements in the initial design stages. With a constant power assumption, one can easily evaluate the power necessary for a specific performance requirement. Very rough estimations can be found by using 'no resistive force' (NRF) model (see Problem 3.3) or 'low speed' (LS) model (see Problem 3.5). For a more accurate power calculation, the general form of the equation of longitudinal motion must be solved.

   In the general case, two approaches can be followed; using the closed form equation or numerical integration. In the first approach, Equation 3.63 is used to obtain the power P for given t and v values. Obviously this must be done by applying a trial and error technique. MATLAB's function '*fsolve*' can be used for this purpose. It finds a solution P^* that satisfies Equation 3.63 for given values of t and v.

It should be noted that to initiate the '*fsolve*' function an initial guess is required. A proper initial value must satisfy $P_s > (kW + cv^2)v$ (see Equation 3.64). The following example shows how to use '*fsolve*' for this problem.

Example 3.5.3

For a vehicle of 1000 kg mass, total rolling resistance force $F_0 = 200$ N and overall aerodynamic coefficient of 0.4, obtain power necessary to reach a speed of 100 km/h during a 10-second acceleration starting from rest.

Solution

The MATLAB program listings used for the solution of this example are given in Figure 3.41. Figure 3.41a is the main program and Figure 3.41b is the function that includes the equation $f(P, t, v) = 0$. The result obtained from this program is P_star = 46,097 W.

```
% Example 3.5.3
% Find a power P to have a desired speed v* at a desired time t*

clc, clear all, close all

global c k m t0 v0 td vd

% Vehicle information:
m=1000;     % Vehicle mass (kg)
c=0.4;      % Aerodynamics overall coefficient
F0=200;     % Rolling resistance force
theta=0;    % Angle of slope (rad)
td=10;      % Desired time (s)
vd=100;     % Desired speed (km/h)
% Initial conditions:   @t=0, v=0
t0=0; v0=0;

vd=vd/3.6;

% Define the coefficient of constant resistive force:
fr=F0/m/9.81;
k=(fr*cos(theta)+sin(theta))*m*9.81;

% Initial guess for P_star:
Ps=(F0+c*vd^2)*vd+1;
% Invoke 'fsolve' for function 'f_353'
P_star=fsolve(@f_353, Ps, optimset('Display','off'))
```

(a)

Figure 3.41 MATLAB programs (a) Main and (b) Function for Example 3.5.3

```
function f=f_353(Ps)

global c k m t0 v0 td vd

% Solution of 3rd order polynomial c*v^3+k*W*v-p=0
See Example 3.5.1

% Pre-calculations:
See Example 3.5.1

% Determine the constant of integration:
sq1=sqrt(v0^2+vm*v0+a);
C=t0-k1*log((vm-v0)/sq1)-k2*atan((2*v0+vm)/c3);
sq1=sqrt(vd^2+vm*vd+a);
f=k1*log((vm-vd)/sq1)+k2*atan((2*vd+vm)/c3)+C-td;
```

(b)

Figure 3.41 (*Continued*)

Alternatively, the equation of motion (Equation 3.68) can be solved by the numerical integration, but as observed in Section 3.6.5 the solution requires the power as an input. In fact, the process examined earlier was to obtain the speed values from a given power value. Here, the process is reversed as the power P is needed for a required speed v^* at a specified time t^*. Thus in order to calculate the power, an iteration loop must be performed in the numerical integration process. The result in one iteration process will be a value v_1 for speed at time t^*; if v_1 happens to be equal to the specified speed v^*, then the given power P is the answer. Otherwise P must be modified until the speed obtained from iteration process equals v^*.

Example 3.5.4

Repeat Example 3.5.3 by using the numerical integration method of Section 3.5.5.

Solution

The MATLAB program of Section 3.5.5 can be modified to include the iteration loop. MATLAB command '*while*' can be used for this purpose. The program will repeat the instructions inside the loop until the condition in the '*while*' statement is not satisfied. The modified program is shown in Figure 3.42.

The output result of this program is printed as:

$$\text{maxv} = 27.7768 \ (\sim 100 \, \text{km/h})$$
$$P = 4.6022e + 004 \ (46,022 \, \text{w})$$

```
% Example 3.5.4
% Power estimation using numerical integration technique based on Figure 3.39

% Vehicle information:
See Example 3.5.3

v0=eps;           % Initial condition
t0=0; tf=10;      % define differentiation interval t0-tf

% Initial value for Power:
Ps=(F0+c*vd^2)*vd+1;

% Iteration loop:
maxv=0;
% Continue iteration until the speed is very close to desired value 'vd'

while abs(maxv-vd) > 0.001 % The answer is acceptable within a small tolerance

% Now invoke ode45:
  [t,v]=ode45(@const_pow, [t0 tf], v0);   % Calls 'const_pow' function

  maxv=max(v);
% Check for velocity:
  if maxv < vd    % then increase power to increase velocity
     P=P*vd/maxv;
  else   % decrease power (with a different rate) to decrease velocity
     P=0.9*P*maxv/vd;
  end
end
% At this point results are acceptable, so print them:
maxv, P
```

Figure 3.42   MATLAB program for power calculation of Example 3.5.4

3.5.7   Time of Travel and Distance

Two important parameters in the vehicle motion are the time duration and the distance the vehicle travels during that time. In this section the equations of motion will be used to find these two parameters. The required time to achieve a specified speed can simply be determined by the direct use of the result of the closed form solution given in Equation 3.63. Alternatively, the numerical integration method can also be used to obtain this time value but the process needs a 'while' loop. In fact, the travel time was already obtained from the numerical integration of the equation of motion. The integration methods advance the time by small steps to the final integration time t_f that is the vehicle's total travel time at the end of the integration process. In other words, in such processes the time is pre-selected and velocity is calculated at the end of that specified period. In the numerical method, therefore, the travel time at a desired speed can be obtained from the time history of motion that is in the form of vehicle speed versus time. Alternatively by using a 'while' statement, the time can be obtained directly. For the determination of the travelled distance S, the following relation can be used:

$$v \, dv = a \, dS \tag{3.69}$$

and after substituting from Equation 3.58, one obtains:

$$dS = \frac{mvdv}{\frac{P^*}{v} - F_0 - cv^2}$$

(3.70)

which is similar to Equation 3.61 and can be integrated similarly. The result reads:

$$S = v_m k_1 \ln(v_m - v)\sqrt{v^2 + vv_m + a} + \frac{a}{v_m} k_1 \ln\sqrt{v^2 + vv_m + a} + k_3 Arc\tan\frac{2v + v_m}{\sqrt{4a - v_m^2}} + C_S$$

(3.71)

with:

$$k_3 = -\frac{v_m^2 - a}{\sqrt{4a - v_m^2}} \cdot k_1$$

(3.72)

and C_S is the constant of integration. Alternatively, to calculate the distance of travel using numerical integration, instead of using the approach of Equation 3.69, it is recalled that velocity is the derivative of travelled distance, that is:

$$\frac{ds}{dt} = v(t)$$

(3.73)

This adds another ordinary differential equation to the one existing before for the velocity (i.e. Equation 3.68). For the numerical integration, the number of differential equations does not make any difference, in fact, the procedure of numerical solution is similar when a set of differential equations are present. In the MATLAB program of Section 3.5.5, only a few changes listed below are necessary:

(a) The two variables must be put together in a single raw matrix (array). Let this array be called x. Then x includes two variables v and S:

$$x = [v \ S]$$

(3.74)

Throughout the program v should be replaced with x.

(b) An initial condition must be given for the vector x. For instance, if the motion is started from the rest at origin, then:

$$x_0 = [eps \ 0]$$

(3.75)

(c) In the separate function file, the additional differential equation has to be included (i.e. Equation 3.73).

(d) To plot the results, the command 'plot(t, x)' plots both variables in one single figure. In order to separate the two plots one must specify how to plot the results.

Changes necessary to the program of Section 3.5.5 are listed in Figure 3.43.

```
% Changes to main.m to include 'Distance'

% Initial condition:
x0=[eps 0];

% Now invoke ode45:
[t,x]=ode45(@const_pow, [t0 tf], x0);    % Note that x replaces v

% To plot the variation of velocity versus time:
% First define which part of x is velocity:
v=x(:, 1);
plot(t,v)
% Or alternatively: plot(t, x(:, 1))

% To plot the variation of distance versus time:
s=x(:, 2);
plot(t,s)
% Or alternatively: plot(t, x(:,2))
```

```
% Necessary changes to the function
function f=const_pow(t,x)          % x replaces v

% Define differential equations to be solved (f=dx/dt).
% x is a vector, so f must be vector too
% Define v:
v=x(1);
f1=(p/v-f0-c*v^2)/m;
f2=v;
% f must be a column vector, so:
f=[f1
   f2];
```

Figure 3.43   Changes required to the MATLAB program of Figure 3.39

Example 3.5.5

For the vehicle of Example 3.5.1, when starting to accelerate from standstill, find:

(a) the time of travel;
(b) the distance travelled when the speed is 100 km/h.

Use both closed form and numerical integration methods.

Solution

(a) By direct evaluation of Equation 3.63 with the data of Example 3.5.1 the time value of 7.326 s is obtained for the closed form solution. For the numerical method, the result of Example 3.5.2 can be used and at the speed of 27.78 m/s the time can be read from Figure 3.40. In the MATLAB

environment by 'zooming in' around the specified speed, (or by using the data cursor in the figure window) the value of time is obtained as 7.328 s. For a direct solution using the numerical integration, a 'while' statement could be used as was shown in Example 3.5.4 but this time to obtain 't' instead of 'P'. The 'check for velocity' segment in the program is changed to:

    if maxv < vd % then increase time of integration to increase velocity
    tf=tf*vd/maxv;
    else % decrease time (with a different rate) to decrease velocity
    tf=0.8*tf*maxv/vd;
    end

and the result is obtained as:

$$tf = 7.326 \text{ s at } maxv = 27.7771 \ (\sim 100 \text{ km/h})$$

(b) A similar approach used in (a) for the time is also applicable for the distance. To obtain the solution by the closed form method for the distance travelled, Equation 3.71 results in 139.02 m.

   The numerical solution using program listings of Figure 3.43 produces the time histories of speed and distance depicted in Figure 3.44. At a speed of 100 km/h the travel distance can be read approximately. By zooming in the figure, (or by using the data cursor in the figure window) the value is 139 m. Alternatively, the 'while' loop given above can also be used to obtain the distance. In fact, the distance and time are produced simultaneously. The result is 139.01 m.
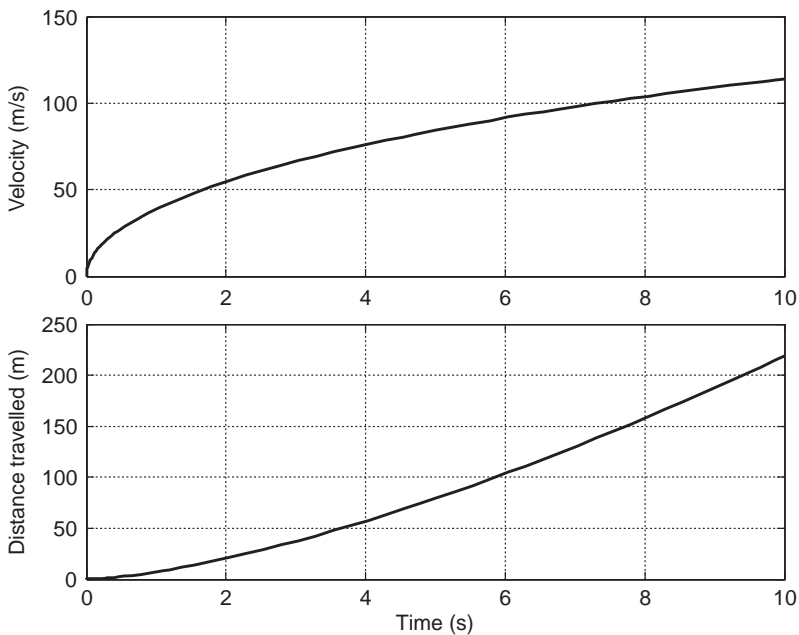
Figure 3.44   Results obtained from the MATLAB program with changes specified in Figure 3.43

3.5.8   Maximum Speed

The maximum speed of vehicle is one of the important factors in the performance analysis. The acceleration of the vehicle shows the increase of the vehicle speed vs time. The maximum speed will occur when the resistive forces equal the tractive force available. Mathematically this means:

$$\frac{dv}{dt} = 0 \tag{3.76}$$

This also means a steady-state condition for the vehicle motion. From the equation of motion of the vehicle, it is clear for such a condition that:

$$F_T(t^*) - F_R(t^*) = 0 \tag{3.77}$$

Since both tractive force F_T and resistive force F_R are changing by the time, there will be an instant t^* in which both forces attain equal values. At this instant the vehicle speed will reach its maximum. If the variation of tractive and resistive forces is drawn in a single figure, the intersection point will indicate the instant t^*. The tractive and resistive forces are functions of velocity v, so a diagram can be constructed for the variation of the forces against velocity. The tractive force for CPP was given in Equation 3.54:

$$F_T(v) = \frac{P^*}{v} \tag{3.78}$$

and the resistive force $F_R(v)$ depends on the assumptions made for the rolling resistance force. For a constant rolling resistance force $f_0 W$ (see Section 3.4.1.5), Figure 3.45 shows the variation of the tractive and resistive forces in a single diagram. The maximum speed of the vehicle is reached where the two forces balance each other. This point is the intersection point of $F_T(v)$ with $F_R(v)$. For the specific condition shown in Figure 3.45, the maximum speed is reached exactly at 50 m/s (180 km/h).
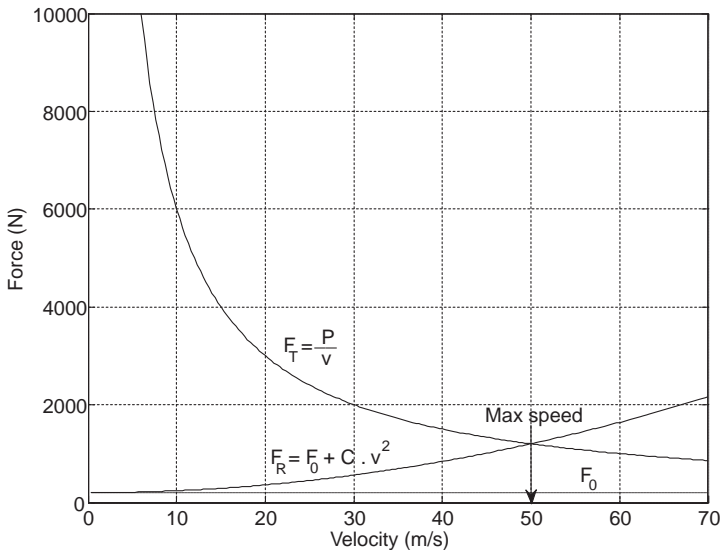
Figure 3.45   The intersection point of tractive and resistive forces gives the maximum speed

To obtain the maximum speed of the vehicle a mathematical solution can also be obtained from Equation 3.77 after substituting the relevant terms for the tractive and resistive forces:

$$\frac{P^*}{v} = F_0 + cv^2 \tag{3.79}$$

A closed form solution for Equation 3.79 is in the following form:

$$v_{\max} = e + h \tag{3.80}$$

in which:

$$e = (a+d)^{\frac{1}{3}} \tag{3.81}$$

$$h = \text{sgn}(a-d)|a-d|^{\frac{1}{3}} \tag{3.82}$$

$$a = \frac{P^*}{2c} \tag{3.83}$$

$$b = \frac{F_0}{3c} \tag{3.84}$$

$$d = (a^2 + b^3)^{0.5} \tag{3.85}$$

Alternatively, Equation 3.79 can be solved numerically using MATLAB functions '*fsolve*' or '*roots*'. The following example will use both methods.

Example 3.5.6

For a vehicle with engine power of 60 kW, constant rolling resistance force of 200 N and overall aerodynamic force coefficient of 0.4, determine the maximum speed:

(a) Use Equation 3.80.
(b) Use MATLAB's '*fsolve*' function.

Solution

In a MATLAB program shown in Figure 3.46, both methods are used one after the other. Both will display 50 m/s for the maximum speed.

```
% MATLAB program to determine Max speed for CPP

Ps=60000;          % power in watts
f0=200;            % rolling resistance force (N)
c=0.4              % total aero force coefficient

%  Case (a): Use Equation 10:
a=Ps/c/2;
b=f0/c/3;
d=sqrt(b^3+a^2);
e=(a+d)^(1/3)
amd=a-d;
h=sign(amd)*abs(amd)^(1/3)
vmax1=e+h

% Case (b): Use MATLAB function 'fsolve'
% define in-line function:
fun=inline('60000-200*v-0.4*v^3', 'v');
%  Initial guess for 'v', v0
v0=20;
vmax2=fsolve(fun, v0, optimset('Display','off'))
```

Figure 3.46   MATLAB program to solve for vehicle maximum speed

3.6   Constant Torque Performance (CTP)

In the previous section we discussed a simplified longitudinal acceleration performance of the vehicle. The major assumption was to consider a constant power demand from the vehicle during the entire motion. This was to simulate a constant load (including the full load) acceleration in which the vehicle is assumed to demand fixed power. In practice, the power demand of the vehicle, however, depends on the torque-speed combination during the acceleration. It is, therefore, necessary to take into the consideration the torque generator's characteristics as well as the vehicle parameters.

There are circumstances in which the torque of the power source is almost constant. Two examples are electric traction motors in their constant torque phase of operation (see Figure 3.4) and modern diesel engines (see Figure 3.3) in their flat torque area. For such cases, the power is not constant and the foregoing discussion cannot be used. Another difference for the constant torque case is the effect of the gearshifts that take place during the acceleration. With a constant torque T from the power source, the tractive force F_{Ti} of the vehicle in a specified gear ratio n_i is a constant:

$$F_{Ti} = \frac{n_i}{r_w} T = cte \qquad (3.86)$$

in which n_i and r_w are the overall gear ratio and the wheel effective radius respectively. At any speed, the resistive force is known and the difference between the tractive and resistive force will generate the acceleration $a(v)$:

$$a(v) = \frac{dv}{dt} = \frac{1}{m}\left(F_{Ti} - F_0 - cv^2\right) \qquad (3.87)$$

The implication from Equation 3.87 is that any gearshift will change F_{Ti} and in turn the acceleration.

3.6.1 Closed Form Solution

In order to find the velocity, Equation 3.87 should be integrated with respect to time. In differential equation form:

$$\frac{dv}{F_{Ti} - F_0 - cv^2} = \frac{dt}{m} \tag{3.88}$$

This is a differential equation that can be integrated by the separation of variables. The closed form solution of Equation 3.88 is of the form:

$$v(t) = \beta \tanh\left(\frac{\beta c}{m}(t - t_0) + \phi_0\right), \quad \beta > 0 \tag{3.89}$$

where:

$$\beta = \sqrt{\frac{F_{Ti} - F_0}{c}} \tag{3.90}$$

$$\phi_0 = \tanh^{-1}\frac{v_0}{\beta} \tag{3.91}$$

The time to reach a specified speed v can be obtained from following relation:

$$t = t_0 + \frac{m}{\beta c}\left(\tanh^{-1}\frac{v}{\beta} - \phi_0\right) \tag{3.92}$$

The travelled distance S, in terms of vehicle speed is given by:

$$S = S_0 + \frac{m}{c}\left(\ln\sqrt{\frac{\beta^2 - v_0^2}{\beta^2 - v^2}}\right) \tag{3.93}$$

In order to apply the results to the motion of a vehicle with a number of gears, consider that the torque-speed diagram of the power source is as shown in Figure 3.47. Let us assume that the vehicle accelerates
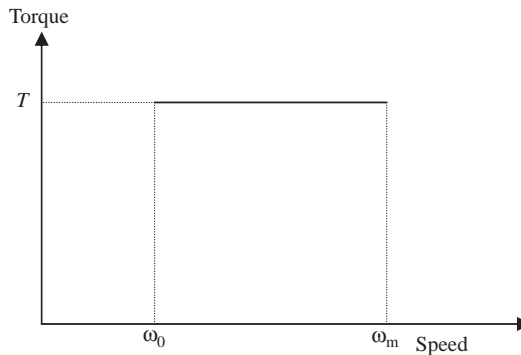
Figure 3.47 Torque-speed diagram of a constant torque power source

up to the speed of ω_m at each gear. In other words, when in first gear the rotational speed reaches ω_m, the gear is shifted to gear 2. The same applies for the 2–3 gear and so on.

The maximum speed at each low and middle gear is when the engine rotational speed is ω_m:

$$v_{\text{max}_i} = \frac{r_w}{n_i}\omega_m \tag{3.94}$$

But this situation for high gears can only happen if the balance of forces is also consistent. The force balance for a high gear n_H is:

$$F_T - F_R(v) = \frac{n_H}{r_w}T - F_0 - cv^2 = 0 \tag{3.95}$$

which results in:

$$v_{\text{max}} = \left[\frac{1}{c}\left(\frac{n_H}{r_w}T - F_0\right)\right]^{0.5} \tag{3.96}$$

This result according to Equation 3.90 is simply equal to β and is only valid if the associated engine speed is less than the maximum speed. Therefore the smaller of results obtained from Equation 3.94 and the value of β must be used. The travel time for each gear is calculated from Equation 3.92, noting that:

$$t_0 = t_{i-1} \tag{3.97}$$

The total travel time at the end of gear number N (to reach ω_m) is:

$$t = \sum_{i=1}^{N} t_i \tag{3.98}$$

A similar approach must be used for the vehicle speed and travel distance at the end of gear number N.

The maximum power for each gear is:

$$P_{\text{max}i} = F_{\text{T}i}v_{\text{max}i} \tag{3.99}$$

With the assumption of no power loss in the driveline, the maximum power for all gears at the maximum speed will be equal, as the power at the maximum speed points is:

$$P_{\text{max}} = T\omega_m \tag{3.100}$$

If the maximum speed at a particular gear is less than the maximum speed ω_m, the actual speed must be used in Equation 3.100.

Example 3.6.1

A diesel engine produces a constant torque of 220 Nm from 1200 to 2800 rpm. A vehicle of mass 2000 kg, with tyre rolling radius of 0.3 m, rolling resistance coefficient 0.02 and overall aero coefficient of 0.5, accelerates on a level road from the rest in its lowest gear with overall ratio of 20 and then shifts successively up to gear 4 with overall ratio of 5. Each successive gear ratio is 0.63 times the previous gear ratio.

In reality, the clutch slip at gear 1 allows the engine speed to differ from corresponding values of the vehicle speed. For the sake of simplicity, however, assume the engine speed at gear 1 can start from zero.

1. Calculate the speeds and travel distances at the end of constant torque curve and the times when these speeds are reached.
2. Plot the variations of engine speed, vehicle acceleration, speed and distance with time.

Solution

A MATLAB program facilitates the solution and with straightforward steps the required outputs can be obtained. The program listing is given in Figure 3.48.

```
% Example 3.6.1

clc, close all, clear all

m=2000;    % Vehicle mass (kg)
fR=0.02;   % Rolling resistance coefficient
Ca=0.5;    % Overall aerodynamic coefficient
rW=0.3;    % Wheel effective radius (m)
nf=4.0;    % Final drive ratio
Tm=220;    % Constant torque (Nm)
wm=1200;   % Minimum engine speed (rpm)
wM=2800;   % Maximum engine speed (rpm)

n_g=[5.0 3.15 1.985 1.25];   % Transmission ratios 1-4
n=n_g*nf;                    % Overall gear ratios
F0=m*9.81*fR;
t0=0; v0=0; s0=0;   % Initial conditions
wmin(1)=0;      % Assume the engine speed can start from zero in gear 1

for i=1: 4    % Loop for gears
   FT(i)=n(i)*Tm/rW;          % Traction force of each gear
   b=sqrt((FT(i)-F0)/Ca);       % Equation 3.90
   phi0=atanh(v0/b);           % Equation 3.91
   vmax(i)=min(wM*rW*pi/n(i)/30, b);                % Maximum  speed of each gear
   tmax(i)=t0+m*(atanh(vmax(i)/b)-phi0)/b/Ca;        % Maximum time of each gear
   smax(i)=s0+m*log(sqrt((b^2-v0^2)/(b^2-vmax(i)^2)))/Ca; % Maximum distance at each gear
   if i<4, wmin(i+1)=30*vmax(i)*n(i+1)/rW/pi; end % Minimum engine speed at next gear

for j=1: 100       % Start the loop for 100 intermediate points at each gear
   w(j, i)=wmin(i)+(j-1)*(wM-wmin(i))/99;  % Divide the speed span into 100 segments
   t(j, i)=t0+(j-1)*(tmax(i)-t0)/99;          % Divide the time span into 100 segments
   v(j, i)=min(b*tanh(b*Ca*(t(j, i)-t0)/m+phi0), b); % values for velocity at each gear
   a(j, i)=(FT(i)-F0-Ca*v(j,i)^2)/m;       % values for acceleration at each gear
   s(j, i)=s0+m*log(sqrt((b^2-v0^2)/(b^2-v(j, i)^2)))/Ca; % values for distance at each gear
end
   t0=tmax(i);   v0=vmax(i);    s0=smax(i); % Set initial conditions for next gear
   % In order to have continuous plots of acceleration and engine speed:
   if i>1, a(1, i)=a(100, i-1); w(1, i)=w(100, i-1); end
```

Figure 3.48 The MATLAB listing of Example 3.6.1

```
    % Plot the results:
    figure (1)
    plot(t(:,i), w(:,i))
    hold on
    grid on
    xlabel('Time (s)')
    ylabel('Engine speed (rpm)')
% repeat plot statements for other variables
    end
```

Figure 3.48   (*Continued*)

(a) Solution to this part is performed in the first loop of program for each gear. At first, the vehicle maximum speed at each gear is calculated as the minimum of kinematic relation (Equation 3.94) and β. These values are then used to determine the time values and distances travelled at the end of each gear engagement phase. The results for time, velocity and distance at the end of each gear are:

Time (s):	0.6164	1.2014	2.7221	6.8327
Velocity (m/s):	4.3982	6.9813	11.0787	17.5929
Distance (m):	1.3557	4.6844	18.4198	77.4139

(b) Once the minimum and maximum of each variable are available, the intermediate points can be determined in a second loop. The loop is designed to calculate 100 points for each variable. The results are plotted in Figures 3.49–3.52
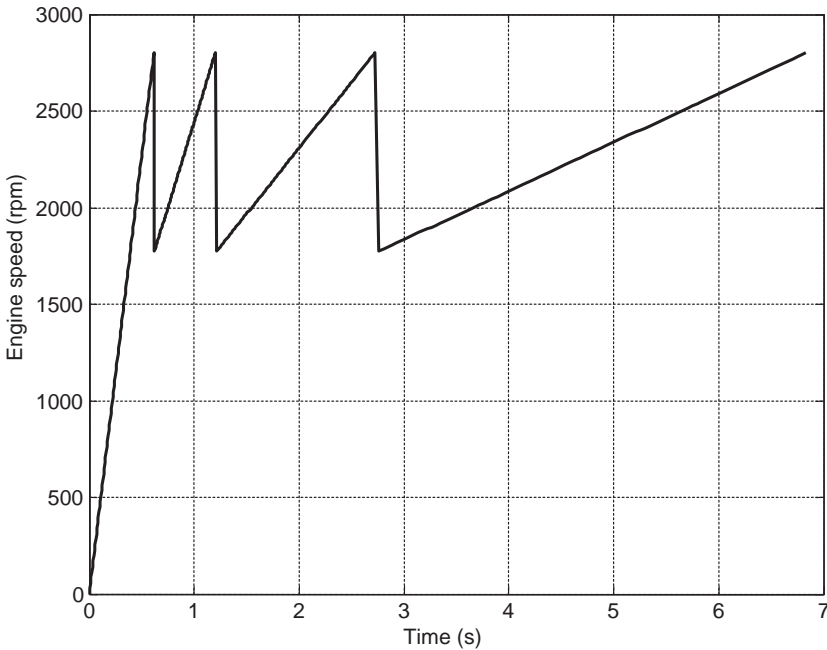
Figure 3.49   Variation of engine speed
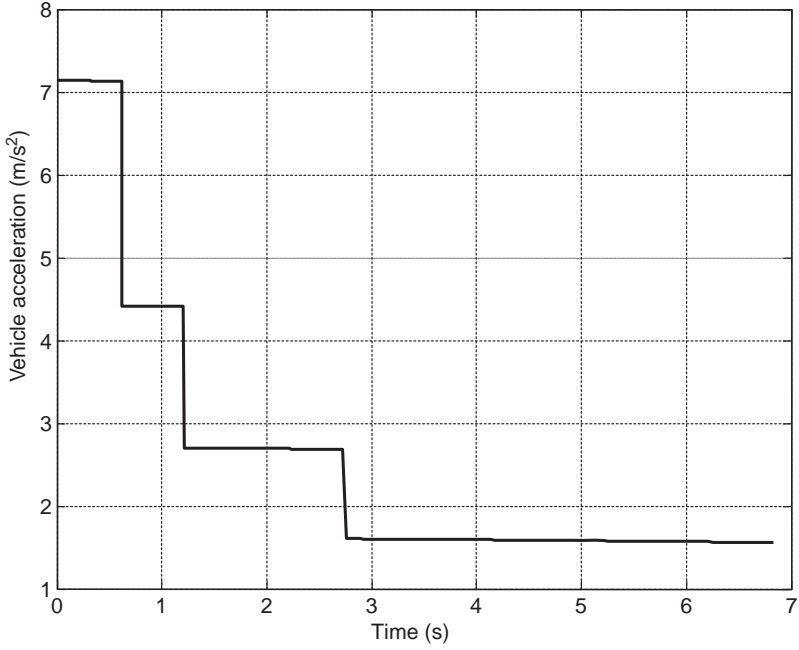
Figure 3.50   Variation of vehicle acceleration
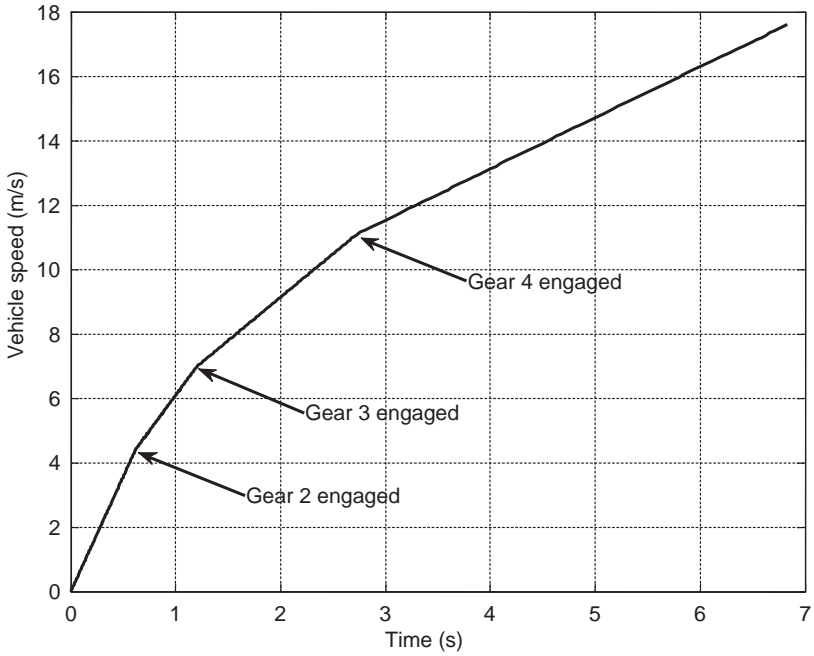
Figure 3.51   Variation of vehicle speed
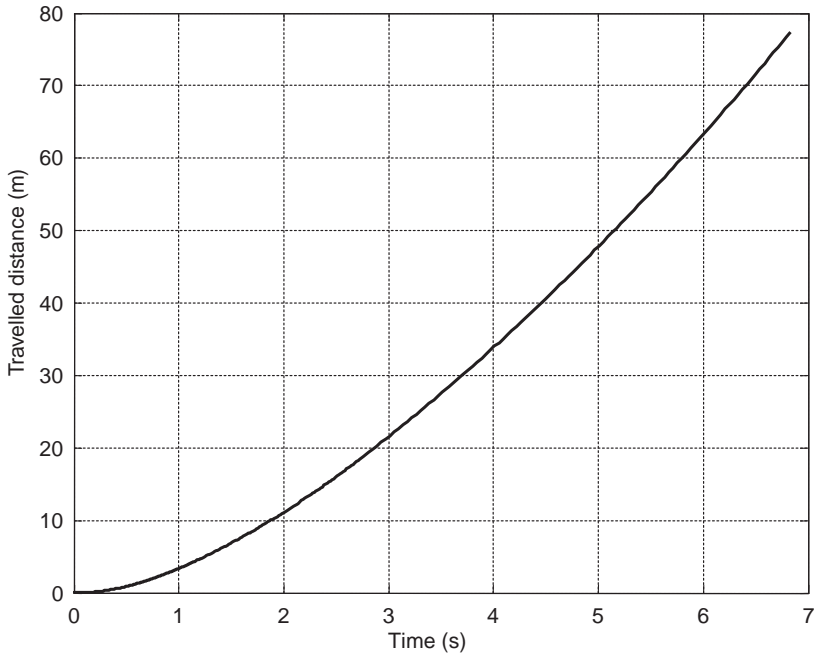
Figure 3.52 Variation of vehicle travelled distance

From Figure 3.50 it can clearly be seen that the acceleration at each gear is almost constant and the variation of velocity is almost perfectly linear. This is due to the low velocity regime in which the aerodynamic force does not play an important role.

3.6.2   Numerical Solutions

For the constant torque equation of motion 3.87, a closed form solution was presented in the previous section. In order to obtain a numerical solution, the method of Section 3.5.5 can be applied with some modifications. The main difference in this case is that the integration must take place at each gear separately. To this end the process for each gear must be repeated, thus there should be a loop with repetition up to the number of gears. The initial conditions at each gear (except gear 1) will be the final results at the previous gear. Another issue in this case is the need for iteration to find the time at which a gear is engaged. This is because the integration at each gear is taking place between two specified times t_0 and t_f. However, the final integration time t_f is related to the maximum speed of the constant torque phase.

A sample MATLAB program is provided in Figure 3.53 in which a loop is considered for four gears ($i = 1: 4$), and the iteration loop is done within a '*while-end*' statement. The function associated with the main program contains the differential equation 3.87. In practice, gearshifts will take some time; nevertheless no delay for gearshifts is included in the program in this case. It would only require a simple modification to include it.

```
% main_t.m
% A sample program to solve Constant Torque Performance (CTP)
% of vehicle in longitudinal motion
% The output of this program is vehicle speed versus time of travel
clc
close all
clear all

global Fti c f0 m          % Fti is traction force at each gear i

% Vehicle information: See Example 3.6.1

f0=fr*m*9.81;
% Initial condition:
v0=eps;
t0=0; tf=10;

we=3000;        % An input larger than wM (for 'while' statement)

for i=1: 4      % For 4 gears
   ni=n(i);
   Fti=Trq*ni/rw;  % Tractive force at gear n(i)

   while abs(we - wM) > 0.001
      [t,v]=ode45(@const_trq, [t0 tf], v0);   % Calls const_trq function
      % Check for rpm at the end of integration
      we=30*ni*max(v)/rw/pi;
      if we>wM           % Not allowed
         tf=tf*wM/we;    % Decrease integration time
      end
   end
   % At this point 'we' is almost equal to 'wM'
   plot(t,v)
   hold on
% Repeat the loop for other gears with following initial conditions:
we=3000;
t0=max(t);
tf=20;
v0=v(end);
end

xlabel('Time (s)')
ylabel('Velocity (m/s)')
grid
```

```
% Function called in program 'main_t.m'
function f=const_trq(t,v)

global Fti c f0 m

f=(Fti-f0-c*v^2)/m;
```

Figure 3.53   MATLAB programs main_t.m and const_trq.m function

Example 3.6.2

For the vehicle of Example 3.6.1, use the numerical integration technique and plot the variation of velocity versus time with successive gearshifts.

Solution

The result of the inclusion of the vehicle data and running the program is illustrated in Figure 3.54. It is identical to Figure 3.51 that was obtained using closed form formulas.
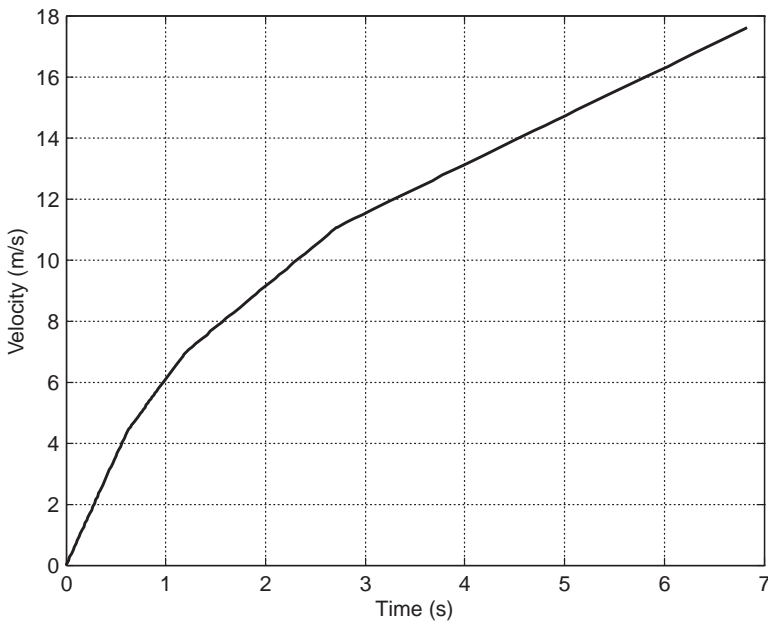
Figure 3.54   The variation of vehicle speed with time

3.7   Fixed Throttle Performance (FTP)

The general longitudinal motion of a vehicle involves the driver's throttle inputs and gearshifts, both of which will have influential effects on the overall performance of the vehicle. Taking into consideration the different inputs from the driver requires a more complicated analysis. One special case in driving already discussed is the full throttle acceleration. In this particular case, the torque-speed characteristics of the engine are usually available and can be used in the analysis. An extension to this case is the fixed throttle acceleration in which instead of 100% throttle input, a fixed part throttle is the input from the driver.
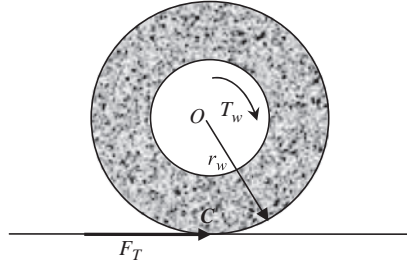
Figure 3.55   The driving wheel

3.7.1   Gearshift and Traction Force

When the throttle is fixed, the quasi-steady engine torque-speed diagram is available and from the MT engine formula (Section 2.6), the part throttle torque-speed relation can be obtained. Full throttle acceleration will be a special case for the analysis and of course, the full throttle curve is usually available for most engines, and analysis can be performed more easily for this case. The engine torque at a constant throttle can be written as:

$$T_e = T_e(\omega_e) \tag{3.101}$$

Assuming no driveline losses (see Section 3.13), the torque at the driving wheels is:

$$T_w = n_g n_f T_e(\omega_e) \tag{3.102}$$

where n_g and n_f are the transmission and final drive gear ratios. According to the free body diagram of the driving wheel shown in Figure 3.55, the tractive force is related to the wheel torque by ignoring the wheel rotational dynamics (Section 3.10):

$$F_T = \frac{T_w}{r_w} = \frac{nT_e(\omega_e)}{r_w} \tag{3.103}$$

This tractive force must be produced by the tyre through the generation of slip between the tyre and the road, provided that sufficient friction is present at the surface. For the time being it will be assumed that the tyre is able to generate the necessary tractive force.

In a certain gear, the tractive force will change according to Equation 3.103 with the engine's rotational speed. With the kinematic relation between the engine speed and the wheel rotational speed, the tractive force at each gear can be related to the wheel rotational speed. A no-slip approximation is considered for the tyre rotation in order to directly relate the forward speed of the wheel centre v to its rotational speed by the simple relation:

$$v = r_w \omega_w = r_w \frac{\omega_e}{n} \tag{3.104}$$

or,

$$\omega_e = \frac{n}{r_w} v \tag{3.105}$$

Therefore, the tractive force at each gear can be directly related to the forward speed of the wheel that is equal to the forward speed of vehicle when no slip is present. At different gear ratios, by using Equations 3.103 and 3.104, different tractive force-speed diagrams can be constructed.

Example 3.7.1

The gear ratios for a five-speed transmission are 4, 2.6, 1.7, 1.1 and 0.72 and the vehicle final drive ratio is 4. The effective radius of the driving wheels is 27 cm.

The full-throttle engine torque-speed is described by following equation:

$$T_e = -4.45*10\text{-}6\,\omega_e^2 + 0.0317\omega_e + 55.24, \ 1000 < \omega_e < 6000\,\text{rpm}$$

(a) Plot the engine torque-speed and power-speed diagrams.
(b) At each gear ratio for different engine speeds, find the corresponding values of v and F_T and plot F_T-v diagram for all gears in a single figure.

Solution

(a) It is a simple task to vary the engine speed ω_e and determine the corresponding T_e values. The result is plotted in Figure 3.56.
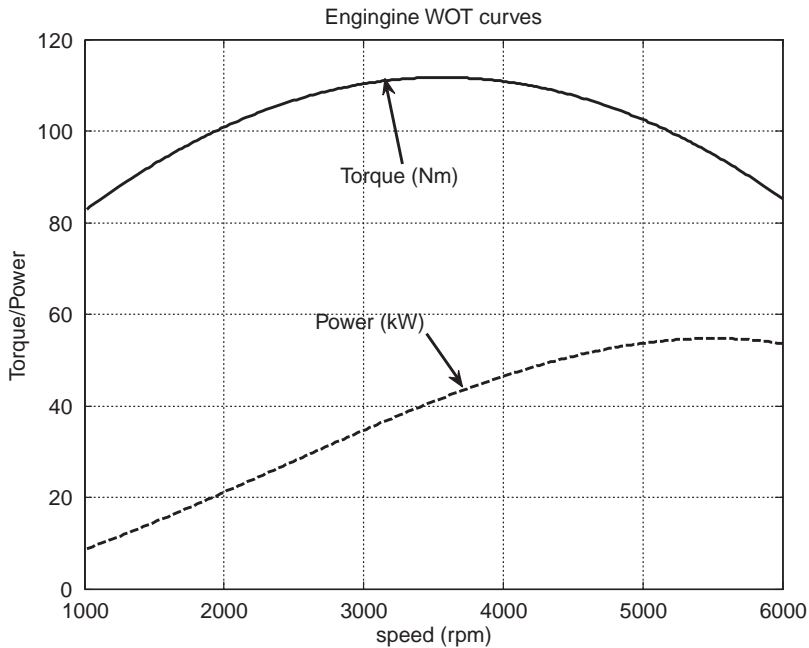
Figure 3.56 WOT engine torque and power variation of Example 3.7.1

(b) The tractive force $F_T(\omega_e)$ and vehicle speed $v(\omega_e)$ can be determined by using Equations 3.103 and 3.104 at any given gear ratio for the different values of engine speed ω_e. The variation of F_T versus v for each gear can then be plotted. The results for all gears are shown in Figure 3.57. In each gear the tractive force follows the pattern of the engine torque-speed variation, and when the gear is upshifted, the force magnitude reduces sharply and the curve flattens.
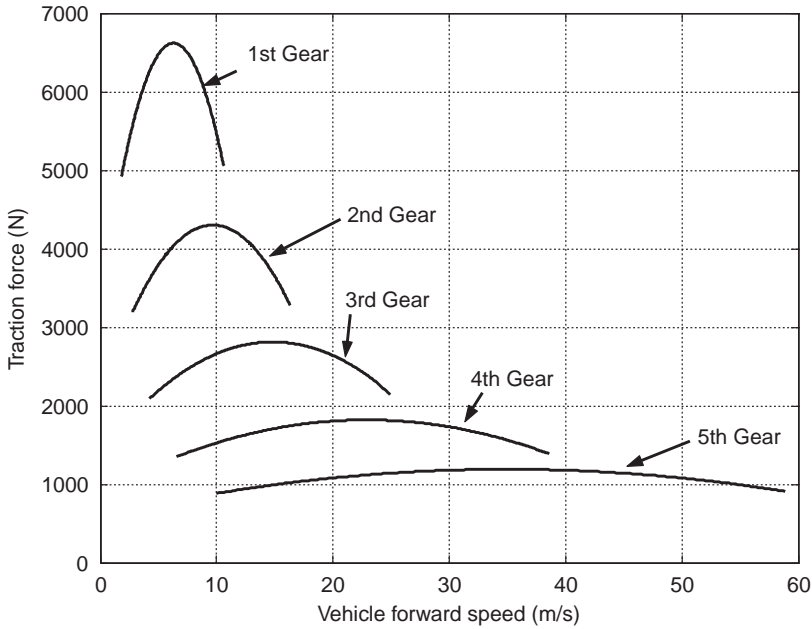
Figure 3.57 Tractive force versus speed at different gears

3.7.2 Acceleration, Speed and Distance

The difference between the tractive force of the vehicle F_{Ti} in a typical gear number i with the resistive force F_R at a specific speed v will generate the acceleration:

$$a(v) = \frac{F_{Ti}(v) - F_R(v)}{m} \qquad (3.106)$$

This equation can be represented by Figure 3.58 for a specific gear ratio. It is clear that the excess force at each gear varies with vehicle speed and the resulting acceleration will also vary with speed. It is also important to note that at low gears the excess force is greater (see Figure 3.57) and produces greater accelerations.

In order to find the velocity, Equation 3.106 can be integrated with respect to time. In differential form it reads:

$$\frac{dv}{F_{Ti}(v) - F_R(v)} = \frac{1}{m} dt \qquad (3.107)$$
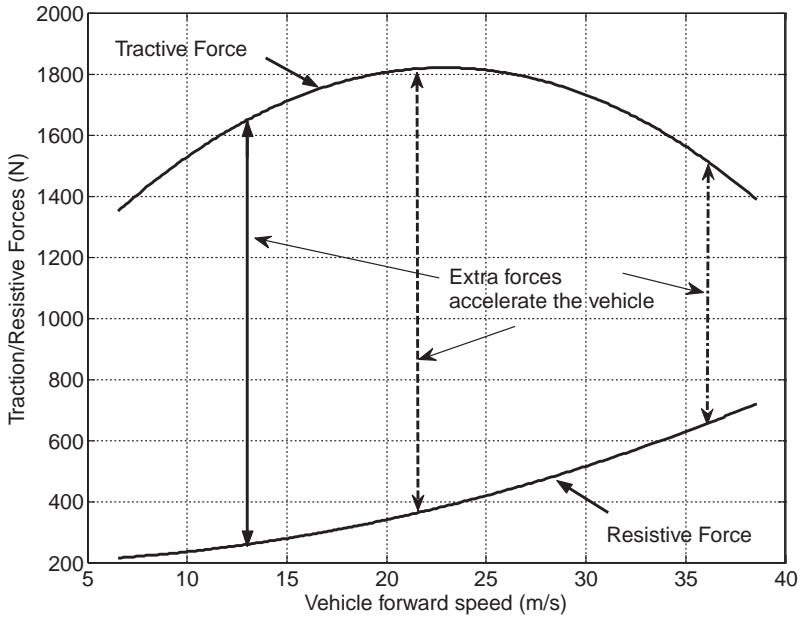
Figure 3.58   The vehicle acceleration is the result of excess force

Theoretically this is a differential equation that can be integrated by separation of variables. Based on our experience in the previous cases in which the tractive force had simpler forms, and also owing to the fact that the engine torque-speed variation usually takes a complex form, looking for a universal closed form solution is not attractive. Nonetheless, there are cases in which the engine torque-speed variation has a relatively simple form and the integration of Equation 3.107 is possible. In general, however, a numerical solution would be preferred.

In order to solve Equation 3.107 numerically, it can be written as a time-based differential equation of the form:

$$\frac{dv(t)}{dt} = \frac{1}{m} [F_{Ti}(t) - F_R(t)] \tag{3.108}$$

Since $v(t)$ is obtained through the numerical integration, $F_{Ti}(v)$ and $F_R(v)$ of Equation 3.106 are available at each instant. The main MATLAB program for this case is similar to the main program of Section 3.6.2, but its accompanying function will differ to some extent. In the main program a similar inner loop for the acceleration up to a certain engine speed (ω_{em}) will be present. Also, an outer loop for gear selection is present as shown in Figure 3.59. It is assumed that the shifts are performed instantly and no delay is involved.

The function for this case must include the instantaneous engine torque and tractive force calculations. For this reason the engine torque-speed formula is needed in the function statements. This information can be shared with the function through the '*global*' statement. In the program of Figure 3.60 a second order polynomial is assumed for the torque-speed of engine (see Example 3.7.1) and its coefficients are given in a vector 'p' that is shared between the main program and the function.

```
% Program to determine Fixed Throttle Performance (FTP)
clc; clear all; close all;

global m c f0 rw ni p   % Share information with the 'function'

% Engine torque formula is: te=p1*we^2+p2*we+p3
% polynomial coefficients are in 'p'
p=[p1 p2  p3];

% Enter proper vehicle parameters:
m=m; rw=rw; fr=fr; c=c;
f0=m*9.81*fr;

% Gearbox and final drive ratios:
ng=[n1, n2, n3, n4, n5]; nf=nf;

x0=[eps  0]; t0=0; tf=20;   % Initial conditions
wem=5500;                   % Engine speed at which gear is shifted

we=6500;          % A value set for the 'while' statement below

for i=1: length(ng)         % Loop for gears
  ni=ng(i)*nf;              % Overall gear ratio at each gear

  while we > wem            % Repeat statements until we=wem

  [t,x]=ode45(@Fixed_thrt, [t0 tf], x0);   % Calls Fixed_thrt function
  v=x(:,1);
  s=x(:,2);
  we=30*ni*v(end)/rw/pi;
    if we>=wem
      tf=tf*wem/we;
    end
  end
% At this point results for gear 'ni' are ready to plot
  subplot(2,1,1),  plot(t,v),  hold on
  subplot(2,1,2),  plot(t,s),  hold on

% Now gearshift is needed. Set the initial conditions for the next gear
  t0=max(t);
  tf=60;                     % set to large values
  x0=[v(end) s(end)];
  we=6500;
end
subplot(2,1,1)
xlabel('Time (s)')
ylabel('Velocity (m/s)')
grid
subplot(2,1,2)
xlabel('Time (s)')
ylabel('Distance (m)')
grid
```

Figure 3.59   Main MATLAB program for fixed throttle performance

```
% Function called in program main_ft.m
function f=Fixed_thrt(t,x)

global m c f0 rw ni p

v=x(1);                    % instantaneous vehicle speed
omega=ni*v*30/rw/pi;       % instantaneous engine speed (rpm)
Trq=polyval(p, omega);     % engine torque at this instant
Fti=Trq*ni/rw;             % instantaneous tractive force at gear n(i)

f1=(Fti-f0-c*v^2)/m;       % Differential equation for speed
f2=v;                      % Differential equation for distance
f=[f1
   f2];
```

Figure 3.60   MATLAB function for fixed throttle performance

Example 3.7.2

For a vehicle with mass of 1000 kg, rolling resistance coefficient of 0.02 and overall aerodynamic force coefficient of 0.35, use the transmission and engine information given in Example 3.7.1.

(a) Plot the variation of vehicle speed and distance versus time.
(b) Plot the variation of acceleration versus time.

Solution

Enter the necessary information such as p, n_f, m, f_R, c and r_w and the main program will be ready for run. No change is needed to the function. The results obtained for speed and distance are given in Figure 3.61.

It is worth noting that at the highest gear (gear 5), as the resistive forces approach the tractive force value, the acceleration approaches zero. The theoretical final speed is, therefore, attained after a substantial time. For this reason, the integration time 'tf' needs be set to large values. This in turn will increase the integration time. Thus, in this example, a tf = 60 seconds is chosen, for which the final speed (a little above 50 m/s) is not actually reached.

The values of vehicle acceleration are calculated inside the '*function*' and not in the main program. For this reason the data is lost when it returns to the main program. In order to find the acceleration, the best way is to regenerate it within the main program from the values of speed available. A subprogram listing below shows how an inner loop can be constructed at the end of each gear loop to calculate acceleration values:

```
v=×(:,1);
  omega=ni*v*30/rw/pi;
  Trq=polyval(p,omega);
  Fti=Trq*ni/rw;
  acc=(Fti-f0-c*v.^2)/m;
  figure(2)
  plot(t, acc')
  hold on
  clear acc
```

Including the subprogram in the main program will generate the plot of Figure 3.62.
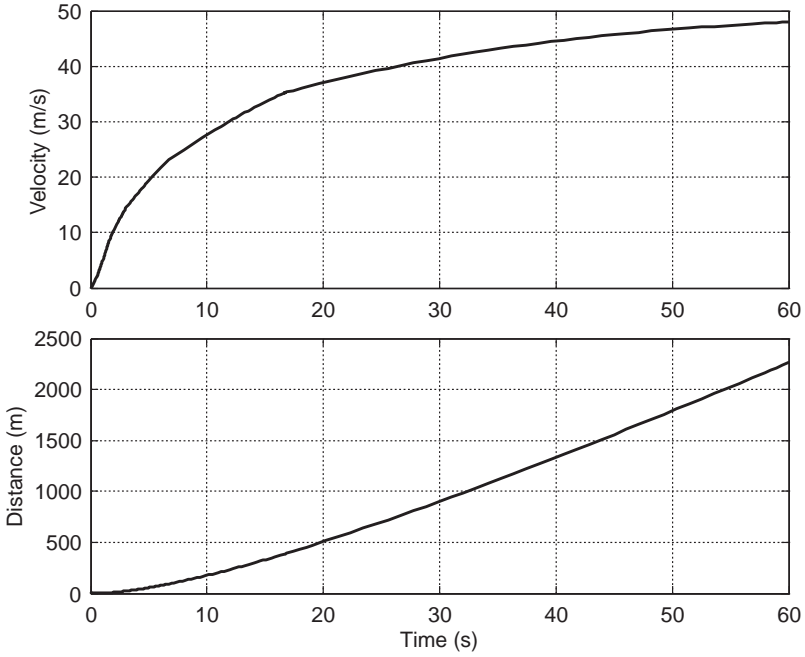
Figure 3.61   Results for velocity and distance of Example 3.7.2
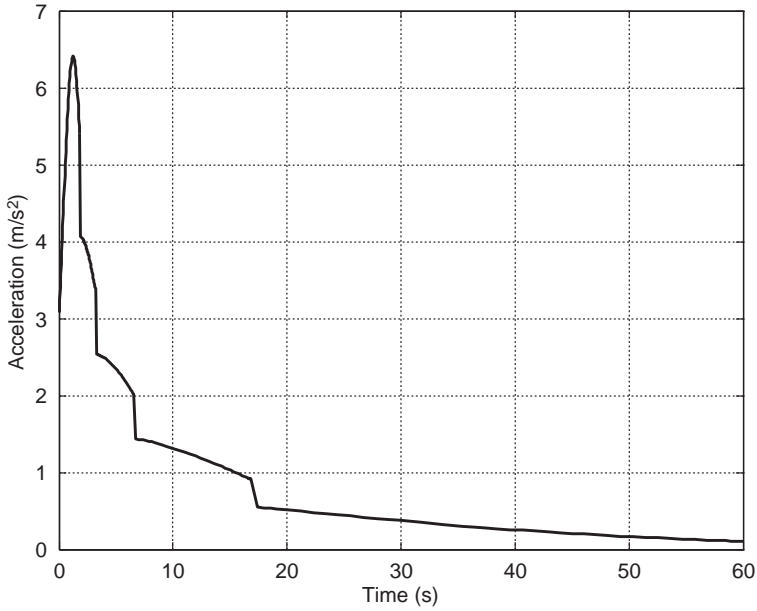
Figure 3.62   Acceleration performance of Example 3.7.2

3.7.3 Shift Times

When a gear should be shifted depends on several factors. In automatic transmissions the decision is made by the controller and in manual transmissions by the driver. In the latter case, the gearshift is performed according to the individual driving style and the engine speed at which the gear is shifted differs for different drivers. In theory, when a new gear is engaged, the vehicle can accelerate up to the limit speed of the engine. In practice, however, this is not the case and every driver changes the gear based on their style of driving at speeds below the maximum. Gearshift issues are discussed in more detail in Chapter 4.

In most transmissions, and especially in manual transmissions, there is an engine torque interruption during a shift. This will eliminate the tractive force and with F_T absent, only resistive forces will act on the vehicle during the shifts and negative accelerations will result (see Figure 3.30). This duration is different for different drivers and even for different gears. In the previous analysis, immediate gearshifts with no torque interruption were assumed. In order to consider the torque break involved in the gearshifts, an inner subprogram should be included in the existing MATLAB program. The main idea is to set the tractive force to zero during this '*tdelay*' time. This is left to the reader as an exercise to apply the necessary changes to the MATLAB program and generate results that are depicted in Figures 3.30 and 3.63 for the vehicle acceleration, speed and distance (see Problem 3.15).

3.7.4 Maximum Speed at Each Gear

The maximum speed at each gear may be reached in two different situations: kinematic limit or dynamic balance point. The kinematic limit is when the tractive force exceeds the resistive force and vehicle can still accelerate but the engine cannot turn faster. A good example is acceleration in low gears at which the tractive force is very high and the resistive forces are very low and the excess force is used to accelerate the
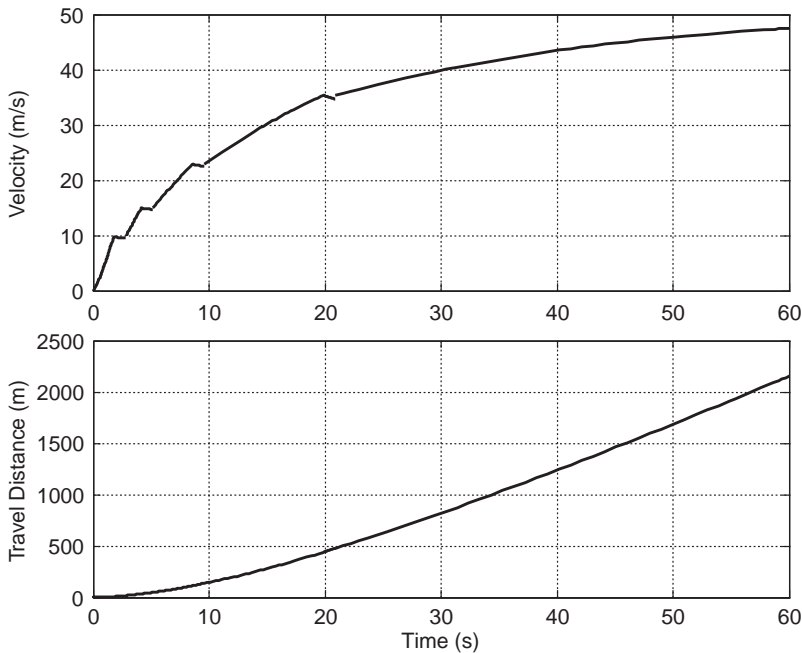
Figure 3.63 Effect of including shift delays

vehicle but the engine speed can reach very high values close to its cut-off point. At this point an upshift is needed, as the forward speed is still low but driveline kinematics imposes a constraint on the motion. Upshifts will allow higher kinematic vehicle speeds but at the same time lower tractive forces and reduced accelerations will occur. In high gears, due to high speeds and low traction forces, there are points at which the resistive force can balance the tractive force. These points, called dynamic balance points, represent steady states for the vehicle motion – even though the vehicle may not remain in this steady condition for long.

Figure 3.64 summarizes these issues for an example vehicle on a level road. At low gears (1, 2 and 3) as seen, there are excess tractive forces at the points of engine maximum speeds. These points are kinematic limit points at which the gear must be shifted. At the highest gear (gear 5), the resistive force grows with speed and at a certain point equals the tractive force. At this point, the dynamic balance is met and vehicle attains its final speed. At gear 4, too, it is sometimes possible to have a dynamic balance point, for example on a slight slope. Also in Figure 3.64 an intersection point would be possible for gear 4 if a slightly higher engine speed were attainable.

At the dynamic balance points where the tractive and resistive forces balance, the equation of motion simply is:

$$F_T(v) - F_R(v) = 0 \qquad (3.109)$$

This equation will be satisfied at a certain forward speed v^* and a corresponding engine speed of ω^*. At each gear n_i, Equation 3.109 should be solved for v^* where the steady state could be achieved (e.g. high gears), but the speed of engine at v^* must be smaller than the engine limit speed ω_{em}, that is:

$$\omega^* = \frac{n_i v^*}{r_w} < \omega_{em} \qquad (3.110)$$
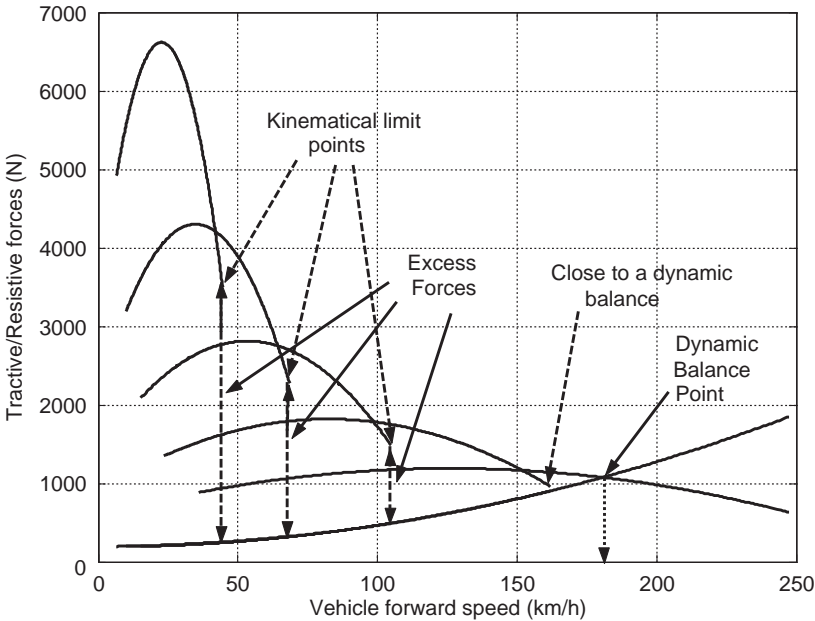
Figure 3.64 Definitions of kinematic limit and dynamic balance points

This process should usually be performed numerically by modifying the existing MATLAB program. However, for some cases where the engine torque-speed relation at a fixed throttle is available, a mathematical solution can also be obtained. Let the engine torque-speed formula be written in the form:

$$T_e(\omega_e) = f(\omega_e) \tag{3.111}$$

Then the solution is obtained from:

$$\frac{n_i}{r_w} f\left(\frac{n_i}{r_w} v^*\right) - F_R(v^*) = 0 \tag{3.112}$$

Example 3.7.3

For the vehicle in Example 3.7.2, investigate the existence of dynamic balance points on a level road for gears 3 and 5.

Solution

The engine torque-speed formula is:

$$T_e = -4.45 \times 10^{-6}\omega_e^2 + 0.0317\omega_e + 55.24$$

In which ω_e is in rpm. This relation in general can be written as (ω_e in rad/s):

$$T_e(\omega_e) = t_1\omega_e^2 + t_2\omega_e + t_3 = f(\omega_e)$$

Substituting in Equation 3.112 and after some manipulations, one finds:

$$(v^*)^2 + k_1 v^* + k_2 = 0$$

in which:

$$k_1 = -\frac{(n_i/r_w)^2 t_2}{c - (n_i/r_w)^3 t_1}$$

$$k_2 = F_0 - n_i\frac{t_3}{r_w}$$

t_1, t_2 and t_3 after conversion to rad/s are found to be 4.1×10^{-4}, 0.3027 and 55.24 respectively. For gear 3 the overall ratio is $n_3 = 1.7 \times 4 = 6.8$ and k_1 and k_2 are:

$$k_1 = -28.103 \text{ and } k_2 = -1195$$

Solving the quadratic equation for v^* results in:

$$v^* = 51.367 \text{ and/or } -23.265$$

With the positive answer, the engine speed must be checked:

$$\omega^* = \frac{n_3}{r_w} v^* = 6.8 \times 51.367/0.27 = 1293.7 \text{ rad/s } (12,354 \text{ rpm!})$$

This is not possible at all! For gear 5, the same procedure will result in:

$$n_5 = 2.88, \; k_1 = -40.882, \; k_2 = -393.03, \; v^* = 48.92 \text{ m/s } (176.1 \text{ km/h}) \text{ and } \omega^* = 4,983 \text{ rpm}$$

which is fine.

3.7.5   Best Acceleration Performance

A question is often raised of how to perform gearshifts to get the best acceleration performance. In practice, achieving higher velocities in less time means higher average accelerations. From a mathematical view point, velocity is the time integral of acceleration:

$$v(t) = \int a(t)dt \qquad (3.113)$$

In a graphical representation, the area under the acceleration curve versus time gives the velocity. For a fixed throttle performance (FTP) (e.g. WOT), the acceleration behaviour of the vehicle is determined with the gearshifts. To see the effect of the choice of the shift point, consider the acceleration performance of a typical vehicle at two different shift speeds shown in Figure 3.65 in an acceleration-speed diagram. Solid lines represent a shift carried out at a certain engine speed where the traction force is equal at two consecutive gears (corresponding to the point of intersection of traction curves of the two gears), whereas the dashed lines belong to a shift at lower engine speeds.

It is clear that the area under the solid lines (A_1) is larger than the area under the dashed lines (A_2). Also if the shift speeds of the dashed lines are further reduced, the area A_2 will also be decreased. Therefore, as the maximum area is A_1 it can be concluded that the concept of gearshifting at the points of intersection with consecutive traction curves, produces higher accelerations. According to Equation 3.113, the area under the acceleration-time equals the speed of the vehicle at the end of the acceleration phase and thus for the area A_1 the speed is maximum.

In the acceleration-time plot, the acceleration curve of each gear will not remain identical when the shift speed varies. This can be seen in the plots of Figure 3.66 for two different shift speeds of 5500 rpm (solid lines) and 4000 rpm (dashed lines). Nonetheless, the area under the acceleration-time curves is still larger overall as the shift rpm is increased. In order to further clarify the effect of the shift rpm, the time to attain a specific speed is a good measure as it indicates the overall acceleration performance. Figure 3.67 shows the velocity-time curves for four different shift rpm 4000, 4500, 5000 and 5500. It is clear that at any speed (a horizontal line), the time to reach that speed is smaller for larger shift speeds. This is shown for speed of 30 m/s (108 km/h). The time to reach the specified speed reduces in a non-linear fashion for example from
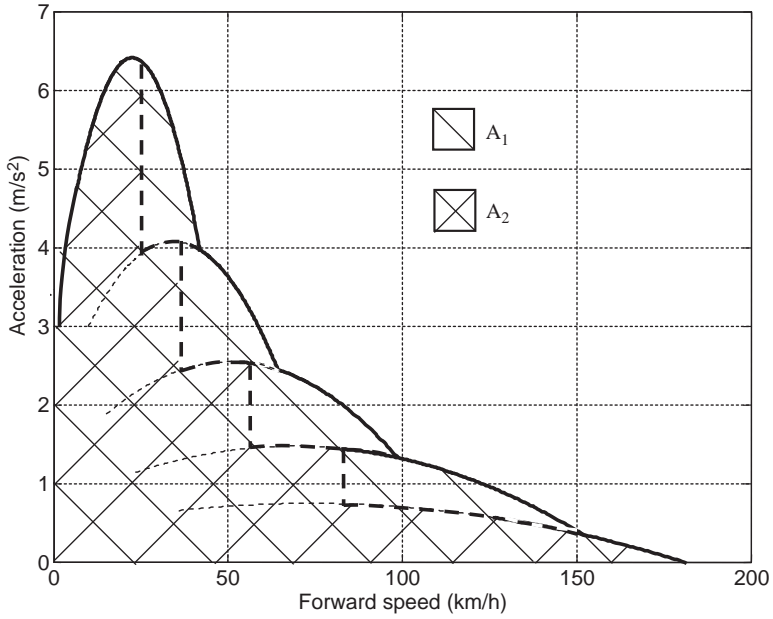
Figure 3.65 Effect of shift rpm on the acceleration performance in *a-v* plot
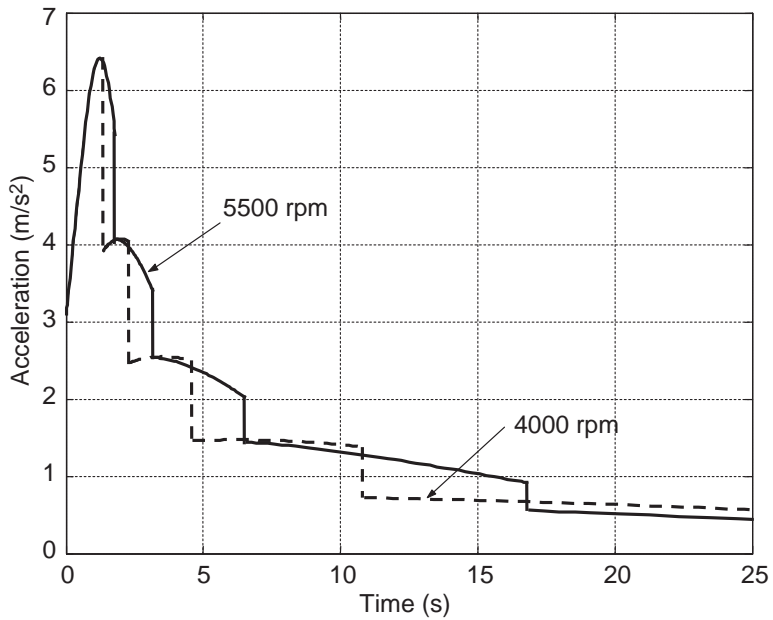
Figure 3.66 Effect of shift rpm on the acceleration performance in *a-t* plot
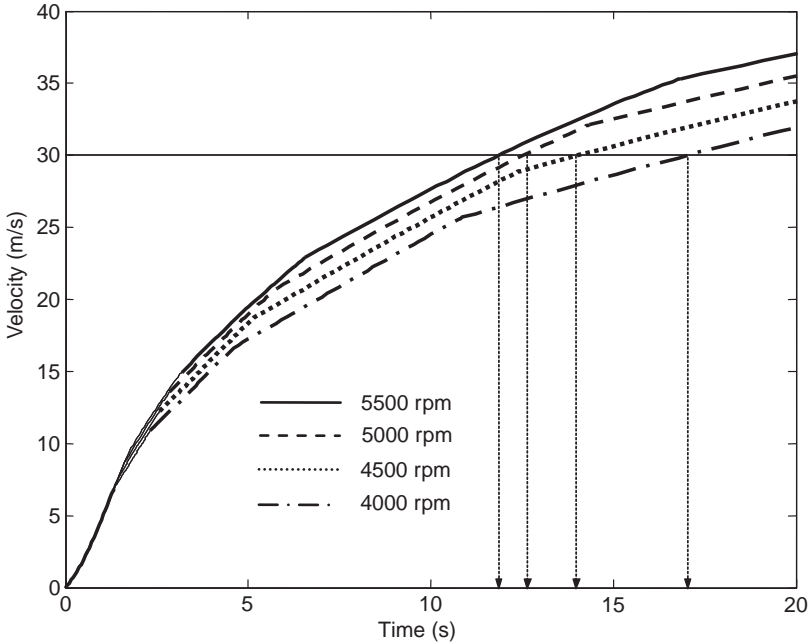
Figure 3.67   Effect of shift rpm on reduction of time to attain a certain speed

4000 to 4500 rpm the time reduces around 3 seconds, whereas from 5000 to 5500 rpm it is reduced around 1 second.

It should be noted that the overall appearance of the acceleration and speed curves are dependent on the transmission gear ratios as well as the vehicle physical properties. In changing any of the parameters, the details of the figures presented above will change, nevertheless the overall behaviour is similar for different configurations.

3.7.6   Power Consumption

The power requirement during the vehicle motion comprises two parts: power to accelerate; and power to overcome resistive forces. The total power used to move the vehicle at a specified speed $v(t)$ is:

$$P(t) = F_T v(t) \tag{3.114}$$

The tractive force F_T can be written as:

$$F_T = ma(t) + F_R \tag{3.115}$$

Therefore:

$$P(t) = ma(t)\,v(t) + F_R v(t) = P_a(t) + P_R(t) \tag{3.116}$$
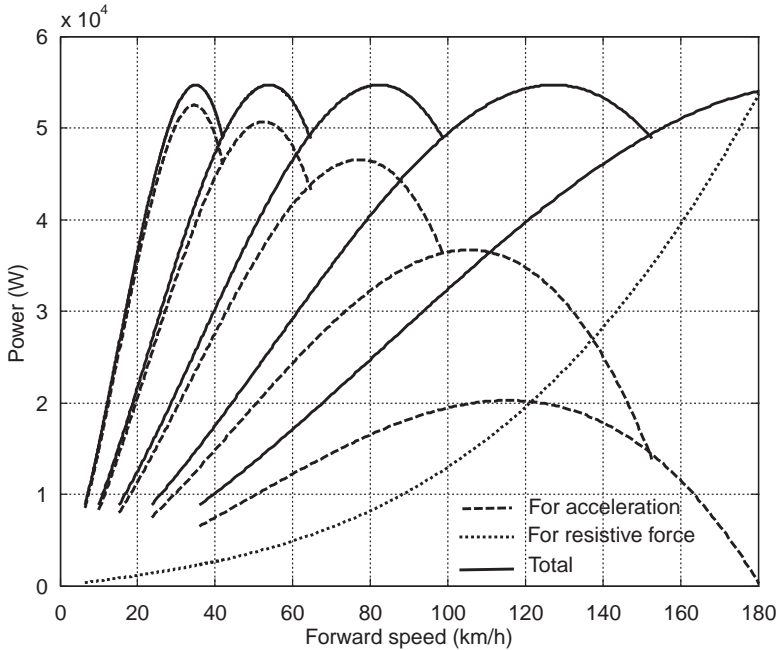
Figure 3.68   A power-speed diagram for WOT acceleration

The first term P_a is the power needed for the vehicle acceleration and the second term P_R is the power to overcome the resistive forces. Equation 3.116 indicates that the power is an instantaneous quantity that varies during the vehicle motion according to the variations of acceleration or speed. It also signifies that for greater acceleration more power is needed.

   During the vehicle motion with a fixed throttle input (e.g. WOT), the variation of power with speed at different gears is shown in Figure 3.68. As the acceleration is higher at lower gears while the speed is low (low resistive forces), the main part of power is used for accelerating and only a small portion is used for resistive forces. Upshifting reduces the acceleration where the speed is high and the resistive forces play an important role; as a result, the share of the power to overcome the resistive forces increases at higher gears. At the final speed (where the acceleration is zero), the total power is devoted to overcoming only the resistive forces.

   The time history of power variation at different gears is shown in Figure 3.69 for a full throttle acceleration with gearshifts at the maximum power point. When a gear is upshifted, the acceleration will drop and as the resistive forces remain unchanged at the specific speed, the power demand will be reduced. In less aggressive driving, the acceleration in low gears often ends in lower engine speeds, and as a result, the power use in low gears is usually much lower than the maximum engine power. It should be noted that the selection of transmission gear ratios can change the results by moving the points in the plots. The effect of gear ratios on the power curves, especially at high gears, will be discussed in Chapter 4.

3.8   Throttle Pedal Cycle Performance (PCP)

In real driving situations, the accelerator pedal is depressed by the driver according to driving requirements. In a vehicle equipped with a manual gearbox, the pedal input even in a high acceleration
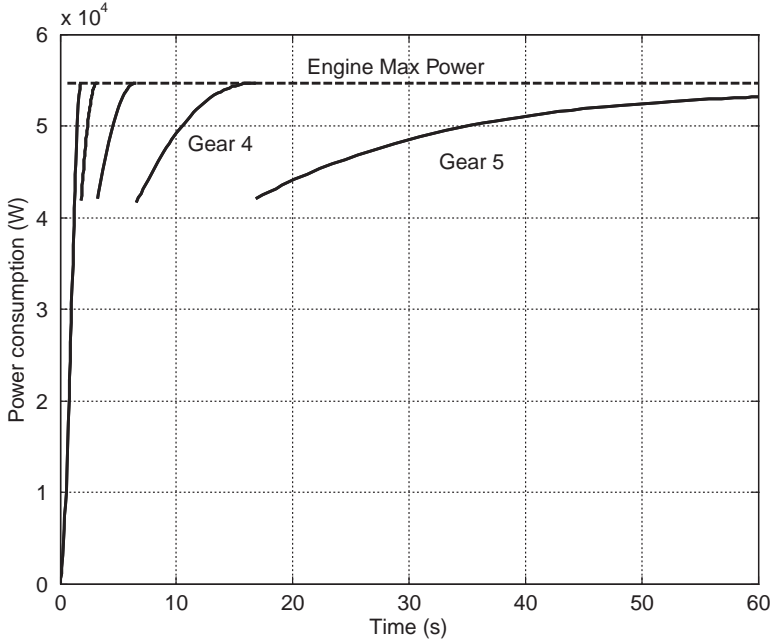
Figure 3.69   Typical power-time diagram for fixed throttle performance
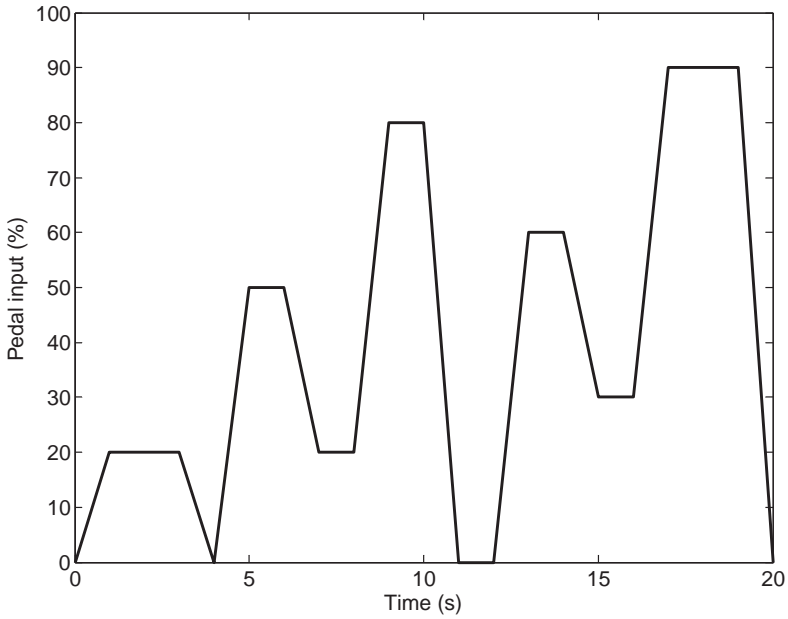
Figure 3.70   A typical time history for accelerator pedal inputs (a pedal cycle)

performance is not kept constant, since at least during gearshifts it is necessary to release the pedal and press it once again. In normal driving conditions, the pedal input varies in different driving situations. Thus in the study of vehicle longitudinal performance, one category of problem is when the input variable is the engine throttle and the output is the resulting vehicle motion.

Drivers' pedal inputs can vary largely owing to diverse driving situations and driving habits. The time history of the pedal variations with time may look like that of Figure 3.70 in which the pedal input varies between 0 (fully closed) to 100 (wide open).

In order to simulate a driving condition under pedal inputs, the engine torque-speed- throttle characteristics will be necessary. This can be in the form of look-up tables or the MT engine formula introduced in Chapter 2.

Moreover, during driving, the gearshifts are also carried out according to the vehicle and engine speeds and driver's selection. In order to include the pedal inputs in the MATLAB programs, it is necessary to do it inside the '*function*' and not inside the main program. The reason is that the pedal inputs are time-dependent and when '*ode*' is called inside the main, all integration steps are performed by the '*function*' and the final results are returned. The following example is designed to illustrate this concept.

Example 3.8.1

The MT engine formula for a passenger car engine is given in Equation 3.2 together with the information of Tables 3.1 and 3.2. For a throttle pedal cycle shown in Figure 3.71, use the vehicle information of Example 3.7.2 and plot the variation of vehicle speed with time. Ignore time delays during the gearshifts.
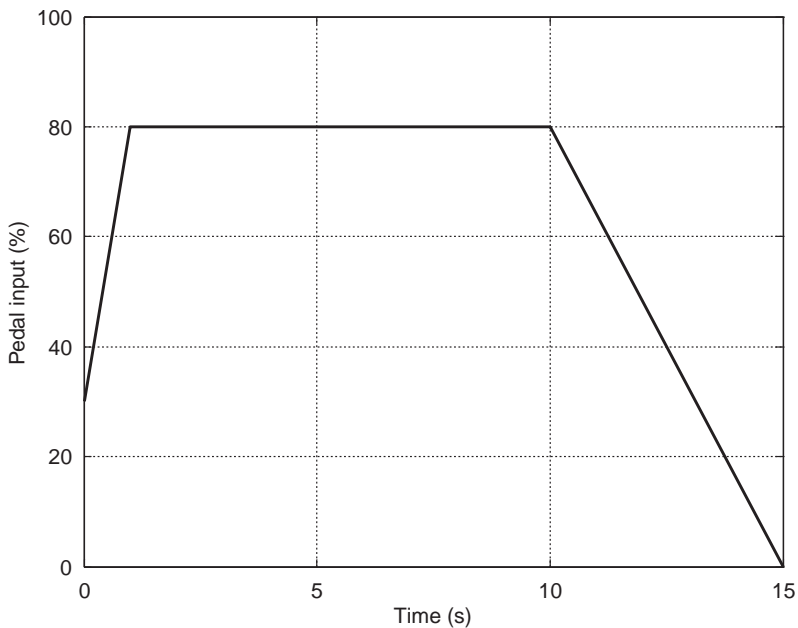
Figure 3.71   Pedal cycle of Example 3.8.1

Solution

```
% Main MATLAB program for Example 3.8.1
global m c f0 rw n p theta t_t wem

m=1000; rw=0.27; fr=0.02; c=0.35;
f0=m*9.81*fr;

% Engine full throttle formula is a second order polynomial:
p=[-0.00000445 0.0317 55.24];

% Define the pedal cycle:
theta=[30 80 80 0];          % Throttle values (%)
t_t=[0 1 10 15];             % Corresponding times (s)

x0=[eps 0]; t0=0; tf=15;
wem=5500;        % Engine upper limit

[t,x]=ode45(@pedal_cyc, [t0 tf], x0)    % Calls pedal_cyc function

% Plot the results
```

(a)

```
% Function called in the main program
function f=pedal_cyc(t,x)

global m c f0 rw n  p theta t_t wem

v=x(1);
s=x(2);
% A loop to specify the gear number:
for i = 5: -1: 1   % Number of gears
   omeg=n(i)*v*30/rw/pi;  % Engine speed at vehicle speed 'v'
  if omeg <= wem  % If engine speed is less than max allowed speed,
   ni=n(i);    % Leave the gear number 'i'
  end
end
omeg=ni*v*30/rw/pi;       % Engine speed at the selected gear

% Find the throttle value 'th':
th=interp1(t_t, theta, t);

% Now calculate the part-throttle torque:
   pow=(1.003*omeg)^1.824;
   den=(1+exp(-11.12-0.0888*th))^pow;
   Trq=polyval(p, omeg)/den;
% Tractive force at gear 'i'
Fti=Trq*ni/rw;

f=[(Fti-f0-c*v^2)/m
                  v];
```

(b)

Figure 3.72   MATLAB programs for Example 3.8.1: (a) Main and (b) the function
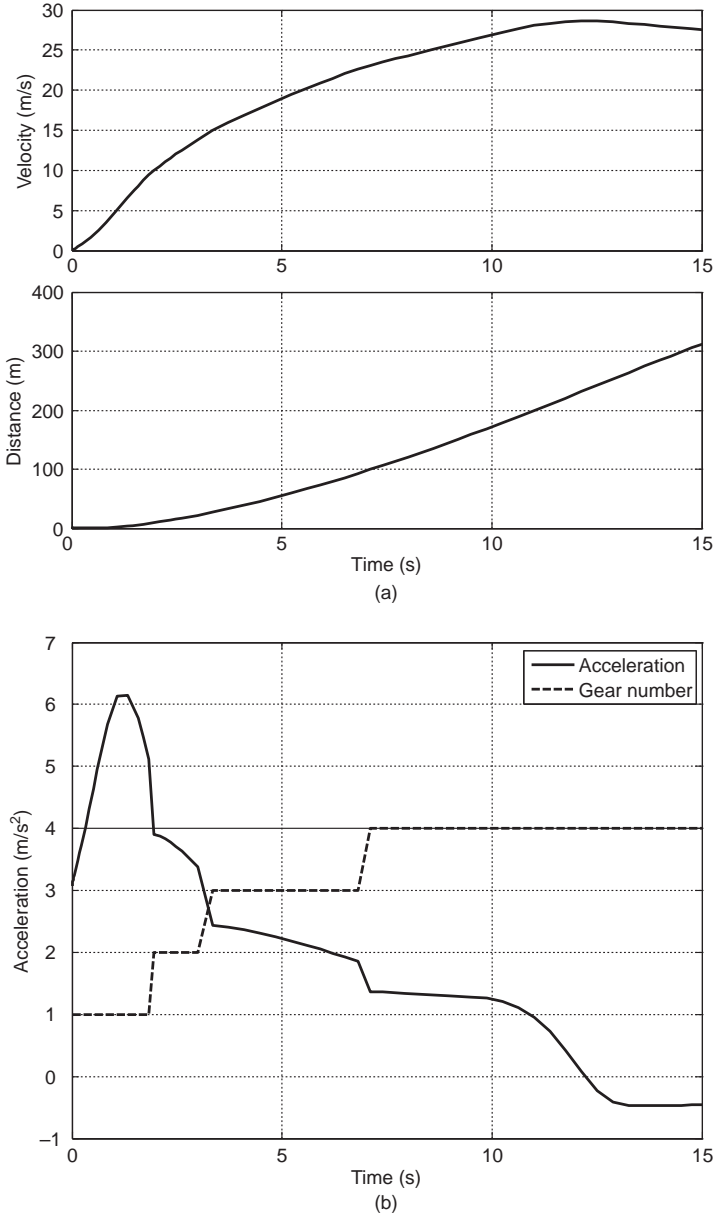
Figure 3.73 (a) Time histories of velocity and distance for Example 3.8.1. (b) Time history of acceleration for Example 3.8.1

The programs shown in Figure 3.72 provide the details of instructions for this case. In the main program, inputs are given and information is passed to the '*function*' by the '*global*' statement. The tricky part is to specify the gear that is engaged. It is assumed each gear is engaged up to the maximum engine speed and then upshifted. It should be noted that in this program the downshifts

are not taken into consideration otherwise another loop should be defined to check for the lower limit of the engine speed and determine the downshifts.

The output results are shown in Figures 3.73a and 3.73b. From the time history of vehicle acceleration, the gearshift points to gears 2, 3 and 4 are clear. Note that the acceleration calculations are similar to those explained in Example 3.7.2.

3.9   Effect of Rotating Masses

When the vehicle accelerates, the wheels, rotating shafts and even the engine accelerates. In other words, in addition to the vehicle body (mass) which needs tractive force to develop its kinetic energy, the rotating inertias also need torques in order that their corresponding kinetic energy is developed. The demanded power produced by vehicle engine is therefore divided and the part that propels the vehicle body is reduced due to the share taken by rotating masses. This will reduce the vehicle acceleration compared with the case with no rotating masses. Consider the torque balance from the engine to the driving wheels through each of the torque-consuming driveline components as shown in Figure 3.74.

The application of Newton's Second Law to the rotational motion of the engine output with regard to Figure 3.74a reads:

$$T_c = T_e - I_e \alpha_e \tag{3.117}$$

This means the clutch torque T_e is what is left from the engine output torque T_e after accelerating the relevant inertias I_e grouped at the engine output shaft (including the engine rotating masses, flywheel,

(a) Engine flywheel

(b) Transmission

(c) Final drive

(d) Axle and wheel
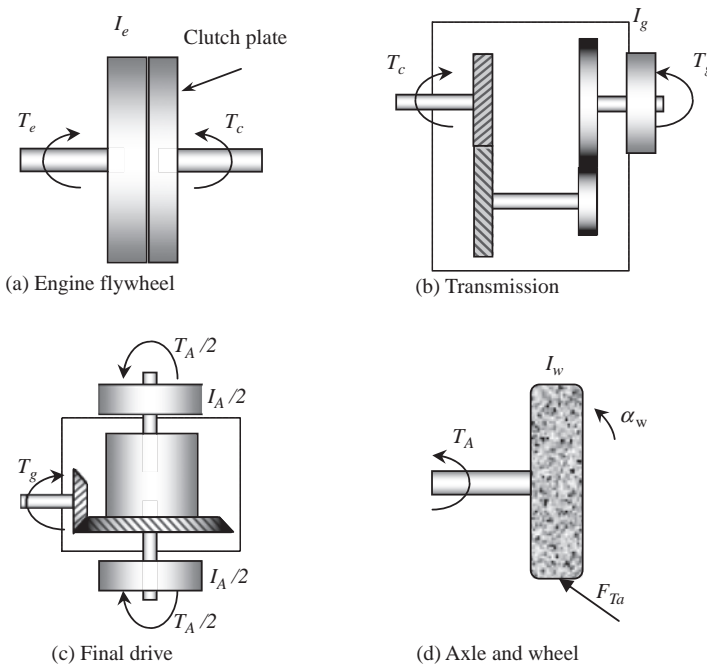
Figure 3.74   Main components of the vehicle driveline

clutch assembly, etc.) with angular acceleration α_e. In Figure 3.74b it is assumed that the inertias of all rotating masses related to the gearbox input and output are summed up as a single inertia I_g at the output shaft of gearbox. Before this inertia, the torque on the output shaft simply is the input torque multiplied by the gearbox ratio n_g:

$$T_T = n_g T_c \tag{3.118}$$

The output torque after the inertia I_g, therefore, is:

$$T_g = T_T - I_g \alpha_T \tag{3.119}$$

where α_T is the angular acceleration of the output shaft of gearbox. For the final drive, according to Figure 3.74c, it is assumed that there is only a single drive axle and all the rotating inertias related to it are collected as a single inertia I_A at the output side of the differential. The governing equation in this case will be:

$$T_A = n_f T_g - I_A \alpha_A \tag{3.120}$$

α_A being the angular acceleration of the final drive output shaft. Finally, the torque output from the final drive reaches the wheel with an overall inertia I_W rotating with the wheel speed ω_w and accelerates it. According to Figure 3.74d, the balance of torques around the wheel centre results in:

$$T_A - F_{Ta} r_w = I_w \alpha_w \tag{3.121}$$

where F_{Ta} is the tractive force available at the tyre–road interface. Since all the shafts are connected, their rotational speeds (or accelerations) are related to the engine rotational speed (acceleration), i.e.:

$$\alpha_e = n_g \alpha_g \tag{3.122}$$

$$\alpha_g = n_f \alpha_A \tag{3.123}$$

Combining all equations results in:

$$F_{Ta} = \frac{n}{r_w} T_e - \frac{1}{r_w} \left(n I_e + \frac{n_f}{n_g} I_g + \frac{I_w + I_A}{n} \right) \alpha_e \tag{3.124}$$

This is the force propelling the vehicle, whereas in the previous discussions the tractive force was simplified as:

$$F_T = \frac{n}{r_w} T_e \tag{3.125}$$

Now, for the longitudinal motion of the vehicle under the action of tractive and resistive forces, the equation of motion reads:

$$F_{Ta} - F_R = ma \tag{3.126}$$

where a is the longitudinal acceleration of the vehicle. F_{Ta} is produced by the tyre through slip generation at contact patch. With slip at the tyre–road interface, the rotational speed of the tyre will differ slightly from the speed of wheel centre divided by the tyre rolling radius (see Section 3.10). Accepting a small

error, the no-slip condition for the tyre will be assumed and that allows the rotational acceleration of the wheel α_w to be directly related to the vehicle acceleration a:

$$a = r_w \alpha_w \tag{3.127}$$

Substituting Equations 3.124, 3.125 and 3.127 into Equation 3.126 yields:

$$F_T - F_R = m\left[1 + \frac{1}{mr_w^2}\left(I_w + I_A + n_f^2 I_g + n^2 I_e\right)\right]a \tag{3.128}$$

which can be written as:

$$F_T - F_R = m_{eq}a \tag{3.129}$$

with:

$$m_{eq} = m\left[1 + \frac{1}{mr_w^2}\left(I_w + I_A + n_f^2 I_g + n^2 I_e\right)\right] \tag{3.130}$$

From Equation 3.130 it is clear that m_{eq} is always larger than m, therefore the vehicle acceleration in the real case will be smaller than that obtained in previous analyses without accounting for the rotating masses. In other words, when the effect of rotating masses is taken into consideration, it is like considering an extra mass for the vehicle. Alternatively, when no rotating masses are considered, a larger tractive force will be available. Figure 3.75 conveys this concept by assuming a single flywheel equivalent to all rotating masses, attached to the driving wheels.

In general, m_{eq} can be written as:

$$m_{eq} = m + m_r \tag{3.131}$$

where m_r is regarded as the equivalent mass of the rotating inertias:

$$m_r = \frac{1}{r_w^2}\left[I(\omega_w) + n_f^2 I(\omega_g) + n^2 I(\omega_e)\right] \tag{3.132}$$

In Equation 3.132 the inertias are defined as:

$I(\omega_w)$ is the sum of all inertias rotating with the speed of driving wheels.
$I(\omega_g)$ is the sum of all inertias rotating with the speed of gearbox output shaft.
$I(\omega_e)$ is the sum of all inertias rotating with the speed of engine.

Large rotating mass   Driving wheel
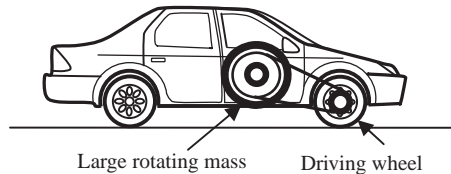
Figure 3.75   Concept of rotating masses

It is important to note that the m_{eq} has different values at different gears, since $n = n_g n_f$ changes with transmission gear ratio n_g. Larger transmission ratios will make m_{eq} larger (by power 2 of n_g). This means in the lowest gear (i.e. gear 1), m_{eq} will have the largest value whereas at highest gear (e.g. gear 5) it will have the smallest value. This is working against the requirements of high accelerations at low gears.

Example 3.9.1

For a vehicle with information given in Table 3.9 and gear information of Example 3.7.2, compare the terms of Equation 3.132. Also evaluate the ratio m_{eq}/m for different gears.

Table 3.9 Data for Example 3.9.1

Vehicle information		Value	Unit
1	Vehicle mass	m	1200	kg
2	Engine attached inertia	I_e	0.25	kg.m^2
3	Gearbox attached inertia	I_g	0.1	kg.m^2
4	Wheel attached inertia	I_w	4	kg.m^2
5	Wheel rolling radius	r_w	27	cm

Solution

Calculation of the individual terms in Equation 3.132 is straightforward. Let us define the existing terms as:

$$\text{Term1} = I_w \left(\frac{1}{r_w}\right)^2, \quad \text{Term2} = I_g \left(\frac{n_f}{r_w}\right)^2 \text{ and Term3} = I_e \left(\frac{n}{r_w}\right)^2$$

The dimensions of each term are kg, thus these terms effectively represent extra masses that are accelerated. The results are summarized in Table 3.10.

As seen from Table 3.10, the effect of terms 1 and 2 altogether is about 6–7% of vehicle mass, whereas the effect of term 3 is something over 70% of the vehicle mass in gear 1 and some 2% in gear 5. The total effect at gear 1 is almost 80% of the vehicle mass. Therefore it is evident that the effect of rotating masses especially at low gears is quite large compared to the vehicle mass itself.

Table 3.10 Equivalent masses of Example 3.9.1

	Parameter		Gear 1	Gear 2	Gear 3	Gear 4	Gear 5
1	Term1	kg	54.8697	54.8697	54.8697	54.8697	54.8697
2	Term2	kg	21.9479	21.9479	21.9479	21.9479	21.9479
3	Term3	kg	877.9150	370.9191	158.5734	66.3923	28.4444
4	Total m_r	kg	954.7325	447.7366	235.3909	143.2099	105.2620
5	m_{eq}	kg	2154.7	1647.7	1435.4	1343.2	1305.3
6	m_{eq}/m		1.7956	1.3731	1.1962	1.1193	1.0877

3.9.1 Corrections to Former Analyses

When m_{eq} is substituted in the equation of vehicle longitudinal motion it will be of the general form:

$$F_T(v) - F_R(v) = m_{eq}(n)\frac{dv}{dt} \tag{3.133}$$

The gear ratio n for a discrete ratio gearbox is a fixed value at a specific gear. For a CVT, however, its value also depends on the speed. Thus, for the two cases of analyses, the following corrections must be made in order that the effect of rotating masses is included.

3.9.1.1 Discrete Gear Ratios

For all cases of constant torque, fixed throttle and throttle pedal cycle, the condition of gear ratio changing during the vehicle motion was discussed. In order to include the effect of rotating masses, the only required change will be the evaluation of the equivalent mass at each engaged gear, as for a particular gear ratio n the equivalent mass $m_{eq}(n)$ is an unchanging quantity. The method of solution for all cases will be similar once the gear ratio is specified.

Example 3.9.2

For the vehicle in Example 3.7.2, investigate the effect of rotating masses on the acceleration of the vehicle. Use the information for rotating masses from Example 3.9.1.

Solution

The inclusion of the equivalent mass in the MATLAB program can be done inside the main loop for the gears in Figure 3.59:

```
Mr1=Iw/(rw^2);
Mr2=Ig*(nf^2)/(rw^2);
for i=1: length(ng)      % Loop for gears
ni=ng(i)*nf;             % Overall gear ratio at each gear
Mr3=Ie*(ni/rw)^2;
m=Mr1+Mr2+Mr3+m0;
f0=m0*9.81*fr;
```

The result is shown in Figure 3.76 for the rotating and non-rotating masses. In gear 1 the difference in acceleration is very large and decreases as the gear number increases. It should be noted that the time of gearshift is also delayed when the rotating masses are included as the engine rpm reaches the shifting rpm later due to lower accelerations.
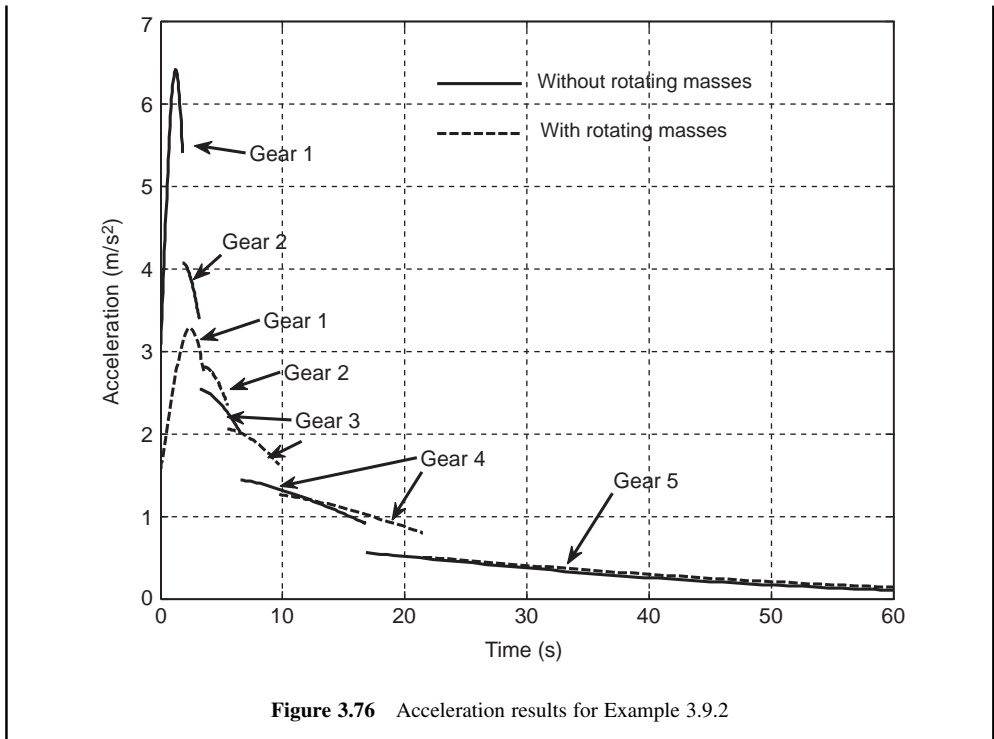
Figure 3.76 Acceleration results for Example 3.9.2

3.9.1.2 Continuous Gear Ratios

The continuous variation of gear ratio was considered in the Constant Power Performance analysis. The equation of motion for this case when the rotating masses are included reads:

$$\frac{dv}{dt} = \frac{1}{m_{eq}(n)} \left[\frac{P}{v} - F_{RR}(v) - F_A(v) \right] \tag{3.134}$$

From the kinematic relation (no slip assumption):

$$n = \frac{\omega_e}{v} r_w \tag{3.135a}$$

but since power is kept constant, there are two different cases:

(a) Torque is also constant: for this case, the engine speed must be fixed too, since torque multiplied by speed equals power. If engine speed is a constant ω_e^*, then for each vehicle speed, say v^*:

$$n = \frac{\omega_e^*}{v^*} r_w \tag{3.135b}$$

At every instant, the velocity values are determined from the integration of Equation 3.134 and the gear ratio n can be evaluated from Equation 3.135b. It should be noted that this equation will result in large values for n at very low speeds, therefore, an upper limit for n should be imposed in the program.

(b) Torque is variable: if the engine torque is variable while the power is constant, it means the engine speed must vary to keep power constant. In this case, Equation 3.135a is unable to produce a result for n unless the variation of engine speed is known. This will require an additional criterion to change the engine speed in a desired manner (e.g. for fuel economy).

Example 3.9.3

For the vehicle in Example 3.5.4, find the effect of rotating masses on the time history of vehicle speed. Use the information in Example 3.9.1 for the rotating masses. Assume a fixed engine rpm of 500 rad/s and a maximum overall gear ratio of 16.

Solution

The instantaneous value of gear ratio n can be calculated from Equation 3.135b and equivalent mass calculations from the statements given in Example 3.9.2 can be used in this case too. It should be noted that the described process must be included within the '*function*' and not inside the main program.

Figure 3.77 compares the effect of including the rotating masses with those of the base case with no rotating masses. It is evident that the vehicle speed is considerably lower when the rotating masses are included.
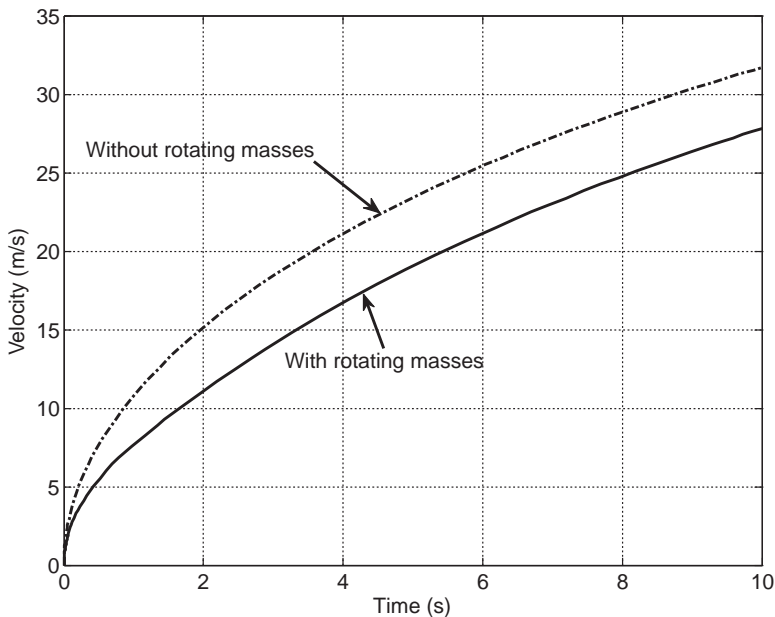
Figure 3.77   Effect of rotating masses on CPP acceleration performance

3.10 Tyre Slip

In the foregoing discussions in order to simplify the relation of the vehicle speed to the wheel rotational speed, the driving wheels were assumed to roll without slipping. In reality, however, this is not the case since according to the discussions in Section 3.3, the traction force is produced by the tyre only if longitudinal slip is developed between the tyre and road surface. In fact, in the real driving situation, the process by which the vehicle motion is built up can be described by the flowchart of Figure 3.78. According to this process, the transformation of the wheel torque to the tyre traction force is accomplished through the generation of tyre slip. This process, in addition to the vehicle longitudinal dynamics, involves the wheel rotational dynamics in which the input torque generates the wheel rotational speed. The rotational motion of a driving wheel can be modelled according to the free body diagram of Figure 3.79.

Application of Newton's Second Law to the rotation of a wheel results in:

$$T_w - F_x r_w = I_w \frac{d\omega_w}{dt} \tag{3.136}$$

in which T_w is the wheel torque, ω_w is the rotational speed of the wheel and I_w is the polar moment of inertia of the wheel including the other rotating parts (see Section 3.9). From Equation 3.11, the tyre slip is:

$$S_x = 1 - \frac{v}{r_w \omega_w} \tag{3.137}$$

Equations 3.136 and 3.137 show the interdependency between the wheel speed ω_w and slip S_x. In fact, Equation 3.136 is a differential equation which, when integrated, leads to values for the wheel rotational speed ω_w. To this end, however, S_x must be available beforehand but it is dependent on the wheel rotational speed (Equation 3.137). With a numerical solution the problem can be resolved by having an initial condition for the vehicle motion, e.g. starting from rest. The wheel rotational speed and vehicle speed are then obtained by simultaneous numerical integration for ω_w and v of the vehicle. The solution of the differential Equation 3.136 together with Equation 3.137 involves rapid fluctuations in the wheel slip and its rotational speed values. In MATLAB to solve this type of

Figure 3.78   The process of the development of vehicle motion from engine torque
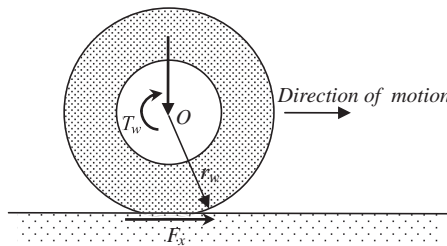
Figure 3.79   Free body diagram of a driving wheel

differential equations one must invoke '*ode15s*' instead of '*ode45*'. There are also other points that must be taken into consideration:

(a) In the equation of longitudinal motion, the tractive tyre force F_x is a function of normal load on the tyre and tyre slip S_x (see Section 3.3):

$$F_x = F_x(F_z, S_x) \qquad (3.138)$$

The Magic Formula could be used for this, for example (see Section 3.3).

(b) The problem is sensitive to the wheel speed initial condition and different initial conditions for ω_w can lead to different output results for the wheel rotational speed, especially at low speeds. A reliable initial rotational speed assumption for the wheel in a motion starting from rest is 100^*eps, which is still a very small value (2.22×10^{-14}).

(c) In practice, S_x during longitudinal acceleration performance is bounded by the $1 \geq S_x \geq 0$ range. Mathematically, however, Equation 3.137 can have results outside the range, e.g. $S_x > 1$ (even very large values) or $S_x < 0$. In programming, therefore, care must be taken to impose the necessary constraints on S_x to keep it within practical limits.

The programming for this problem is left to the reader and typical speed and acceleration results are given below as a reference. The time history of vehicle speed looks like that shown in Figure 3.80. This figure also shows the equivalent centre of wheel speed that is wheel rotational speed times its radius. It is clear that the equivalent speed must be greater than the vehicle speed due to the wheel slip. The time history of vehicle acceleration is depicted in Figure 3.81 together with the same results for the case with no wheel slip. It is noted that there is a short delay in the response of the vehicle owing to
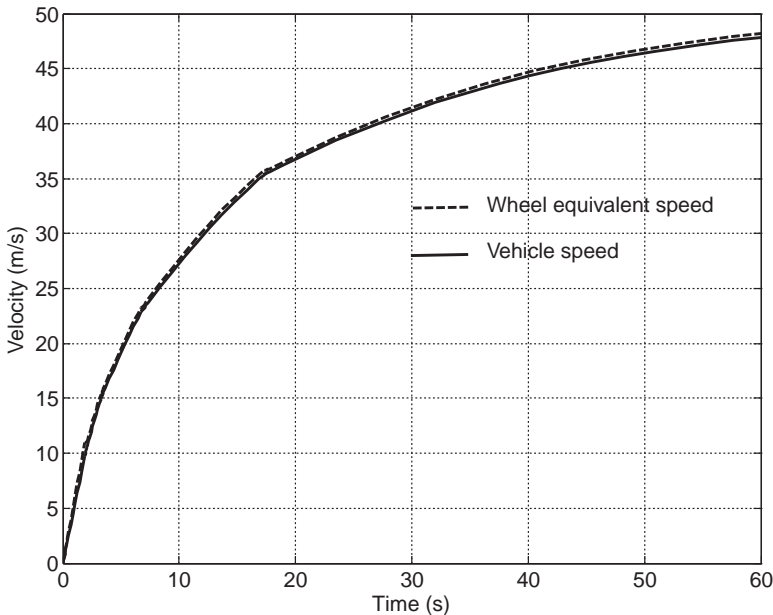
Figure 3.80   Vehicle and wheel equivalent speeds with wheel dynamics
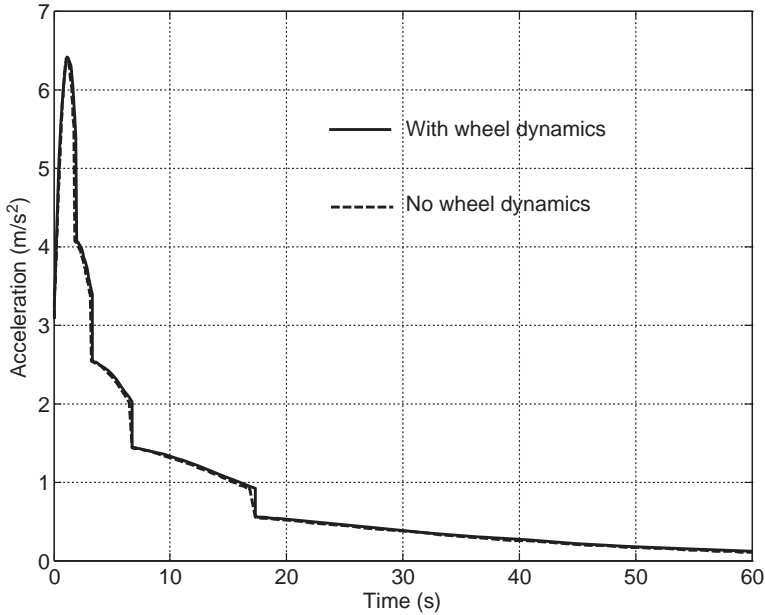
Figure 3.81   Vehicle acceleration with and without wheel dynamics

the wheel dynamics. In fact, with the wheel dynamics in effect, the tyre tractive forces build up after the tyre slip is generated.

3.11   Performance on a Slope

So far the vehicle motion was assumed to take place on a level road only for the sake of simplicity. In this section, the effect of motion on a slope will be discussed. It should be noted that the intention is to see what happens to the vehicle performance (e.g. speed or acceleration) when it moves on a sloping road. Another area of interest is to examine the grade capability of a vehicle – which will be discussed in Chapter 4.

The vehicle motion on a slope can be viewed from the following perspectives:

- How will a vehicle accelerate?
- What is the maximum vehicle speed at each gear?
- What is the maximum slope a vehicle can move on at a specified speed?
- What is the vehicle performance on a road of variable slope?

The FBD of a vehicle on a sloping road was shown in Figure 3.36 with all forces acting on it and the governing equation of motion was shown to be of the form:

$$m\frac{dv}{dt} = F_T - W(f_R \cos\theta + \sin\theta) - cv^2 \tag{3.139}$$

Depending on the nature of the tractive force F_T the solution method will be different as it was discussed in previous sections.

3.11.1   Constant Power Performance (CPP)

For the constant power case, there is no concern about the gear ratios and with the inclusion of the angle θ in the equation of motion, the performance can be analyzed during vehicle acceleration. The acceleration performance and maximum speed of vehicle on the slope will obviously be reduced due to the increase in resistive forces. The MATLAB program of Figure 3.39 already includes the slope terms and can be used without any change. In order to find the maximum slope on which the vehicle can move with a specified speed, the same MATLAB program for finding maximum speed can be used. In fact, with an iteration procedure the input slope can be varied until the specified maximum speed is reached.

Example 3.11.1

For the vehicle in Example 3.5.2, obtain the time histories of velocity and acceleration for slopes of 0, 10 and 20 degrees.

Solution

Using the MATLAB program of Figure 3.39 for the specified slopes will produce the results shown in Figure 3.82.
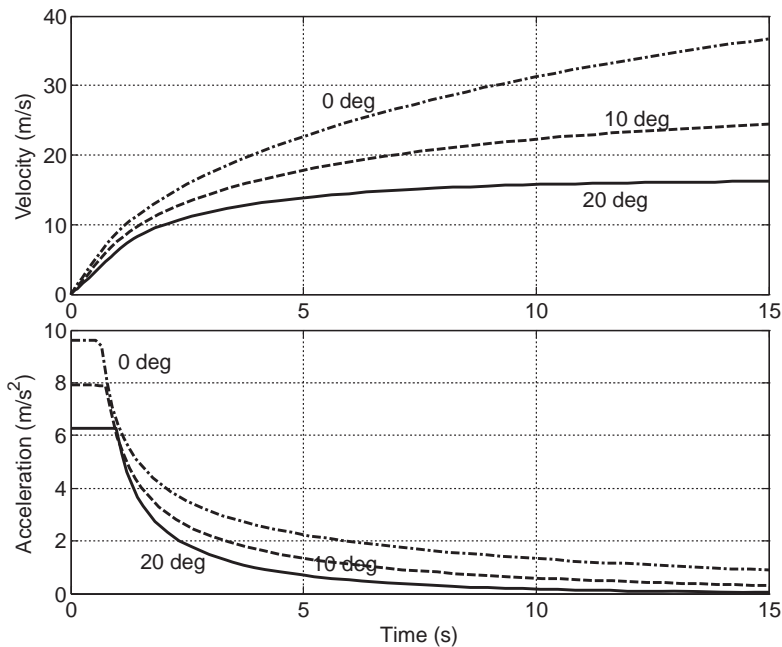
Figure 3.82   Results of Example 3.11.1

3.11.2   *Constant Torque Performance (CTP)*

In this case, the gearshifts occur and it is necessary to examine if the vehicle can ascend a slope in a certain gear. In each gear, therefore, there is a certain maximum slope that vehicle can move at a constant speed. In order that the vehicle can maintain the speed in a specific gear n_i right after an upshift, the force balance must be positive at the time of gearshift, i.e.:

$$\frac{n_i}{r_w}T - F_0 - c[v_{\max}(i-1)]^2 > 0 \tag{3.140}$$

where:

$$F_0 = W(f_R \cos\theta + \sin\theta) \tag{3.141}$$

and $v_{\max}(i-1)$ is the maximum speed of previous gear prior to the gearshift. If Equation 3.140 is not satisfied at gear i, the vehicle cannot keep the final speed of previous gear and either a lower maximum speed is achieved or a downshift to a lower gear is required. The maximum achievable vehicle speed in each gear n_i can be written as (Equation 3.96):

$$v_{\max}(i) = \left[\frac{1}{c}\left(\frac{n_i}{r_w}T - F_0\right)\right]^{0.5} \tag{3.142}$$

provided that the term in the parenthesis is positive – otherwise gear n_i cannot be maintained and a downshift would be necessary. In addition, the resulting value from Equation 3.142 must be less than or equal to the kinematic speed limit:

$$v_{\max}(i) \le \frac{r_w}{n_i}\omega_m \tag{3.143}$$

In fact, the minimum of the two results obtained from Equations 3.142 and 3.143 is the maximum speed in that gear. The required changes for the inclusion of slopes in the MATLAB programs are straightforward.

Example 3.11.2

For the vehicle in Example 3.6.2, plot the time variation of velocity for successive gearshifts at slopes 0, 5 and 10 degrees.

Solution

Inclusion of slope in the calculations is simply done by replacing 'f0' in Figure 3.53 with:

f0 = m*9.81*(fr*cos(theta) + sin(theta))

The result of running the program is depicted in Figure 3.83. It is clear that the vehicle can accelerate even in gear 4 on the slopes of 0 and 5 degrees, whereas on the 10-degree slope the gearshift from 3 to 4 will result in a negative acceleration that eventually may need a downshift to 3 again. This can be seen by examining Equation 3.140 as the results given in Table 3.11 indicate that
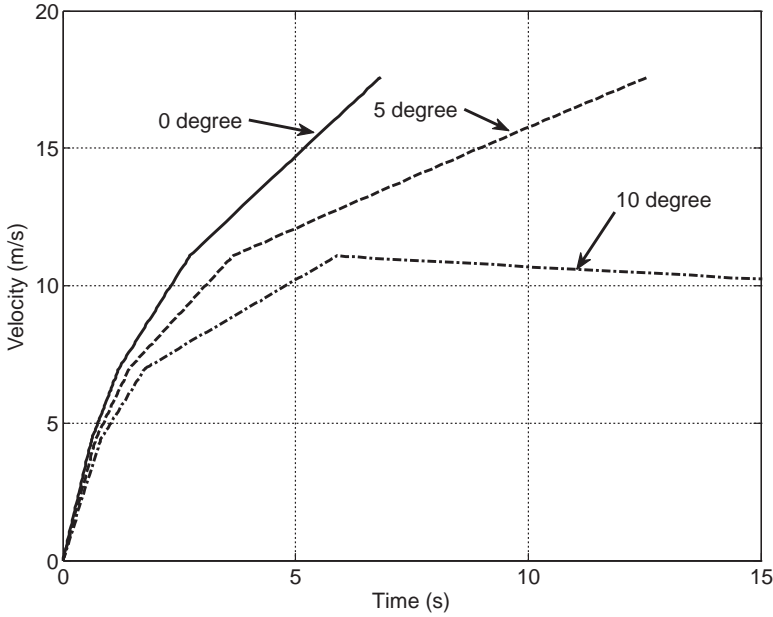
Figure 3.83   Results of Example 3.11.2

on a 10-degree slope, a gearshift to 4 results in a negative force balance which means in this gear the vehicle will decelerate.

Table 3.11   Force balance (Equation 3.140) over slopes (N)

Gear	1	2	3	4
5-deg slope	12566	7125	3686	1475
10-deg slope	10873	5432	1993	−217

3.11.3   Fixed Throttle (FT)

For this case too, the concept is similar to those discussed in previous sections and the force balance condition for any gear to maintain a positive acceleration after an upshift on a slope is:

$$\frac{n_i}{r_w} T_e(\omega_i, \theta) - F_0 - c[v_{max}(i-1)]^2 > 0 \tag{3.144}$$

where $T_e(\omega_i, \theta)$ is the engine torque at a given throttle input θ and at engine rpm ω_i immediately after shifting to n_i. If this condition is not satisfied for a gear n_i, the resultant force in the direction of motion will be negative after an upshift, and a downshift might be necessary if the engine speed is reduced to a low value ω_L. A steady state maximum vehicle speed is also attainable for those gears not satisfying Equation 3.144 but at a lower value than that of the previous gear. In any case, the constraint for the engine speed (Equation 3.143) should not be violated.

Example 3.11.3

Repeat Example 3.7.2 for slopes of 5 and 10 degrees. Also evaluate the force balance of Equation 3.144 to show which gear can maintain a positive acceleration.

Solution

The inclusion of slopes in the MATLAB program is similar to the previous example and the time histories of velocity and distance for the three cases are presented in Figure 3.84. On the flat road all the gears generate positive accelerations. On the 5-degree slope the fifth gear cannot maintain a positive acceleration and on a 10-degree slope even the fourth gear has similar problems so that gear 5 is not engaged. The results of Equation 3.144, summarized in Table 3.12, are produced at the maximum engine torque and support those of Figure 3.84.
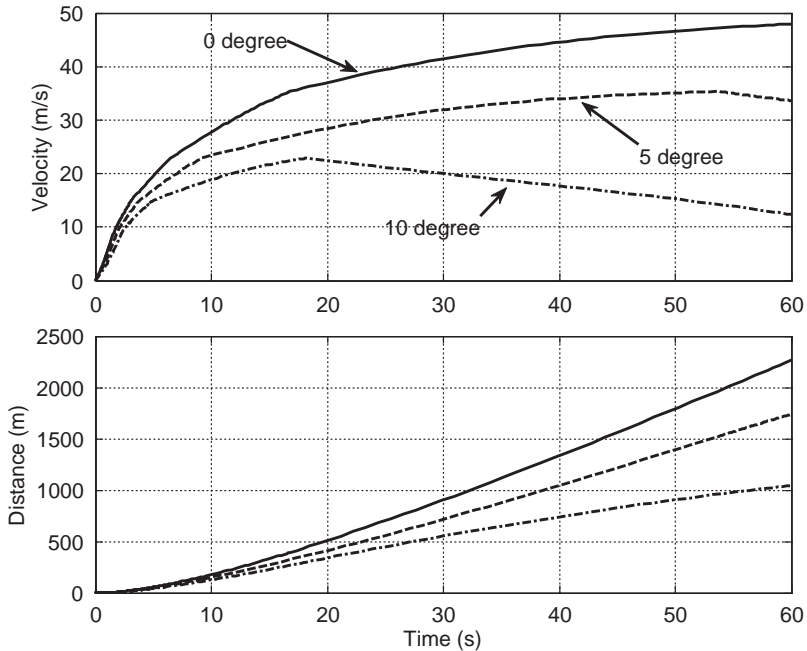
Figure 3.84   Time histories of velocity and distance for Example 3.11.3

Table 3.12   Force balance (Equation 3.144) over slopes (N)

Gear	1	2	3	4	5
5-deg slope	5569	3219	1684	587	−296
10-deg slope	4722	2373	838	−260	−629

3.11.4 Variable Slopes

If the vehicle motion involves several piecewise-constant slopes, the solution can be divided into several solutions for each slope. The initial conditions for every slope are the final results of the previous slope. In general, the slope can be expressed as a varying elevation-distance function and it must be defined inside the MATLAB '*function*'.

Example 3.11.4

The vehicle of Example 3.11.3 starts accelerating from rest and just before gearshift to 5 enters a slope of 10 degrees and continues with gear 4. Knowing that a downshift must be carried out when the engine speed reduces to 2000 rpm, determine the distance travelled on the slope before a downshift to gear 3 is necessary.

Solution

This problem can be solved in two parts. In the first part, the vehicle motion on a level road is considered and its speed before upshift to gear 5 can easily be obtained (see Example 3.7.2). The result is 35.343 m/s. The second part is the vehicle motion on a 10-degree slope at gear 4 with this initial speed. The distance up to the point when the engine speed reduces to 2000 rpm is the answer. The MATLAB program of Figure 3.59, modified to include the slope, needs a small change in the integration loop as shown in Figure 3.85. The distance travelled is found to be 1555 m after 70 seconds on the slope, when the speed is 46.3 km/h and the engine speed is 2000 rpm.

```
wlow=2000;        % Set low engine rpm
we=1500;          % A value (less than 'wlow') for 'while' statement
t0=0; tf=80;
x0=[35.3429 0];   % Speed just before entering on the slope

for i=4: 4                  % Only gear 4

   while we – wlow <      0.001    % Repeat statements until we ≅ wlow

   [t,x]=ode45(@Fixed_thrt, [t0 tf], x0);
   v=x(:,1);
   we=30*ni*v(end)/rw/pi; % Engine speed at the end of integration process
    if we < wlow
        tf=tf*we/wlow;              % Integration time should be reduced
    elseif we-wlow>=0.01            % A small margin for fast convergence
        tf=tf*we/wlow;
        we=1500;
   end
   end
s=x(:,2);
   end
```

Figure 3.85   Changes to the MATLAB program for Example 3.11.4

3.12   Vehicle Coast Down

Vehicle coast down is a condition in which the transmission is disengaged (gear in neutral) and the vehicle is left to roll freely from a particular speed and come to a stop under the action of the resistive forces. A coast down test is very useful when measuring the characteristics of resistive forces acting during vehicle motion. On a level road, the resistive forces comprise the driveline rotational frictions, the rolling resistance and the aerodynamic force. From a coast down test, the time history of vehicle speed can be obtained. In order to exclude the effects of air movements on the results, the tests are usually performed in still, no-wind air conditions. The mathematical modelling of vehicle motion previously developed can be applied to this type of vehicle motion with no motive force from the prime mover and the gradual deceleration of the vehicle under the action of the resistive forces only. The equation of longitudinal motion in a coast down situation will be simpler owing to the absence of the tractive force:

$$m\frac{dv}{dt} = -F_{RR} - cv^2 \tag{3.145}$$

in which F_{RR} is the rolling resistance force and the term cv^2 is the aerodynamic force. If the time history of the vehicle speed is available, the two unknowns can be determined. However, the solution depends on the nature of the resistive forces especially the rolling resistance that can be considered a constant or as a function of speed. These will be considered in following sections.

3.12.1   Constant Rolling Resistance

Assuming a constant rolling resistance force is a common practice in many cases, i.e.:

$$F_{RR} = f_R W = F_0 \tag{3.146}$$

From the time history of vehicle speed it is possible to determine the rolling resistance coefficient f_R and aerodynamic coefficient c.

3.12.1.1   Simple Model

With only a simple test we can estimate the 'F_0' and 'c' values. This test consists of two high speed and low speed parts. Two sets of data are recorded at high speed and low speed cases. Each set consists of an incremental velocity change defined as v_{H1} and v_{H2} at high speed and v_{L1} and v_{L2} at low speed. The incremental velocity can be as small as 5 km/h. The time increments over which the velocity increments occur are called Δt_H and Δt_L. The mean velocities at each case are defined as:

$$v_H = \frac{v_{H1} + v_{H2}}{2} \tag{3.147}$$

$$v_L = \frac{v_{L1} + v_{L2}}{2} \tag{3.148}$$

The mean decelerations at each velocity are defined as:

$$a_H = \frac{v_{H2} - v_{H1}}{\Delta t_H} \tag{3.149}$$

$$a_L = \frac{v_{L2} - v_{L1}}{\Delta t_L} \tag{3.150}$$

The equations of motion (Equation 3.145) for the low and high speeds can be expressed in terms of the above definitions as:

$$ma_H = -F_0 - cv_H^2 \tag{3.151}$$

$$ma_L = -F_0 - cv_L^2 \tag{3.152}$$

At low speeds it is quite reasonable to ignore aerodynamic force and Equation 3.152 can be simplified to:

$$F_0 = m\frac{v_{L1} - v_{L2}}{\Delta t_L} \tag{3.153}$$

This is an equation suitable for calculating the rolling resistance force. Substituting Equation 3.153 into Equation 3.151 and using Equations 3.148 and 3.150 results in:

$$c = \frac{4m}{\Delta t_L \Delta t_h} \cdot \frac{\Delta t_L(v_{H1} - v_{H2}) - \Delta t_H(v_{L1} - v_{L2})}{(v_{H1} + v_{H2})^2} \tag{3.154}$$

If incremental velocities in both low speed and high speed are taken equal, i.e.:

$$\Delta v = v_{H1} - v_{H2} = v_{L1} - v_{L2} \tag{3.155}$$

then the results for F_0 and c simplify to:

$$F_0 = m\frac{\Delta v}{\Delta t_L} \tag{3.156}$$

$$c = \frac{4m}{\Delta t_L \Delta t_h} \cdot \frac{(\Delta t_L - \Delta t_H)\Delta v}{(v_{H1} + v_{H2})^2} \tag{3.157}$$

Example 3.12.1

The coast down test result for a vehicle with mass of 1600 kg is given in Table 3.13. Calculate the rolling resistance force F_0 and the coefficient of aerodynamic force c.

Table 3.13   Vehicle coast down test results

	Speed (km/h)	Time (s)
1	110	0
2	100	4.1
3	30	54.5
4	20	64.0

<div style="border:1px solid black;">

Solution

The incremental speeds at low and high speeds are both equal to 10 km/h. Calculations are straightforward; convert speeds to m/s and the results are:

$$F_0 = 1084 \, \text{N} \, (f_R = 0.0691)$$

$$c = 0.7243$$

</div>

3.12.1.2   Analytical Model

For the general coast down case, the equation of motion can be integrated analytically. Equation 3.145 can be written as:

$$c_m dt = - \frac{dv}{v^2 + 1/f^2} \tag{3.158}$$

in which:

$$c_m = \frac{c}{m} \tag{3.159}$$

$$f = \sqrt{\frac{c}{F_0}} \tag{3.160}$$

Integration of Equation 3.158 results in:

$$Arc \tan vf = \frac{c_m}{f} (t_0 - t) + Arc \tan v_0 f \tag{3.161}$$

In general, at time t_0 the speed is v_0, but is always possible to take $t_0 = 0$, therefore:

$$Arc \tan vf = - \frac{e}{m} t + Arc \tan v_0 f \tag{3.162}$$

where:

$$e = \sqrt{cF_0} \tag{3.163}$$

If test data for two points, say, points 1 and 2, are available, then:

$$Arc \tan v_1 f = - \frac{e}{m} t_1 + Arc \tan v_0 f \tag{3.164}$$

$$Arc \tan v_2 f = - \frac{e}{m} t_2 + Arc \tan v_0 f \tag{3.165}$$

Equations 3.164 and 3.165 constitute a set of two non-linear equations for the two unknowns e and f. With an iteration technique like MATLAB's '*fsolve*', the equations can be solved and once e and f are obtained,

the aerodynamic coefficient c and rolling resistance coefficient f_R can simply be calculated from:

$$c = ef \tag{3.166}$$

$$f_R = \frac{e}{fmg} \tag{3.167}$$

An interesting result from this method is the evaluation of vehicle mass from a coast down test. Hence, if a further data point is available, then three equations can be solved for three unknowns e, f and m.

Example 3.12.2

A selection of data recorded in the coast down test for a light duty truck is given in Table 3.14. Use four rows of the table to evaluate rolling resistance coefficient f_R, aerodynamic force coefficient c and vehicle mass m. If the frontal area is 2.5 square metres and the air density is 1.2 kg/cubic metre, calculate the drag coefficient.

Table 3.14 Vehicle coast down test results

Speed (km/h)	110	100	90	80	70	60
Time (sec)	0	4	9	14.3	20.7	28
set	1	2	3	4	5	6

Solution

A MATLAB program consisting of a main program and a function as shown in Figure 3.86 is suitable to solve the problem. Four sets of data are needed for the calculation of the unknowns. The following sets are chosen:

(a) sets: 1, 3, 5 and 6
(b) sets: 1, 2, 4 and 6
(c) sets: 1, 2, 3 and 5
(d) sets: 1, 3, 4 and 5

The results obtained for all cases are summarized in Table 3.15.

Table 3.15 Results for Example 3.12.2

Case	c	f_R	m	C_D
a	0.99	0.020	1767	0.66
b	0.94	0.0199	1672	0.627
c	0.98	0.020	1752	0.653
d	0.98	0.020	1752	0.653

```
% MATLAB program 'maincdfr.m'
% Program for the calculation of Cd and Frr from Coast-down data
% Data is in the form of a two-column table of t and v test values

clear all, close all, clc

global v t i j k

% In the solution four rows of data are used at a time: Row 1 and rows i, j and k
% Enter values for i, j and k:
i=?; j=?; k=?;

% Input data
v=[110 100 90 80 70 60].';
t=[0 4 9 14.3 20.7 28].';

% Initial guess for variables:
% Solution requires a guess for the three variable x(1), x(2) and x(3)
% Note that C=x(1)*x(2), fR=x(2)/x(1) and m=x(3)
x0=[7  0.05  1750];

% Set options for 'fsolve'
options=optimset('TolFun',1.e-10, 'MaxFunEvals', 1.e+6);

x=fsolve(@cdfrr, x0, optimset('fsolve'))

c=x(1)*x(2)
fR=x(2)/x(1)
m=x(3)
```

(a)

```
% MATLAB function 'cdfrr.m' called from maincdfrr.m

function f=f(x)
global v t i j k

c=x(1);
d=x(2);
m=x(3);
a=1/sqrt(m*9.81);
b=1/m/a;
f(1)=atan(v(i)*a*c/3.6)-atan(v(1)*a*c/3.6)+b*d*t(i);
f(2)=atan(v(j)*a*c/3.6)-atan(v(1)*a*c/3.6)+b*d*t(j);
f(3)=atan(v(k)*a*c/3.6)-atan(v(1)*a*c/3.6)+b*d*t(k);
```

(b)

Figure 3.86   MATLAB programs (a) main and (b) function for Example 3.12.2

3.12.2   Rolling Resistance as a Function of Speed

In general, the resistive force can be written (see Section 3.4.1.5) in the form of:

$$F_R = F_0 + f_v v + c v^2 \tag{3.168}$$

The two first terms on the right-hand side represent the rolling resistance force which is considered as a linear function of the vehicle speed. It should be noted that the rolling resistance may also involve a speed-squared term, however, that part will be included in the aerodynamic force. In order that the unknowns F_0, f_v and c are evaluated, the speed-time history obtained from the test must produce the variation of total resistive force versus velocity. To this end, the basic form of the equation of motion in a coast down test reads:

$$m \frac{dv}{dt} = -F_R \tag{3.169}$$

Thus by differentiating the time history of vehicle velocity with respect to time, the resistive force versus time will be obtained. If a quadratic curve is fitted to the F_R-v data, it will have the form:

$$F_R = a + bv + cv^2 \tag{3.170}$$

from which the unknowns F_0, f_v and c can be evaluated by a simple comparison of Equations 3.168 and 3.170. It is worth noting that this technique can be applied for powers of speed more than 2. For example, it is possible to include an extra term with a power of 3 for speed v and use the same procedure to obtain the unknown coefficients. The drawback of this method is its sensitivity to the accuracy of test data owing to the differentiation involved in the process. In order to avoid such errors, a more sophisticated non-linear curve fitting techniques must be used.

3.12.3   Inertia of Rotating Masses

At the start of a coast down test, the vehicle has a certain initial velocity and all driveline rotating components have their respective rotational speeds. The total mechanical energy E of the system at the starting instant, therefore, consists of kinetic energies of vehicle body together with those of the rotating inertias:

$$E = \frac{1}{2} m v^2 + \frac{1}{2} \sum I_i \omega_i^2 \tag{3.171}$$

The second term can be written for the rotating components including wheels, axles, propeller shaft and gearbox output shaft (it is assumed that the gear is in neutral and clutch is disengaged, so the input shaft and gears inside the gearbox are not rotating). Thus:

$$\sum I_i \omega_i^2 = I_{wA} \omega_w^2 + n_f^2 I_p \omega_w^2 = I_{eq} \omega_w^2 \tag{3.172}$$

in which I_{wA} is the sum of all rotating inertias with the wheel speed and I_p is the sum of those rotating inertias with the speed of differential input shaft (or gearbox output shaft):

$$I_{eq} = I_{wA} + n_f^2 I_p \tag{3.173}$$

Assuming no slip for the tyres, one can write:

$$\omega_w = \frac{v}{r_w} \tag{3.174}$$

Equation 3.171 thus can be simplified to:

$$E = \frac{1}{2}mv^2 + \frac{1}{2}I_{eq}\left(\frac{v}{r_w}\right)^2 = \frac{1}{2}\left(m + \frac{I_{eq}}{r_w^2}\right)v^2 \tag{3.175}$$

This energy will be dissipated by the work done by resistive forces acting on the vehicle, until the vehicle comes to a complete stop. The work of the resistive forces is:

$$U = \int F_R ds = \int F_{RR} ds + \int F_A ds \tag{3.176}$$

where s is the distance travelled. For the case of a constant rolling resistance force, between any two points 1 and 2, it can be written:

$$\Delta U = U_2 - U_1 = \int_1^2 f_R W ds + \int_1^2 cv^2 ds \tag{3.177}$$

The first integral results:

$$\int_1^2 f_R W ds = f_R W \int_1^2 ds = f_R W A_1 \tag{3.178}$$

in which A_1 is the area under the v-t diagram:

$$A_1 = s_2 - s_1 = \Delta s = \int_1^2 ds = \int_1^2 v dt \tag{3.179}$$

and can be determined from summing up the surface between times t_1 and t_2. The second integral in Equation 3.177 can be changed to a time domain integral:

$$A_2 = \int_1^2 v^2 ds = \int_1^2 v^3 dt \tag{3.180}$$

This is the area under the v^3-t diagram and can be obtained by processing the original data. Thus the total work of Equation 3.177 is:

$$\Delta U = U_2 - U_1 = A_1 f_R W + A_2 c \tag{3.181}$$

The energy change between any two instants is:

$$\Delta E = \frac{1}{2}\left(m + \frac{I_{eq}}{r_w^2}\right)(v_2^2 - v_1^2) \tag{3.182}$$

This must be equal to the work done by the resistive forces within this period:

$$\frac{1}{2}\left(m + \frac{I_{eq}}{r_w^2}\right)|v_2^2 - v_1^2| = A_1 f_R W + A_2 c \tag{3.183}$$

In Equation 3.183 all parameters are known but I_{eq}, therefore:

$$I_{eq} = \left(2\frac{A_1 f_R W + A_2 c}{|v_2^2 - v_1^2|} - m\right)r_w^2 \tag{3.184}$$

For the speed-dependent rolling resistance assumption, too, a similar procedure can be followed. Also it should be noted that the equivalent rotating inertia of Equation 3.173 does not include the rotating masses with engine speed (gearbox input shaft). If a special coast down test is carried out with the gear engaged in an arbitrary gear with only the clutch pedal depressed, then from the test results the full value of rotating masses as seen on the driving wheels can be determined by the method explained in this section.

Example 3.12.3

Use the information of Example 3.12.2 and calculate the equivalent inertia at the driving wheels of the rotating masses. Tyre rolling radius is 38 cm.

Solution

According to Equation 3.184, information for every two points can be used to determine the equivalent inertia for the rotating masses. If data for any two neighbouring points are used, the result will be those listed in Table 3.16. There are negative values for the inertia which is unacceptable and this reflects errors in the data and inaccuracy of calculations between two adjacent points. The average value from the table is some $1.5 \, \text{kg} \, \text{m}^2$. A close result can also be obtained if A_1 and A_2 are the sums of all surfaces from $t = 0$ to $t = 28$. The results are:

$$A_1 = 639, \; A_2 = 365430 \text{ and } I_{eq} = 1.41 \text{ kg.m}^2.$$

Table 3.16   Solution with any two adjacent points

Speed (km/h)	110	100	90	80	70	60
Time (s)	0	4	9	14.3	20.7	28
A_1 (Eq. 3.179)	0	116.7	132.0	125.1	133.3	131.8
A_2 (Eq. 3.180)	0	99923	92646	70487	58642	43732
I_{eq} (Eq. 3.184)	–	−7	15.2	−6.2	4.8	0.85

3.13   Driveline Losses

In the preceding discussions the assumption was made that the driveline system is ideal in such a way that all the power transmitted by the driveline will be delivered to the wheels. In practice, however, every component in the driveline will involve losses due to internal friction. The torque necessary to overcome the friction multiplied by speed of rotation of the component results in the power lost to the friction of that component.

3.13.1   Component Efficiencies

Consider a torque-transmitting component shown in Figure 3.87. The input and output powers are:

$$P_i = T_i \omega_i, \; P_o = T_o \omega_o \tag{3.185}$$
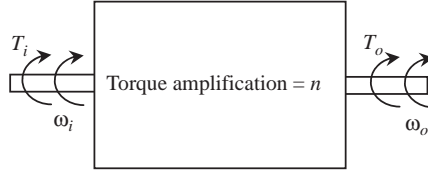
Figure 3.87   A torque-carrying component

Due to the rigid connections between the input and the output (flexibilities are ignored), the output rotational speed is related to the input speed by:

$$\omega_o = \frac{1}{n}\omega_i \tag{3.186}$$

The input energy is:

$$E_i = \int P_i dt = \int T_i \omega_i dt = n\int T_i \omega_o dt \tag{3.187}$$

The efficiency of the torque transfer is defined as the ratio of the output to the input energies:

$$\eta = \frac{E_o}{E_i} = \frac{\displaystyle\int T_o \omega_o dt}{n\displaystyle\int T_i \omega_o dt} \tag{3.188}$$

At constant speed and torque inputs, this simplifies to:

$$\eta = \frac{T_o}{nT_i} = \frac{T_o}{T_o^*} \tag{3.189}$$

in which T_o^* is the output torque at the ideal (no power loss) condition. Thus, it is concluded that when there is energy loss in a component, the output torque will be reduced with respect to the ideal output torque by a factor smaller than 1, defined as the efficiency of that component, i.e.:

$$T_o = \eta T_o^* \tag{3.190}$$

which also leads to:

$$P_o = \eta P_i \tag{3.191}$$

The torque loss T_L and power loss P_L for the component are:

$$T_L = T_o^* - T_o = n(1 - \eta)T_i = \frac{1 - \eta}{\eta}T_o \tag{3.192}$$

$$P_L = P_i - P_o = (1 - \eta)P_i = \frac{1 - \eta}{\eta}P_o \tag{3.193}$$
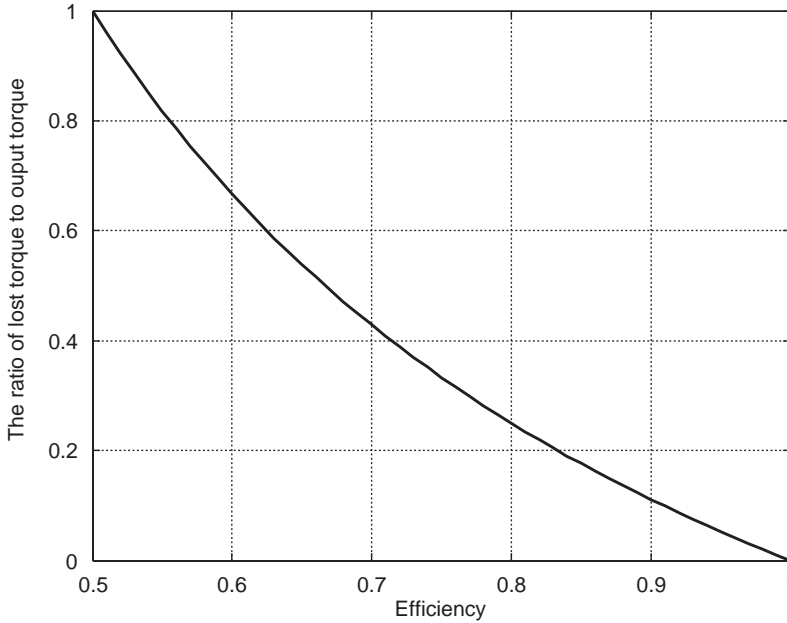
Figure 3.88   The variation of the ratio of torque loss to output torque with efficiency

Figure 3.88 shows the ratio of torque loss T_L to the output torque T_o with the variation of efficiency. For efficiencies less than 0.5 the output torque is less than the torque loss (see Equation 3.192).

   In the above discussions, a constant speed was considered at the time of a constant torque delivery and the dependency of the power loss on the speed of rotation or the value of torque was not considered. In fact, friction in the moving parts is of two different natures: dry and/or viscous. The former is independent of relative speed between the moving parts and once the movement starts, it remains proportional to the load (kinetic friction). Viscous friction, however, is speed-dependent and increases as the relative speed of moving parts increase.

   The dry friction is often assumed to be linearly dependent on the load ($F = \mu N$). Examples of this type of friction in a driveline are contact friction between gear teeth and friction in bearings. When larger torques are transferred, the contact forces on the gear teeth increase and lead to larger friction forces. The same also goes for bearing loads. Speed-dependent friction is typically due to churning and pumping losses of the lubricant which increase with rotational speed. These losses are not usually affected by the amount of torque that is transmitted. There is also another type of loss that is almost constant, regardless of rotational speed or transmitted torque – sliding friction in seals typically behave this way.

   In general, the efficiency of a component, therefore, must be considered to depend on speed and load, i.e.:

$$\eta = \eta(T, \, \omega) \tag{3.194}$$

In practice, however, it is a common to assume the efficiency is a constant value. In fact, it is an approximation to the real losses in the drivetrain system. This assumption means that increasing the
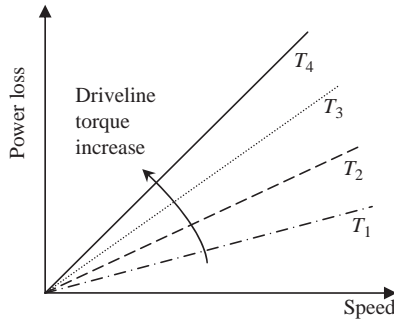
Figure 3.89   Power loss changes with speed and torque

speed of rotation at a specified torque (power increase) will only increase the power loss in the component (Equation 3.193) and will not influence the torque loss (Equation 3.192). Conversely at a specified speed, torque increase will increase both the torque and power losses. As Figure 3.89 summarizes, along a line of a certain torque T_i the torque loss is constant but the power loss increases with speed.

For the vehicle driveline with several components, the wheel torque is:

$$T_w = \eta_c \eta_g \eta_j \eta_d \eta_a \eta_w T_w^* = \eta_{ov} T_w^* \tag{3.195}$$

in which η_{ov} is the overall efficiency and subscripts c, g, j, d, a and w stand for clutch, gearbox, joint (universal or constant velocity), differential, axles and wheels respectively. T_w^* is the ideal wheel torque:

$$T_w^* = n_g n_f T_e = n T_e \tag{3.196}$$

It should be noted that the clutch efficiency treatment for the transient phase is different from what is considered here, nevertheless the concept will be similar (see Section 4.5.5).

Example 3.13.1

Repeat Example 3.7.2 assuming the efficiencies of the driveline components are 0.97 for the gearbox, 0.94 for the final drive and 0.90 for the rest of components combined.

Solution

The inclusion of Equations 3.195 and 3.196 in the MATLAB program is a simple task. The component efficiencies must be defined in the main program and the overall efficiency (say '*etov*') must be shared with the '*function*' in '*global*' statement. The tractive force is simply modified to Fti=etov*Trq*ni/rw;. The result of the modified program is compared with those of Example 3.7.2 in Figure 3.90.
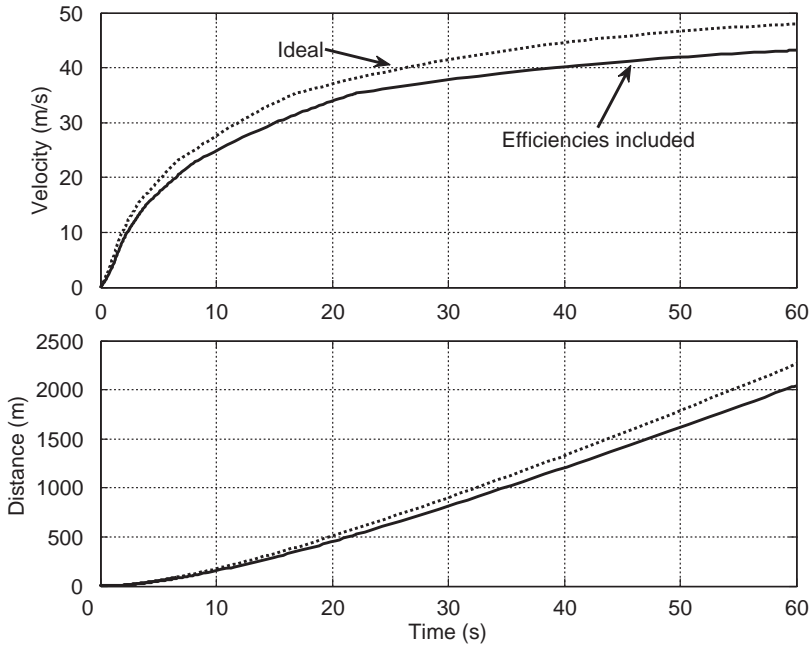
Figure 3.90   Effect of efficiencies on the vehicle performance of Example 3.7.2

Example 3.13.2

A vehicle test shows that when the engine torque is 100 Nm, at a certain engine speed, a wheel torque of 1200 Nm is produced. With overall gear ratio of 15, calculate the driveline efficiency and the torque loss.

Solution

From Equations 3.195 and 3.196:

$$\eta_{ov} = \frac{T_w}{nT_e} = \frac{1200}{15 \times 100} = 0.8$$

and the lost torque is:

$$T_L = nT_e - T_w = 1500 - 1200 = 300 \, Nm$$

Alternatively:

$$T_L = \frac{1 - 0.8}{0.8} \times 1200 = 300$$

3.13.2   Torque Flow Direction

The driveline efficiency depends on the direction of torque flow. The foregoing discussion applies to the case when the engine torque is transmitted by the driveline to turn the wheels. In the cases when the accelerator pedal is suddenly released during the vehicle motion on a level road or when vehicle is moving downhill, the energy flow is reversed. In the former case, the kinetic energy of vehicle and turning parts is used to overcome the resistive forces and in the latter case the gravitational force is also helping vehicle motion. In both cases, with engaged gears and zero throttle, the engine will run in its braking regions. Thus, in these cases the efficiency equation must be written the other way round, that is:

$$T_e = \eta'_a \, \eta'_d \, \eta'_j \, \eta'_g \, \eta'_c \, T_e^* = \eta'_{ov} T_e^* \tag{3.197}$$

in which,

$$T_e^* = \frac{T_w}{n_g \, n_f} = \frac{r_w F_T}{n} \tag{3.198}$$

The notation of using primes in Equation 3.197 emphasizes that in the reverse direction the efficiency is not necessarily the same as the other direction. The torque loss in driveline this time will be:

$$T_L = T_w - nT_e = (1 - \eta'_{ov})T_w \tag{3.199}$$

3.13.3   Effect of Rolling Resistance

In order to move the vehicle from rest, friction in the driveline must be overcome before the vehicle can start to move. Suppose the vehicle is pushed from rest with the gearbox disengaged until it starts to move. The question is whether or not this amount of force is related to the driveline torque or power loss. In fact, this force is just the rolling resistance force that also includes the non-loaded driveline rolling frictions. Therefore, it should not be confused with the driveline losses during the torque delivery.

The objective of the engine torque is to move the vehicle, but throughout the driveline it overcomes friction, and eventually before turning the wheel, it has to overcome the rolling resistance torque. In other words, the total torque loss in the driveline is the summation of component torque losses T_{CL} and rolling resistance torque T_{RR}:

$$T_L = T_{CL} + T_{RR} \tag{3.200}$$

The output torque used for moving the vehicle is:

$$T_w = T_o^* - T_L \tag{3.201}$$

Since the rolling resistance is already included in the resistive forces against the vehicle motion, substituting Equation 3.200 in 3.201 is not correct and the rolling resistance term must be excluded. Thus the output torque at driving wheels is:

$$T_w = T_o^* - T_{CL} \tag{3.202}$$

For a given overall efficiency η_{ov} the component torque losses can be evaluated as:

$$T_{CL} = nT_e(1 - \eta_{ov}) \tag{3.202}$$

This is what was previously considered as the total torque loss. It should also be noted that the unloaded torque losses of the driveline have already been considered in the rolling resistance, and the efficiency of

the wheel η_w defined earlier represents only those torque losses in the tyre in addition to rolling resistance torque (e.g. tyre slip).

Example 3.13.3

In Example 3.13.2 the effect of rolling resistance was ignored in determining the efficiency of the driveline. For a rolling resistance force of 200 N and tyre rolling radius of 30 cm, determine the true efficiency.

Solution

The component losses should be calculated. The total torque loss is:

$$T_L = 1500 - 1200 = 300 \text{ Nm}$$

From Equation 3.200:

$$T_{CL} = T_L - T_{RR} = 300 - 0.3 \times 200 = 240 \, Nm$$

From Equation 2.203:

$$\eta_{ov} = 1 - \frac{T_{CL}}{T_w^*} = 1 - \frac{240}{1500} = 0.84$$

This is 4% higher than before.

3.14   Conclusion

In this chapter, the basics of vehicle longitudinal dynamics studies were discussed and various forms of the vehicle motion were studied. The tractive force generation by the tyres and its dependence on tyre slip were discussed. The natures of resistive forces against vehicle motion were also described and characterized. The equations of vehicle motion in different forms were developed, starting with the simplest forms and gradually adding other terms.

   Closed form analytical solutions were presented where such solutions are available. These forms are helpful for quick estimations of the approximate performance. For more detailed studies, numerical integrations are preferred and several examples using MATLAB programs are provided. Several example problems were worked out in order to facilitate the understanding of the physics of vehicle motion in different cases. Students are encouraged to become more familiar with the details by reworking the example problems and writing MATLAB programs. Problems in Section 3.16 will further help students build their knowledge on the subjects.

3.15   Review Questions

3.1 Describe the torque-generating properties of engines and motors used in automotive applications.
3.2 Explain the tractive force generation of a tyre with a sliding friction force of rubber on a surface.

3.3 Explain why the Magic Formula representation of the tyre tractive force is different from a simple curve fitting of tyre data.

3.4 Propose a method by which the tractive force of tyre could be maintained at its maximum during the vehicle motion.

3.5 What are the tyre rolling resistance moment and force? How are they related?

3.6 Describe the influencing factors in the tyre rolling resistance generation.

3.7 Explain the main sources of aerodynamic force.

3.8 What are the aerodynamic moments?

3.9 The power delivery from the prime mover to the wheels can be achieved in different ways. Describe the constant power, constant torque and constant throttle cases and how they can be justified.

3.10 List the assumptions involved in the CPP method and explain why they are needed.

3.11 Explain how the final speed of a vehicle is achieved and mathematically how long it takes to attain the maximum speed.

3.12 The maximum speed of a vehicle in each gear is influenced by both kinematic and dynamic factors. Explain how.

3.13 How would you propose to shift the gears in order that a better acceleration performance is achieved?

3.14 Explain why the rotating masses inside the vehicle powertrain would reduce the vehicle acceleration.

3.15 Describe the necessity of having tyre slip for vehicle motion and the cause and effect relationship between the wheel torque and traction force.

3.16 Why is a coast down vehicle test useful? Estimate the length of a road needed for a test speed of 150 km/h.

3.17 What are the basic natures of the torque and power losses of the driveline components? Explain the dependency of the losses on the speed and load.

3.16 Problems

Problem 3.1

The rolling resistance force is reduced on a slope by a cosine factor ($\cos \theta$). On the other hand, on a slope, the gravitational force is added to the resistive forces. Assume a constant rolling resistance force and write the parametric forms of the total resistive force for both cases of level and sloping roads. At a given speed v_0:

(a) Write an expression that ensures an equal resistive force for both cases.
(b) Solve the expression obtained in (a) for the parametric values of corresponding slopes.
(c) For the coefficient of rolling resistance equal to 0.02, evaluate the values of the slopes obtained in (b) and discuss the result.

Result:

(a) $f_R(1 - \cos \theta) = \sin \theta$

Problem 3.2

For the vehicle of Example 3.4.2:

(a) Calculate the overall aerodynamic coefficient for the same temperature at altitude of 1000 m.
(b) Repeat (a) for the same altitude at temperature 30 °C.

(c) At the same altitude of (a), at what temperature does the drag force increase by 20%?
(d) At the same temperature of (a), at what altitude does the drag force reduce by 20%?

Problem 3.3

In order to have a rough estimation of the performance of a vehicle, it is proposed to ignore the resistive forces to obtain the No-Resistive-Force (NRF) performance.

(a) Derive the governing equations of vehicle longitudinal motion for speed $v(t)$ and distance $S(t)$ by ignoring all resistive forces for the CPP (see Section 3.5).
(b) For a vehicle of mass 1.2 ton, determine the required engine power P to achieve an acceleration performance of 0–100 km/h during 10, 8 or 6 seconds.
(c) Evaluate the power increase factors from 10 seconds to t^* seconds defined as $[P/P_{10} = [P(t*) - P(10)]/P(10)]$, for $t^* = 8$ and 6.

Results:

(a) $v = \sqrt{v_0^2 + \dfrac{2Pt}{m}}$, $S = \dfrac{m(v^3 - v_0^3)}{3P}$,
(b) 46.3, 57.9 and 77.2 kW.
(c) 0.25 and 0.67.

Problem 3.4

Use the results of Problem 3.3:

(a) Write the expression for the specific power P_s (in W/kg) of a vehicle to reach a certain speed v (km/h) from the rest at a certain acceleration time t.
(b) Plot the variation of P_s versus t from 6 to 10 seconds. Repeat the result for three speeds of 80, 90 and 100 km/h.
(c) Are the results dependent on the vehicle properties?

Problem 3.5

At very low speeds the aerodynamic force is small and may be ignored. For example, at speeds below 30 km/h, the aerodynamic force is one order of magnitude smaller than the rolling resistance force. For such cases categorized as Low-Speed (LS), ignore the aerodynamic force and for the CPP assume a constant rolling resistance force F_0.

(a) Integrate the equation of motion (Equation 3.58 with $c = 0$) and use the initial condition of $v = v_0$ at $t = t_0$ to obtain an expression for the travel time in terms of speed.
(b) For a vehicle of 1000 kg mass and total rolling resistance force of 200 N, when starting to move from standstill, plot the variation of vehicle speed against elapsed time up to 10 seconds and compare it with the results of NRF model (Problem 3.3). The engine power is 50 kW.

Results:

$$(a)\; t = t_0 + \frac{m(v_0 - v)}{F_0} + m\frac{P}{F_0^2}\ln\frac{P - F_0 v_0}{P - F_0 v}$$

Problem 3.6

For the vehicle of Problem 3.5 and using the LS method, find the required power for the 0–100 km/h acceleration to take place in 7 seconds.
Result: 58,849 W.
   Hint: The following statements in MATLAB can be used with a proper initial guess for x0.

fun=inline('7−1000*×*log(×/(×−(100/3.6/200)))+ 1000*(100/3.6/200)');
×=fsolve(fun, ×0, optimset('Display','off')); (×= P/F0^2)

Problem 3.7

For the vehicle of Problem 3.5 using the LS method determine the power requirements for a performance starting from rest to reach speed v at time t, for three cases of $v = 80$, 90 and 100 km/h for accelerating times varying from 6 to 10 seconds. Plot the results in a single figure.

Problem 3.8

The power evaluation for the NRF case (Problem 3.3) is a simple closed-form solution but it is not accurate. The LS method (Problems 3.5–3.7) produces more accurate results especially in the low speed ranges. By generating plots similar to those of Problem 3.7 show that an approximate equation of $P = P_{\mathrm{NRF}} + 0.75F_0v$ can generate results very close to those of LS method.

Problem 3.9

For the LS case, use $vdv = adS$ that relates the speed to acceleration and distance, substitute for acceleration in terms of speed.

(a) Integrate to obtain an expression for travel distance S in terms of velocity v.
(b) Derive the equation for a motion starting at a distance S_0 from origin with velocity v_0.
(c) Simplify the expression for a motion stating from rest at origin.

Results:

$$(a)\ S = C - mF_0\left[p_1^2\ln(P - F_0v) + 0.5v_1^2 + p_1v_1\right],\ (c)\ S = mF_0\left(p_1^2\ln\frac{p_1}{p_1 - v_1} - 0.5v_1^2 - p_1v_1\right)$$

$$\text{With } p_1 = \frac{P}{F_0^2} \text{ and } v_1 = \frac{v}{F_0}.$$

Problem 3.10

A vehicle of 1200 kg mass starts to accelerate from the rest at origin. If power is constant at 60 kW, for a LS model with $F_0 = 200$ N, determine the travel time and distance when speed is 100 km/h. Compare your results with those of the NRF model.
Results:

$$t = 8.23 \text{ s}, S = 153.65 \text{ m for LS and } t = 7.72 \text{ s and } S = 142.9 \text{ m for NRF}.$$

Problem 3.11

In Problem 3.8 a close approximation was used for the power estimation of LS method. For the general case including the aerodynamic force, the approximation given by $P = P_{NRF} + 0.5F_R v$ is found to work well.

For the vehicle of Example 3.5.3, plot the variations of power versus acceleration times similar to those of Problem 3.8 and compare the exact solutions with those obtained from the proposed method.

Problem 3.12

According to the solutions obtained for CTP (see Section 3.6) it turned out that at each gear, the acceleration is constant to a good degree of approximation (see Figure 3.50). Thus a simpler solution can be obtained by considering an effective resistive force for each gear that reduces the problem to a Constant Acceleration Approximation (CAA). In each gear assume the resistive force acting on the vehicle is the average of that force at both ends of the constant torque range. Write the expressions for the average speed at each gear v_{av}, the average resistive force R_{av}.

(a) Show that the acceleration, velocity and distance at each gear are $a_i = \frac{1}{m}(F_{Ti} - R_{av})$, $v_i(t) = a_i(t - t_0) + v_{0_i}$ and $S_i = 0.5a_i(t-t_0)^2 + v_{0_i}(t - t_0) + S_{O_i}$, in which $v_{0_i} = v_{max}(i - 1)$ and $S_{0_i} = S_{max}(i - 1)$ are the initial speed and distance from origin for each gear for $i > 1$ and v_0 and S_0 for i = 1.
(b) Repeat Example 3.6.1 by applying the CAA method.

Problem 3.13

A 5th overdrive gear with overall ratio of 3.15 is considered for the vehicle in Problem 3.12, and the torque is extended to 3400 rpm. Obtain the time variations of acceleration, velocity and travel distance for the vehicle by both CAA and numerical methods and plot the results.

Problem 3.14

In Example 3.5.2 impose a limit for the traction force of $F_T < 0.5\,W$ and compare the results.

Problem 3.15

For a vehicle with transmission and engine information given in Example 3.7.2, include a 1-second torque interruption for each shift and plot similar results. To this end, include a subprogram with listing given below at the end of loop for each gear:

```
% Inner loop for shifting delay:
if i<5 % No delay after gear 5!
t0=max(t);
tf=t0 + tdelay;
×0=[v(end) s(end)];
p=[0 0 0]; % No traction force
[t,×]=ode45(@Fixed_thrt, [t0 tf], ×0);
v=×(:,1);
s=×(:,2);
```

end
% Now plot the results
p=[p1 p2 p3 p4]; % Set back the engine torque

Problem 3.16

Repeat Problem 3.15 with a different shifting delay for each gear of the form 1.5, 1.25, 1.0 and 0.75 seconds for 1–2, 2–3, 3–4 and 4–5 shifts respectively. (Hint: For this you will need to change the program.)

Problem 3.17

Repeat Example 3.7.2 for a different shifting rpm.

(a) Shift all gears at times when the engine speed is 4500 rpm.
(b) Shift the gears at 4500, 4000, 3500 and 3000 rpm for shifting 1–2, 2–3, 3–4 and 4–5 respectively. (Hint: For this part you will need to change the program.)

Problem 3.18

In Example 3.7.3, investigate the possibility of having a dynamic balance point in gear 4. If no steady state point is available, find a new gear ratio to achieve a steady state.

Problem 3.19

Repeat Example 3.7.2 with transmission ratios 3.25, 1.772, 1.194, 0.926 and 0.711.

Problem 3.20

In the program listing given for Example 3.7.2, no constraint is imposed for the lower limit of engine speed and at low vehicle speeds the engine rpm will attain values less than its working range of 1000 rpm.

(a) For the existing program try to find out at what times and vehicle speeds the engine speed is below 1000 rpm.
(b) Modify the program to ensure a speed of at least 1000 rpm for the engine. How are the results affected?

Problem 3.21

In a vehicle roll-out test on a level road, the variation of forward speed with time is found to be of the form:

$$v = a \tan(b - dt),$$

where a, b and d are three constants.

(a) Assume an aerodynamic resistive force in the form of $F_A = cv^2$ and derive an expression for the rolling resistance force F_{RR}.
(b) Write an expression for the total resistive force acting on the vehicle.

Result:

$$\text{(b) } F_R = md(a + v^2/a)$$

Problem 3.22

Two specific tests have been carried out on a vehicle with 1300 kg weight to determine the resistive forces. In the first test on a level road and still air, the vehicle reaches a maximum speed of 195 km/h in gear 5. In the second test on a road with slope of 10%, the vehicle attains a maximum speed of 115 km/h in gear 4. In both tests the engine is working at WOT at 5000 rpm, where the torque is 120 Nm.

(a) If the efficiency of the driveline is 90% and 95% at gears 4 and 5 respectively, determine the overall aerodynamic coefficient and the rolling resistance coefficient.
(b) If the gearbox ratio at gear 5 is 0.711 and the wheel effective radius is 320 mm, assume a slip of 2.5% at first test and determine the final drive ratio.
(c) Calculate the ratio of gear 4 (ignore the wheel slip).

Results:

$$\text{(a) } c = 0.314, f_R = 0.014, \text{ (b) } n_f = 4.24, \text{ (c) } n_4 = 1.206$$

Problem 3.23

For a vehicle with specifications given in Table P3.23, engine torque at WOT is of the following form:

$$T_e = 100 + a(\omega_e - 1000) - b(\omega_e - 1000)^2, \ a = 0.04, \ b = 8 \times 10^{-5}, \ \omega_e < 6000 \, rpm$$

The driveline efficiency is approximated by $0.85 + i/100$ in which i is the gear number.

(a) Determine the maximum engine power.
(b) What is the maximum possible speed of the vehicle?
(c) Calculate the maximum vehicle speed at gears 4 and 5.

Table P3.23   Vehicle information

Vehicle mass		1200 kg
Rolling Resistance Coefficient		0.02
Tyre Rolling Radius		0.35 m
Final drive Ratio		3.5
Transmission Gear Ratio 1		4.00
Gear Ratio 2		2.63
Gear Ratio 3		1.73
Gear Ratio 4		1.14
Gear Ratio 5		0.75
Aerodynamic Coefficient	C_D	0.4
Frontal Area	A_f	2.0 m^2
Air density	ρ_A	1.2 kg/m^3

Table P3.24

	Parameter	Gear 1	Gear 2	Gear 3	Gear 3	Gear 5	
1	Engine speed						rpm
2	Engine torque						Nm
3	Maximum vehicle speed						km/h

Results:

$$\text{(a) } 69,173 \text{ W; (b) } 170.6 \text{ km/h; (c) } 169.9 \text{ and } 142.6 \text{ km/h}$$

Problem 3.24

For the vehicle of Problem 3.23, find the following:

(a) For a constant speed of 60 km/h over a slope of 10%, which gears can be engaged?
(b) For case (a), in which gear is the input power minimum?
(c) On this slope, what would be the maximum vehicle speed in each gear?

Hint: Table P3.24 is useful for solving this problem.

Problem 3.25

The vehicle of Problem 3.23 is moving on a level road at the presence of wind with velocity of 40 km/h. Assume $C_D = C_{D0} + 0.1|\sin \alpha|$, in which α is the wind direction relative to the vehicle direction of travel. Determine the maximum vehicle speed in gear 4 for:

(a) a headwind ($\alpha = 180$)
(b) a tailwind ($\alpha = 0$)
(c) a wind with $\alpha = 135$ degree.

Results:

$$\text{(a) } 142.5; \text{ (b) } 192.0; \text{ (c) } 140.5 \text{ km/h.}$$

Problem 3.26

Two similar vehicles with exactly equal properties are travelling on a level road but in opposite directions. Their limit speeds are measured as v_1 and v_2 respectively. Engine torque at WOT is approximated by following equation:

$$T_e = 150 - 1.14 \times 10^{-3} (\omega\text{-}314.16)^2$$

Determine the aerodynamic drag coefficient C_D and wind speed in direction of travel v_w:

(a) By writing a parametric tractive force equation in terms of vehicle speed for both vehicles.
(b) Then write a parametric resistive force equation in terms of speed for both vehicles.

Table P.3.26

Transmission Gear Ratio	0.9
v_1	180
v_2	200

(c) Equate the two equations for each vehicle and use the numerical values of Problem 3.23 for m, f_R, A_f, ρ_A, r_W and the additional information given in Table P3.26.

Results:

$$0.25 \text{ and } 19.32 \text{ km/h}$$

Problem 3.27

While driving uphill in gear 4 on a road with constant slope θ, the vehicle of Problem 3.23 reaches its limit speed v_U at an engine speed of Ω at a still air. The same vehicle is then driven downhill on the same road in gear 5, while keeping the engine speed same as before. Engine powers for uphill and downhill driving are P_U and P_D respectively. The tyre slip is roughly estimated from equation $S_x = S_0 + P \times 10^{-2}$ (%) where S_0 is a constant and P is power in hp.

Assume a small slope angle and use the additional data given in Table P3.27 to determine:

(a) uphill and downhill driving speeds
(b) road slope

Results: (a) 116.9 and 165.1 km/h; (b) 9.4%.

Problem 3.28

For the vehicle of Problem 3.23, find the following:

(a) Derive a general parametric expression for the value of speed v^* at the maximum attainable acceleration.
(b) Use the numerical values and determine the values of v^* at each gear.
(c) Calculate the maximum accelerations at each gear.

Results:

$$(a) \ v^* = \frac{30 n_i^2}{\pi \, r_W^2} \frac{\eta_d (a + 2000b)}{2 \left(c + \eta_d b \frac{30^2}{\pi^2} \frac{n_i^3}{r_W^3} \right)}$$

(b) 9.06, 13.38, 18.51, 21.45 and 17.88 m/s; (c) 4.07, 2.59, 1.55, 0.796 and 0.298 m/s^2.

Table P.3.27

Uphill power	P_U	90	hp
Downhill power	P_D	10	hp
Tyre basic slip	S_0	2.0	%
Gear progression ratio n_4/n_5	C_4	1.4	

Problem 3.29

In Section 3.9 the effect of rotating masses were discussed and equations for including this effect in the acceleration performance of a vehicle were developed. From an energy consumption point of view, when the vehicle is accelerated to the speed of v, the rotating inertias will be at rotational speeds related to v (ignore the tyre slip).

(a) Write the kinetic energies for the vehicle body mass m and rotating masses I_e, I_g and I_w.
(b) From the kinematic relations, relate the rotational speeds to the vehicle speed.
(c) Write the energy terms in terms of vehicle speed v.
(d) Write the total energy of vehicle as: $E_t = 0.5 m_{eq} v^2$.
(e) Determine the equivalent mass m_{eq} and compare it with Equation 3.130.

Problem 3.30

For a tyre with the Magic Formula information given in Table 3.3:

(a) Plot the longitudinal force (F) against slip (s) for both traction and brake regions at normal load values 1.0, 2.0, 3.0 and 4.0 kN (all in a single figure).
(b) Plot coefficients of tyre-road friction for case (a).
(c) At slip ratios 5, 10, 20 and 50%, plot the variation of F_x versus F_z (max $F_z = 5$ kN).
(d) Differentiate the Magic Formula with respect to slip to find the value of slip at which the force is maximum. Verify your results by comparing them with those of case (a).
(e) In order to have an impression of the influence of different factors in the Magic Formula tyre model, try the following for the above tyre in (a) at a normal load of 3.0 kN:
   (i) Multiply coefficient B by 0.8, 1.0 and 1.2 while keeping the other coefficients unchanged. Plot all three results in a single figure.
   (ii) Repeat i for coefficient C.
   (iii) Repeat i for coefficient D.
   (iv) Repeat i for coefficient E.

Problem 3.31

The vehicle of Problem 3.23 is moving with a constant speed of 100 km/h. Use the tyre data of Table 3.3 for each of the two driving wheels and for a front/rear weight distribution of 60/40, determine:

(a) Longitudinal slip (in percentage) of the tyres for both cases of FWD and RWD.
(b) Repeat (a) for a 5-degree grade.
(c) Repeat (a) for a level road with adhesion coefficient of 0.4 (ignore the load transfer).

Further Reading

The analysis of the performance of vehicles in the longitudinal direction in terms of accelerations and speeds been dealt with in many automotive texts. This is not surprising since in practice it has always been one of the most highly debated areas in comparing vehicles – indeed, technical journals and magazines have seemed obsessed with 0 to 60 mile/h times and top speeds even if these aspects of performance cannot actually be used safely on the roads.

A good introduction to the subject which takes a slightly different approach from this book is provided by Gillespie [4]. In Chapter 2, he derives the basic equations and discusses power and traction limited acceleration performance. In Chapter 4, he goes on to discuss in more detail the road loads – both rolling

resistance and aerodynamic – which affect longitudinal performance. Gillespie's book, written in the USA in 1992, provides good clear explanations of the fundamentals of vehicle performance – and the only problem for current students is the use of non-SI units which makes the numerical examples somewhat difficult to follow.

Lucas's book, *Road Vehicle Performance* [5], arose from lecture courses at Loughborough University of Technology. It is interesting because it gives a comprehensive analysis of vehicle performance, and links it to the practical issues of measurements both on the road and on laboratory-based dynamometers. Although it is now rather dated since it was written in 1986, the principles are of course all still relevant and he discusses some useful information on manual vs automatic gearboxes and fuel consumption calculations. It is targeted at undergraduate and graduate students but again has the drawback of using non-SI units.

The text by Guzzella and Sciaretta on vehicle propulsion systems [6] also provides an excellent introduction to vehicle performance in Chapters 2 and 3. It is a modern book, updated in 2007, and based on lectures at the Swiss Federal Institute of Technology (ETH), Zurich. It is useful as a companion to this book because the authors use examples in MATLAB and Simulink, and in particular describe some interesting case studies in the Appendix. They also introduce the QSS toolbox package which was developed at ETH, and which may be downloaded from http://www.idsc.ethz.ch/Downloads/qss.

References

[1] SAE (1978) *Vehicle Dynamics Terminology*. SAE J670e, Society of Automotive Engineers.
[2] Bakker, E., Nyborg, L. and Pacejka, H.B. (1987) Tyre Modelling for Use in Vehicle Dynamics Studies, SAE Paper 870421.
[3] Wong, J.Y. (2001) *Theory of Ground Vehicles*, 3rd edn. John Wiley & Sons, Inc., ISBN 0-470-17038-7.
[4] Gillespie, T.D. (1992) *Fundamentals of Vehicle Dynamics*. SAE, ISBN 1-56091-199-9.
[5] Lucas, G.G. (1986) *Road Vehicle Performance*. Gordon and Breach, ISBN 0-677-21400-6.
[6] Guzzella, L. and Sciarretta, A. (2005) *Vehicle Propulsion Systems: Introduction to Modelling and Optimisation*. Springer, ISBN 978-3-549-25195.

4

Transmissions

4.1 Introduction

The function of the vehicle transmission is to transfer engine power to the driving wheels of the vehicle. Changing gears inside the transmission allows matching of the engine speed and torque with the vehicle's load and speed conditions. In manual transmissions the driver must shift from gear to gear, whereas in automatic transmission the shifting is performed by a control system. There has been a gradual refinement in gearbox design over recent decades and a move towards an increasing number of gear ratios to improve overall performance and efficiency.

The chapter starts by analyzing conventional transmissions – manual gearboxes, clutches and gear ratio calculations. Then, recent developments in transmissions are reviewed and analyzed – these include Automated Manual Transmissions (AMT), Dual Clutch Transmissions (DCT) and Continuously Variable Transmissions (CVT). Their technical benefits are summarized along with the commercial issues which influence their use in current vehicle design. Two of the main trends which have influenced the increasing use of more sophisticated gearboxes have been the demands for both improved driveability and improved fuel efficiency.

4.2 The Need for a Gearbox

Vehicles are traditionally equipped with gearboxes and differentials. The number of gears in vehicle transmissions range from three for older cars to five, six and even eight in newer ones. The differential provides a constant torque amplification ratio (final drive) and acts as a power split device for left and right wheels. The role of a gearbox is to provide different torque amplification ratios from the engine to the wheels when necessary at different driving conditions. The characteristics of IC engines were studied in detail in Chapter 2 and the torque generation behaviour of electric motors was discussed in Chapter 3. In this section, one question that will be looked at is whether with any of these torque generators, it is possible to omit the gearbox?

Consider a case in which the torque source is directly connected to a driving wheel. With reference to Figure 4.1 and ignoring the effect of rotating masses (see Section 3.9), we further assume that enough friction is available at tyre–road contact area (see Section 3.3), so the available tractive force is:

$$F_T = \frac{T_S}{r_w} \tag{4.1}$$
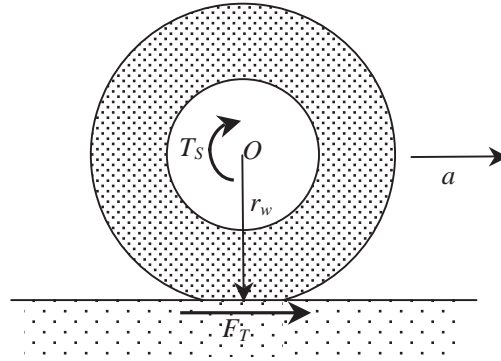
Figure 4.1   The tractive force resulting from a torque acting at the wheel centre

where T_S and r_w are the torque source and effective tyre radius respectively. For a vehicle of mass m, the acceleration resulting from this traction force is simply:

$$a = \frac{F_T}{m} = \frac{T_S}{mr_w} \tag{4.2}$$

An accepted benchmark for the overall performance of a vehicle is the 0–100 km/h time. A guideline value for this characteristic can be considered as 10 seconds. Hence the average acceleration of the vehicle during this period is:

$$a_{av} = \frac{\Delta v}{\Delta t} = \frac{100/3.6}{10} \approx 2.7 \, m/\sec^2 \tag{4.3}$$

For a typical vehicle with a mass of 1000 kg and wheel radius of 30 cm, the average torque required at wheel centre will be:

$$T_{av} = ma_{av}r_w = 710 \, Nm \tag{4.4}$$

From the discussions of Chapter 3 (e.g. Section 3.7), we found that the maximum acceleration occurs at start of motion and is up to 2–3 times the average acceleration. With a maximum acceleration of $2.5a_{av}$ the maximum torque at the wheel is:

$$T_{\max} = 2.5T_{av} = 1775 \, Nm \tag{4.5}$$

For a vehicle with specifications considered, an average power of 60 kW (80 hp) would be reasonable. Typical 60 kW IC engines and electric motors are compared in Table 4.1 in terms of the maximum torques they generate. Obviously for our example vehicle, compared to what is needed to produce

Table 4.1   Gear ratios for different power sources

Power source (60 kW)	Max torque (Nm)	Overall gear ratio (n)	Gearbox ratio (n_g)
SI engine (Petrol)	100–120	15–18	4.3–5.1
CI engine (Diesel)	170–200	9–10	2.6–2.9
Electric motor	250–500	3.5–7	1–2

required acceleration, all the torque sources have insufficient torque and are not suitable to be directly connected to the driving wheels. With an overall gear ratio n from the torque source to the driving wheels, torque amplification results. Values of n shown in the third column of Table 4.1 can generate the required acceleration for that specific torque source. With a final drive ratio n_f of 3.5, the gearbox ratio n_g is given in the last column of the table. In fact, the overall ratio is the gearbox ratio times the final drive ratio:

$$n = n_g \times n_f \tag{4.6}$$

This gear ratio can produce the maximum acceleration but it is not useful as the vehicle speed increases. The vehicle speed from the kinematic relation ignoring the tyre slip (see Section 3.10) is:

$$v = \frac{\omega_S}{n} r_w \tag{4.7}$$

in which ω_S is the speed of the power source. For our example vehicle equipped with an SI engine for a maximum speed of 6000 rpm, the maximum vehicle speed at overall ratio of 15 will be 45 km/h. Thus, in order to operate at higher speeds, the gear ratio must be reduced. The kinematic limitation explained above makes several gear reductions necessary during vehicle acceleration to its final speed. The gearbox is, therefore, required for this purpose. For electric motors it is possible to have no additional gear ratio and a single ratio can be used. For example, with a maximum speed of 8000 rpm and with a single gear ratio of 5, a speed of 180 km/h can be reached.

4.3   Design of Gearbox Ratios

Vehicle motion in different conditions is governed by the way power is transmitted from its source to the wheels. Gearbox ratios must be designed to match the vehicle motion with the torque generator's characteristics. In the case of an IC engine, the diverse working conditions of the engine make it very important to have proper gear ratios for good overall performance of the vehicle. Low gears are used at low speeds and should provide high tractions for accelerating and hill climbing. High gears, on the other hand, are used at higher speeds and must allow proper matching between engine torque-speed characteristics with vehicle acceleration and speed. Since the requirements for the lowest and highest speed gears are totally different, each will be considered separately.

4.3.1   Lowest Gear

The first or the lowest gear is used when highest acceleration is needed, or when the road load is high, such as on a slope. Since the gear ratio amplifies the engine torque, a large ratio will produce large wheel torques. With reference to the discussions in Section 3.3, however, the tractive force generated by a tyre is limited. Hence, increasing the gear ratio is limited by the tyre–road friction characteristics. Using Equation 3.22 for the tractive force including the driveline efficiency η_d is:

$$F_T = \frac{n \eta_d T_e}{r_w} \tag{4.8}$$

Assuming the limitation for the tractive force is, say, F_{Tmax}, the overall gear ratio n_L for the lowest gear can be written as:

$$n_L = \frac{r_w F_{T_{\max}}}{\eta_d T_e} \tag{4.9}$$
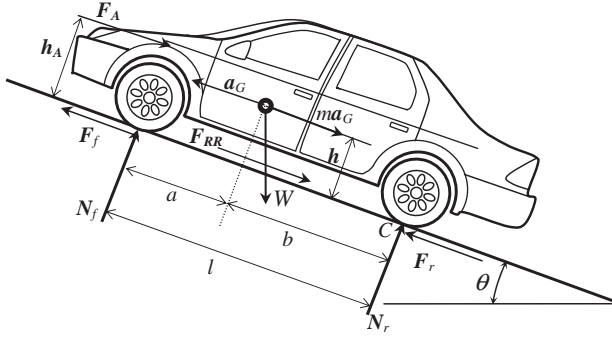
Figure 4.2 Free body diagram of vehicle

Referring to Figures 3.14 and 3.15, the maximum tractive force can be written as:

$$F_{T_{max}} = \mu_p W_{Axle} \tag{4.10}$$

where μ_p is the maximum coefficient of adhesion in tyre–road interface and W_{Axle} is the load on the driving axle. Thus:

$$n_L = \frac{r_w \mu_p}{\eta_d T_e} W_{Axle} \tag{4.11}$$

In order to find the axle load, consider the free body diagram of a vehicle travelling on a road of slope θ shown in Figure 4.2. The equations of motion in the longitudinal and vertical directions are:

$$F_f + F_r - F_A - F_{RR} - W \sin \theta = ma_G \tag{4.12}$$

$$W \cos \theta - N_f - N_r = 0 \tag{4.13}$$

where F_f and F_r are front and rear tractive forces, F_A and F_{RR} are aerodynamics and rolling resistance forces and W is the vehicle gravitational force (weight). The aerodynamic force is acting at a height of h_A whereas the vehicle centre of mass is located at height h. Taking moments about the contact point of the rear wheel (point C) results in:

$$lN_f + h(ma_G + W \sin \theta) + h_A F_A = bW \cos \theta \tag{4.14}$$

Combining Equations 4.12–4.14 leads to:

$$N_f = \frac{b}{l} W \cos \theta - \frac{h}{l}(F_T - F_{RR}) - \frac{\Delta h}{l} F_A \tag{4.15}$$

$$N_r = \frac{a}{l} W \cos \theta + \frac{h}{l}(F_T - F_{RR}) + \frac{\Delta h}{l} F_A \tag{4.16}$$

where:

$$\Delta h = h_A - h \tag{4.17}$$

$$F_T = F_f + F_r \tag{4.18}$$

Since Δh is usually small, and at low speeds the aerodynamic force is also small, the last terms in Equations 4.15 and 16 can be ignored. N_f and N_r are the axle loads at the front and rear respectively. For a front wheel drive (FWD) vehicle, only F_f will br present and for a rear wheel drive (RWD), only F_r will be present. For a four-wheel drive (4WD) vehicle both tractive forces at front and rear will be acting. The axle loads in Equations 4.15 and 16 are still dependent on the total tractive force F_T as can be seen. Assuming the tractive force has its maximum limiting value proportional to the axle load, substituting from Equation 4.10 into Equations 4.15 and 4.16 for FWD and RWD vehicles will result in:

$$N_f = \frac{b + hf_R}{l + \mu_p h} W \cos \theta, \quad \text{(for FWD only)} \tag{4.19}$$

$$N_r = \frac{a - hf_R}{l - \mu_p h} W \cos \theta, \quad \text{(for RWD only)} \tag{4.20}$$

The coefficient of rolling resistance is:

$$f_R = \frac{F_{RR}}{W \cos \theta} \tag{4.21}$$

Substituting Equations 4.19 and 4.20 into Equation 4.11 will result in:

$$n_L(FWD) = \mu_p \frac{b + hf_R}{l + \mu_p h} \cdot \frac{r_w}{\eta_d T_e} W \cos \theta \tag{4.22}$$

$$n_L(RWD) = \mu_p \frac{a - hf_R}{l - \mu_p h} \cdot \frac{r_w}{\eta_d T_e} W \cos \theta \tag{4.23}$$

n_L is the largest gear ratio and its maximum value is found at zero slope $\theta = 0$. Equations 4.22 and 4.23 can be rearranged as:

$$n_{L_{F/R}} = k_{F/R} \frac{r_w}{\eta_d T_e} \mu_p W \tag{4.24}$$

in which F/R stands for F or R for FWD or RWD respectively, and:

$$k_F = \frac{b + hf_R}{l + \mu_p h}, \quad k_R = \frac{a - hf_R}{l - \mu_p h} \tag{4.25}$$

Equation 4.24 can be used to calculate the largest gear ratio, however, the value of T_e must be available. In fact, the engine torque does not have a constant value and it depends on the engine speed and throttle position (see Section 3.2.1). In order to find a suitable value for engine torque, let us rewrite Equation 4.24 as:

$$\frac{n_{L_{F/R}} \eta_d T_e}{r_w} = k_{F/R} \mu_p W \tag{4.26}$$

The left-hand side is the traction force resulting from the engine torque and the right-hand side expression is the limiting value for the tractive force due to the tyre–road friction. Since the maximum tractive force on the left is generated at the maximum of engine torque, therefore in Equation 4.24 the maximum of engine torque is used. If a gear ratio larger than that obtained from Equation 4.24 is used, the tyres will slip at maximum engine torque, nevertheless it is common practice to use a value of 10–20% larger. This will

allow maximum tyre traction to be generated at lower engine torques. This is more practical since to gain maximum traction, it is not necessary to have a full throttle.

Example 4.3.1

For a vehicle with the information given in Table 4.2:

Table 4.2 Vehicle information of Example 4.3.1

Tyre rolling radius	0.30 m
Coefficient of rolling resistance	0.02
Engine maximum torque @ 2800 rpm	120 Nm
Vehicle mass	1200 kg
Maximum road adhesion coefficient	0.9
Weight distribution F/R	58/42%
CG height to wheelbase ratio h/l	0.30
Driveline efficiency	85%

(a) Calculate the low gear ratio for both cases of FWD and RWD.
(b) For front/rear weight distributions 60/40, 55/45 and 50/50 vary the road adhesion coefficient from 0.5 to 1.0 and plot the ratio of k_R to k_F.
(c) For the weight distribution of case (b), plot the variation of gear ratios versus variation of μ_p from 0.7 to 1.0.

Solution

For (a), from row 6 of Table 4.2, $a/l = 0.42$ and $b/l = 0.58$. From Equation 4.25:

$$k_F = \frac{b/l + f_R h/l}{1 + \mu_p h/l} = \frac{0.58 + 0.02 \times 0.3}{1 + 0.9 \times 0.3} = 0.461$$

$$k_R = \frac{a/l - f_R h/l}{1 - \mu_p h/l} = \frac{0.42 - 0.02 \times 0.3}{1 - 0.9 \times 0.3} = 0.567$$

$$n_L(FWD) = k_F \frac{r_w}{\eta_d T_e} \mu_p W = 0.461 \times \frac{0.3}{0.85 \times 120} \times 0.9 \times 1200 \times 9.81 = 14.37$$

$$n_L(RWD) = k_R \frac{r_w}{\eta_d T_e} \mu_p W = 17.67$$

For (b), a simple MATLAB$^{\circledR}$ program can generate the results. The output plots are shown in Figure 4.3. It is clear that k_R is greater than k_F at most practical cases.

For (c), the plot is shown in Figure 4.4. As can be seen for RWD, the vehicle gear ratios are larger, which implies that under similar road conditions, larger traction forces can be produced at the rear wheels. It should be noted that this result is due to dynamic conditions when the vehicle accelerates

or on slopes where the load transfer from front to rear takes place. The difference between FWD and RWD layouts increases with increasing *a/l* ratio.
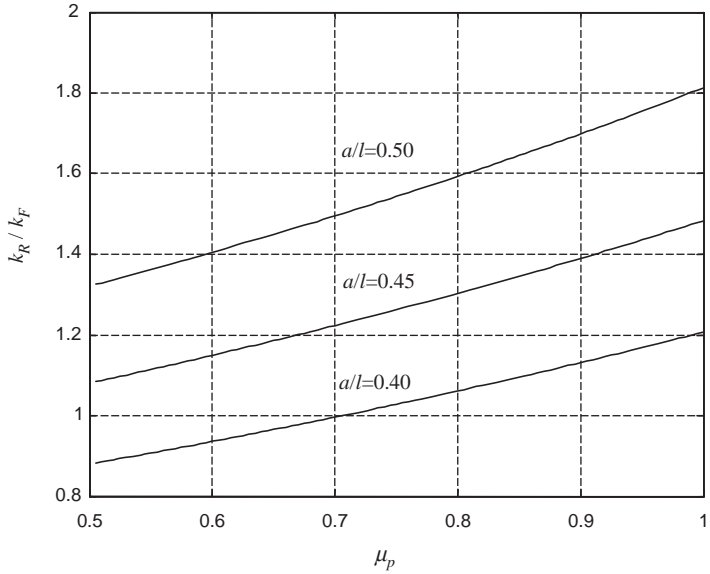
Figure 4.3   Variation of ratio k_R/k_F with adhesion coefficient μ_p
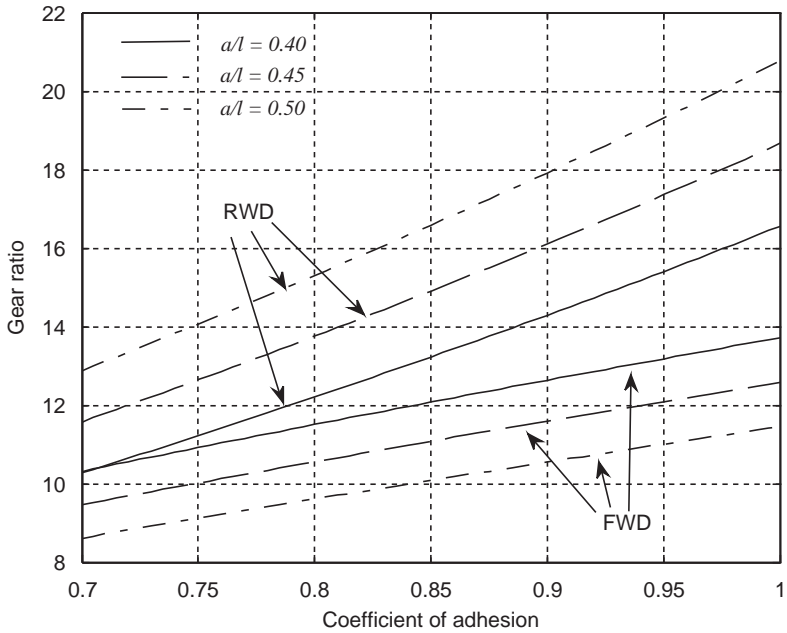
Figure 4.4   Variation of overall gear ratio with adhesion coefficient μ_p

4.3.1.1 Gradability

The maximum grade a vehicle can negotiate depends on two factors: first, the limitation of road adhesion and, second, the limitation of the engine torque. In order to consider the limitation of road friction, the right-hand side of Equation 4.26 with the inclusion of the slope angle, dictates the maximum traction force:

$$F_{T_{\max}} = k_{F/R}\mu_p W \cos\theta \qquad (4.27)$$

and this must overcome the resistive forces F_R,

$$F_R = F_A + F_{RR} + W\sin\theta \qquad (4.28)$$

Assuming the vehicle moves at low speed, then the aerodynamic force will be negligible. Thus for a constant speed of travel on a slope θ we have:

$$F_{T_{\max}} - F_R = k_{F/R}\mu_p W \cos\theta - (f_R\cos\theta + \sin\theta)W = 0 \qquad (4.29)$$

or the maximum slope travelable for the vehicle is:

$$\tan\theta = k_{F/R}\mu_p - f_R \qquad (4.30)$$

The limitation of the engine torque is not in general critical to gradeability as it is always possible to increase the gear ratio to increase the tractive force. If the torque is limited, the left-hand side of Equation 4.26 dictates the maximum traction force. At low speeds:

$$F_{T_{\max}} = \frac{n_{L_{F/R}}\eta_d T_e}{r_w} = (f_R\cos\theta + \sin\theta)W \qquad (4.31)$$

which can be solved for θ. The minimum of the values obtained from Equations 4.30 and 4.31 will be the gradeability of the vehicle at low speeds.

Example 4.3.2

For the vehicle of Example 4.3.1:

(a) Determine the climbable slope for both cases of FWD and RWD.
(b) Plot the variation of gradable slopes with the variation of μ_p at different a/l ratios (use the road friction limitation).

Solution

(a) For a FWD vehicle from Equation 4.30, the slope angle can be determined using the information from the previous example:

$$\tan\theta = 0.461 \times 0.9 - 0.02 = 0.3949, \quad \text{or,} \quad \theta = 21.55\,\text{deg.}$$

If the torque limitation is imposed, the result from Equation 4.31 will be:

$$\frac{n_{L_F}\eta_d T_e}{r_w W} = 0.415 = 0.02 \cos\theta + \sin\theta \text{ that gives the answer } \theta = 23.37 \text{ deg.}$$

For the RWD case, the result is: $\tan\theta = 0.4903$, or, $\theta = 26.12$ deg. for the limitation on friction. The torque limitation results: $0.510 = 0.02 \cos\theta + \sin\theta$ with $\theta = 29.5$ deg. Therefore the grading angle for FWD is 21.55 deg. and for RWD it is 26.12 deg.

(b) Gradable slopes plotted in Figure 4.5 show that RWD vehicle has better gradeability for different designs over roads with given coefficients of adhesion.
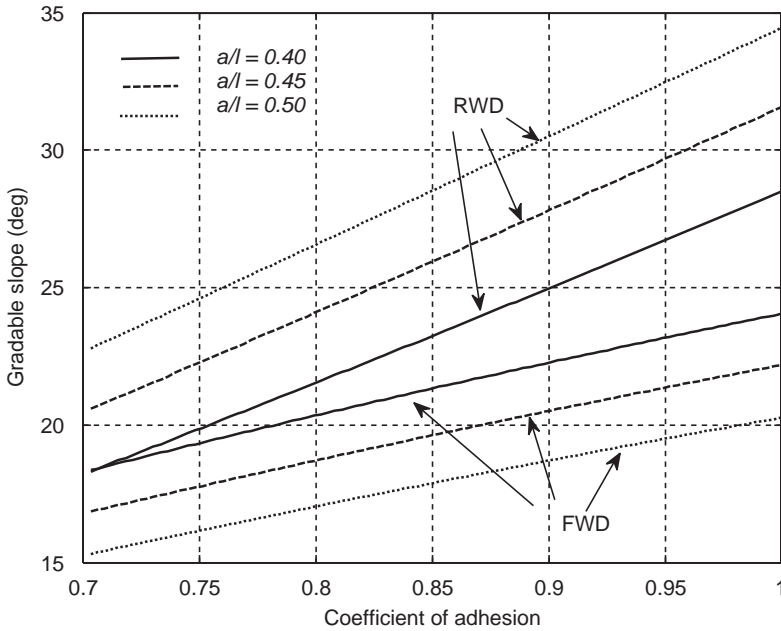
Figure 4.5   Gradable slopes versus the adhesion coefficient at different weight distributions

4.3.2   Highest Gear

The highest gear is usually used for cruising at high speeds. The maximum vehicle speed is attained at the top gear as a result of the dynamic balance between the tractive and resistive forces (see Section 3.7.4). From the kinematic point of view, the maximum speed of a vehicle in the highest gear n_H will occur at a certain engine speed ω_e^* so:

$$n_H = \omega_e^* \frac{r_w}{v_{\max}} \tag{4.32}$$
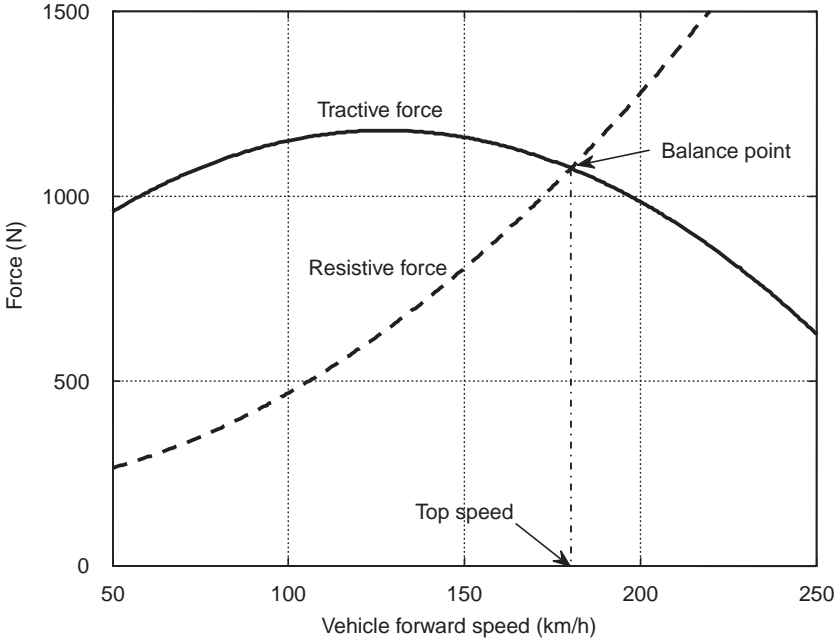
Figure 4.6 Top speed of vehicle at the balance point

If the tyre slip S_x is also taken into account (see Section 3.3), the modified equation will be:

$$n_H = \omega_e^* \frac{r_w}{v_{\max}} (1 - S_x) \tag{4.33}$$

For a target top speed of v_{max} if ω_e^* was known, the gear ratio n_H could simply be calculated. However, ω_e^* is the result of the power balance between the engine and resistive forces which is dependent on the design parameters including the gear ratio.

The highest gear in the gearbox (e.g. 5th) sometimes is designed by assuming ω_e^* to be about 10% higher than the engine speed at the point of maximum engine power, then the final gear is designed by arranging it to be an overdrive (see Section 4.3.2.2) of up to 30% [1]. For the design of the highest gear, it is reasonable to consider a full throttle condition for the top speed of vehicle, therefore the WOT curve of engine can be used to find the dynamic balance point. In general, as Figure 4.6 illustrates, the intersection of the tractive and resistive force diagrams defines the balance point at which a steady state condition results and the vehicle speed will remain constant.

The variation of tractive force can be written as (Equation 4.8):

$$F_T(\omega_e) = \frac{n_H \eta_d T_e(\omega_e)}{r_w} \tag{4.34}$$

in which $T_e(\omega_e)$ is the engine WOT curve. Since the vehicle speed is related to the engine speed by the kinematic relation (Equation 4.32 or 4.33), the variation of tractive force with speed can be obtained.
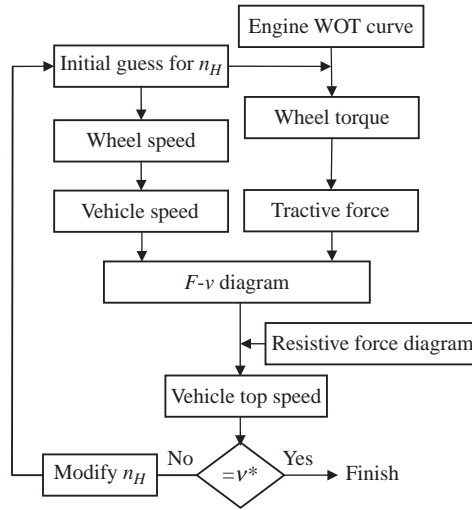
Figure 4.7 Flowchart to obtain n_H

Equation 4.34 indicates that the tractive force is dependent on the gear ratio n_H, thus without knowing it, the tractive force cannot be constructed. If the design value of the top speed (say, v^*) is given, an iterative procedure starting with an initial value for n_H can be used, the tractive and resistive forces can be constructed and the intersection of the two curves gives the top speed. If this value is equal to v^*, the initial guess for n_H is correct, otherwise its value should be modified and the procedure repeated. The flowchart of Figure 4.7 illustrates this procedure.

An alternative and somewhat simpler approach is also available to calculate the highest gear. According to the resistive force diagram of Figure 4.8, at a specified top speed of v^* the resistive force has a value F^*
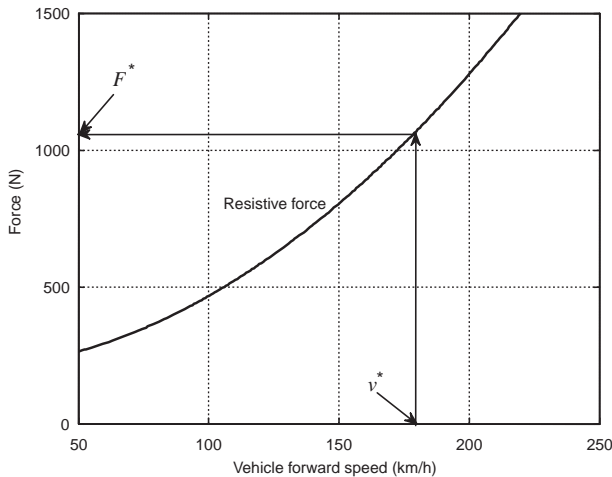
Figure 4.8 The tractive force is equal to the resistive force at the final speed
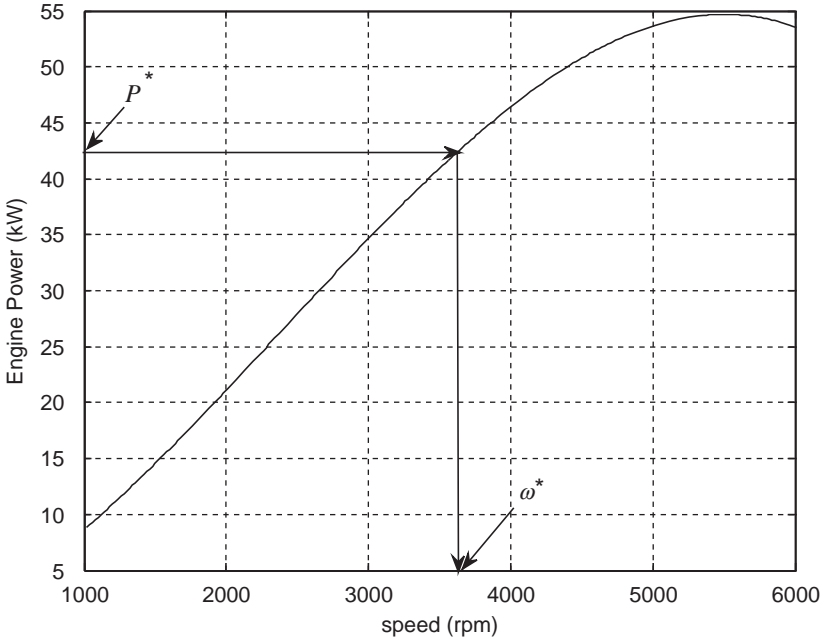
Figure 4.9   Finding the engine working speed at the top speed of the vehicle

which is also equal to the tractive force at this point. Therefore, with known values for the tractive force and the top speed, the required power P^* will also be known:

$$P^* = F^* v^* / \eta_d \tag{4.35}$$

This power also includes the driveline losses (see Section 3.13) and the engine provides the total power sum P^*. In the engine WOT power-speed curve, a horizontal line at P^* value intersects the curve and gives an engine speed ω_e^* (see Figure 4.9). Then, from Equation 4.32 (or 4.33), the high gear ratio n_H can simply be obtained.

Example 4.3.3

A vehicle with mass of 1000 kg, overall aerodynamic coefficient of 0.35 and tyre rolling radius of 30 cm, has an engine WOT torque-speed formula of the form:

$$T_e = -4.45 \times 10^{-6} \omega_e^2 + 0.0317 \omega_e + 55.24$$

in which ω_e is in rpm. The intention is to have a top speed of 180 km/h for the vehicle. Design the high gear ratio, if the coefficient of rolling resistance is 0.02. Ignore the driveline losses and tyre slip.

Solution

The total resistive force and power at the top speed are:

$$F^* = f_R W + c v_{max}^2 = 0.02 * 1000 * 9.81 + 0.35 * 50^2 = 1071.2 \, N$$

$$P^* = 1071.2 \times 50 = 53560 \, W$$

The engine speed for this power can be obtained by solving the equation:

$$53560 = (-4.45 \times 10^{-6} \omega_e^2 + 0.0317 \omega_e + 55.24) \omega_e \times \pi/30$$

The term $\pi/30$ is necessary to convert the ω_e term to rad/s. The solution can be found by trial and error or by using MATLAB function '*fsolve*'. The result is $\omega_e = 4975 \, rpm$. The overall gear ratio then can be found by using Equation 4.32.

$$n_H = \omega_e^* \frac{r_w}{v_{max}} = 4975 \times \frac{0.3\pi}{50 \times 30} = 3.13$$

4.3.2.1 Design for Maximum Speed

The standard resistive force/power curves for a given vehicle are fixed in the *F-v* or *P-v* relationships. The tractive force/power curves, however, vary with the gear ratio (Equation 4.8). The dynamic balance points, therefore, will also vary with the variation of the high gear ratio. Figure 4.10 illustrates the variation of traction/power diagrams and the resulting top speed points with the variation of the gear ratio. It shows that the maximum top speed is achievable at the maximum power point. Other top speeds at the points where the tractive and resistive force/power diagrams intersect are lower than this maximum value. In other words, there is one gear ratio for which the top speed is attained at the maximum power of engine and this speed is the maximum speed achievable.

Mathematically, at the balance point, according to Equation 4.35:

$$\eta_d P^* = (f_R W + c v_{top}^2) v_{top} \qquad (4.36)$$

which simply shows that the top speed v_{top} is maximum where the power P^* is maximum. This belongs to a certain gear ratio n_H^* and if this ratio is either increased or decreased, the maximum speed will be reduced. Figure 4.11 shows this effect for two larger and smaller ratios which have similar final speeds.

Example 4.3.4

For the vehicle in Example 4.3.3, find the gear ratio in order to achieve the maximum possible speed.

Solution

The maximum power point can be found from the full throttle torque-speed equation of the engine. Mathematically from:

$$\frac{dP}{d\omega_e} = \frac{d}{d\omega_e}\left[(-4.45 \times 10^{-6}\omega_e^2 + 0.0317\omega_e + 55.24)\omega_e \times \pi/30\right] = 0$$

or from numerical solutions one obtains:

$$P_{max} = 54.7\,\text{kW}, \; \omega_{P_{\max}} = 5500\,\text{rpm},$$

From Equation 4.36:

$$54700 = (0.02 \times 1000 \times 9.81 + 0.35 \times v_{top}^2)v_{top}$$

The steady-state speed is:

$$v_{top} = 50.4\,\text{m/s}\,(181.4\,\text{km/h})$$

Finally Equation 4.32 results in:

$$n_H = \omega_e^* \frac{r_w}{v_{\max}} = 5500 \times \frac{0.3\pi}{50.4 \times 30} = 3.43$$
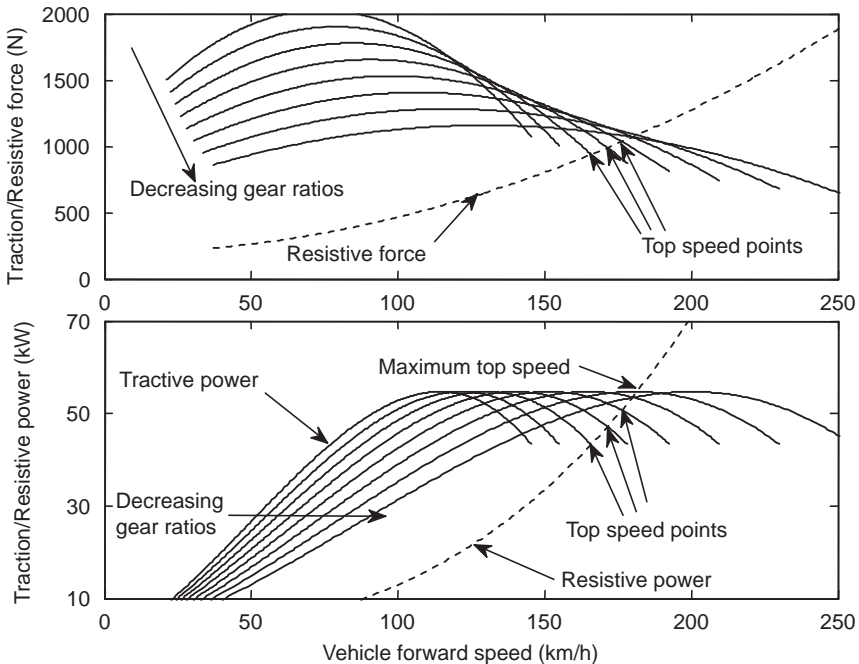
Figure 4.10 Traction/power diagrams, the variation of top speed with change of gear ratio
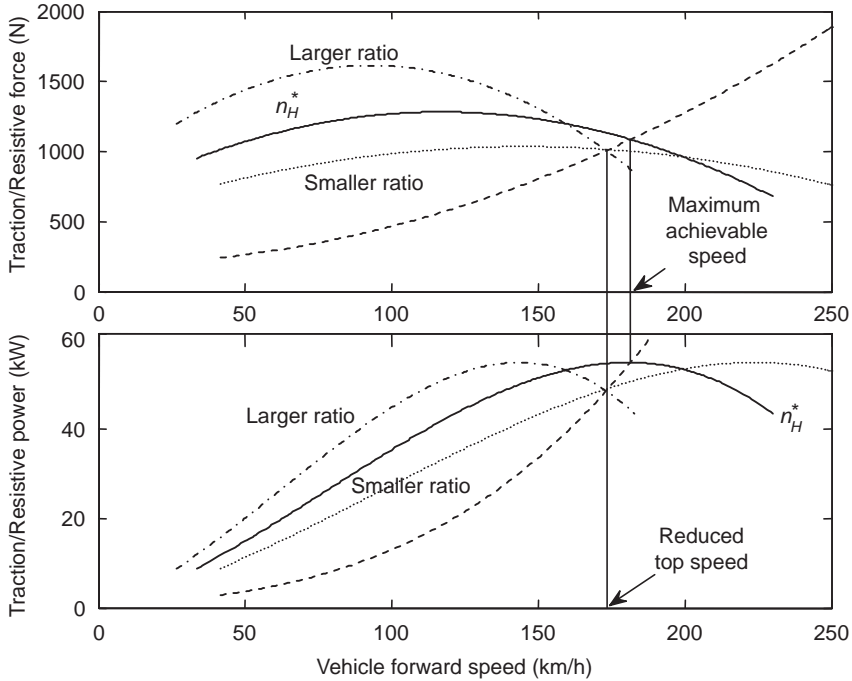
Figure 4.11 Reduction of maximum speed with changing gear ratio n_H^*

4.3.2.2 Overdrive

In Figure 4.11 it can be seen that the top speed was reduced for gear ratios smaller or larger than n_H^*. When n_H is larger than n_H^* (dash-dotted curves), the top speed will occur at higher engine speeds. This will force the engine to work at fuel-inefficient points (see Chapter 5). On the other hand, when n_H is smaller than n_H^* (dotted lines), the engine speed will be lower while the top speed could still be similar to the case of Figure 4.11. This is called *overdrive* and will move the engine working points to fuel-efficient regions as well as reducing engine noise for passengers. The term 'overdrive' indicates that the transmission output turns with higher speed than the engine speed. The amount of overdrive is chosen in different cars depending on other design and intended operating usage conditions. A value of 10–20% appears to be a typical practical design [2]. In mathematical form, a 10% overdrive results in:

$$n_H = 0.9 \times n_H^* \tag{4.37}$$

Example 4.3.5

For the vehicle in Example 4.3.4, design a 10% overdrive high gear.

Solution

According to Equation 4.47:

$$n_H = 0.9 \times n_H^* = 0.9 \times 3.43 = 3.1$$

It can be observed from comparing this result with the result of Example 4.3.3 (with $nH = 3.13$) that a 10% overdrive has not significantly altered the top speed of vehicle notably (181 km/h has become 180) whereas the engine speed has reduced considerably from 5500 rpm to slightly below 5000 (about 10%).

4.3.2.3   Reserve Power

With an overdrive, the maximum power of the engine is not available for use in the high gear since the force balance is achieved below the maximum power. For reasons of providing better vehicle performance at the times when an extra load is acting (like a head wind or a slope), it is useful to keep some reserve power to be utilized at such circumstances. An obvious solution is to have the installed power of the engine greater than the designed power. With a greater installed power, the reserve power and tractive force will be increased but the maximum speed of the vehicle will also increase.

In practice, at any working speed, extra traction and power are available at a larger gear ratio. For example, the dotted curve of Figure 4.12 represents gear ratio *A* which is larger than the gear ratio *B* shown
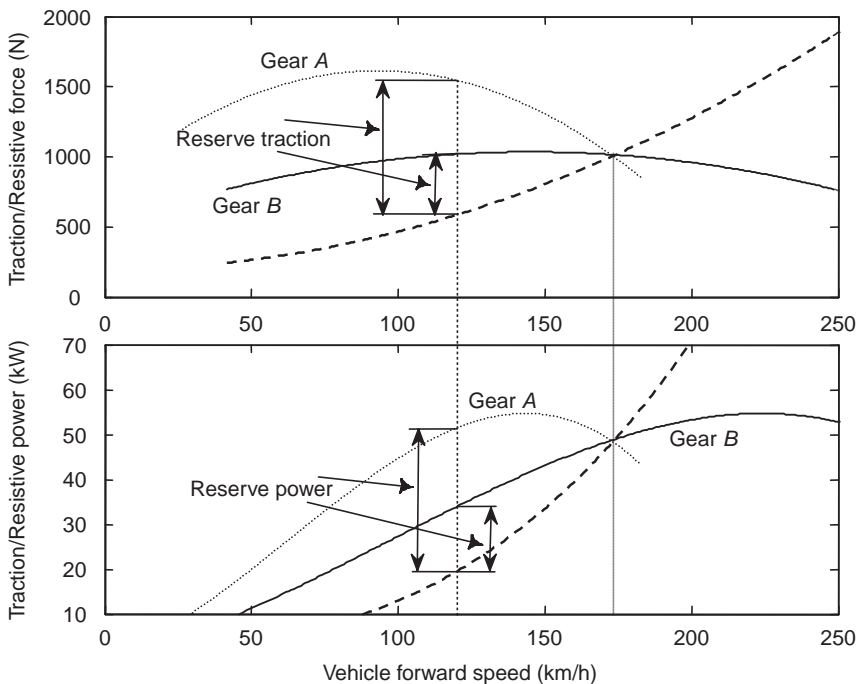
Figure 4.12   Power and tractive force reserves

in the solid curve but both gears have an equal maximum speed. At a specific speed (e.g. 120 km/h), the reserve power and tractive force are greater for gear A. If the vehicle needs a greater acceleration capability even at its high gear (like a sports car), then this type of gear ratio design would be preferred. In a passenger car, however, an overdrive (e.g. gear B) is more appropriate and in practice when the load is high, a downshift could provide more reserve power and tractive force during vehicle motion. In this case, the gear A can be regarded as 4th gear and the gear B as the 5th gear. Further considerations are also needed for the design of the high gear. One good approach, for example, is to have enough torque and traction in the high gear to be able to maintain it at lower speeds. In other words, having the largest possible speed span at the highest gear makes the driving more comfortable and pleasant.

4.3.3 Intermediate Gears

The gear ratio of the gearbox is the mechanism by which the vehicle and engine speeds are kinematically related. For stepped ratio transmissions, moving from a high gear to a low gear or vice versa must be carried out by shifting through the intermediate gears. By ignoring the tyre slip (Equation 4.7):

$$\omega_e = \frac{n}{r_w} v \tag{4.38}$$

For different gear ratios this relation expresses a family of lines with slopes equal to the n/r_w a ratio as shown in Figure 4.13. In each gear, the variation of engine speed with vehicle speed is prescribed by its relevant line. When the gear is shifted, the working point moves on to another point on another line but at the same vehicle speed.

During a gearshift, the torque transmission is interrupted by the clutch action and the engine speed starts to fall. When a new gear is engaged, the engine speed is changed to a new value (in an upshift to a lower speed and in a downshift to a higher speed). In practice, during the shift, the vehicle speed will be reduced
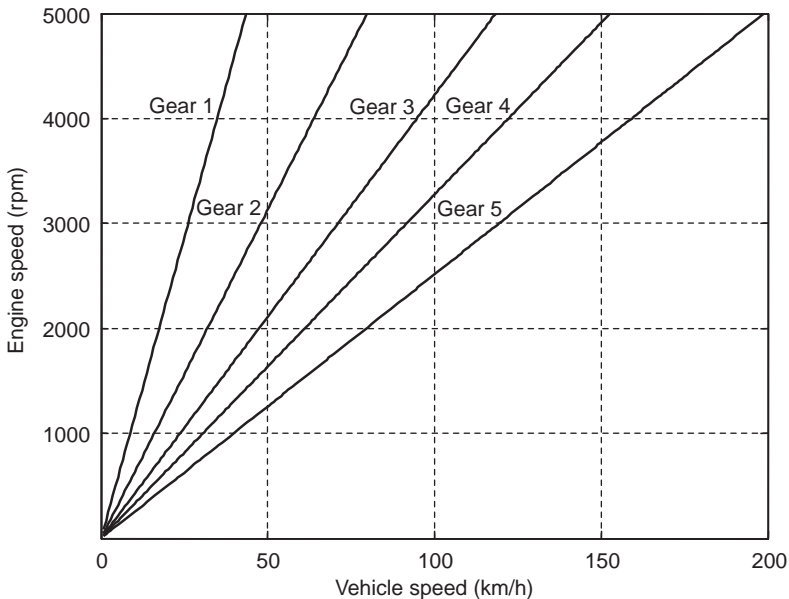
Figure 4.13 Kinematic relation between engine and vehicle speeds
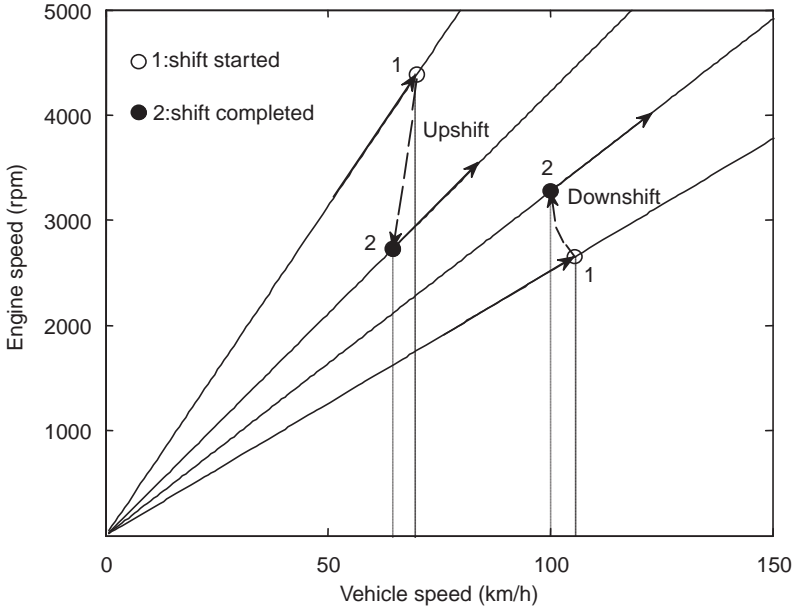
Figure 4.14   Upshift and downshift in an engine-vehicle speed diagram

slightly under the action of resistive forces and in the absence of the tractive force. Therefore, during an upshift or a downshift, as Figure 4.14 illustrates, the engine and vehicle speeds must move from point 1 to point 2. The location of point 2 depends on the shifting speed. If the shift is carried out slowly, the engine speed will drop further and vehicle speed will also reduce more.

For a vehicle under normal driving conditions, a standard shift will take a certain time. Knowing this time period, point 2 can be located and the gear ratio can be determined from the slope of a line from origin to that point. With the selected gear ratio and a standard shift, the kinematic relation will be re-established and the engine and vehicle speeds will match exactly. Conversely, if a different shifting is carried out, the point 2 will depart from the designed location and a mismatch will occur between the engine and vehicle speeds. This is accommodated by the clutch slip and the engine is gradually adjusted to the relevant speed. For initial design values, there are standard methods for the determination of intermediate gears that will be discussed in the coming sections.

4.3.3.1   Geometric Progression Method

This method represents an ideal case in which the gearshift takes place at a constant speed. In addition, it is assumed that there is an engine working range between a high engine speed ω_H and a low engine speed ω_L as shown in Figure 4.15. According to this figure, for a 5-speed gearbox, at points 1 and 2 the kinematic relations are:

$$\omega_H = \frac{n_1}{r_w} V_{12} \tag{4.39}$$

$$\omega_L = \frac{n_2}{r_w} V_{12} \tag{4.40}$$
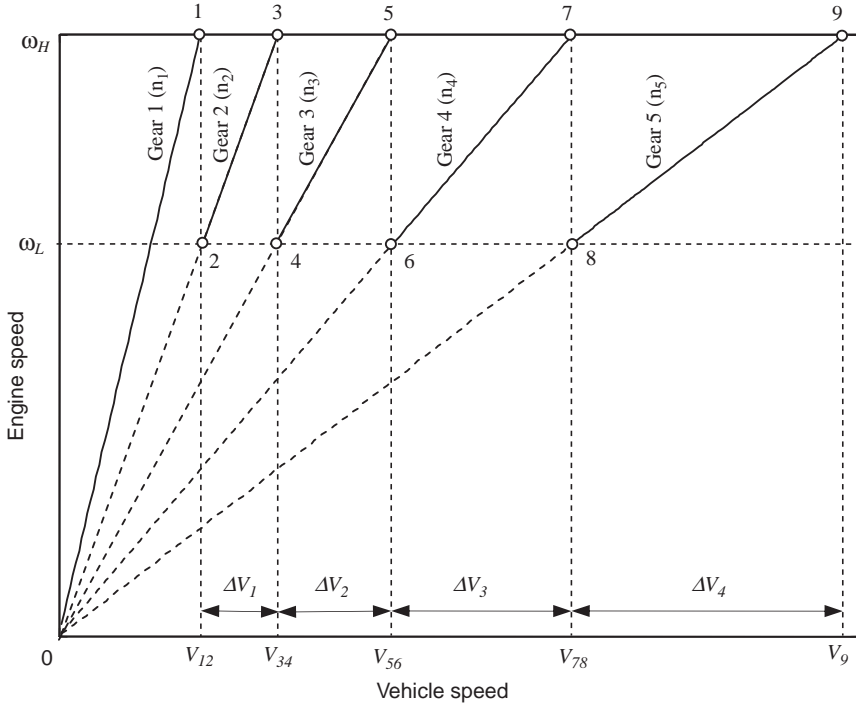
Figure 4.15 Geometric progression speed diagram

As a result:

$$\frac{\omega_H}{\omega_L} = \frac{n_1}{n_2} \tag{4.41}$$

Repeating the same procedure for points 3 and 4 leads to:

$$\frac{\omega_H}{\omega_L} = \frac{n_2}{n_3} \tag{4.42}$$

and for all ratios, one writes:

$$\frac{n_1}{n_2} = \frac{n_2}{n_3} = \frac{n_3}{n_4} = \frac{n_4}{n_5} = \frac{\omega_H}{\omega_L} = C_{gp} \tag{4.43}$$

in which C_{gp} is the geometric progression constant and has a typical value of around 1.5. Multiplying the equalities in Equation 4.43 results in:

$$\frac{n_1}{n_2} \times \frac{n_2}{n_3} \times \frac{n_3}{n_4} \times \frac{n_4}{n_5} = \frac{n_1}{n_5} = C_{gp}^4 \tag{4.44}$$

or:

$$C_{gp} = \sqrt[4]{\frac{n_1}{n_5}} \tag{4.45}$$

In general, for an *N*-speed gearbox:

$$C_{gp} = \sqrt[N-1]{\frac{n_L}{n_H}} \qquad (4.46)$$

and from Equation 4.43:

$$n_i = n_{i+1}C_{gp}, \quad i = 1, 2, \ldots, N-1 \qquad (4.47)$$

It should be noted that ω_H and ω_L are only dummy variables and are not involved in the final results.

Example 4.3.6

For the vehicle in Example 4.3.3, use the low gear ratios of Example 4.3.1 and determine the intermediate gear ratios for a five-speed gearbox.

Solution

From the results of Examples 4.3.1 and 4.3.3, we have:
For a FWD vehicle: $n_H = 3.13$ and $n_L = 12.21$, hence:

$$C_{gp} = \sqrt[4]{\frac{12.21}{3.13}} = 1.405 \text{ and } n_4 = n_5C_{gp} = 3.13 \times 1.405 = 4.40, n_3 = 6.18 \text{ and } n_2 = 8.69$$

For a RWD vehicle: $n_H = 3.13$ and $n_L = 15.02$, therefore:

$$C_{gp} = \sqrt[4]{\frac{15.02}{3.13}} = 1.480 \text{ and } n_4 = n_5C_{gp} = 4.63, \; n_3 = 6.86 \text{ and } n_2 = 10.15$$

4.3.3.2   Progressive Design

The geometric progression method produces larger speed ranges (ΔVs) for higher gears and smaller speed ranges for lower gears, as can be seen in Figure 4.15. In mathematical form, the ratio of the speed range can be represented as:

$$\frac{\Delta V_{i+1}}{\Delta V_i} = C_{gp} \qquad (4.48)$$

In the traction-speed curves, the ratio of differences in tractive forces at three consecutive gears also follows a similar pattern:

$$\frac{\Delta F_i}{\Delta F_{i+1}} = C_{gp} \qquad (4.49)$$

In passenger cars it is desirable to provide larger traction differences at low gears and smaller differences at high gears. In the speed diagram this will have opposite effect of reducing the differences in speed ranges.

In the geometric progression pattern of Equation 4.43, the ratio of any two consecutive gears was a constant. If the tractive force difference ratio of Equation 4.49 is changed for different gears, then the ratio of any two consecutive gears will be different:

$$\frac{n_i}{n_{i+1}} = C_i \tag{4.50}$$

In the progressive design, the consecutive ratios C_i are related by a constant factor k:

$$C_{i+1} = k\, C_i \tag{4.51}$$

Multiplication of the ratios C_i together equals the ratio of first to the last gear, that is:

$$\frac{n_1}{n_2} \times \frac{n_2}{n_3} \times \frac{n_3}{n_4} \times \cdots = \frac{n_L}{n_H} \equiv C_1 C_2 C_3 \cdots C_{N-1} \tag{4.52}$$

Substituting from Equation 4.51 and after simplification results in:

$$C_{gp}^{N-1} = C_1^{N-1} k^{(1+2+\cdots+N-2)} \tag{4.53}$$

This can be solved for C_1:

$$C_1 = C_{gp} k^{1-\frac{N}{2}}, \; N > 2 \tag{4.54}$$

For a five-speed gearbox, it reduces to:

$$C_1 = C_{gp} k^{-1.5} \tag{4.55}$$

Values for other C_i can be calculated by using Equation 4.51. The lowest and highest gear ratios are available and other gear ratios can be determined once the values of C_i have been calculated. In terms of the lowest gear:

$$n_2 = \frac{n_1}{C_1}, \quad n_3 = \frac{n_2}{C_2} = \frac{n_1}{C_1 C_2}, \quad n_{i+1} = \frac{n_i}{C_i} = \frac{n_1}{C_1 C_2 \cdots C_i} \tag{4.56}$$

or in terms of the highest gear:

$$n_i = \prod_{j=i}^{N-1} C_j\, n_N, \quad i = 1, 2, \cdots, N-1 \tag{4.57}$$

The design can now be completed if the factor k is known. A value of $k = 1$ provides a geometric progression and for values less than unity, a progressive design is achieved. Small variations in k have large effects on the speed range of each gear as Figure 4.16 illustrates for a five-speed gearbox. Reducing the value of k results in the reduction of gear ratios (slopes of inclined lines) in a non-linear fashion. For example, for $k = 0.8$, the last ΔV becomes very small.

In the traction-speed diagram of Figure 4.17, two cases of $k = 1.0$ (geometric) and $k = 0.9$ (progressive) have been compared in terms of tractive force distribution for the gears of a five-speed gearbox. As is clear, the differences between ΔFs of the two methods at gears 1–2 and 4–5 are large but at gears 2–3 and 3–4 are close to one another.

Values of k below 0.8 will place the 4th gear very close to gear 5 in a five-speed gearbox as seen in Figure 4.16; this is not practical, thus the working range for k can be considered as:

$$0.8 < k < 1.0 \tag{4.58}$$
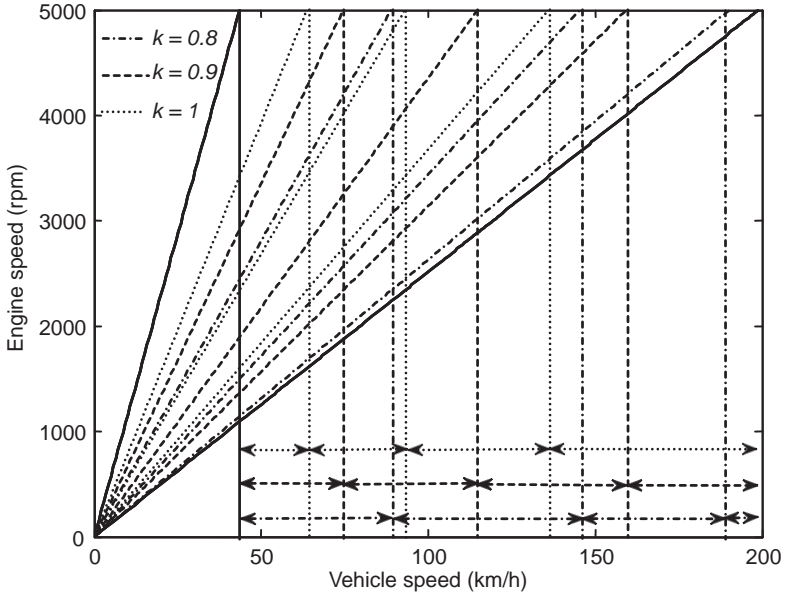
Figure 4.16   Speed diagram for different values of k
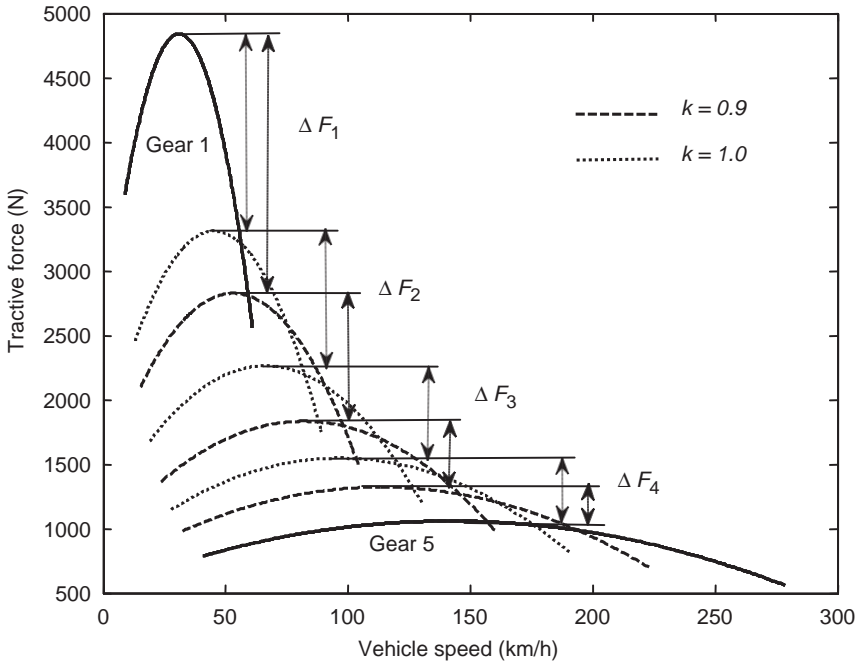
Figure 4.17   Traction-speed diagrams for geometric and progressive designs
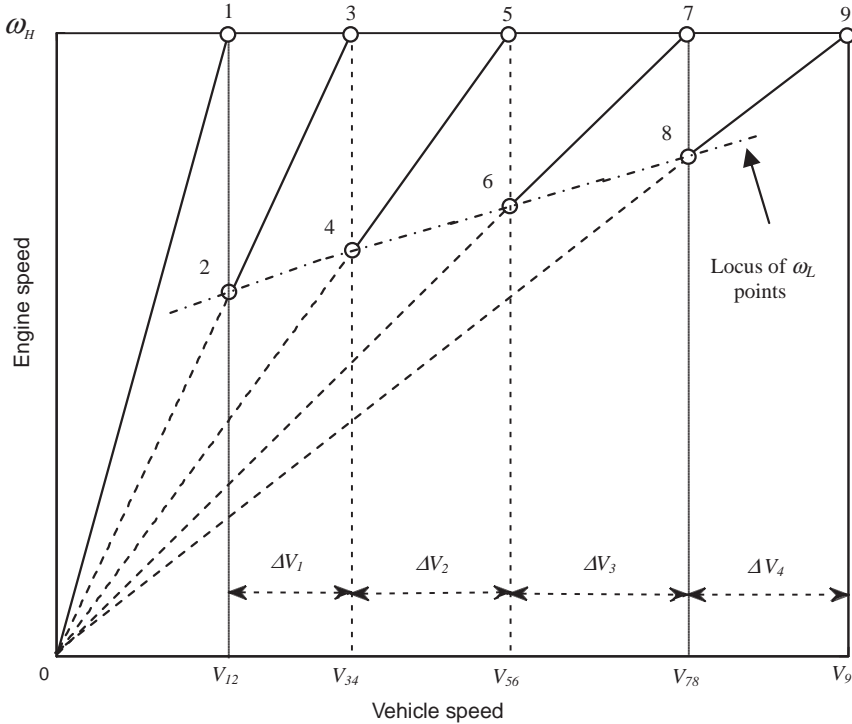
Figure 4.18 Speed diagram for progressive gear ratios

In contrast, with the geometric progression method in which a low engine speed line was present in the speed diagram for all gears, for the progressive method, each gear will have a certain low speed point as shown in Figure 4.18. The locus of ω_L points is an ascending curve (close to a line) and indicates that shifting time is decreasing with gear number increase.

Example 4.3.7

Determine the progressive intermediate gear ratios for the vehicle in the previous example using $k = 0.9$.

Solution

For a FWD vehicle we have: $n_H = 3.13$ and $n_L = 12.21$, and $C_{gp} = 1.405$. From Equation 4.55:
$C_1 = 1.405 \times 0.9^{-1.5} = 1.646$

Other C ratios are calculated from Equation 4.51:

$$C_2 = 1.646 \times 0.9 = 1.481, \quad C_3 = 1.333, \quad C_4 = 1.200$$

Equation 4.57 will be used to determine the intermediate gear ratios:

$$n_i = 3.13 \times \prod_{j=i}^{N-1} C_j, \quad n_2 = 3.13 \times C_2 C_3 C_4 = 7.42, \quad n_3 = 5.01, \quad n_4 = 3.76$$

For a RWD vehicle we have: $n_H = 3.13$ and $n_L = 15.02$ and $C_{gp} = 1.480$ thus:

$$C_1 = 1.733, \quad C_2 = 1.560, \quad C_3 = 1.404, \quad C_4 = 1.264, \text{ and}$$

$$n_2 = 8.67, \quad n_3 = 5.56, \quad n_4 = 3.96$$

4.3.3.3 Equal ΔVs

One particular type of progressive gear ratio selection is to set all ΔVs equal. With reference to Figure 4.18:

$$\Delta V = V_{i+2} - V_i, \quad i = 1, 3, 5, \ldots \tag{4.59}$$

The velocities V_i of points i using a kinematic relation is:

$$V_1 = \frac{\omega_H}{n_1} r_w, \; V_3 = \frac{\omega_H}{n_2} r_w, \ldots \tag{4.60}$$

Equating the first two ΔVs results in:

$$\frac{1}{n_2} - \frac{1}{n_1} = \frac{1}{n_3} - \frac{1}{n_2} \tag{4.61}$$

or,

$$n_2 = \frac{2 n_1 n_3}{n_1 + n_3} \tag{4.63}$$

and from next equality:

$$n_3 = \frac{2 n_2 n_4}{n_2 + n_4} \tag{4.63}$$

It can be proven that the general relation is:

$$n_i = \frac{2 n_{i-1} n_{i+1}}{n_{i-1} + n_{i+1}} \tag{4.64}$$

The ratio C_i therefore is:

$$C_i = \frac{n_i}{n_{i+1}} = \frac{2 n_{i-1}}{n_{i-1} + n_{i+1}} \tag{4.65}$$

It is a simple task to show that:

$$C_i = 2 - \frac{1}{C_{i-1}} \tag{4.66}$$

Further manipulation gives:

$$C_i = \frac{iC_1 + 1 - i}{(i-1)C_1 + 2 - i} \tag{4.67}$$

Application of Equation 4.52 with substitution from Equation 4.67 leads to the following relation for C_1:

$$C_1 = 1 + \frac{C_{gp}^{N-1} - 1}{N - 1} \tag{4.68}$$

That can provide an equation for n_2:

$$n_2 = \frac{N-1}{N-2+C_{gp}^{N-1}}n_1 \tag{4.69}$$

Then in general, any of gear ratios can be obtained from:

$$n_i = \frac{N-1}{N-i+(i-1)C_{gp}^{N-1}}n_1 \tag{4.70}$$

Noting that $C_{gp}^{N-1} = \frac{n_L}{n_H}$, for a five-speed gearbox, the intermediate gear ratios can be found as:

$$n_i = \frac{4n_L n_H}{(5-i)n_H + (i-1)n_L} \tag{4.71}$$

Example 4.3.8

Determine the intermediate gear ratios for the vehicle in the previous example using the Equal ΔV progressive method.

Solution

For a FWD vehicle we have: $n_H = 3.13$ and $n_L = 12.21$. From Equation 4.71:

$$n_2 = \frac{4 \times 3.13 \times 12.21}{(5-2) \times 3.13 + (2-1) \times 12.21} = 7.08$$

Other gear ratios are calculated similarly:

$$n_3 = 4.98, \quad n_4 = 3.85$$

For a RWD vehicle we have: $n_H = 3.13$ and $n_L = 15.02$ and intermediate gear ratios will be:

$$n_2 = 7.70, \quad n_3 = 5.18, \quad n_4 = 3.90$$

Table 4.3 Some vehicle performance measures

Measure	Metric units	US units	Typical range
Time to accelerate from rest to speed V	0–100 km/h	0–60 mph	6–10 s
Time to accelerate from speed V_1 to speed V_2	80–120 km/h	60–90 mph	6–10 s
Time to travel first x distance	200 m	660 feet	10–14 s
Time to travel first y distance	400 m	1/4 mile	15–20 s

4.3.4 Other Influencing Factors

Owing to different driving conditions for different vehicle designs, the gear ratios may need adjustments to the initial design values. Practical test driving by experienced drivers can help to improve the performance of the vehicle by gear ratio refinements. A simple measure is the 0–100 km/h or 0–60 mph time which has become an accepted benchmark to describe the maximum acceleration performance of vehicles. Another important benchmark is the 80–120 km/h time as it relates to the ability of vehicle to overtake quickly. The time to cover 400 m or a quarter of mile time is another commonly used measure of a vehicle's performance. Table 4.3 summarizes some of these performance measures.

Example 4.3.9

For the vehicle in Example 4.3.3 the intermediate gear ratios using three different methods were designed in Examples 4.3.6–4.3.8. Compare the 80–120 km/h times for all three designs for both FWD and RWD vehicles.

Solution

The MATLAB program of Example 3.7.2 of Chapter 3 can be modified for this example. First, it must include a small loop to check which gears can produce the required speed of 120 km/h within the permitted engine speed range. Second, in the '*while*' statement the engine speed at speed 120 km/h should replace the maximum engine speed. Required modifications are given in Figure 4.19. Using this program, the speed-time performance can be obtained for each of the three gear sets for both cases of FWD and RWD. The results are summarized in Table 4.4 in which N/P stands for 'not possible'.

Table 4.4 80–120 km/h times (s) for Example 4.3.9

Gear	Geometric		Progressive		Equal ΔV	
	FWD	RWD	FWD	RWD	FWD	RWD
3	N/P	N/P	8.50	N/P	8.55	8.29
4	9.73	9.18	12.14	11.21	11.70	11.47
5	16.86	16.86	16.86	16.86	16.86	16.86

```
% MATLAB program for Example 4.3.9
% Modifications to the MATLAB program of Example 3.7.2

Vsp=120/3.6;   % Specified vehicle speed
Trq=max(te);  % Maximum engine torque
eta=1.0;                   % Driveline efficiency

% Check which gear can accelerate the vehicle up to Vsp
for i=5: -1: 1
  ni=ng(i)*nf;
  Ft(i)=eta*Trq*ni/rw;             % Tractive force at gear n(i)
  vmaxi=[sqrt((Ft(i)-f0)/c),       % From force balance
  wem*rw*pi/ni/30];         % Kinematical
  vmax(i)=min(vmaxi);        % Minimum of the two
  if vmax(i) > Vsp, ig=i; end
end

for i=ig: 5  % Repeat for all gears that can reach Vsp
   ni=ng(i)*nf;
   wvmax=30*ni*Vsp/rw/pi;        % Engine speed at Vsp

  while we>wem
  [t,x]=ode45(@Fixed_trt, [t0 tf], x0);    % Calls Fixed_thrt function
      v=x(:,1);
      s=x(:,2);
      we=30*ni*max(v)/rw/pi;
      if we>=wvmax
          tf=tf*wvmax/we;
      end
   end
end
```

Figure 4.19   MATLAB program of Example 4.3.9

4.4   Gearbox Kinematics and Tooth Numbers

Once the gearbox ratios are available, the next step in gearbox design would be the determination of the number of gear teeth based on the speed or torque ratios r_s and r_T defined as:

$$r_s = \frac{\omega_o}{\omega_i} \tag{4.72}$$

$$r_T = \frac{T_o}{T_i} \tag{4.73}$$

in which the subscripts i and o stand for input and output respectively. Note that the gear ratio of a gearbox earlier denoted by n is exactly equal to r_T. In an ideal gearbox with no power loss, the input and output powers are equal:

$$P_i = T_i \omega_i = P_o = T_o \omega_o \tag{4.74}$$
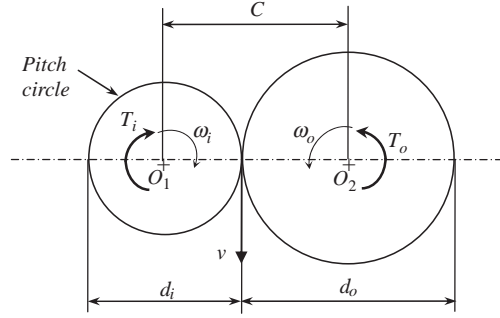
Figure 4.20   Terminology used for two running gears

Therefore:

$$r_s \cdot r_T = 1 \tag{4.75}$$

Thus in an ideal gearbox the speed and torque ratios are inverse of each other. For a couple of meshed gears, the torque ratio according to Figure 4.20 is:

$$r_T = \frac{T_o}{T_i} = \frac{\omega_i}{\omega_o} = \frac{v/d_i}{v/d_o} = \frac{d_o}{d_i} \tag{4.76}$$

For a gear, the pitch diameter can be expressed in terms of the teeth number N:

$$d = mN \tag{4.77}$$

in which m is the module of the gear; the same result could be obtained by expressing in terms of diameteral pitch. Hence:

$$r_T = \frac{N_o}{N_i} \tag{4.78}$$

For a gearbox with a number of meshed gears, the overall torque ratio is:

$$r_T = \frac{\omega_i}{\omega_2} \times \frac{\omega_2}{\omega_3} \times \cdots \times \frac{\omega_{n-1}}{\omega_o} = \frac{\omega_i}{\omega_o} = r_1 r_2 \cdots r_{n-1} r_n \tag{4.79}$$

It should be noted that in a gearbox some of the ratios are unity since they belong to two gears on a compound shaft with a common angular speed. Equation 4.79 can be written in terms of the tooth numbers of the gears with substituting from Equation 4.78 for individual gear meshes.

In the process of selecting the tooth numbers in a gearbox, the tooth numbers of the pinion and the gear must be selected such that interference is prevented. The minimum number of teeth for pinion N_P and the maximum number of teeth for the gear N_G are given by following equations [3, 4]:

$$N_P = \frac{2\cos\psi}{(1+2n)\sin^2\phi_t}\left[n + \sqrt{n^2 + (1+2n)\sin^2\phi_t}\right] \tag{4.80}$$

$$N_G = \frac{N_P^2 \sin^2\phi_t - 4\cos^2\psi}{4\cos\psi - 2N_P\sin^2\phi_t} \tag{4.81}$$

$$\phi_t = Arc\tan\left[\frac{\tan\phi_n}{\cos\psi}\right] \tag{4.82}$$
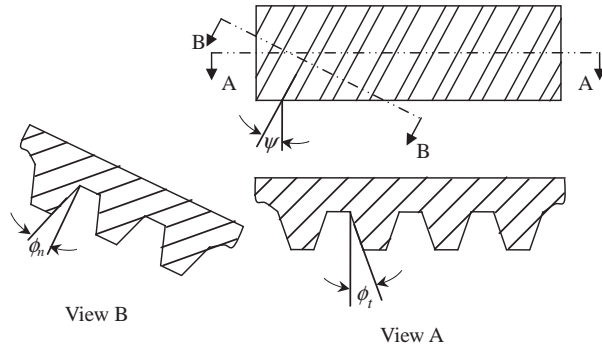
Figure 4.21 Terminology of gears

in which ψ, ϕ_n and ϕ_t are the helix angle, normal and tangential pressure angles of helical gears respectively (see Figure 4.21) and n is equal to the ratio of N_G/N_P. For spur gears $\psi = 0$ and the pressure angle ϕ must be used. Using these equations, the results obtained for spur and helical gears are provided in Tables 4.5 and 4.6.

For the example of spur gears, if a pressure angle of 20 degree and N_P with 15 teeth is selected, then N_G cannot have more than 45 teeth. Furthermore, for pressure angles of 20 and 25 degrees, the smallest numbers of teeth that can be selected regardless of the number of gear teeth are 18 and 12 respectively.

4.4.1 Normal Gears

The normal design for gears used in manual transmissions nowadays is the constant mesh design (see Section 4.5). There are two types of gearbox designs according to the number of shafts. In the first design, only two input and output shafts are used as schematically shown in Figure 4.22a. Each gear mesh denoted by 1, 2, etc. is a power transfer route in the transmission for each gear ratio and is selected through a shifting mechanism. In this type of gearbox, the input and output shafts are not in line, and hence it is suitable only for FWD transaxle applications. The second type uses three shafts, namely, the input shaft, layshaft and output shaft. Figure 4.22b schematically shows a five-speed gear set of this kind transferring power in gear 3. In this case a gear ratio involves two meshing pairs, one is the input pair denoted by '0' and the other is any other of gear pairs 1, 2, etc. that is selected. This gear set is suitable for RWD applications as the input and output shafts are in line.

Design of the tooth numbers of gears for the transaxle gear set involves the design of individual pairs but with a constraint for the centrelines of gear pairs:

$$C_1 = C_2 = \cdots = C \tag{4.83}$$

Table 4.5 N_P and N_G for spur gears

Pressure angle ϕ	20°						25°			
Minimum of N_P	13	14	15	16	17	18	9	10	11	12
Maximum of N_G	16	26	46	101	1310	∞	13	32	250	∞

Table 4.6 N_P and N_G for helical gears with normal pressure angle of 20

Helix angle ψ	20°					25°				
Minimum of N_P	11	12	13	14	15	10	11	12	13	14
Maximum of N_G	14	15	51	208	∞	13	24	57	1410	∞

In terms of tooth numbers:

$$C_i = \frac{m}{2}(N_{P_i} + N_{G_i}) \tag{4.84}$$

With equal modules Equation 4.83 results in:

$$N_{P_1} + N_{G_1} = N_{P_2} + N_{G_2} = \cdots \tag{4.85}$$

For the layshaft gear sets, Equation 4.85 also applies but in addition the gear ratio in each gear is a combination of two ratios:

$$n_i = n_0 n_i^* \tag{4.86}$$

in which (see Figure 4.23):

$$n_0 = \frac{N_2}{N_1} \tag{4.87}$$

$$n_i^* = \frac{N_{Gi}}{N_{Pi}} \tag{4.88}$$

(a) Transaxle gear set

(b) Layshaft gear set
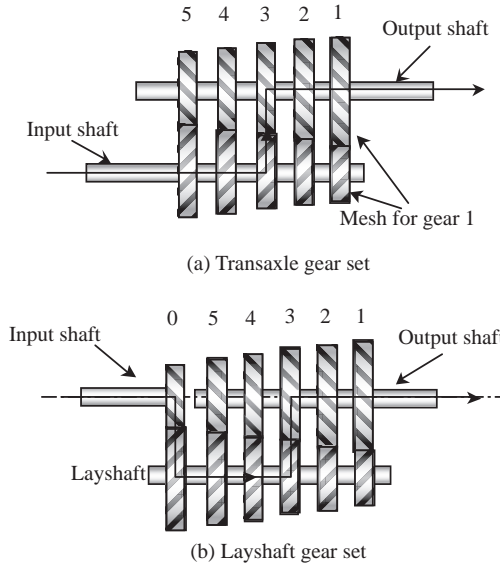
Figure 4.22 Layouts of manual gearboxes
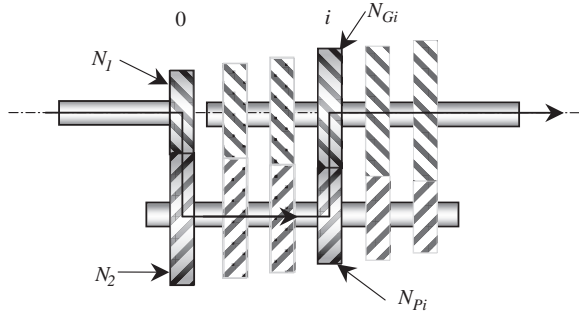
Figure 4.23   Gear numbers in the selected gear i

Therefore:

$$n_i = \frac{N_2}{N_1} \cdot \frac{N_{Gi}}{N_{Pi}} \qquad (4.89)$$

The following examples illustrate how to use the above equations to design the gear teeth numbers.

Example 4.4.1

Design gear numbers for a layshaft gearbox with a low gear ratio of 4. Gears are of helical type with a helix angle of $25°$ and normal pressure angle of $20°$.

Solution

From Equations 4.89 and 4.85:

$$n_1 = \frac{N_2}{N_1} \cdot \frac{N_{G1}}{N_{P1}} = 4 \text{ and } N_1 + N_2 = N_{P1} + N_{G1}$$

A table can be constructed for some possible values of two ratios $\frac{N_2}{N_1}$ and $\frac{N_{G1}}{N_{P1}}$ as shown in Table 4.7. If the first row is selected, we will have:

$$N_2 = 1.25N_1, \; N_{G1} = 3.2N_{P1} \text{ and } N_1 + N_2 = N_{P1} + N_{G1} = N$$

Combining the two provides: $\begin{cases} 2.25N_1 = N \\ 4.2N_{P1} = N \end{cases}$

Table 4.7   Some possible alternative ratios for Example 4.4.1

	$\dfrac{N_2}{N_1}$	$\dfrac{N_{G1}}{N_{P1}}$	n_1
1	1.25	3.2	4
2	1.60	2.5	4
3	2	2	4

Since N, N_1 and N_{P1} are all integer numbers, therefore N must also be a minimum integer of multipliers 2.25 and 4.2, or $N = 63k$, $k = 1, 2, \cdots$

$$\text{For } k = 1, \quad \begin{cases} N_1 = 28 \\ N_{P1} = 15 \end{cases}, \quad \begin{cases} N_2 = 35 \\ N_{G1} = 48 \end{cases}$$

Note that teeth number of 15 is permissible for this type of gear.

If the same procedure is used to determine the tooth numbers for the second row of the table, the result will be:

$$\begin{cases} 2.6N_1 = N \\ 3.5N_{P1} = N \end{cases}, \quad N = 91k, \ k = 1, 2, \cdots$$

And the smallest gears are: $\begin{cases} N_1 = 35 \\ N_{P1} = 26 \end{cases}, \quad \begin{cases} N_2 = 56 \\ N_{G1} = 65 \end{cases}$

The results for the three alternatives are summarized in Table 4.8. As is clear, the results of the third case are smaller gears and make a smaller gearbox.

Table 4.8   Solutions to the alternative ratios for Example 4.4.1

	$\dfrac{N_2}{N_1}$	$\dfrac{N_{G1}}{N_{P1}}$	N_1	N_2	N_{P1}	N_{G1}	ΣN
1	1.25	3.2	28	35	15	48	126
2	1.60	2.5	35	56	26	65	182
3	2	2	11	22	11	22	66

The three options presented in the example were not the only choices one could have, for instance 3 and 4/3, 2.4 and 5/3, etc. are other options. In order to find the best solution for the problem, a table similar to Table 4.8 should be constructed and every possible choice must be investigated.

In general, the same procedure can be used to determine the tooth numbers for the other gear pairs. It should be noted, however, that in a layshaft gearbox for all engaged gears, the first ratio $\frac{N_2}{N_1}$ is the same. Thus the solutions for all gear ratios are dependent on each other and the solution must be obtained in an interrelated procedure. It should also be mentioned that the kinematic solution discussed in this section is a part of general solution in which the gears must be designed also for their structural integrity and durability in power transmission.

4.4.2   Epicyclic Gear Sets

The basic parts in automatic transmissions responsible for the gear ratios are planetary or epicyclic gear sets. Figure 4.24 shows a typical planetary gear set consisting of a sun gear S, a ring gear R and a number of planets P that have their rotation centres on a common carrier called the planet carrier C.

The ring gear has internal teeth and the other gears all have external teeth. The rotations of the planets are not of direct importance but the motions of their centres produce the rotation of the carrier which is important. The three angular speeds in a planetary set ω_S, ω_R and ω_C can be related to one
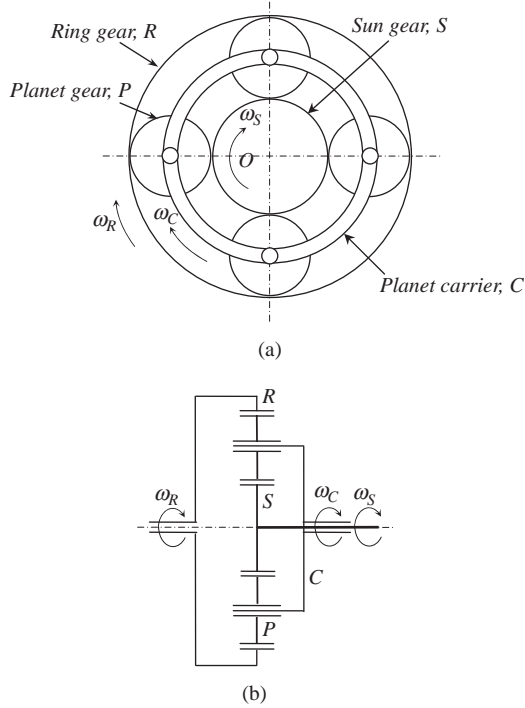
Figure 4.24   A typical planetary gear set (a) schematic, and (b) stick diagram

another via the rotations of planet gears. Defining the angular speed of a planet ω_P (positive clockwise) gives:

$$\omega_P = \frac{R_R \omega_R - R_S \omega_S}{2R_P} \tag{4.90}$$

in which R stands for the radius and is differentiated by the relevant subscripts. The carrier speed ω_C can be written as:

$$\omega_C = \frac{v_P}{R_C} \tag{4.91}$$

where v_p is the velocity of the planet centre:

$$v_P = \frac{R_R \omega_R + R_S \omega_S}{2} \tag{4.92}$$

Thus:

$$\omega_C = \frac{R_R \omega_R + R_S \omega_S}{2(R_S + R_P)} \tag{4.93}$$

If all radii are expressed in terms of the gear modules, Equations 4.93 and 90 can be written in terms of tooth numbers:

$$\omega_C = \frac{N_R \omega_R + N_S \omega_S}{2(N_S + N_P)} \tag{4.94}$$

$$\omega_P = \frac{N_R \omega_R - N_S \omega_S}{2N_P} \tag{4.95}$$

Note that all angular speeds are taken as positive clockwise (see Figure 4.24).

Example 4.4.2

The sun, ring and planet gears in a planetary set have 30, 80 and 20 teeth respectively. The sun and ring are rotating at 100 and 50 rpm respectively. Determine the rotational speed of the carrier if:

(a) the sun and ring both are rotating clockwise;
(b) the sun is rotating clockwise but the ring is rotating counter-clockwise.

Solution

From Equation 4.94, for (a):

$$\omega_C = \frac{80 \times 50 + 30 \times 100}{2(30 + 20)} = 70 \, rpm \, (CW)$$

and for (b):

$$\omega_C = \frac{80 \times (-50) + 30 \times 100}{2(30 + 20)} = -10 \, rpm \, (CCW)$$

It should also be noted that an epicyclic gear set is a two degree-of-freedom device with two inputs and one output. In other words, if only one of the three angular speeds ω_S, ω_R and ω_C were given, the system would be in an indeterminate state and the two other speeds could not be determined. When a planetary gear set is used as a vehicle gearbox, it must have one input and one output at a time. To this end, one degree of freedom must effectively be removed by fixing one of the three main rotating parts. For instance, if the ring gear is held stationary and the input is given to the sun gear, then the planet carrier will turn as the output of the system. For this configuration $\omega_R = 0$ and the overall gear ratio will be:

$$n = \frac{\omega_i}{\omega_o} = \frac{\omega_S}{\omega_C} = \frac{2(N_S + N_P)}{N_S} = 2 + \frac{2N_P}{N_S} \tag{4.96}$$

Two other useful input–output options are also possible and a summary of all three cases and their relevant gearbox ratios are presented in Table 4.9.

Table 4.9 Input–output alternatives of an epicyclic gear set

	Stationary	Input	Output	Overall gear ratio n
1	R	S	C	$n_1 = 2(1 + \dfrac{N_P}{N_S})$
2	S	C	R	$n_2 = \dfrac{N_R}{2(N_S + N_P)}$
3	C	S	R	$n_3 = -\dfrac{N_R}{N_S}$

The three gear ratios of Table 4.7 are related by following equation:

$$n_3 = -n_1 n_2 \tag{4.97}$$

This also leads to:

$$n_1 n_2 = \frac{N_R}{N_S} \tag{4.98}$$

Furthermore from the geometry of the set it is clear that:

$$N_R = N_S + 2N_P \tag{4.99}$$

This will result in alternative relations for the gear ratios:

$$n_1 = 1 + \frac{N_R}{N_S} \tag{4.100}$$

$$n_2 = \frac{N_R}{N_S + N_R} \tag{4.101}$$

$$n_1 = 1 - n_3 \tag{4.102}$$

$$n_2 = \frac{n_3}{n_3 - 1} \tag{4.103}$$

An epicyclic gear set as seen has only limited number of gear ratios. For vehicle applications, therefore, multiple sets must be used in order to produce 4, 5 or more ratios (see Section 4.6.1).

Example 4.4.3

An epicyclic gear set is designed with a first ratio of 4. Determine the other ratios of the set.

Solution

From Equation 4.102:

$$n_3 = 1 - n_1 = 1 - 4 = -3$$

Then from Equation 4.102:

$$n_2 = \frac{-3}{-3 - 1} = 0.75$$

Example 4.4.4

An epicyclic gear set is designed with a first ratio of 3.4. Determine the tooth numbers for all gears in the set.

Solution

The third ratio is:

$$n_3 = 1 - n_1 = 1 - 3.4 = -2.4$$

From the third row of Table 4.7:

$$n_3 = -\frac{N_R}{N_S} = -2.4$$

From Equation 4.92:

$$N_R = N_S + 2N_P = 2.4N_S.$$

Thus:

$$1.4N_S = 2N_P.$$

Or:

$$7N_S = 10N_P$$

The first choice could be:

$$N_P = 14, \quad N_S = 20, \quad N_R = 48$$
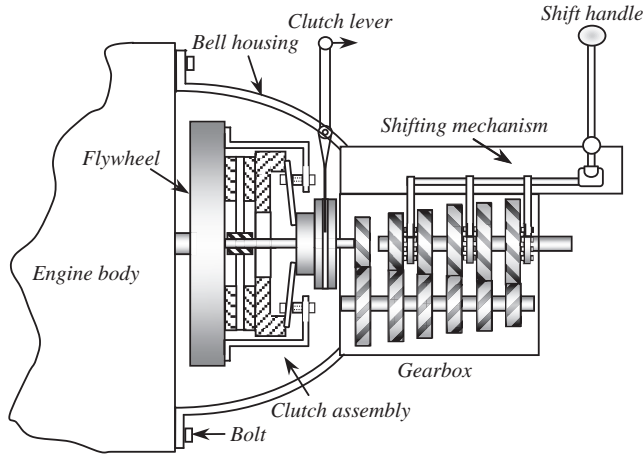
Figure 4.25   Manual transmission assembly

4.5 Manual Transmissions

Manual transmissions are the oldest kind of gearbox designs used in automobiles and were used for decades before automatic transmissions were introduced. Nevertheless, these transmissions are still popular due to their simplicity, low cost and high efficiency. The name 'manual' implies that the shifting from gear to gear must be performed manually by the driver. Although the manual transmissions are inherently the most efficient transmissions, their usage depends on the drivers' abilities and frequent manual operation is needed, for example, in urban traffic.

4.5.1 Construction and Operation

As Figure 4.25 illustrates, the transmission casing is directly bolted to the engine body through the bell housing which contains a space to accommodate the clutch system. The clutch assembly is bolted to the engine flywheel and the input shaft of the transmission receives power through the clutch plate. In fact, when the clutch is engaged, the input shaft of the transmission turns with the clutch at the same speed as the engine. Shifting is performed by means of a shifting mechanism when the transmission input is disconnected from the engine and a gear is selected by the shift lever.

The operation of the clutch is illustrated in Figure 4.26. The clutch is activated when the clutch pedal is depressed and the gear lever is pulled back, causing the release bearing to push the diaphragm spring. The seesaw effect of the spring pulls back the pressure plate and releases the clutch plate. The input shaft of transmission is directly fitted into the clutch plate through the splines and thus the two rotate with the same speed. In other words, although the clutch plate is placed inside the clutch system, it is effectively linked to the gearbox.

There are two basic types of gear change: moving a gear to mesh the opposing gear, or moving a linking member to deliver torque to already meshing gears. The former type called the 'sliding-mesh' type is now an obsolete shifting method and its concept is shown in Figure 4.27a. The second type that is used in all modern manual transmissions is the 'constant-mesh' design and its construction is schematically shown in Figure 4.27b. Both figures illustrate a layshaft type gearbox with in-line input and output shafts. The output shaft for both cases is splined. In the sliding-mesh type, the inside of the gear is also splined and can slide over the shaft. When the clutch is disconnected, the gear is moved to mesh with the opposing
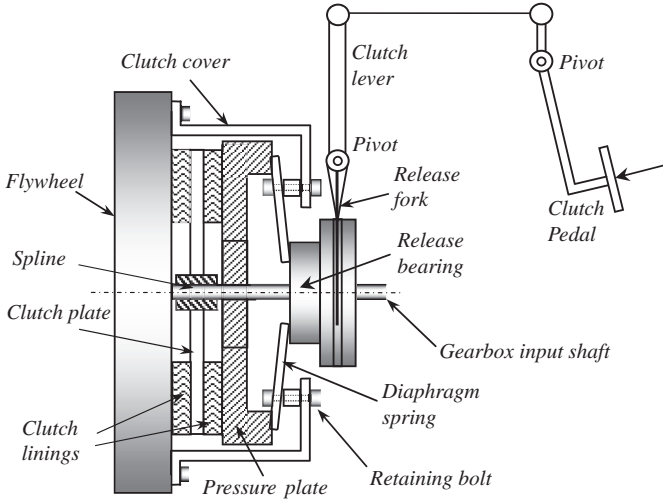
Figure 4.26 Details of the clutch mechanisms

gear on the layshaft. Then, by releasing the clutch, the power will be transferred to the output shaft. In the constant mesh type the two opposing gears are in constant mesh (a pair for each gear ratio), but the gear on the output shaft has a hole in the centre and is not connected to the shaft and no torque is delivered between the two. The power transfer is done through a sliding collar with a spline in its core and dog teeth over its sides (see Figure 4.27b). The collar is always turning with the output shaft through the splines and when it is shifted to the side, its dog teeth fit into the matching teeth on the side of the gear and the three (shaft, collar and gear) connect to each other and power is transferred.

As the gear and output shaft in constant mesh design turn with different speeds prior to their engagement, there should be a means by which the speeds are synchronized. This device is called the 'synchronizer'. Figure 4.28 shows the concept of using two matching conical surfaces that come into gradual contact as the collar slides towards the gear. When the two elements get close, the speeds gradually synchronize and the dog teeth subsequently engage.

The gear selection and shifting mechanism is illustrated in Figure 4.29 in three views (front, top and left). For a typical five-speed transmission there are usually three forks that control the three collars and each collar is used to engage two gears when it slides to left or right. The forks are fixed on three rods that
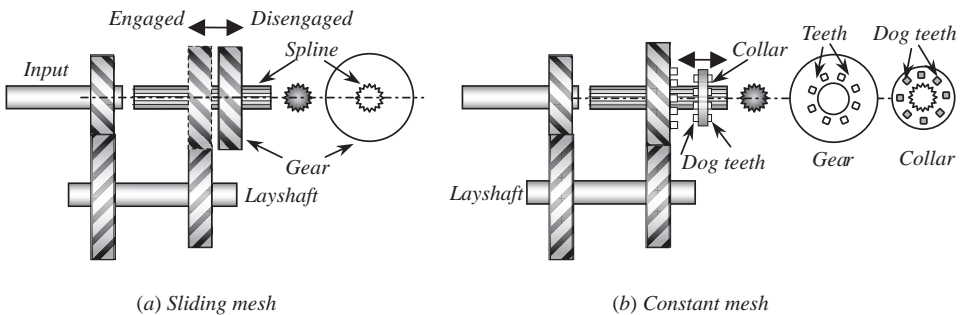
Figure 4.27 Sliding mesh and constant-mesh gear meshing methods
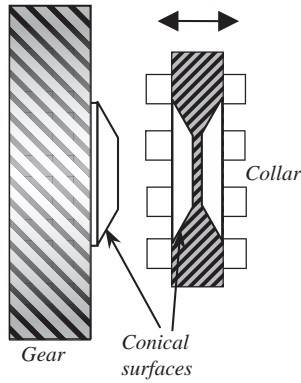
Figure 4.28   Synchronizing concept

can move back and forth. The relevant rod is chosen by the left–right movement of the shift handle. Then the choice between the two gears related to a collar is made by the fore–aft movement of the gear lever or shift handle.

4.5.2   Dry Clutches

A dry clutch is usually used with a manual gearbox for gear shifting. With reference to Figure 4.30, the engine torque is transmitted to the gearbox input shaft through the clutch plate locked between flywheel and pressure plate. The clutch assembly is bolted to the flywheel and as a result the pressure plate is always turning at engine speed. When the clutch is engaged, the spring force F is applied to the pressure plate forcing it against the clutch plate. Both sides of the clutch plate friction surfaces will receive the same force and produce half of the torque each.
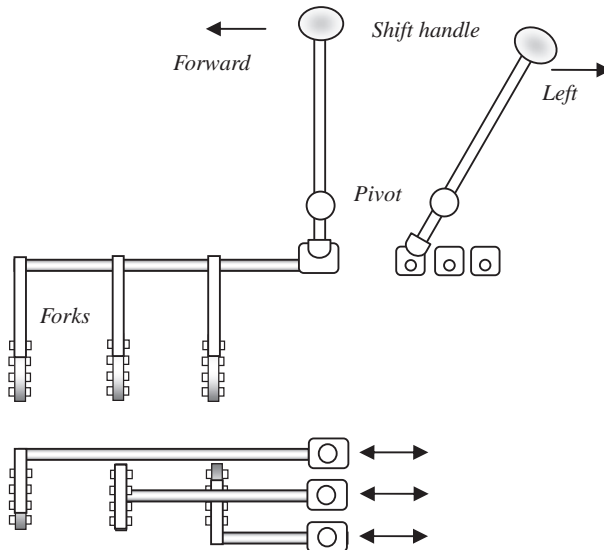
Figure 4.29   Shifting mechanism
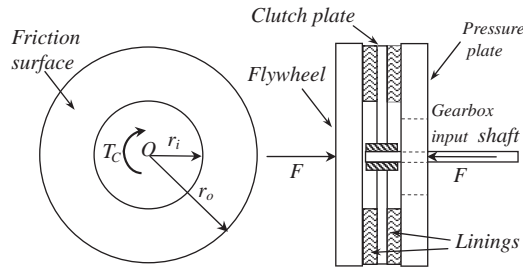
Figure 4.30   Friction surfaces of a clutch plate

The basic mechanism for torque generation in the clutch plate is the existence of a normal load and slip that together produce friction forces at distances from the plate centre and result in a torque. The amount of torque of the clutch plate, therefore, depends on the normal force and slip values. During the clutch release these will vary with time and a transient torque transmission will result, starting from zero up to the torque capacity of the clutch. The transient behaviour is dealt with in Section 4.5.4 and in the next sections the nature of dry friction and the clutch torque capacity will be considered.

4.5.2.1   Dry Friction

According to the classic Coulomb friction model, when the surfaces of two bodies are in contact under the pressure of an external load W (see Figure 4.31), three cases may exist for a force F applied to a body in order to move it along the surface:

(a) F is small and no relative motion is produced. In this case, the friction force F_f is simply:

$$F_f = F \tag{4.104}$$

(b) F is large enough to bring the body to the point of slip. The friction force in this case is:

$$F_f = \mu_S N = \mu_S W \tag{4.105}$$

where μ_S is the static coefficient of friction.

(c) The body skids (with a constant speed) over the surface. The friction force can be expressed as:

$$F_f = \mu_k N = \mu_k W \tag{4.106}$$
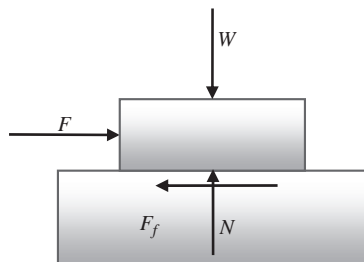
Figure 4.31   Two bodies with dry friction between them
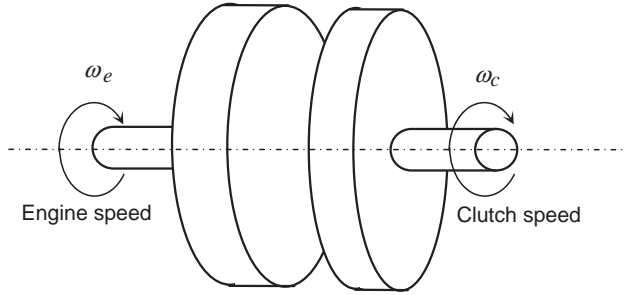
Figure 4.32   Engine and clutch speeds during the clutch engagement

where μ_k is kinetic coefficient of friction and is normally smaller than μ_S. For F larger than F_f the body will accelerate. In summary, by increasing the force F the friction force varies in the following range:

$$0 \leq F_f \leq \mu_S N \tag{4.107}$$

Even this simple model for dry friction F_f, has a non-linear nature when relative motion exists, because at speeds close to zero the value of coefficient of friction is close to the static value and at larger speeds it has its kinetic value. The coefficient of friction is influenced by parameters such as the types of contact surfaces, the relative velocity of the mating surfaces and the load. If the simple Coulomb friction model is considered, in the vicinity of zero speed, a transition from kinetic to static coefficient of friction must be included. For the clutch system before and during the engagement the flywheel rotates with engine speed ω_e and the clutch plate with speed ω_c as shown in Figure 4.32. The relative speed during the engagement period is:

$$\omega_s = \omega_e - \omega_c \tag{4.108}$$

Therefore, the coefficient of friction for the clutch can be expressed as:

$$\mu = \mu(\omega_s) \tag{4.109}$$

Simple models assume a linear transition from kinetic to static coefficient in the following form [5]:

$$\mu = \mu_S - \alpha \omega_s \tag{4.110}$$

in which α is a constant. Exponential transition is an alternative model in the form of [6]:

$$\mu = \mu_k + (\mu_S - \mu_k)e^{-\beta \omega_s} \tag{4.111}$$

where β is a constant. A smoothing approach has also been used with Equation 4.112 in order that the same equation can be used for cases in which ω_s can switch from positive to negative values and vice versa [7]:

$$\mu = \left[\mu_k + (\mu_S - \mu_k)e^{-\beta|\omega_s|}\right] \cdot \tanh(\sigma \omega_s) \tag{4.112}$$

where σ is a constant value. Figure 4.33 illustrates the variation of coefficient of friction by using values $\beta = 2$, $\sigma = 50$, $\mu_S = 0.4$ and $\mu_k = 0.25$ for Equation 4.112.

This model produces values of kinetic coefficient at most of the working points and the transition to the static friction occurs at very small slips. There are also friction models for the clutch that do not
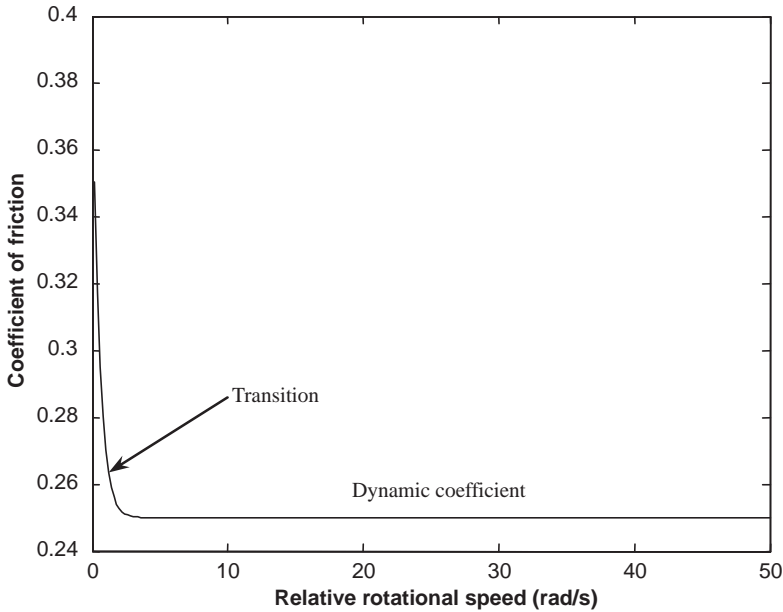
Figure 4.33 Variation of friction coefficient with relative rotational speed

obey the Coulomb friction concept. The clutch torque T_c is taken as a factor of engine torque T_e and slip speed [8]:

$$T_c = T_e \cdot \omega_s \cdot f(\delta_B, \omega_s) \tag{4.113}$$

The function f is dependent on the release-bearing displacement δ_B and slip speed, and is typically obtained through experiments.

4.5.2.2 Torque Capacity

The torque-transferring capacity of a dry clutch can be evaluated by a physical modelling approach. Figure 4.34 depicts a circular band of thickness dr on the friction surface of the clutch plate. Out of this strip an infinitesimal element of area dA is taken between two radial lines from the centre, making a small angle $d\theta$. The enlarged view of this element is also shown in Figure 4.34. The application of an
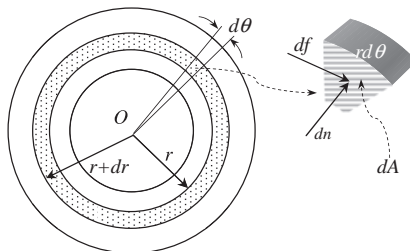
Figure 4.34 An infinitesimal element on the friction surface

axial force F (Figure 4.30) creates a pressure distribution on the contact elements. Owing to circumferential symmetry with regard to angle θ, the pressure is identical at all points lying on a specific radius.

Therefore, the pressure distribution is dependent on radius r only:

$$p = p(r) \tag{4.114}$$

The normal force acting on the element dA is:

$$dn = p(r)dA = r\,p(r)dr\,d\theta \tag{4.115}$$

The resulting frictional force using the Coulomb friction model (see Section 4.5.2.1) is:

$$df = \mu dn \tag{4.116}$$

where μ is the coefficient of kinetic friction between the linings and the flywheel or pressure plate surfaces. To evaluate the torque transmission capacity of a clutch, the kinetic value of the coefficient is used since the clutch plate transmits the torque by slip. Different lining materials produce different friction coefficients ranging up to 0.5. A typical approximate value for a vehicle clutch application is 0.3 [9]. The contribution of clutch torque by the surface element is:

$$dT = rdf \tag{4.117}$$

The total normal force acting on a clutch plate face can be found by integrating the infinitesimal normal forces over the whole friction surface, that is:

$$F = \int_r\int_\theta dn = \int_r r\,p(r)\int_\theta d\theta\,dr = 2\pi\int_{r_i}^{r_o} r\,p(r)dr \tag{4.118}$$

The total torque resulting from the friction elements on one side of clutch plate is the summation of infinitesimal torques dT. The whole torque transmission capacity of a clutch system is twice the capacity of one side, thus:

$$T = 2\int_r\int_\theta dT = 4\mu\pi\int_{r_i}^{r_o} r^2 p(r)dr \tag{4.119}$$

The results of Equations 4.118 and 4.119 depend on the pressure distribution $p(r)$. Two different criteria exist for modelling the pressure variation on the clutch plate, namely uniform pressure and uniform wear.

Uniform Pressure Criterion
When two surfaces are in good uniform contact, it is reasonable to assume a uniform pressure distribution on all contact points. For the contact between the clutch plate and the flywheel or pressure plate surfaces, especially when the liners have flat surfaces, the contact can be regarded as uniform. The axial load applied by the clutch spring is also distributed evenly around the pressure plate. Therefore, a uniform pressure distribution can be assumed for the clutch plate friction surfaces. Defining this uniform pressure as p_u, Equations 4.118 and 119 can then be integrated to find the total axial force F_{up} and transmitted torque T_{up} for the uniform pressure case:

$$F_{up} = 2\pi p_u\int_{r_i}^{r_o} r\,dr = \pi(r_o^2 - r_i^2)p_u \tag{4.120}$$

$$T_{up} = 4\mu\pi\, p_u \int_{r_i}^{r_o} r^2 dr = \frac{4}{3}\mu\pi(r_o^3 - r_i^3)p_u \tag{4.121}$$

For a certain outside diameter, the torque capacity will be maximum when the inner diameter is zero, i.e. an entire circular plate. It means that when a uniform pressure distribution exists, the torque transmitting capacity can be increased by extending the friction surface towards the inner areas. Since the clutch spring force is the main factor in torque capacity, it is useful to express the torque in terms of the spring force. Combining Equations 4.120 and 4.121 will lead to:

$$T_{up} = \mu F_{up}\, r_{eq} \tag{4.122}$$

where:

$$r_{eq} = \frac{8}{3}\left(r_{av} - \frac{r_i r_o}{4r_{av}}\right) \tag{4.123}$$

or alternatively:

$$r_{eq} = \frac{4}{3}r_o\left(1 + \frac{k_r^2}{1 + k_r}\right) \tag{4.124}$$

in which r_{av} is the average radius of friction surface and k_r being the ratio of inner to outer radii:

$$k_r = \frac{r_i}{r_o} \tag{4.125}$$

Uniform Wear Criterion

When an abrasive material is rubbed against a surface, the amount of particles separated from the material is proportional to the length of the path. In a clutch plate, materials located at distances further from the centre will experience more wear than those closer to the centre. The wear on the other hand depends on the normal load applied. In mathematical form, the amount of wear w can be taken to be proportional to both the pressure p and path length s:

$$w = kps \tag{4.126}$$

k is the proportionality constant. The path length for the friction material located at radius r on the clutch plate in one revolution is $s = 2\pi r$ and thus the wear of clutch friction material in one turn is:

$$w = 2\pi\, kpr \tag{4.127}$$

The application of uniform wear criterion is to take w of Equation 4.127 to be a constant value w^* at all radii to obtain:

$$p(r) = \frac{w^*}{2\pi\, rk} \tag{4.128}$$

which indicates the maximum pressure p_m will occur at the minimum radius r_i. The variation of pressure in radial direction is shown in Figure 4.35.

Eliminating w^* will result in the pressure distribution for uniform wear case:

$$p(r) = \frac{r_i}{r}p_m \tag{4.129}$$
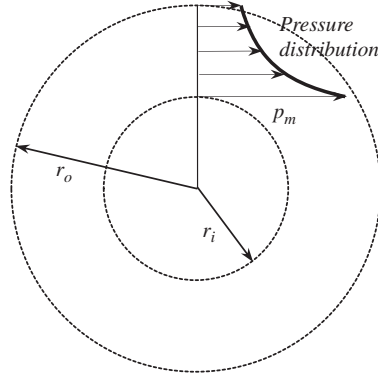
Figure 4.35   Radial pressure distribution

The existence of uniform wear means that regardless of the location, all parts of the material experience equal wear. This will result in a uniform and flat surface for the clutch friction material during its working life. Note that when a flat parallel friction surface exists, the uniform pressure assumption is also valid. Substituting Equation 4.129 into Equations 4.118 and 4.119 will provide the axial load and torque capacity for the uniform wear case:

$$F_{uw} = 2\pi\, r_i\, p_m \int_{r_i}^{r_o} dr = 2\pi\, r_i (r_o - r_i) p_m \tag{4.130}$$

$$T_{uw} = 4\mu\pi\, r_i\, p_m \int_{r_i}^{r_o} r\, dr = 2\mu\pi\, r_i (r_o^2 - r_i^2) p_m \tag{4.131}$$

According to Equation 4.130, when an axial spring force F is applied, for a certain outer diameter the maximum pressure p_m will vary with the variation of the inner radius. Simple differentiation with respect to r_i results that at the inner radius $r_i^* = 0.5 r_o$, p_m will be minimum,

$$p_m = \frac{2F}{\pi r_o^2} \tag{4.132}$$

The torque capacity of the clutch for a certain value of outer diameter varies with the variation of the inner radius, as shown in Figure 4.36, and has a maximum value close to $r_i = 0.6\, r_o$. The exact value can be found by differentiation of Equation 4.131 with respect to r_i leading to $r_i = \sqrt{3} r_o/3$.

   Similar to the case of uniform pressure, the clutch torque can be written in terms of spring force:

$$T_{uw} = 2\mu F_{uw} r_{av} \tag{4.133}$$

Comparing to Equation 4.123, for this case:

$$r_{eq} = 2r_{av} \tag{4.134}$$

4.5.2.3   Other Considerations

In practice, the surfaces of used clutch plates look fairly uniform and flat. Does this mean that the pressure distribution belongs to the uniform wear or uniform pressure? When the pressure is uniform over the
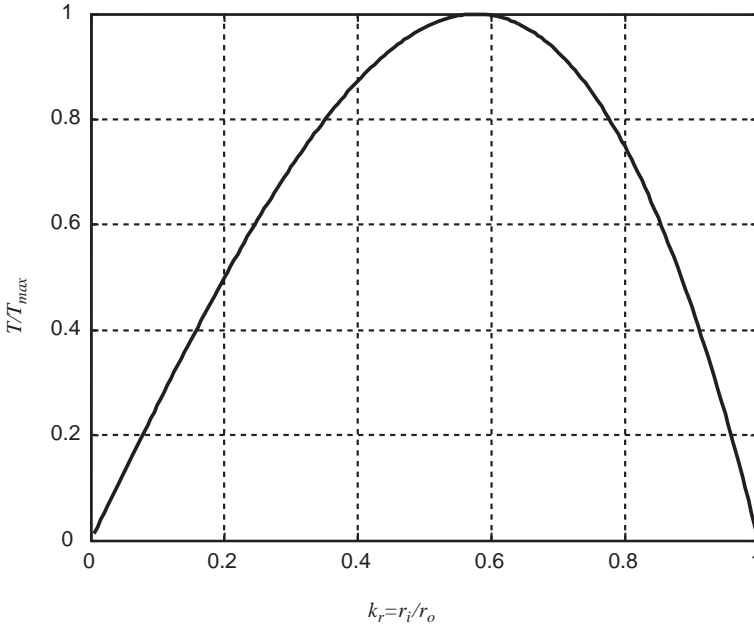
Figure 4.36 Variation of clutch torque with radius ratio

surface, particles near the outer radius wear out faster than those near inner radius. As such, the pressure distribution will no longer remain uniform since the wear particles relieve the pressure when they disappear. Then, the pressure will be borne by the remaining particles, mostly at the inner radii. This results in higher pressures at the inner radii and lower presuures at the outer radii, which is the case of uniform wear. On the other hand, if the wear in the particles of clutch plate is uniform, the surface must remain flat and parallel, which provides the condition for uniform pressure distribution. Therefore, the pressure distribution can be either of two cases and can change from one to another.

One important point is that the clutch spring force is equal for both the uniform pressure and uniform wear case, no matter which case of pressure distribution exists. Therefore, when the spring load is selected, it must be suitable for both cases. With equal spring force, the torque capacity of the two cases can be compared. For instance, the ratio k_T of torques can be obtained from Equations 4.121 and 4.131:

$$k_T = \frac{T_{up}}{T_{uw}} = \frac{r_{eq}}{2r_{av}} \tag{4.135}$$

It is a simple task to show that the ratio of torque capacities at uniform pressure and uniform wear can be expressed in terms only of radius ratio k_r:

$$k_T = \frac{4}{3}\left[1 - \frac{k_r}{(1+k_r)^2}\right] \tag{4.136}$$

This relation simply shows that at two extremes for k_r, namely $k_r = 0$ and $k_r = 1$, the torque ratios are $\frac{4}{3}$ and 1 respectively. The variation of torque ratio for whole range of variation of radius ratio is illustrated in Figure 4.37, and shows that for equal spring loads the torque capacity at uniform pressure case is
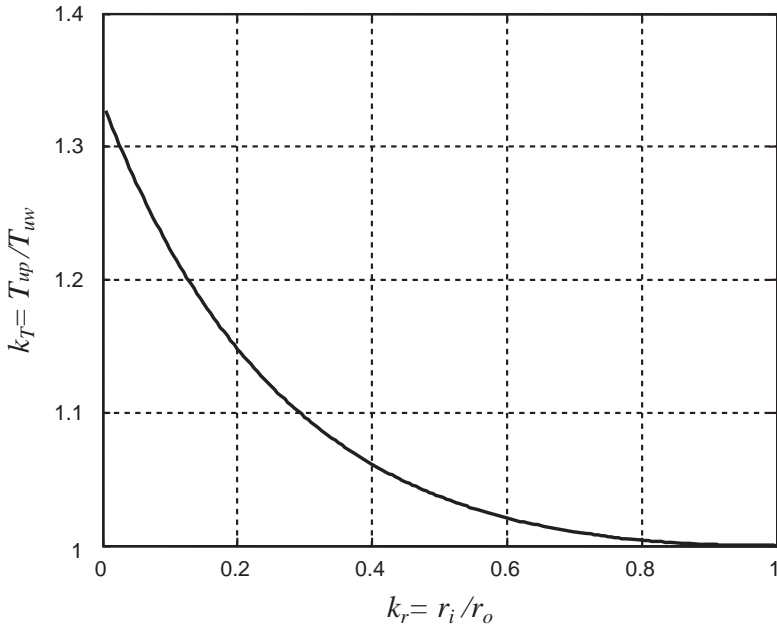
Figure 4.37   Torque ratio k_T versus radius ratio k_r (Equation 4.136)

always greater than that of uniform wear. It is also useful to see the differences in the practical range of k_r between 0.5 and 0.8.

$$k_T = \begin{cases} 1.037 & \text{for } k_r = 0.5 \\ 1.004 & \text{for } k_r = 0.8 \end{cases} \tag{4.137}$$

This shows a difference of somewhere between 0.4% and 3.7% for the torque capacities in the two cases of uniform pressure and uniform wear. Owing to this small difference, designing for either case will lead to similar results. Leaving a small margin for uncertainties in the value of coefficient of friction, it is reasonable to design using the uniform wear criterion.

The torque capacity discussed so far has been the ability of clutch to transfer torque at the time of clutch engagement. When the clutch is locked up, the coefficient of static friction μ_s must be applied. For the locked-up clutch, therefore, the torque capacity is considerably higher than when it slips.

Example 4.5.1

A clutch is designed for a torque capacity of 200 Nm. The coefficient of friction is 0.4 and the outer clutch plate diameter must be a maximum of 200 mm:

(a) Calculate the inner radius for keeping the maximum pressure as small as possible.
(b) Determine the maximum pressure.
(c) Evaluate the spring force.
(d) Find the maximum torque capacity of the clutch.

Solution

The uniform wear criterion will be used.

(a) In order to keep the value of p_m a minimum, the inner diameter must be taken to be half of the outer diameter: $d_i = \frac{1}{2}d_o = 0.1\,m$

(b) Maximum pressure can be calculated using Equation 4.131:

$$p_m = \frac{T_{uw}}{2\mu\pi\,r_i(r_o^2 - r_i^2)} = 212207\,Pa$$

(c) The spring force can be evaluated using Equation 4.132: $F = \dfrac{\pi\,p_m r_o^2}{2} = 3333.3\,N$

(d) The maximum torque capacity will occur at uniform pressure case. From Equation 4.122 and using the spring force:

$$p_u = \frac{F}{\pi(r_o^2 - r_i^2)} = 141471\,Pa$$

and torque capacity from Equation 4.123 is: $T_{up} = \dfrac{4}{3}\mu\pi(r_o^3 - r_i^3)p_u = 207.4\,Nm$

Lining Grooves

The grooves on the clutch linings help it cool down and also act as channels for removed particles to guide them out and leave a clean friction surface. The areas the grooves occupy, however, reduce the total friction area of the clutch linings. The rivet holes on the linings have also the same effect. A question may arise as to what extent this area reduction can influence the torque capacity of a clutch system. In order to answer this question, a simple model shown in Figure 4.38 is considered. For the sake of simplicity, the grooves are taken in pure radial directions which are different from those in practice which often have angled directions.

Assuming n grooves on the plate, the Equations 4.118 and 4.119 will become:

$$F = (2\pi - n\alpha)\int_{r_i}^{r_o} rp(r)dr \tag{4.138}$$

$$T = 2\mu(2\pi - n\alpha)\int_{r_i}^{r_o} r^2 p(r)dr \tag{4.139}$$

The parameters of the grooved surface will be denoted by a prime symbol and those of full friction surface with no prime. For the case of uniform pressure, assuming an identical clutch spring for the two models, results in:

$$F'_{up} = \frac{1}{2}(2\pi - n\alpha)(r_o^2 - r_i^2)p'_u \equiv F_{up} \tag{4.140}$$

Comparing with Equation 4.120:

$$p'_u = \frac{2\pi}{2\pi - n\alpha}p_u \tag{4.141}$$
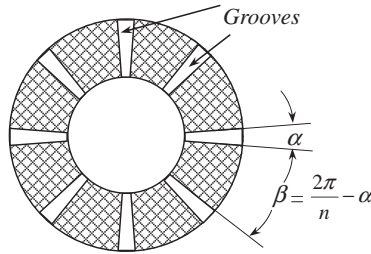
Figure 4.38   Grooves on the facing of a clutch plate

which simply shows the pressure is higher since the same force is applied on a smaller surface. Evaluating the torque capacity results in:

$$T'_{up} = \frac{2}{3}\mu(2\pi - n\alpha)(r_o^3 - r_i^3)p'_u \qquad (4.142)$$

Substituting from Equation 4.141 gives:

$$T'_{up} = \frac{4}{3}\mu\pi(r_o^3 - r_i^3)p_u = T_{up} \qquad (4.143)$$

Therefore no change occurs to the torque capacity when grooves are included on the surface and the only effect is the pressure increase due to the surface reduction. It is a simple task to show that for the uniform wear case too, a similar result will exist.

Energy Loss
The energy loss due to friction in a clutch is the work done by friction forces. The infinitesimal work dW of the friction forces can be written as:

$$dW = T_c(t) \cdot d\theta \qquad (4.144)$$

where:

$$d\theta = \omega_s(t)dt \qquad (4.145)$$

and ω_s is the slip speed of clutch mating surfaces. Thus:

$$dW = T_c(t)\omega_s(t)dt \qquad (4.146)$$

and,

$$E_{loss} = \int dW = \int T_c(t)\omega_s(t)dt \qquad (4.147)$$

The power loss due to friction is:

$$P_{loss}(t) = T_c(t)\omega_s(t) \qquad (4.148)$$

The energy and power losses can be calculated if instantaneous torque and speed of clutch are available.
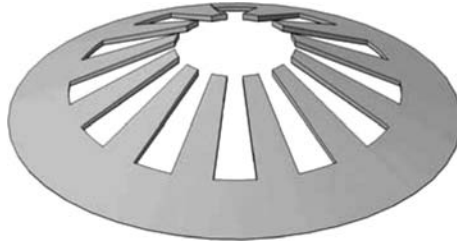
Figure 4.39 A simple form of diaphragm spring

4.5.3 Diaphragm Springs

Diaphragm springs are used in dry clutches to exert necessary force for the generation of friction torque. These springs are of conical shell form with a number of slots cut out in the upper part as schematically shown in Figure 4.39. Different circular or square holes are made at the bottom parts of the slots (not shown in Figure 4.39) to hold pivots or retaining bolts. The tips of so-called fingers come into contact with the release (or throw-out) bearing when clutch pedal is depressed (see Figure 4.40). At the engaged stage the release bearing is held away from the diaphragm spring's fingers. The diaphragm spring can be regarded as two separate springs joined together. The lower part of spring of Figure 4.39 is a Belleville spring and the upper part consists of several flat springs (fingers). The clamping force of the clutch is generated only by the Belleville part of the diaphragm spring.

4.5.3.1 Function

The bottom part (outer rim) of the spring is in contact with the pressure plate. When the clutch is depressed, the release bearing pushes the fingers and the spring is pulled back (like a seesaw) and moves the pressure plate away from the clutch plate (see Figure 4.40).

Three forces are important in the clutch system: the pedal force; the bearing force; and the spring force. The pedal force F_P applied by the driver's foot is amplified by the leverage and a force F_L is generated and transferred to the clutch lever input (see Figure 4.40). Once again this force is amplified and the bearing force F_B results. The bearing force is transmitted to the spring and causes the spring force on the clutch
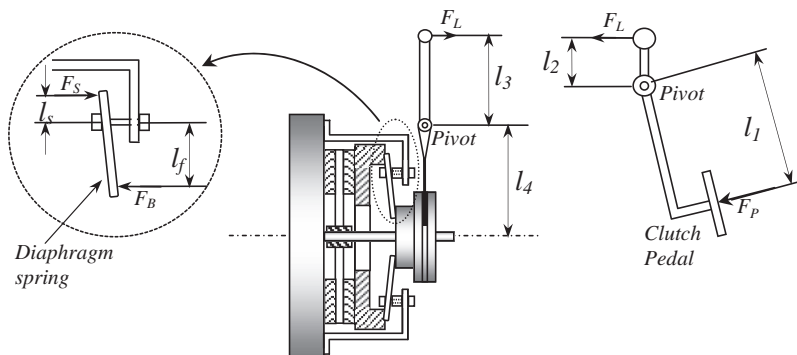
Figure 4.40 Details of a clutch system
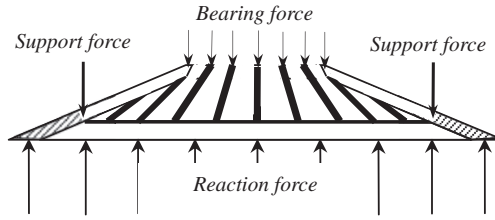
Figure 4.41   Forces acting on the diaphragm spring

plate to decrease. The bearing force is related to the pedal force based on the geometry shown in Figure 4.40:

$$F_B = \frac{l_1 \cdot l_3}{l_2 \cdot l_4} F_P \qquad\qquad (4.149)$$

4.5.3.2   Spring Forces

Three groups of forces acting on the clutch spring are schematically illustrated in Figure 4.41. These include those exerted by the release bearing on the finger tips, those exerted by the retainers at the spring holes (support forces), and the reaction forces from the pressure plate.

The forces acting on the pressure plate are reaction forces from the spring and the clutch plate that balance each other. Hence, the force that compresses the clutch plate between the pressure plate and the flywheel is in fact equal in magnitude to the reaction force on the spring and is called the 'clamp load'. In the engaged state with no bearing force, the diaphragm spring pivots over its slot rings and its outer rim forces the pressure plate tightly against the clutch plate with force F_S due to a preload. In fact, before the clutch assembly is bolted to the flywheel, as illustrated in Figure 4.42a, the diaphragm spring is free and the cover will remain at a distance δ_0 from the flywheel surface. Bolting the cover to the flywheel forces the spring into a pre-loaded condition shown in Figure 4.42b.

The application of the bearing force will cause the bearing to move towards the flywheel by bending the spring fingers. The change of the bearing force F_B with its displacement δ_B has a non-linear characteristic as shown in Figure 4.43 for a typical small passenger vehicle. Since the bearing load releases the clutch from engagement, this force is commonly called the 'release load'.

The force exerted on the clutch plate by the pressure plate, i.e. the spring force F_S, results from tensioning the spring between the outer rim and the retainers. In fact, the spring fingers are not involved in the generation of this force. In order to obtain a better understanding of how the spring force is generated, consider the clutch system of Figure 4.44 in which the cover is rigidly fastened to a flat surface and a disk is
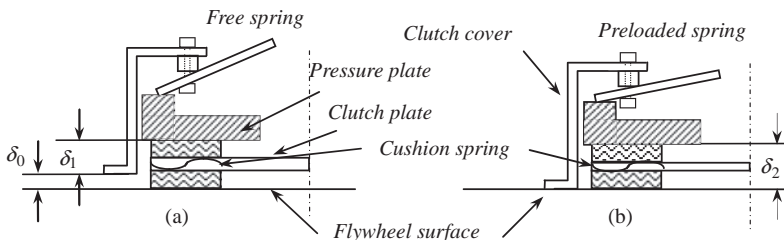
Figure 4.42   The clamp force resulting from preload
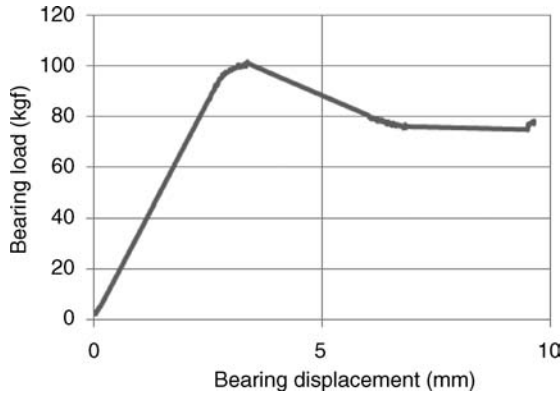
Figure 4.43 Typical bearing force (release load) variation

put under the pressure plate instead of the clutch plate. In the beginning, the displacement δ relative to the reference line is zero when no force is applied. The application of force will cause a displacement δ.

The variation of the spring load F_S with the spring travel δ_S is typically of the form shown in Figure 4.45. It increases up to a peak with increase in the displacement, then starts to decline to a minimum and afterwards increases exponentially. With reference to Figure 4.42 when a clutch plate is placed between the pressure plate and the flywheel, the pressure plate will undergo an initial displacement $\delta_S^* = \delta_2 - \delta_1$, due to the contraction of the clutch plate cushion springs. On the clamp load diagram (Figure 4.45), the load at the displacement δ_S^* describes this situation. For a new clutch plate, the thickness of linings is a maximum and the preload point on the diagram, called the 'set load' point, will be at the far right. By the time the linings wear out, the initial displacement gradually reduces and brings the working point to the left, up to the points at which the plate rivets come into contact with the surface of flywheel (or pressure plate). This is indicated by 'wear-in load' in Figure 4.45. This range from the minimum to the maximum displacement, which is typically of the order of 2 mm, is called the 'wear-in area'. The shaded segment of Figure 4.45, therefore, should not be used.

In order to release the clutch plate, the pressure plate must be moved away from the flywheel which means the spring's displacement must increase relative to its initial value of δ_S^*. In Figure 4.45, this means moving further to the right. To move the pressure plate away from the flywheel and release the clutch plate, no force can be applied from the inner part and hence, the releasing force is applied to the bearing in the opposite direction! When the bearing force acts on the diaphragm spring's fingers during the disengagement stage, due to the pivoting action, the spring contact force, i.e. the clamp load F_C, is reduced.
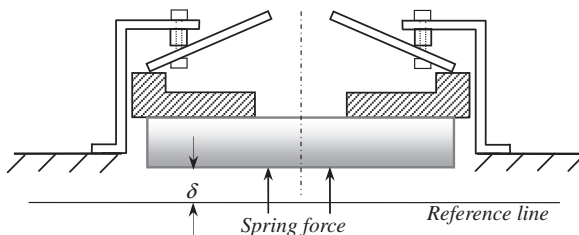
Figure 4.44 Definition of spring force
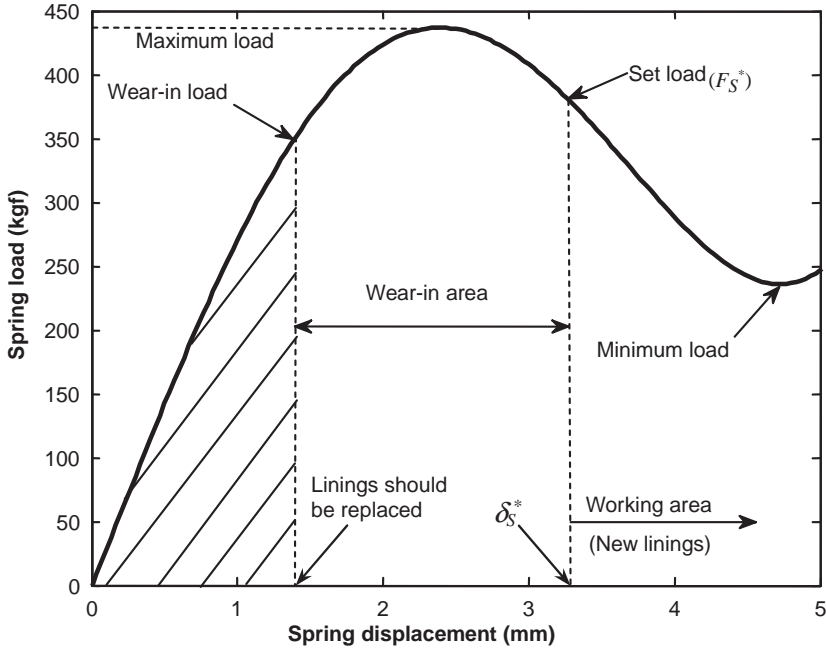
Figure 4.45   Typical force-deflection curve of diaphragm spring

Assuming a symmetrical loading on the spring, Figure 4.41 is simplified by taking only a segment shown in Figure 4.46 in which the shaded part is the spring body and the unshaded part represents the finger. To make it simple, it is assumed this segment supports the full load of the diaphragm spring as a whole. This segment is in static equilibrium under the action of several forces. The segment is supported at the pivot S by unknown forces. The clamp force F_C and the friction force F_X are acting at the pressure plate's contact point C. The bearing force F_B acts at the finger tip and at the cuttings (shaded areas) there are forces (not shown) that are all moved to the pivot point S together with their resulting moments M_S about S.

The moment balance about point S is (positive clockwise):

$$F_C l_s + F_B l_f = M_S + F_X h \tag{4.150}$$
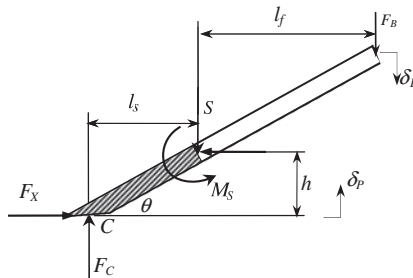
Figure 4.46   Free body diagram of a diaphragm spring's segment

F_X is the friction force at point C, thus:

$$F_X = \mu F_C \tag{4.151}$$

Therefore, Equation 4.150 can be rewritten as:

$$F_C l_s \left(1 - \mu \frac{h}{l_s}\right) + F_B l_f = M_S \tag{4.152}$$

The term $\mu \frac{h}{l_s}$ is small compared to unity (some 2–5%) and it is reasonable to ignore it. On the other hand, the moment M_S in fact is the spring's resistance to the applied load and increases when the spring deflection δ_S increases. In other words, it is equal to the moment of the spring's elastic force about the point S:

$$M_S = l_s F_S(\delta_S) \tag{4.153}$$

Thus, the clamp force equation in general can be written as:

$$F_C(\delta_P) = F_S(\delta_S) - k_s F_B(\delta_B) \tag{4.154}$$

in which k_s will be called the 'seesaw gain':

$$k_s = \frac{l_f}{l_s} \tag{4.155}$$

and δ_B is the releasing bearing displacement, δ_P is the pressure plate lift-off displacement and δ_S is the total spring deflection:

$$\delta_S = \delta_S^* + \delta_P \tag{4.156}$$

Referring to Figure 4.42, the initial deflection δ_S^* of the spring is:

$$\delta_S^* = \delta_2 - \delta_1 \tag{4.157}$$

Typical variations of F_B versus δ_B and F_S versus δ_S are shown in Figures 4.43 and 4.45. In order to be able to use Equation 4.154, the two displacements δ_B and δ_P must be related and belong to a unique working condition of the spring. Theoretically, this relationship can be obtained by the application of the virtual work principle to the spring of Figure 4.46. If a virtual displacement Δ_B is applied at the point of action of F_B, the other forces will also experience virtual displacements Δ for F_X, Δ_P for F_C and Δ_θ for M_S as shown in Figure 4.47.

Since the whole system is in equilibrium, the net virtual work done by all forces and moments should be nil. In mathematical form:

$$F_C \Delta_P + F_B \Delta_B - M_S \Delta_\theta - F_X \Delta = 0 \tag{4.158}$$

According to Figure 4.47 and assuming small Δ_θ, the virtual displacements can readily be related:

$$\Delta_\theta = \frac{1}{l_s} \Delta_P \tag{4.159}$$

$$\Delta = \frac{h}{l_s} \Delta_P \tag{4.160}$$
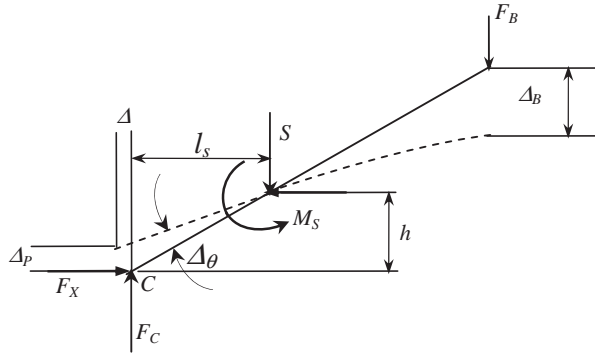
Figure 4.47   Virtual displacements

Therefore:

$$F_B \Delta_B + \left(F_C - \frac{M_S}{l_s} - F_X \frac{h}{l_s} \right) \Delta_P = 0 \tag{4.161}$$

Substituting for the parenthesis from Equation 4.150 gives:

$$\frac{\Delta_B}{\Delta_P} = \frac{l_f}{l_s} = k_s \tag{4.162}$$

With a small deflection approximation, the total displacements δ_B and δ_P can be related by:

$$\delta_B = k_s \delta_P \tag{4.163}$$

Owing to the non-linear behaviour of the spring, however, the actual relationship is not linear. A typical dependency of the pressure plate's displacement δ_P on the bearing displacement δ_B for a passenger car clutch is shown in Figure 4.48. A linear approximation is also considered together with a dead zone in which the pressure plate is insensitive to the bearing displacement.
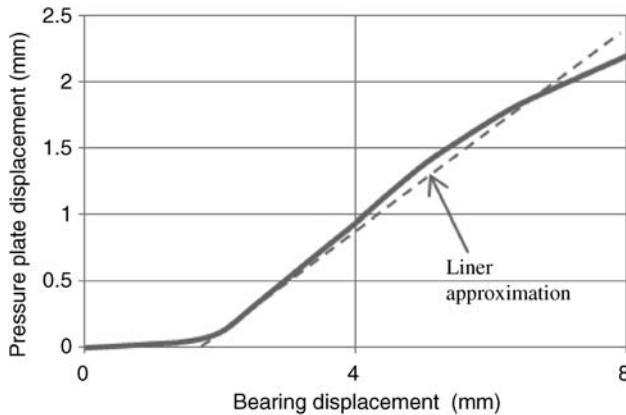
Figure 4.48   Relationship between the pressure plate and bearing displacements
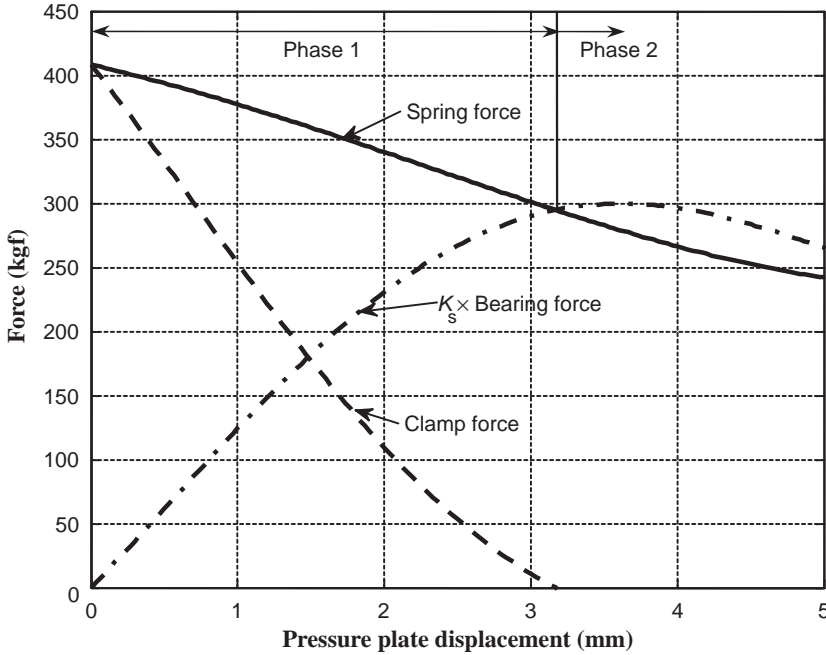
Figure 4.49 Variation of the clamp load with pressure plate displacement

With a linear relation of Equation 4.164, the clamp force of Equation 4.154 can be rewritten as:

$$F_C(\delta_P) = F_S(\delta_S^* + \delta_P) - k_s F_B(k_s \delta_P) \tag{4.164}$$

On the other hand, the clamp load is simultaneously acting on the clutch plate causing its cushion springs to deflect (see Figure 4.42). Thus, the clamp load can also be related to the cushion springs deflection characteristics. During the clutch disengagement two phases will exist; the first phase is the clamp load reduction and second phase is the pressure plate and clutch plate separation. In the first phase, the clamp load reduces from its initial value of F_S^* to nil, and causes the cushion spring inside the pressure plate to expand to its initial deflection δ_C^* (see Figure 4.42):

$$\delta_C^* = \delta_0 + \delta_1 - \delta_2 \tag{4.165}$$

Using Equation 4.157 one finds:

$$\delta_S^* + \delta_C^* = \delta_0 \tag{4.166}$$

Therefore, the total displacement of pressure plate in the first phase, just before disengagement, is δ_C^*. At the end of first phase the clamp load disappears. This instant identifies the start of the second phase at which the clutch plate and pressure plate begin to separate (pressure plate lift-off). A typical variation of the clamp load during phase 1 according to Equation 4.164 can be seen in Figure 4.49.

4.5.3.3   MG Formula

Equation 4.164 is useful when the variations of the spring and bearing forces with relevant displacements are available. Such information can be obtained from clutch tests. The test equipment applies independent

Figure 4.50   Clutch test equipment

forces to the finger tips and pressure plate in order to measure the bearing and spring forces. A clutch under test is shown in Figure 4.50 and a typical test result is given in Figure 4.51. The graphs illustrate the hysteresis behaviour of the spring due to the inherent internal friction.

As the spring force results from the Belleville part of the spring, the mathematical equation for the force-displacement curve of such springs has usually been used to express the behaviour of a diaphragm spring. Research work was carried out at the Department of Automotive Engineering, IUST, in which the test results for several clutch springs were used in order to develop a more accurate relationship between
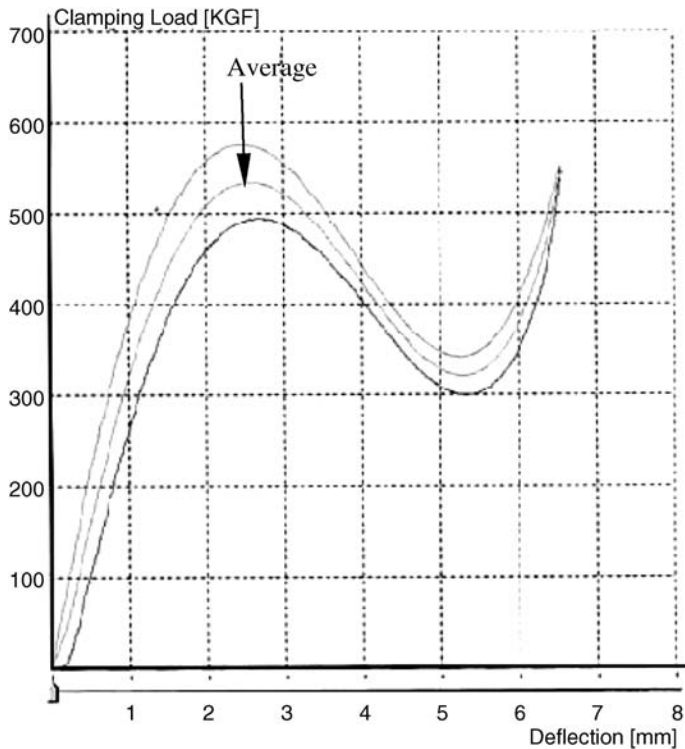
Figure 4.51   Typical test results for spring force

the spring force and its displacement. The final result was found to be applicable to all tested springs belonging to C and D segment automobiles as well as light truck clutches. The spring force-displacement equation which will be called the *MG formula* (stands for Mashadi-Ghyasvand), that uses the basic Belleville equation with several modifications, is of the following form:

$$F_S = \frac{4000E}{1-v^2} \cdot \frac{t^3}{D_o^2} \cdot \frac{k_2}{k_1} \cdot (1+0.153k_3) \cdot \delta_s \qquad (4.167)$$

in which δ_S is the spring deflection (mm) and F_S is calculated in kgf. The other parameters are:

$$k_1 = \frac{6}{\pi \times LnR} \cdot \frac{(R-1)^2}{R^2} \qquad (4.168)$$

$$k_2 = \frac{D_o - D_{eff}}{D_o - D_i} \qquad (4.169)$$

$$k_3 = \left(\frac{2\delta_s + t}{t}\right) \cdot \left(\frac{h - 1.45\delta_s}{t}\right) \cdot \left(\frac{h - k_4\delta_s}{t}\right) \qquad (4.170)$$

$$k_4 = \frac{t}{5} \qquad (4.171)$$

$$R = \frac{D_o}{D_{eff}} \qquad (4.172)$$

$$D_{eff} = 0.98D_b \qquad (4.173)$$
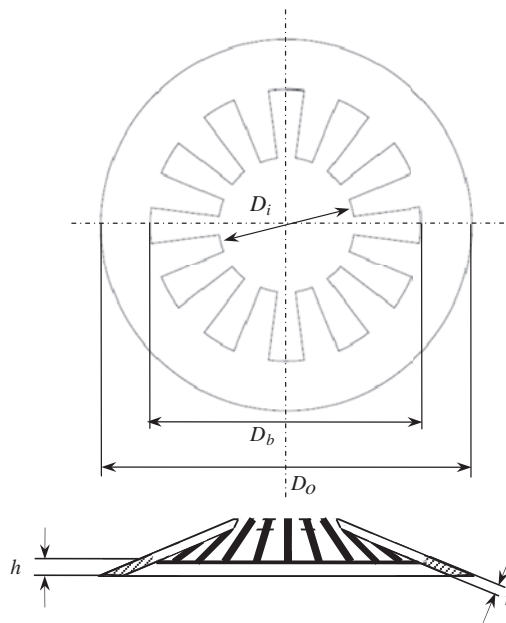
Figure 4.52 The geometry of diaphragm spring
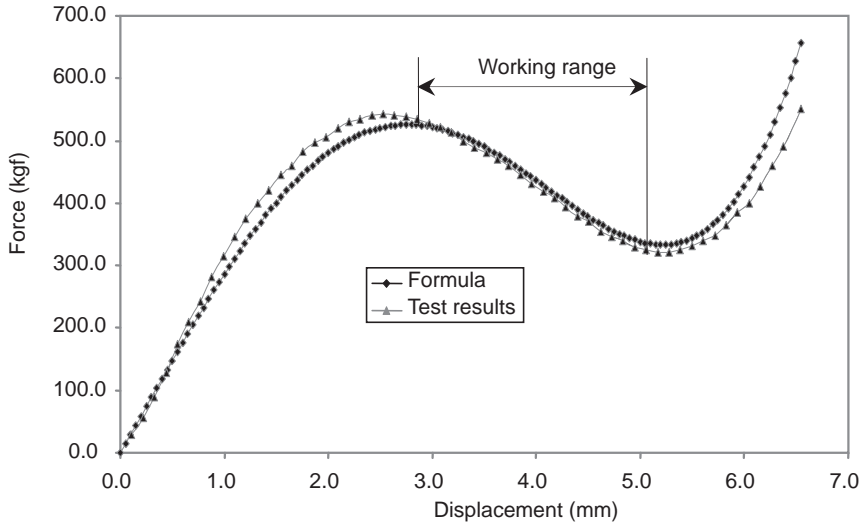
Figure 4.53 Comparison of test data with results of spring MG formula

The definition of geometrical parameters can be found in Figure 4.52. E and v in Equation 4.167 are modulus of elasticity (MPa) and Poisson's ratio of the spring material respectively. A comparison is made between the results of the MG formula with the experimental measurements in Figure 4.53. The central part of the figure which describes the working area of the spring shows good agreement.

A similar equation for the release load (bearing force F_B) versus the bearing displacement δ_B is also obtained in the following form:

$$F_B = \frac{250E}{1 - v^2} \cdot \frac{t^3}{D_o^2 \cdot k_1} \cdot (1 + 0.133 k_3') \cdot \delta_B \tag{4.174}$$

in which:

$$k_3' = \left(\frac{\delta_B - 0.1t}{t}\right) \cdot \left(\frac{h - 2.2\delta_B}{t}\right) \cdot \left(\frac{h - k_4'\delta_B}{t}\right) \tag{4.175}$$

$$k_4' = \frac{t}{6} \tag{4.176}$$

Example 4.5.2

The information for a passenger car clutch is given in Table 4.10.

(a) Plot the F_S-δ_S and F_B-δ_B curves using the MG formula.
(b) Calculate the seesaw gain k_s.
(c) Plot the variation of clamp force inside the first plot of F_S-δ_S.
(d) Calculate the initial deflection δ_C^*.

Table 4.10 Clutch data for Example 4.5.2

Parameter	Value	Unit
Inner diameter D_i	62	mm
Outer diameter D_o	206	mm
Belleville inner diameter D_b	171.3	mm
Spring thickness t	2.3	mm
Belleville height h	3.47	mm
Set point deflection δ_S^*	3.5	mm
Modulus of elasticity	207	MPa
Poisson's ratio	0.3	–

Solution

(a) With a simple MATLAB program the required curves can be plotted. The results are given in Figure 4.54.

(b) Referring to Figure 4.52:

$$l_s = \frac{D_o - D_b}{2}, \quad l_f = \frac{D_b - D_i}{2} \quad \text{and} \quad k_s = \frac{l_f}{l_s} = \frac{D_b - D_i}{D_o - D_b} = 3.15$$
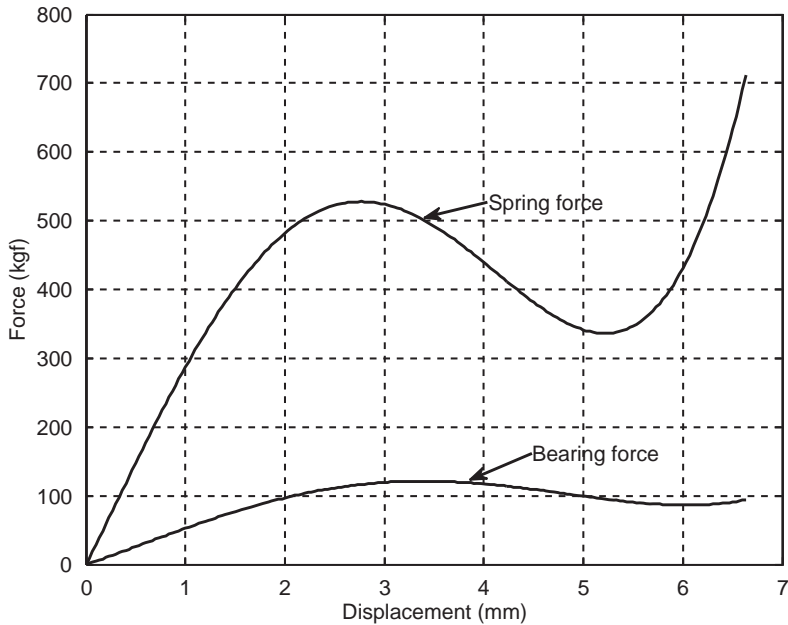
Figure 4.54 Spring and bearings forces of Example 4.5.2 (a)

(c) Using Equation 4.164, the variation of clamp load is obtained and then plotted against the variation of pressure plate displacement. Figure 4.55 shows the result. Note that in Figure 4.49 a similar result was plotted against the bearing displacement. It should also be noted that the graphs are invalid after the clamp load vanishes (shaded area).

(d) According to Equation 4.166:

$$\delta_0 = \delta_S^* + \delta_C^* = 4.5 \text{ mm}$$

Therefore:

$$\delta_C^* = \delta_0 - \delta_S^* = 4.5 - 3.5 = 1 \text{ mm}.$$
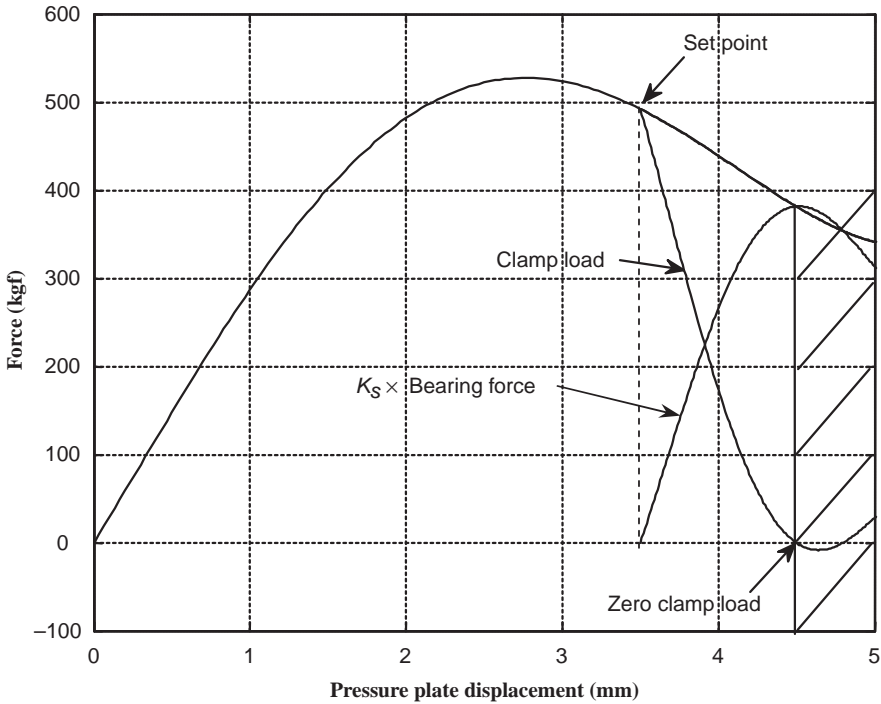
Figure 4.55   Clamp load versus pressure plate displacement

4.5.4   Clutch Engagement Dynamics

In a vehicle equipped with a manual gearbox, for a gearshift it is necessary to press and hold the clutch pedal in order to disconnect the engine from the driveline. When the gear is shifted, then releasing the clutch will let the flywheel and gearbox input shaft gradually attain equal speeds. During this period, torque is generated between the sliding surfaces due to friction which is controlled by the normal force applied to the mating surfaces. The speed variations of the two mating surfaces are dependent on the dynamics of the process influenced by the values of the load and the inertia of input and output. Figure 4.56 depicts a typical speed variation during clutch release with the first gear engaged.
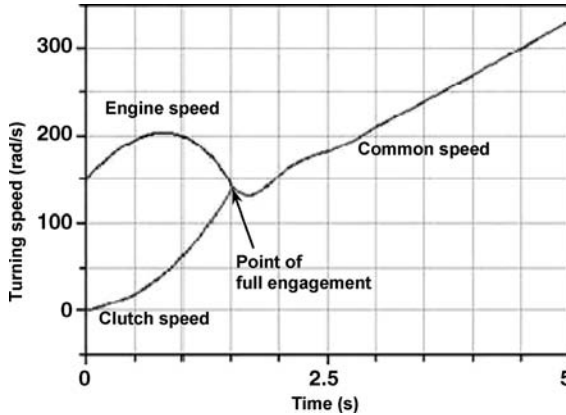
Figure 4.56   Engine and clutch speeds during clutch release

The clutch release is performed by gradually lifting the pedal which will increase the spring force on the surfaces. The resulting torque T_c is proportional to the applied force F (see Equations 4.122 or 4.133):

$$T = KF \tag{4.177}$$

K is the proportionality constant equal to $\mu\, r_{eq}$ or $2\mu\, r_{av}$ for the uniform pressure or uniform wear respectively. Let T_e be the flywheel input torque, i.e. the torque received from the engine side, and T_L the load torque on the clutch, i.e. from the driveline. Figure 4.57 depicts the free body diagram of the flywheel and clutch plate with torques T_e and T_L as input and load torques as well as T_c as the friction torque acting on contact surfaces. The inertia properties are described by I_e as the overall inertia of input shaft and all connecting parts, and I_d as the overall inertia of the output shaft and all connecting parts.

The driveline equivalent inertia I_d referred to the clutch plate can be written as (see Figure 4.58):

$$I_d = I_c + \frac{I_g}{n_g^2} + \frac{I_w + mr_w^2}{n^2} \tag{4.178}$$

in which I_c is the inertia of clutch shaft and all connected masses, I_g is the equivalent inertia of gearbox output shaft and differential input shaft, and I_w is the inertia of wheels and axles combined.
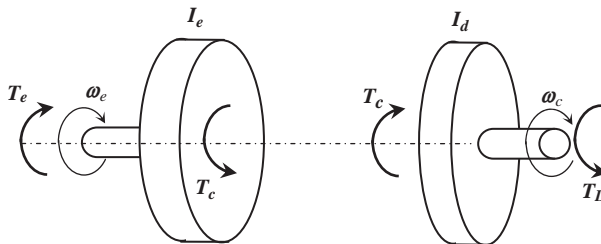
Figure 4.57   Free body diagrams of clutch mating plates
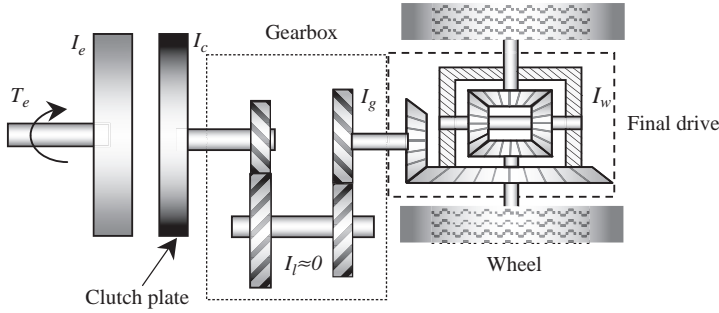
Figure 4.58   Inertias in a vehicle driveline

n_g and n are the gearbox and overall transmission gear ratios, m is the vehicle mass and r_w is the wheel effective radius.

The dynamic equations for the two sides during the clutch engagement are (see Figure 4.57):

$$T_e - T_c = I_e \frac{d\omega_e}{dt} \tag{4.179}$$

$$T_c - T_L = I_d \frac{d\omega_c}{dt} \tag{4.180}$$

It should be noted that in these equations the elasticity of input and output shafts as well as the damping torques in the bearings have been ignored for the sake of simplicity; these will be dealt with in Chapter 6. The input and load torques are time-varying in general; the input torque variations depend on the throttle input, whereas the load torque is dependent on the vehicle's external loads.

The power flow in the clutch system is also important. A part of engine power P_e is transferred to the clutch (P_c) and some part is consumed by the rubbing friction surfaces (P_f). These are:

$$P_e = T_e \omega_e \tag{4.181}$$

$$P_c = T_c \omega_c \tag{4.182}$$

$$P_f = T_c \omega_s = T_c(\omega_e - \omega_c) \tag{4.183}$$

In order to determine the power relationships, let us begin with the difference $P_e - P_f$:

$$P_e - P_f = P_e - T_c \omega_s = T_e \omega_e - T_c(\omega_e - \omega_c) \tag{4.184}$$

This can be simplified by using Equations 4.179 and 4.182:

$$P_e - P_f = P_c + \frac{d}{dt}\left(\frac{1}{2} I_e \omega_e^2\right) \tag{4.185}$$

Thus the clutch power P_c is *not* the difference between the input power and friction power, since a part of input power is also used to change the kinetic energy of the flywheel. Note that the power flow is instantaneous, as is clear from the differentiation sign of Equation 4.185. Therefore, it is only in the steady-state condition that a power balance equation from input to the output can be written. In other conditions, the energy term is important. A misunderstanding is sometimes seen in the literature of taking the engine and clutch powers to be equal at times close to clutch lock-up. Equation 4.185 clearly shows

that this assumption is far from being true, unless the engine speed is kept constant. Note that P_f will vanish as it approaches lock-up.

Clutch efficiency during engagement can be defined as:

$$\eta_c = \frac{E_i - E_{loss}}{E_i} = \frac{E_L}{E_i} \tag{4.186}$$

where the input energy E_i, energy at lock-up E_L and energy loss E_{loss} are:

$$E_i = \frac{1}{2}I_e\omega_e^2(0) + \frac{1}{2}I_d\omega_c^2(0) + \int_0^{t_L} P_e dt \tag{4.187}$$

$$E_L = \frac{1}{2}(I_e + I_d)\omega_e^2(t_L) \tag{4.188}$$

$$E_{loss} = \int_0^{t_L} P_f dt \tag{4.189}$$

where t_L is the time when the speeds of flywheel and clutch plate become equal and the full engagement or clutch lock-up is achieved. After lock-up, Equations 4.179 and 4.180 can be combined to obtain:

$$T_e - T_L = (I_e + I_d)\frac{d\omega_e}{dt} \tag{4.190}$$

Equation 4.190 is the governing equation for engine dynamics after the clutch lock-up.

In order to evaluate T_L, one should consider the external loads acting on the vehicle, details of which were discussed in Chapter 3. These comprise rolling resistance, aerodynamic, and grade forces. With the assumption of no wheel slip (see Section 3.10), the load torque can be written as:

$$T_L = \frac{r_w}{n}(F_{RR} + F_A + F_G) \tag{4.191}$$

The variation of the clutch force with time depends on two factors; one is the spring's force-displacement behaviour and the second is the way the clutch pedal is released. The former can be obtained from the characteristics of the diaphragm spring (Section 4.5.3) and the latter is an input to the model. Details of the dynamic behaviour of clutch engagement require information on the throttle inputs and clutch release regime and will be discussed in the following sections.

4.5.4.1 Uniform Clutch Release

Let us assume the clamp force of clutch varies linearly with the release bearing's displacement, then for a uniform release of clutch, the clutch force can be considered to increase linearly with time by a constant factor k_F, i.e.,

$$F(t) = k_F t \tag{4.192}$$

Equation 4.192 is valid only for times when the force does not exceed its limiting value F_{max}:

$$t \le t_r = \frac{F_{max}}{k_F} \tag{4.193}$$
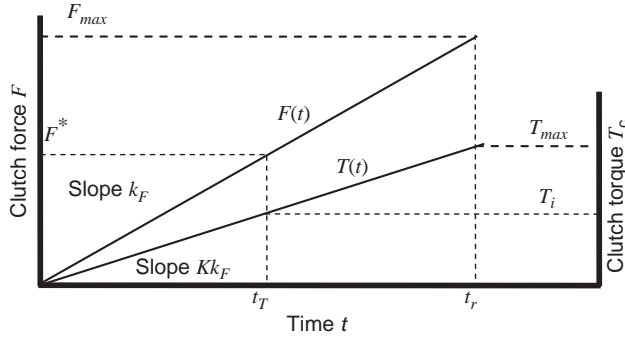
Figure 4.59 Clutch force and torque time variations (linear assumption)

The output torque will also grow linearly with time by factor Kk_F (see Equation 4.177):

$$T_c(t) = Kk_F t \tag{4.194}$$

The variations of the clutch force and torque for these linear assumptions can be illustrated in graphical form of Figure 4.59.

Considering the fact that the maximum clutch torque is delivered at the maximum clutch force, for input torques smaller than the maximum torque, the time t_T at which the friction torque becomes equal to the input torque will always be smaller than t_r, the time of the maximum force. In other words, when the clutch starts to engage, the clutch torque reaches the input value before the clutch is completely released. The time t_T depends on the value of input torque T_i:

$$t_T = \frac{T_i}{Kk_F} \tag{4.195}$$

The clutch force at the end of this phase is (see Figure 4.59):

$$F^* = F(t_T) = \frac{T_i}{K} \tag{4.196}$$

At this time, the clutch torque is equal to the input torque, but the clutch output speed is still below the input speed. This means the full power is not delivered to the output since the same input torque is transmitted to the output but at a lower speed. Further release of the clutch will increase the spring force and in turn also increase the clutch torque up to its maximum limit. With known characteristics for T_c and T_L, Equation 4.180 can be integrated to find the clutch rotational speed before lock-up:

$$\omega_c(t) = \omega_c(0) - \frac{1}{I_d} T_L t + \frac{1}{2I_d} Kk_F \, t^2 \tag{4.197}$$

The vehicle acceleration and speed during this period are:

$$a(t) = \frac{r_w}{nI_d}[Kk_F t - T_L] \tag{4.198}$$

$$v(t) = v(0) + \frac{r_w}{n}\left[\omega_c(0) - \frac{1}{I_d} T_L t + \frac{1}{2I_d} Kk_F t^2\right] \tag{4.199}$$

The distance travelled can also be found from:

$$s(t) = s(0) + v(0)t + \frac{r_w}{n}\left[\omega_c(0)t - \frac{1}{2I_d}T_Lt^2 + \frac{1}{6I_d}Kk_Ft^3\right] \tag{4.200}$$

Also from Equation 4.179:

$$\int_0^t T_e(t)dt = T_Lt + I_d\,\omega_c(t) - I_e[\omega_e(0) - \omega_e(t)] \tag{4.201}$$

The integral on the left side depends on the throttle input and engine speed and in general is difficult to obtain. After lock-up the speed of the engine and clutch can be found by the integration of Equation 4.190:

$$\omega_e(t) = \omega_e(t_L) + \frac{1}{I_e + I_d}\int_{t_L}^t (T_e - T_L)dt \tag{4.202}$$

where t_L is the lock-up time.

There is a subtle issue regarding the rolling resistance part of the load torque in the equations of this section. In fact, on a level road, no load will act on the vehicle as long as a motive force is not present. Thus for those instants with no clutch torque, no load torque should be considered. Also as long as the clutch torque is less than the rolling resistance torque, the net motive torque on the clutch plate must be zero. In other words, the rolling resistance torque alone cannot produce a negative acceleration.

Constant Engine Torque

If a constant engine torque T^* is assumed to be delivered during the clutch engagement, then the integral of Equation 4.201 and engine speed $\omega_e(t)$ can readily be obtained from Equations 4.179 and 4.194:

$$\int_0^t T_e(t)dt = T^*t \tag{4.203}$$

$$\omega_e(t) = \omega_e(0) + \frac{1}{I_e}T^*t - \frac{1}{2I_e}Kk_Ft^2 \tag{4.204}$$

The time t_L at which the two speeds become identical (lock-up time) can be found by equating Equations 4.201 and 4.203:

$$t_L = \frac{\beta}{2\alpha} + \frac{1}{2\alpha}\sqrt{\beta^2 + 4\alpha\gamma} \tag{4.205}$$

where:

$$\alpha = \left(\frac{1}{2I_e} + \frac{1}{2I_d}\right)Kk_F \tag{4.206}$$

$$\beta = \frac{1}{I_e}T^* + \frac{1}{I_d}T_L \tag{4.207}$$

$$\gamma = \omega_e(0) - \omega_c(0) \tag{4.208}$$

The angles the engine and clutch plate revolve (in radians) are found by integrating Equations 4.204 and 4.197:

$$\theta_e(t) = \omega_e(0)t + \frac{1}{2I_e}T^* t^2 - \frac{1}{6I_e}Kk_F t^3 \tag{4.209}$$

$$\theta_c(t) = \omega_c(0)t + \frac{1}{6I_d}Kk_F t^3 - \frac{1}{2I_d}T_L t^2 \tag{4.210}$$

The speed of flywheel after lock-up can be found from:

$$\omega_e(t) = \omega_e(t_L) + \frac{1}{I_e + I_d}(T_e - T_L)(t - t_L) \tag{4.211}$$

The clutch efficiency during engagement is determined by using Equations 4.187 and 189 then substituting in Equation 4.186. The input and loss energies are:

$$E_i = \frac{1}{2}I_e\omega_e^2(0) + \frac{1}{2}I_d\omega_c^2(0) + T^* t_L\left[\omega_e(0) + \frac{1}{2I_e}T^* t_L - \frac{1}{6I_e}Kk_F t_L^2\right] \tag{4.212}$$

$$E_{loss} = Kk_F\left[\frac{1}{2}\gamma + \frac{1}{3}\beta t_L - \frac{1}{4}\alpha t_L^2\right]t_L^2 \tag{4.213}$$

Example 4.5.3

Consider a 1 second time for a uniform release of clutch pedal and assume that the engine torque during this period is kept constant. The vehicle is at a standstill and a gradual start-up on a level road is required.

(a) Calculate the clutch lock-up time.
(b) Plot the variation of engine and clutch speeds up to the lock-up point.
(c) Plot the variations of engine and clutch torques.
(d) Plot the variations of components of powers.

Table 4.11   Data for Example 4.5.3

Parameter	Value	Unit
Input inertia I_e	0.25	kgm^2
Clutch inertia I_c	0.05	kgm^2
Gearbox output inertia I_g	0.1	kgm^2
Wheels and axles inertia I_w	2.0	kgm^2
Vehicle mass	1000	kg
Wheel radius	30	cm
Gearbox ratio	3.5	–
Final drive ratio	4	–
Rolling resistance coefficient	0.02	–
Engine input torque (constant)	60	Nm
Maximum engine torque	110	Nm
Engine initial speed	1000	rpm

(e) Determine the clutch efficiency during the engagement.
(f) Discuss the results.

   Data are given in Table 4.11.

Solution

K and k_F are not given. We assume the clutch is designed for the maximum engine torque which leads to: $Kk_F = \dfrac{T_{\max}}{t_r} = 110$

```
% Example 4.5.3

close all, clear all, clc

% Inputs:
Ie=0.25; Ic=0.05; Ig=0.1; Iw=2; m=1000; rw=0.3;
ng=3.5; nf=4;
tr=1.0;    % Clutch release time
frr=0.02;  % Rolling resistance coef
Temax=110; % maximum engine torque
Tstar=60;  % Constant engine torque input
omegae0=1000;      % Initial engine speed (rpm)
theta=0;   % Slope (deg)

% pre-calculations
Ig=Ig/ng^2; Iw=Iw/(nf*ng)^2; Iv=m*(rw/nf/ng)^2;
Id=Ic+Ig+Iw+Iv;
Ka=Temax/tr;
theta=theta*pi/180;
Tl=m*9.81*(frr*cos(theta)+sin(theta))*rw/nf/ng;

% Solution of Part (a)
alpha=Ka*(0.5/Ie+0.5/Id);
beta=Tstar/Ie+Tl/Id;
gama=omegae0*pi/30;
tlock=beta/2/alpha+sqrt(beta^2+4*alpha*gama)/2/alp
ha;

% solution of Part (b)
for i=1: 200
    t(i)=i*tlock/200;
    temp=Ka*t(i)^2/2;
    omegae(i)=omegae0*pi/30-temp/Ie+Tstar*t(i)/Ie;
    omegac(i)=temp/Id-Tl*t(i)/Id;
end
subplot(2,1,1)
plot(t, omegae*30/pi)
hold on
plot(t, omegac*30/pi, '--')
ylabel('Rotational speed (rpm)')
grid
```

Figure 4.60   MATLAB program for Example 4.5.3

```
% Example 4.5.3 (continued)
% Solution of Part (c)
for i=1: 200
    Tc(i)=Ka*t(i);
end
Te=Tstar*ones(200,1);
subplot(2,1,2)
plot(t, Te)
hold on
plot(t, Tc ,'--')
xlabel('Release time (s)')
ylabel('Torque (Nm)')
grid

% Solution of Part (d)
for i=1: 200
    Pe(i)=Te(i)*omegae(i);
    Pc(i)=Tc(i)*omegac(i);
    Pf(i)=Tc(i)*omegae(i)-Pc(i);
    Pl(i)=Tl*omegac(i);
    P(i)=Pe(i)-Pl(i)-Pf(i);
end
figure
subplot(2,1,1)
plot(t, Pe/1000)
hold on
plot(t, Pc/1000 ,'--')
plot(t, Pl/1000 ,'-.')
plot(t, Pf/1000, '.')
ylabel('Power (kW)')
grid
subplot(2,1,2)
plot(t, P/1000)
xlabel('Release time (s)')
ylabel('Power (kW)')
grid

% Solution of part (e): clutch efficiency
Ei=0.5*Ie*(omegae0*pi/30)^2+…
Tstar*tlock*(omegae0*pi/30+Tstar*tlock/2/Ie-
Ka*tlock^2/6/Ie);
Eloss=Ka*(gama/2+beta*tlock/3-
alpha*tlock^2/4)*tlock^2;
etac=(Ei-Eloss)*100/Ei;
```

Figure 4.60   (*Continued*)

A simple MATLAB program can be written to calculate the variables. Figure 4.60 provides a sample program for this purpose. The answer to (a) using this program is: $t^* = 1.067$ sec.
The results of (b) and (c) are plotted in Figure 4.61. The results of (d) are plotted in Figure 4.62. The result of (e), the efficiency of clutch during engagement is 44.7%.

(f) The speed of the engine increases while the clutch torque is small, and then decreases with the increase of the clutch torque. The clutch speed, on the other hand, grows steadily to reach the engine speed. The clutch torque increases linearly with time, but as is clear from the lower subplot

of Figure 4.62, its maximum exceeds the maximum torque of engine (110 Nm). The reason is that the release time of 1 second for the uniform increase of clutch force was not sufficient for the speeds to become equal. At 1 second the torque attains the 110 Nm limit and should not increase further. Thus, the results after 1 second are not valid.
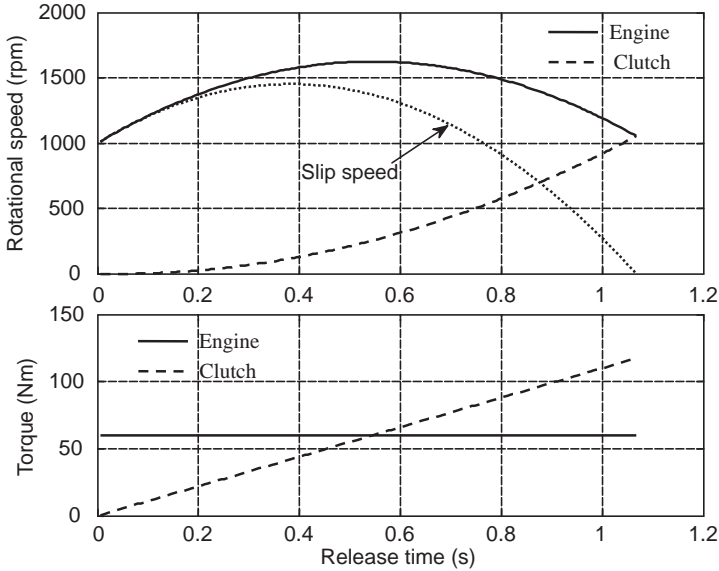
Figure 4.61   Answers to (b) and (c) of Example 4.5.3
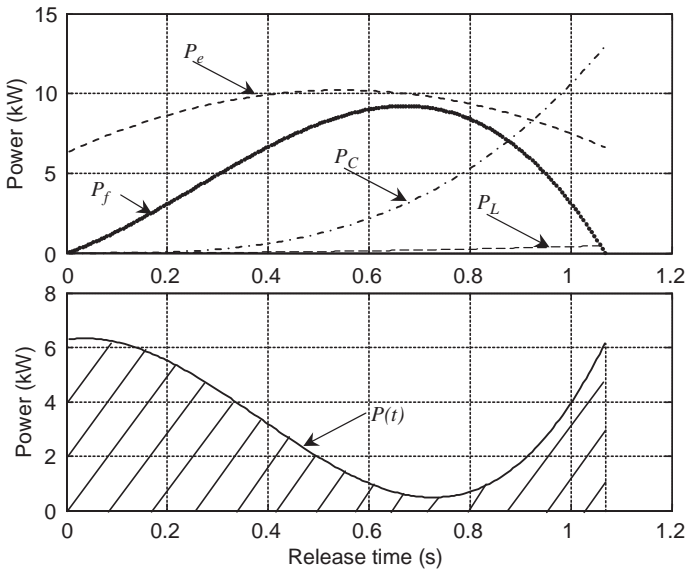
Figure 4.62   Answers to (d) of Example 4.5.3

The power variations, on the other hand, show that the friction power grows steadily up to around 0.65 sec and declines afterwards with decreasing slip speed. The surface under the net instantaneous power depicted in the lower subplot indicates the net energy transmitted to the system by the engine. Therefore, the remaining engine power is lost to friction or external load on the vehicle. The power lost to friction (P_f) is large compared to the power consumed by the external load (P_l).

Note that the clutch power slightly after 0.9 second is larger than the input power from the engine. This is because the clutch plate is receiving not only a part of engine power, but also a considerable amount of kinetic energy from the flywheel (this is why the engine speed decreases). In Equation 4.185 with a negative engine acceleration and decreasing friction power, the clutch plate receives additional power and its power value is higher than the engine power.

Constraint on Torque

We earlier noticed that the torque will grow higher than its maximum limit unless a constraint is imposed on it:

$$T_c = \begin{cases} Kk_F & \text{for} \quad t \le t_r \\ T_{\max} & \text{for} \quad t > t_r \end{cases} \tag{4.214}$$

For the constant clutch torque region, the engine and clutch speed variations are:

$$\omega_e(t) = \omega_e(t_r) + \frac{1}{I_e}(T^* - T_{\max})(t - t_r); \quad t > t_r \tag{4.215}$$

$$\omega_c(t) = \omega_c(t_r) + \frac{1}{I_d}(T_{\max} - T_L)(t - t_r); \quad t > t_r \tag{4.216}$$

Vehicle acceleration, velocity and travelled distance during this period are:

$$a(t) = \frac{r_w}{nI_d}[T_{\max} - T_L] \tag{4.217}$$

$$v(t) = v(t_r) + \frac{r_w}{nI_d}[T_{\max} - T_L](t - t_r) \tag{4.218}$$

$$s(t) = s(t_r) + v(t_r)(t - t_r) + \frac{r_w}{2nI_d}[T_{\max} - T_L](t - t_r)^2 \tag{4.219}$$

The new lock-up time t_L^* at which the two speeds become identical is:

$$t_L^* = t_r + \frac{I_e I_d[\omega_e(t_r) - \omega_c(t_r)]}{(I_e + I_d)T_{\max} - I_d T^* - I_e T_L} \tag{4.220}$$

Example 4.5.4

Repeat the previous example with a constraint imposed on the clutch torque. In addition to (a) plot of speeds; (b) plot of torques; also (c) plot the variations of vehicle acceleration, speed and travelled distance with time.

Solution

Small changes to the previous program can include the torque constraint. A sample program for these changes is given in Figure 4.63. The results obtained with this program are depicted in Figures 4.64 and 4.65.

The lock-up time t_L^* becomes only slightly longer than t_L: $t_L^* = 1.071\,s$

The overall trends of parameters are similar to previous results. Although the torque limitation is applied, no significant changes occur due to the very short period of time involved.

```
% Example 4.5.4

% Solution of Part (a)
     temp=Ka*tr^2/2;
     omegae_tr=omegae0*pi/30-temp/Ie+Tstar*tr/Ie;
     omegac_tr=(temp-Tl*tr)/Id;
tstar=tr+Id*Ie*(omegae_tr-omegac_tr)/(Temax*(Id+Ie)-
Tstar*Id-Tl*Ie);
if tstar < tr
     alpha=Ka*(0.5/Ie+0.5/Id);
     beta=Tstar/Ie+Tl/Id;
     gama=omegae0*pi/30;
     tstar=beta/2/alpha+sqrt(beta^2+4*alpha*gama)/2/alpha;
end

% solution of Part (b)
for i=1: 200
  t(i)=i*tstar/200;
   if t(i) <= tr
      temp=Ka*t(i)^2/2;
      omegae(i)=omegae0*pi/30-temp/Ie+Tstar*t(i)/Ie;
      omegac(i)=temp/Id-Tl*t(i)/Id;
      Acc(i)=(2*temp/t(i)-Tl)*rwpn/Id;
      v(i)=omegac(i)*rwpn;
      s(i)=(temp*t(i)/3/Id-Tl*t(i)^2/2/Id)*rwpn;
      j=i;
   else
      omegae(i)=omegae(j)+(Tstar-Temax)*(t(i)-t(j))/Ie;
      omegac(i)=omegac(j)+(Temax-Tl)*(t(i)-t(j))/Id;
      Acc(i)=(Temax-Tl)*rwpn/Id;
      v(i)=v(j)+Acc(i)*(t(i)-t(j));
      s(i)=s(j)+(v(j)+v(i)/2)*(t(i)-t(j));
   end
end
```

Figure 4.63   Changed parts of program for Example 4.5.4
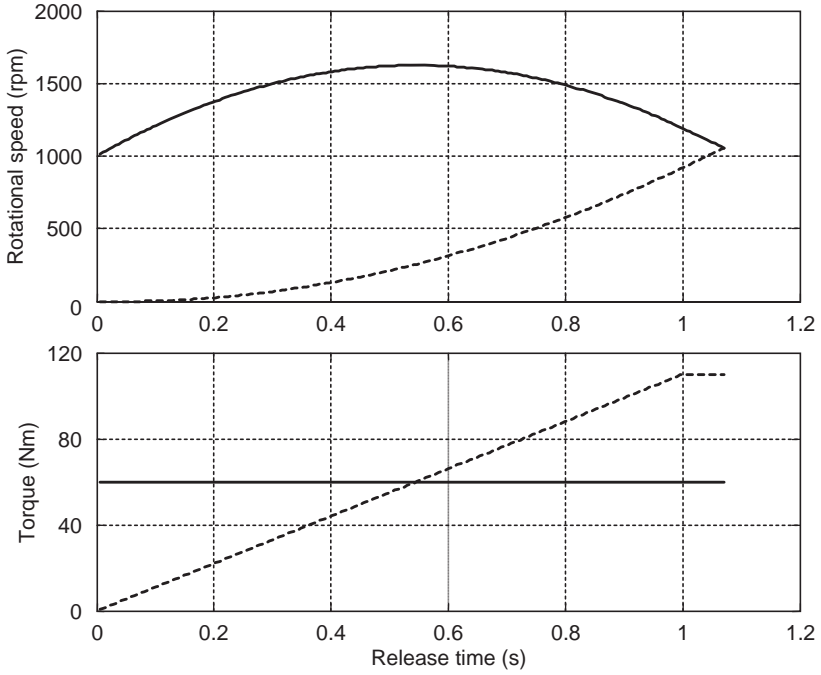
Figure 4.64 Answers to (a) and (b) of Example 4.5.4
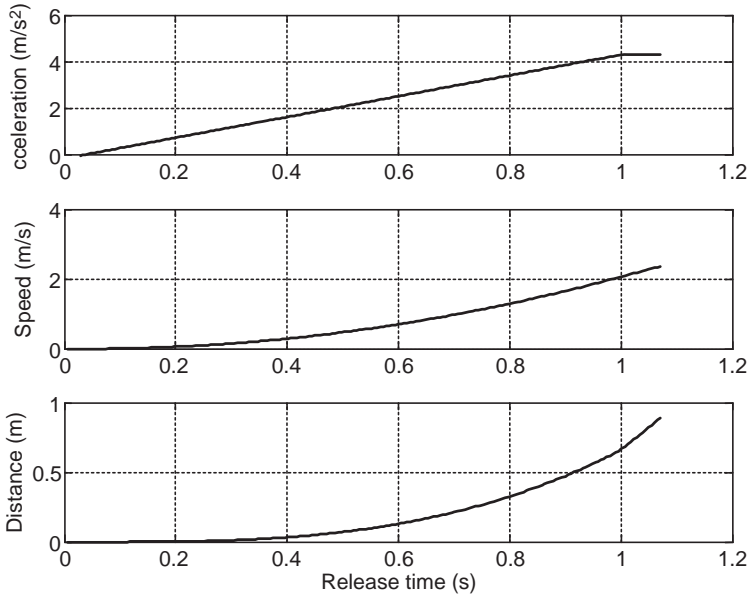
Figure 4.65 Answers to (c) of Example 4.5.4

Throttle Inputs

In practice, the clutch engagement is performed by controlling the throttle at the same time as the clutch pedal is released. In this way the engine torque is controlled in accordance with power requirements which comprise the power generated by the clutch torque on the output shaft and the dissipated power due to friction.

With a uniform clutch release assumption, the clutch torque variations will be similar to those described before. For different throttle inputs, different scenarios can be considered:

- *Sudden throttle*: In this case, a throttle value of θ_0 is applied instantly as the releasing is underway.
- *Constant throttle*: In this case, a throttle value of θ_0 is assumed to be applied before the releasing is performed. Therefore, prior to the release, the engine speed is higher than sudden throttle case.
- *Variable throttle*: In this case, the throttle is assumed to vary in an exponential form according to the load on the vehicle and final throttle value θ_f is chosen by the operator. The relation is:

$$\theta_e(t) = \theta_i + (\theta_f - \theta_i) \cdot (1 - e^{bt}) \tag{4.221}$$

$$b = a + c \cdot \frac{T_L}{T_{e_{\max}}} - d.\frac{\theta_i}{100} \tag{4.222}$$

in which θ_i is the initial throttle input and coefficients a, c and d are three constants.

Owing to the complexity of engine behaviour following throttle inputs, no closed form solution is available for this case. A computer program, therefore, is needed for the solution of governing differential equations. Similar problems were solved in Chapter 3 and the same program structure can also be used in the current case.

Example 4.5.5

For the vehicle in Example 4.5.3, consider a sudden throttle input of 35% at the start-up and repeat the calculations. The MT engine formula coefficients and full throttle engine data are available in Tables 3.1 and 3.2 of Chapter 3.

Additional information is provided in Table 4.12.

Table 4.12 Additional data for Example 4.5.5

Parameter	Value	Unit
Coefficient of dynamic friction	0.20	
Initial engine speed	1000	rpm
Average clutch radius	15	cm

Solution

A main MATLAB program is generated together with two MATLAB functions to solve the differential equations. The structure of the programs is similar to previous examples and comments inside the program listings given in Figures 4.66 and 4.67 are self-explanatory.

Results obtained from these programs are illustrated in Figures 4.68–4.70. Solid lines in general belong to engine outputs and dashed lines are for clutch outputs. The outputs for the rotational speeds and torques of clutch and engine depicted in Figure 4.68 show quite similar results to those of previous examples with constant torque. The reason is that the torque has a very small variation and the amplitude is close to that of Example 4.5.4.

The lock-up time in this case is 1.091 s, again very close to the previous result. Power elements depicted in Figure 4.69 are also quite similar to those in Example 4.5.4. In this case, the number of turns of flywheel and clutch plate are also calculated and shown in Figure 4.70.

```
% Example 4.5.5
% Sudden throttle input

clc; clear all; close all;

global p Tcmax Tl Ie Id th0 thm ar b mud
global wer tet p

% Additional Inputs:
rc_av=0.15;    % clutch plate average radius
mus=0.3;       % static coefficient of friction
mud=0.2;       % dynamic coefficient of friction
thm=35;        % throttle limit

% Engine full throttle (WOT) information
te=[80 98 100 105 107 109 110 109 104 97];
ome=[1000 1500 2000 2500 3000 3500 4000 4500 5000 5300];
Temax=max(te);
% Fit a curve to WOT data
[p,s]=polyfit(ome,te,2);

% Precalculations
Ig=Ig/ng^2; Iw=Iw/(nf*ng)^2; Iv=m*(rw/nf/ng)^2;
Id=Ic+Ig+Iw+Iv;
K=2*mud*rc_av;       % 2*mud*Raverage
Tcmax=Temax;                 % Clutch torque limit
Fcmax=Temax/K;       % Clutch force limit
a=Fcmax/tr;
Ka=K*a;
ar=a*rc_av;
theta=theta*pi/180;
rwpn=rw/nf/ng;
Tl=m*9.81*(frr*cos(theta)+sin(theta))*rwpn;

% set values for sudden throttle input:
th0=thm; b=0;

% Initial conditions for integration:
x0=[w0*pi/30 0 0 0];  % [w_e w_c theta_e theta_c]
t0=0; tf=1.5;
```

Figure 4.66 Main MATLAB program for Example 4.5.5

```
% Example 4.5.5 (continued-1)

% Main loop for finding lockup time
w_e=x0(1);
w_c=1.5*we;
while w_c – w_e > 0.05

[t,x]=ode45(@Example_455_f,[t0 tf], x0);

w1=x(:,1); w2=x(:,2);
i=length(w1);
w_e=w1(i); w_c=w2(i);
 if w_c >= w_e
   if w_e<0
     tf=tf*0.8;
   else
      tf=0.95*tf;
   end
 else
    tf=tf*1.05;
    w_c=600;
 end
end

% Figure 1.1: rotational speed-time
subplot(2,1,1)
plot(t, x(:,1)*30/pi), hold on, plot(t, x(:,2)*30/pi,'--'), grid
xlabel('Time (s)')
ylabel('Rotational speed (rpm)')

% Regenerate the results:
wei=x(:,1); wci=x(:,2);
for j=1: i
 thr=th+(thm-th)*(1-exp(-b*t(j))); if thr>100, thr=100; end
% calculate engine torque from MT formula:
 wer=30*wei(j)/pi;
 pow=(1.003*wer)^1.824;
 den=(1+exp(-11.12-0.0888*thr))^pow;
 Te(j)=polyval(p,wer)/den;
 tet=Te(j);
% Estimate engine throttle opening
 thet(j)=fsolve(@partfind, thr ,optimset('Display','off',
'TolFun', 0.1));
 delomeg=abs(wei(j)-wci(j));
 torq(j)=Ka*t(j);
% limit the torque
 if torq(j)>Tcmax, torq(j)=Tcmax; end
 Pe(j)=wei(j)*tet;
 Pc(j)=wci(j)*torq(j);
 Pf(j)=torq(j)*wei(j)-Pc(j);
 Pl(j)=Tl*wci(j);
 P(j)=Pe(j)-Pl(j)-Pf(j);
end
% Plot other figures
```

Figure 4.66   (*Continued*)

```
function f=Example_455_f(t,x)

global p Tcmax Tl Ie Id th thm ar b mud

thr=th+(thm-th)*(1-exp(-b*t));
if thr>100, thr=100; end
% Calculate engine torque at given w_e and throttle
   wer=x(1)*30/pi; % engine speed
   pow=(1.003*wer)^1.824;  % MT formula
   den=(1+exp(-11.12-0.0888*thr))^pow; % MT formula
Te=polyval(p,wer)/den;  % MT formula
% Calculate clutch torque
Tc=2*mud*ar*t;
if Tc>Tcmax, Tc=Tcmax; end

f=[(Te-Tc)/Ie,
   (Tc-Tl)/Id,
   x(1),
   x(2)];

% Function to find the throttle opening at given torque and speed
function f=partfind(x)

global wer tet p

   pow=(1.003*wer)^1.824;
   den=(1+exp(-11.12-0.0888*x))^pow;
   f=tet-polyval(p,wer)/den;
```

Figure 4.67 MATLAB functions for Example 4.5.5

The clutch efficiency during the engagement in this case can be found by including the following additional integrations in the function:

delomeg=abs(×(1)−×(2));
f(5)=Te*×(1);
f(6)=Tc*delomeg;

and the following statements in the main program:

Ei=×(i,5)+0.5*Ie*(w0*pi/30)^2;
Eloss=×(i,6);
etac=(Ei−Eloss)*100/Ei;

The result is 45.5%.
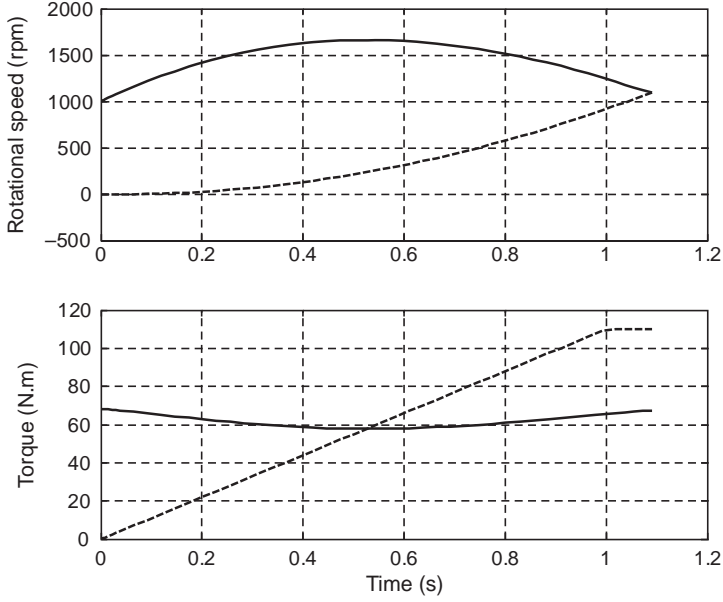
Figure 4.68   Engine and clutch speeds and torques of Example 4.5.5
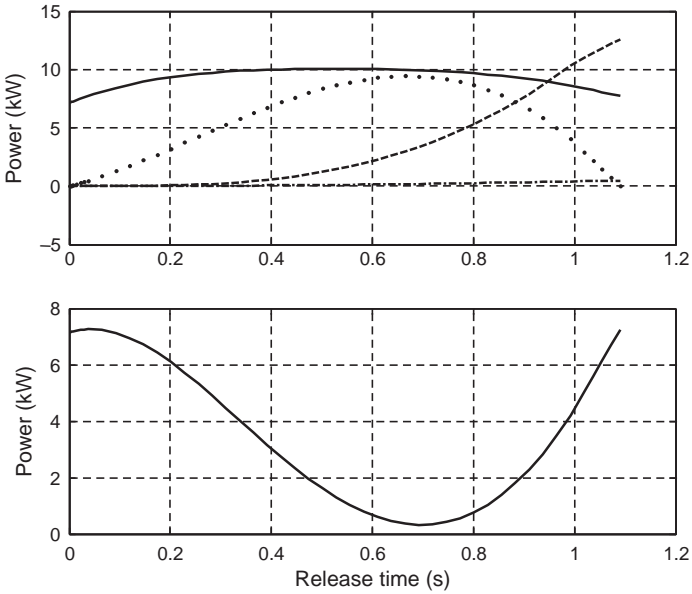
Figure 4.69   Power elements (see Figure 4.62) of Example 4.5.5
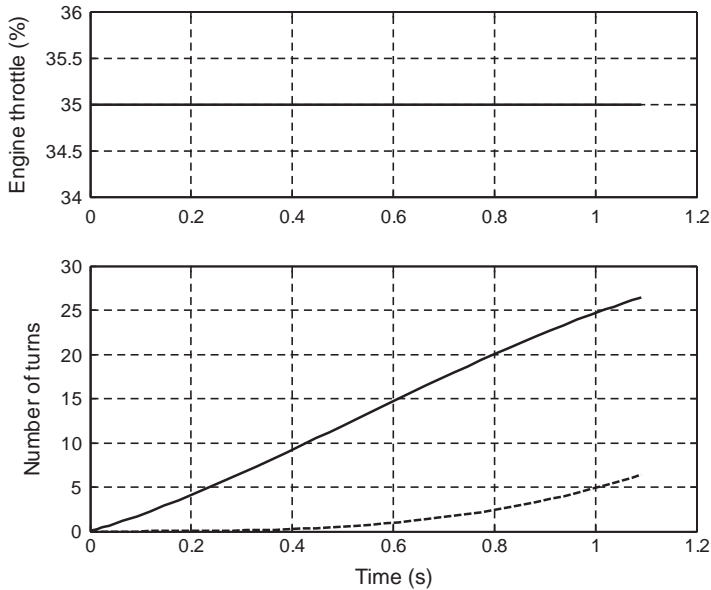
Figure 4.70   Engine throttle, engine and clutch turns of Example 4.5.5

Note that the similarities between the answers of Example 4.5.4 and the current example are due to the identical vehicle parameters and the choice of 35% throttle input that produced similar torque inputs. The maximum torque of the MT engine model is 113 Nm, whereas in Example 4.5.4 it was 110. Therefore only small differences exist between the results of the two cases. This example was designed to show that the assumption of a constant engine torque is reasonable.

Example 4.5.6

Repeat Example 4.5.5 for an exponential throttle input with values of a, c and d equal to 3, 3 and 2 respectively. The vehicle in this case is initially at rest on an uphill road with a slope angle of 10 degrees. For this case consider a pedal release time of 1.5 sec and a final throttle value of 50%.

Solution

With small modifications to the programs of Example 4.5.5 (not provided), the results shown in Figures 4.71–4.73 are obtained. Since the vehicle is facong uphill, a backward motion occurs as shown by negative clutch speed of Figure 4.71. The 50% throttle is enough to prevent engine speed falling below 1000 rpm at the time of lock-up. The power curves of Figure 4.72 indicate that the instantaneous power becomes negative at times.
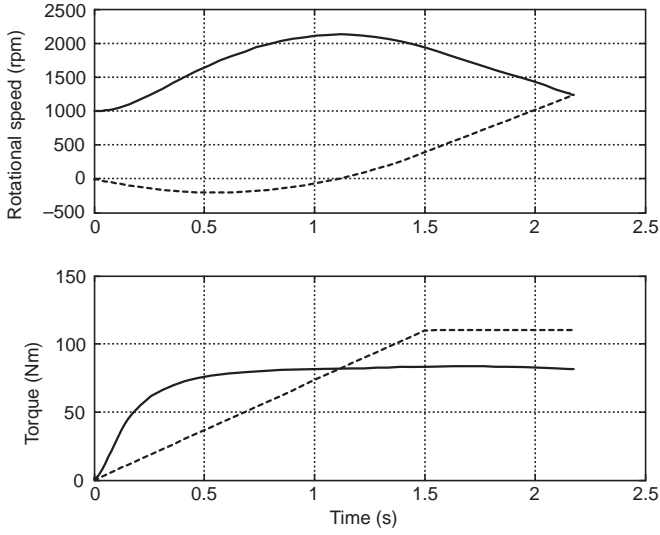
Figure 4.71   Engine and clutch speeds and torques of Example 4.5.6
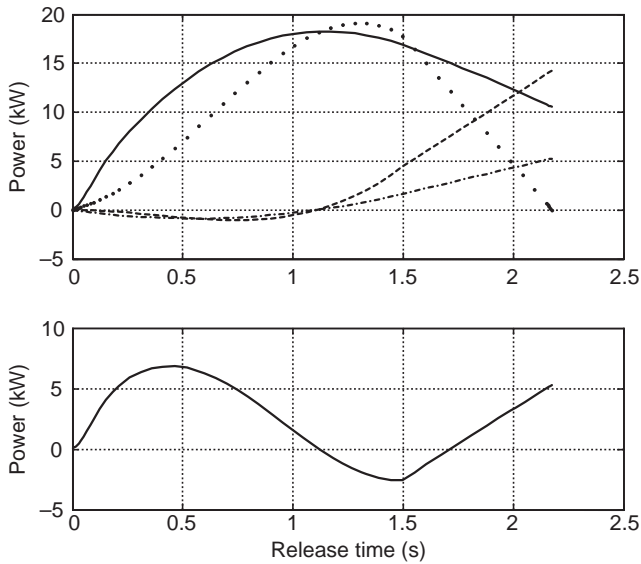
Figure 4.72   Power elements (see Figure 4.62) of Example 4.5.6
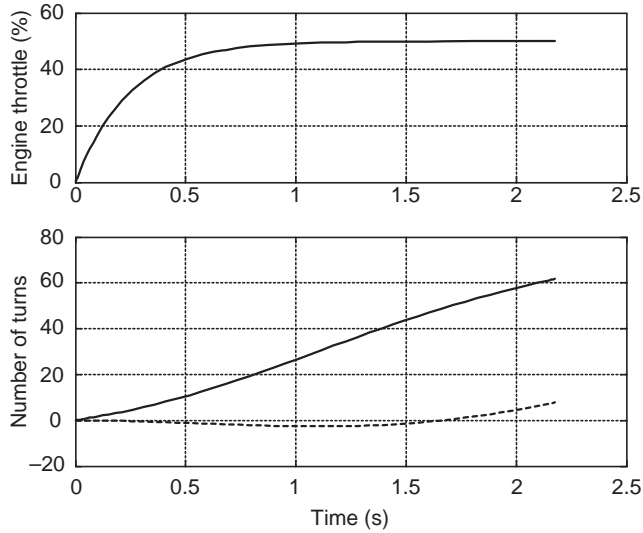
Figure 4.73 Engine throttle, engine and clutch turns of Example 4.5.6

4.5.4.2 Pedal Release

The most realistic case for clutch dynamics would be to consider the clutch pedal travel instead of the clutch force variation during the engagement. To this end, the relationship between the pedal travel and the release bearing travel can be obtained similar to Equation 4.149 (see Figure 4.40). Assuming rigid arms, the displacement δ_B of release bearing is related to pedal travel x_P by:

$$\delta_B = \frac{l_2 \cdot l_4}{l_1 \cdot l_3} x_P = k_{BP} x_P \tag{4.223}$$

Making use of Equation 4.163, one will find the relationship between the pressure plate displacement δ_P and the pedal travel x_P:

$$\delta_P = \frac{1}{k_s} \delta_B = \frac{k_{BP}}{k_s} x_P = k_{PP} x_P \tag{4.224}$$

Now according to Equation 4.164, the clamp force F_C can be determined from the pedal travel x_P. Thus, the clutch dynamics will depend on the time history of pedal travel $x_P(t)$ during clutch release. In order to analyze the clutch dynamics by pedal travel, the following examples are presented.

Example 4.5.7

The measured lever arms of a clutch system in a vehicle are given in Table 4.13.

(a) Calculate the overall gain from the pedal travel to pressure plate displacement.
(b) For a maximum displacement of 13 cm for the clutch pedal, determine the pressure plate displacement.

Table 4.13   Clutch system information for Example 4.5.7

Parameter	l_1	l_2	l_3	l_4	l_f	l_s
Value (mm)	330	60	130	30	43	14

Solution

The answer to (a) can be found from Equations 4.163, 4.223 and 4.224:

$$k_s = \frac{l_f}{l_s} = \frac{43}{14} = 3.071$$

$$k_{BP} = \frac{l_2 \cdot l_4}{l_1 \cdot l_3} = \frac{60 \times 30}{330 \times 130} = 0.042$$

$$k_{PP} = \frac{k_{BP}}{k_s} = \frac{0.042}{3.071} = 0.0137$$

The answer to (b) simply is:

$$\delta_P = k_{PP}x_P = 0.0137 \times 130 = 1.8\,mm$$

Example 4.5.8

For the clutch of Example 4.5.7, the information on the MG formula is provided in Table 4.14. If a linear pedal release in 2 seconds is considered:

(a) Determine displacement δ_{BC} that takes place before the release bearing comes into contact with the spring fingers.
(b) Plot the time variations of the clamp load and displacements.

Table 4.14   Clutch data for Example 4.5.8

Parameter	Value	Unit
Inner diameter D_i	46	mm
Outer diameter D_o	164	mm
Bellville inner diameter D_b	134.5	mm
Spring thickness t	2	mm
Bellville height h	2.75	mm
Set point deflection δ_S^*	3	mm
Modulus of elasticity	207	MPa
Poisson's ratio	0.3	–

Solution

A linear pedal release in 2 seconds means that the maximum displacement of 13 cm has travelled linearly:

```
% Example 4.5.8
global Ds ks t k1 k2 kp3 De Nu E h

% Input data
Di=46; De=164; Dt=134.5; t=2; h=2.75;
Nu=0.3; E=207; % Giga Pascal
l1=330; l2=60; l3=130; l4=30;
Ds=3;    % set point
tr=2.;   % Pedal release time
pt=130;  % Pedal travel

% Pre-calculations
Dteff=0.98*Dt; R=De/Dteff;
k1=6*((R-1)/R)^2/pi/log(R);
k2=(De-Dteff)/(De-Di);
lf=(Dt-Di-t)/2; ls=(De-Dt-t)/2;
ks=lf/ls; kbp=l2*l4/l1/l3; kpp=kbp/ks; kxp=pt/tr;

% Determine the bearing displacement 'dbstar' at release-start point
dbstar=fsolve(@Example_458_f, 1.5, optimset('Display','off'));
tstar=dbstar/kbp/kxp; % total time for full engagement

% Calculate the spring force
dt=tstar/200;
for i=1:200
   time(i)=i*dt;
   db(i)=time(i)*kbp*kxp;
   ds(i)=Ds+time(i)*kpp*kxp;
   k3=(2*ds(i)+t)*(h-1.45*ds(i))*(h-0.4*ds(i))/t^3;
   k4=4000*E*k2*t^3/k1/(1-Nu^2)/De^2;
FS(i)=k4*ds(i)*(1+0.153*k3);
   kp3=(db(i)-0.1*t)*(h-2.2*db(i))*(h-t*db(i)/6)/t^3;
   k4=250*E*t^3/k1/(1-Nu^2)/De^2;
FB(i)=k4*db(i)*(1+0.133*kp3);
Fc(i)=FS(i)-ks*FB(i);
end
plot(tr-time, FS), hold on, plot(tr-time, ks*FB, '--'),
plot(tr-time, Fc, '-.'), grid
xlabel('Time (s)'), ylabel('Force (kgf)')
figure
plot(tr-time, ds, '--')
hold on

dt=tr/200;
for i=1:200
   time(i)=i*dt;
   db(i)=time(i)*kbp*kxp;
end
plot(tr-time, db), grid
xlabel('Time (s)'), ylabel('Displacement (mm)')
```

Figure 4.74   MATLAB program for Example 4.5.8

$$x_P(t) = \frac{130}{2}t = 65\,t$$

Therefore: $\delta_B = k_{BP}x_P = 0.042*65\,t = 2.73\,t$

For the pressure plate displacement, however, we need to find out when the bearing comes into contact with the fingers. This happens just before the clamp force starts to build up from zero. From Equation 4.164 the transition point is:

$$F_S\left(\delta_S^* + \frac{\delta_B}{k_s}\right) - k_s F_B(\delta_B) = 0$$

which is a nonlinear function and must be solved numerically (or by trial and error) to obtain δ_B^*, that is the total displacement of the bearing from start of contact between the clutch plate and pressure plate to completion of the engagement. Hence, the rest of bearing travel δ_{BC} is to bring the pressure plate into contact with the clutch plate, i.e.,

$$\delta_{BC} = 130k_{BP} - \delta_B^*$$

In the time domain it is:

$$t_{BC} = 2 - \frac{\delta_B^*}{65k_{BP}}$$

The pressure plate displacement is zero up to this time and after that it is:

$$\delta_P(t) = k_{PP}x_P(t - t_{BC}) = 0.0161 \times 65(t - t_{BC}) = 1.047(t - t_{BC}),\ t > t_{BC}$$

When the time history of the displacements is known, the clamp force can be obtained from Equation 4.164.

A MATLAB program is useful for solving the equations given above. A sample program is provided in Figure 4.74. The function used to determine δ_B^* is shown in Figure 4.75.

Parameters δ_B^*, δ_{BC} and t_{BC} calculated by the program are:

$$\delta_B^* = 2.49\,mm,\ \delta_{BC} = 2.97\,mm \text{ and } t_{BC} = 1.087\,s$$

```
% Function for Example 4.5.8
function f=Example_458_f(x)

global Ds ks t k1 k2 kp3 De Nu E h
    ds=Ds+x/ks;
    db=x;
    k3=(2*ds+t)*(h-1.45*ds)*(h-0.4*ds)/t^3;
    k4=4000*E*k2*t^3/k1/(1-Nu^2)/De^2;
FS=k4*ds*(1+0.153*k3);
    kp3=(db-0.1*t)*(h-2.2*db)*(h-t*db/6)/t^3;
    k4=250*E*t^3/k1/(1-Nu^2)/De^2;
FB=k4*db*(1+0.133*kp3);
f=FS-ks*FB;
```

Figure 4.75   MATLAB function for Example 4.5.8
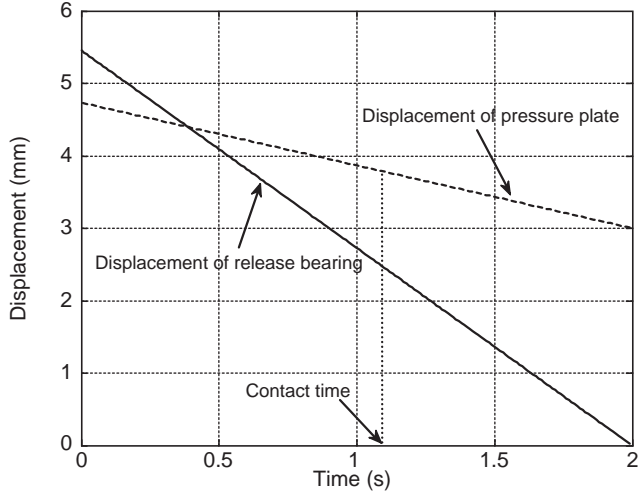
Figure 4.76   Time histories of clutch displacements

Therefore, when the pedal is fully depressed, the bearing displacement is 5.456 mm. Releasing the pedal up to 1.087 seconds, only brings the pressure plate in contact with the clutch plate and clutch engagement starts here. So far the bearing has displaced 3 mm whereas the pressure plate has displaced 0.943 mm (Figure 4.76). In the remaining time of 0.9 seconds the engagement takes place and the clamp force increases from zero to its maximum of 406 kgf (Figure 4.77) that is equal to spring force at its set point.
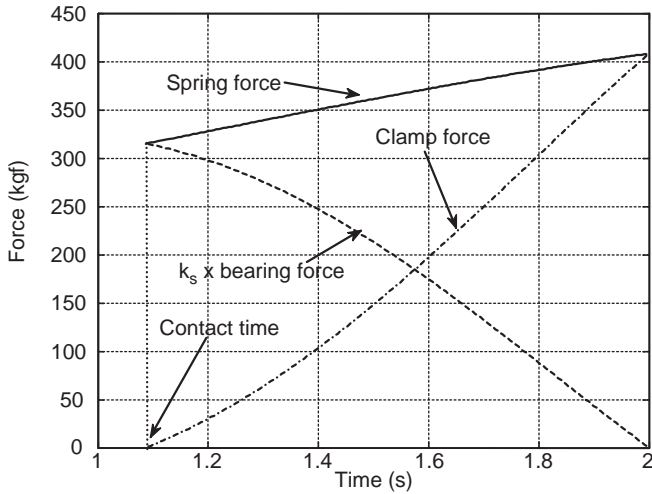
Figure 4.77   Time histories of clutch forces

Example 4.5.9

Use the information of Examples 4.5.3, 4.5.7 and 4.5.8 and simulate the clutch dynamics by releasing the clutch pedal when a constant engine torque is maintained.

Solution

A suitable program for this example is a combination of programs written for Examples 4.5.5 and 4.5.8. Modifications are needed since the program of Example 4.5.5 was for throttle input whereas for the current example a constant torque is assumed.

Preparing this program is left to the reader and only the results are given here. The time variations of the rotational speeds as well as torques of engine and clutch plate are illustrated in Figure 4.78. Since the engagement phase starts after around 1.1 sec, and the torque input is present from the start, the engine speed increases close to 4000 rpm until the release period begins and the clutch torque opposes the input torque. The clutch torque is determined from the clamp load and the coefficient of friction, and as a result it grows to large values but the torque limit is imposed at 110 Nm (max. of engine torque). The plot of power items given in Figure 4.79 shows a similar trend in the engagement phase, but with larger values of friction power that produce negative power flows during this stage.

The efficiency of the clutch engagement is found to be 40.1%.
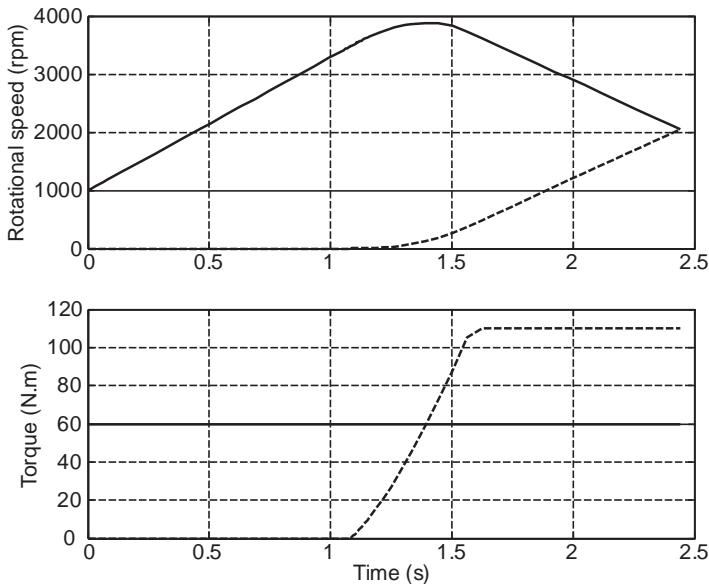
Figure 4.78   Turning speeds and torques of Example 4.5.9
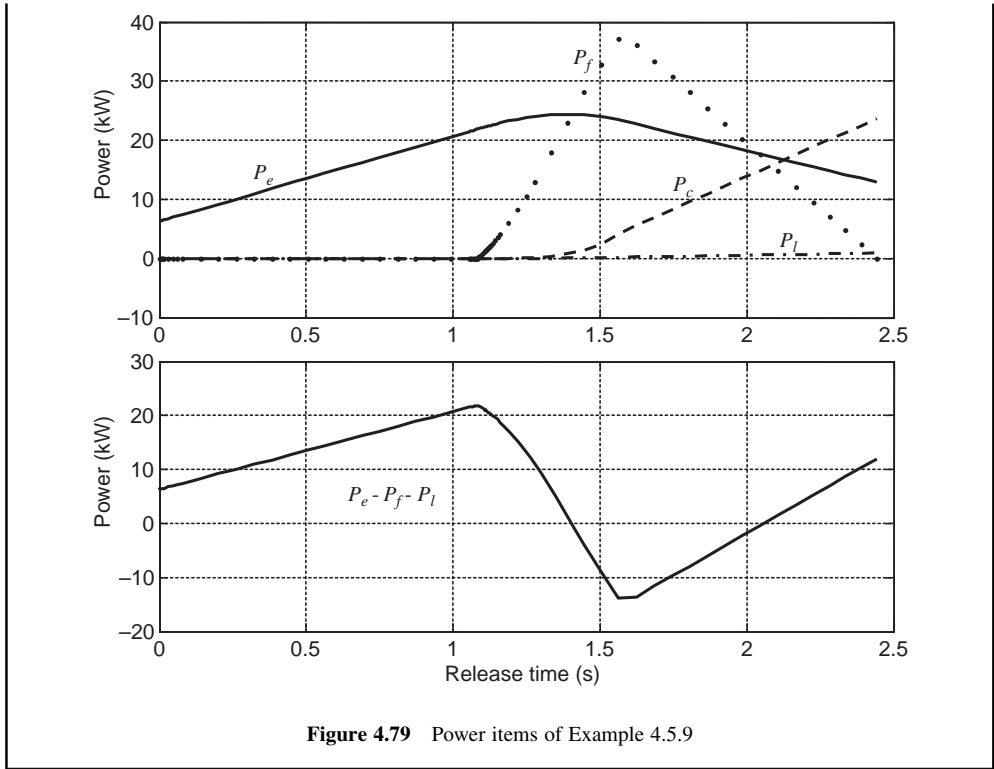
Figure 4.79   Power items of Example 4.5.9

4.5.4.3   Remarks

The clutch controls the power transfer from engine to the vehicle and vice versa. The complicated natures of the friction and spring load make clutch modelling difficult. Two issues are important to note: the clutch torque magnitudes and direction of energy flow and these will be discussed in the following section.

Clutch Input and Output Torques

The torque model based on the Coulomb friction for the clutch results in clutch torques larger than the engine torque. The clutch torque is related linearly to the normal load on the friction surface which itself is the result of the clutch pedal release. Therefore, the clutch force of this model has nothing to do with the engine torque. Nonetheless, the clutch torque being larger than the engine torque is explainable by considering the following example. Imagine a large flywheel to replace the engine. At time zero, the flywheel is charged and the clutch starts to engage. The clutch torque will be generated due to friction while there is no input torque. Thus the clutch torque can exist with no input torque and this means the clutch torque is independent of the input torque. In fact, the clutch is receiving energy from the flywheel due to its change in momentum. This is also happening in the vehicle case with the engine attached to the flywheel, and the lost energy of flywheel is replaced by the engine's energy. According to Equation 4.185:

$$P_c = P_e - P_f - I_e \omega_e \alpha_e \tag{4.225}$$

which shows that the clutch receives energy from the flywheel (the last term is positive when the engine speed decreases) even if the engine produces no power. The limitation on the clutch torque with the
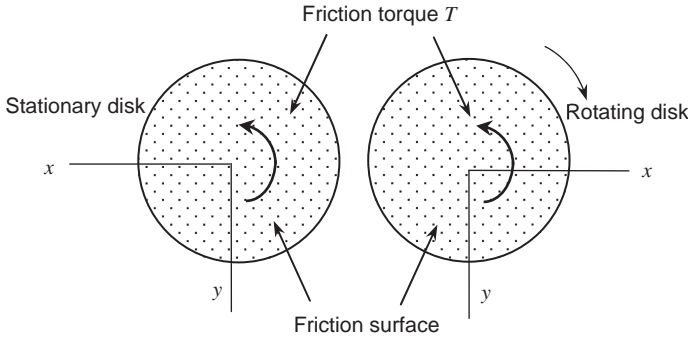
Figure 4.80   Direction of friction torques on disk pairs

Coulomb friction model is based on its design capacity. Assuming the design capacity to be equal to the maximum engine torque, it means that whatever the input torque of engine is, the clutch can develop its torque up to the *maximum* engine torque.

Direction of Power Flow

The power flow is not always from the engine to the gearbox and can be other way round. In order to analyze the direction of the power flow, let us consider two disks, one stationary and the other rotating. If the two disks are brought into contact, the friction torques over the two surfaces will act in opposite directions. According to Figure 4.80 for the rotating disk (around the z axis), the friction torque acts opposite to the direction of relative rotation, but for the stationary disk the torque is in the direction of relative rotation. In other words, the negative torque on the rotating disk consumes its power ($P = [-T]\omega < 0$) and torque transmitted to the stationary disk delivers energy to it and can make it turn until the relative speed is zero. Thus the power flow is from the one with higher speed towards that with lower speed.

Defining the speed difference for two rotating disks with speeds ω_2 and ω_1 as:

$$\Delta\omega = \omega_2 - \omega_1 \qquad (4.226)$$

For positive $\Delta\omega$ the power flow is directed from disk 2 towards disk 1, and for negative $\Delta\omega$ it is vice versa. One example for energy transfer from clutch to the engine is during a downshift of gears in which the engine speed increases during the clutch release. This means that the engine receives energy via the clutch. The reason is that when a lower gear is engaged, the rotation of wheels will effectively turn the clutch plate at higher speeds than the engine speed.

4.6   Automatic Transmissions

With an automatic transmission, a driver no longer needs to worry about gear selection during driving and thus it makes driving a car easier. In the past, conventional automatics were used with control systems which were not reliant on electronics. With recent progress in automotive electronics, however, new types of automatic transmission systems have been proposed. One simple concept is the automation of a manual transmission (AMT), which allows the controlled use of the well-developed manuals that also have largest efficiency. Other automatic derivations from manuals are double (twin) clutch transmissions (DCT) with the attractive feature of having continuous torque flow. More details will be discussed in the next sections.
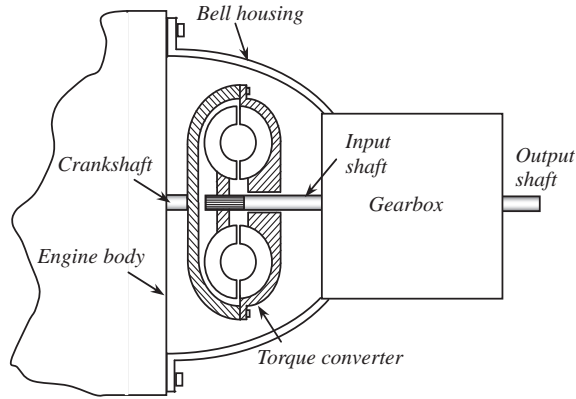
Figure 4.81   Overall construction of a conventional automatic

4.6.1   Conventional Automatics

In a conventional automatic transmission, the clutch is replaced with a fluid coupling or torque converter to eliminate engaging/disengaging action during gear change. A completely different gearing system, called a planetary or epicyclic gears (see Section 4.4.2), is used to perform gear ratio changes instead of using conventional gears. These changes make the conventional automatics totally different from the manuals internally although the external shape may look similar to a manual transmission as Figure 4.81 shows.

   The gears used in conventional automatics are made up of epicyclic gears. An epicyclic gear set was introduced in Section 4.4.2 and was shown to be able to produce several ratios from which three ratios were useful (two forward and one reverse). Thus in a multi-speed transmission, several epicyclic gear sets are needed. In fact, when the two sets of such gears are connected to each other, *coupled gears* result. In a planetary coupling the number of ratios increases, but unfortunately not all of the ratios are useful. The reason is that the overall gear ratio from input to the output of the gearbox will depend on all of the gears that are connected. Therefore, in order to achieve the required gear ratios for a transmission (e.g. 1–5), the gear teeth for all the planetary sets must be designed in relation to one another. The function of torque converter and control of transmission are discussed in the following subsections.

4.6.1.1   Torque Converter

The principle of operation of a *fluid coupling* is the transfer of momentum from a working fluid (oil) to a turbine. An impeller (pump) with several vanes is fixed to the crankshaft and when an engine rotates, a working fluid is accelerated, moving from low radius to higher radius along the vanes (see Figure 4.82). At the outlet of the vane, the fluid with a high momentum hits the blade of a turbine that is attached to the input shaft of the gearbox. The momentum is transferred to the turbine while the fluid returns to the low radius with low velocity and exits the turbine blade. The working fluid once again enters to the impeller inlet channel and the cycle starts over and fluid continuously circulates between the two. When the input shaft of transmission is not rotating while the engine is turning, the fluid is under tension but there is no mechanical connection between the engine and the gearbox. This slip in the fluid coupling allows the vehicle to stop while the engine is running. A torque from the engine is, however, applied to the gearbox input through the fluid coupling. When the engine is idling, the torque is small but still in this basic form of torque converter, and the vehicle tends to move if it is in gear. This motion is referred to as creep – and it is
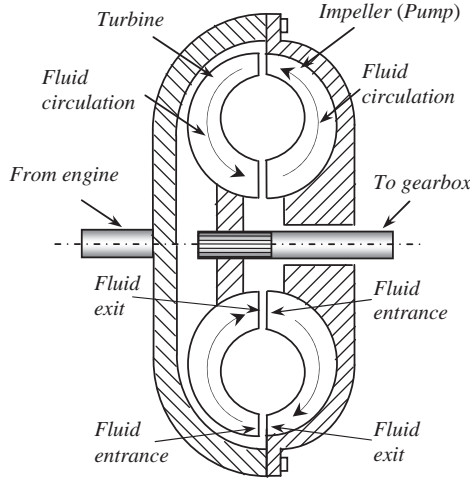
Figure 4.82   Schematic of a fluid coupling

viewed as a desirable feature of vehicles with automatic transmissions. With increasing engine speed, the torque transferred to the gearbox will increase and the vehicle will accelerate away smoothly.

By adding a third member known as a stator (reactor) to the fluid coupling, its performance is enhanced. The stator is a small vane wheel mounted on a freewheel (one-way clutch) and is placed between the pump and turbine. The stator directs the oil exiting the turbine blades to enter the impeller channels and save energy and fluid momentum. The torque transfer in a torque converter has complicated characteristics that can be related to the speed ratio defined as:

$$k_\omega = \frac{\omega_T}{\omega_P} \tag{4.227}$$

A typical variation of the torque ratio k_T (the ratio of the turbine torque T_T to pump torque T_P) with the speed ratio of a torque converter is shown in Figure 4.83. It is clear that when the speed of turbine is low
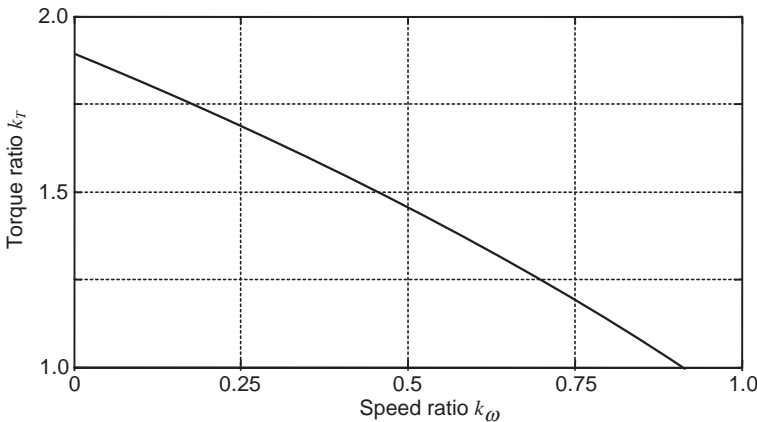
Figure 4.83   Torque amplification property of a torque convector
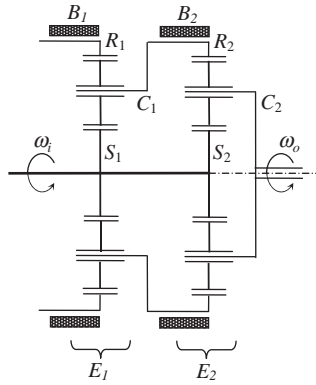
Figure 4.84 Coupling of planetary gear sets

relative to the speed of the impeller, the torque transferred to the turbine is even higher than the input torque. This is due to the momentum of the working fluid *relative* to the turbine and when the turbine has lower speeds, the momentum increases and causes greater energy transfers. This is a property that acts like a reduction gear and is useful in producing higher acceleration.

4.6.1.2 Control

A planetary gear set as explained in Section 4.4.2 works as a gearbox with an input and an output, once one of the three members is fixed. Fixing the external member in the epicyclic gear set is done by an actuation device called a *band brake* that encircles and holds the ring gear from outside. In an automatic transmission with several gear sets, several band brakes are also needed. For example, in the coupled system of Figure 4.84 with two epicyclic gear sets E_1 and E_2, two band brakes B_1 and B_2 can control the power transfer process. Activating B_1 will cause the output on C_2 to take influence from C_1 as well as S_2. When B_2 is activated, the output will only be directed from S_2 to C_2. Each route has its own speed and torque ratio from input to the output. In addition to band brakes, other types of clutches are also used in automatic transmissions to control the torque transfer routes. Therefore, in a conventional automatic transmission, the gear connections are fixed and the gear ratios are obtained only by activating different clutches and brakes that fix and release some components in the transmission.

Another issue in the control of automatic transmissions is when to shift a gear. For this task the control system must use the driving information available during the vehicle motion in order to make a proper decision on shifting the gear. The two basic pieces of information required are the engine speed and load. When engine speed is too low, a downshift is requested and when it is too high, an upshift is necessary. This, however, depends also on the engine load because, for example, when the load is high, the engine should work at higher speeds than when the load is low. One good indication of the load on the engine is the driver's throttle input. Driving on slopes, at high speeds or with high accelerations are examples of high loads on the engine, all of which require high throttle inputs. In most traditional automatic transmission, gear selections are determined based on the shift patterns related to engine speed and throttle input. A typical pattern is illustrated in Figure 4.85 consisting of three areas: low-speed low-throttle; high-speed high-throttle; and midrange areas. The solid line is for upshifts and the dashed line is for downshifts. The difference between the two lines is to prevent frequent upshift/downshifts. The shifting patterns for all gears are not similar and they also depend on the engine torque-speed map.
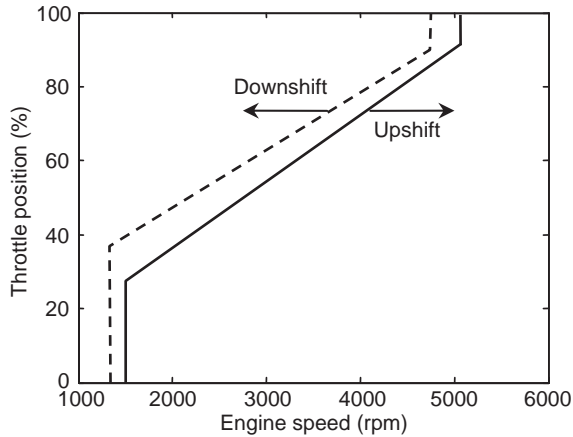
Figure 4.85 Typical shifting patterns of automatic transmissions

4.6.2 AMTs

An automated manual transmission (AMT) combines the benefits of both manual and automatic transmissions, i.e. the high efficiency of manuals with the ease of use of automatics. With the help of electronic controls an AMT can be developed from the manual gearbox. The clutch actuation which is the difficult part of gear changing process is performed automatically, making gear shifting more comfortable. The mechanical connection between selector lever and transmission is also eliminated and gearshifts are executed automatically (shift-by-wire). Compared to an automatic transmission, AMT offers advantages including the ability of using existing manual transmission manufacturing facilities, leading to lower production costs and still enjoying their high efficiency and lower weight. The main disadvantage of an AMT is the interruption of torque flow during shift actuation.

Converting a manual transmission to AMT requires two main tasks:

- Installing three actuator systems for the three actions a driver usually performs: 1 for clutching plus 2 for two movements in gear selection (see Figure 4.86).
- Adding a control unit to make shifting decisions.

Gearshifting decisions can be very influential on the performance and fuel economy of the vehicle. Automation of gear shifting for a manual transmission, therefore, requires a decision-making algorithm based on practical working conditions.

4.6.3 DCTs

For manual transmissions, despite the high efficiency, the torque interruption is an inherent disadvantage. During a gear shift, the clutch is activated to separate the engine torque from the gearbox in order that meshing between the gears can be accomplished by a sliding motion. When the new gear is selected, the clutch is released to re-establish the torque flow to the wheels. With this type of sliding engagement, in manual gearboxes the torque interruption from the engine to the wheels is inevitable.

Another transmission designed based on the concept of the manual gearbox is the double clutch transmission (DCT). A DCT is basically a layshaft-type gearbox with two input shafts and therefore, it needs one clutch for each shaft. Hydraulic and electronic systems are used to control the clutches. The technical challenge is to establish very precise control of the coordination between one clutch
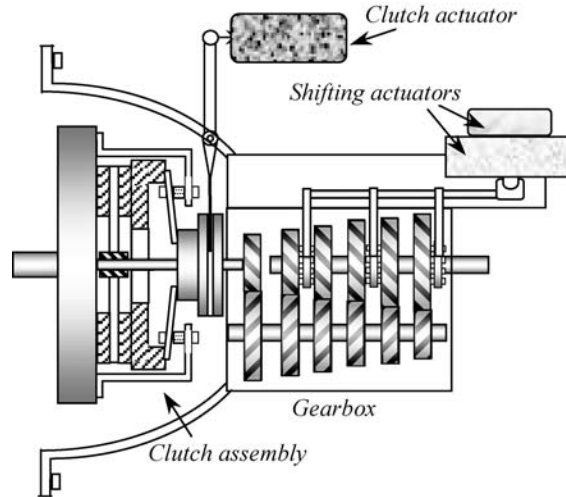
Figure 4.86   Actuators for AMT

disengaging and another clutch engaging. In DCT designs, usually the odd gears are mounted on one shaft and the even gears on the other shaft. By using this arrangement, the gearshift can be performed without torque interruption from engine to the wheels. Due to the fact that in DCTs, the disengagement of a gear and engagement of the new gear happen simultaneously, the discontinuity of a gearshift is eliminated to a great extent. This results in smooth accelerations during gearshifts in comparison with manual and even automatic transmissions.

In contrast to automatic transmissions in which torque converters deliver the engine torque to the gearbox, dry clutches or multi-plate wet clutches are used in DCTs. In addition to the fact that overall driveability is improved, one of the most important motives of the automotive industry for investment in DCTs is the benefit in fuel consumption reduction.

4.6.3.1   Function

DCTs consist of two input shafts and two power paths for the even and odd gear numbers. On the input end, each input shaft has a clutch to allow power interruption for shifting. Figure 4.87 is a schematic demonstration of a 6-speed DCT. One distinguishing feature of a DCT is its coaxial input shafts with one solid shaft (shaft 1) positioned inside the other hollow shaft (shaft 2). Each shaft has a clutch of its own and receives power from the engine through that clutch. Three gears are attached to shaft 1 and rotate with it. Since the gearbox is of constant mesh type, three pairs of meshed gears of shaft 1 (two of them located on lower shaft and the other one on the upper shaft) constitute the odd gears 1, 3 and 5 of the gearbox. Shaft 2 has only two gears fixed to it, but again three gears on the upper and lower shafts are meshed with these two gears and make the even gears 2, 4 and 6 of the gearbox. The lower and upper shafts are also the two output shafts of the gearbox and power flow to these shafts is established by selecting the gear by engaging the gear selector to the specified gear. In fact, like a typical layshaft gearbox, the gears on the output shaft rotate freely until they are connected to the shaft by the gear selector. Therefore, only one gear is connected to the output at a time.

The main difference between a traditional manual gearbox and a DCT is that in the former the gear selection cannot be performed without disengaging the engine from the transmission, whereas in a DCT the next gear can be identified and pre-selected without power interruption. For example, as shown in Figure 4.87, if the vehicle is already in gear 2, then clutch 2 is engaged and shaft 2 is transmitting power
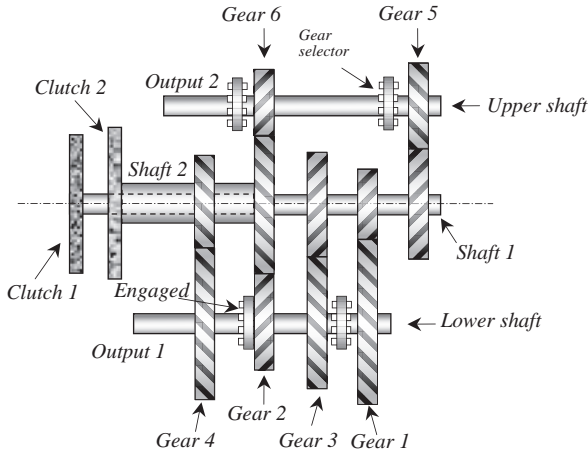
Figure 4.87   Schematic of a 6-speed DCT

through gear 2 to the output shaft 1. Now if the intention is to select gear 3, the selector between gears 1 and 3 is moved towards gear 3. Since the output shaft 1 is rotating, gear 3 will start to rotate after selection and will rotate the mating gear on the input shaft 1. This will also cause the clutch 1 to rotate while it is not engaged. The same thing could be done if gear 1 was to be selected. Therefore, pre-selecting a gear in a DCT will force the free clutch to rotate.

To shift the gear after pre-selection, the two clutches must swap over – releasing the active one and engaging the free one. In our example, the engine power will be transmitted through shaft 1 and gear 3 to the lower output shaft. The other gear selector is still connected to gear 2 and thus the input shaft 2 will also rotate freely due to the rotation of gear 2. In a DCT there are two paths for torque flow and especially during a gearshift the torque flow is complex. It is dependent on several parameters such as: clutch clamp forces, layshaft angular velocity and the type of gearshift (upshift or downshift). Another important factor during a gearshift is clutch force regulation. Due to the fact that both clutches simultaneously engage/ disengage, if the pressure profiles are not appropriate, high torque variations must be avoided by careful control design or they will result in unwanted longitudinal acceleration inputs to the vehicle and its passengers.

An uninterrupted torque flow in DCT requires both clutches to slip in order to transfer torques. The ratio of clutch angular velocities is determined by the ratio of engaging gears. Upshifts and downshifts are carried out in two distinct phases, namely, torque and inertia phases. When a gearshift signal is initiated, in an upshift the torque phase takes place first and is followed with the inertia phase. In a downshift, the order of the two phases is reversed, starting with the inertia phase followed by the torque phase. In the event of an upshift, the engine torque is gradually transferred from the off-going clutch to the on-coming clutch (target gear). In order to reduce clutch wear due to angular speed difference between the clutch input and output ends, it is necessary to modulate the clutch slip accurately.

4.6.3.2   Upshift Performance

To start the vehicle motion from rest, clutch 1 should be activated with the first gear selected. Upshift from first to second gear is performed by pre-selecting the gear 2 and switching the clutches. This action is done by the shifting controller. In order that a fast and smooth gearshift is obtained, the forces on the clutches and throttle must be controlled precisely. Figures 4.88 and 4.89 illustrate a typical upshift performance from 1st to 2nd gear. In the beginning, the off-going clutch (clutch 1) is engaged with the engine and its
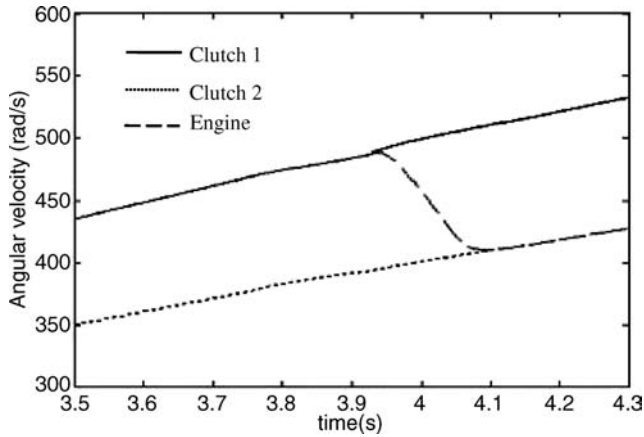
Figure 4.88   Angular speeds during upshift from 1st to 2nd gear

angular velocity is equal to engine angular velocity. At this time, the angular speed of the on-coming clutch (clutch 2) is less than that of the off-going clutch due to gear ratios. The clamp force of the off-going clutch is gradually reduced to the value where the clutch starts to slip. This in turn will cause the transmitted torque to drop and engine speed tends to increase. The clamp force of on-coming clutch will increase instead, producing slip and receiving part of engine torque. If the clamp force is excessive, the engine speed will reduce and a torque backlash from clutch 1 to engine will occur. The clamping forces are, therefore, regulated so that the receiving torque is switched from clutch 1 to clutch 2 smoothly. This phase ends when the torque is fully transmitted through clutch 2. The torque flow is thus achieved, but the transmission speed ratio is not changed during this phase. If no regulation is applied to the clamp forces, the transmission output torque will drop to the lowest value during the torque phase due to shift transients.

In the inertia phase that follows the torque phase, the main purpose is the synchronization of the engine speed with that of the clutch 2. In fact, this clutch is transmitting the power but with large slips.

The output torque variations during the upshift can be seen in Figure 4.89. No interruption in torque transmission is the advantage of this gearbox during the gearshift.
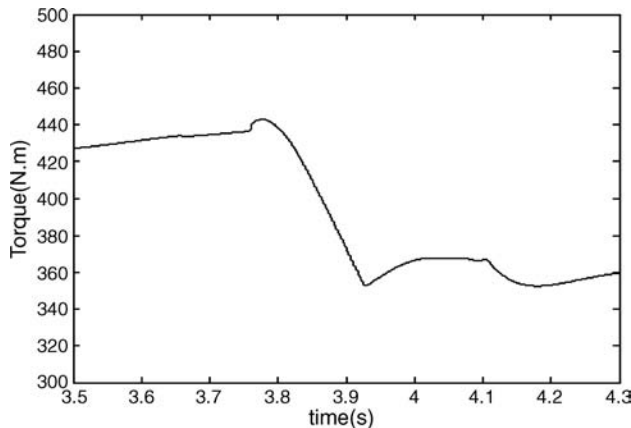
Figure 4.89   Transmission output torque during upshift from 1st to 2nd gear
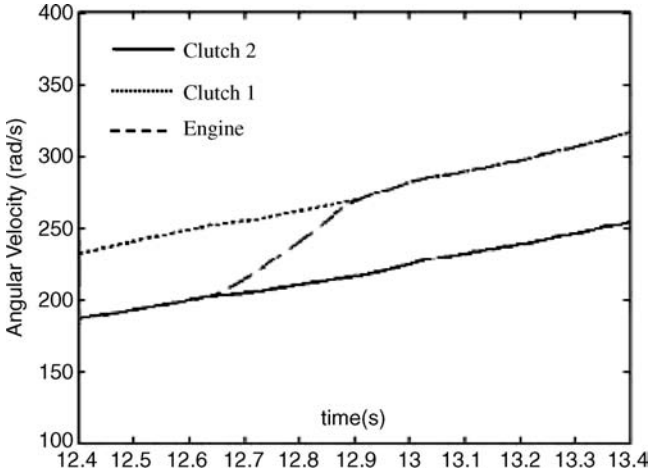
Figure 4.90   Angular speeds during downshift from 2nd to 1st gear

4.6.3.3   Downshift Performance

A downshift is more complex than an upshift especially at high gears, because in a downshift the on-coming clutch's angular velocity is greater than that of the engine, so that in the absence of suitable synchronization, torque backlash to the engine is very likely. This can cause a large transient in the powertrain system which is undesirable for the vehicle occupants and possibly harmful to the components, especially the gears and shafts. In the downshift case, the subsequent gear is pre-selected and turns with output shaft 1. This time the inertia phase must occur first since the rotational speed of the on-coming clutch (clutch 1) is larger than engine speed and if the clamp force in this clutch is increased, torque will flow in the reverse direction. When the clamp force of the off-going clutch (clutch 2) is decreased, the torque acting on the engine will be reduced, causing the engine to speed up. This will adjust the engine speed closer to the speed of clutch 1 but at the expense of reducing the transmitted torque. In order to maintain the torque and at the same time to accelerate the engine, the throttle can be further opened. This will help to achieve speed synchronization during the inertia phase. During the torque phase the clamp force at the on-coming clutch (clutch 1) is increased and the clamp force at the off-going clutch (clutch 2) is decreased simultaneously until the whole engine torque is transferred through the on-coming clutch. A gear 2 to gear 1 downshift is more severe than the others and a sample downshift performance is shown in Figures 4.90 and 4.91.

4.7   CVTs

Continuously variable transmissions (CVT) are based on a well-established concept to transmit power from one rotating shaft to another with continuously variable speeds. The basic idea can be understood from a simple arrangement of two similar cones with a flat belt wrapped around them as illustrated in Figure 4.92. As the belt is moved along the parallel axes of the cones, x varies and for a given rotational speed ω_1 of input shaft, the output angular speed ω_2 can be obtained by assuming no slip:

$$\omega_2 = \frac{x}{h-x}\omega_1 \tag{4.228}$$
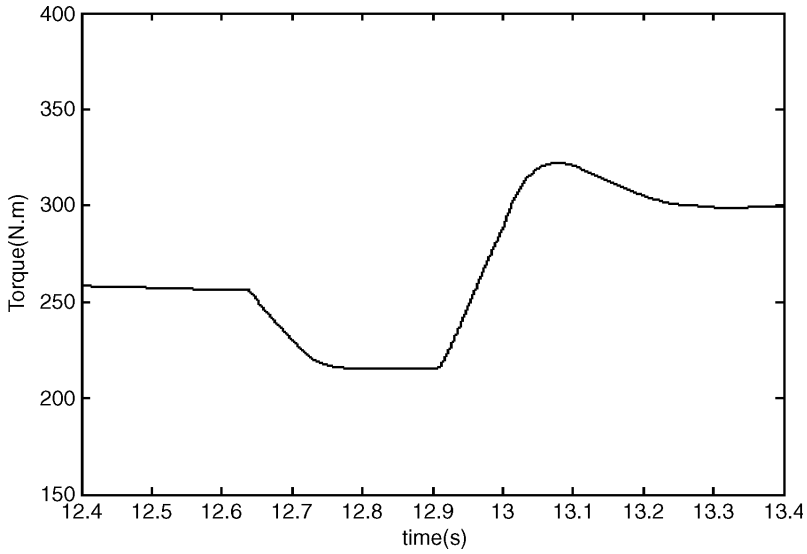
Figure 4.91   Transmission output torque during downshift from 2nd to 1st gear

Figure 4.93 depicts the variation of dimensionless output speed $\frac{\omega_2}{\omega_1}$ with the variation of dimensionless input displacement $\frac{x}{h}$ according to Equation 4.228. For a fixed value of input angular speed, the output speed ranges continuously from very small values near zero up to large values. This property of CVTs is useful in many applications in which the benefits of providing different gear ratios in addition to smooth shifting between ratios are required.

Simple concepts like that of Figure 4.92 may work in some applications, but in automotive applications, due to the high duty cycles and durability requirements only a few types of CVTs have proved successful in practice.
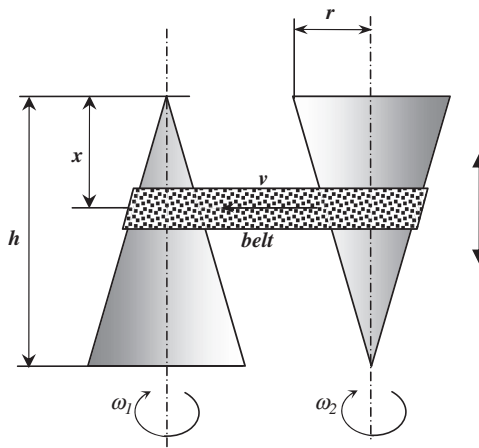
Figure 4.92   A conceptual CVT
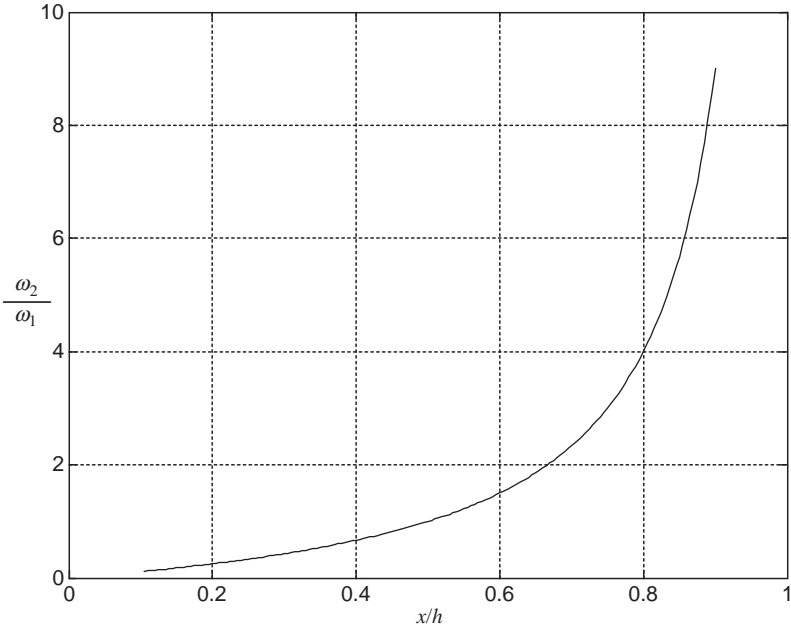
Figure 4.93   Variation of speed ratio versus displacement ratio

4.7.1   Classification

CVTs used in vehicles may be classified in different ways. The classification shown in the flowchart of Figure 4.94 divides CVTs according to the nature of producing the output torque. Details of each classification will be discussed in the separate sections that follow.
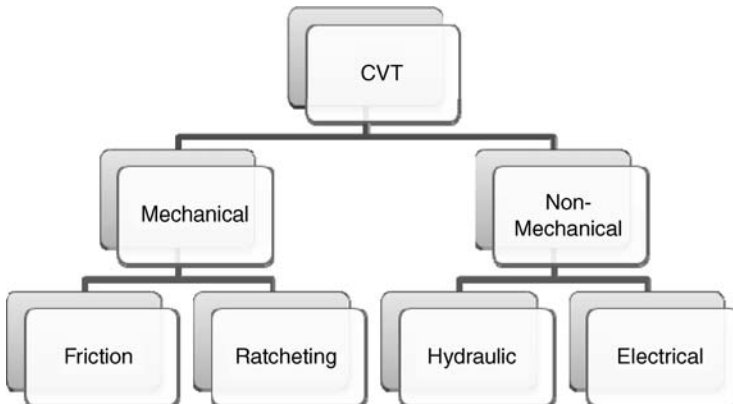
Figure 4.94   A classification for automotive CVTs
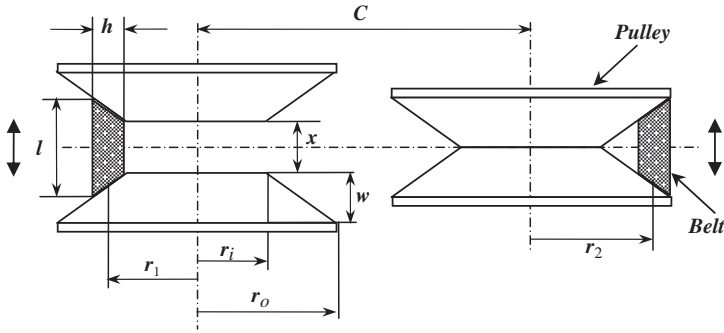
Figure 4.95 Geometry of a typical belt CVT

4.7.2 Friction CVTs

As the name implies, friction CVTs produce torque based on friction between mating surfaces, by means of belts or rollers. Two types of friction CVTs which are currently used in automobiles are the belt and toroidal CVTs. A belt CVT system is similar to standard belt-pulley drive with the exception that the pulleys are not fixed and are able to move apart. The geometry of a belt type CVT is shown in Figure 4.95. Both pulleys have fixed axes of rotation at a distance C from each other. The sides of each pulley are controlled to move apart or together laterally, but the displacements of each pulley is the opposite of the other. The situation shown in Figure 4.95 is an extreme case when the sides of left pulley are fully apart and sides of right pulley fully closed.

Assuming no slip between the belt and pulleys, the speed ratio between the drive and driven pulleys can be written as:

$$\frac{\omega_o}{\omega_i} = \frac{r_1}{r_2} = \frac{A - x}{B + x} \tag{4.229}$$

in which x is the distance between the two sides of the drive pulley and:

$$A = \frac{2r_o - h}{2(r_o - r_i)} \cdot l \tag{4.230}$$

$$B = \frac{2r_i + h}{2(r_o - r_i)} \cdot l \tag{4.231}$$

Displacement x is bounded between the two extremes:

$$0 \leq x \leq x_m = l \left\{ 1 - \frac{h}{r_o - r_i} \right\} \tag{4.232}$$

The speed ratio at these extremes is:

$$\frac{\omega_o}{\omega_i}(x = 0) = \frac{2r_o - h}{2r_i + h} \tag{4.233}$$

$$\frac{\omega_o}{\omega_i}(x = x_m) = \frac{2r_i + h}{2r_o - h} \tag{4.234}$$
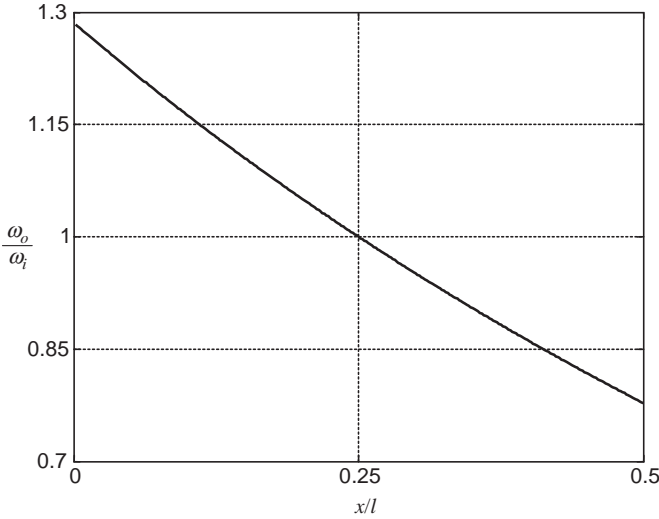
Figure 4.96   Typical variation of speed ratio in belt CVT

which are the inverse of each other. Since the trivial condition of $r_o > r_i + h$ is always satisfied, the speed ratio at $x = 0$ is always larger than its value at $x = x_m$. The speed ratio becomes equal to unity at $x = \frac{1}{2} x_m$. In order to increase the overall ratio of the CVT, the difference between the outer and inner radii should be increased. The variation of the speed ratio with the variation of lateral displacement x is illustrated in Figure 4.96 for the special case of $x_m = \frac{1}{2} l$.

The torque transmitted by a standard rubber belt pulley system is through the tensioning of a belt that produces larger tensions in the direction of rotation and small tensions at the loose end (see Figure 4.97a). The torque, therefore, results from the difference between the tensions at both ends multiplied by the effective radius. Due to the limitations of rubber belts, it is common in automotive applications to use steel belts as the means of transferring torque. One type of such belts is called a 'push belt', which in addition to the tension in front end of the belt, produces a compressive (push) force at the trailing end (see Figure 4.97b). This push force contributes to the torque transmission of the CVT. A push belt has a composite structure comprising two major components. One is a series of V-shaped steel segments that, when assembled, resemble a V belt shape. The segments come into contact with the pulleys and bear all contact forces. The other element in a push belt is a number of thin flat steel belt layers that together make a
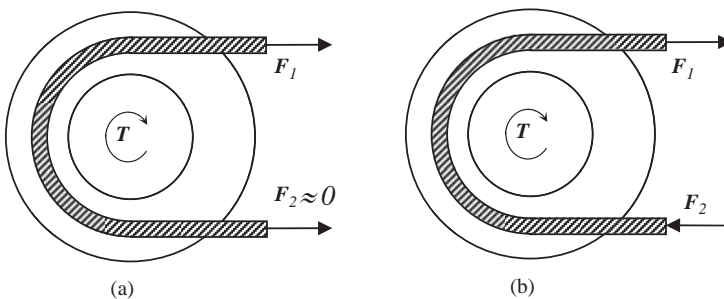
Figure 4.97   Rubber belt (a) and push belt (b)
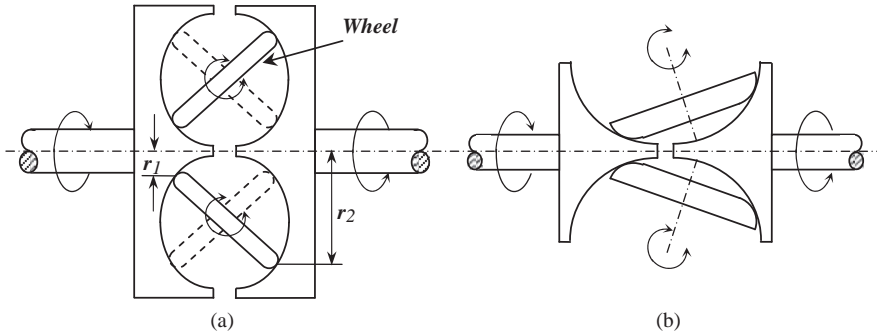
Figure 4.98   Full toroidal (a) and half toroidal (b) CVT types

band to stack the segments and constitute a uniform steel belt. These belt layers withstand the tensile forces in the push belt.

One other friction CVT used in vehicle transmissions is the toroidal type in which free wheels or rollers are placed between cavities of two disks and relate the rotations of two input and output shafts. Figure 4.98 shows the schematics of two variations from this type, namely 'full toroidal' and 'half toroidal' CVTs. The inside surfaces of the disks are spherical and the wheels or rollers in addition to their spin can oscillate laterally and change the radii of the contact points of input and output disks and in turn the speed ratio of the CVT.

One of main problems in friction CVTs is the friction generated at the contacting points. Friction is used to generate traction forces at the contact region which in turn generates a torque. But friction has two problems: build-up of heat and sensitivity to wear. In order to resolve these problems, lubricating oil can be used but this will reduce the friction and torque capacity of the CVT. The friction force depends on the coefficient of friction and normal load. Increase in normal load can compensate for the reduction of coefficient of friction provided that the oil can withstand high pressures and temperatures. Special traction oils have the required properties and are used for this purpose.

4.7.3   Ratcheting CVTs

A ratchet is a device that produces rotation in one direction regardless of the direction of the input rotation. This produces an intermittent output from a non-uniform and even oscillatory input. Ratcheting gearboxes are based on the concept of producing the output rotation from a series of discontinuous rotations summed up at the output. For this purpose the gearbox is constructed from a number of similar mechanisms. In order to understand the concept, consider a four-bar mechanism shown in Figure 4.99. If a constant
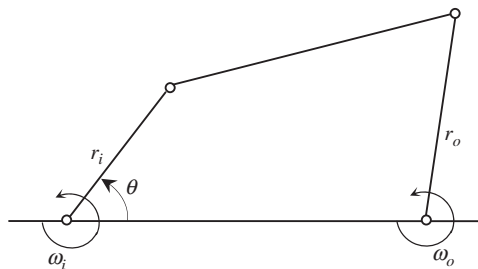
Figure 4.99   A four-bar mechanism
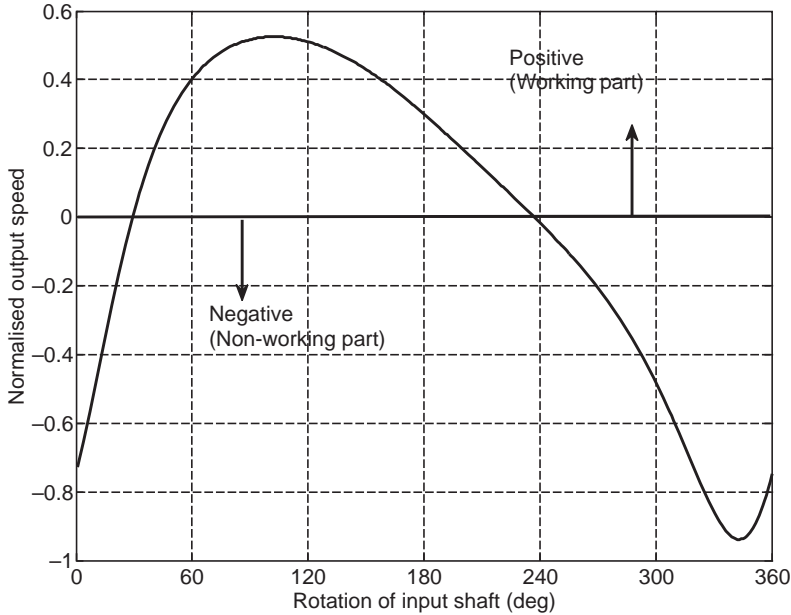
Figure 4.100 The normalized output speed of a typical four-bar mechanism

input angular speed ω_i is applied to the mechanism, an output angular speed ω_o will result. Depending on the geometry, the output could be similar to that shown in Figure 4.100 in normalized form (i.e., ω_o divided by ω_i). Since the output in a gearbox must rotate in the same direction of the input, only positive parts of the output are acceptable. In addition, the gearbox should have a fixed ratio with rotation of the input shaft.

If several mechanisms of equal geometry are used in such a way that their input linkages are connected to the same input shaft in timed angles, several of output angular speeds will be available as shown in Figure 4.101 for only four mechanisms. Now if one-way clutches (or free wheels) are used at the outputs, in such a way that at certain moments each clutch engages and disengages, the overall output of the system will look like that shown in Figure 4.102. This output, although irregular (similar to engine output torque irregularities), has an average and can be used in practice as a gearbox output.

The four-bar linkage was only an example of how a mechanism can be used to build a gearbox, several other mechanisms have this potential and some might perform better. For example, if the output of a mechanism at a certain span of input angles is almost flat, then the gearbox output from such a mechanism is more desirable and fewer mechanisms are necessary to build the gearbox. This explanation shows how a gearbox can be constructed, but the main issue is whether it can act as a CVT. To this end if the mechanism can be altered during the work, the gearbox will change ratio and a CVT characteristic can result. Consider, for instance, the same four-bar mechanism of Figure 4.99, but with an adjustable input arm depicted in Figure 4.103. Changing the input arm length will change the speed ratio of the mechanism and if it is done continuously, a CVT is effectively achieved.

4.7.4 Non-Mechanical CVTs

Two important types of non-mechanical CVTs are based on hydraulic and electrical components. A hydraulic system comprising a pump and a hydraulic motor constitutes a gearbox, since the pump produces oil flow and turns the motor. Thus the input mechanical power is first transformed to fluid power
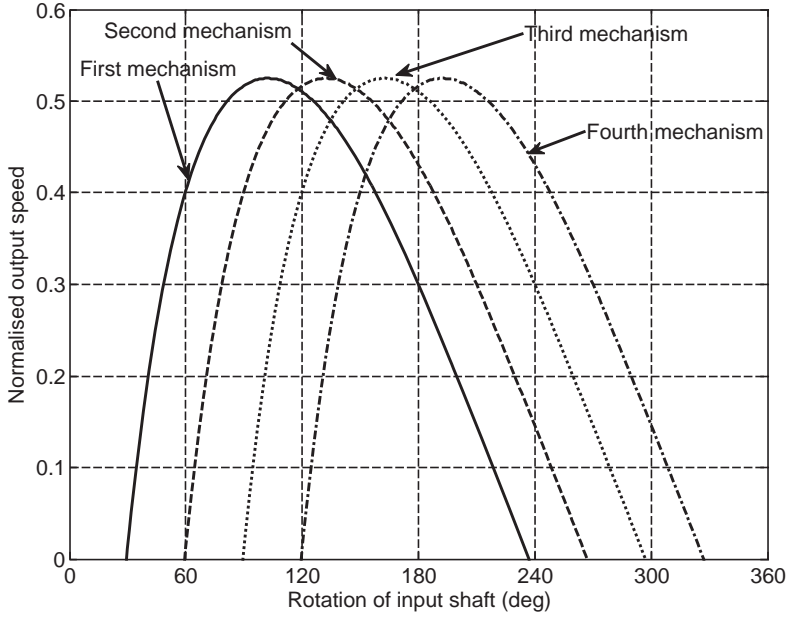
Figure 4.101   Outputs of several mechanisms
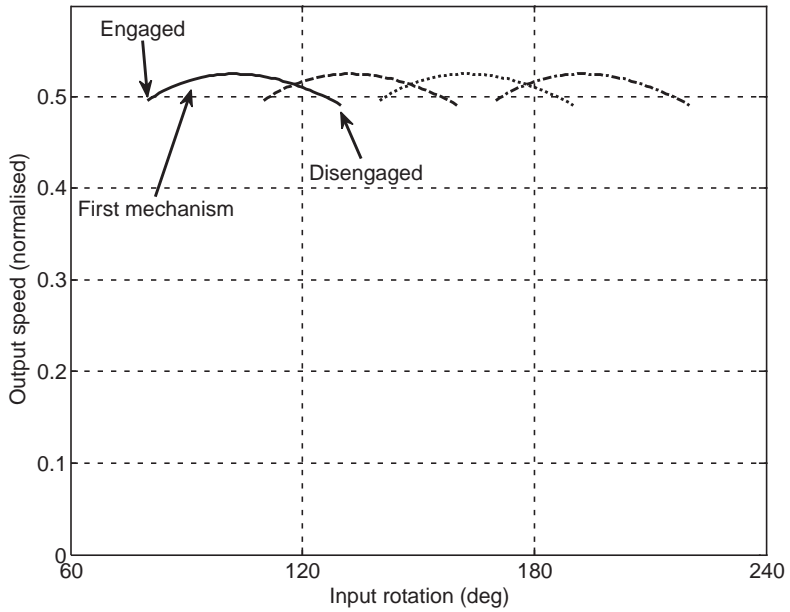
Figure 4.102   Output of the system with one-way clutches
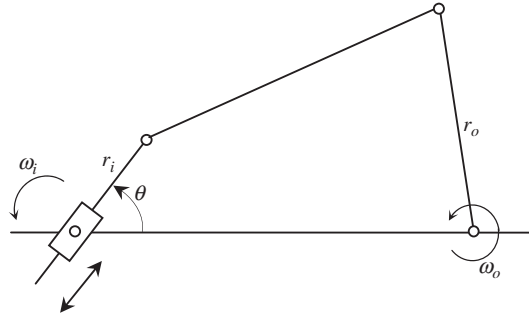
Figure 4.103 A four-bar mechanism with adjustable input arm

by the pump and once again to mechanical power by the motor. Converting such a system to a CVT is done simply by selecting the pump and/or motor of variable displacement type. Figure 4.104a shows a simplified representation of a hydraulic CVT in which the engine (E) rotates the variable displacement pump (P). The fluid is sucked from tank (T) to the pump and fed to the hydraulic motor (HM) and returned to the tank again. Such a system is referred to as a hydrostatic transmission and has been used successfully in off-road vehicle applications.

An electric system consisting of a generator and a motor is quite similar to the hydraulic gearbox. The mechanical input power can rotate the generator and produce electric current that in turn can drive an electric motor and produce mechanical power at the output. Converting this system to a CVT is achieved by using electric power circuits that control the motor's voltage (or frequency). Figure 4.104b schematically shows an electrical system consisting of a generator (G) and an electric motor (M) connected by a controller.

Although these systems may look very simple and practical, nevertheless due to heavy weights and power losses resulting from double energy transformation involved, they have not been widely used in automobile applications. However, with the remarkable growth of interest in electric vehicles in the early years of the twenty-first century, this situation is set to change.

4.7.5 Idling and Launch

Interruption of torque from the engine to the driveline is necessary when the vehicle is at rest with the engine running. For manual transmissions a clutch disconnects the torque but it is not enough on its own and the gearbox must have a neutral condition to allow idling comfortably when clutch is released. For vehicle launch from standstill, the clutch allows the engagement of the necessary gear and then
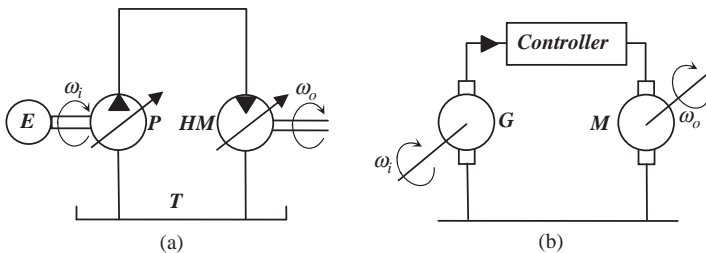
Figure 4.104 Non-mechanical CVT types (a) hydraulic and (b) electrical

acceleration is achieved by releasing the clutch. In automatic transmissions the torque converter makes both the idling and launch possible. For most CVTs there are a range of gear ratios between the upper and lower values and the torque interruption from the engine is necessary at idling. This needs an additional device such as a torque converter or friction clutch. The launch from standstill can also be handled with such device. Some CVT systems produce gear ratios ranging from zero to the highest ratio. The zero ratio makes idling possible as there is no (zero) torque transfer from engine at this particular gear ratio (neutral). These systems are called infinitely variable transmissions (IVT).

4.8   Conclusion

This chapter covered aspects of the transmission design including gear ratios, tooth numbers, clutch torque capacity and dynamics. Gearbox ratio estimation was divided into three parts of low, high and intermediate gears and several methods for the determination of ratios were discussed. The evaluation of the dry clutch torque delivering capacity was studied and design issues were discussed. Useful semi-empirical equations provided for the clutch force (MG formula) to facilitate analytical solutions as well as more realistic simulations of clutch engagement. The clutch dynamics were simulated in some detail, although this particular subject has attracted further detailed attention particularly in relation to DCT designs.

The construction and basics of operation of transmissions were considered and the differences between manual and automatic transmissions were summarized. Automatic transmissions comprising the conventional automatics and automated manuals (AMTs) were described. The recent developments of DCT transmissions as improved versions of AMTs was explained and the DCT performance during the upshift and downshift actions was discussed. Further details on the quality of shiftings involve the control of clutch forces, slips and throttle regulation. CVTs were described and classified and an overview of the functioning of different types was provided. More advanced subjects such as DCT and CVT dynamics and control are beyond the scope of this book.

4.9   Review Questions

4.1 Explain the reasons why a gearbox is needed for the vehicle. When would it be possible to use only one reduction gear?

4.2 Why are the design methods for the lowest and highest transmission gear ratios different?

4.3 Describe the method of designing the lowest gear in the transmission.

4.4 Explain the factors on which the gradeability of the vehicle at low speed depends.

4.5 Describe the method of designing the highest gear in the transmission.

4.6 Explain how to design the highest gear to achieve the maximum possible vehicle speed.

4.7 A student proposes a design method in which the intermediate gears are evenly spaced between the lower and higher gear ratios. What is wrong with this suggestion?

4.8 What is the idea behind the geometric progression method?

4.9 Describe the progressive design method of intermediate gear ratios.

4.10 How does the equal ΔV method differ from the progressive method?

4.11 Describe the two types of meshing in manual transmissions.

4.12 In manual transmissions explain why synchronization is necessary and how is it performed.

4.13 What is the difference between the transaxle and layshaft manual transmissions?

4.14 The first student says that the gears inside a manual transmission stop rotating once the clutch is depressed. The second student believes the gears will stop only when the transmission is in neutral. Which student is correct?

4.15 In friction clutches describe the two criteria for the pressure distribution and their justification.

4.16 Compare the torque capacity of a dry clutch at both working conditions and discuss which case is more appropriate for clutch design.

4.17 Describe the operation of a friction clutch system by drawing a schematic figure.

4.18 Explain why the clutch plate is released when the release bearing is pressed towards the engine.

4.19 A student believes the pedal force of a clutch is at maximum when the clutch is new and linings are thick. What is your comment?

4.20 Explain how the clamp force of the clutch varies when the pedal is depressed.

4.21 Explain how it is possible to have the clutch torque larger than the input engine torque.

4.22 Describe the construction of manual and conventional automatic transmissions.

4.23 Describe the operation of a torque converter.

4.24 A student suggests using a torque converter in manual transmissions to replace the clutch. Does this work?

4.25 Explain why several planetary gear sets are required in conventional automatics.

4.26 Describe the method of gear selection in conventional automatics.

4.27 Describe the method of converting a manual to an AMT. What are the advantages of AMTs over manuals and conventional automatics?

4.28 What is the main difference between a DCT and an AMT? What are the advantages of DCTs over the conventional automatics?

4.29 Describe the operation of a DCT.

4.30 Explain why the upshift and downshift controls are different in a DCT.

4.31 Describe the classification of CVTs and specify which types are used in practice.

4.10   Problems

Problem 4.1

Explain why the term $N_f + N_r$ of Equations 4.19 and 4.20 is not necessarily equal to $W_{\cos\theta}$ and discuss the conditions of equality.

Problem 4.2

Repeat Example 4.3.2 and show that for lower adhesion coefficients of below 0.7, FWD vehicle can have better gradeability results than RWD vehicle.

Problem 4.3

For a vehicle with information given in Table P4.3:

(a) Find an expression for the overall high gear ratio for the case in which the maximum vehicle speed occurs at the engine speed corresponding to the maximum engine torque.

Table P4.3   Vehicle information of Problem 4.3

1	Aero drag coefficient	c
2	Rolling resistance coefficient	f
3	Tyre rolling radius	R
4	High gear ratio	n
5	Maximum engine torque	T^*
6	Engine speed at max torque	Ω^*
7	Torque at max engine power	T_P
8	Engine speed at max power	Ω_P
9	Vehicle mass	m

(b) Repeat (a) for the case where the maximum vehicle speed occurs at the engine speed corresponding to the maximum engine power.

Result: (a) $T^* n^3 - fmgRn^2 - cR(R\Omega^*)^2 = 0$

Problem 4.4

For the vehicle in Example 4.3.3 design the highest gear ratio in the manner described below and compare the result with those of Examples 4.3.3–4.3.4.

First design gear 4 at the engine speed 10% above the speed at the maximum power and then design gear 5 with a 25% overdrive.

Problem 4.5

Prove Equation 4.37 for the overdrive gear ratio by writing the kinematic equation of vehicle motion. State the assumptions involved in this process.

Problem 4.6

In a 4WD vehicle the wheel torques at front and rear axles are distributed such that the ratio of front to rear axle torques is given by r.

(a) Assume the rear wheels are at the point of slip and derive an expression for the maximum negotiable slope of the vehicle (assume equal gear ratios for front and rear and ignore the rolling resistance).
(b) Repeat (a) assuming the front wheels are at the point of slip.
(c) For both cases of (a) and (b) derive expressions for the limits of torque ratio r.
(d) Use numerical values 2.5, 0.5, 1.2, 0.8 and 0.02 for l, h, a, μ and f_R to evaluate the limits of r.

Result: (a) $\tan \theta = \mu(1+r) \dfrac{a - h f_R}{l - \mu(1+r)h}$ (d) $r \leq 0.57$ and $r \geq 0.57$

Problem 4.7

A method shown in Figure P4.7 is proposed for the evaluation of intermediate gearbox ratios. It includes two low speed levels for the engine with the definition of $\Omega_{L_2} = \alpha \Omega_{L_1}$ ($\alpha > 1$).

(a) Find expressions for C_{g_1} and C_{g_2}.
(b) Find expressions for n_2, n_3 and n_4 in terms of C_{g_i}.
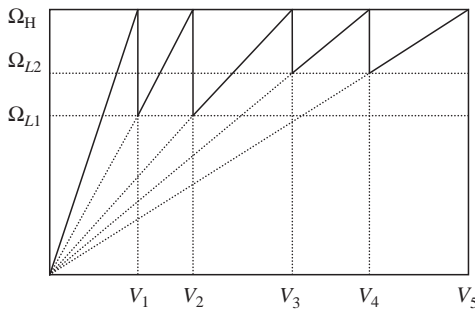
Figure P4.7   Engine-vehicle speed diagram of Problem 4.7

(c) Examine the difference between the average of C_{g_1} and C_{g_2} with C_{gp} of geometric progression.

(d) Show that for $\alpha = 1$ this method is identical to conventional geometric progression.

Results: (a) $C_{g2} = \sqrt{\alpha}C_{gp}$ and $C_{g1} = \frac{1}{\sqrt{\alpha}}C_{gp}$.

Problem 4.8

A method is proposed for the evaluation of intermediate transmissions ratios presented in Figure P4.8. With the assumption of $\Omega_{L_2} = \alpha\Omega_{L_1}$ $(\alpha\rangle 1)$, $\alpha - 1 = t$, $n_1/n_5 = N$.

(a) Find an expression for the calculation of $C_g = \frac{\Omega_H}{\Omega_{L_1}}$ in terms of N and t (or α).

(b) Find expressions for n_2, n_3 and n_4 in terms of known parameters.

(c) Show that for $\alpha = 1$ the above results are identical to conventional geometric progression.

Result: (a) $C_g^4 - tC_g^3 - tC_g^2 - N\alpha^2 = 0$
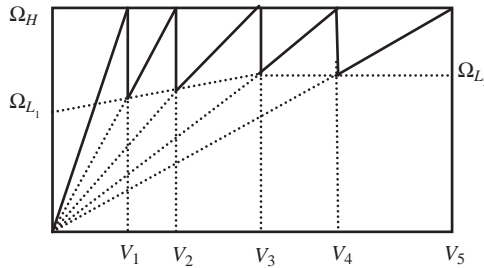
Figure P4.8   Engine-vehicle speed diagram of Problem 4.8

Problem 4.9

Repeat Problem 4.8 for the following engine-vehicle speed diagram in Figure P4.9.

Result: (a) $C_g^4 - t(C_g^3 + C_g^2 + C_g + 1) - N = 0$
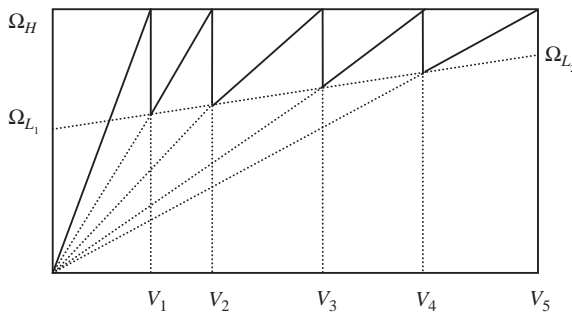
Figure P4.9   Engine-vehicle speed diagram of Problem 4.9

Problem 4.10

In a vehicle clutch, the inner and outer disk radii are r and R respectively, while the maximum spring force is F^*.

(a) Write an expression for ΔT, the difference between delivered torque at the two cases of constant pressure and uniform wear in terms of the uniform wear torque.
(b) Calculate the ratio $\frac{r}{R}$ for the three cases of $\Delta T = 1\%$, 5% and 10% of the torque of constant wear.
(c) Draw the variation of $\Delta T/T_{uw}$ versus $\frac{r}{R}$.

Result: (b) $\left[\dfrac{1}{3} - \dfrac{4Rr}{3(R+r)^2}\right]T_{uw}.$

Problem 4.11

For the clutch of Problem 4.10:

(a) Is there an answer for r for having equal torques at both cases of uniform pressure and uniform wear? Explain why.
(b) With μ being the coefficient of friction, find an expression for the maximum difference between the clutch torques in the two cases.

Result: (b) $\dfrac{1}{3}\mu F^*R.$

Problem 4.12

If the sum of groove angles on the clutch plate lining is θ (radians), show that the actual maximum pressure on the material is $\dfrac{1}{1-\frac{\theta}{2\pi}}$ times its theoretical value with no grooves, for both uniform pressure and uniform wear.

Problem 4.13

During the clutch release in gear 1, the clutch force is increased linearly from zero to the maximum of 5000 N. The variations of the engine and clutch rotational speeds are of the form shown in Figure P4.13.
   For information given in Table P4.13, determine the clutch efficiency.
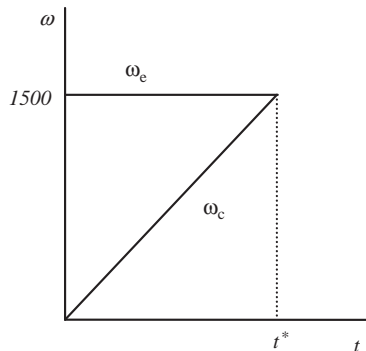
Figure P4.13   Engine-clutch speed diagram of Problem 4.13

Table P4.13 Information for Problem 4.13

Parameter		Value	Unit
1	Engine maximum torque	100	Nm
2	Lock-up time t^*	1	s
3	Average clutch radius	20	cm
4	Dynamic coefficient of friction	0.4	–
5	Engine rotating inertia	0.25	kgm^2

Problem 4.14

The driver of a vehicle decides to gearshift from gear 1 to gear 2 when the travelling speed reaches 36 km/h. At the time driver releases the clutch pedal the engine is idling.

(a) Determine the rotational speeds of engine, clutch plate and driving wheels at the time the clutch starts to be released (use Table P4.14).
(b) Specify the torque flow direction if the driver:
   (i) just releases the clutch pedal;
   (ii) increases the engine speed before releasing the clutch pedal.
(c) Plot a rough variation of the engine and clutch plate speeds versus time during the gearshift for two cases when the driver attempts to:
   (i) accelerate right after gearshift;
   (ii) maintain a uniform speed.
(d) Is it possible to gearshift without using the clutch? Explain how.

Result: (a) $\omega_e \approx 1000$ *rpm*, $\omega_c = 2578.3$ *rpm* and $\omega_w = 286.5$ *rpm*.

Table P4.14 Information for Problem 4.14

Engine idle speed	1000 rpm
Tyre rolling radius	33 cm
Overall ratios at 1st, 2nd and 3rd gears	14, 9 and 6

Problem 4.15

For a 4WD vehicle the CG is at equal distances from the front and rear axles and the CG height to the ground is half of the same distance. For $\mu_P = 1$, assume equal driveline efficiencies for driving with front or rear wheels and determine the ratio of FWD to RWD low gear ratios

$$k = \frac{N_L]_{FWD}}{N_L]_{RWD}}.$$

Result: $k \approx 0.6$.

Problem 4.16

The gear ratio of a layshaft gearbox in gear 1 is 3.85:1. Two options with sub-ratio combination 1.75×2.2 and 1.925×2 are proposed for the determination of tooth numbers (in each case the left figure is input gear mesh ratio and the second figure is the output gear mesh ratio). The distance between the centrelines of the

upper and lower shafts has to be larger than 100 mm but as small as possible. Gear modules must be larger than 1 mm with spacing of 0.25 mm (e.g. 1.25, 1.50, etc.). Find the tooth numbers for all four gears for both given options and select the best answer.

Problem 4.17

For the vehicles with given properties in Table P4.17:

(a) Determine the maximum grade each vehicle can climb.
(b) At the grade found in (a), what percentage of maximum engine power is utilized at speed of 30 km/h?
(c) At the grade found in (a), what percentage of maximum engine torque is utilized at speed of 30 km/h?

Table P4.17   Vehicle information of Problem 4.17

	Parameter	Unit	Vehicle 1 (RWD)	Vehicle 2 (FWD)
1	Distribution of weight F/R	(%)	55/45	60/40
2	Rolling resistance coefficient		0.02	0.02
3	Tyre rolling radius	(m)	0.30	0.30
4	High gear ratio		*13.0*	*12.0*
5	Maximum engine torque	(Nm)	150.0	150.0
6	Engine speed at max torque	(rpm)	3000	3000
7	Torque at max engine power	(Nm)	120.0	120.0
8	Engine speed at max power	(rpm)	5000	5000
9	Vehicle mass	(kg)	1200	1150
10	CG height to ground	(m)	0.6	0.6
11	Friction coefficient		0.8	0.8
12	Wheel base	(m)	2.2	2.2

Problem 4.18

The information for a passenger car clutch spring is given in Table P4.18:

(a) Plot the F_S-δ_S and F_B-δ_B curves using the MG formulae.
(b) Calculate the seesaw gain k_s.
(c) Plot the variation of clamp force inside the first plot of F_S-δ_S.
(d) Calculate the initial deflection δ_C^*.

Table P4.18   Clutch information of Problem 4.18

Parameter	Value	Unit
Inner diameter D_i	34	mm
Outer diameter D_o	185	mm
Bellville inner diameter D_b	151	mm
Spring thickness t	2.3	mm
Bellville height h	3.4	mm
Set point deflection δ_S^*	3.4	mm
Modulus of elasticity	206	MPa
Poisson's ratio	0.3	–

Problem 4.19

For the vehicle with given specifications in Table P4.19.1, the engine is off. For the two cases of uphill and downhill, determine the maximum grade vehicle can stop without slipping, if:

(a) only gear 1 is engaged;
(b) only the handbrake on the front wheels is activated;
(c) only the handbrake on the rear wheels is activated;
(d) only the footbrake is activated;
(e) gear 1 is engaged together with the handbrake acting on front wheels;
(f) gear 1 is engaged together with the handbrake acting on rear wheels.

Table P4.19.1   Vehicle information of Problem 4.19

	Parameter	unit	value
1	Tyre rolling radius	m	0.30
2	High gear ratio		14
3	Engine braking torque @ 0 rpm	Nm	30
4	Vehicle mass	kg	1200
5	Maximum road friction coef.		0.8
6	Weight distribution F/R (FWD)		58/42
7	Weight distribution F/R (RWD)		55/45
8	CG height to wheelbase ratio h/l		0.35
9	Coefficient of rolling resistance f_R		0.02

Compare the results for both cases of FWD and RWD by filling in Table P4.19.2.

Table P4.19.2   Proposed table for filling in the results

		Results for Maximum grade (deg)			
		Uphill		Downhill	
		FWD	RWD	FWD	RWD
1	Case a				
2	Case b				
3	Case c				
4	Case d				
5	Case e				
6	Case f				

Problem 4.20

The intention is to investigate the existence of a certain grade and friction coefficient for which both FWD and RWD vehicles with same properties generate equal traction forces.

(a) In the expression for the tractive forces of FWD and RWD vehicles ignore the hf_R term and find a condition for friction coefficient which guarantees equal traction forces for the both cases.
(b) Using the result of (a) prove that for both cases: $\tan \theta = 0.5\mu_P$.
(c) Use $\frac{a}{l} = 0.45$ and $\frac{b}{h} = 2.0$ and calculate the values of μ_P and θ.

(d) Retain the hf_R term and repeat case (a) and show that the result in (b) is still valid and that the friction coefficient must satisfy the condition: $\mu_P = 2f_R + \frac{4}{11}$ if values in (c) are used.

Problem 4.21

In the expressions for the tractive forces of FWD and RWD vehicles, ignore the hf_R term and derive equation for slope in the form of $\tan\theta = \dfrac{c}{d/\mu_P + e}$ and then:

(a) Find values c, d and e for both cases given $\frac{a}{l} = 0.45$ and $\frac{b}{h} = 2.0$.
(b) From a mathematical point of view investigate the possibility of a maximum grade each type of vehicle can negotiate by differentiating θ with respect to μ_P and find θ_{max} for each case.
(c) Draw the variation of θ versus μ_P for both cases (evaluate θ values for μ_P up to 4).
(d) What would be the values of θ_{max} for each case in the real practice? (Suggest a practical μ_{max}.)

Problem 4.22

In the derivation of Equations 4.212 and 213 the limitation on the clutch torque was not included. Derive the equations for the clutch efficiency when considering this limitation.

Further Reading

In contrast to the enormous number of books on engines, textbooks devoted to transmissions are relatively rare. It is not clear why this huge discrepancy has occurred – particularly since developments in transmissions have had a major impact on vehicle design, especially over recent years – and yet informative texts on multispeed automatics, dual clutch transmissions and CVTs are not available.

The best introduction to automotive transmissions is probably Chapter 13 in Happian Smith (ed.), written by Vaughan and Simner [10]. They provide an excellent overview of the fundamentals of transmissions and describe the functional aspects of different components without going into the analysis. Details of gear design and manual gearbox design are provided in Stokes' 1992 texts [11, 12].

Other useful descriptive material is available in Heisler [13] and Gott [14] but both these texts are now dated and do not cover any of the interesting developments over the past two decades. The most comprehensive text on automotive transmissions is by Naunheimer et al. [15] which is a recent update of an earlier 1999 book [2]. It is aimed more at the practising professional engineer than the student market and so it remains rather expensive. However, it is a definitive text; as well as covering the basic vehicle performance, it also provides detailed design information on gears, shafts, bearings and synchronizers. It describes manual, automatic gearboxes and torque converters and introduces overall aspects of the commercial design, development and testing processes associated with transmission manufacture.

References

[1] Wong, J.Y. (2001) *Theory of Ground Vehicles*, 3rd edn. John Wiley & Sons, Inc., ISBN 0-470-17038-7.
[2] Lechner, G. and Naunheimer, H. (1999) *Automotive Transmissions: Fundamentals, Selection, Design and Application*. Springer, ISBN 3-540-65903-X.
[3] *Shigley's Mechanical Engineering Design*, 8th edn. McGraw-Hill, 2006, ISBN 0-390-76487-6.
[4] Mabie, H.H. and Reinholtz, C.F. (1987) *Mechanisms and Dynamics of Machinery*, 4th edn. John Wiley & Sons, Inc. ISBN 0-471-02380-9.
[5] Lhomme, W. et al. (2008) Switched Causal Modeling of Transmission with Clutch in Hybrid Electric Vehicles, *IEEE Transactions on Vehicular Technology*, 57 (4).

[6] Berger, E.J. (2002) Friction Modeling for Dynamic System Simulation, *Applied Mechanics Review*, 55 (6): 535–577.

[7] Duan, C. (2004) Dynamic Analysis of Dry Friction Path in a Torsional System. PhD dissertation, The Ohio State University.

[8] Amari, R., Tona, P. and Alamir, M. (2009) A Phenomenological Model for Torque Transmissibility During Dry Clutch Engagement, paper presented at 18th IEEE International Conference on Control Applications, Saint Petersburg, Russia, July.

[9] Newbold, D. and Bonnick, A.W.M. (2005) *A Practical Approach to Motor Vehicle Engineering and Maintenance*. Elsevier Butterworth-Heinemann, ISBN 0-7506-6314-6.

[10] Happian Smith, J. (ed.) (2002) *An Introduction to Modern Vehicle Design*. Butterworth-Heinemann, ISBN 07506-5044-3.

[11] Stokes, A. (1992a) *Gear Handbook: Design and Calculations*. Butterworth-Heinemann, ISBN 07506-149-9.

[12] Stokes, A. (1992b) *Manual Gearbox Design*. Butterworth-Heinemann, ISBN 07506 0417 4.

[13] Heisler, H. (2002) *Advanced Vehicle Technology*, 2nd edn. Butterworth Heinemann, ISBN 07506-5131-8.

[14] Gott, P.G. (1991) *Changing Gears: The Development of the Automatic Transmission*. SAE, ISBN 1-56091-099-2.

[15] Naunheimer, H., Bertsche, B., Ryborz, J., Novak, W., Fietkau, P. and Kuchle, A. (2010) *Automotive Transmissions: Fundamentals, Selection, Design and Application*, 2nd edn. Springer, ISBN 978-3642162138.

5

Fuel Consumption

5.1 Introduction

Fuel efficiency and emissions have become extremely important issues in the design of automobiles in order to reduce petroleum consumption and emissions that result in greenhouse effect and global warming. Overall, there are three phases involved in the conversion of fossil fuels to the delivery of useful work in controlling the motion of the vehicle in typical driving conditions. Two of these were introduced and discussed in Chapter 1 and described as:

- well-to-tank (see Figure 1.1a);
- tank-to-wheels (see Figure 1.1b)

The third phase involves the conversion of power delivered at the vehicle wheel into useful work to power the vehicle over its range of normal operating conditions. Further energy losses are associated with this phase, in particular, due to tyre rolling resistances, aerodynamic drag and friction of the non-driven rotating components. Analysis of the vehicle powertrain system in typical driving scenarios depends heavily on the details of the driving schedule, involving grades, stop-start progress, traffic, acceleration and deceleration phases, etc. Consequently, there has been a lot of interest worldwide in developing standard driving cycles. These claim to be representative of typical driving conditions in different countries in, for example, urban, mixed urban, highway conditions, and they provide reference conditions so that different vehicles can be compared on a fair basis.

This chapter focuses on the second and third phases – and in particular on the calculation of the fuel consumption of the vehicle in normal driving situations. The fuel consumption of a vehicle is controlled by two main factors, namely the operating loads and the engine efficiency. The former depends on how the vehicle is used whereas the latter depends how the fuel is transformed into the work within the engine, which is often described by an engine fuel efficiency map. The loads on the vehicle vary with acceleration and climbing grades, air resistance, and the rolling resistance of the tyres. Improving efficiency, therefore, involves reducing the loads on the vehicle by proper management of vehicle performance and motion, as well as improving the efficiency of the whole powertrain and its components. Operation of the engine at peak efficiency points involves analysis of the powertrain system to ensure that the transmission is well matched to the prime mover.

The aim of this chapter is to introduce the fundamentals of vehicle fuel consumption and its calculation during normal driving. It starts with engine's fuel consumption characteristics and the dependence of fuel consumption on the engine's operating conditions. Vehicle driving cycles are universally used for standard measurements of vehicle fuel consumption and emissions, and example calculations are

presented. The effect of gearbox shifting on engine working points when driving in different cycles is described and methods of automated gearshifts and their policies in fuel consumption reduction are also discussed.

5.2   Engine Energy Consumption

The detailed energy losses in an IC engine have already been described in previous chapters – they include combustion processes, heat loss processes, pumping losses, power to drive ancillaries such as alternator, air conditioner and steering pump, etc. From the point of view of fuel consumption calculations, an overall summary of the engine properties is required. This information can be presented in several ways to quantify the fuel consumption at, for example, different engine speeds, torques and throttle conditions. The most common technique to summarize the overall engine fuel efficiency is the brake specific fuel consumption (BSFC) map.

5.2.1   BSFC Maps

The brake specific fuel consumption (BSFC) of an engine is a measure of the fuel consumption under a certain working condition. It is defined as an instantaneous ratio:

$$BSFC(t) = \frac{Rate\ of\ fuel\ consumption}{Engine\ output\ power} = \frac{\dot{m}(t)}{P_e(t)} \qquad (5.1)$$

where:

$$\dot{m}(t) = \frac{d}{dt}m(t) \qquad (5.2)$$

$$P_e(t) = T(t) \cdot \omega(t) \qquad (5.3)$$

in which m is the instantaneous mass of the fuel, and T and ω are the engine torque and speed respectively. Power P_e in Equations 5.1 and 5.3 is the brake engine power which is the mechanical output power at the crankshaft.

Using SI units, Equation 5.1 results in kg/J (kilogram per joule), however, in practice, units of grams per kilowatt-hour (kWh) are used. Conversion from kg/J to g/kWh is:

$$\text{BSFC}\left[\frac{kg}{J}\right] \times 3.6 \times 10^9 = \text{BSFC}\left[\frac{g}{kWh}\right] \qquad (5.4)$$

The conversion from metric to US customary units can be obtained from:

$$\text{BSFC}\left[\frac{g}{kWh}\right] \times 1.644 \times 10^{-3} = \text{BSFC}\left[\frac{lb}{hph}\right] \qquad (5.5)$$

An engine operating point (EOP) can be indicated in the engine torque-speed diagram by a specific point according to the values of torque and speed, as illustrated in Figure 5.1. For example, the point EOP_1 results from a throttle input of θ_1 at output power P_1 with torque T_1 and speed ω_1. Each EOP has its own BSFC value according to the working condition of the engine.

If load on the engine varies, the operating point will vary and, as a result, in the torque–speed chart, an infinite number of EOPs exist for all possible working conditions of the engine. For each point on the chart a corresponding BSFC value will be available. It happens that several of EOPs in the torque–speed plane
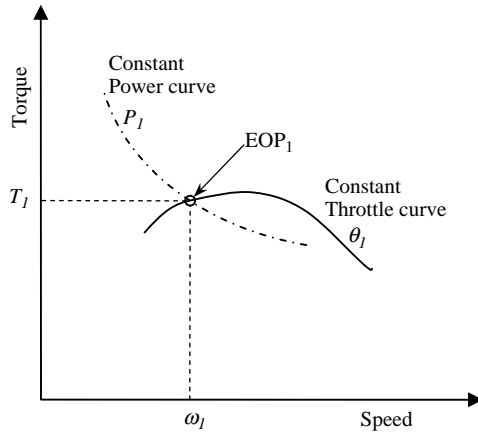
Figure 5.1 An engine operating point (EOP)

take identical BSFC values. If these equal BSFC points are connected to each other, they will generate a curve that is a locus for a specific BSFC value. This can be repeated for all other similar points and eventually loci of constant BSFC points or iso-BSFC points result. This is called the BSFC map of an engine and a schematic map of this kind is shown in Figure 5.2.

Specifying fuel consumption by the BSFC figure has a big advantage in that the BSFC values over a wide range of engine sizes remain similar. The reason is that BSFC is largely dependent on engine design factors such as compression ratio and fuel type. Therefore, for a family of engines with similar fuel type
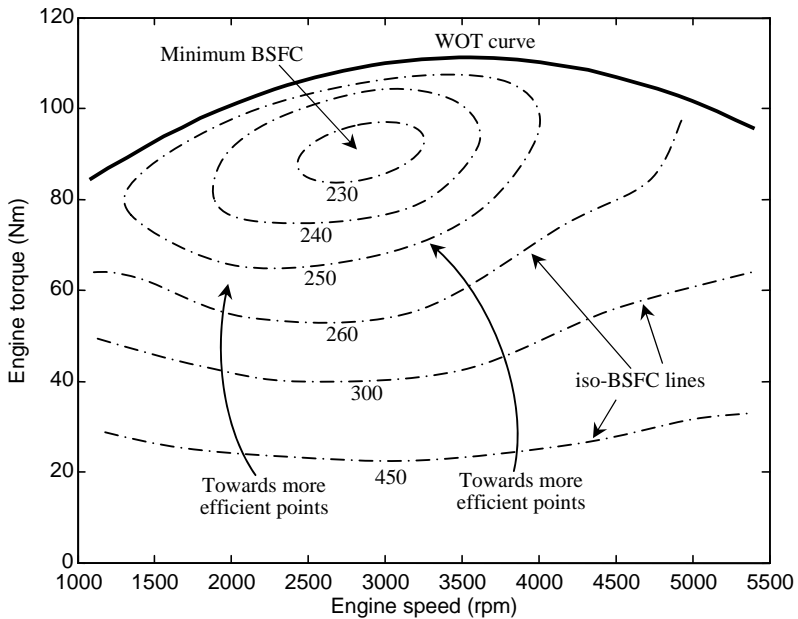
Figure 5.2 A schematic BSFC map

and compression ratios, the overall values for BSFC will be similar. Diesel engines have smaller BSFC values compared to petrol engines.

5.2.2 BSFC and Engine Efficiency

The engine fuel efficiency η_{fe} is defined as the ratio of energy produced by the engine E_e to the fuel energy supplied to that engine E_f, i.e.:

$$\eta_{fe} = \frac{E_e}{E_f} \tag{5.6}$$

Any fuel has an energy density or specific energy defined by the fuel energy divided by its mass:

$$E_{fs} = \frac{E_f}{m_f} \tag{5.7}$$

It is determined in a standardized test procedure in which a known mass of fuel is fully burned with air, and the thermal energy released by the combustion process is absorbed by a calorimeter as the combustion products cool down to their original temperature.

In order to relate the engine efficiency to BSFC, Equation 5.1 can be rewritten in the following form:

$$\frac{d}{dt}m(t) = BSFC(t)P_e(t) \tag{5.8}$$

Integrating Equation 5.8 will require the time history of BSFC together with the instantaneous power of engine. If at a particular period of time or under a particular working condition, the BSFC value remains unchanged, say $BSFC^*$, then for this particular case one finds:

$$m_f = BSFC^* E_e(t) \tag{5.9}$$

Substituting from Equation 5.6 gives:

$$m_f = \eta_{fe} BSFC^* E_f \tag{5.10}$$

Combining Equations 5.10 and 5.7 gives:

$$\eta_{fe}^* = \frac{1}{E_{fs} \times BSFC^*} \tag{5.11}$$

Equation 5.11 indicates that the engine efficiency is inversely proportional to the BSFC and fuel specific energy values. It also shows that the engine efficiency is not a constant value and depends on the engine working conditions and in fact on the instantaneous BSFC values.

E_{fs} basically has units of J/kg, but for Equation 5.11, it is convenient to convert E_{fs} to kWh/g by multiplying it by 2.78×10^{-10}.

Example 5.2.1

An engine is running at a steady condition in which the BSFC is 350 g/kWh. For a fuel specific energy of 0.0122 kWh/g, determine the engine efficiency.

Solution

The solution is a simple use of Equation 5.11:

$$\eta_{fe}^* = \frac{1}{E_{fs} \times BSFC^*} = \frac{1}{0.0122 \times 350} = 0.2342 \quad (23.42\%)$$

Example 5.2.2

The minimum BSFC values for two typical gasoline and diesel engines together with their specific energies are given in Table 5.1. Compare the maximum efficiencies for the two typical engines.

Table 5.1 Typical engine specifications for Example 5.2.2

Engine type	Minimum BSFC $\left(\frac{g}{kWh}\right)$	Specific energy $\left(\frac{MJ}{kg}\right)$
Diesel	200	43
Petrol	225	44

Solution

When using Equation 5.11, the specific energy values must be converted to kWh/g, hence:

$$\eta_{fe}^*(Diesel) = \frac{1}{E_{fs} \times BSFC^*} = \frac{1}{43 \times 2.78 \times 10^{-4} \times 200} = 0.4183 \quad (41.83\%)$$

$$\eta_{fe}^*(Petrol) = \frac{1}{44 \times 2.78 \times 10^{-4} \times 225} = 0.3634 \quad (36.34\%)$$

5.3 Driving Cycles

The fuel consumption or emissions for an engine depends on the way an engine is operated, which in turn depends on the vehicle operation. The vehicle operation itself is dependent on several factors such as driving pattern, gearshifts and road loads. Suppose two engine designs for a vehicle are available and designer wants to compare the performance of the two engines in terms of fuel economy and emissions when installed on a specific vehicle. Obviously both engines must be tested in similar fashion through a comprehensive test procedure so they can be compared. Driving cycles have been designed so that all test vehicles follow identical driving patterns in order that the test results for fuel consumption and pollution can be comparable.

A driving cycle is a speed-time history of vehicle motion designed to represent a real-world driving pattern. Cycle time lengths are different and could range up to 2000 seconds or more depending on the test
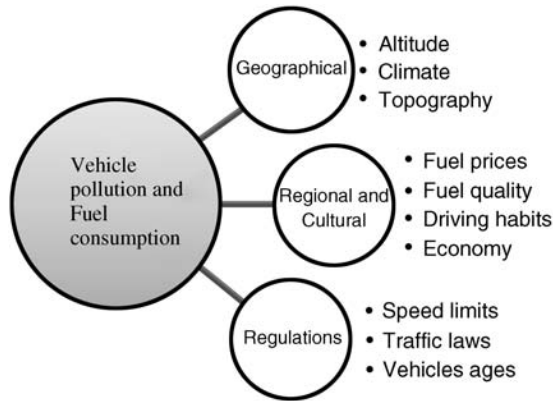
Figure 5.3   Different influential parameters on the fuel consumption and pollution of vehicles

purposes. The designs of driving cycles are based on different data collection methods [1], including realistic driving sequences that represent the normal operation of the vehicle. The driving cycles are intended to provide a compromise between real driving conditions and the repeatable measurements in the laboratory scale, with an acceptable accuracy.

Engine performance is highly dependent on geographical, cultural and legislation factors (see Figure 5.3). It is greatly influenced by the climatic variations (see Section 2.8.3). Different global regions have various climatic conditions in terms of air pressure, temperature and humidity. Road loads are different in various areas due to topographic differences. Some areas are flat and others are mountainous, thus the gravitational forces play different roles in exerting loads on engines. Driving habits in different countries also vary due to cultural, economic and traffic regulations. Local fuel prices can also affect driving styles. Average age and technology of the automobiles on the road are two other factors that create differences in the fuel consumption comparisons. The quality of fuels also plays a role in the fuel consumption and pollution generation. For all these reasons, the driving cycles for different global regions should vary if realistic estimations and comparisons are to be made. Driving cycle construction methods are different although the objectives are the same. Several countries have designed their own driving cycles based on regional influential factors.

5.3.1   Typical Driving Cycles

Over the past two decades several test procedures have been developed and standardized by different countries in various global regions. The most common test procedure in Europe for light duty vehicle type approval is the New European Driving Cycle (NEDC), shown in Figure 5.4. The driving cycle consists of two parts, ECE15 and EUDC, that correspond to urban and highway driving conditions. The ECE15 test cycle simulates an approximate 4 km urban trip at an average speed of 18.7 km/h and at a maximum speed of 50 km/h. Its duration is 780 seconds. The same part of the ECE15 driving cycle is repeated four times to obtain an adequate driving distance and engine temperature. The EUDC cycle represents a more aggressive cycle with some high speed driving at a maximum speed of 120 km/h. Its duration is 400 seconds at an average speed of 62.6 km/h and 7 km distance. Since the year 2000, the 40 seconds idle period at the beginning of the European driving cycle (EC2000) has been omitted. Thus, the emissions during the cold start are included in the driving cycle and this makes NEDC a more realistic test procedure.
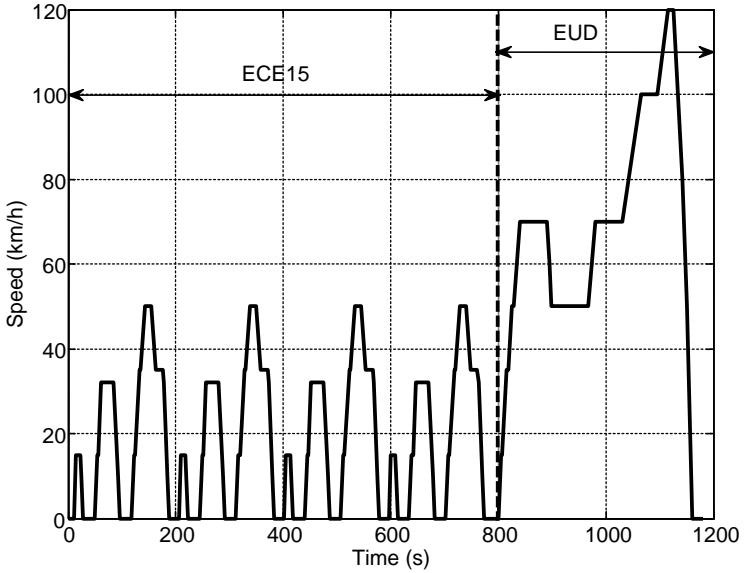
Figure 5.4   New European driving cycle (NEDC)

The FTP (Federal Test Procedure) established by the U.S. Environmental Protection Agency (EPA) is another example of a driving cycle, shown in Figure 5.5. The FTP test cycle, simulates 11.4 miles (17.7 kilometres) of driving at an average speed of 21.2 mph (34.1 km/h). The test involves a cold start after the engine's idle period, a hot start, and a combination of urban and highway conditions.
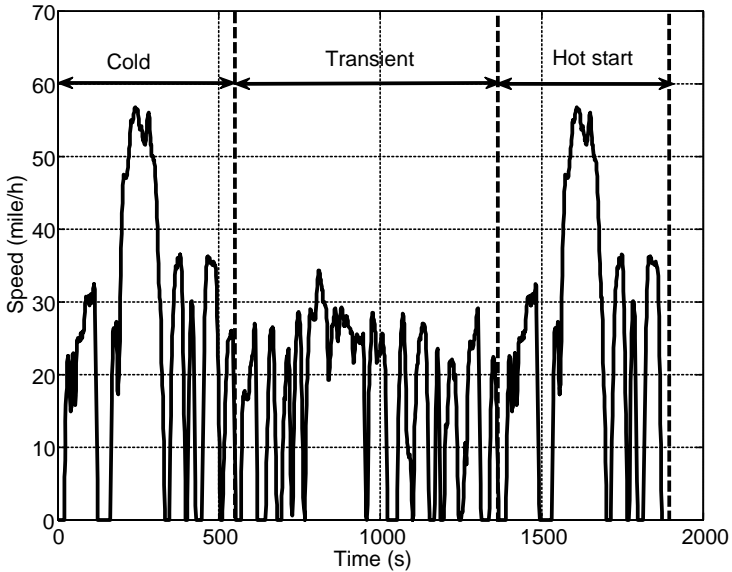
Figure 5.5   FTP-75 driving cycle

The applicability of the standard driving cycles to the real-world driving patterns is also debatable. There have been efforts to design new driving cycles which claim to be more representative of real-world driving behaviour [2–4].

5.3.2   Calculations

Driving cycles can be compared based on the statistical information available. Despite the fact that only speed versus time is given in a driving cycle, from rather simple calculations, other important motion parameters such as acceleration and travel distance can be obtained, for example:

$$a(t) = \frac{d}{dt} v(t) \tag{5.12}$$

$$S(t) = \int v(t)\, dt \tag{5.13}$$

Thus from a given driving cycle, the variation of acceleration $a(t)$ and distance $S(t)$ can be produced by the differentiation and the integration of vehicle speed respectively. Other useful parameters can also be calculated, such as:

- average speed
- average acceleration
- total time
- maximum speed
- maximum acceleration
- other statistical measures.

Once the acceleration and distance are obtained from the speed variations (Equations 5.12 and 5.13), the average speed v_{av} and average acceleration a_{av} during a cycle are:

$$v_{av} = \frac{1}{T} \int_0^T v(t)\, dt = \frac{S}{T} \tag{5.14}$$

$$a_{av} = \frac{1}{T} \int_0^T a(t)\, dt \tag{5.15}$$

in which T is the total travel time and S is the total travel distance. It should be noted that a_{av} obtained from Equation 5.15 also accounts for negative accelerations due to braking. Sometimes it is useful to find the average positive acceleration a_{av}^+ in order to get an estimation of how dynamic the driving cycle is.

Example 5.3.1

An idealized driving cycle is given in Figure 5.6:
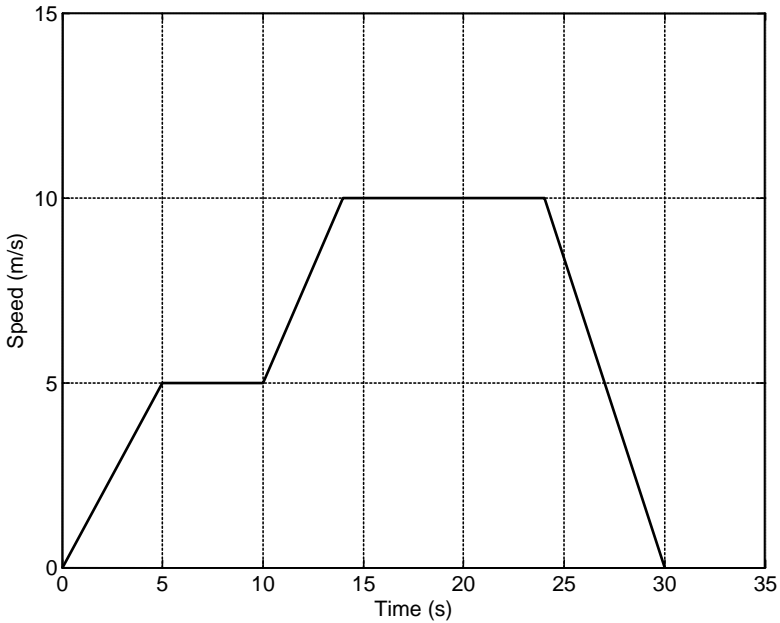
Figure 5.6 Driving cycle of Example 5.3.1

(a) Plot the variation of acceleration and travel distance with time.
(b) Determine average speed, average overall acceleration and average positive acceleration.

Solution

Since the speed-time profile includes only constant speed and constant acceleration parts, the calculation of acceleration simply involves obtaining the slopes at different points. The result is plotted in Figure 5.7.

Finding the distance is also simple. The distance at every given time is the total area under the speed curve from time zero to that specific time. This can simply be done by calculating the triangular and rectangular sub-areas under the curve. The result is shown in Figure 5.8.The average speed can be calculated by dividing the total distance by the total time:

$$v_{av} = \frac{197.5}{30} = 6.583 \quad (m/s)$$

The average acceleration is determined simply from the variation of acceleration (Figure 5.7) by summing up the area under the curve relative to zero acceleration. The result is:

$$a_{av} = \frac{1}{30}(1 \times 5 + 1.25 \times 4 - 1.67 \times 6) = -6.7 \times 10^{-4} \approx 0 \quad (m/s^2)$$
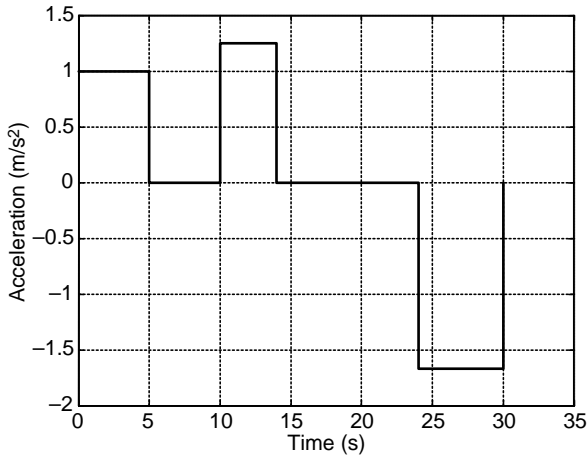
Figure 5.7   Vehicle acceleration time history of Example 5.3.1
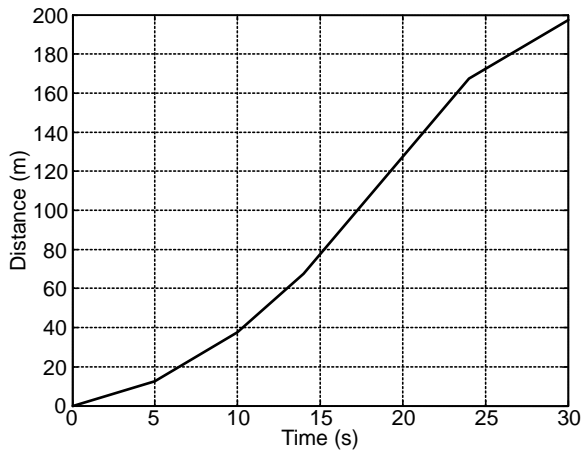
Figure 5.8   Variation of travelled distance with time of Example 5.3.1

The average positive acceleration takes only positive accelerations into account, thus it consists only of the first two terms of average acceleration:

$$a_{av}^+ = 0.333 \quad (m/s^2)$$

5.3.3   Vehicle Tests

Test cycles are performed on chassis dynamometers and the vehicle is constrained to follow a speed-time pattern specified by the driving cycle. A driver controls the throttle in order that the vehicle speed remains

as close to the specified speed as possible and in the meantime the emissions and fuel consumption data are recorded. Chassis dynamometers simulate the road loads and thus the test results can be considered as if the vehicle were driving on a real road.

Manufacturers' quoted fuel consumption figures are determined using standard laboratory tests on chassis dynamometers. These tests do not include several variables including road profile, traffic and weather conditions, driving style and vehicle speed, load and conditions. Such figures therefore cannot be exactly interpreted as the fuel consumption a vehicle might achieve under actual operating conditions, and are only reference values in order to compare with other manufacturers' figures.

5.4   Vehicle Fuel Consumption

Fuel consumption is a fundamental engineering measure and is useful because it is related directly to the goal of decreasing the amount of fuel required to travel a given distance. The terms *fuel economy* and *fuel consumption* are both used to classify the efficiency of how fuel is used in vehicles. These terms are defined as:

- Fuel economy is a measure of how far a vehicle will go with a given amount of fuel (e.g. per litre or gallon) and is expressed in kilometre per litre or miles per gallon (mpg). This is mostly the term used in North America.
- Fuel consumption is in fact the inverse of the fuel economy and is defined as the amount of fuel consumed in driving a given distance (e.g. 100 km or 100 miles) and is measured in litres per 100 kilometres (or gallons per 100 miles).

The fuel is the source of the energy for a vehicle and the work done by the vehicle is at the expense of the fuel consumption. Part of the energy E_c a vehicle consumes during its travel is transformed to kinetic energy E_k and the rest, E_R is lost due to resistive forces. In mathematical form this is:

$$E_c = E_k + E_R \tag{5.16}$$

In conventional vehicles with no energy regeneration, even the kinetic energy gained during accelerating will be transformed into heat when a vehicle is eventually stopped. Thus the total energy consumption of the conventional vehicle is what the engine produces:

$$E_c(t) = E_e(t) = \int_0^t P_e(t)dt \tag{5.17}$$

Only a fraction of the fuel energy, E_f is transformed to mechanical power by the engine and the rest is lost (E_L), or:

$$E_f = E_e + E_L \tag{5.18}$$

The engine fuel efficiency η_{ef} was defined as the ratio of energy produced by the engine to the energy supplied to that engine (Section 5.2.2). Energy is also lost within thevehicle driveline system (E_D) and the remaining energy E_w reaches to the wheels. Thus:

$$E_e = E_w + E_D \tag{5.19}$$

The overall driveline efficiency is defined as:

$$\eta_D = \frac{E_w}{E_e} = 1 - \frac{E_D}{E_e} \tag{5.20}$$

The overall efficiency of vehicle motion from fuel to wheel is therefore:

$$\eta_{fw} = \frac{E_w}{E_f} = \frac{E_w}{E_e} \cdot \frac{E_e}{E_f} = \eta_D \cdot \eta_{fe} \tag{5.21}$$

The transformation of wheel energy into vehicle energy involves the interactions between the road and the tyre. Another portion of energy is lost by the tyres through rolling resistance and slip. The portion related to the rolling resistance has been taken into consideration in the longitudinal dynamics (see Chapter 3) and that of the slip can be included in the tyre efficiency:

$$\eta_t = \frac{E_v}{E_w} \tag{5.22}$$

where:

$$E_v = \int_0^t F_T(t) \, v(t) \, dt \tag{5.23}$$

$$E_w = \int_0^t T_w(t) \, \omega_w(t) \, dt \tag{5.24}$$

in which the motion energy E_v is the energy that the vehicle gains during the motion and E_w is the energy delivered to the driving wheels during the same period. The overall efficiency of vehicle from fuel to longitudinal motion, therefore, becomes:

$$\eta_{fv} = \eta_t \cdot \eta_D \cdot \eta_{fe} \tag{5.25}$$

Combining Equations 5.21 and 5.22 results in:

$$E_f = \frac{E_v}{\eta_{fv}} \tag{5.26}$$

This means if the values for the energy of motion E_v and overall efficiency η_{fv} are available, the fuel energy E_f can be determined readily. Knowing the caloric energy content or specific energy of a fuel E_{fs} (joule/kg), the consumed fuel mass m_f is obtained simply from Equations 5.7 and 5.26:

$$m_f = \frac{E_f}{E_{fs}} = \frac{E_v}{\eta_{fv} E_{fs}} \tag{5.27}$$

The overall efficiency η_{fv} is the inherent property of vehicle main components and is assumed to be available from test results. The motion energy E_v depends on the travelling pattern of the vehicle in which the time variation of speed is known. The method of determining E_v from driving time histories will be discussed in following section.

5.4.1 Map-free Fuel Consumption

If a constant efficiency for the engine is assumed, the engine efficiency map is replaced by a single average value for the engine performance. This will provide simple estimations for the vehicle fuel consumption. In general, driving cycles include various kinds of speed-time variations that can be divided into three
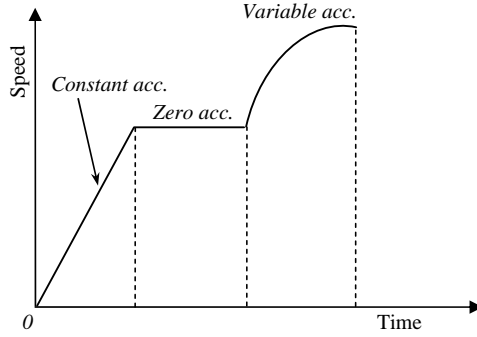
Figure 5.9   Different types of speed variations

types: zero, constant and variable acceleration regimes as shown in Figure 5.9. The dynamic equation of vehicle longitudinal motion in simple form is (see Chapter 3):

$$F_T - F_R = m\frac{dv}{dt} \tag{5.28}$$

in which F_T and F_R are the tractive and resistive forces acting on the vehicle and m is the vehicle mass including the effect of rotating inertias (see Section 3.9). The resistive force F_R is in general dependent on speed and can be determined once the speed-time history is available. The details of evaluating E_v for each driving regime depend on the right-hand side of Equation 5.28 and will be discussed in the following sub-sections.

5.4.1.1   Zero Acceleration

The result of the application of Equation 5.28 for zero acceleration is:

$$F_T = F_R \tag{5.29}$$

Thus from Equation 5.23:

$$E_v = \int_0^t F_R v \, dt \tag{5.30}$$

Note that the speed is also constant at this period and therefore for a time duration of Δt,

$$E_v = F_R v \, \Delta t \tag{5.31}$$

At a constant speed v, F_R is also a constant value and the energy E_v only increases with time.

5.4.1.2   Constant Acceleration

For a constant acceleration a, the tractive force F_T is:

$$F_T = F_R + ma \tag{5.32}$$
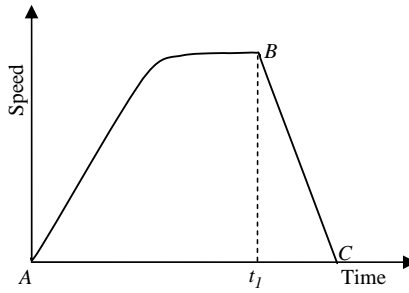
Figure 5.10   A sample trip

Substituting into Equation 5.23 leads to:

$$E_v = ma\,S + \int_0^t F_R v\,dt \tag{5.33}$$

in which S is the distance travelled and the integral term can be evaluated from the driving cycle information and resistive force values.

5.4.1.3   Variable Acceleration

Consider a segment in which a vehicle starts a variable acceleration from speed v_0 at time $t = t_0$ and ends at time t and speed v. The fuel consumption in such a trip can be calculated based on the equations obtained earlier. To this end, substituting Equation 5.28 into Equation 5.23 results in:

$$E_v(t) = \frac{1}{2}m(v^2 - v_0^2) + \int_0^t F_R v\,dt \tag{5.34}$$

The first term on the right is the net kinetic energy of vehicle during the motion and is obtained from the two end speeds. The second term must be determined using driving cycle information and resistive force values.

It should be noted that Equations 5.31, 5.33 and 5.34 are valid only for those segments of trips with no deceleration. The reason simply is that the kinetic energy gained during acceleration cannot be recuperated during deceleration, therefore it will be lost if the vehicle stops. For further clarification consider the vehicle trip illustrated in Figure 5.10 which comprises one acceleration segment starting from point A (origin) to point B and one deceleration segment from B to C. If Equation 5.34 is used to evaluate the energy E_v of vehicle, the first term on the right-hand side vanishes since the vehicle speed at both ends are nil. This result is not acceptable since if the same equation between points A and B was evaluated first, a positive sum would be calculated and since this amount of energy will be lost during deceleration while the engine is not producing power, i.e. the throttle is closed and the engine will produce braking torque if the transmission is engaged, or will work in idle if the transmission is disengaged, the total kinetic energy corresponds only to the part with no deceleration.

Example 5.4.1

A trip is designed in two linear acceleration and deceleration segments shown in Figure 5.11. The vehicle weighs 1200 kg and the overall efficiency from fuel to longitudinal motion is 25%.
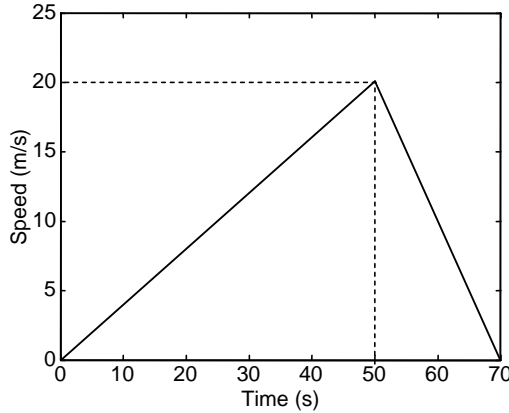
Figure 5.11   Trip for Example 5.4.1

Resistive forces against the vehicle motion can be estimated from equation:

$$F_R = 200 + 0.4v^2$$

If the fuel has the caloric energy content of 44 MJ/kg and density of 800 kg/m^3, calculate the fuel consumption in l/100 km on this particular trip.

Solution

The motion energy E_v can be obtained from either Equations 5.33 or 5.34. The second terms of both equations are identical. The evaluation of the first term on the right-hand side of equations is straightforward. From Equation 5.33 the travelled distance can be obtained by integration (or simply the area under the curve):

$$S(50) = \int_0^{50} v\, dt = \int_0^{50} 0.4\, t\, dt = 500\, m$$

The first term thus results in:

$$term\, 1 = maS = 1200 \times \tfrac{20}{50} \times 500 = 0.24 \times 10^6\, J$$

From Equation 5.34:

$$term\, 1 = \tfrac{1}{2} \times 1200 \times (20^2 - 0) = 0.24 \times 10^6\, J$$

that is exactly the same. For the second term, the variation of speed with time must be substituted.

$$term\, 2 = \int_0^{50} (200 + 0.4v^2)v\, dt = \int_0^{50} \{200 + 0.4(0.4t)^2\}(0.4t)dt = 0.14 \times 10^6$$

Thus the total energy is 0.38 MJ. The fuel mass for the trip can be calculated from Equation 5.32:

$$m_f = \frac{E_v}{\eta_{fv}E_{cf}} = \frac{0.38}{0.25 \times 44} = 0.0345 \text{ kg}$$

The fuel volume simply is $V_f = 43.13$ cc $= 0.043$ l.

In order to convert it to l/100 km, the total travelled distance in one cycle is needed. At the end of the cycle:

$$S(70) = S(50) + \int_0^{20} (20 - t)dt = 700 \, m$$

Thus for a $700 \, m$ trip 0.043 l of fuel is consumed, for 100 km the fuel consumption is 6.14 l.

5.4.2   Map-based Fuel Consumption

In practice, as discussed in Section 5.2, the engine performance varies in different working conditions. BSFC as a measure of engine fuel consumption depends on the operating condition of the engine. On the other hand, engine efficiency was related to the fuel consumption measure (BSFC) in Section 5.2.2, by assuming a particular working condition for an engine in which the BSFC was a constant value (Equation 5.11). The fuel mass used to produce an amount of engine output energy E_e can be obtained from Equations 5.6 and 5.10 in the following form:

$$m_f = BSFC^* E_e \tag{5.35}$$

This result is valid if the BSFC can be treated as a constant value. During a brief period of vehicle motion, it would be reasonable to assume it is a constant value $BSFC^*$. In such cases, eliminating E_e from Equation 5.35 by making use of Equations 5.21 and 5.22 results in:

$$m_f = \frac{E_v BSFC^*}{\eta_D \eta_t} \tag{5.36}$$

Equation 5.36 is valid only for a short period of time in which BSFC is assumed to remain constant. Therefore, in order to make use of this result for a driving cycle, the cycle must be divided into short time periods. In this way, Equation 5.36 can be evaluated separately for each time period and the total fuel consumption during a cycle can be obtained by summing up those small segments. A 1 second period is found to be appropriate for divisions of driving cycles in terms of simplicity and accuracy. A 1 second period makes the calculations very simple since the energy of each component at every division i can be replaced by its power, i.e.:

$$E(i) = P(i)\Delta t = P(i) \tag{5.37}$$

Evaluation of Equation 5.36 requires the calculation of two parameters E_v and BSFC at each period. A useful equation that can be used to evaluate E_v for each division is of the form:

$$E_v(i) = F_T(i)v(i) = \eta_D \eta_t P_e(i) \tag{5.38}$$
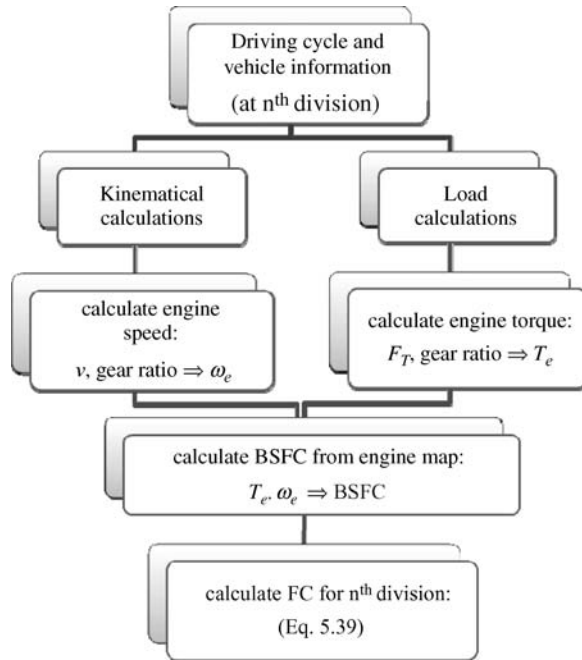
Figure 5.12 Flowchart of calculating fuel consumption at each division

Thus combining Equations 5.36 and 5.38 gives:

$$m_f(i) = P_e(i) \cdot BSFC(i) \tag{5.39}$$

$P_e(i)$ is simply $T_e(i)$ times the values of $\omega_e(i)$ that are also used to determine the BSFC (i) from the engine map. Calculation of BSFC requires the engine data at different working conditions as discussed in Section 5.2. Figure 5.12 shows the general procedure involved in the calculation of the fuel consumption at each division of the driving cycle.

In order to evaluate fuel consumption, again similar acceleration regimes to those explained in Section 5.4.1 can be used, with the exception that in a short time period of 1 second, acceleration can always be regarded as either constant or zero.

5.4.2.1 Zero Acceleration

Zero acceleration or constant speed portions are present in several driving cycles. For a segment in a driving cycle with constant speed, N divisions can be made (see Figure 5.13). For division i the tractive force is obtained from Equation 5.28, then the equation of motion of the driving wheel is (see Section 3.10):

$$T_w(i) - F_T(i)r_w = I_w\dot{\omega}_w(i) \tag{5.40}$$

The wheel torque can be written as (see Section 3.13.2):

$$T_w(i) = n \cdot \eta_D \cdot T_e(i) \tag{5.41}$$

in which n and η_D are the overall gear ratio and efficiency of driveline respectively.
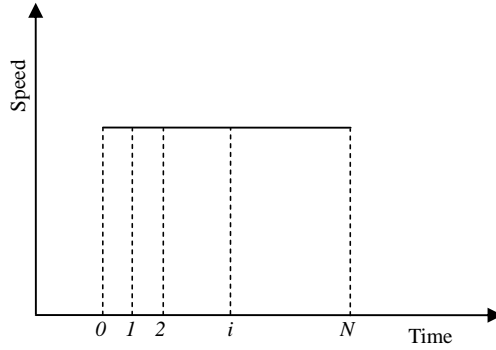
Figure 5.13   Constant speed portions of a driving cycle

The vehicle speed v is directly related to the wheel rotational speed (see Section 3.10):

$$v(i) = r_w(1 - S_x)\omega_w(i) \tag{5.42}$$

in which S_x is the longitudinal slip of the driving wheel. Since v is constant, the right-hand side of Equation 5.40 vanishes and by using Equations 5.40 and 41, one simply finds:

$$T_e(i) = \frac{r_w}{n \cdot \eta_D} \cdot F_T(i) \tag{5.43}$$

Engine speed for this time division can be obtained using Equation 5.42:

$$\omega_e(i) = \frac{n}{r_w(1 - S_x)} \cdot v(i) \tag{5.44}$$

With values obtained for the engine speed and torque at this particular point i, the BSFC value can be read from the engine map. E_v for this division then can be obtained from Equation 5.38 and used in Equation 5.39 to calculate the fuel mass for the ith time division.

If BSFC is given in kg/J and power in Watts, the fuel mass for division i will result in units of kg/s. However, it is a common practice to represent BSFC in g/kWh. For this reason, it is necessary to convert the result of Equation 5.39 dividing it by 3.6×10^6, the result will be in grams of fuel in a time span of 1 second. The fuel mass for the whole cycle is then obtained by summing up all the individual fuel masses:

$$m_f = \sum_{i=1}^{N} m_f(i) \tag{5.45}$$

Fuel consumption (FC) can be converted to g/100 km by dividing the fuel mass by the vehicle speed and multiplying the result by an appropriate factor. Having the density of the fuel ρ_f, its volume can be calculated:

$$FC = \frac{m_f}{v \cdot \rho_f} \times 10^2 \quad \left(\frac{l}{100\,km}\right) \tag{5.46}$$

In Equation 5.46, v must be in km/h, m_f in g/h and fuel density in kg/m^3. It is also worth noting that for all divided segments the speed is equal and, as a result, the fuel consumption will be identical for all

divisions. Thus it is sufficient to calculate the fuel mass only for one single division and multiply it by the number of divisions to obtain the total fuel consumption.

Example 5.4.2

The vehicle in Example 5.4.1 is driven over a 10-second segment of a cycle with constant speed of 45 km/h. At this particular point of operation, the engine BSFC is 330 g/kWh. Driveline and tyre efficiencies are 0.95 each. Determine the fuel consumption in l/100 km.

Solution

From Equation 5.28:

$$F_T = F_R = 200 + 0.4v^2 = 262.5 \text{ N}$$

Engine power can be calculated from Equation 5.38:

$$P_e = \frac{F_T v}{\eta_D \eta_t} = \frac{262.5 \times 12.5}{0.95 \times 0.95} = 3636 \ W$$

Fuel mass in one second of motion is (Equation 5.39):

$$m_f(i) = P_e(i) \cdot BSFC(i) = \frac{3636 \times 330}{3.6 \times 10^6} = 0.3333 \text{ g/s}$$

The total mass is therefore 3.333 grams in 10 seconds. m_f in one hour is 1200 grams so:

$$FC = \frac{m_f}{v \cdot \rho_f} \times 10^2 = \frac{1200 \times 100}{45 \times 800} = 3.3 \ \left(\frac{l}{100 \, km} \right)$$

5.4.2.2   Constant Acceleration

Constant acceleration portions may be present in some driving cycles; or if a segment of a driving cycle with variable acceleration is divided into short time spans, the acceleration in such spans can be regarded as constant (see Figure 5.14).

For this case, the tractive force in division i is obtained from Equation 5.32. Since v is not constant, the right-hand side of Equation 5.40 can be derived from Equation 5.44 (a zero S_x is assumed) and by using Equations 5.40–42 results in:

$$T_e(i) = \frac{r_w}{n \cdot \eta_D} \cdot \left[F_T(i) + \frac{I_w}{r_w^2} \cdot a(i) \right] \tag{5.47}$$

Engine speed for division i can be obtained from Equation 5.44; however, since the vehicle speed is not constant, its average value at each division is used. The rest of the procedure is similar to that of the
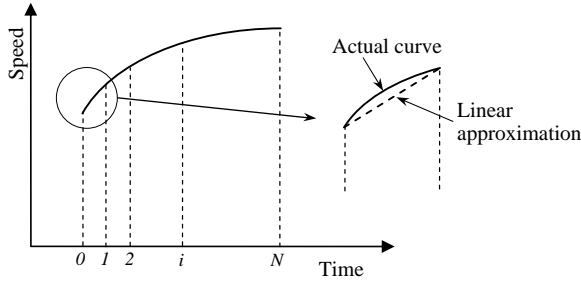
Figure 5.14 Constant acceleration approximation

zero acceleration case and the fuel mass can be calculated for each division and then summed up for all segments.

5.4.3   Effect of Rotating Masses

Accelerating the vehicle body takes place not only in longitudinal direction but also involves simultaneously accelerating the wheels, axles and other rotating elements, around their rotating axes. In fact, a mass that moves with speed v and rotates with speed ω has two energy components:

$$E = \tfrac{1}{2}mv^2 + \tfrac{1}{2}I\omega^2 \tag{5.48}$$

The first term in the energy equation is for the translating motion and the second term is for the rotating motion. In the discussions so far, the second term arising from the rotation of driveline components was not considered. In order to include this effect, we refer to discussions in Section 3.9, and it will suffice to substitute the vehicle mass in Equation 5.28 with an equivalent mass m_{eq} (see Section 3.9.1):

$$m_{eq} = m + m_r \tag{5.49}$$

where:

$$m_r = \frac{1}{r_w^2} \left[I(\omega_w) + n_f^2 I(\omega_g) + n^2 I(\omega_e) \right] \tag{5.50}$$

in which $I(\omega_w)$ is the sum of all inertias rotating with speed of driving wheels, $I(\omega_g)$ is the sum of all inertias rotating with speed of gearbox output shaft and $I(\omega_e)$ is the sum of all inertias rotating with the speed of the engine.

5.5   Shifting Effects

Many approaches have been attempted to improve the fuel economy of a vehicle, including optimization of the engine performance itself such as intake and fuel injection systems, increasing volumetric efficiency, optimizing the combustion chamber, etc. With the application of these methods, the performance of the engine will be directly affected and the fuel consumption map will be modified to include more areas of fuel efficient points.

In addition to these techniques which obviously influence the function of the engine itself, it is possible to optimize the manner in which the engine is utilized during driving. Improvement of the powertrain system is a means of optimizing the engine operating regimes. Possible modifications of powertrain systems can be divided into hardware and software categories. The hardware modifications affect the structure

and mechanism of the powertrain system and involve the selection of different transmission types and gear ratio designs. Software modifications include the design of gearshifting schedules to optimize shift points. This is based on controlling the time spent at the most efficient engine operation points (EOPs).

5.5.1 Effect of Shifting on EOP

Operating at a particular EOP depends on the control of the input parameters, namely the throttle (or accelerator pedal) and gear ratios. In order to observe how EOPs change when the gear is changed, the engine torque–speed map will be considered from various perspectives. Engine torque and speed are dependent on vehicle kinematics and loads. The basic equations are (see Chapter 3):

$$\omega_e = \frac{nv}{r_w} \tag{5.51}$$

$$T_e = \frac{F_T r_w}{n} \tag{5.52}$$

$$F_T = F_R + m\frac{dv}{dt} \tag{5.53}$$

in which F_T and F_R are the tractive and resistive forces acting on the vehicle, and n is the overall gear ratio from engine to the driving wheels. m in Equation 5.53 is regarded as the equivalent mass including the effect of rotating inertias (see Section 5.4.3). It should be noted that no tyre slip was assumed in deriving Equations 5.51 and 5.52 and also ideal efficiency was considered for the drivetrain. The engine torque and speed are related by the engine characteristic equation with the general form:

$$T_e = f(\omega_e, \theta) \tag{5.54}$$

The overall resistive force is speed dependent (see Section 3.4):

$$F_R = g(v) \tag{5.55}$$

Thus, Equations 5.51–5.55 show that once the vehicle speed (and its time history) have been specified, two control parameters, namely the gear ratio n and throttle θ, will govern the engine working points. The combination of these two inputs produces various possibilities for the engine operation selected by the drivers. Schematic relations of Figure 5.15 explain the processes involved in the changing of operating points according to Equations 5.56–5.60.

The engine torque-speed map can be viewed from three different perspectives: (1) throttle variations; (2) power variations; and (3) specific fuel consumption. Figure 5.16 illustrates these three views in a single figure. Moving over solid lines shows the constant throttle case, whereas dashed lines represent constant power lines. Figure 5.16 indicates that to take the engine EOP close to a minimum fuel consumption value, only limited choices for throttle opening and engine power exist. It is also clear that low and high powers are far from efficient points.

Gearshifts are carried out in order to change the EOPs, with different objectives such as:

1. Use more engine power to accelerate: this action will move EOP across the power lines.
2. Increase engine torque when more traction is required: this action will move EOP upwards.
3. Take EOP towards more efficient areas: this action will move EOP towards lower BSFC points.
4. Move away from very low and very high engine speeds: this action will move EOP towards the middle areas.
5. Use the engine braking torque: this action is usually carried out by closing the throttle completely and EOP moves downwards below the zero torque line (not shown in Figure 5.16).
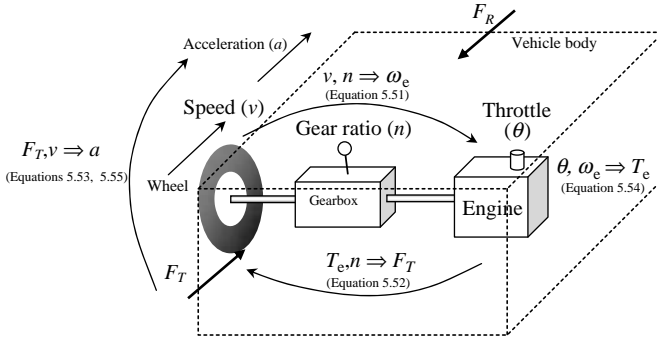
Figure 5.15 Interrelations between the parameters according to Equations 5.56–5.60
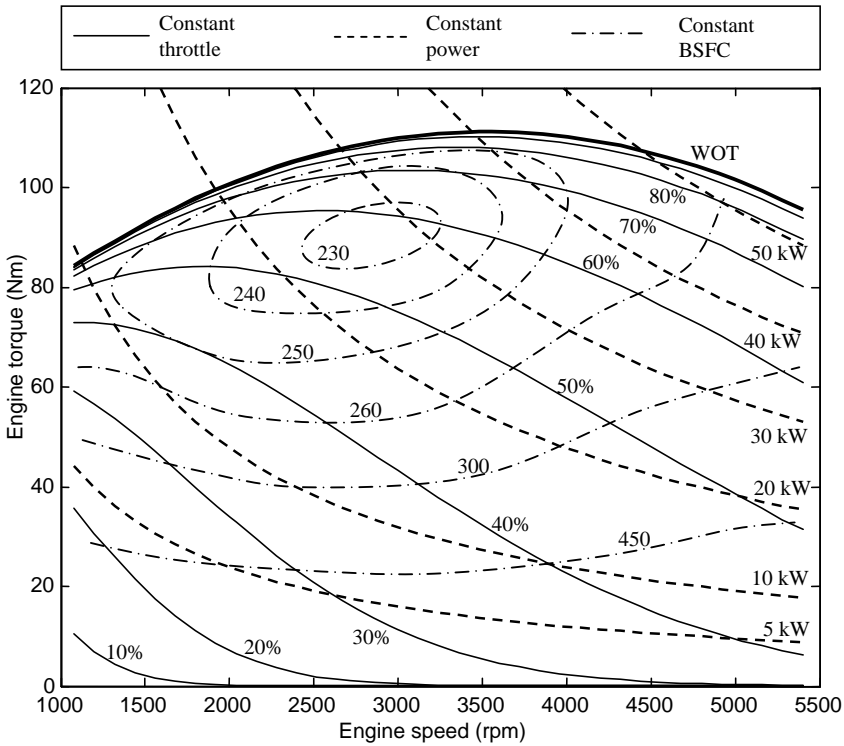
Figure 5.16 Engine torque–speed diagram and influential parameters

All of the above-mentioned objectives can be achieved in different ways. The two available control inputs are throttle input and transmission gear ratio. If throttle input is kept unchanged during the gearshift, then the EOP will move along the constant throttle lines (Figure 5.17). Otherwise the EOP moves in any direction according to the throttle input and gear ratio.
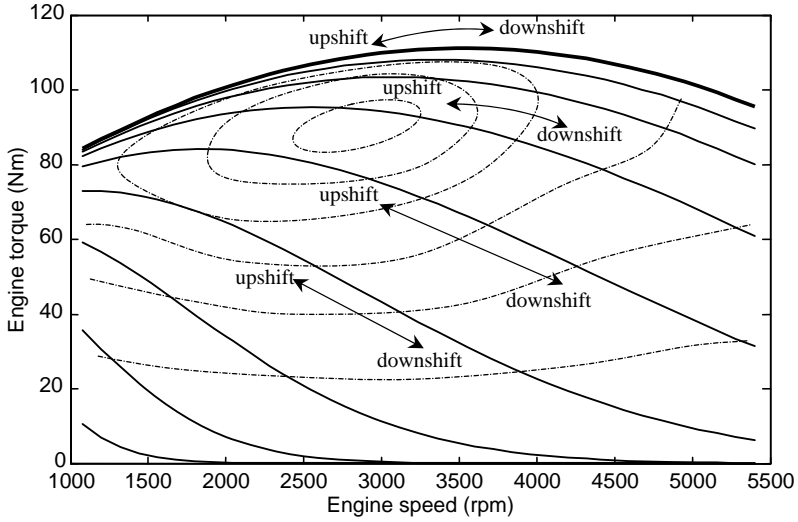
Figure 5.17 Fixed throttle shifting

Sometimes a gearshift is performed when a constant load is acting on the vehicle. In such circumstances, the output power of engine is kept constant and the EOP is moved along the constant power lines as shown in Figure 5.18.
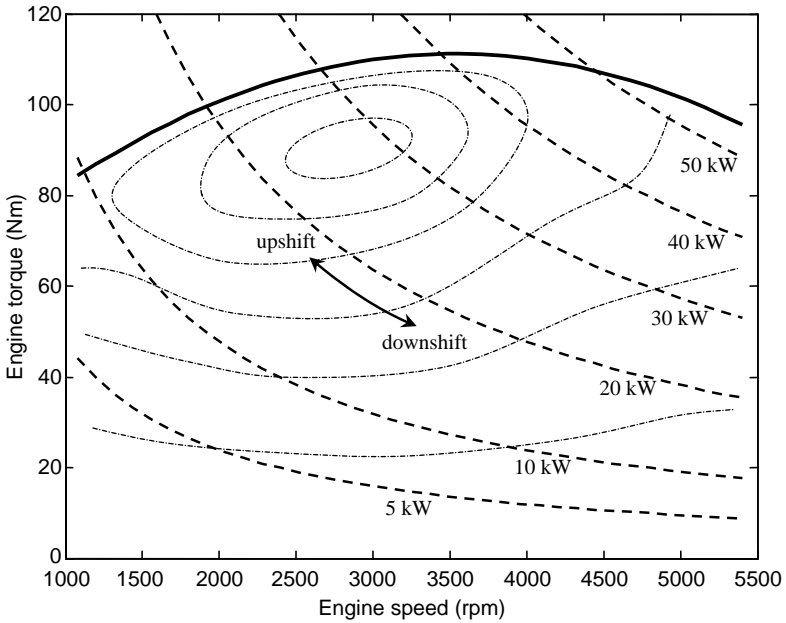
Figure 5.18 Constant power shifting

Example 5.5.1

The vehicle of Example 5.4.1 is moving with a speed of 90 km/h at gear 3 while the engine throttle is wide open. The engine WOT torque-speed formula is of the form:

$$T_e = -4.45 \times 10^{-6}\omega_e^2 + 0.0317\omega_e + 55.24$$

The overall gear ratios for gear 3 and 4 are 6.86 and 4.63 respectively and the tyre rolling radius is 30 cm. If, at this instant, gear is shifted to 4:

(a) Determine the new EOP and compare it with the old EOP.
(b) Compare the vehicle acceleration in the two cases.

Solution

From Equation 5.51, the engine speed at gear 3 is:

$$\omega_3 = \frac{n_3 v}{r_w} = \frac{6.86 \times 90/3.6}{0.3} \times \frac{30}{\pi} = 5459 \, (rpm)$$

Engine torque at this speed is:

$$T_3 = -4.45 \times 10^{-6} \times 5459^2 + 0.0317 \times 5459 + 55.24 = 95.7 \, Nm$$

When the shift to gear 4 is carried out, the engine speed and torque will change to:

$$\omega_4 = \frac{4.63 \times 90/3.6}{0.3} \times \frac{30}{\pi} = 3684 \, (rpm) \quad \text{and} \quad T_3 = 111.6 \, Nm$$

Thus the EOP is moved along the WOT curve to the left since an upshift is performed. This gearshift was to move the EOP away from a high engine speed (item (4) in the list of objectives on p. 361). The vehicle acceleration for each case can be determined from Equation 5.53. The resistive force for both cases is identical:

$$F_R = 200 + 0.4v^2 = 200 + 0.4 \times (90/3.6)^2 = 450 \, \text{N}$$

$$a_3 = \frac{1}{m}\left(\frac{nT_e}{r_w} - 450\right) = \frac{1}{1200}\left(\frac{6.86 \times 95.7}{0.3} - 450\right) = 1.45 \, m/s^2$$

$$a_4 = \frac{1}{1200}\left(\frac{4.63 \times 111.6}{0.3} - 450\right) = 1.06 \, m/s^2$$

5.5.2 Efficient Operating Points

There are several EOPs on a certain BSFC contour that apparently have similar fuel consumption values. From the definition of engine BSFC, however, it is understood that the fuel consumption is dependent on

the power output of the engine as well. From Equation 5.1, the instantaneous fuel consumption can be expressed in the following form:

$$\dot{m}(t) = BSFC(t) \cdot P_e(t) \tag{5.56}$$

Equation 5.56 indicates that at a given BSFC, the instantaneous fuel consumption depends not only on the BSFC value, but also on the output power. In other words, in order to reduce the vehicle fuel consumption, it is necessary not only to direct the engine towards lower BSFC values, but also at the same time to use lower output powers.

Example 5.5.2

The vehicle in Example 5.5.1 with gearbox information given in Table 5.2 is travelling at a speed of 85 km/h. The MT formula coefficients (see Chapter 2) for the engine with the full throttle equation of Example 5.5.1 are given in Table 5.3. The minimum BSFC point for the engine is located at $(T = 90, \omega = 2700)$.

Table 5.2 Gearbox information for Example 5.5.2

	Gear		Value
1	3rd ratio	n_3	5.56
2	4th ratio	n_4	3.96
3	5th ratio	n_5	3.13

Table 5.3 Coefficients of MT formula for Example 5.5.2

Coefficient	A	B	C	D
Value	-11.12	0.0888	1.003	1.824

(a) Find an ideal ratio that can bring the EOP close to the minimum BSFC point.
(b) Calculate the required engine throttle for case (a).
(c) Which of the actual vehicle gears is more suitable for similar dynamic performance and fuel economy?

Solution

(a) From Equation 5.51 the gear ratio according to the target engine speed at the specified point is:

$$n = \frac{r_w \omega}{v} = \frac{0.3 \times 2700}{85/3.6} \times \frac{\pi}{30} = 3.59$$

(b) This ratio will match the vehicle speed with required engine speed. However, in order that the engine torque also coincides with the specified torque of 90 Nm, the engine throttle must be

adjusted. From the MT formula with two input values of engine speed and torque, the throttle can be obtained by a trial and error procedure. The result is 56% throttle opening (see Example 4.5.5). (c) Apparently the gear ratio 3.59 is somewhere between gears 4 and 5 but closer to gear 4. In order to see how dynamically close the gears 4 and 5 are to the ideal gear ratio, the vehicle acceleration can be examined. The resistive force is:

$$F_R = 200 + 0.4 \times (85/3.6)^2 = 423 \, \text{N}$$

Vehicle acceleration at the ideal gear is:

$$a = \frac{1}{1200} \left(\frac{3.59 \times 90}{0.3} - 423 \right) = 0.545 \, m/s^2$$

The engine speeds for gears 4 and 5 at specified vehicle speed are:

$$\omega_4 = 2976 \, rpm, \omega_5 = 2352 \, rpm$$

In order to produce similar acceleration at both gears, torques are obtained as (assuming no driveline loss):

$$T_4 = 81.7 \, Nm \quad \text{and} \quad T_5 = 103.3 \, Nm$$

Figure 5.19 illustrates the EOPs for ideal ratio ($\boxtimes$), 4th ratio ($\oplus$) and 5th ratio ($\otimes$) respectively. In terms of BSFC, the two resulting EOPs for 4th and 5th gears are located at points with not too different BSFC values, but smaller for gear 4. Since the power level for both gears is equal to 25.45 kW (and why is this?), therefore, for a similar dynamic performance gear 4 will have lower fuel consumption.
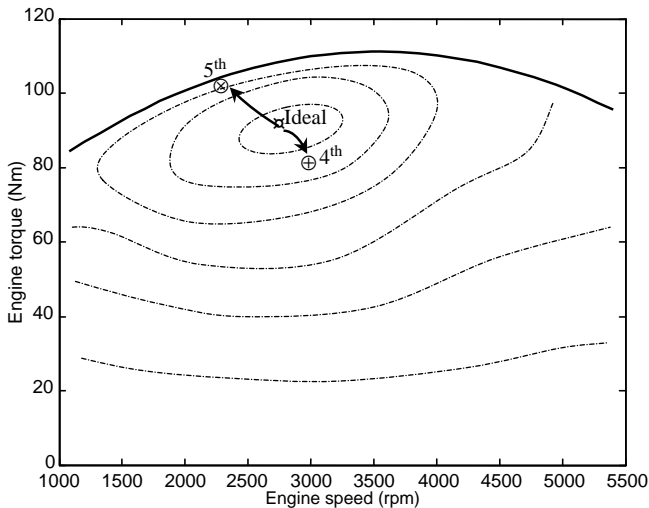
Figure 5.19   Effect of gear ratio on EOP of Example 5.5.2
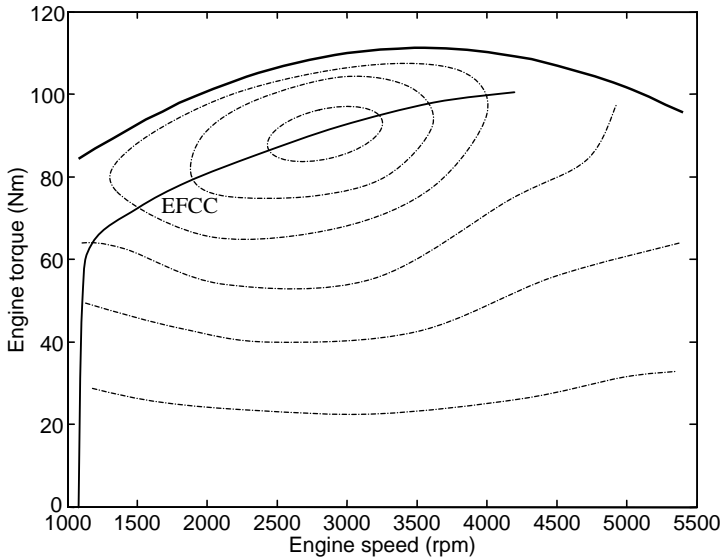
Figure 5.20   A typical efficient fuel consumption curve (EFCC)

A fuel efficient point on a BSFC contour is, therefore, the point with a minimum power requirement. With this concept, the Efficient Fuel Consumption Curve (EFCC), which is also called the Optimum Operating Line (OOL), is obtained from the engine torque–speed map by connecting all the fuel efficient points on different contours. In other words, at each engine power, the intersection of the constant power curve with the lowest fuel consumption contour gives a fuel efficient point for that power. Connecting all the points for different powers produces the EFCC curve. Figure 5.20 illustrates a typical EFCC curve for an engine. Tracking the EFCC in all engine output powers leads to the minimum achievable fuel consumption of the vehicle. In other words, if all EOPs could be located on the EFCC during a specific trip, all requested output powers will have been utilized with minimum BSFCs.

Tracking the EFCC of an engine requires a gearbox with unlimited gear ratios, so that the change of transmission ratio does not lead to a sudden change of engine speed and torque. Hence, a continuously variable transmission (CVT) is required to track the EFCC with minimum error. Despite the fact that the mechanical efficiency of CVTs in general is less than that of common manual gearboxes, nevertheless this type of transmission can reduce fuel consumption by making it possible to travel smoothly along the EFCC and thus select engine operating points near to optimum working conditions by continuously changing the gear ratio.

Example 5.5.3

Suppose that the vehicle in Example 5.5.2 is equipped with a CVT gearbox. The aim is to retain the EOP at the minimum BSFC point with torque–speed specifications given previously.

For the two speeds of 70 and 100 km/h:

(a) If the speeds are meant to remain constant, can the minimum BSFC point be held?
(b) Calculate the gearbox ratios and throttle openings for the two given constant speeds.
(c) Propose better EOPs to improve the fuel economy.

Solution

(a) The answer in general is no. The reason is that when the EOP is moved over the given point, both engine torque and speed are specified. According to the discussions in Section 5.5.1 and the procedure shown in Figure 5.15, a vehicle will attain an acceleration as a result of a balance between the tractive and resistive forces. In order to have a constant speed, the tractive force must equal the resistive force at that speed. In practice, such a case can only happen accidentally.

(b) The gear ratios can be determined as before by using Equation 5.51. This solution relies only on the engine speed corresponding to the specified EOP. The results for the two speeds are $n_{70} = 4.36$ and $n_{100} = 3.05$. In order to obtain the necessary throttle openings, the condition of tractive–resistive force balance must be met. The resistive forces for the two speeds are obtained as $F_{R70} = 351.2\,N$ and $F_{R100} = 508.6\,N$. Equating the tractive forces to the resistive forces, the engine torques are found to be $T_{e70} = 24.2\,Nm$ and $T_{e100} = 50.0\,Nm$ for the two cases. The EOPs of the two cases are illustrated in Figure 5.21 (points A and B). As is clear, the EOPs are located in very poor fuel efficiency areas especially that for the 70 km/h speed. Again, using the MT formula with two input values of engine speed and torque, the throttle values can be obtained. The results are 32.6% and 40% throttle openings respectively.

(c) Since the speeds are meant to remain constant, maintaining a constant power in each case will keep the traction force unchanged ($F_T \cdot v = \eta_D P_e$) which in turn does not change the speed of motion. Thus, moving the EOP over a constant power curve towards the EFCC (points C and D in Figure 5.21) can improve the fuel economy.
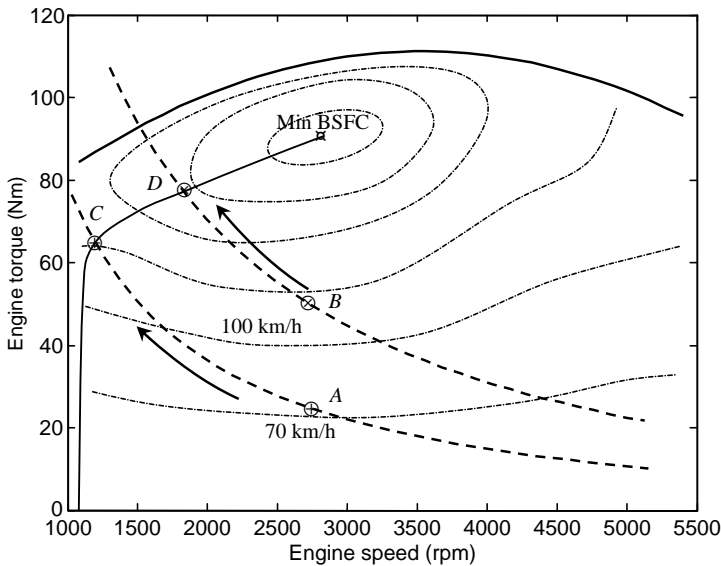
Figure 5.21   Effect of gear ratio on EOP of Example 5.5.3

5.6   Software

Determining the vehicle fuel consumption in general requires the engine, the BSFC map, vehicle and driving information. Accurate calculations need additional information regarding the components' performances and efficiencies. Inclusion of driving cycles in the calculations will add to the complexity of the calculations. When engine pollution is to be determined in addition to the fuel consumption, further engine maps regarding different pollutants should also be included as inputs. All these will make the calculations more complex than one could manage without the aid of software packages.

5.6.1   Solution Methodologies

Two different methodologies are available in determining the fuel consumption and emissions of a vehicle. These are called *forward-facing* and *backward-facing* methodologies. The forward-facing methodology resembles a real vehicle's motion that involves the driver's input commands and the resulting vehicle motion. Details of such longitudinal motions of vehicle were discussed in Chapter 3. Figure 5.22 summarizes the input–output relations for a forward-facing methodology. In a forward-facing method, differential equations of motion have to be solved in order to obtain the vehicle and component states. Therefore, this type of solution is a dynamic solution in which all time-dependent phenomena are dealt with.

In the backward-facing method, as the name implies, the problem is to find 'unknown inputs' to the system that have led to a 'known output' for the system. In vehicle motion the output is typically the time history of speed (driving cycle) and the input values such as the throttle and gear ratios are calculated. A driving cycle is, therefore, the input of the backward-facing solution. Figure 5.23 shows the flowchart of a backward-facing solution.

The input driving cycle is used to first determine the motion kinematics such as vehicle acceleration and travel distance as well as the components' kinematics such as rotational speeds of engine and transmission. In the next step, the loads on the vehicle and components must be evaluated so that the engine load is found. Once the engine rotational speed and load are known, the EOP is obtained and from engine performance data, the fuel consumption and emissions can be determined.

Obtaining the system kinematics and also the dynamic loads requires the differentiation of the input of the time–speed history (to obtain acceleration). A practical way to simplify this process is to divide the cycle time into small time spans and in each time span consider a constant acceleration. With this assumption, evaluation of system parameters can be carried out simply by algebraic equations (see Figure 5.12). Because efficiency maps used in backward-facing simulations are generally obtained by
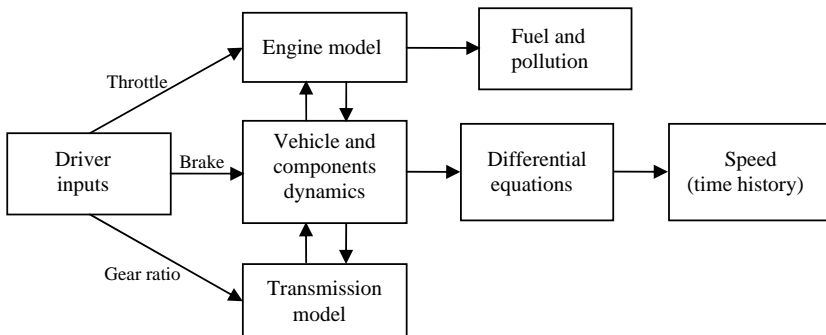
Figure 5.22   Forward-facing solution methodology
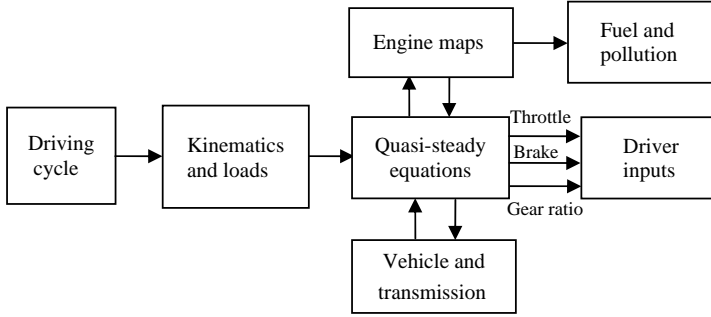
Figure 5.23 Backward-facing solution methodology

steady state testing, dynamic effects are not included and this is why these methods of solution are called quasi-steady solutions.

In real-world driving, if a driver wants to follow a predefined pattern like a driving cycle, the input parameters must be adjusted by receiving feedbacks from the output. In other words, the driver acts like a controller that closes the loop of the system from input to the output. Simulation in a forward-facing solution in which the input to the system is the accelerator pedal, will lead to a time history of vehicle speed but not necessarily a predefined driving cycle. In other words, in order to follow a specified driving cycle, a closed loop control system is needed to apply appropriate pedal angles at each instant so that vehicle speed versus time follows the desired pattern. In chassis dynamometer tests, a similar problem is solved since the driver must adjust the inputs according to the speed errors.

Vehicle simulators that use a forward-facing approach include a driver model, which determines the speed error as the difference between the required speed from the driving cycle input and the current speed, to estimate the appropriate throttle and brake commands so that the vehicle follows the input cycle with minimum error. Although the forward-facing solutions include all dynamic effects, backward simulations are easier to use since they do not need a closed loop control.

5.6.2   ADVISOR®

ADVISOR® is an acronym for ADvanced VehIcle SimulatOR, a simulation software package designed for the analysis of the performance and fuel economy of conventional, electric, and hybrid vehicles. The simulation environment is MATLAB® and Simulink®. ADVISOR® was designed to analyze vehicle powertrains, focusing on power flows among the components, and its main outputs are fuel consumption and vehicle exhaust emissions.

The software was first developed in 1994 by the US National Renewable Energy Laboratory (NREL) and its benchmarking began in 1995. Between 1998 and 2003, it was downloaded free of charge by more than 7,000 individuals, corporations, and universities worldwide. The input data to ADVISOR® is mostly empirical, relying on quasi-steady drivetrain component input–output relationships measured in the laboratory, and using data collected in steady state tests. The transient effects such as the rotational inertia of drivetrain components are considered in the calculations. This software was intended to be used to estimate vehicle fuel economy and investigate how conventional, hybrid, or electric vehicles use energy throughout their drivetrains. Also, it was used to determine the exhaust emissions produced on a driving cycle.

ADVISOR® is called a backward-facing vehicle simulation since the flow of information is back through the drivetrain, from tyre to axle, to gearbox, and so on. It approximates the continuous behaviour of a vehicle as a series of discrete steps. During each step the components are assumed to be in a steady state and calculations are performed at a time scale of 1 second. This assumption allows the use of

power-usage or efficiency maps for the components, which are derived from steady-state tests in the laboratory. This main assumption, however, does not allow investigation of detailed, drivetrain dynamics of short duration. Examples are vibrations, electric field oscillations and similar dynamics with a time scale of less than 1 second. The input to the software is required speed (driving cycle), and it determines drivetrain torques, speeds, and powers required to meet that prescribed vehicle speed. ADVISOR$^®$ is an open source software in a MATLAB/Simulink environment and the user can modify it according to their requirements. The software was copyrighted by DOE/MRI/NREL to protect the integrity of the code because the download included the full source code, GUI, all non-proprietary data files in the ADVISOR$^®$ library, and complete documentation. However, NREL initiated the commercialization of ADVISOR$^®$ in 2003 and currently this software is no longer available in the public domain. Comments on the currently available software packages for powertrain analysis and fuel consumption calculations were included in Section 1.5 in Chapter 1.

5.7   Automated Gearshifts

An important subject in automatic gearshifting is designing a schedule which determines gear selection points according to a pre-defined strategy. Designers and researchers have investigated various kinds of strategies in order to reduce the fuel consumption and improve the fuel economy without sacrificing vehicle performance. Automation of gearshifts for transmission relies on decision-making algorithms depending on the vehicle's operating conditions. Gearshift decisions can be made based on two criteria: either the engine's working state or the driver's intention. The first criterion is based on moving the engine operating point towards points at which higher efficiency, lower fuel consumption or lower emissions are achieved. The engine torque and speed at any operating condition are used to determine the shift decision, with engine load and speed as two inputs similar to a conventional automatic transmission. In the second criterion, in addition to what is useful as far as the engine performance is concerned, driver's demands are also taken into account [5].

5.7.1   Engine State

Decision-making can be performed according to the engine state and load on the vehicle as is typically done in automatic transmissions. Engine life, efficiency, emissions and fuel consumption are key factors under normal operating conditions. The upper and lower speed limits of engine are limiting factors under certain working conditions. Torque capacity and output power are two governing factors at most operating points. Engine maps provide the necessary information regarding the possible movement towards optimum operating conditions and throttle value is an input element that controls the amount of available power and torque. In this case of shifts based on the engine state, only the dynamic working conditions of the engine will determine the shift decisions. To this end, a controller is needed to read the state parameters and issue a decision to maintain a gear, upshift or downshift according to the shifting strategy.

   The engine load can generally be estimated according to the throttle value. The higher throttle value indicates more load on the engine and hence, more torque necessary to overcome the load. The governing laws for gearshifts, based on the engine state, can be built in accordance with an expert operator's judgement, taking into account the requirements of the engine in realistic driving conditions.

5.7.2   Driver's Intentions

The intentions of a driver are interpreted from the driver's actions during driving. Among the various parameters under the driver's control, accelerator pedal displacement and brake pedal force are the two important ones. A rather hard push on the accelerator (a large positive displacement) will mean the driver's intention is to increase acceleration and the release of the accelerator (negative displacement) will

mean the opposite. Brake pedal displacements will always indicate an intention to reduce speed and eventually shift down a gear.

Gearshifts based on driver's intention need an inference system in order that the driver's actions are translated into shift decisions demands. The accelerator pedal input includes three types of information, namely:

- pedal location;
- rate of displacement;
- direction of displacement.

The output of the system is an indication of the driver's desire of how to proceed driving in terms of acceleration. The shifting controller should take all input information and issue the shift command accordingly.

5.7.3 Combined Shifting

Doing gearshifts based only on the engine state is good for fuel economy but will not necessarily satisfy the driver in terms of drivability. Shifting the gears only according to the driver's demands, on the other hand, will often make the fuel consumption worse. A compromise solution, therefore, is to take into consideration both the engine state and the driver's intention. It is, however, a complicated task to combine two contradictory requests simultaneously. The best compromise solution is to produce the power requested by the driver and at the same time try to place the EOP as close to the EFCC as possible.

5.7.4 Controller

Making decisions on gearshifts and the position of the engine operating point (EOP) is performed by a control unit. By considering a range of factors selected by the system designer (e.g. engine speed, engine load, vehicle speed, throttle angle, accelerator pedal angle and brake pedal angle, etc.) and according to the shifting strategy, the control unit determines a suitable shift action which can be to shift up a gear, to shift down a gear or no shift.

With a manual gearbox, the gearshift decision is one of the successful human control operations associated with normal driving. Although sophisticated non-linear controllers seem to work well for the decision-making of gearshifts, nevertheless the human-controlled operation is accepted as satisfactory in most cases. Thus, it is expected that a rule-based controller (e.g. a Fuzzy Logic controller) would work very well for this purpose.

The main objective for the controller could be selecting the engine operating points as close to the EFCC as possible, on various road conditions and for all inputs applied by the driver. This strategy, however, may cause behaviours unexpected by the driver such as unexpectedly increasing or decreasing the engine speed for different pedal inputs. This strategy does not take into consideration the driver's demands and only accounts for fuel economy. As stated above, in order to have a compromise, the control strategy must consider both the driver's demand and the fuel consumption at the same time. A controller based on both the engine state and the driver's intention is able to recognize the driver's intention to increase or decrease the speed and to incorporate it in the gearshift decision-making. This will in turn provide better performance using more engine power in acceleration and engine brake torque in the deceleration phases.

A controller algorithm consisting of two layers as shown in Figure 5.24 could perform the required task. In the first layer (lower layer), the outputs 'engine state' and 'driver's intention' are determined by having state inputs 'torque' and 'speed' on one hand (left), and intention inputs 'brake', 'accelerator pedal position and speed' on the other (right). In the second layer (upper layer), by receiving the two inputs 'engine state' and 'driver's intention', a controller makes the decision to shift by the commands to upshift, downshift or maintain state.
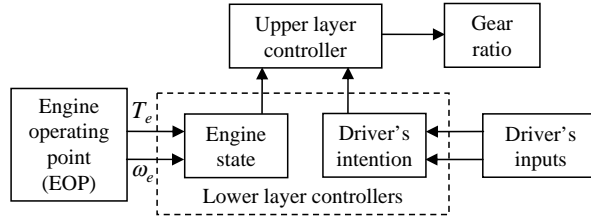
Figure 5.24 Schematic of two-layer controller operation

5.7.5 Multigear Transmission Concept

In Section 5.5.2, the EFCC curve was introduced and it was explained that a continuously variable transmission can be used to direct the engine to follow the curve. The question is whether it is possible to develop a geared transmission which can resemble the CVT performance. Obviously, following the EFCC exactly like a CVT is an impossible task for transmissions with finite gear ratios. Hence, a multigear transmission concept is introduced in order to make the analysis feasible, regardless of the technological barriers. Increasing the number of intermediate gears provides less difference between two adjacent ratios and in turn less amount of EOP jump during the shifts. More intermediate ratios can help the EOPs to smoothly move to a neighbouring point and the system to track the EFCC more accurately, but of course too many gear ratios need frequent shift actions. Moreover, the existence of many shift actions causes large amounts of shift delays and torque losses – both of which degrade the fuel economy. Hence, the increase of intermediate gear numbers should not exceed a certain number.

In order to find out how many gears is enough, a number of investigations were carried out using the Advisor® software and the result was that a transmission with 16 gear steps could be considered a multigear transmission. The intermediate ratios were calculated using the geometrical method (see Section 4.3.3) between the lowest and highest gear ratios. For the multigear transmission with 16 gear ratios, simulation results include the traces of EOPs that are recorded in the engine torque–speed map of Figure 5.25. The EFCC is also plotted in the same figure to make a comparison with the density of EOPs. The investigation of the trace of EOPs shows that the application of a 16-gear transmission has clearly made it possible for the points to lie close to the EFCC [6]. As the gear ratios of this virtual transmission are
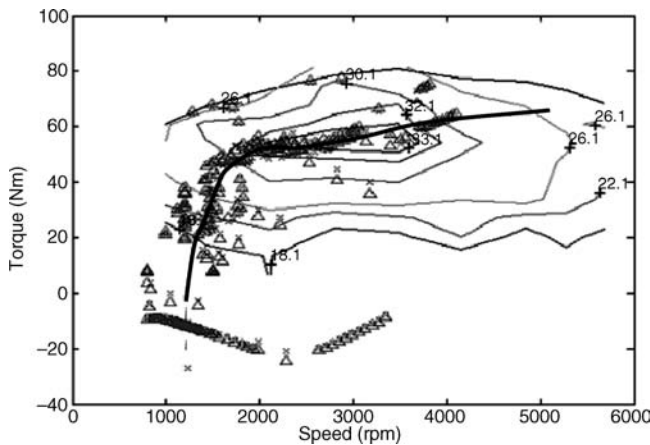
Figure 5.25 EOP placement for a 16-gear manual transmission
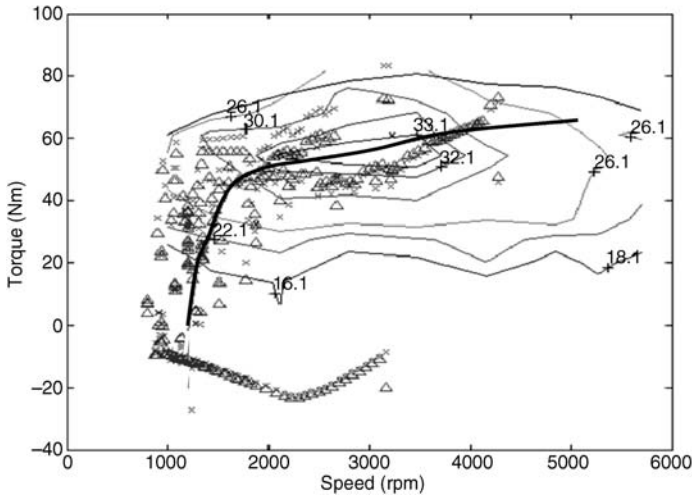
Figure 5.26 EOP placement of a five-speed annual transmission

not as many as a CVT, EOP jumps are inevitable; nevertheless they have been placed in such a way that the EFCC curve can be regarded as the mean value of the points.

For the sake of comparison, the output for a five-speed manual gearbox is also generated. Figure 5.26 shows the EOP placement together with the EFCC curve. It is clear that for the five-speed transmission the EOPs are scattered at some distance away from the EFCC.

5.8 Other Solutions for Fuel Efficiency

Obviously the process of Well-to-Wheel (see Section 1.1) is a fairly inefficient process and more work needs to be done in order to make it more acceptable. Two major approaches to increase the total efficiency of the process are related to the two main phases of Well-to-Tank and Tank-to-Wheel. Improving the Well-to-Tank efficiency is not related to the automotive industry but can be done by optimizing each portion of the upstream processes. Also substituting alternative primary energy sources instead of fossil fuels with higher energy efficiency could be useful.

Improving the Tank-to-Wheel efficiency is a bigger area for improvements since the vehicle powertrain system and especially the engine have very low fuel efficiency (see Chapter 2).

Three approaches are feasible to realize powertrain improvements. In the first approach the improvement of the efficiency of the individual powertrain components is taken into consideration. This approach has always been used by the designers and manufacturers of the powertrain components in the past and still remains one of the main challenges in the future.

The second approach is an energy management point of view that suggests making best use of components during the vehicle motion by taking advantage of the opportunities already existing in the conventional propulsion system. The third approach looks at alternative powertrain concepts that can make best use of energy sources in the vehicle and add the capability to recover the kinetic and potential energy of the vehicle that otherwise will be lost.

5.8.1 Powertrain Component Improvements

Various methods for fuel economy improvement by enhancing the efficiency of individual driveline components have been studied and employed over recent years, and researchers, designers and

Table 5.4 Powertrain component improvement areas

	Area of improvement	Description	Typical range of reduction in fuel consumption
1	Weight reduction	Lightweight materials – optimum packaging	Up to 30%
		Aerodynamic improvement	Up to 10%
2	Engine improvements	Variable valve timing	Up to 15%
		Direct injection and turbo-charging (petrol)	Up to 25%
		High pressure injection (diesel)	Up to 30%
		Other improvements	Up to 10%
3	Transmission	Twin-clutch 6 and higher speeds, CVT	Up to 15%

manufacturers will continue to tackle these issues in the years to come. These improvements can be realized in almost every aspect of vehicle design and the main items can be categorized into the three parts of weight, engine and transmission improvements. A rough estimation of the typical range of fuel consumption reduction is given in Table 5.4.

5.8.2 Lightweight Vehicles

Although making the vehicle weight lighter has been a major design goal over recent years, actually the inclusion of many comfort and safety devices has caused the vehicle weight to increase and, in future, weight reduction will continue to be one of the important issues. The direct link between vehicle weight and fuel consumption is obvious since the vehicle is accelerated and the power P_a used for this purpose simply is given in Equation 3.116:

$$P_a = mav \qquad (5.57)$$

in which m, a and v are the vehicle mass, acceleration and speed respectively. If the kinetic energy absorbed by the vehicle ($E = \frac{1}{2}mv^2$) was reversible, then a large vehicle mass would not be disadvantageous from an energy point of view. In real practice, however, this energy cannot be fully regained even in hybrid vehicles with regenerative possibility (see Chapter 7). Lightweight construction is thus an important influencing factor in reducing energy consumption. From the vehicle performance viewpoint, too, a larger vehicle mass is always disadvantageous since it results in lower attainable accelerations. Moreover, as the rolling resistance force against the vehicle motion is dependent on the mass of the vehicle (see Section 3.3), reducing the mass will in turn reduce the resistive force and improve the fuel economy.

Example 5.8.1

The mass of the vehicle of Example 5.4.1 is reduced by 10%. Consider this vehicle on the trip shown in Figure 5.11. The overall efficiency from fuel to longitudinal motion is unchanged but the rolling resistance force is reduced due to the weight reduction.

Calculate the reduction in the fuel consumption in l/100 km for this mass reduction.

Solution

The solution is similar, only the mass and the rolling resistance force must be modified. The mass is: $m = 1200 \times 0.9 = 1080$ kg. The rolling resistance is: $F_{RR} = 200 \times 0.9 = 180$ N.

The result for the first term is:

$$term\,1 = maS = 1080 \times \tfrac{20}{50} \times 500 = 0.216 \times 10^6 \, J$$

The second term is:

$$term\,2 = \int_0^{50} (180 + 0.4v^2)v\,dt = \int_0^{50} \{180 + 0.4(0.4t)^2\}(0.4t)dt = 0.13 \times 10^6 \, J$$

The total energy is 0.346 MJ. The fuel mass is:

$$m_f = \frac{E_v}{\eta_{fv}E_{cf}} = \frac{0.346}{0.25 \times 44} = 0.0315 \, \text{kg}$$

The fuel consumption is obtained as 5.63 l in 100 km, that is 10% lower than for the original vehicle. It should be noted that the linear dependency observed in this example is due to the low speeds involved and the map-free technique used.

Vehicle weight is also crucial for safety issues as in an accident a lower kinetic energy must be absorbed for a lighter vehicle. Reducing vehicle weight, therefore, is always advantageous in terms of safety, performance and fuel economy.

Lightweight design can be achieved with different methods focusing on appropriate material usage of, for example, steel, aluminium and plastics. Major technology areas are the downsizing of all possible vehicle components. Proper loading of components is another important issue since lower loads on the part will reduce its dimensions. Another area of work is X-by-wire systems in which a remote mechanical actuation is replaced by transferring a signal to the location and actuating with an electric device. Due to uncertainties of electric and electronic devices, in most cases a mechanical back-up is also necessary to ensure safety. One potential way to optimize the weight is to eliminate electric system uncertainty and remove the mechanical back-up from such systems. Optimum reduction of the weight cannot be achieved by only using lightweight and high-strength materials, but also by optimum utilization of installation space and optimum component packaging.

One more area of challenge in vehicle body design is to reduce the aerodynamic drag force (see Section 3.3) that is a resistive force in front of vehicle and consumes power. As the powertrain efficiency is improved through weight reduction, aerodynamic losses represent a greater share of total losses.

5.8.3 Engine

Despite the current trend in the direction of electric drive systems, both the spark-ignition (SI) and compression-ignition (CI) engines are still far from reaching the end of their life. This emphasizes that the efficiency of the internal combustion engine will remain critical in future vehicle applications. Losses in the engine are the single greatest source of inefficiency in vehicles. Many approaches are known to be feasible to improve the fuel economy of an engine; including the optimization of the intake and fuel injection systems, increasing the volumetric efficiency, optimizing the combustion chamber, etc. Through the application of these methods, the structure and performance of the engine will be directly affected and the fuel consumption map (Figure 5.2) will be likewise amended so that more areas of the torque-speed map are assigned to fuel-efficient points.

More improvements are needed in the part–load efficiency of IC engines as this determines the actual fuel consumption in normal driving conditions. Compared to the peak efficiency of CI or SI engines (below 40%), the part-load efficiencies are much lower on average (below 20%). Engine

downsizing is important in reducing the size which will allow better packaging and weight reduction that is in line with the total vehicle weight reduction. A measure of engine sizing is its power-to-volume ratio and with downsizing a specific power output up to 70 kW per litre or even higher is now reasonable.

5.8.3.1 Gasoline Engines

Two major areas of improvement for SI engines are direct fuel injection and downsizing by using supercharging. The development potential of the SI engine is therefore considerable as the expectation of the improved combustion performance from these developments is in the order of 25% with a corresponding benefit in fuel consumption, and the resulting reduction in cylinder displacement is up to 40%. In addition, variable valve trains (VVT) and variable compression ratio (VCR) offer significant potential for fuel economy. Alternative fuels such as natural gas and hydrogen are compatible with SI engine technology and if the problems related to the infrastructure needed for using these fuels are solved, the proper combustion systems for these fuels will be easy to develop.

5.8.3.2 Diesel Engines

Modern CI engines have large power/weight ratios and their exhaust emissions have been reduced considerably over the years. In comparison to SI engines, CI engines have on average some 30% higher efficiencies and this is useful in reducing the overall fuel consumption of vehicles. Higher torque development at low rpm is another advantage of diesel engines. The downsizing of diesel engines and further reduction of friction losses will increase their potential for fuel economy. This can be done, for example, by increasing turbocharging rates, intercooling and variable valve train concepts. Advanced fuel injection systems with a variable injection-hole will reduce the exhaust emissions substantially. To increase the degree of downsizing, in-cylinder peak pressure must increase, which needs advanced supercharging and improved materials. Greater emission reduction over a wide operation in the part-load range in the engine is expected with homogeneous charge compression ignition (HCCI) without full load fuel consumption penalties.

5.8.4 Transmission

The vehicle transmission is influential in vehicle fuel economy in both hardware and software categories. Possible modifications of the transmission systems can also be divided into these two areas. First, a portion of the mechanical power generated by the engine is lost inside the transmission and not used to propel the wheels. From this viewpoint, the vehicle transmission is a power consumer and can be improved in order to become more efficient. These hardware modifications affect the structure and mechanism of the powertrain system and involve the selection of different transmission types and gear ratio designs. These types of conceptual and structural modifications of transmission system are believed to improve the fuel economy by up to 10%.

The second contribution of the transmission in vehicle fuel consumption is the way it forces the engine to operate by controlling the speed of the engine relative to the vehicle speed. In this way, it would be possible to optimize the manner in which the engine is utilized during various driving conditions. Automatic transmissions have for years accomplished this task and shifted the gears automatically in a predefined fashion.

The task of changing gears in the optimum way depends both on the hardware and software of the transmission systems. A limited number of transmission gear ratios restricts the potential for ideal adjustments of the engine operating points. In fact, the operating point of an engine jumps when a gear is changed in stepped ratio transmissions whether in manual transmission (MT) or automatic transmission

(AT) modes. To be able to follow the efficient or ideal operating curve (EFCC) of an engine (see Section 5.5.2), a CVT-type transmission (see Section 4.6) is required. CVTs allow the continuous running of the engine at its optimal operating points without any interruption in power transfer. Therefore, even with ideal software programming, the optimum engine operation is not possible by using the traditional manual and automatic transmissions with a limited number of gear ratios.

On the other hand, the fuel economy is directly dependent on the efficiency of the transmission itself. Manual transmissions are simplest and are the most efficient transmissions available. Automated manual transmissions (AMT), therefore, offer the possibility for improvements in fuel economy of up to 5% owing to their high efficiency and controlling the engine operating points. These systems still have two major drawbacks of torque interruption and not being able to ideally control the engine working points. Conventional automatic transmissions have considerably lower efficiencies compared to manuals and thus their fuel economy is lower. The adoption of torque converter locks and six or more ratios, however, will mitigate the low efficiency issue.

Further possibilities are also opened up by new transmission technologies and by increasing the number of gears (six or eight speeds) as well as eliminating the torque transfer interruption. Double-clutch transmission (DCT) with seamless shifting points has significant potential for development. This technology is based on manual transmission hardware but uses two parallel transmissions for odd and even gears (see Section 4.7). This system offers the comfort of a conventional automatic transmission with the efficiency of a manual transmission and thus results in more fuel savings.

From an integrated powertrain perspective, it is important to note that the overall performance of a powertrain is dependent on matching the engine with the transmission. In practice, the engine designer should consider the shortcomings of conventional stepped ratio transmissions (automatic or manual) and include a broad speed range to allow matching to road speed. Conversely, a transmission designer should consider the operating range of the engine in determining the number of ratios in the transmission. An ideal integrated powertrain design will lead to the more efficient operation of whole system.

5.9 Conclusion

The fundamentals of vehicle fuel consumption evaluation were discussed in this chapter. The engine working points were shown to have different energy performances and efficiencies that are usually expressed by engine BSFC maps. There are points with higher efficiency on the engine map and operating close to these points will result in efficient driving with less fuel consumption.

Two mechanisms by which the engine operating points (EOPs) can be placed in the desired locations on the torque–speed map are the transmission gear ratios and the engine throttle opening. In each driving situation, power is demanded and for each power demand there is an efficient fuel consumption point on the map. Connecting all these points produces a curve called the efficient fuel consumption curve (EFCC). In order to obtain minimum fuel consumption, the controller should try to adjust the throttle and gear ratio in order to select the EOP close to the EFCC. A CVT was shown to be the only transmission type that can locate the EOPs over the EFCC curve. For other types of transmission with limited number of gear ratios, the EOPs cannot follow the EFCC and will be scattered around it.

It was shown that the calculation of fuel consumption for a typical driving cycle involves a large volume of information related to the engine and the vehicle that is not manageable in calculations by hand. For this reason, several software packages have been developed that provide the necessary aids for the determination of vehicle fuel consumption and exhaust pollution. It should be emphasized that even with the help of software, a large number of data inputs regarding the engine and vehicle components performances including engine maps and component efficiencies are necessary. This information must be obtained through design procedures or laboratory tests.

Further potential for the improvement of vehicle fuel economy were discussed including lightweight vehicles, engine and transmission developments. Off all the solutions, engine improvements and weight decrease have considerable further potential for reducing the fuel consumption.

5.10 Review Questions

5.1 Describe why the BSFC is a varying quantity during engine operation.

5.2 Where is the minimum BSFC point of an engine map?

5.3 What is the engine fuel efficiency? Can it in general be related to the BSFC?

5.4 Why are the driving cycles necessary?

5.5 What factors are the driving cycles dependent on?

5.6 Describe the difference between the map-free and map-based fuel consumption determination.

5.7 What is the basic assumption in map-based fuel consumption evaluation?

5.8 Why should the rotating masses of the vehicle be considered in fuel consumption estimation?

5.9 Describe the objectives of gearshifting.

5.10 Explain how an EFCC curve is constructed from an engine BSFC map.

5.11 Explain whether it is possible to fix the EOP of engine on the minimum BSFC point during vehicle motion.

5.12 Explain how an EFCC curve can be followed in a real vehicle.

5.13 Is it possible to obtain a good fuel economy by trying to keep the EOP as close to the minimum BSFC point as possible?

5.14 Describe forward-facing and backward-facing vehicle simulation methodologies. Which one provides more realistic outputs?

5.15 Explain the engine state and the driver's intentions in gearshifting decision-making. How can both taken into consideration in automatic gearshifts?

5.16 Describe the concept of a multigear transmission and its effect on gearshift strategy. Is it feasible to increase the number of gear ratios without limit?

5.17 What are the benefits of mass reduction in the vehicle?

5.18 The fuel consumption figures produced by an on-board trip computer are in practice different from the actual vehicle fuel consumption the driver measures. Assuming the estimation method of computer has few errors, explain the reasons for the existing differences.

5.11 Problems

Problem 5.1

Use the information given in Section 5.3.1 and show that the average speeds over the NEDC and FTP-75 cycles are almost equal.

Problem 5.2

For the NEDC cycle determine:

(a) Plot the variation of acceleration with time.
(b) Plot the time history of distance travelled.
(c) Specify the maximum and average of vehicle acceleration.
(d) Repeat (c) only for the positive values.

Results: (c) $a_{max} = 1.04$ and $a_{av} = 0$ m/s^2; (d) $a_{max} = 1.04$ and $a_{av} = 0.124$ m/s^2.

Problem 5.3

Repeat Example 5.4.1 for the first part of trip as a sine function of the form:

$$v = 10 + 10 \sin\left(\frac{\pi}{50}t - \frac{\pi}{2}\right)$$

Problem 5.4

Repeat Example 5.4.1 for the driving cycle given in Figure P5.4. For the constant speed portion use the information in Example 5.4.2.
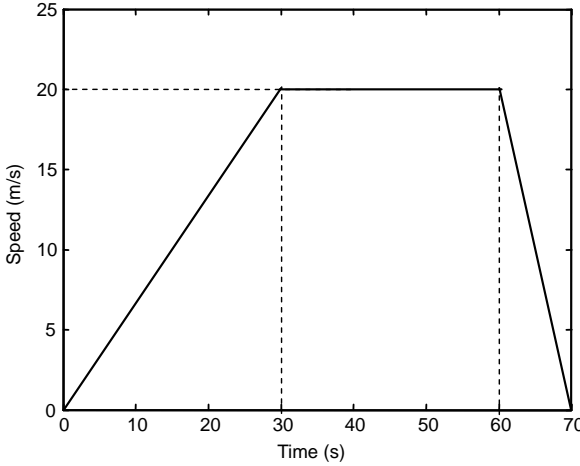
Figure P5.4   Driving cycle of Problem 5.4

Problem 5.5

Determine the map-free fuel consumption in l/100 km for a vehicle of 1500 kg mass if the driving cycle in Figure P5.5 is repeatedly used. Due to the low speeds, the driving resistance can be assumed to be a constant value of 250 N. The overall driveline efficiency from fuel caloric energy contents to traction power at the drive shafts can be assumed as a constant value of 20%. The fuel has the caloric energy content of 40 MJ/kg and density of 800 kg/m^3.

Result: 5.2 l/100 km.
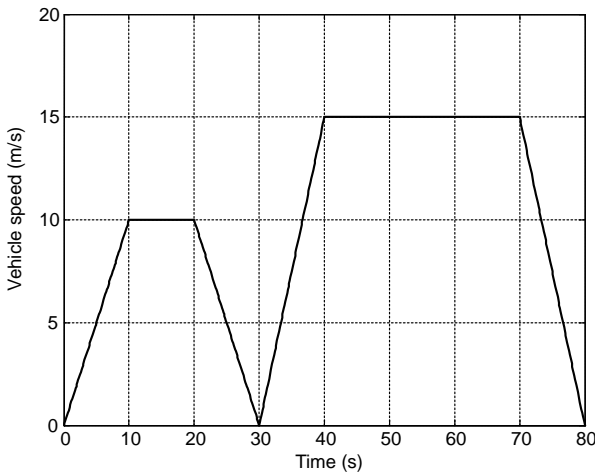
Figure P5.5   Driving cycle of Problem 5.5

Problem 5.6

Repeat Problem 5.5 for the driving resistance in the form of

$$F_R = 0.02W + 0.5v^2.$$

Problem 5.7

Estimate the map-free fuel consumption in l/100 km for a vehicle with 1300 kg weight from the urban part of NEDC driving cycle. Driving resistance is $F_R = 0.015W + 0.4v^2$ and the overall efficiency can be assumed to be the constant value of 30%, from fuel caloric energy contents to traction power on the drive shafts. The fuel has the caloric energy content of 40 MJ/kg and density of 800 kg/m³.

Problem 5.8

In order to examine the effect of carrying cargo on the fuel consumption, consider the vehicle in Problem 5.5 is carrying a weight of 50 kg. How much in percentage will increase its fuel consumption? Repeat this for weights of 100 and 150 kg.

Problem 5.9

Repeat Example 5.5.2 for travelling speeds of 70 and 100 km/h.

Problem 5.10

The efficient fuel consumption curve of an engine is approximated by the equation below:

$$T_{opt}(\omega) = T_e^*(1 - e^{\frac{-\omega_e}{1865}}), \omega_e < \text{rpm}$$

A vehicle with information given in Table P5.10 is equipped with a CVT. The vehicle is to follow the simple driving cycle given in Figure P5.10, while engine is tracking the efficient fuel consumption curve.

(a) Ignore the low speed effects and assume that engine speed starts from 1000 rpm when the vehicle starts to move from the rest and at this moment determine the initial transmission gear ratio.
(b) Determine the overall driveline ratios at the engine speeds of 1000 to 5000 rpm at increments of 50 rpm and plot the result (n versus ω).
(c) Use the kinematic relation at a specified speed and calculate the transmission gear ratios at speeds of 5 to 20 m/s and plot n versus speed.

Result: (a) n_g=3.74

Table P5.10 Information for Problem 5.10

1	Vehicle mass	1000	kg
2	Tyre rolling radius	30	cm
3	Final drive ratio	5	
4	Driveline efficiency	0.85	
5	Rolling resistance coefficient	0.02	
6	T_e^*	100	Nm
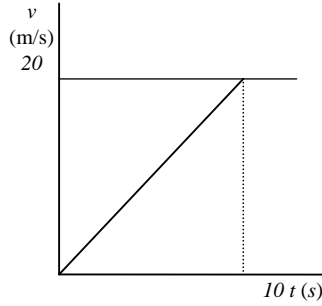
Figure P5.10   Driving cycle of Problem 5.10

Problem 5.11

In a micro-hybrid system the intention is to eliminate engine flywheel inertia in order to improve the fuel economy. To see the effectiveness of such concept, consider a simple driving cycle shown in Figure P5.5 and use the information in Tables P 5.11.1 and 5.11.2 to find (assume no energy is lost during a gearshift):

(a) total energy spent to accelerate the flywheel in one cycle;
(b) average power loss (due to deceleration of flywheel);
(c) fuel consumed due to flywheel dynamics in one cycle;
(d) fuel consumption in l/100 km;
(e) percentage of fuel economy in a vehicle with an 8 l/100 km fuel consumption.

Results: (a) 49,414 J; (b) 618 W.

Table P5.11.1   Transmission information

Gear ratios		Max speed (km/h)
1st gear ratio	3.250	30
2nd gear ratio	1.772	50
3rd gear ratio	1.194	70
Final drive ratio	4.0	

Table P5.11.2   Additional information for Problem 5.11

Flywheel's moment of inertia	1	kgm^2
Engine idle speed	800	rpm
Tyre rolling radius	30	cm
Fuel energy content	40	MJ/kg
Fuel density	0.8	kg/l

Problem 5.12

In order to examine the effect of driving aggressiveness on the vehicle fuel consumption, consider the vehicle and trip of Example 5.4.1 and increase the acceleration by having the maximum speed at 40 seconds (see Figure P5.12). Repeat this for accelerating times of 30, 20, 10 and 5 seconds and plot the variation of fuel consumption with acceleration.
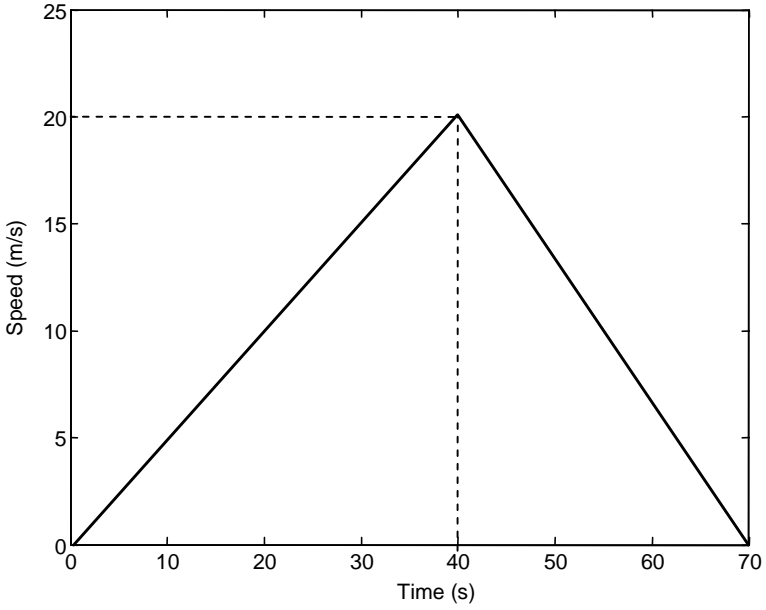
Figure P5.12   Driving cycle of Problem 5.12

Problem 5.13

To study the effect of aggressive driving at higher speeds, Figure P5.13 is suggested. Use the information of Problem 5.4 and compare the increase in fuel consumption for maximum speeds of 15, 20, 25 and 30 m/s.
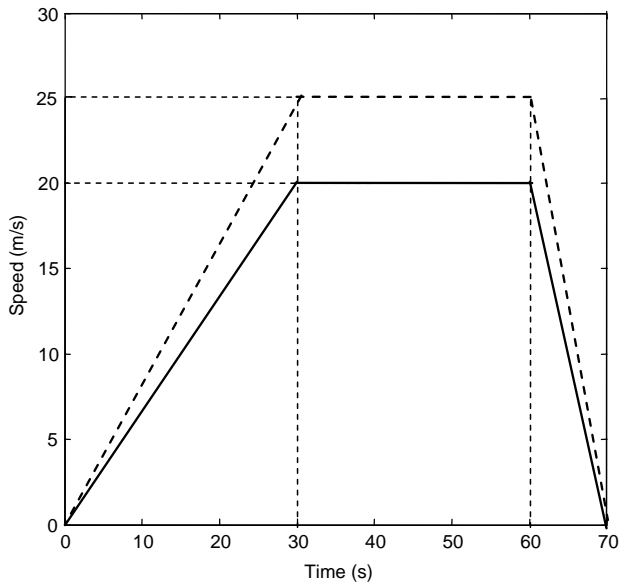
Figure P5.13   Driving cycle of Problem 5.13

Further Reading

Fuel economy has always been of interest to vehicle designers – although in some markets it has until recently been of secondary importance – the focus on large 'gas-guzzling' engines developed in the USA for many years is an example of this. Analysis of fuel consumption features in Lucas's book [7] and he discusses vehicle design features which can be used to minimize fuel usage.

Over the past couple of decades, however, the most significant feature of vehicle design has been the need to control emissions and optimize energy usage; fortunately, these two objectives have been reasonably compatible. Emissions targets have been relentlessly driven downwards by government legislation around the world; energy usage has been driven downwards by a combination of global pressures on energy supplies coupled with consumer pressures for economic transportation. Standardized driving cycles have become a universally accepted – if controversial – method of comparing the fuel economy performance of vehicles This worldwide interest has resulted in literally thousands of journal papers and conference articles addressing the issues, but to date, very few text books. The book by Guzzella and Sciaretta [8] stands out as an excellent reference on the analysis of fuel consumption and the use of driving cycles in comparing powertrain systems.

The term 'fuel economy' has traditionally been associated with the usage of petrol and diesel by conventional spark-ignition (SI) or compression-ignition (CI) engines. We will return to this subject in Chapter 7 under the more general heading of 'energy consumption'. It is central to the motivation for investigating hybrid powertrain systems that they might offer improved energy efficiency compared with conventional powertrains; hence, it is essential that we have robust and reliable techniques for analysing IC engine powertrains as a benchmark for comparisons.

There are two useful books which make a considered attempt to look forward to future developments. The textbook by Fuhs [9] is excellent reference on hybrid vehicle technology; it is up-to-date and Chapter 3 contains a comprehensive summary of all the hybrid vehicles available in 2009 – most of these are prototype developments and over 100 vehicles are described! Another particularly interesting section is Chapter 12 entitled 'Mileage Rating' which gives a thorough summary of testing techniques and procedures.

The book by Mitchell et al. [10] takes a much broader view of the future of personal transportation. These industry experts 're-imagine' what personal transportation of the future could look like – with 'vehicles' that are green, smart, connected and fun to drive. Electric drive systems, wireless communication, links to infrastructure information, smart infrastructure recharging, etc. are all discussed as contributing to personal mobility in our cities. This is a fascinating and sometimes controversial text, but it certainly encourages some challenging forward thinking.

References

[1] Niemeier, D.A. et al. (1999) *Data Collection for Driving Cycle Development: Evaluation of Data Collection Protocols*. California Department of Transportation.

[2] Lina, J. and Niemeier, D.A. (2002) An Exploratory Analysis Comparing a Stochastic Driving Cycle to California's Regulatory Cycle, *Atmospheric Environment*, 36: 5759–5770.

[3] Andre, M. et al. (2006) Real-World European Driving Cycles, for Measuring Pollutant Emissions from High- and Low-Powered Cars, *Atmospheric Environment*, 40: 5944–5953.

[4] Hung, W.T. et al. (2007) Development of a Practical Driving Cycle Construction Methodology: A Case Study in Hong Kong, *Transportation Research Part D*, 12: 115–128.

[5] Mashadi, B., Kazemkhani, A. and Baghaei, L.R. (2007) An Automatic Gearshifting Strategy for Manual Transmissions, *Proceedings of IMechE, Part I, Journal of Systems and Control Engineering*, 221(15): 757–768.

[6] Mashadi, B. and Baghaei, L.R. (2007) *A Fuel Economy-Based Gearshifting Strategy*. EAEC.

[7] Lucas, G.G. (1986) *Road Vehicle Performance*. Gordon and Breach, ISBN 0-677-21400-6.

[8] Guzzella, L. and Sciarretta, A. (2005) *Vehicle Propulsion Systems: Introduction to Modelling and Optimization*. Springer, ISBN 978-3-549-25195.

[9] Fuhs, A.E. (2009) *Hybrid Vehicles and the Future of Personal Transportation*. CRC Press, ISBN 978-1-4200-7534-2.

[10] Mitchell, W.J., Borroni-Bird, C.E. and Burns, L.D. (2010) *Reinventing the Automobile: Personal Mobility for the 21st Century*. MIT Press, ISBN 978-0-262-01382-6.

6

Driveline Dynamics

6.1 Introduction

The vehicle driveline is a dynamic system consisting of inertia and elastic components and when it is subjected to excitations, mechanical resonances occur. These span a large range of frequencies and are generally referred to as noise, vibration and harshness (NVH). Vehicle drivelines with manual transmissions are lightly damped and tend to be more prone to vibration. Driveline torsional frequencies are in general excited by changes in torque which arise from engine or driver inputs.

There are many sources of driveline excitation and in general the disturbing inputs can be categorized into two types: sudden/discrete and persistent. The first category includes throttle inputs, tip-in/tip-out and sudden changes in the engine torque. The second type may arise from engine torsional/torque fluctuations or from worn or misaligned components in the driveline such as Hooke's joints. The driveline vibrations are sometimes categorized as engine speed, vehicle speed or acceleration related. Free play between the components or gear lash will often exacerbate driveline torsional oscillations.

The lowest frequency driveline oscillation (longitudinal vehicle oscillation) is called vehicle shunt. This phenomenon arises from high rate of pedal application to change the driveline torque instantly. The existence of a large gear backlash in the driveline will amplify this type of oscillation starting with an initial jerk. The driver can, therefore, distinguish the longitudinal oscillations and this reduces the driver's subjective perception of the vehicle's performance. Vehicle shunt is commonly followed by torsional vibrations of the entire powertrain, referred to as shuffle. These oscillations that usually are below 10 Hz correspond to the fundamental driveline resonance frequencies and are mainly caused by the compliances of drivetrain.

Throttle tip-in is defined as a fast depression of throttle and tip-out as a sudden release of throttle; these are two common excitations of vehicle driveline oscillations. They often occur on hill climbing or in downhill motion and are typically more problematic for vehicles with manual transmissions since, unlike automatic transmissions, they do not have viscous damping within the driveline. The vibration induced by the impacts of gear pairs is another mechanism of high frequency driveline vibration. In certain conditions, it is called gear rattle and is an impulsive phenomenon in which the unloaded gears knock each other and the result is an undesirable rattle noise.

The aim of this chapter is to analyse the driveline dynamics and understand the design issues relating to driveline NVH.

6.2 Modelling Driveline Dynamics

The transient response of vehicle driveline has a significant influence on the driver's subjective impression of the vehicle performance. It is very difficult to define objective parameters, which describe the driveline

dynamics and which therefore strongly influence the driveability of vehicles. Hence, although the analysis of vehicle driveline dynamics is fairly straightforward in that it is similar to many other examples of engineering multibody systems, the interpretation of the results poses difficulties. In order to better understand the dynamic behaviour of the powertrain and reduce unwanted oscillations, analysis and modelling are required. The aim is that computer simulations should produce practical design information for the designers for the refinement and tuning of the driveline parameters.

6.2.1 Modelling Methods

Various methods and techniques are available for modelling physical systems. For mechanical systems, the direct application of Newton's laws of motion is the most common approach and leads to the governing equations of motion. The ability to draw accurate free body diagrams (FBD) is a crucial part of this traditional approach. On the other hand, Kane's approach to dynamics analysis [1] is based on system energies; it is advantageous in that it does not involve unnecessary unknown internal forces and moments, and the governing equations of motion are generated in the form of a set of first order differential equations ready for numerical solution.

Other modelling tools like the block diagram (BD) method or signal flow graphs (SFG) are graphical methods used in modelling dynamic systems. In fact, all such methods are derivations from the law of conservation of energy and can be applied to any physical systems. The graphical methods, BD and SFG, are based on the flow of signals in a dynamic system. An alternative approach is called the bond graph method, in which the flow of energy is taken into consideration.

In this approach, a physical system is represented by simple symbols that indicate the power flow paths or *bonds*. There are basic elements in bond graphs, like other modelling methods, that are connected to one another and a network structure results. Application of the basic laws to the bond graph construction generates the governing equations of the system. Like Kane dynamics, the bond graph approach also generates the equations of motion in the form of first order differential equations that can be readily solved. One main advantage of bond graph modelling is its ability to model multiple energy systems such as electromechanical systems.

In this chapter, the modelling of a driveline system is carried out by the application of the bond graph technique. For those not familiar with the subject, a brief introduction is provided for the bond graph technique in Appendix A for quick reference. This will suffice for the simple models that are developed here. Interested readers should refer to specialist books or materials for more information [2–4].

Example 6.2.1

For a torsional vibrating system consisting of a rotating inertia J, a torsional spring K_T and a torsional damper B_T shown in Figure 6.1, derive the equations of motion:

(a) Apply Newton's law.
(b) Use the bond graph method.
(c) Compare the results.
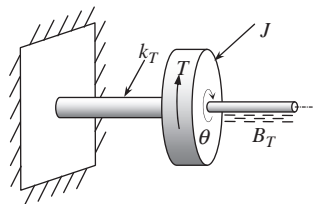
Figure 6.1   A torsional vibrating system

Solution

This system is a torsional equivalent of the well-known mass-spring damper system.

(a) For the displacement θ of the inertia J, the governing equation of motion according to the FBD of Figure 6.2 is obtained by combining the individual equations:
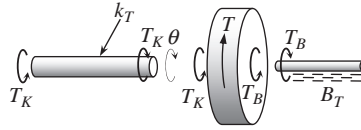
Figure 6.2 The free body diagram of a torsional vibrating system

$$J\ddot{\theta} = T(t) - T_K - T_B, T_K = K_T\theta, T_B = B_T\dot{\theta}$$

The result is:

$$J\ddot{\theta} + B_T\dot{\theta} + K_T\theta = T(t)$$

(b) The details of applying the bond graph technique to this system are available in Appendix A (Example A.4.3). The result is a set of equations given below:

$$\frac{dp_1}{dt} = S_e - k_2q_2 - R_3\frac{p_1}{I_1}$$

$$\frac{dq_2}{dt} = \frac{p_1}{I_1}$$

in which:

$$S_e = T, \ I_1 = J, \ k_2 = k_T, \ R_3 = B_T, \ p_1 = J\dot{\theta} \text{ and } q_2 = \theta$$

(c) The equations derived from bond graph are already in state-space form and suitable for solution using several techniques. The equation resulting from the direct application of Newton's law is a second order differential equation. This can be transformed to two first order equations by using the definitions: $x_1 = J\theta$ and $x_2 = J\dot{\theta}$. The result is:

$$\frac{dx_1}{dt} = x_2$$

$$\frac{dx_2}{dt} = T - \frac{k_T}{J}x_1 - \frac{B_T}{J}x_2$$

Substituting $p_1 = x_2$ and $q_2 = x_1/J$, the two sets become identical.

6.2.2 Linear Versus Non-linear Models

In reality, all physical systems are non-linear systems to different degrees and obtaining their accurate responses to input excitations over a wide range requires the development of non-linear models. The vehicle driveline is a complex dynamical system comprising many non-linear sub-systems and elements. As a result, the governing equations of motion of the vehicle driveline, in general, are highly non-linear and comprise a set of non-linear differential equations. Closed form solutions are in general not available for such equations and only numerical integration techniques are workable. Results obtainable from non-linear models are mainly restricted to time history solutions from which it is often difficult to provide useful design information. Non-linearities in the driveline dynamics include:

- non-linearities of component behaviour, for example, stiffness (spring), non-linearity of shafts and dry friction between two rotating elements;
- free plays and backlash;
- non-linearities of engine torque variation with throttle inputs and speed.

Linear analysis offers the analyst a wide range of outputs which potentially provide a design insight into vehicle dynamics problems. Much of the knowledge relating to the understanding of dynamic behaviour of systems is based on linear properties that allow powerful linear analysis tools such as eigenvalue extraction, frequency response analysis, etc. to be applied to the system model. When large deformations, speeds or accelerations are involved, it becomes more likely that non-linearities are significant and the application of linear tools is no longer valid. Nevertheless, situations exist in which the behaviour of the non-linear elements can be regarded as linear. For instance, if the relative displacements of the subsystems remain small, the mechanical characteristics can be rather well described by linear functions. Therefore, in such conditions it is possible to define linear models for which linear equations of motion can be derived. The general advantages of treating the system as a linear system are listed below:

- Linear models are easy to work with (i.e., equations of motion can easily be derived and solved).
- Closed form solutions for the equations of motion are possible.
- Linear analytical tools such as frequency response, eigenvalue solution, steady-state/transient analyses, and linear control theory can be employed for the interpretation of system behaviour.

The general assumptions involved in the linear description of driveline system models may be itemized as follows:

- The behaviour of system components is linear.
- The inputs or excitations are small.
- All resulting output displacements, speeds and accelerations are small.

In many practical working conditions these assumptions are true and thus the linear models are reliable. The modelling techniques for both linear and non-linear systems are similar but working with non-linear models is difficult. Linear models, in contrast, are easy to deal with and the designer is able to apply a wide range of linear analysis tools to extract design information from them. In this chapter the modelling and discussions will be limited only to linear models as dealing with non-linear behaviour of components is beyond the scope of this book.

6.2.3 Software Use

There are now several multi-body systems dynamics packages available with which the equations of motion of vehicle driveline models for any complexity of problem can be generated and solved. These

codes usually perform static solutions, kinematic and dynamic analyses, and the outputs are time histories and/or animations.

For vehicle driveline modelling, software packages include: Adams/Driveline [5], AMESim [6], Dymola [7], GT-Suite [8], Modelica [9], SimDrive [10] and VALDYN [11]. These packages offer standard libraries for typical elements in the vehicle driveline and the user can employ their graphical interfaces to develop the driveline model by putting together the elements of a driveline system.

Although the usefulness and the power of these packages have been well proven, nevertheless the appropriateness of using them in students' learning phase is debatable. Two main disadvantages are, first, they need a considerable level of expertise, as the development of the model and extraction of results can often be time-consuming, and second, the user is unaware of the relations between the system components as no parametric relations are presented. The main advantage of purpose-built driveline simulations, on the other hand, is that they are easier to use and allow quick studies to be undertaken. Students on the driveline-related courses can learn more through building their own models and obtaining their solutions. The more sophisticated packages can be used for commercial design purposes and final tuning of driveline parameters.

6.3   Bond Graph Models of Driveline Components

A *word bond graph* is a simple representation of a system by using the bond graph *arrows* to demonstrate the relations of the system components. For the vehicle driveline system, such a representation is illustrated in Figure 6.3 for a typical FWD vehicle. This word bond graph shows at a glance the transfer of the energy through the components of a driveline system. If the bond graph of each subsystem or component of the driveline is replaced in the word bond graph, the actual bond graph of the system obtained. Thus, this simple representation of the system can be used as the starting point for preparation of the complete bond graph of the driveline.

6.3.1   The Engine

The engine excitations resulting from the torque pulses caused during the power strokes are sources of driveline oscillations. The engine is a complicated system with a large number of mechanisms and elements so that constructing a full bond graph for the engine, therefore, is a complicated task.

A simplified model of an engine, however, can be considered by assuming it to be a source of mechanical power with quasi-steady characteristics. In this form, the internal dynamics of the engine are
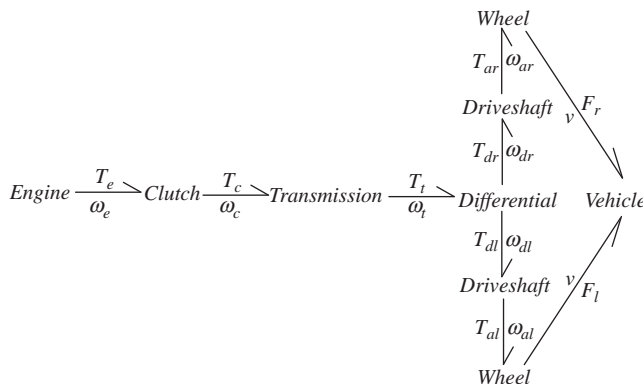
Figure 6.3   A word bond graph for vehicle driveline
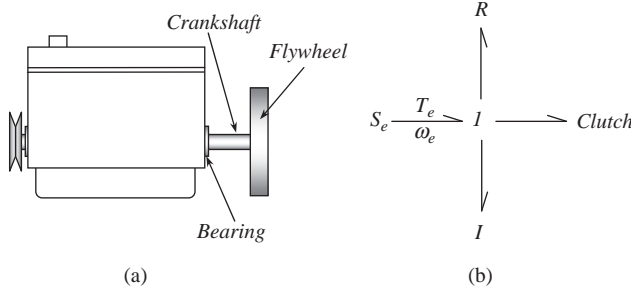
Figure 6.4 Schematic model (a) and simple bond graph of engine (b)

not taken into consideration and only its steady torque-speed characteristic is given as input to the driveline system. This simplified engine model consists of a crankshaft mounted on a bearing and connected to a flywheel (see Figure 6.4a). The total inertia connected to the engine includes the flywheel, crankshaft and the clutch assembly that rotate with the engine speed. Bearing friction can also be included in the model. The bond graph of such a simple engine is depicted in Figure 6.4b, inertia by the I element and the bearing friction by the R element.

It was assumed that the crankshaft was a rigid element; if an elasticity is to be included for the crankshaft between the bearing and the flywheel (i.e. the shaft can twist between these two points), the bond graph model can be modified to that shown in Figure 6.5 with the C element as the elasticity of the crankshaft.

6.3.2   The Clutch

The clutch plays an important role in transmission torsional vibrations. It typically consists of dry friction damping and torsional spring effects. The clutch works in two phases: fully engaged and transient phases (see Chapter 4). In the fully engaged phase, the dry friction does not have any influence except in extreme cases with large torques above the capacity of clutch so that slip occurs. In the engaged case the circumferential (torsional) clutch spring stiffness (see Figure 6.6) is influential in driveline vibrations.
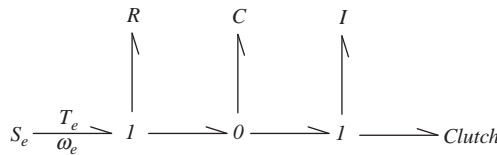
Figure 6.5 Engine bond graph with elasticity
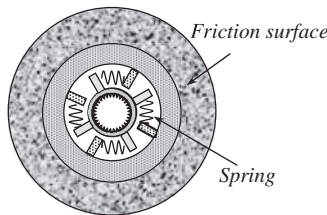
Figure 6.6 Schematic of a clutch plate and its springs
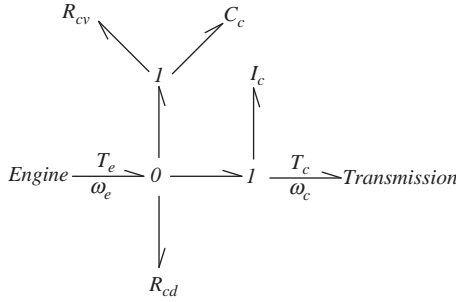
Figure 6.7 Bond graph of the clutch

The transient release phase, in which the power flow from the engine to the transmission takes place gradually, involves both dry friction and spring stiffness effects.

In the bond graph of Figure 6.7, the C element is to account for the circumferential springs and the upper R element (R_{cv}) represents a viscous damping for the springs. The lower R element (R_{cd}) represents the damping of friction surface which should be removed for the fully engaged phase. Finally, the I element is to model an equivalent rotating inertia in the clutch output (including spline and attachments). In fact, the springs in reality have stiffness, inertia and damping all combined. For modelling purposes, these three properties are treated separately as ideal elements.

6.3.3   The Transmission

The transmission contains several elements including shafts, gears and bearings. Constructing a bond graph for a gearbox, therefore, requires a detailed analysis of the system components. It is, however, possible to consider the gearbox as a simple system with rigid elements having only inertia and friction. In this way, the inertia can be assumed to act only at the input or only at the output of the gearbox. Figure 6.8 clarifies this concept. In Figure 6.8a a simple gearbox including an input shaft, a layshaft and an output shaft is considered. The inertias of the three shafts (including the gears) are I_1, I_2 and I_3 respectively, and n_1 and n_2 are the gear ratios between the two mating gears. With the assumption of rigid shafts and gears, the two cases of Figure 6.8b and c are possible. The lumped inertias I_B and I_C are:

$$I_B = \frac{1}{n^2}\left(n^2 I_1 + n_2^2 I_2 + I_3\right) \tag{6.1}$$

$$I_C = n^2 I_B \tag{6.2}$$

In only one gear ratio, a transmission acts like a transformer. Since other gear ratios are also selectable, a *Modulated* transformer (MTF) is used to indicate the changing character of the gear ratio. The bond graphs

| (a) | (b) | (c) |
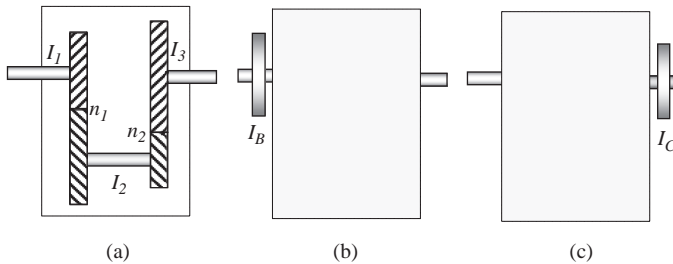
Figure 6.8 Lumped inertia models for a gearbox
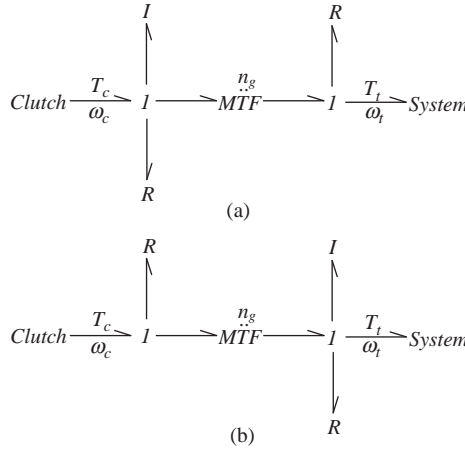
Figure 6.9   Bond graphs of gearbox with lumped inertia at (a) input shaft and (b) output shaft

for the simplified models of a gearbox are shown in Figure 6.9. The R elements are the bearings at the input and output shafts of the transmission and n_g is the transmission gear ratio.

6.3.4   Propeller and Drive Shafts

A propeller shaft (rear-wheel drive (RWD) layout only) or a driveshaft can be considered as an elastic element with lumped inertia and friction elements. The inertia and the friction elements can be included at one or two ends. In Figure 6.10, the inertia and the friction elements are considered to be present at both input and output ends. In order to include an internal damping in the elastic element, a common flow joint is used.

6.3.5   The Differential

A differential is a device to allow the two wheels on an axle to assume different speeds while the vehicle is turning. An open differential has the components shown in Figure 6.11. It has an input shaft with torque T_p and speed ω_p, and two output shafts with torques and speeds of T_L, T_R, ω_L and ω_R.

   A differential including six gears, shafts and bearings, is a complicated system for modelling. A complete bond graph of the differential can be constructed by considering the details of the system.
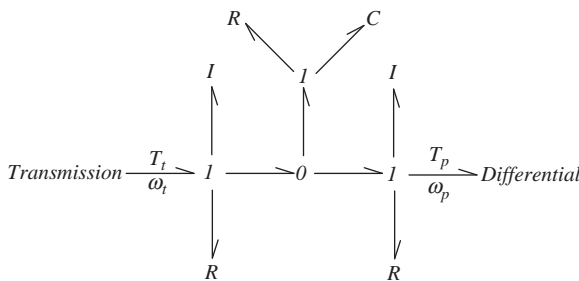
Figure 6.10   Bond graph of a propeller or drive shaft
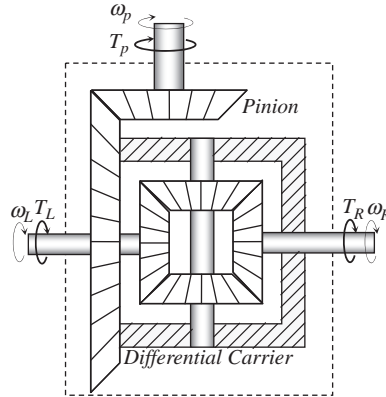
Figure 6.11   Main components of the vehicle differential

The resulting bond graph, however, will not be useful for driveline modelling. In order to use a simple differential model, the relations between input and outputs must be taken into consideration. In an open differential, the torques at output shafts are equal to half the input torque, while the speeds are different but related. Assuming no power loss in the differential, the output power must be equal to the input power:

$$P_L + P_R = P_i \tag{6.3}$$

In terms of the torques and speeds:

$$T_L \omega_L + T_R \omega_R = T_p \omega_p \tag{6.4}$$

Taking into account the torque relation $T_L = T_R = \frac{1}{2} T_p$ we obtain:

$$\omega_L + \omega_R = 2\omega_p \tag{6.5}$$

In fact, a differential provides half the input torque at each shaft but does not double the speeds, which makes it different from a transformer. This phenomenon is not one that can be modelled by any of the basic components available for bond graphs. Thus a new element must be defined for a differential which has the property of halving the effort but the flows must comply with Equation 6.5. Since this property resembles that of the transformer, the element will be called a Differential Transformer or DTF for short. The bond graph for a DTF is depicted in Figure 6.12.

The overall bond graph of a differential including the inertia properties and viscous friction in the bearings is depicted in Figure 6.13 by using a DTF element. Note that the TF element used at the input is
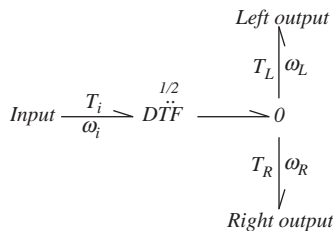
Figure 6.12   Bond graph of DTF element
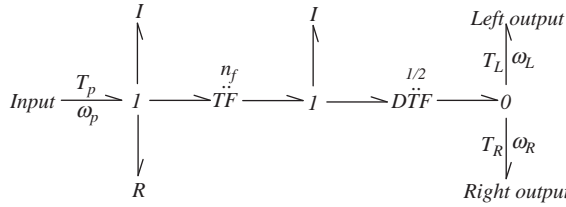
Figure 6.13   Bond graph of a differential

for the final drive ratio between the pinion and crownwheel gears. The first I element belongs to the input shaft whereas the second one is for the crownwheel and carrier. Inertias and frictions for output shafts can also be included in the bond graph.

6.3.6   The Wheel

The wheel component includes the rim, rigid rotating parts and the tyre. A full dynamic model of the wheel accounts for the tyre deformations, wheel slip and road interactions. These are complicated phenomena due to the complex structure of the tyre and force generation mechanism. A simple model that includes the rigid body wheel properties and tyre deformation is schematically shown in Figure 6.14. F_x, W and T_W are the tractive force, wheel load and wheel torque respectively. The wheel has effective radius r_W, mass m_W and inertia I_W. It is assumed that the deformation of the tyre takes place at the contact surface and since the tyre material has a visco-elastic property, a combined elasticity and damping are considered to account for its deformation and internal damping.

   The bond graph of the wheel with properties explained above is produced and depicted in Figure 6.15. Note that the input energy first causes the rigid parts to turn, then transforms to a force at the road level
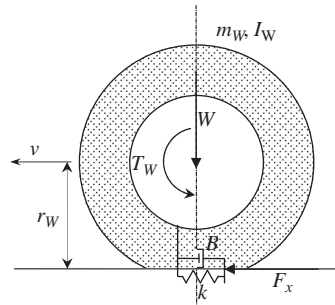
Figure 6.14   Model of wheel and tyre deformation
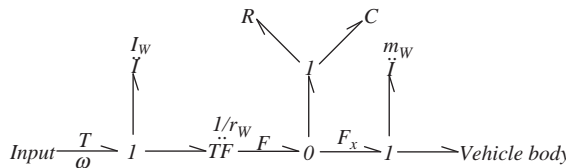
Figure 6.15   Bond graph of wheel and tyre
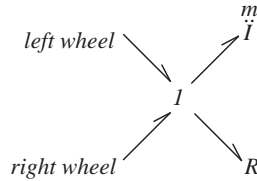
Figure 6.16   Bond graph of vehicle body

where it deforms the tyre. Then, the remaining energy results in the tractive force which moves the wheel mass and the remaining effort is passed to the vehicle body.

6.3.7   Vehicle

For a conventional two wheel drive (2WD) vehicle, the motive force results from those forces generated by the two tyres. The vehicle mass imposes an inertia force against the motive force together with the resistive forces acting in the same direction. The bond graph of the vehicle body, therefore, is very simple as illustrated in Figure 6.16.

6.4   Driveline Models

Once the bond graph models of different components are available, the full driveline bond graph can easily be constructed by putting together the bond graphs of the components. The resulting bond graph involves details of the vehicle driveline components and it is expected that it can provide an account of the accurate behaviour of the system. Nonetheless, working with such model could be difficult due to complicated equations and because the detailed information required is difficult to obtain in practice. On the other hand, not all of parameters have critical effects on the behaviour of the driveline and sometimes simple models can demonstrate the fundamental properties of the system. Therefore, in addition to the full driveline model, it is also intended to develop simplified driveline models with less complexity but at acceptable levels.

6.4.1   Full Driveline Model

In the process of developing a full driveline model, some simplifications can be performed by merging similar properties of two adjacent elements (e.g. their inertias). The result will look like the bond graph of Figure 6.17. In this model, the elasticity of engine crankshaft has been ignored.

6.4.2   Straight-Ahead Motion

The motion of a vehicle in the longitudinal direction is of major importance when the driveline vibrations are studied. Thus if it is assumed that the vehicle moves only straight ahead, then the differential plays no other role than to produce the final drive ratio and the two left and right wheels can be combined. The resulting bond graph for such motions will be of the form shown in Figure 6.18. In the following sections only straight-ahead motion will be considered.

6.4.3   Rigid Body Model

Assuming all the driveline components are rigid elements with no elasticity, then all the C elements in the bond graph vanish. The bond graph of Figure 6.19 results from removing the 0 nodes with C elements in the bond graph of Figure 6.18, and combining any two adjacent 1 nodes resulting from this process.
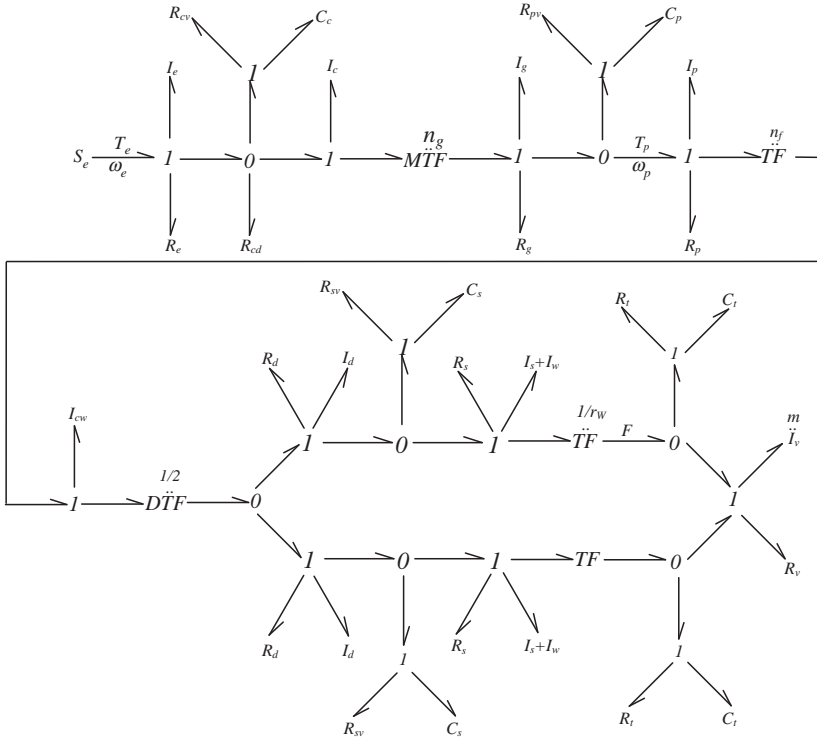
Figure 6.17   Bond graph of vehicle driveline system
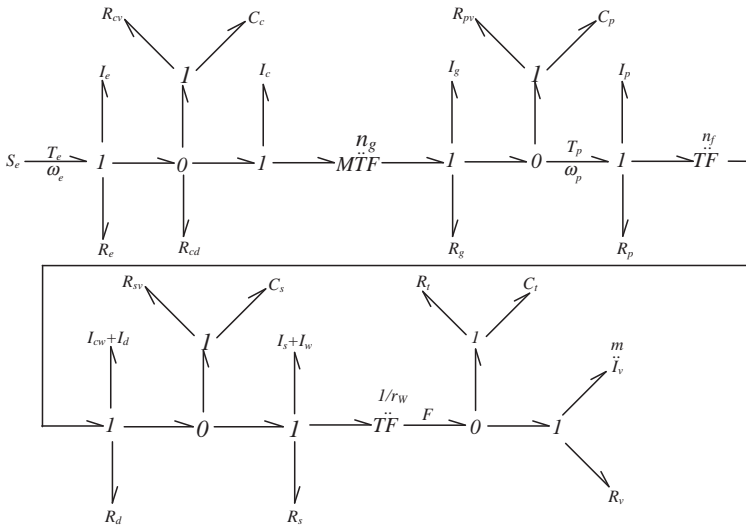
Figure 6.18   Bond graph of driveline system in straight-ahead motion
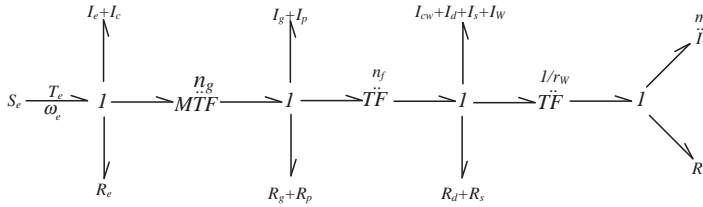
Figure 6.19   Bond graph of rigid body driveline

The bond graph of Figure 6.19 can be simplified by using the equivalent I (and R) rule for transformers (see Appendix, Section A.4.5). Note that two sequential transformers can be replaced by one transformer by simple multiplication of the modules of the two transformers. The resulting bond graph is shown in Figure 6.20. I_{eq} and R_{eq} in the bond graph are obtained from the following equations:

$$I_{eq} = I_v + \frac{1}{r_W^2}\left[I_{cw} + I_d + I_s + I_W + n_f^2(I_g + I_p) + n^2(I_e + I_c)\right] \tag{6.6}$$

$$R_{eq} = R_v + \frac{1}{r_W^2}\left[R_d + R_s + n_f^2(R_g + R_p) + n^2 R_e\right] \tag{6.7}$$

Equation 6.6 represents the effect of rotating inertia discussed in Section 3.9. From the simple bond graph of Figure 6.21 the equation of motion is:

$$\frac{dp_{eq}}{dt} = e_{eq} = \frac{n_g n_f}{r_W} T_e - R_{eq}\frac{p_{eq}}{I_{eq}} \tag{6.8}$$

Recalling that p_{eq} is vI_{eq}, Equation 6.8 can be written as:

$$I_{eq}\frac{dv}{dt} = \frac{n_g n_f}{r_W} T_e - R_{eq} v \tag{6.9}$$

which is in the form of $F_T - F_R = m_{eq}a$ of Equation 3.129 for vehicle longitudinal motion, including the effect of rotating masses.

6.4.4   Driveline with Clutch Compliance

If all the components are considered as rigid parts, but only clutch compliance is taken into consideration, the bond graph of driveline in a straight-ahead motion becomes that shown in Figure 6.21.
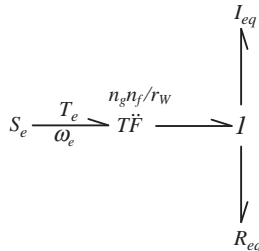
Figure 6.20   Simplified bond graph of rigid body driveline in straight-ahead motion
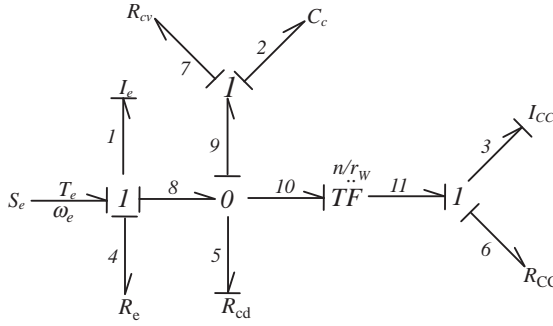
Figure 6.21   Bond graph of driveline with only clutch compliance

The transformers are combined and the two end elements I_{CC} and R_{CC} can be determined from the following equations with the same terminology as those of Figure 6.18:

$$I_{CC} = I_v + \frac{1}{r_W^2}\left[I_{cw} + I_d + I_s + I_w + n_f^2(I_g + I_p) + n^2 I_c\right] \qquad (6.10)$$

$$R_{CC} = R_v + \frac{1}{r_W^2}\left[R_d + R_s + n_f^2(R_g + R_p)\right] \qquad (6.11)$$

The equations of driveline motion according to the bond graph (with causal strokes inserted) of Figure 6.21 are as follows:

$$\frac{dp_1}{dt} = T_e - \frac{p_1}{I_1} R_e - T_1 \qquad (6.12)$$

$$\frac{dq_2}{dt} = \frac{p_1}{I_1} - \frac{k_2}{R_{CV}} q_2 - \frac{n}{r_W}\frac{p_3}{I_3} \qquad (6.13)$$

$$\frac{dp_3}{dt} = \frac{n}{r_W} T_1 - \frac{p_3}{I_3} R_{CC} \qquad (6.14)$$

in which:

$$T_1 = k_2 q_2 + R_{CV}\dot{q}_2 \qquad (6.15)$$

6.4.5   Driveline with Driveshaft Compliance

If rigid components are considered for all parts except the driveshafts which are taken as elastic elements, the overall bond graph of Figure 6.18 in straight-ahead motion will reduce to the bond graph of Figure 6.22.

$$I_{Eq} = I_e + I_c + \frac{1}{n^2}(I_{cw} + I_d) + \frac{1}{n_g^2}(I_g + I_p) \qquad (6.16)$$

$$R_{Eq} = R_e + \frac{1}{n^2} R_d + \frac{1}{n_g^2}(R_g + R_p) \qquad (6.17)$$

$$I_{DC} = I_v + \frac{1}{r_W^2}(I_s + I_w) \qquad (6.18)$$

$$R_{DC} = R_v + \frac{1}{r_W^2} R_s \qquad (6.19)$$
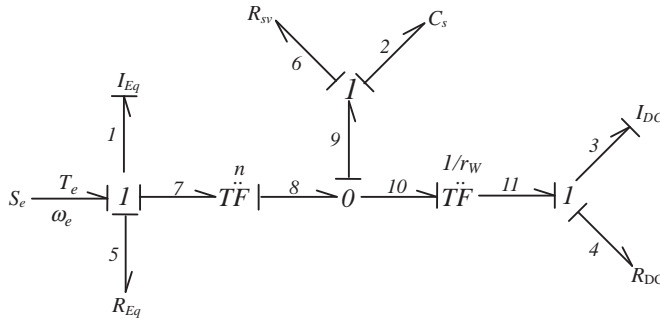
Figure 6.22 Bond graph of driveline with only driveshaft compliance

The equations of motion of the driveline according to Figure 6.22 are:

$$\frac{dp_1}{dt} = T_e - \frac{p_1}{I_1}R_{Eq} - T_1 \tag{6.20}$$

$$\frac{dq_2}{dt} = \frac{1}{n}\frac{p_1}{I_1} - \frac{1}{r_W}\frac{p_3}{I_3} \tag{6.21}$$

$$\frac{dp_3}{dt} = \frac{1}{r_W}T_1 - \frac{p_3}{I_3}R_{DC} \tag{6.22}$$

In which:

$$T_1 = \frac{1}{n}(k_2 q_2 + R_{Sv}\dot{q}_2) \tag{6.23}$$

6.4.6   Driveline with Clutch and Driveshaft Compliances

In the two preceding sections, the compliances of the clutch and driveshaft alone were considered to be unaccompanied by the other. In this section both compliances will be included in a single driveline model, as shown in Figure 6.23.

The two end elements I_{CDC} and R_{CDC} as well as two equivalent inertia and damping I_{deq} and R_{deq} can be determined from the following equations with the same terminology of Figure 6.18:

$$I_{CDC} = I_v + \frac{1}{r_W^2}(I_s + I_w) \tag{6.24}$$

$$R_{CDC} = R_v + \frac{1}{r_W^2}R_s \tag{6.25}$$

$$I_{deq} = I_d + I_{cw} + n_f^2(I_g + I_p) + n^2 I_c \tag{6.26}$$

$$R_{deq} = R_d + n_f^2(R_g + R_p) \tag{6.27}$$
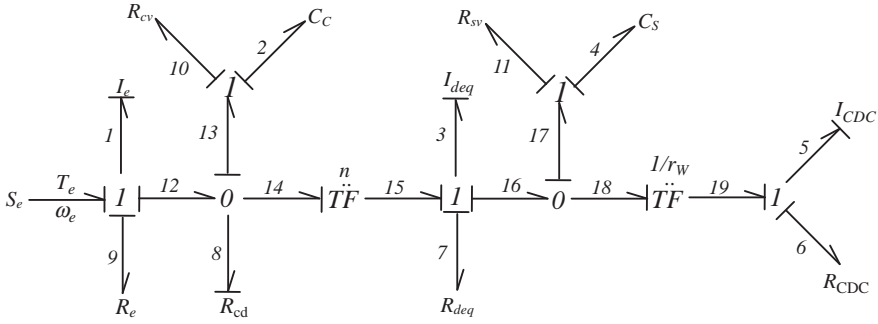
Figure 6.23   Bond graph of driveline with clutch and driveshaft compliances

The equations of motion of the driveline according to Figure 6.23 are:

$$\frac{dp_1}{dt} = T_e - \frac{p_1}{I_1}R_e - T_1 \tag{6.28}$$

$$\frac{dq_2}{dt} = \frac{p_1}{I_1} - \frac{T_1}{R_{Cd}} - n\frac{p_3}{I_3} \tag{6.29}$$

$$\frac{dp_3}{dt} = nT_1 - \frac{p_3}{I_3}R_{deq} - T_2 \tag{6.30}$$

$$\frac{dq_4}{dt} = \frac{p_3}{I_3} - \frac{1}{r_W}\frac{p_5}{I_5} \tag{6.31}$$

$$\frac{dp_5}{dt} = \frac{1}{r_W}T_2 - \frac{p_5}{I_5}R_{CDC} \tag{6.32}$$

in which:

$$T_1 = k_2 q_2 + R_{Cv}\dot{q}_2 \tag{6.33}$$

$$T_2 = k_4 q_4 + R_{Sv}\dot{q}_4 \tag{6.34}$$

6.5   Analysis

Driveline models with different elastic elements were constructed and the governing equations of motions were derived in the preceding sections. In this section, the equations of the system will be solved to observe the effects of compliances in the driveline on the system oscillations.

It is assumed that changes in engine torque due to throttle variations provide inputs to cause driveline oscillations. Sudden throttle changes such as tip-in (fast depression of throttle) and tip-out (sudden release of throttle) are two common excitations of vehicle driveline leading to large changes in vehicle acceleration. In the following sections for different driveline models, it will be assumed that the vehicle is at a steady motion and suddenly the throttle is changed and the resulting oscillations will be observed.

6.5.1 Effect of Clutch Compliance

Equations of motion of the vehicle driveline can be written in more familiar form by substituting into Equations 6.12–6.15 the equivalent values $p_1 = I_e \omega_e$, $p_3 = m_{eq} v$ and $q_2 = \theta_C$. The results are:

$$I_e \frac{d\omega_e}{dt} = T_e - R_e \omega_e - T_1 \tag{6.35}$$

$$\frac{d\theta_C}{dt} = \omega_e - \frac{n}{r_W} v \tag{6.36}$$

$$m_{CC} \frac{dv}{dt} = \frac{n}{r_W} T_1 - R_{CC} v \tag{6.37}$$

$$T_1 = k_C \theta_C + R_{Cv} \dot{\theta}_C \tag{6.38}$$

Solution of above equations can be obtained either by a MATLAB® or a Simulink® program. The MATLAB program will be similar to those used in previous chapters to simulate systems with of differential equations. The following example is solved by such a program written in the MATLAB environment.

Example 6.5.1

For a vehicle with driveline parameter values given in Table 6.1 and an engine MT formula parameters of Example 5.5.2, use a driveline model with only clutch compliance in the fully engaged phase:

Table 6.1 Numerical values for driveline parameters

Element	Name	Value	Units
I_e	Flywheel inertia	0.30	kgm^2
I_c	Clutch inertia	0.04	kgm^2
I_g	Transmission output inertia	0.05	kgm^2
I_p	Inertia at differential input	0.01	kgm^2
I_{cw}	Crownwheel inertia	0.10	kgm^2
I_d	Differential output inertia	0.10	kgm^2
I_s	Driveshaft output inertia	0.50	kgm^2
I_W	Wheel inertia	2.00	kgm^2
k_C	Clutch stiffness	500	Nm/rad
k_S	Driveshaft stiffness	10000	Nm/rad
R_e	Damping of crankshaft	0.01	Nms/rad
R_{Cv}	Internal damping of clutch	10	Nms/rad
R_g	Damping in transmission	0.50	Nms/rad
R_p	Damping in differential input	0.50	Nms/rad
R_d	Damping in differential output	0.10	Nms/rad
R_S	Damping of driveshaft output	0.1	Nms/rad
R_{Sv}	Internal damping of driveshaft	200	Nms/rad
R_v	Damping in vehicle motion	20	Ns/m
m	Vehicle mass	1200	kg
n_g	Transmission ratios (gear 1)	3	-
n_f	Final drive ratio	4	-
r_W	Tyre effective radius	30	cm
m	Vehicle mass	1200	kg

(a) Find steady values for state variables at speed of 5 m/s.
(b) At t = 1s the throttle is suddenly fully depressed. Find the variations of engine speed, clutch spring depression angle, vehicle speed and acceleration.

Solution

(a) Steady state values of system states can simply be obtained from Equations 6.35–6.37 by equating them to zero. The results for the fully engaged clutch ($R_C = \infty$) are:

$$\omega_{e0} = \frac{n}{r_W} v0$$

$$\theta_{C0} = \frac{r_W R_{CC}}{n k_C} v0$$

The value of engine torque to maintain steady motion is:

$$T_{e0} = R_e \omega_{e0} + k_C \theta_{C0}$$

(b) For this part two MATLAB programs are needed, one main program and one function including the system differential equations. Typical programs for this purpose are provided in Figures 6.24 and 6.25.

```
% Example 6.5.1
% A sample program to investigate the driveline vibrations with only Clutch
compliance

clc, close all, clear all

global thrtl Te0 RCv kC Ie rW n Rcc mcc Re p

% Vehicle information (see Table 6.1):
m=1200; Ie=0.3; Ic=0.04; Ig=0.05; Icw=0.1; Ip=0.01; Id=0.1; Is=0.5; Iw=2;
kC=500;
Re=0.01; RCv=10; Rg=0.5; Rd=0.1; Rp=0.02; Rs=0.1; Rv=20; ng=3.0;
nf=4.0; rW=0.3;
n=ng*nf;

% Engine Full throttle information:
te=[80 98 100 105 110 112 109 111 104 96.6];
ome=[1000 1500 2000 2500 3000 3500 4000 4500 5000 5300];
% Fit a curve to WOT data
[p,s]=polyfit(ome,te,2);

% Define equivalent mcc and Rcc:
mcc=m+(Icw+Id+Is+Iw+(Ig+Ip)*nf^2+Ic*n^2)/rW^2;
Rcc=Rv+(Rd+Rs+(Rg+Rp)*nf^2)/rW^2;
```

Figure 6.24   MATLAB program listing of Example 6.5.1

```
        % Initial conditions:
        v0=5;
        omegae0=v0*n/rW;
        thetac0=Rcc*v0*rW/n/kC;
        x0=[omegae0 thetac0 v0];
        Te0=Re*omegae0+Rcc*v0*rW/n;            % Steady torque

        % Specify throttle value:
        thrtl=100;

        % Specify differentiation interval t0-tf:
        t0=0; tf=5;

        % Invoke ode15s (stiff equations):
        [t,x]=ode15s(@driveline_cc, [t0 tf], x0);   % Calls 'driveline_cc' function

        % Plot the variation of parameters versus time
        plot(t,x(:,1)*30/pi),
        xlabel('Time (s)')
        ylabel('Engine speed (rpm)')
        grid
        figure
        plot(t,x(:,2)*180/pi)
        xlabel('Time (s)')
        ylabel('Clutch spring angle (degree)')
        grid
        figure
        plot(t,x(:,3))
        xlabel('Time (s)')
        ylabel('Vehicle speed (m/s)')
        grid
        % Example 6.5.1 (continued)
        % Generate the acceleration
        j=length(t);
        for i=1: j
            a(i)=(-Rcc*x(i,3)+kC*x(i,2)*n/rW)/mcc;
        end
        figure
        plot(t,a)
        xlabel('Time (sec)')
        ylabel('Vehicle acceleration (m/s2)')
        grid
```

Figure 6.24 (*Continued*)

It is worth noting that the equations of motion describe an oscillatory system and instead of '*ode45*' function, '*ode15s*' for stiff differential equations is used for integration.

The outputs of the programs are illustrated in Figures 6.26–6.29.

```
% Function called in Example 6.5.1
function f=driveline_cc(t,x)

global thrtl Te0 RCv kC Ie rW n Rcc mcc Re p

omegae=x(1);
thetac=x(2);
v=x(3);
    if t<1
        Te=Te0;
    else
    % Engine MT formula
    pow=(1.003*omegae*30/pi)^1.824;
    den=(1+exp(-11.12-0.0888*thrtl))^pow;
    Te=polyval(p,omegae*30/pi)/den;
    end

    f2=omegae-v*n/rW-omc;
    T1=kC*thetac+RCv*f2;
    f1=(Te-Re*omegae-T1)/Ie;
    f3=(-Rcc*v+T1*n/rW)/mcc;

    f=[f1
       f2
       f3];
```

Figure 6.25   MATLAB function of Example 6.5.1
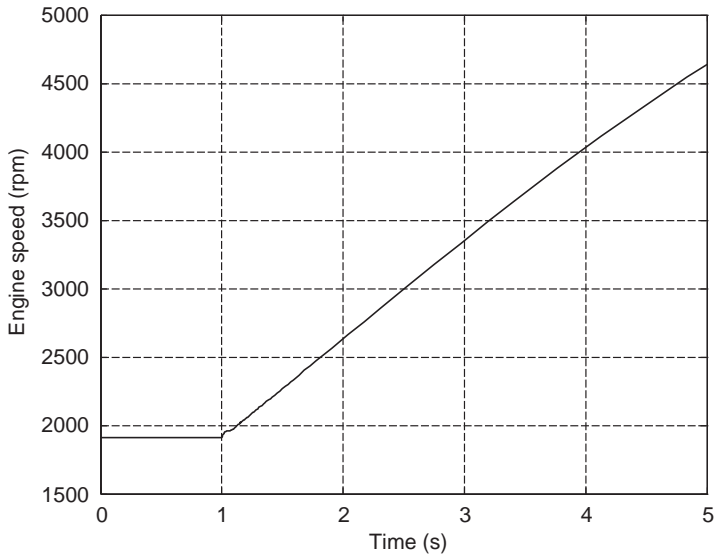
Figure 6.26   Variations of engine speed for sudden throttle input of Example 6.5.1
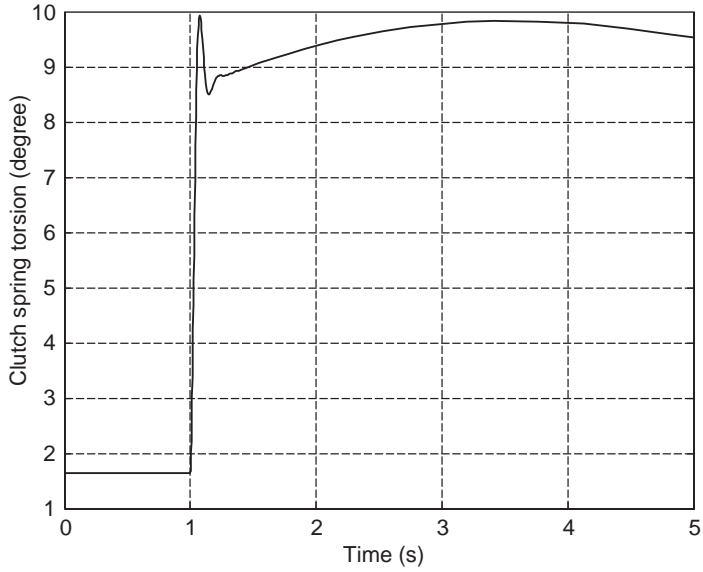
Figure 6.27   Variations of clutch spring torsion for sudden throttle input of Example 6.5.1
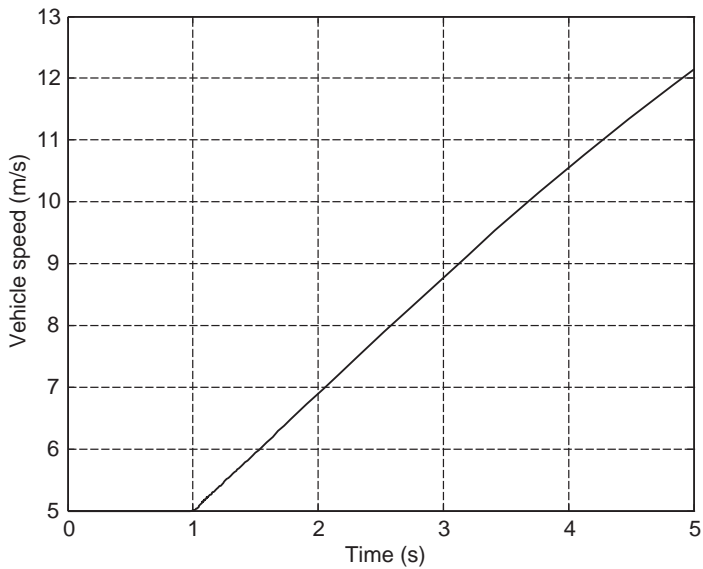
Figure 6.28   Variations of vehicle speed for sudden throttle input of Example 6.5.1
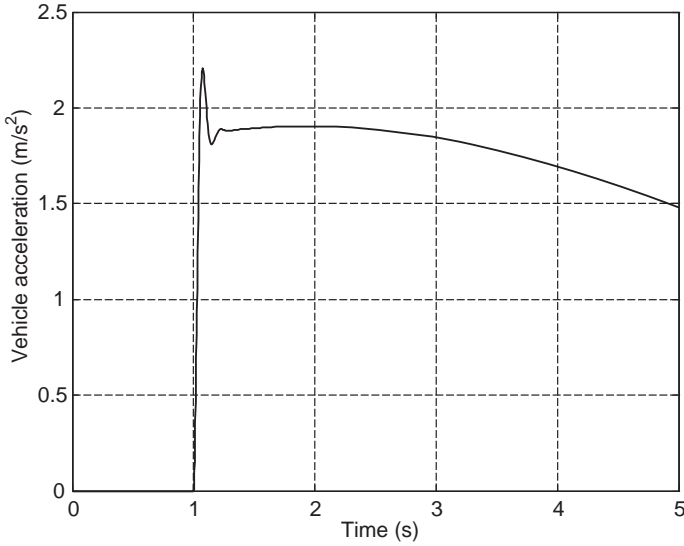
Figure 6.29   Variations of vehicle acceleration for sudden throttle input of Example 6.5.1

6.5.2   *Effect of Driveshaft Compliance*

The equations of motion of the vehicle driveline in simplified form for this case are:

$$I_{Eq}\frac{d\omega_e}{dt} = T_e - R_{Eq}\omega_e - T_1 \tag{6.39}$$

$$\frac{d\theta_s}{dt} = \frac{1}{n}\omega_e - \frac{1}{r_W}v \tag{6.40}$$

$$m_{DC}\frac{dv}{dt} = \frac{n}{r_W}T_1 - R_{DC}v \tag{6.41}$$

with:

$$T_1 = \frac{1}{n}(k_S\theta_S + R_{Sv}\dot{\theta}_S) \tag{6.42}$$

which are very similar to equations when only the clutch compliance was present. Thus the solution method is exactly similar.

Example 6.5.2

For the vehicle of Example 6.5.1 use a driveline model with only driveshaft compliance:

(a) Find steady values for state variables at speed of 5 m/s.
(b) At $t = 1$s the throttle is suddenly fully depressed. Find the variations of engine speed, driveshaft torsion angle, vehicle speed and acceleration.

Solution

The MATLAB program of Figures 6.24 and 6.25 can simply be modified for this case. The main changes are for the initial conditions and derivative equations inside the function file.

(a) Initial conditions or steady values of state variables read:

$$\omega_{e0} = \frac{n}{r_W} v0$$

$$\theta_{S0} = \frac{r_W R_{DC}}{k_S} v0$$

The initial steady value of engine torque is:

$$T_{e0} = R_{Eq}\omega_{e0} + \frac{1}{n} k_S \theta_{S0}$$

(b) The results for this case are plotted in Figures 6.30–6.33. It is clear that the initial and final conditions for this case are exactly equal to those of previous section and only the oscillations are different.
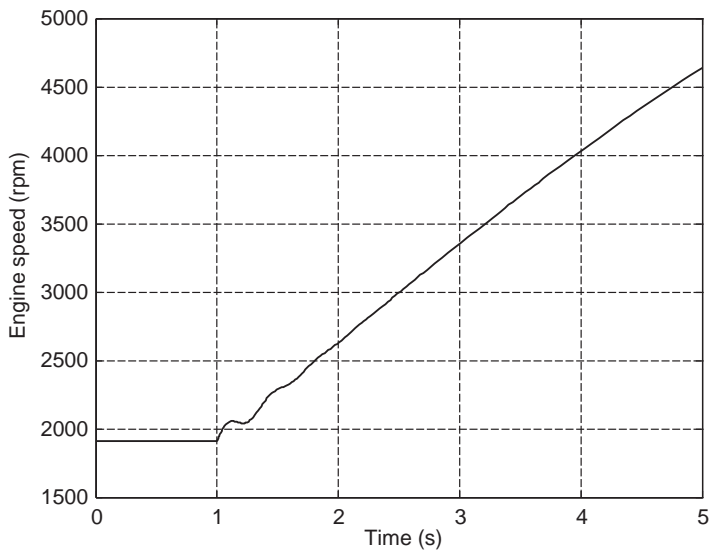
Figure 6.30 Variations of engine speed for sudden throttle input of Example 6.5.2
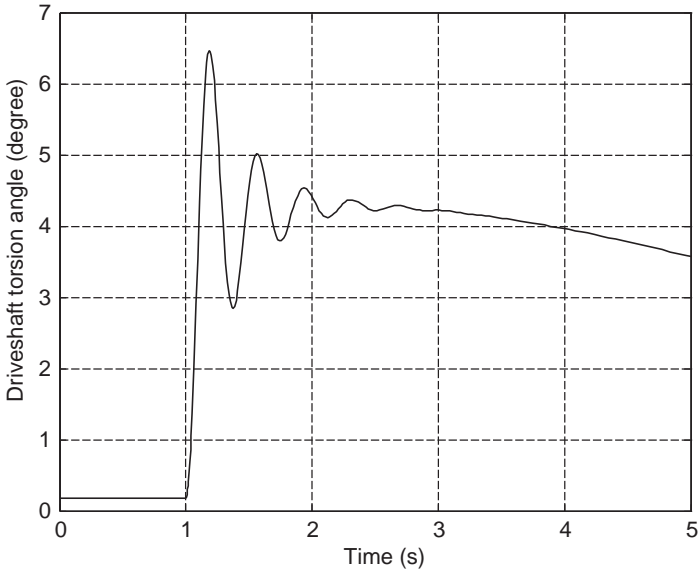
Figure 6.31 Variations of driveshaft torsion for sudden throttle input of Example 6.5.2
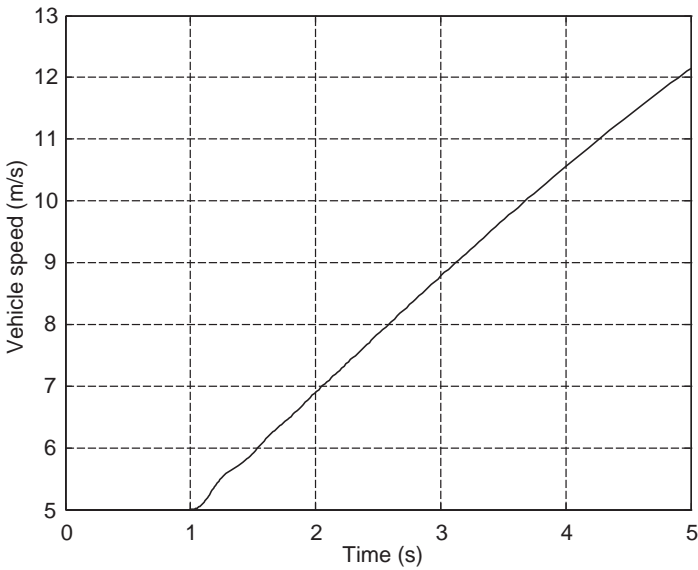
Figure 6.32 Variations of vehicle speed for sudden throttle input of Example 6.5.2
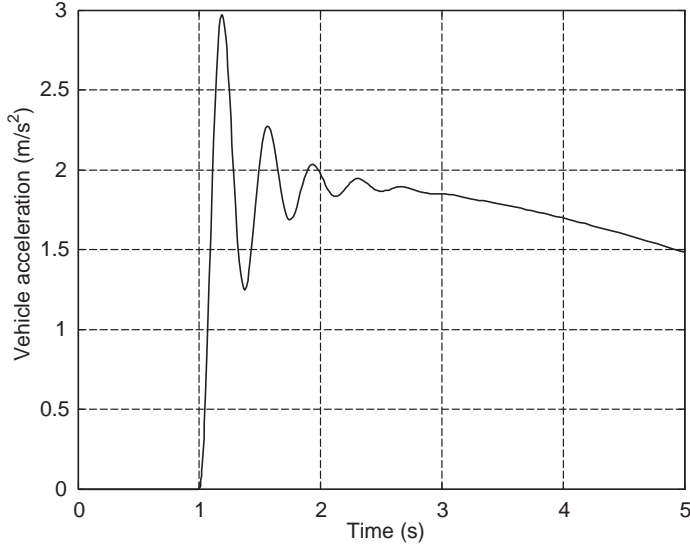
Figure 6.33   Variations of vehicle acceleration for sudden throttle input of Example 6.5.2

6.5.3   *Effect of Clutch and Driveshaft Compliances*

The equations of motion of driveline for this case are (see Equations 6.28–6.32):

$$I_e \frac{d\omega_e}{dt} = T_e - R_e \omega_e - T_1 \tag{6.43}$$

$$\frac{d\theta_C}{dt} = \omega_e - \frac{T_1}{R_{Cd}} - n\omega_d \tag{6.44}$$

$$I_{deq} \frac{d\omega_d}{dt} = nT_1 - R_{deq}\omega_d - T_2 \tag{6.45}$$

$$\frac{d\theta_S}{dt} = \omega_d - \frac{v}{r_W} \tag{6.46}$$

$$I_{CDC} \frac{dv}{dt} = \frac{1}{r_W} T_2 - v R_{CDC} \tag{6.47}$$

in which:

$$T_1 = k_C \theta_C + R_{Cv}\dot{\theta}_C \tag{6.48}$$

$$T_2 = k_S \theta_S + R_{Sv}\dot{\theta}_S \tag{6.49}$$

Example 6.5.3

For the vehicle of Example 6.5.1 use a driveline model with both clutch and driveshaft compliances:

(a) Find the steady values for state variables at speed of 5 m/s.
(b) At t = 1s the throttle is suddenly fully depressed. Find the variations of engine speed, clutch torsion, driveshaft torsion, vehicle speed and acceleration.

Solution

(a) The steady-state values are obtained by equating the time derivatives of Equations 6.43–6.49 to zero. The results are:
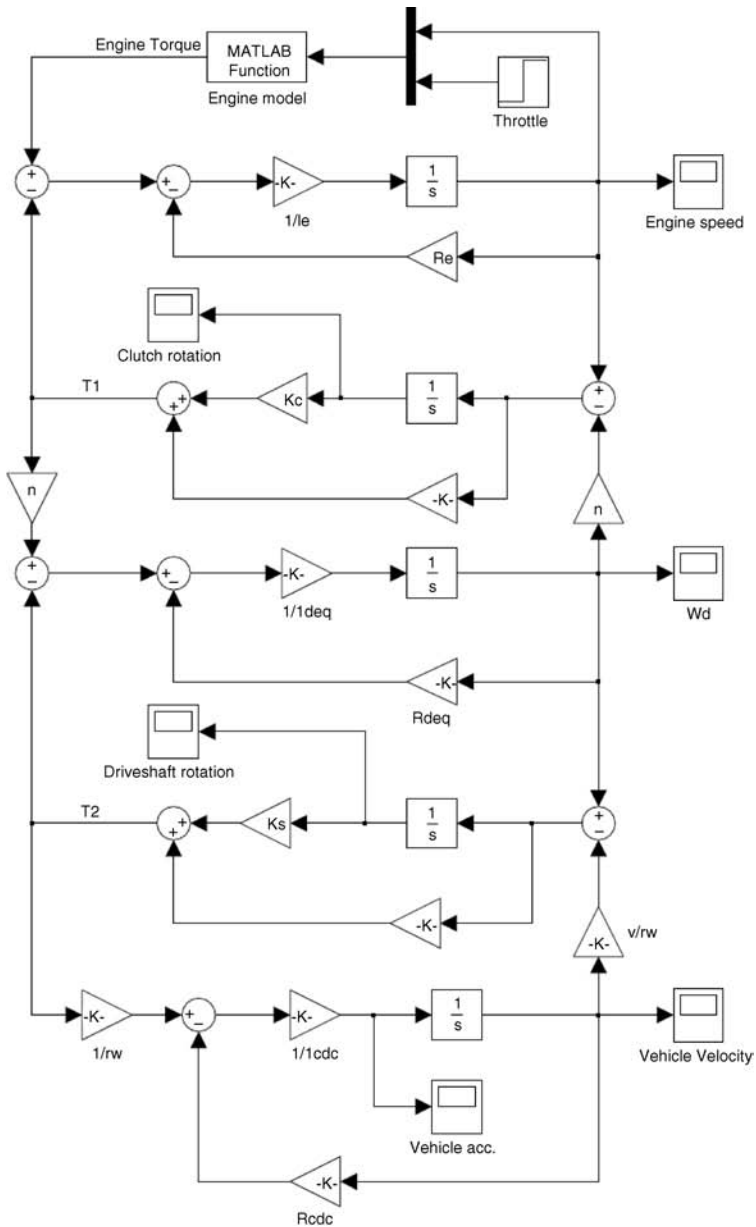
Figure 6.34 Simulink model for driveline including clutch and driveshaft compliances
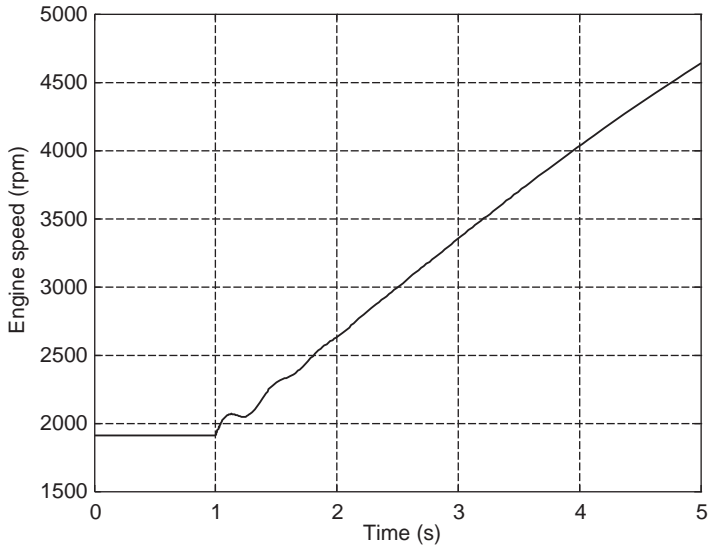
Figure 6.35   Variations of engine speed for sudden throttle input of Example 6.5.3

$$\omega_{e0} = \frac{n}{r_W} v0$$

$$\theta_{S0} = \frac{r_W R_{CDC}}{k_S} v0$$
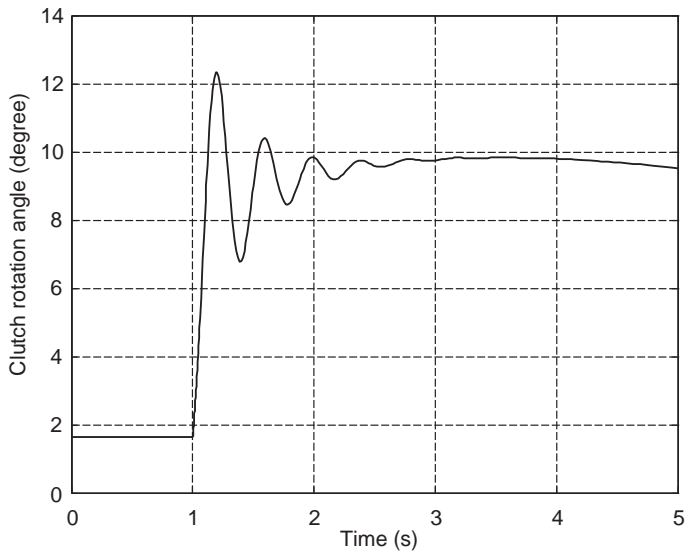
Figure 6.36   Variations of clutch spring torsion for sudden throttle input of Example 6.5.3
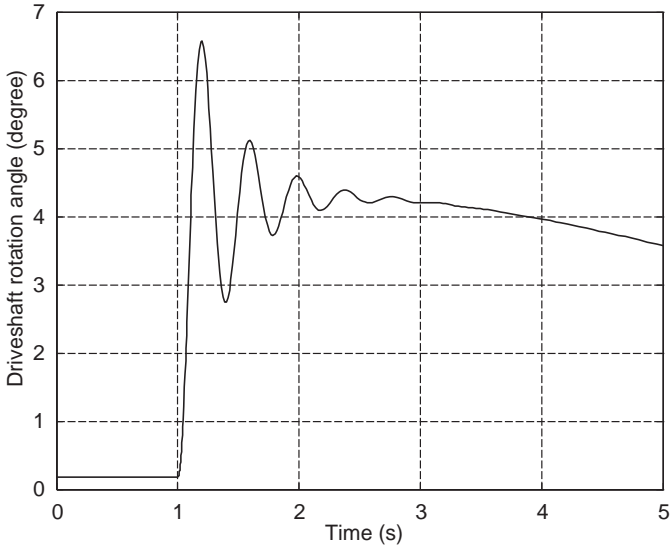
Figure 6.37   Variations of driveshaft torsion for sudden throttle input of Example 6.5.3

$$\theta_{C0} = \frac{r_W k_S \theta_{S0} + R_{deq}}{n r_W k_C} v0$$

The initial steady value of engine torque is:

$$T_{e0} = R_e \omega_{e0} + k_C \theta_{C0}$$
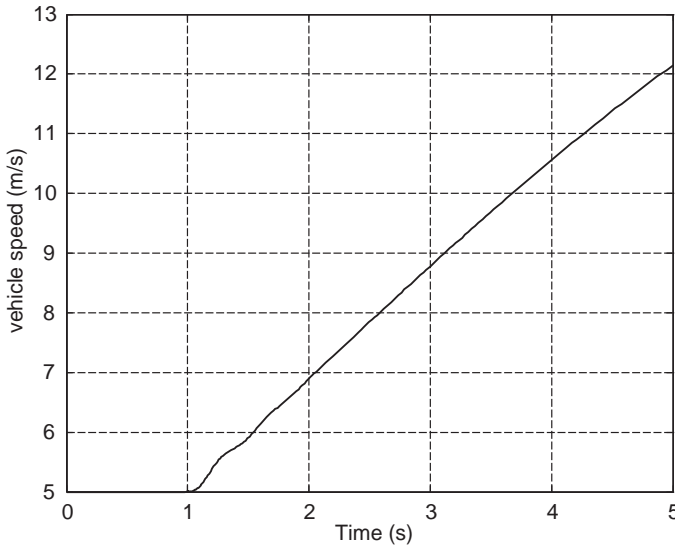
Figure 6.38   Variations of vehicle speed for sudden throttle input of Example 6.5.3

(b) As an alternative method to our solutions in two previous examples, let us this time use Simulink. A model for this purpose is shown in Figure 6.34. The output results are given in Figures 6.35–6.39.
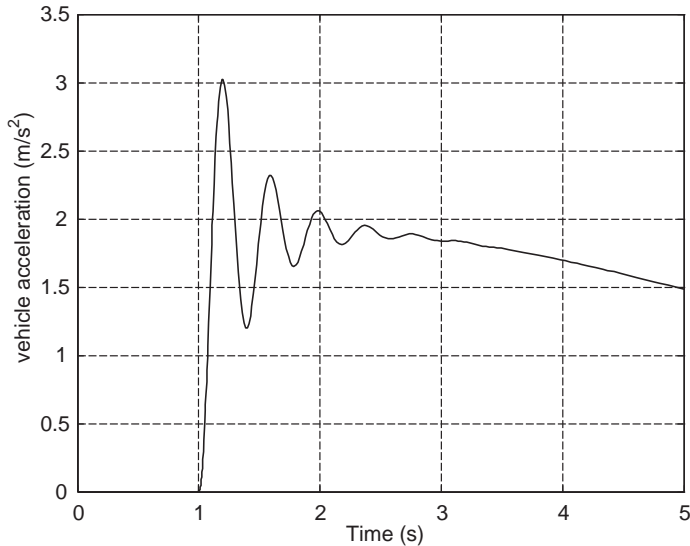
Figure 6.39   Variations of vehicle acceleration for sudden throttle input of Example 6.5.3

6.5.4   Frequency Responses

The equations of motion for the driveline models are all in the form of a set of first order ordinary differential equations that can easily be written in state space form. With the use of specialized software such as MATLAB, obtaining the frequency response analysis is rather simple. In addition to useful information regarding the frequencies and damping ratios of the driveline systems, transfer functions between inputs and outputs can also be produced. This can help in performing additional linear analyses studies and controller designs for active elements.

The state space representation of a system is in the basic form of:

$$\frac{dX}{dt} = AX + BU \tag{6.50}$$

in which X is an $n \times 1$ column matrix containing the system state variables, U is an $m \times 1$ column matrix containing the system inputs, A is an $n \times n$ square matrix and B is an $n \times m$ matrix. Elements of A and B are obtained from the governing equations of the system.

If specific system outputs given in an $r \times 1$ column matrix, Y is chosen, it can be represented by following expression:

$$Y = CX + DU \tag{6.51}$$

with C and D as two $r \times n$ and $r \times m$ matrices. The following examples in this section are designed to familiarize the reader with developing models for frequency response analysis.

Example 6.5.4

For the three driveline models developed in Sections 6.5.1, 6.5.2 and 6.5.3 derive the state space matrices. Engine torque T_e is input whereas vehicle speed and acceleration are outputs.

Solution

(a) Model with clutch compliance: for this case Equations 6.35–6.37 can be written in the form of Equation 6.50. Matrices A and B are:

$$
A = \begin{bmatrix}
-\dfrac{R_e + R_{Cv}}{I_e} & -\dfrac{k_C}{I_e} & \dfrac{nR_{Cv}}{r_W I_e} \\[2mm]
1 & 0 & -\dfrac{n}{r_W} \\[2mm]
\dfrac{nR_{Cv}}{r_W I_{CC}} & \dfrac{nk_C}{r_W I_{CC}} & -\dfrac{R_{CC}}{I_{CC}}
\end{bmatrix}, \quad B = \begin{bmatrix} \dfrac{1}{I_e} \\[2mm] 0 \\[1mm] 0 \end{bmatrix}
$$

Matrices C and D must be generated for the two outputs v and a and the input T_e:

$$
C = \begin{bmatrix}
0 & 0 & 1 \\[2mm]
\dfrac{nR_{Cv}}{r_W I_{CC}} & \dfrac{nk_C}{r_W I_{CC}} & -\dfrac{R_{CC}}{I_{CC}}
\end{bmatrix}, \quad D = \begin{bmatrix} 0 \\ 0 \end{bmatrix}
$$

(b) Model with driveshaft compliance: for this case Equations 6.39–6.41 are used. Matrices A and B this time are:

$$
A = \begin{bmatrix}
-\dfrac{R_{Eq} + \dfrac{1}{n^2} R_{Sv}}{I_{Eq}} & -\dfrac{k_S}{n I_{Eq}} & \dfrac{R_{Sv}}{n r_W I_{Eq}} \\[4mm]
\dfrac{1}{n} & 0 & -\dfrac{1}{r_W} \\[3mm]
\dfrac{R_{Sv}}{n r_W I_{DC}} & \dfrac{k_S}{r_W I_{DC}} & -\dfrac{R_{Sv} + r_W^2 R_{DC}}{r_W^2 I_{DC}}
\end{bmatrix}, \quad B = \begin{bmatrix} \dfrac{1}{I_{Eq}} \\[2mm] 0 \\[1mm] 0 \end{bmatrix}
$$

Matrices C and D for the same input and outputs are:

$$
C = \begin{bmatrix}
0 & 0 & 1 \\[2mm]
\dfrac{R_{Sv}}{n r_W I_{DC}} & \dfrac{k_S}{r_W I_{DC}} & -\dfrac{R_{Sv} + r_W^2 R_{DC}}{r_W^2 I_{DC}}
\end{bmatrix}, \quad D = \begin{bmatrix} 0 \\ 0 \end{bmatrix}
$$

(c) Model with both clutch and driveshaft compliances: for this case Equations 6.43–6.47 are used and thus the matrices A and B include five rows:

$$
A = \begin{bmatrix}
-\dfrac{R_e + R_{Cv}}{I_e} & -\dfrac{k_C}{I_e} & \dfrac{nR_{Cv}}{I_e} & 0 & 0 \\[3mm]
1 & 0 & -n & 0 & 0 \\[3mm]
\dfrac{nR_{Cv}}{r_W I_{deq}} & \dfrac{nk_C}{I_{deq}} & -\dfrac{R_{Sv} + n^2 R_{Cv} + R_{deq}}{I_{deq}} & -\dfrac{k_S}{I_{deq}} & \dfrac{R_{Sv}}{r_W I_{deq}} \\[3mm]
0 & 0 & 1 & 0 & -\dfrac{1}{r_W} \\[3mm]
0 & 0 & \dfrac{R_{Sv}}{r_W I_{CDC}} & \dfrac{k_S}{r_W I_{CDC}} & -\dfrac{R_{Sv} + r_W^2 R_{CDC}}{r_W^2 I_{CDC}}
\end{bmatrix}, \quad B = \begin{bmatrix} \dfrac{1}{I_e} \\[2mm] 0 \\[1mm] 0 \\[1mm] 0 \\[1mm] 0 \end{bmatrix}
$$

Matrices C and D for the same input and outputs are:

$$C = \begin{bmatrix} 0 & 0 & 0 & 0 & 1 \\ 0 & 0 & \dfrac{R_{Sv}}{r_W I_{CDC}} & \dfrac{k_S}{r_W I_{CDC}} & -\dfrac{R_{Sv} + r_W^2 R_{CDC}}{r_W^2 I_{CDC}} \end{bmatrix}, \quad D = \begin{bmatrix} 0 \\ 0 \end{bmatrix}$$

Example 6.5.5

For the driveline models with the state space matrices obtained in previous example, use the driveline information of Example 6.5.1:

(a) Determine the frequencies and damping ratios for each driveline model.
(b) Plot the Bode diagrams for the outputs for the third driveline model.

Solution

(a) The frequencies and damping ratios depend only on the matrix A of each system. In the MATLAB environment a simple command '[wn, z]=damp(A)' produces the results by displaying natural frequencies (wn) and damping ratios (z).

For the three driveline models, the values of natural frequencies and damping ratios are summarized in Table 6.2.

(b) The state space from can be converted into a MATLAB system by using the following command:

$$sys = ss(A,\ B,\ C,\ D);$$

Then the Bode plot is simply obtained by issuing command: '*bode(sys)*'. For the third driveline model the result is illustrated in Figure 6.40.

Table 6.2 Frequencies and damping ratios of Example 6.5.5

Item	Modes	Clutch compliance	Driveshaft compliance	Clutch and driveshaft compliances
Natural Frequency (rad/s) [Hz]	First	0.073 [0.012]	0.073 [0.012]	0.073 [0.012]
	Second	47.75 [7.6]	17.03 [2.7]	16.97 [2.6]
	Third	47.75 [7.6]	17.03 [2.7]	16.97 [2.6]
	Fourth	–	–	66.11 [10.5]
	Fifth	–	–	201.87 [32.1]
Damping ratio	First	1	1	1
	Second	0.478	0.175	0.165
	Third	0.478	0.175	0.165
	Fourth	–	–	1
	Fifth	–	–	1

Figure 6.40   Bode plots of system outputs for Example 6.5.5
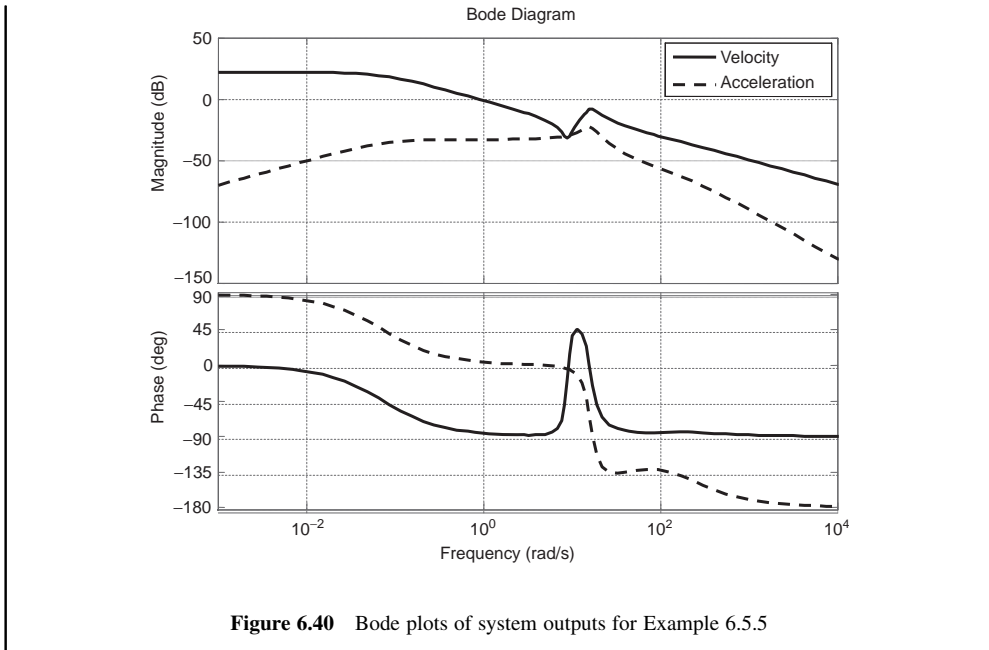
6.5.5   Improvements

In the design process with the help of software simulations, the driveline parameters can be altered to get better responses in terms of driveline oscillations at different working conditions. The potential approaches that are possible for reducing driveline vibrations in general are:

1. Tuning the system natural frequencies by changing the stiffnesses or inertias of the components.
2. Adjusting the damping of the driveline system. Viscous damping in the system decreases the amplitude of the oscillations and must be adjusted to the desired values to obtain faster responses and at the same time low amplitude oscillations.
3. Regulating the input power to the system by controlling the engine torque.

Engine torque fluctuations can be a source of excitation of driveline vibration. Engine torque fluctuations can initiate or magnify the oscillations. Passive crankshaft torsional dampers are useful in reducing the amplitude of vibrations. These include very simple rubber dampers or sophisticated dual-mass systems. The appropriate control of engine torque also can lead to smooth power transfers at different driving conditions. Engine management systems can achieve this by controlling the throttle and ignition for smoothing the torque outputs. The controller calculates a spark advance or fuel injection timing as well as the throttle position that is needed in order to counteract the torque changes and reduce the overall driveline vibrations.

6.6   Conclusion

In this chapter, the modelling of the vehicle driveline was discussed and the development of several models using bond graph method was presented. This method allows the inclusion of the detailed component properties of the driveline system. The derivation of the governing equations is

straightforward and the resulting equations are in the form of a set of first order ordinary differential equations that are suitable for direct numerical integration. MATLAB/Simulink programs were used to demonstrate the method of solving system equations for three different cases including stiffness of clutch plate, stiffness of driveshaft and both stiffnesses together.

   Other analysis techniques are also available, once the equations of motion are derived. These include state space and frequency response analyses. The study of driveline behaviour can be extended by observing the effect of changing parameters on the oscillation of the system and modification of parameter values in order to reduce the vibrations.

6.7   Review Questions

6.1 Describe why vehicle drivelines are prone to vibration.
6.2 Explain the difference in concept of the bond graph method with other methods such as block diagrams and signal flow graphs.
6.3 Explain why there are two friction elements in the bond graph of a clutch plate.
6.4 What is a modulated transformer?
6.5 Explain how the inertia is lumped on one side of an element. Does it make any difference about which side to include?
6.6 Is the vehicle differential a true transformer? Why?
6.7 Explain why the final steady values for Examples 6.5.1, 6.5.2 and 6.5.3 are similar.
6.8 Describe how the system natural frequencies can be obtained once the equations of motion are derived.
6.9 What are the practical ways of reducing the driveline vibrations at the design stage?
6.10 What are the practical ways of reducing the vehicle vibration during operation?

6.8   Problems

Problem 6.1

For a single cylinder internal combustion engine with a schematic diagram shown in Figure P6.1:

(a) Explain clearly how many *transformers*, *gyrators*, *inertia elements*, *capacitor elements* and *resistor elements* you find in the bond graph.
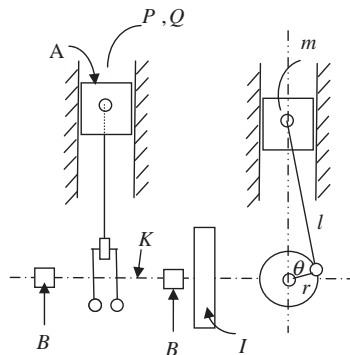
Figure P6.1   Schematic diagram of engine for Problem 6.1

(b) Construct the complete bond graph, number it and insert the causal strokes.

(c) Specify the state variables of the system.

Problem 6.2

For a two-cylinder internal combustion engine with a schematic diagram shown in Figure P6.2:

(a) Construct the bond graph.

(b) Assign the causal strokes and specify the state variables.
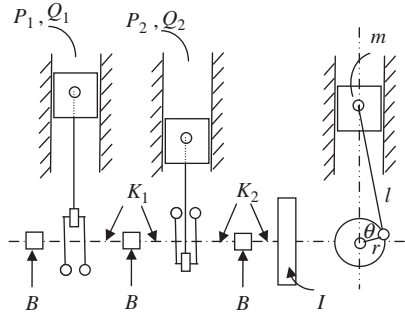
Figure P6.2 Schematic diagram of engine for Problem 6.2

Problem 6.3

For a four-cylinder internal combustion engine with a schematic diagram shown in Figure P6.3:

(a) Construct the bond graph.

(b) Assign causal strokes and specify the state variables.
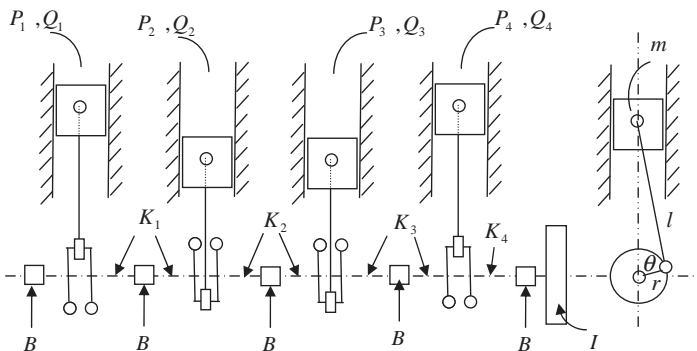
Figure P6.3 Schematic diagram of engine for Problem 6.3

Problem 6.4

Consider a five-speed constant mesh gearbox as shown in Figure P6.4:

(a) Construct a bond graph for the system when gear 1 is engaged.
(b) Insert causal strokes and then specify the state variables.
(c) What changes will occur to the bond graph when another gear is engaged? Explain why.
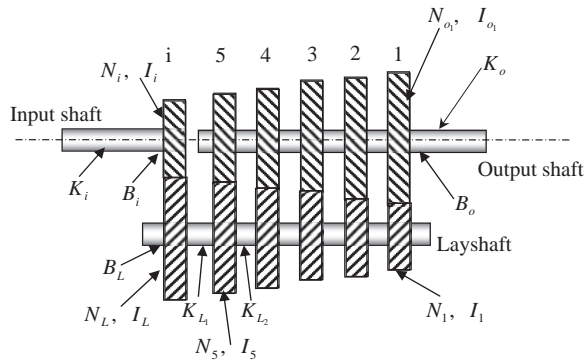
Figure P6.4   Schematic diagram of gearbox for Problem 6.4

Problem 6.5

For a vehicle differential with details shown in Figure P6.5:

(a) Draw a complete bond graph.
(b) Assign proper causal strokes.
(c) Specify the appropriate state variables.
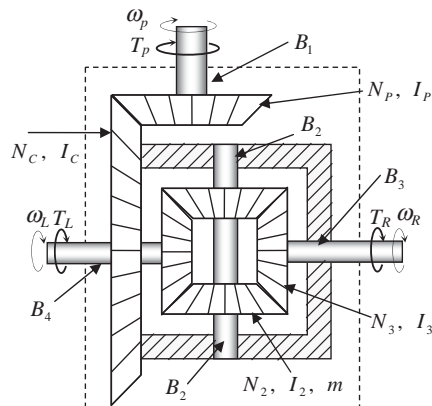
Figure P6.5   Schematic diagram of differential for Problem 6.5

Problem 6.6

For the planetary gear set shown in Figure P6.6, construct the bond graph for following cases:

(a) When the Carrier C is fixed (T_R input and T_S output).
(b) When the Sun S is fixed (T_R input and T_C output).
(c) When the Ring R is fixed (T_S input and T_C output).
(d) Write the equations of motion of system in case (a).
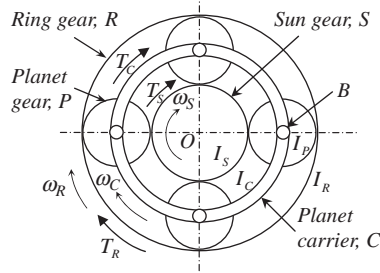
Figure P6.6   Schematic diagram of epicyclic gear set for Problem 6.6

Problem 6.7

A rigid body model of the driveline is represented as a simplified model in Figure P6.7 by ignoring damping:

(a) Derive the equations of motion of the system (note the differential causalities).
(b) Find the equation for the angular acceleration α_W of the wheel
(c) Find an expression for the overall gear ratio n that maximizes α_W
(d) Is the result useful?
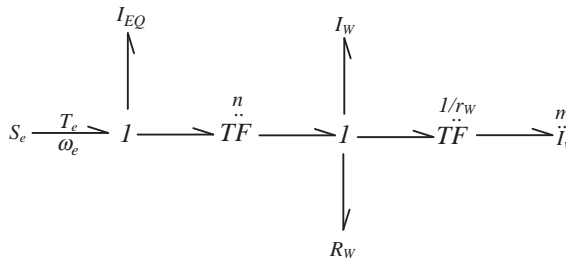
Figure P6.7   Rigid body bond graph model of Problem 6.7

Problem 6.8

Repeat Examples 6.5.1, 6.5.2 and 6.5.3 for an initial speed of 15 m/s and gear ratio of 2.

Problem 6.9

Repeat Examples 6.5.1, 6.5.2 and 6.5.3 for an initial speed of 10 m/s and a sudden release of the accelerator pedal. In this case the engine will generate a braking torque that can be modelled by the relation $T_{be} = -0.1\omega_e$ (ω_e in rad/s).

Problem 6.10

Repeat Problem 6.9 for an initial speed of 15 m/s and gear ratio of 2.

Problem 6.11

Repeat Examples 6.5.1, 6.5.2 and 6.5.3 for a 3 second pulse of throttle shown in Figure P6.11. Use the braking torque of Problem 6.9.
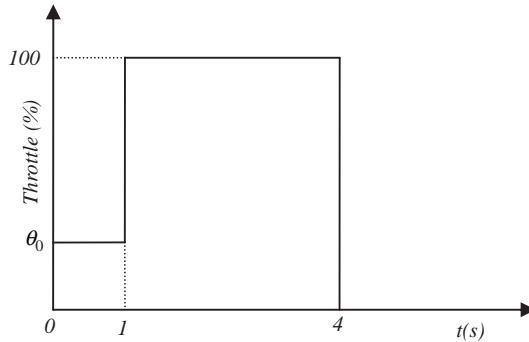
Figure P6.11   Throttle pulse of Problem 6.11

Problem 6.12

Consider the bond graph of a whole vehicle for straight ahead motion and ignore propeller shaft elasticity.

(a) Simplify it by combining the elements around the middle transformers.
(b) Insert causal stokes and specify the state variables of system.
(c) Derive the equations of motion of the resulting bond graph.

Problem 6.13

Consider the bond graph of whole vehicle in straight-ahead motion.

(a) Simplify it by combining the elements around the transformers.
(b) For (a), insert causal strokes and specify the state variables of system.
(c) Derive the equations of motion of system.

Problem 6.14

Consider the rigid-body model of driveline.

(a) Compare the system of Problem 6.7 with the rigid-body model and determine R_W and I_{EQ}.
(b) Specify which components have been ignored.
(c) Describe what the system of Problem 6.7 is telling you and if it is comparable to what was discussed in Chapter 3.

Further Reading

The torsional behaviour of the interconnected components in a driveline is important in controlling the overall refinement of the powertrain system and its effects on noise, vibration and harshness (NVH).

There are several methods for tackling this dynamic problem, and the method adopted in this book is the bond graph approach. Although there are several texts available, the best and most comprehensive introduction to the bond graph method is that by Borutzky [4]. Although there have been plenty of published studies of automotive driveline dynamics, little of this work has found its way into reference books. However, there is a good section in Kienke [12] (Chapter 5 in that book) which provides a simple driveline analysis using a Newtonian approach, and then goes on to discuss control issues relating to functionality and driveability.

References

[1] Kane, T.R. and Levinson, D.A. (1985) *Dynamics: Theory and Applications*. McGraw-Hill Book Company, ISBN 0-07-037846-0.

[2] Karnopp, D.C., Margolis, D.L. and Rosenberg, R.C. (1990) *System Dynamics: A Unified Approach*. John Wiley & Sons, ISBN 0-471-62171-4.

[3] Mukherjee, A. and Karmakar, R. (1999) *Modeling and Simulation of Engineering Systems Through Bond Graphs*. CRC Press, ISBN 978-0849309823.

[4] Borutzky, W. (2010) *Bond Graph Methodology: Development and Analysis of Multidisciplinary Dynamic System Models*, Springer, ISBN 978-1848828810.

[5] http://simcompanion.mscsoftware.com/infocenter/index?page=content&id=DOC9381&cat=2010_ADAMS_DOCS&actp=LIST.

[6] http://www.keohps.com/keohps_english/Amesim.htm.

[7] http://www.3ds.com/products/catia/portfolio/dymola.

[8] http://www.gtisoft.com/applications/a_Vehicle_driveline.php.

[9] https://www.modelica.org/libraries/PowerTrain.

[10] http://www.mathworks.com/products/simdrive/.

[11] http://www.ricardo.com/en-gb/What-we-do/Software/Products/VALDYN/.

[12] Kienke, U. and Nielsen, L. (2000) *Automotive Control Systems: For Engine, Driveline and Vehicle*. Springer, ISBN 3-540-66922-1.

7

Hybrid Electric Vehicles

7.1   Introduction

Conventional powertrain systems with a single power source based on fossil fuels have dominated vehicle design for the past decade. In recent years, however, fuel economy and pollution concerns have caused hybrid powertrain systems to be seen as one of the alternative approaches to powertrain design. Commercial interest in hybrid vehicle technology has grown at a much more dramatic rate than was predicted a decade ago. Around that time, many industry observers were substantially more optimistic about a major leap from current petroleum-based technology straight to hydrogen, fuel cells and biofuel systems. However, it is now widely accepted that hybrid vehicles will have a significant role to play over the next couple of decades as these other technologies continue to be developed.

The growth in interest in hybrid technology has been driven by increasing concerns about the environment and fuel efficiency savings. Petrol emissions in a car can release harmful gases into the air that can contribute to the 'greenhouse effect', damaging the environment's protective ozone layer and causing global warming. In addition, petrol is a limited natural resource with potential supply problems in future. Although hybrid vehicles are still reliant on petrol, they offer the flexibility to enhance the fuel economy and emissions of vehicles without sacrificing vehicle performance factors such as safety, reliability and other conventional vehicle features. This has prompted researchers to develop innovative hybrid powertrain configurations and generate design guidelines on component sizing and control strategies.

Hybrid electric vehicles attempt to combine the benefits of petrol engines and electric motors – the engine provides most of the vehicle's power, and the electric motor provides additional power when needed for accelerating and overtaking. This allows a smaller, more efficient internal combustion engine to be used and to be operated near its optimal efficiency range. The electric power for the electric motor is generated not only from the engine but also from regenerative braking that converts otherwise wasted energy from braking into electricity and stores it in the battery.

This chapter is aimed at providing an overall understanding of the main issues of hybrid drivetrains with special emphasis on the power flow and power management.

7.2   Types of Hybrid Electric Vehicles

A hybrid electric vehicle (HEV) is a vehicle fitted with an internal combustion engine and an electric motor. Hybrid vehicles can be designed in different types, a variety of technologies ranging from those using the internal combustion engine as major driving power and those using the electric motor as the main driving source (see Table 7.1). This makes it difficult to group hybrid vehicles into one category and it is

Table 7.1 Range of hybrid vehicles

Conventional vehicle	Hybrid vehicles			Pure electric vehicle
	Motor assist vehicle	Hybrid electric vehicle	Plug-in electric vehicle	

possible that more diversified hybrid vehicles will be developed in the future, as hybrid technologies mature.

7.2.1 Basic Classification

Hybrid vehicles are traditionally divided into two basic types, namely *series* and *parallel*, based on the way the two power sources are utilized in the vehicle. In the series type, the vehicle is mechanically driven by an electric motor and the internal combustion engine is used to produce electric energy. In the parallel type, the mechanical power is delivered to the wheels by either the IC engine or electric motor alone or by both together.

7.2.1.1 The Series Hybrid

In a series hybrid vehicle, an electric motor is responsible for propelling the vehicle. The necessary electric energy is basically produced by a generator that is mechanically driven by an IC engine. Thus, in this type of hybrid system, the main energy source is still the fossil fuel that is used by the IC engine and is transformed into the electric energy that is either stored in the battery pack or directly drives the electric motor that propels the vehicle. This means that in this type of hybrid vehicle the installed IC engine does not drive the vehicle directly and mechanically.

Figure 7.1 illustrates a typical series hybrid configuration in which the main components can be distinguished. The mechanical power from the engine (ICE) drives a generator (G) and the resulting electric current is rectified, and through an electronic converter it is used to either charge the battery pack (B) or drive an electric motor (MG) that can also work as a generator. The motor is controlled by a power electronic device called a motor controller (MC). The mechanical power produced by the motor usually drives the vehicle through a torque amplification device (TAD) attached to the wheels (e.g. a transmission, reduction gear or final drive).
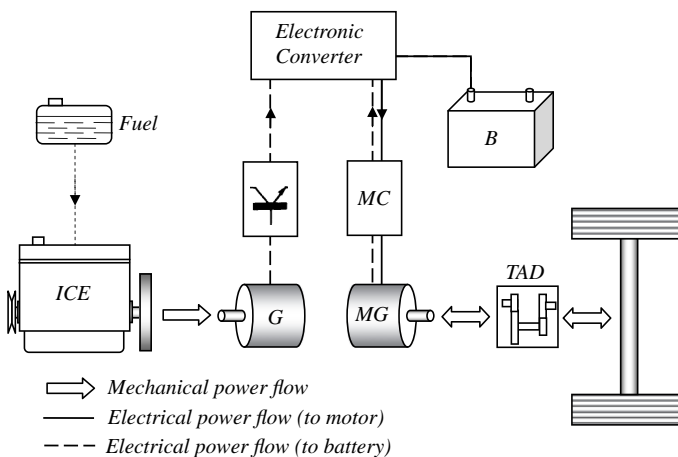
Figure 7.1 A typical series hybrid configuration

It can be argued that the conversion of the IC engine's mechanical power to electrical power and then back to mechanical power will result in more power losses compared with a conventional vehicle with similar engine. This is in general true, however, there are two reasons that might make the series hybrid more efficient than a conventional vehicle. One is the regenerative power obtained from the vehicle kinetic or potential energy (e.g. braking or gravitational forces). The other benefit of the series hybrid vehicles is the independence of the engine operation on the instantaneous vehicle load and speed which allows the engine to work under its most efficient conditions. However, the drawback of the series hybrid vehicle is its large electric motor that is the only source of traction and must generate the total motive force for the vehicle.

The regenerative power is obtained from the electrical power generated by the MG when it is driven by the wheels during braking or downhill travel. The MG acts as a generator, and the electric current (dashed line in Figure 7.1) is absorbed by the battery pack if it is not already fully charged. This two-way mechanical energy flow is shown by the double-ended arrows of Figure 7.1.

7.2.1.2 The Parallel Hybrid

The parallel hybrid type with the example configuration shown in Figure 7.2 uses two different mechanical power flows to propel the vehicle. The mechanical power of either of the two sources can drive the wheels individually or the two sources can work simultaneously and *in parallel*. The connection of the two mechanical powers is performed in a distributing device MPD that controls the split of power in different ways. The mechanical power from the engine can be fully supplied to the driving wheels or at the same time to the MG (in generator mode). The mechanical output of the MG (in motor mode) alone, can be sent to the wheels or it can be added to the output of the ICE. In regenerative mode, the mechanical power from the wheels drives the MG (in generator mode) and the electrical energy supplied to the battery. In other words, in a parallel hybrid system the mechanical system must incorporate a power-combining device and a regeneration scheme so that the vehicle can be propelled by any combination of the two sources and so that the battery can be recharged either by the engine or by the kinetic energy of the vehicle.

One benefit of the parallel hybrid layout is the lower energy conversion losses since, unlike the series configuration, engine power is directly transferred to the driving wheels. However, the direct connection of the engine to the wheels can also be regarded as a disadvantage due to the associated transient engine operation in inefficient working conditions. In addition, the direct connection of engine to the driving
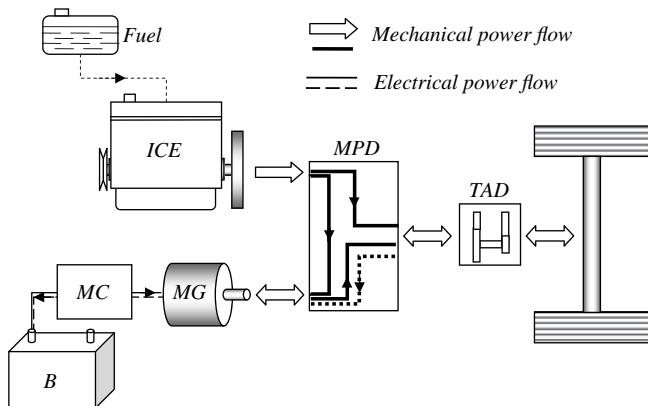
Figure 7.2 A typical parallel hybrid configuration

wheels requires a transmission that was absent in the series case. In terms of electric components, in this case, only one MG is used whereas in series configuration there was an additional generator.

7.2.2 Basic Modes of Operation

Both series and parallel hybrid electric vehicles provide several modes of operation depending on the availability of the power sources. The central philosophy in using different modes of operation is to keep the energy usage as low as possible. To this end, therefore, the goal would be the optimal use of the three sources of energy (fossil fuel, battery and vehicle mechanical energy). Typically when the vehicle is started, the ICE is off and the electric energy acts as driving source. The ICE takes over to power the vehicle at cruising speeds and during heavy accelerating or when additional power is needed, the electric energy is also used to propel the vehicle. When the vehicle is stopped for more than a certain period, the ICE is shut off automatically so that energy is not wasted in idling. In these cases the battery continues to power the accessory systems, such as the air conditioning and in-vehicle electrics.

The basic modes of operation can be listed as follows:

1. *Pure ICE (Engine-only) mode*: In this mode, the ICE produces the full power for vehicle motion and no power is used from the batteries.
2. *Pure electric (Electric-only) mode*: In this mode, the ICE produces no power (turned off) and the full power for vehicle motion is taken from the batteries.
3. *Hybrid mode*: The power for vehicle motion in this mode is taken simultaneously from both ICE and batteries.
4. *ICE plus charging mode*: In this mode of operation, the ICE not only produces the power for vehicle motion, but also to recharge the battery.
5. *Regeneration mode*: The kinetic energy of vehicle during braking (or its potential energy during downhill motion) can be used to turn the electric motors and produce electricity. Using energy from the wheels to turn the motor slows the vehicle down. This energy is produced when the battery can accept it and is stored for later use in electric or hybrid mode. In this mode, the ICE is off and the battery is charged by the MG in its generator mode.
6. *Charging mode*: There are cases when the vehicle is at a standstill and no power is used for its motion. In these circumstances if the battery needs recharging, then the ICE is turned on to power the generator and charge the battery.
7. *Hybrid charging mode*: In this case the battery needs more recharging energy than is available through regeneration and the ICE generator units will also contribute to producing electricity during braking.

Table 7.2 summarizes the modes of operation for both series and parallel hybrid types and the components that participate in each mode.

Table 7.2   Component participation in different operation modes

Mode	Title	Series Hybrid			Parallel Hybrid	
		ICE	G	MG	ICE	MG
a	Pure ICE	✓	✓	✓	✓	-
b	Pure electric	-	-	✓	-	✓
c	Hybrid	✓	✓	✓	✓	✓
d	ICE + charging	✓	✓	✓	✓	✓
e	Regeneration	-	-	✓	-	✓
f	Charging	✓	✓	-	✓	✓
g	Hybrid charging	-	✓	✓	-	✓

7.2.3   *Other Derivatives*

The parallel configuration provides more flexibility in allowing various power flow schemes between the two mechanical power generators. On the other hand, the series configuration also offers some benefits, as discussed earlier, thus combining the two layouts potentially creates even more design opportunities for hybridization.

Many types of hybrid designs have been developed which incorporate the basic concepts discussed earlier, combined with distinct concepts for motive force and power management. No agreed classification for the hybrid designs is available and in most cases a variety of commercial terms is also used. Some types are identified by their technical layout and some by the way in which they use the electric energy. The former types will be considered in the current section and the latter concepts will be discussed in a later section.

7.2.3.1   **Series-Parallel Hybrids**

A series-parallel hybrid (SPH) configuration is the most common layout in which the benefits of both series and parallel layouts are integrated into a combined system. In an SPH the vehicle must be able to run in both series and parallel modes. In series mode, the traction is produced by the electric motor and the engine power is only used to recharge the battery. For this reason, a generator must be included in the design.

In parallel modes, the IC engine and electric motor can either work independently or together. In addition, the IC engine can contribute tractive power as well as recharging the battery. This combination takes advantage of the efficiency range of the electric motor in the vehicle's low speed range, and the IC engine works in the higher speed ranges of vehicle motion.

Various layouts can be found for the SPH configuration depending on the mechanical power distribution (MPD) system involved. The mechanical power distributor can be used to combine the mechanical power of the ICE and MG as well as splitting the power for generator use as shown in Figure 7.3. Alternatively, the MPD can be used between the ICE and generator, while connecting the motor directly to the driveline. The torque amplification device (TAD) such as a transmission or reduction gear can be placed either before or after the MPD.
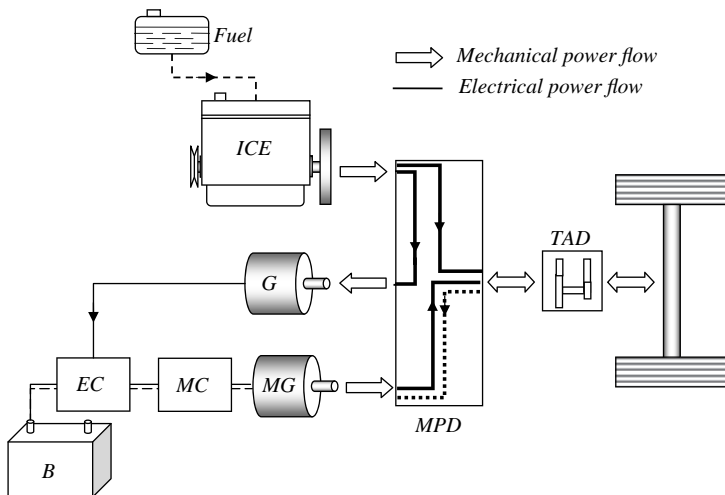
Figure 7.3   A typical series-parallel hybrid configuration

7.2.3.2 Power Split Hybrids

The series-parallel types of HEVs are also sometimes called power split hybrid systems, owing to the special transmissions used to combine the mechanical power from two power sources. Power split designs usually use two motor/generator (MG) units in their configurations in order to exercise sufficient control of both speeds and torques in the system. A combination of two MGs allows the engine to drive one of them as a generator to either charge the battery or supply power to the other motor.

Of the numerous power split transmission designs, two configurations known as single mode and dual mode power split transmissions have been commercially successful. The single mode term refers to the fact that there is only one way in which the power is split between the mechanical and electrical paths. A dual mode arrangement has more than one epicyclic gear unit and introduces clutches into the drivetrain which can be used to change the power flow through the system.

The Toyota Hybrid System (THS) is used in cars such as the Prius and Camry hybrid models and its power split device (PSD) enables the engine to operate at its efficient regions, independent of the vehicle speed and in fact it provides an electronically controlled transmission with continuously variable gearing. The power split device, which is a planetary (or epicyclic) gear unit (see Section 7.3), controls the ratio of power going directly to the wheels and to the generator in a continuously variable way (see Figure 7.4). Consequently, there are still energy conversion losses due to the transmission efficiency.

The FHS system, developed by Ford, Volvo and Aisin (Figure 7.5), is very similar to the THS except that one of the MG units is connected to the epicyclic planetary gear via an additional set of 'output gears'. An alternative version of the single mode design by NexxtDrive (Figure 7.6), employs two epicyclic gears in conjunction with two MG units. This arrangement offers potential efficiency benefits over the single planetary gear systems because there is more flexibility in controlling the balance of power flows through the mechanical and electrical branches. It has an important benefit of providing two points at which the electrical path transmits zero power, and therefore incurs no losses [1].

The GM Allison design (AHS) is based on a dual mode arrangement (Figure 7.7) that uses two epicyclic gear units and two clutches. One of the modes remains exactly the same as for the single mode system but the other – the compound split mode – effectively splits the input power into two paths and then recombines them at the second epicyclic unit. A GM/Daimler Chrysler/BMW consortium has released a dual mode system with the arrangement shown in Figure 7.8, offering four fixed gear ratios. It incorporates three epicyclic gear units, linked together via clutches, and although it appears rather complex at first sight, it nevertheless only involves the mechanical content and overall size associated with a modern, multispeed automatic transmission.
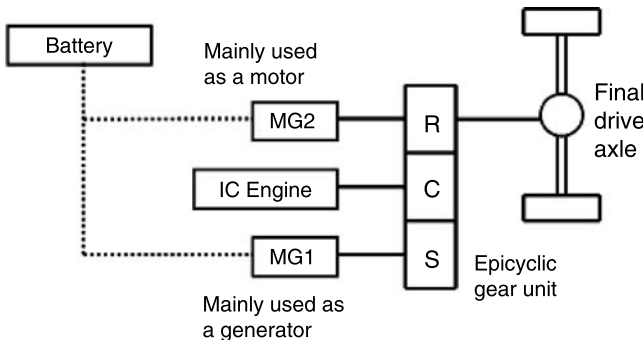
Figure 7.4   Toyota Prius, THS arrangement
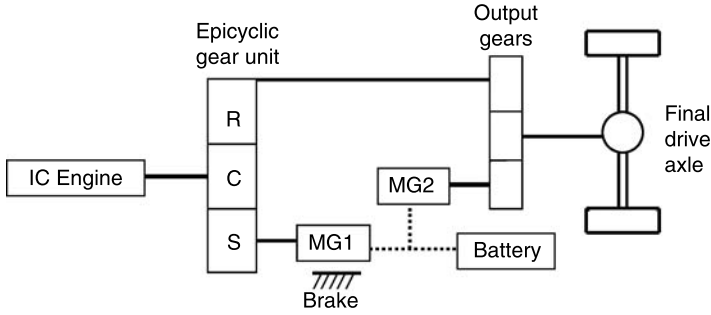
Figure 7.5 Ford, Volvo, Aisin, FHS arrangement
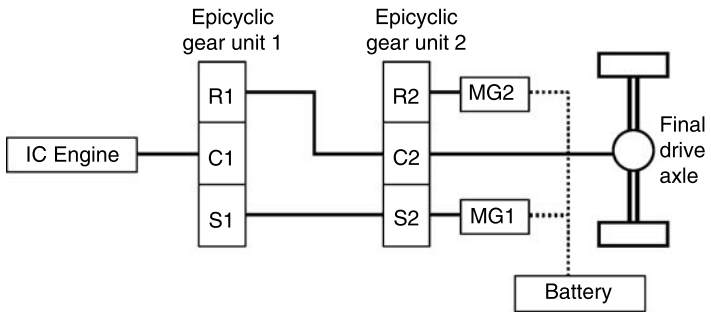
Figure 7.6 NexxtDrive arrangement

7.2.3.3 Plug-In Hybrids

Electric vehicles (EVs), that use a battery as the only source of energy, must plug into the electric grid to recharge their batteries. HEVs rely on the energy from fossil fuels and their batteries are charged by a generator driven by the ICE. A hybrid vehicle that can also receive electric power from the grid to charge its batteries is called a 'plug-in hybrid electric vehicle' or PHEV in short. The size of the battery defines the vehicle's range that can be achieved in electric mode. Therefore, PHEVs need larger battery packs when compared to other HEVs in order to increase their battery working range. In addition to increasing the battery capacity, modification to the vehicle controller and energy management
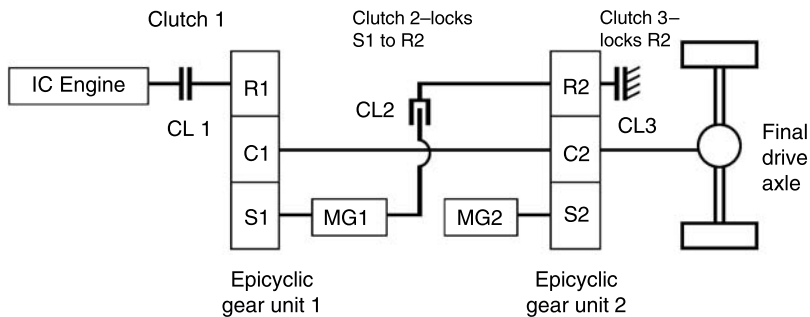
Figure 7.7 GM Allison AHS arrangement
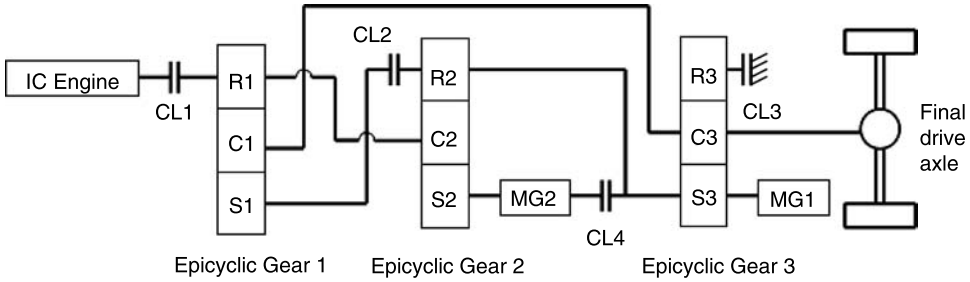
Figure 7.8 GM/Daimler Chrysler/BMW power split arrangement

system is also necessary. Additionally, owing to lower electricity costs during night time, recharging the battery at night will be advantageous not only to the vehicle owners, but also to the electricity providers.

7.2.4 Degree of Hybridization

In an electric hybrid vehicle with two different power sources, the balance between the sources can be quantified by a simple criterion defined as the degree of hybridization (DOH):

$$DOH = \frac{P_E}{P_T} \tag{7.1}$$

in which P_E and P_T are the electric and total installed powers. The electric installed power refers to the maximum power of the electric motor(s) and the total power is the sum of the maximum engine power (P_{ICE}) and motor power. Typical variations of the DOH for different engine and motor powers are illustrated in Figure 7.9. Different definitions may also be found in the literature such as the ratio of motor power to ICE power (P_E/P_{ICE}) which results in higher DOH values.

A different way of classifying HEVs is simply to refer to those utilizing the highest DOH values as full hybrids and those with small values of DOH as light (or micro) hybrids. HEVs with average DOH values are categorized as mild hybrids. In this type of classification, the architectures of hybrid vehicles are not important and so two hybrid vehicles with similar layouts may fall into different categories according to their DOH values. Nonetheless, no specific figures have been agreed for the three hybrid categories and designation of a vehicle into them remains a matter of choice.

7.2.4.1 Full Hybrids

A large degree of hybridization in a full hybrid electric vehicle means that a large electric motor must be used. But this is not the only requirement since a full hybrid needs to allow 'electric-only' driving which means the battery must also be large enough for this purpose. In addition, the full hybrid designs provide a full range of hybrid operations including engine start-stop, regenerative braking and motor assist motion.

7.2.4.2 Mild Hybrids

HEV designs with a lower degree of hybridization, even with a similar architecture to that of full parallel hybrids, are often regarded as mild hybrids. In a mild hybrid, only the engine is responsible for moving the vehicle, however, at high loads the motor(s) can assist the engine in producing the motive force. Therefore, mild HEV designs provide engine start/stop, electric assist driving and even regenerative braking, but do not allow driving with the electric motor only.
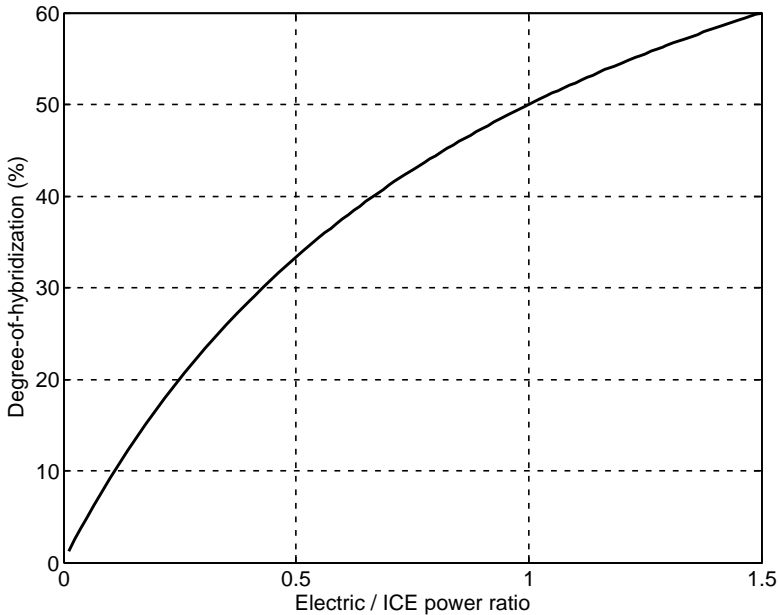
Figure 7.9   The variation of the DOH with electric to engine power ratio

7.2.4.3   Light/Micro Hybrids

A light hybrid is an HEV with an oversized starter motor that can also be used as a generator, usually called an integrated starter-generator (ISG) or a belted alternator starter (BAS). The ISG must be capable of acting as a motor to crank the engine and drive the belt-driven accessories when the engine is off. Recharging the battery can also be done by the ISG at low engine loads.

Light hybrids are capable of stop/start and regenerative charging functions. Shutting the engine off whenever the vehicle is not moving improves the fuel economy by a few percent. The implementation of a mild hybrid on a vehicle requires only small modifications including a larger electric motor generator and an oversized battery together with simple power electronics.

The term 'micro hybrid' is used to differentiate some vehicles in the mild family. In fact, a micro hybrid vehicle is the simplest kind of HEV with very low DOH. The most common definition for a micro hybrid vehicle is a 'start-stop system' in which the IC engine is turned off when the vehicle pulls to a stop, and is restarted when the driver accelerates. Like mild hybrids, ISG systems are used and thus similar functions are available. Some micro hybrids, in addition to the start-stop function, use some degree of regenerative braking to charge the battery.

Figure 7.10 compares the four types of HEVs in terms of their functionalities. It should be noted that in general, hybrid vehicles lie in a spectrum between micro and full hybrids and it is sometimes hard to differentiate between the two neighbouring types.

7.3   Power Split Devices

The transmission design has been a crucial issue in the success of hybrid vehicles. Specific types of transmissions, also often referred to as power split devices (PSD), are of particular importance. A PSD is a mechanical device that makes it possible to control the power share between the ICE and electric motor(s)

Figure 7.10 Comparison of basic functions among different hybrid types

in a hybrid system. In Section 7.2.3.2 it was briefly explained how the power split hybrids are categorized (see Figures 7.4 to 7.8). In this section, the functioning of a PSD will be discussed in more detail.

7.3.1 Simple PSD

The simplest PSD mechanism is the planetary gear system (or epicyclic system) which has three input/output shafts (see Section 4.4.2). This mechanism, that is widely used in conventional automatic transmissions, is used by Toyota as a power split device in their THS hybrid systems (see Figure 7.4). Figure 7.11 illustrates a typical epicyclic gear set in a schematic form as well as a simplified 'stick diagram'.

In the THS system, the engine output shaft is directly connected to the carrier C, motor/generator number 1 (MG1) is connected to the sun S and motor/generator number 2 (MG2) is connected to the Ring R. Denoting the angular speeds of engine, MG1 and MG2 as ω_e, ω_1 and ω_2 respectively, the kinematic relationship among the three angular speeds is (Equation 4.90):

$$(N_S + N_R)\omega_e = N_S\omega_1 + N_R\omega_2 \tag{7.2}$$

According to the free body diagrams of gears in an epicyclic set (Figure 7.12), the quasi-static relations among the torques applied at input/outputs are (the dynamic and frictional effects are ignored):
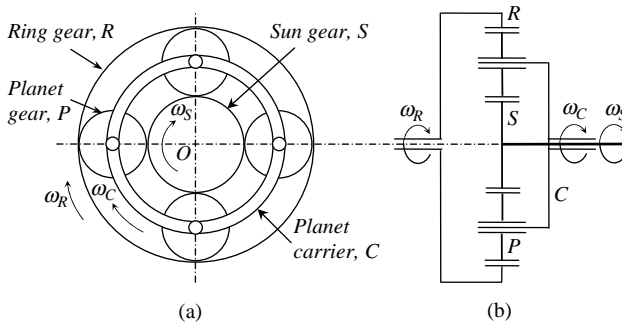
Figure 7.11 A typical planetary gear set (a) schematic and (b) stick diagram
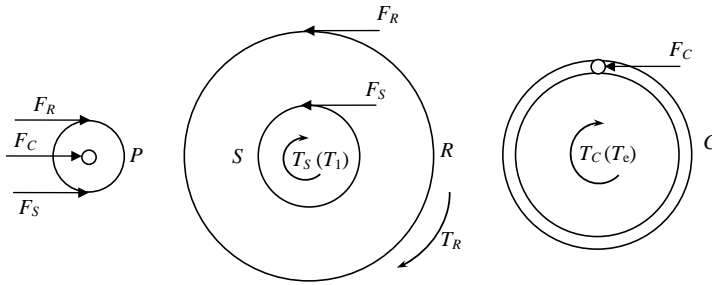
Figure 7.12   Free body diagrams of epicyclic gear components

$$T_R N_S = T_1 N_R \tag{7.3}$$

$$T_1 = -\frac{N_S}{N_S + N_R} T_e \tag{7.4}$$

$$T_R = -\frac{N_R}{N_S + N_R} T_e \tag{7.5}$$

The minus signs in Equations 7.4 and 7.5 imply that the torque equilibrium cannot be obtained with three torques applied in the clockwise direction as shown in Figure 7.12. If T_e is applied counter-clockwise, equilibrium is obtained.

Summing Equations 7.4 and 7.5 leads to:

$$T_C + T_S + T_R = 0 \tag{7.6}$$

which is an obvious conclusion since the PSD system is at equilibrium under the action of the external torques. In terms of engine and motor torques:

$$T_e + T_1 + T_R = 0 \tag{7.7}$$

7.3.1.1   Speed Constraints

Equation 7.2 is the governing relation between the three speed components in a simple PSD system. These three speeds are in fact physical parameters of the vehicle motion and are related to the engine, motor and vehicle speeds. It is clear that Equation 7.2 is acting like a constraint on the speeds of the main vehicle components and does not allow each speed component to vary independently.

On the other hand, the engine and two motors/generators each have speed limitations. The engine can work only in one direction from idle speed up to its limiting speed, whereas the two motors/generators work in both directions from their lower (negative) up to upper (positive) limiting speeds.

The constraint imposed by Equation 7.2 is representative of an inclined line connecting the three speeds ω_e, ω_1 and ω_2 placed at relevant geometric locations. Figure 7.13 illustrates this geometry together with limitations for the speeds of components. The three vertical lines from left to right represent the axes for the speeds of MG1, engine and MG2 respectively, drawn at relative distances proportional to N_R and N_S. Two possible working lines are included in Figure 7.13 to clarify the concept. The following example uses numerical values for the parameters.

As the speed of the MG2 can vary continuously, the vehicle speed which is proportional to this speed will also vary accordingly. Therefore, this type of PSD acts like a continuously variable transmission (CVT).
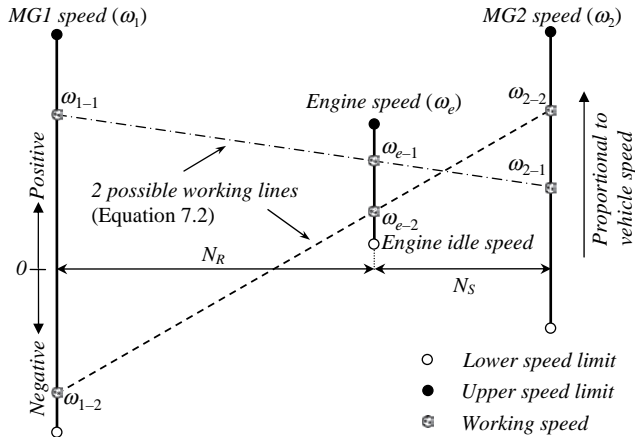
Figure 7.13   Speed constraints in a simple PSD system

Example 7.3.1

In a PSD the tooth numbers for the ring and sun gears are 78 and 30 respectively. The ring gear is directly connected to the shaft of MG2 and to the driving wheels through a reduction gear with overall ratio of $n_f = 4$. For a wheel radius of 30 cm, find the speeds of MG1 and MG2:

(a) if the vehicle is at rest and the engine is off;
(b) if the vehicle is at rest and the engine is at idle (1000 rpm);
(c) if the vehicle is moving forward at 60 km/h and the engine is at idle;
(d) if the vehicle is moving forward at 160 km/h and the engine is at 4000 rpm.

Solution

According to Equation 7.2, the relation of MG1 rotational speed with engine and MG2 speeds is:

$$\omega_1 = \left(1 + \frac{N_R}{N_S}\right)\omega_e - \frac{N_R}{N_S}\omega_2$$

On the other hand, the speed of MG2 is directly related to the vehicle speed:

$$\omega_2 = \frac{n_f}{r_W}v$$

Substituting in the first relation and using the given information results in:

$$\omega_1 = 3.6\omega_e - 91.956v$$

Table 7.3 Numerical results of Example 7.3.1

Case	ω_e(rpm)	v (km/h)	ω_1(rpm)	ω_2(rpm)
a	0	0	0	0
b	1000	0	3600	0
c	1000	60	−1917	2122
d	4000	160	−313	5659

in which ω_e and v are in rpm and km/h respectively. The numerical results for the four cases are summarized in Table 7.3.

This constraint causes some limitations on the operation of components, for example, the engine, as it forces them to work at a specific speed. For instance, at low vehicle speeds, the engine cannot work at its highest speed. The speed limit for the engine is dictated by the speed of the MG1. At the highest speed for the MG1, the engine speed will be located below its maximum speed as shown in Figure 7.14. The relation for this limiting speed is:

$$\omega_{e_{Max}} = \frac{1}{N_S + N_R}\left(N_R\omega_2 + N_S\omega_{1_{MAX}}\right) \tag{7.8}$$

7.3.1.2 Power Flow

It is a simple task using Equations 7.2 to 7.5 to show that:

$$T_e\omega_e + T_1\omega_1 + T_R\omega_R = 0 \tag{7.9}$$

or simply:

$$P_e + P_1 + P_R = 0 \tag{7.10}$$

This demonstrates the conservation of power and at the same time the power splitting feature of the device. The power received by the vehicle is the summation of the engine and battery power minus the lost power:

$$P_V = P_e + P_B - P_L \tag{7.11}$$

Assuming no power losses (the inclusion of power losses is considered in Problem 7.2), the total power delivered to the wheels is the summation of PSD output and MG2 power (see Figure 7.4):

$$P_V = -P_R + P_2 \tag{7.12}$$
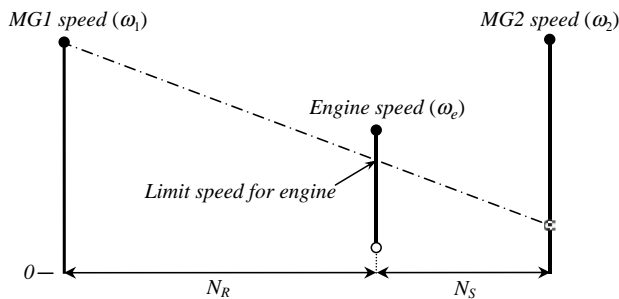
Figure 7.14 Speed limit for engine at low vehicle speeds

The minus sign for P_R is necessary to adjust its torque sense with its rotation. Substituting from Equation 7.10 will result in:

$$P_V = P_e + P_1 + P_2 \tag{7.13}$$

$$P_B = P_1 + P_2 \tag{7.14}$$

According to Equation 7.11 if the vehicle power P_V is larger than the engine power P_e, the battery is also transmitting power through MG1 or MG2 (Equation 7.14). Conversely, if P_e is larger than P_V, then MG1 or MG2 act in generator mode and receive power from the engine to recharge the battery. It is important to note that we have assumed the PSD output shaft (ring gear R) is directly connected to MG2 and thus only the speed of MG2 is identical to the output speed of PSD and its torque T_2 is independent of PSD output torque T_R.

Example 7.3.2

For the vehicle in Example 7.3.1, the resistive force on a level road is given by $F_R = 300 + 0.25v^2$ (v in m/s). The engine is working at full throttle and its torque-speed curve is given by:

$$T_e = -4.45 \times 10^{-6}\omega_e^2 + 0.0317\,\omega_e + 55.24, \quad 1000 < \omega_e < 6000\,\text{rpm}$$

For the case (d) in Example 7.3.1, assume the vehicle is at a steady motion.

(a) Calculate the torque and power of each component.
(b) Specify the direction of flow of power in the system.

Solution

(a) Since the speed is steady, the torque acting on the common shaft of the ring gear and MG2 at the given speed is:

$$T_O = \frac{F_R r_W}{n} = \frac{(300 + 0.25v^2)r_W}{n} = 59.537\,\text{Nm}$$

From the engine torque equation at the given rpm we obtain $T_e = 110.84$ Nm. From Equation 7.5 the PSD output torque can be determined: $T_R = -80.051\,Nm$.

  The minus sign indicates that the direction of engine rotation is opposite that of MG2. The torque of engine is larger than what is needed and the extra torque at output shaft ($80.051 - 59.537 = 20.514$) is absorbed by MG2. The torque of MG1 from Equation 7.3 is -30.79 Nm.

  The power of each component is simply its torque multiplied by its speed:

$$P_e = 110.84 \times 4000 \times \frac{\pi}{30} = 46{,}429W$$

$$P_1 = -30.79 \times (-313) \times \frac{\pi}{30} = 1009W$$

$$P_2 = -20.514 \times 5659 \times \frac{\pi}{30} = -12{,}156W$$

Since the rotating direction of MG2 is different from its torque direction, it is in generator mode and has a negative power.

(b) Vehicle power demand P_V is equal to: $P_V = F_R v = 35,281\,W$.

   The engine power is greater than the demand power, therefore, the battery is charged with power $P_B = P_V - P_e = -11,147\,W$ (Equation 7.11). In fact, MG2 takes $12,156\,W$ of engine power and delivers it to the battery. MG1, on the other hand, works in motor mode and receives $1,009\,W$ of battery power. The balance of power towards the battery, therefore, is $P_B = -12,156 + 1,009 = -11,147\,W$ as Equation 7.14 indicates.

7.3.1.3   Power Circulation

In the 'engine-only' mode no power is received from the battery, nevertheless owing to speed dependencies through the PSD, the engine power cannot be delivered directly to the driving wheels. In such circumstances MG1 and MG2 will either work as generators or motors. This causes mechanical power to be transformed into electrical power and back again by the two electrical machines. In Example 7.3.2 we observed the circulation of $1009\,W$ of power.

   Figure 7.15 illustrates two possible cases for the power circulation in 'engine-only' mode. In Figure 7.15a a fraction of the mechanical power from the engine is taken by MG1 and converted to electrical energy that is received by MG2 and converted in mechanical energy and delivered to the driving wheels. Figure 7.15b shows the power circulation in the opposite direction.

   For the cases of 'engine-only' mode shown in Figure 7.15a, the circulating power P_{Cir} is equal to the power of MG1 for case (a) and the power of MG2 for case (b). If no power loss is considered for this mode of operation, then P_B vanishes and from Equation 7.14:

$$P_{Cir} = |P_1| = |P_2| \tag{7.15}$$

Making use of Equations 7.5 and 7.9 will result in:

$$\frac{P_{Cir}}{P_e} = \left| 1 - \frac{N_R}{N_R + N_S} \frac{\omega_2}{\omega_e} \right| \tag{7.16}$$

The variation of power circulation ratio P_{Cir}/P_e versus speed ratio ω_2/ω_e for the gear numbers of Example 7.3.1 is depicted in Figure 7.16.
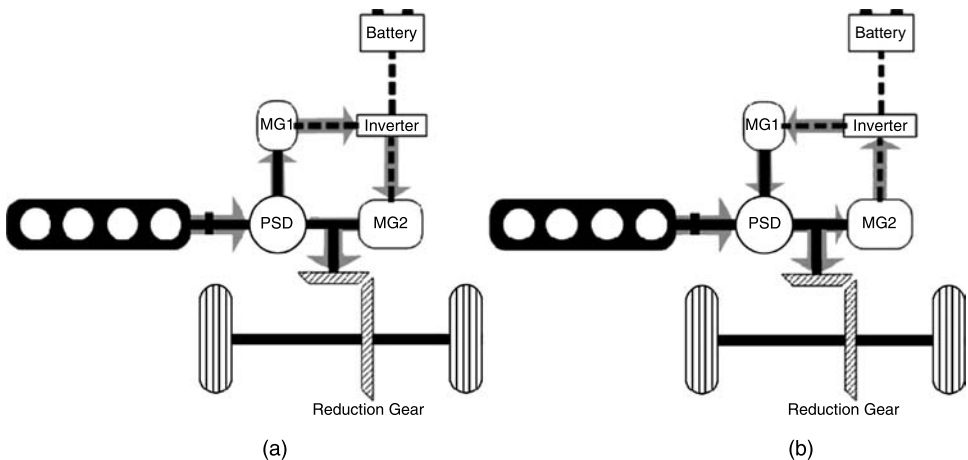
Figure 7.15   Power circulation
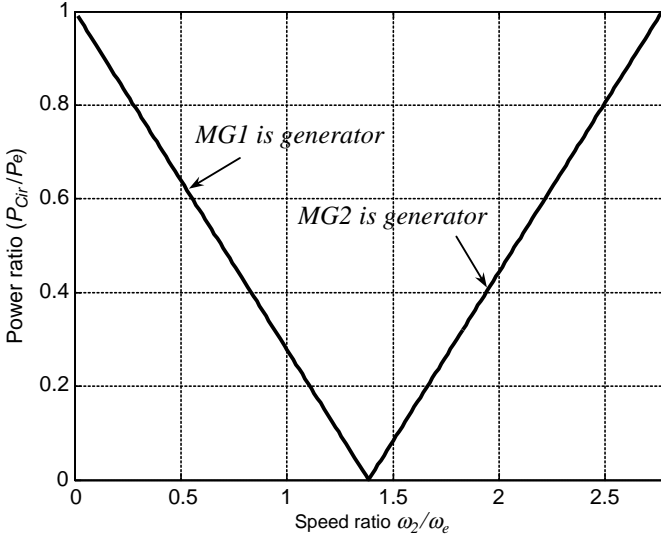
Figure 7.16   Variation of power circulation ratio with speed ratio

It is obvious that in practice, power circulation will generate power loss due to inefficiencies involved in converting between mechanical power and electrical power.

Example 7.3.3

For the vehicle in Example 7.3.2 with 1500 kg mass, the engine is working at full throttle and the vehicle is accelerating at a speed of 120 km/h. Assume no power losses and for 'pure-engine' mode:

(a) Calculate the vehicle acceleration.
(b) Determine the power circulation of the system using component powers.
(c) Determine the power circulation using Equation 7.16.

Solution

(a) For maximum acceleration, the engine must work at maximum torque. From the engine torque equation we obtain: $T_e = 111.7 \, \text{Nm}$ and $\omega_e = 3562 \, \text{rpm}$.

Since no power is taken from the battery, the total power demand of the vehicle is produced by the engine, thus: $F_T = \frac{T_e \omega_e}{v} = 1250 \, \text{N}$. Vehicle acceleration therefore is:

$$a = \frac{F_T - F_R}{m} = 0.45 \, \frac{m}{s^2} \, .$$

(b) The torque acting on the common shaft of ring gear and MG2 is:

$$T_O = \frac{F_T r_W}{n} = 93.737 \, \text{Nm}$$

According to the procedure explained in Example 7.3.1, the torques and speeds are obtained as:

$$T_1 = -31.026 \text{ Nm}, \quad T_R = -80.668 \text{ Nm}$$
$$\omega_1 = 1787.7 \text{ rpm}, \quad \omega_2 = 4244.1 \text{ rpm}$$

The output torque of the PSD (T_R) is less than the total output torque (T_O). The balance is the torque of MG2:

$$T_2 = 93.737 - 80.668 = 13.069 \text{ Nm}.$$

The component powers are:

$$P_1 = -5.8\,kW, P_2 = 5.8\,kW \text{ and } P_{Cir} = 5.8\,kW$$

which indicates that MG1 and MG2 are acting as the generator and motor respectively.

(c) The speed ratio in Equation 7.16 is 1.1916 and the right-hand side is:

$$1 - \frac{N_R}{N_R + N_S} \frac{\omega_2}{\omega_e} = 0.1394 \text{ and } P_{Cir} = 5.8\,kW.$$

7.3.1.4 Maximum Driving Force

Assuming sufficient friction is available at the tyre contact area, the driving force of the vehicle results from the torque available at the driving wheels. The maximum torque delivered to the wheels is the summation of torques generated at the PSD output (T_R) and MG2 torque (T_2) multiplied by their gear ratios. Therefore, the torque delivered to the driving wheel with different gear ratios n_1 and n_2 for PSD output and for MG2 (see Figure 7.5) is:

$$T_W = n_1 T_R + n_2 T_2 \tag{7.17}$$

The output of the PSD in turn is the result of interaction between the engine torque and MG1 torque. Using Equation 7.5, we obtain:

$$T_W = \frac{n_1 N_R}{N_S + N_R} T_e + n_2 T_2 \tag{7.18}$$

For the case when the PSD output and MG2 are both on a single shaft, the available driving force is:

$$F_T = \frac{n_f}{r_W} \left(\frac{N_R}{N_S + N_R} T_e + T_2 \right) \tag{7.19}$$

Depending on the mode of vehicle operation, therefore, the maximum traction force varies. In battery-only mode, the engine is off and only T_2 will be present in Equation 7.19. In engine-only mode, however, due to power circulation, the T_2 term will still be present.

Example 7.3.4

The vehicle of Example 7.3.3 is accelerating at full throttle from a standstill with an engine idle speed of 1000 rpm. Other necessary information is provided in Table 7.4.

Table 7.4   Additional data for Example 7.3.4

Parameter	Description	Value	Unit
$T_{m\max}$	Maximum torque of MG2	400	Nm
r_{Wf}	Front axle weight ratio	0.6	–
μ	Tyre-road adhesion coefficient	0.9	–

Assume no power loss and for 'engine-only' mode, plot the variation of vehicle speed, acceleration, traction force, component torques and component powers versus time.

Solution

Solving this problem requires a large number of calculations and therefore it is helpful to write a program for it. The following comments are useful before starting to solve the problem:

1. Although the vehicle is in engine-only mode, the circulating power is present and both motor/generators are involved.

```
% Example 7.3.4 (Main program)

clc, clear all, close all

global m n rW k1 k2 Pcir T1 Tmmax FTmax

NR=78; NS=30;   % Tooth numbers
n=4;       % Final gear ratio
rW=0.3;    % Effective tyre radius
m=1500;    % Vehicle mass
Tmmax=400;   % Maximum motor torque
FWR=0.6;   % Front weight ratio
mio=0.9;   % Tyre-road adhesion coefficient
vm0=eps;    % Initial vehicle speed (m/s)
omega_e0=1000; % Initial engine speed (rpm)

FTmax=mio*FWR*m*9.81;  % Maximum tractive force
k2=NR/NS; k1=1+k2;     % See Example 7.3.1
omega_2=30*n*vm0/rW/pi; % See Example 7.3.1
omega_1=k1*omega_e0-k2*omega_2;% See Example 7.3.1

Te=-4.45e-6*omega_e0^2+0.0317*omega_e0+55.24;
TR0=-NR*Te/(NR+NS);     % Initial torque TR
T1=NS*T20/NR;           % Initial torque T1
Pe0=pi*Te*omega_e0/30;  % Initial engine power (Watt)
S_ratio=omega_2/omega_e0;
Pratio=abs(1-S_ratio*k2/k1);    % Equation 7.16
Pcir=-Pe0*Pratio*30/pi;    % W*30/pi is used also in the function
% Call function 'v_find' to integrate the dv/dt term (See Chapter 3)
[t,v]=ode45(@v_find, [0 20], vm0);
```

Figure 7.17   Main MATLAB® program listing for Example 7.3.4

```
% Example 7.3.4 (Main program) – Continued
% Now vehicle speed versus time is at hand and every other information
% must be reconstructed. This is done in following loop:
Pcir0=-Pe0*Pratio*30/pi;    % Initial value for circulating power
(W*30/pi)
T10=NS*TR0/NR;  % Initial value for MG1 torque
for i=1: length(v)
  vm=v(i);
omega_2(i)=30*n*vm/rW/pi;
omega_1(i)=Pcir0/T10;       % See comment 4
omega_e(i)=(omega_1(i)+k2*omega_2(i))/k1;
Te(i)=-4.45e-6*omega_e(i)^2+0.0317*omega_e(i)+55.24;
TR(i)=-k2*Te(i)/k1;
T1(i)=TR(i)/k2;
Pe(i)=pi*Te(i)*omega_e(i)/30;
FT(i)=Pe(i)/vm;     % See comment 3
if FT(i)>FTmax, FT(i)=FTmax; end    % Limit the traction force
Tout(i)=FT(i)*rW/n;     % Total torque on the PSD output shaft
T2(i)=Tout(i)+TR(i);    % Calculate MG2 torque (TR is negative)
if T2(i)>Tmmax          % Limit the MG2 torque
   T2(i)=Tmmax;
   Tout(i)=T2(i)-TR(i); % Equation 7.19
   FT(i)=n*Tout(i)/rW;     % Correct the tractive force
end

S_ratio=omega_2(i)/omega_e(i);
Pratio=1-S_ratio*NR/(NR+NS);
Pcir1(i)=Pe(i)*Pratio;     % Circulating power Equation 7.16
T10=T1(i);
FR=300+0.25*vm^2;       % Calculate the resistive force
a(i)=(FT(i)-FR)/m;      % Calculate acceleration
P1(i)=pi*T1(i)*omega_1(i)/30;  % MG1 power
PR(i)=pi*TR(i)*omega_2(i)/30;  % PSD output
power
P2(i)=pi*T2(i)*omega_2(i)/30;  % MG2 power
end

% Now plot the figures.
```

Figure 7.17   (*Continued*)

```
% Example 7.3.4 (Function)

function vdot=v_find(t,v)

global m n rW k1 k2 Pcir T1 Tmmax FTmax

vm=v;
omega_2=30*n*vm/rW/pi;
omega_1=Pcir/T1;
omega_e=(omega_1+k2*omega_2)/k1;
Te=-4.45e-6*omega_e^2+0.0317*omega_e+55.24;
```

Figure 7.18   MATLAB function program listing

```
Pe=pi*Te*omega_e/30;
S_ratio=omega_2/omega_e;
Pratio=abs(1-S_ratio*k2/k1);
Pcir=-Pe*Pratio*30/pi;
FT=Pe/vm;
FT(FT>FTmax)=FTmax;
Tout=FT*rW/n;
TR=-k2*Te/k1;
T1=T2/k2;
T2=Tout+TR; % Equation 7.17
if T2>Tmmax
  T2=Tmmax;
  Tout=T2-TR;
  FT=n*Tout/rW;
end
FR=300+0.25*vm^2;
vdot=(FT-FR)/m;
```

Figure 7.18   (*Continued*)

2. The initial condition of zero vehicle speed results in a zero speed for MG2 and thus at the start of calculations, MG2 cannot absorb and deliver the circulation power to the wheels. It can be assumed that the traction force is at its maximum at time zero.

3. Assumption of no power loss lets us use $F_T v = P_e$ at every instant (note that vehicle is in 'engine-only' mode).

4. ω_2 (= ω_m) is directly related to vehicle speed, whereas ω_1 must be determined from the circulating power (note that the circulating power is also equal to MG1 power).
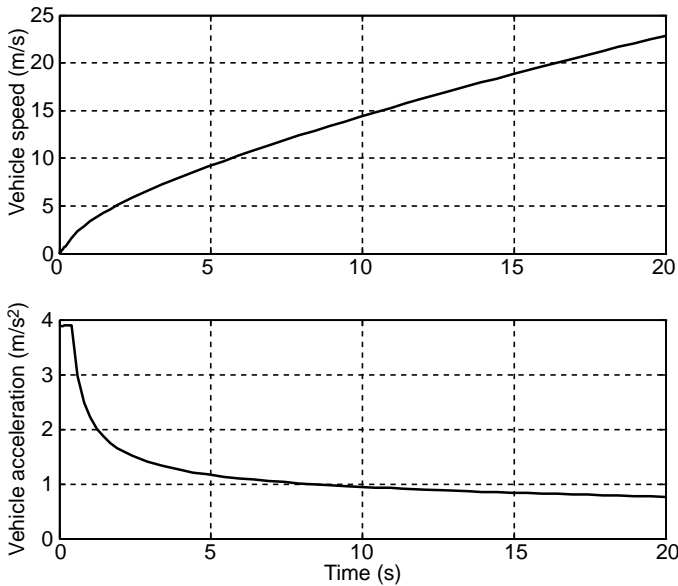
Figure 7.19   Variations of vehicle speed and acceleration
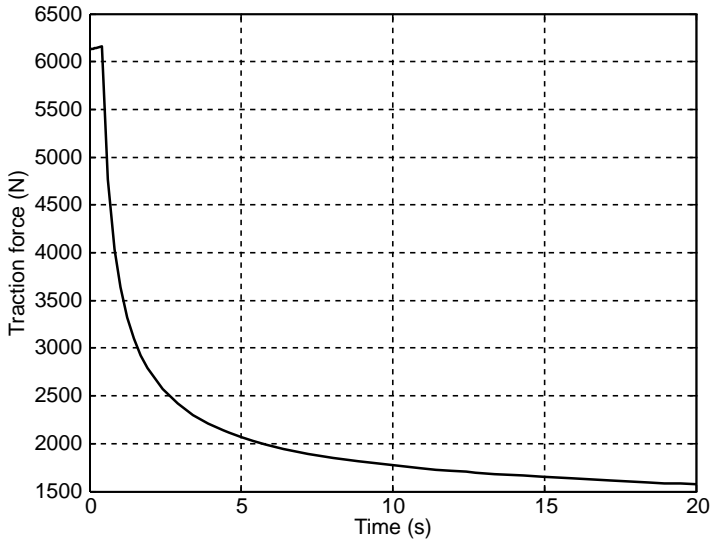
Figure 7.20 Variation of total vehicle tractive force

A MATLAB program is provided for the solution of Example 7.3.4 with listings given in Figures 7.17 and 7.18. The solution involves numerical integration to obtain the vehicle speed and for this reason a function named 'v_*find*' is shown in the main program. The comments are included in the programs to make them self-explanatory. Results are plotted in Figures 7.19–7.23.
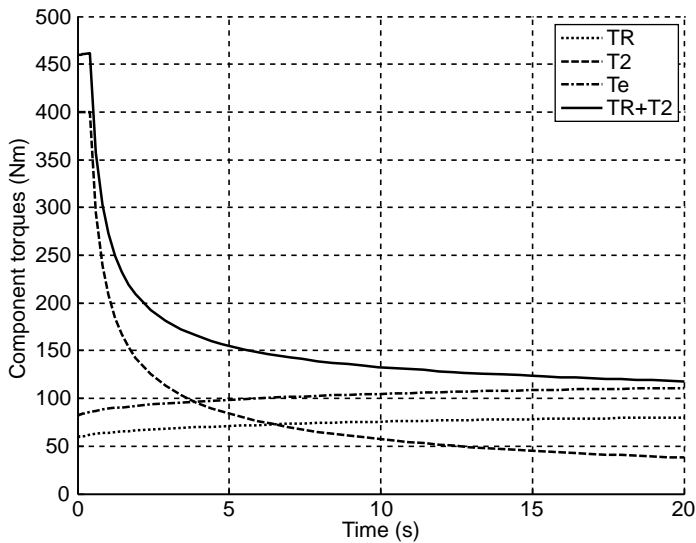
Figure 7.21 Variations of component torques
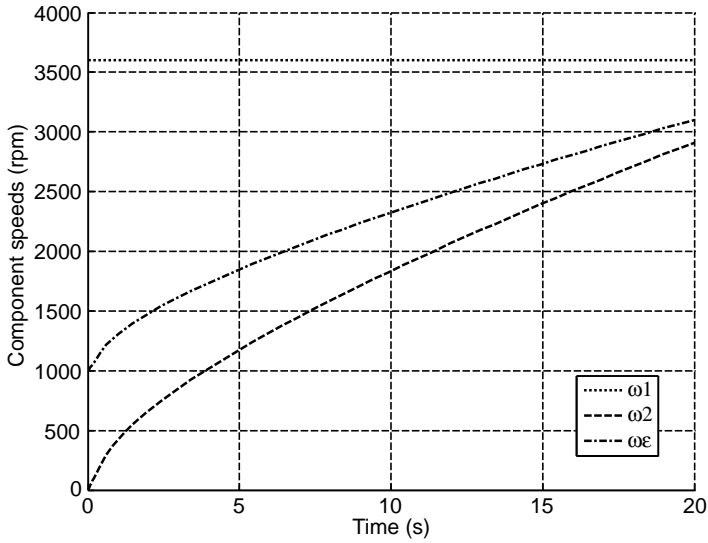
Figure 7.22   Variations of component speeds
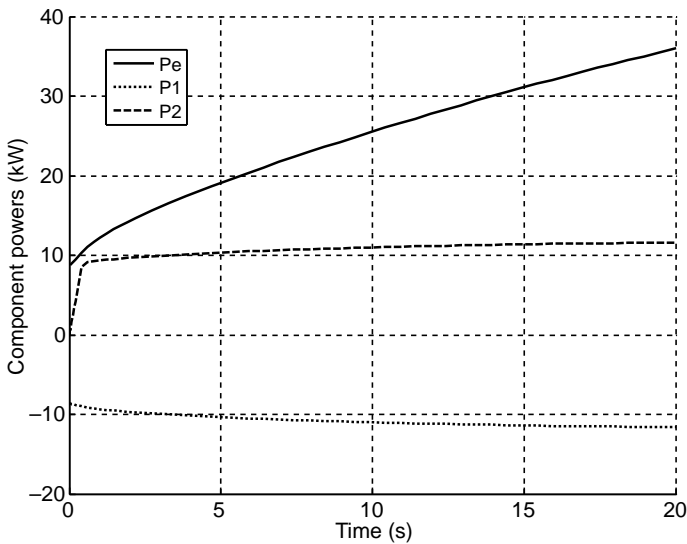
Figure 7.23   Variations of component powers

7.3.2   EM Compound PSD

The PSD system of Section 7.3.1, despite the simple construction, imposes limitations on the power management and operation of the vehicle. In Section 7.2.3.2 several types of PSDs were discussed. The objectives of new designs are to introduce more flexibility to the operation of the hybrid system and power flow schemes.
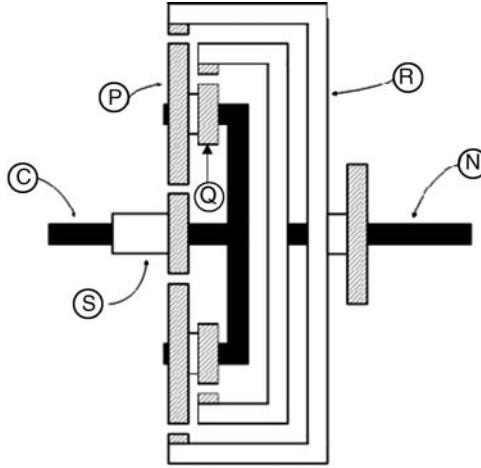
Figure 7.24 Layout of EM compound PSD

A PSD design, developed at Iran University of Science & Technology (IUST), is a compact device that is based on a planetary gear set and incorporates an additional input shaft for MG2. The layout of this device is called *easier management* or EM PSD (EM also stands for Emadi-Mashadi) is depicted in Figure 7.24 (also see [2]). An input shaft 'N' connected to a second ring gear is the additional feature of the simple planetary gear set.

Kinematic relationships for this device can be written as follows:

$$\omega_{MG1} = (1+m)\omega_e - m\omega_R \tag{7.20}$$

$$\omega_{MG2} = (1-n)\omega_e + n\omega_R \tag{7.21}$$

in which:

$$m = \frac{N_R}{N_S} \tag{7.22}$$

$$n = \frac{2mk_P}{2m + (k_P - 1)(m - 1)} \tag{7.23}$$

$$k_P = \frac{N_Q}{N_P} \tag{7.24}$$

Graphical representations of Equations 7.20 and 7.21 can be seen in Figure 7.25 for a PSD layout with $k_P < 1$ (like Figure 7.24). The two left and right vertical lines and the engine line constitute the Equation 7.20 which is exactly equal to Equation 7.2 of the simple PSD system. The three right-hand side vertical lines, on the other hand, represent the relation defined by Equation 7.21.

For values of k_P larger than unity, the two right-hand side vertical lines change over. At $k_P = 1$, the EM-PSD will be identical to the simple PSD.
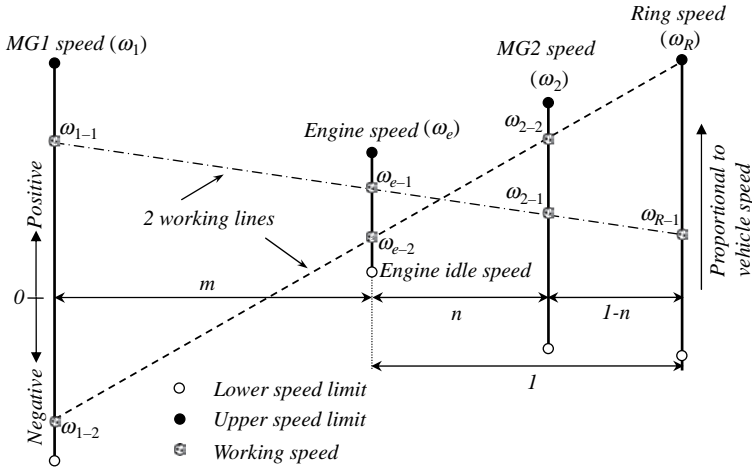
Figure 7.25   Speed constraints in EM PSD system

Example 7.3.5

Use the information of Example 7.3.1 and find the speeds of MG1 and MG2 for the four cases of the same example. Obtain the results for two cases with the radius ratio of small planet gear to the larger planet gear of $k_P = 0.75$ and $k_P = 1.5$.

Solution

Similar to Example 7.3.1, the speed of vehicle is directly related to the speed of PSD output which in this case is the ring gear R. The rotational speed of the ring gear is:

$$\omega_R = \frac{n_f}{r_W} v$$

According to Equations 7.20 and 7.21, the relations of MG1 and MG2 speeds with engine and ring gear speeds are available. So once the speed of ring gear from vehicle speed is calculated, the required speeds are easily found. The numerical results for the four cases are summarized in Table 7.5.

It can be seen that the speed values of MG1 are identical with those of Example 7.3.1.

Table 7.5   Numerical results of Example 7.3.5

Case	ω_e(rpm)	v (km/h)	$k_P = 0.75$		$k_P = 1.5$	
			ω_1(rpm)	ω_2(rpm)	ω_1(rpm)	ω_2(rpm)
a	0	0	0	0	0	0
b	1000	0	3600	187.5	3600	−300
c	1000	60	−1917	1912	−1917	2459
d	4000	160	−313	5348	−313	6157

7.3.2.1 Torque and Power

The quasi-static torque equilibrium of the device is of the form:

$$T_e + T_{MG1} + T_{MG2} + T_R = 0 \tag{7.25}$$

Assuming no power loss in the device results in:

$$P_e + P_{MG1} + P_{MG2} + P_R = 0 \tag{7.26}$$

Substituting from Equations 7.20 and 7.21 into Equation 7.26 leads to:

$$nT_{MG2} - mT_{MG1} + T_R = 0 \tag{7.27}$$

Then by using Equation 7.25, one obtains the following equations for the torques of MGs:

$$T_{MG1} = -\frac{n}{m+n}T_e + \frac{1-n}{m+n}T_R \tag{7.28}$$

$$T_{MG2} = -\frac{m}{m+n}T_e - \frac{1+m}{m+n}T_R \tag{7.29}$$

The total power demand from the vehicle motion is produced by the engine and the battery and in this case is only delivered through the main ring gear (see Figure 7.24):

$$P_V = P_e + P_B = -P_R \tag{7.30}$$

Substituting from Equation 7.26, the result is:

$$P_V = P_e + P_{MG1} + P_{MG2} \tag{7.31}$$

which leads to:

$$P_B = P_{MG1} + P_{MG2} \tag{7.32}$$

This confirms the fact that the exchange of power with the battery is performed by MG1 and MG2 together.

Example 7.3.6

For the vehicle and PSD of Example 7.3.5, repeat Example 7.3.2 and at a steady motion for the case (d) of Table 7.5:

(a) Calculate the torque and power of each component.
(b) Specify the direction of flow of power in the system.

Solution

(a) The torques acting on the shaft of ring gear and the engine torque at the given speed for both cases of k_P are $T_R = 59.537$ Nm and $T_e = 110.84$ Nm (see Example 7.3.2).

From Equations 7.28 and 7.29, the MG1 and MG2 torques can be obtained. The power of each component is found by simply multiplying its torque by its speed. The engine power is $P_e = 46.429$ kW.

The other results are provided in Table 7.6.

Table 7.6 Numerical results of Example 7.3.6

Case	n	T_1(Nm)	T_2(Nm)	P_1(kW)	P_2(kW)	P_B(kW)
$k_P = 0.75$	0.81	−29.662	−21.641	0.972	−12.12	−11.147
$k_P = 1.5$	1.30	−32.367	−17.936	1.061	−12.21	−11.147

(b) Vehicle power demand P_V is equal to $P_V = F_R v = 35,281\,W$ for both cases.

The engine power is greater than the demand power, therefore, the battery is charged with power $P_B = P_V - P_e = -11,147\,W$ (Equation 7.30). In fact, MG2 takes part of the engine power and delivers it to the battery. MG1, on the other hand, works in motor mode and receives power from the battery. The balance of power to the battery, therefore, is: $P_B = P_{MG1} + P_{MG2} = -11,147\,W$ (a negative sign means the battery receives power).

7.3.2.2 Power Circulation

In 'engine-only' mode the power source is only from the engine while the power is delivered to the output through the ring gear R only. Thus, if power loss is ignored:

$$P_e + P_R = 0 \tag{7.33}$$

$$P_{MG1} + P_{MG2} = 0 \tag{7.34}$$

Equation 7.34 represents the power circulation between MG1 and MG2 during 'engine-only' mode of vehicle motion, that is:

$$P_{cir} = |P_{MG1}| = |P_{MG2}| \tag{7.35}$$

Making use of Equations 7.20, 7.28 and 7.33 (or Equations 7.21, 7.29 and 7.33), one finds the following expression for the circulating power as a fraction of engine power:

$$\frac{P_{cir}}{P_e} = \left| 1 - \frac{2n(m+1)}{m+n} + \frac{mn}{m+n} \times \frac{\omega_R}{\omega_e} + \frac{(1+m)(n-1)}{m+n} \times \frac{\omega_e}{\omega_R} \right| \tag{7.36}$$

In general, at two points with speed ratios of either $1 + \frac{1}{m}$ or $1 - \frac{1}{n}$, the circulating power vanishes. The former point depends only on parameter m that is dependent on the layout of original epicyclic set (see Equation 7.22). This point with a speed ratio of greater than unity is always physically possible. The latter point is dependent on the relative sizes of planet gears in the EM-PSD and for values of $n < 1$ will lie on the negative side of speed ratio axis and will not be present in forward vehicle motions. $n = 1$ refers to the case when the two PSD systems are identical.

The variation of power ratio of Equation 7.36 with the variation of speed ratio $\frac{\omega_R}{\omega_e}$ for different values of parameter n is plotted in Figure 7.26. The parameter m is taken equal to 2.6 that refers to tooth numbers $N_S = 30$ and $N_R = 77$. It is clear that for values of $n > 1$ the circulating power is reduced considerably in some working regions compared to the original PSD system.

Example 7.3.7

For the vehicle and conditions of Example 7.3.3 and the PSD of Example 7.3.5, determine the power circulation of the system.
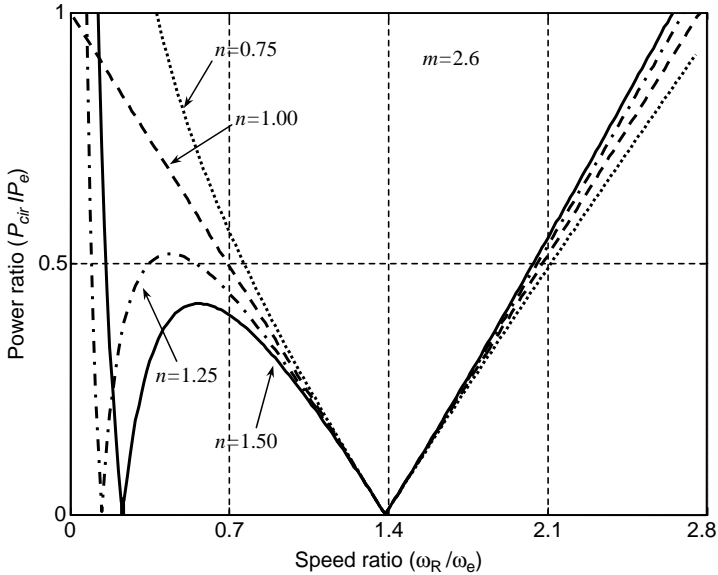
Figure 7.26 The variation of circulating power ratio versus speed ratio for EM-PSD

Solution

The vehicle acceleration is 0.45 m/s^2 with $T_e = 111.7$ Nm and $\omega_e = 3562$ rpm. The torque acting on the output shaft (main ring gear) is 93.737 Nm (see Example 7.3.3).

According to procedure explained in Example 7.3.3, the results are obtained and summarized in Table 7.7 for both k_P values.

Table 7.7 Numerical results of Example 7.3.7

Case	n	ω_1(rpm)	ω_2(rpm)	T_1(Nm)	T_2(Nm)	P_1(kW)	P_2(kW)	P_{cir}(kW)
$k_P = 0.75$	0.81	1788	4116	−31.744	13.787	−5.943	5.943	5.943
$k_P = 1.5$	1.30	1788	4449	−30.021	12.064	−5.620	5.620	5.620

7.4 HEV Component Characteristics

Hybrid electric vehicles employ electric motors either to power the vehicle in pure-electric mode or to assist the IC engine during brief periods of high torque demands. On the other hand, electric generators are used to recapture the energy of a vehicle during braking to recharge the battery. A substantial advantage of a hybrid vehicle, however, is the optimum use of its power-generating components. IC engines and electric machines each have their own operating characteristics that influence the whole performance and efficiency of an HEV. In hybrid vehicle designs, therefore, maximizing the overall efficiency and reducing the vehicle emissions are major goals.

7.4.1 The IC Engine

The internal combustion engine is still a dominant source of power in a hybrid electric vehicle. The influential characteristics of an engine include its torque-speed performance, efficiency behaviour and pollution. The performance characteristics of IC engines were discussed in detail in Chapter 2 and fuel consumption issues were analyzed in Chapter 5. Those readers who are familiar with materials covered in Chapters 2 and 5 will have no difficulty in following the subject of this chapter.

7.4.2 Electric Machines

Electric machines are well-established components in conventional vehicles as starters and alternators, for cranking of the engine and producing electricity to charge the battery. In HEVs, however, the electric machines play more important roles as they deliver greater power for extended durations.

Different electric machines depending on their construction will have different characteristics. Two key features of electric machines from a HEV design point of view are their torque-speed and efficiency characteristics. Various types of DC or AC machines have been developed and each type has found its best place in the industry. The range of electric motors used in HEV designs includes separately excited DC motors, permanent-magnet synchronous and induction AC motors, brushless DC (BLDC) and switched reluctance motors.

In general, AC motors are less expensive and maintenance-free, but they require more sophisticated power electronics. But owing to higher power density and higher efficiency of AC motors, these types of motors are used in the majority of HEV applications.

7.4.2.1 Motor Torque

The distinctive property of electric motors compared to IC engines is that they produce torque from zero speed. The torque-speed characteristics of different types of motors in general depend on their construction, but they typically contain two phases of constant-torque and constant-power controlled by using power electronics.

Figure 7.27 shows a typical variation of motor torque and power with shaft speed. With increasing supply voltage to the motor while the flux is kept constant, the motor speed increases and a high constant torque is obtained. At the point where the motor voltage equals the source voltage, the constant-torque phase ends and during the second phase, at that constant voltage the flux decreases and constant maximum power is maintained. This feature is very useful when the motor is used as a vehicle traction motor since it can produce large driving forces at low vehicle speeds (even at zero speed and without needing a clutch) and can produce high acceleration up to the maximum available power of the motor.

7.4.2.2 Motor Efficiency

An electric motor receives electric power and converts it to mechanical power. In any physical system the output power is always less than the input power due to power losses through the energy flow components. According to Figure 7.28 a part of the electric input power P_E will be lost all the way through the inverter to the motor and inside the motor itself. Defining this power loss P_L, the output mechanical power P_M will be:

$$P_M = P_E - P_L \tag{7.37}$$
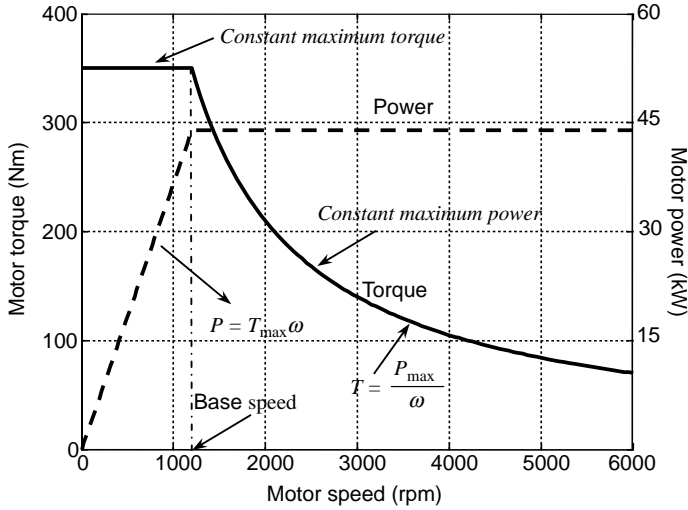
Figure 7.27 Typical maximum performance curves of HEV electric motors

The motor efficiency η_M at every working condition is defined as the ratio of output power to input power:

$$\eta_M = \frac{P_M}{P_E} = 1 - \frac{P_L}{P_E} \tag{7.38}$$

The power loss, therefore, can be expressed in terms of input power:

$$P_L = (1 - \eta_M)P_E \tag{7.39}$$

When the motor efficiency is determined through laboratory tests, it turn out that the efficiency is dependent on the working condition of the motor and is not a constant value. In a mathematical representation:

$$\eta_M = \eta_M(T, \omega) \tag{7.40}$$

In the motor T-ω plane, the efficiency of each working point has a discrete value. There will be several points with an identical efficiency value, so that when these points are connected to one another, an
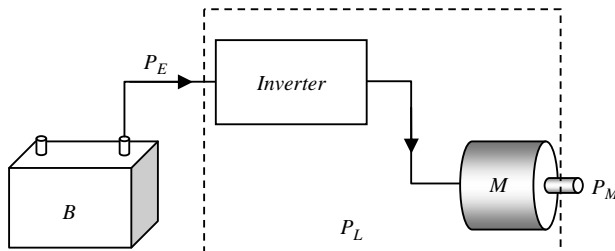
Figure 7.28 Power flow from battery to motor output
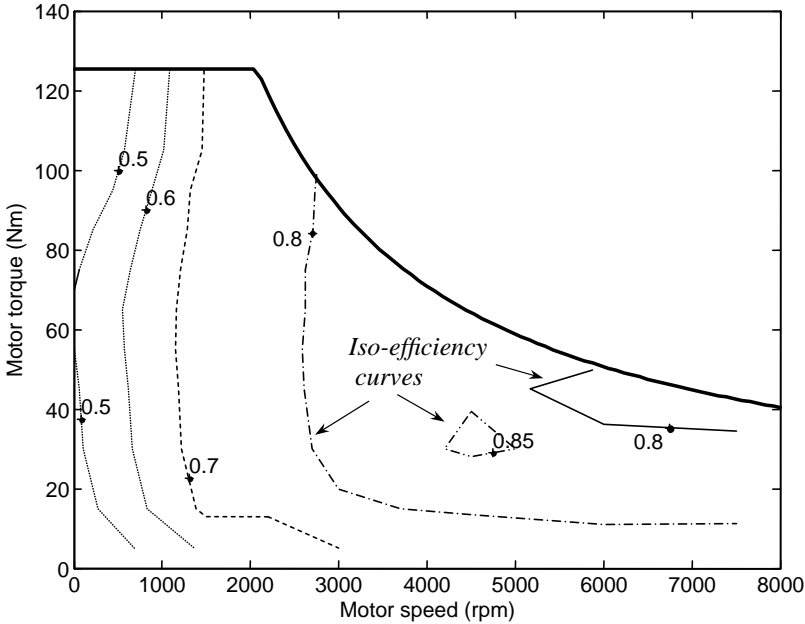
Figure 7.29   A typical motor efficiency map

iso-efficiency curve will appear. Repeating this process for other equal efficiency points, generates an 'efficiency map' for the motor. A typical efficiency map for an electrical motor is provided in Figure 7.29.

For a generator, the power direction of Figure 7.29 reverses and the electric power received at battery terminals P'_E is:

$$P'_E = P_M - P'_L \tag{7.41}$$

where P'_L is the power loss in generator mode. Similar to the motor, the efficiency is defined:

$$\eta_G = \frac{P'_E}{P_M} = 1 - \frac{P'_L}{P_M} \tag{7.42}$$

$$P'_L = (1 - \eta_G)P_M = (1 - \eta_G)\eta_M P_E \tag{7.43}$$

If it is assumed that the power loss is independent of the direction of power flow, then equating the right-hand sides of Equations 7.39 and 7.43 leads to:

$$\eta_G = 2 - \frac{1}{\eta_M} \tag{7.44}$$

Example 7.4.1

Table 7.8 includes efficiency figures obtained for an electric motor in its motoring phase of operation. The intention is to use this information and generate similar result for the generating phase of the same motor. Use Equation 7.44 and build efficiency plots for generating phase.

Table 7.8 Motor efficiency values of Example 7.4.1

Torque (Nm)	0	5	15	30	45	55	65	75	85	95	105	124
Speed (rpm)						Efficiency						
0	0.1	0.4	0.45	0.48	0.49	0.5	0.51	0.49	0.46	0.4	0.37	0.32
1500	0.1	0.62	0.72	0.75	0.76	0.76	0.75	0.75	0.74	0.74	0.71	0.71
2200	0.1	0.62	0.72	0.75	0.76	0.76	0.75	0.75	0.74	0.74	0.71	0.71
3000	0.1	0.7	0.79	0.83	0.84	0.84	0.84	0.84	0.83	0.83	0.82	0.71
4500	0.1	0.71	0.82	0.86	0.85	0.84	0.8	0.84	0.83	0.83	0.82	0.71
6000	0.1	0.74	0.84	0.84	0.74	0.84	0.8	0.84	0.83	0.83	0.82	0.71
7500	0.1	0.76	0.83	0.83	0.74	0.84	0.8	0.84	0.83	0.83	0.82	0.71
9000	0.1	0.76	0.83	0.83	0.74	0.84	0.8	0.84	0.83	0.83	0.82	0.71

Solution

A MATLAB program is provided for the solution of this example. The program listing is given in Figure 7.30. The main part of solution makes use of MATLAB '*contour*' function. The comments are included in the program to make it self-explanatory and the resulting plot can be seen in Figure 7.31.

```
% Example 7.4.1
% Motor and generator efficiencies

clc, close all, clear all

% Motor torque vector corresponding to columns of efficiency table
mg_trq=[0  5  15 30 45 55 65 75 85 95 105 124]; % Nm

% motor and inverter efficiency table
motor_eff =[...
0.1 0.40  0.45  0.48  0.49  0.50  0.51  0.49  0.46  0.40  0.37  0.32  % 0
0.1 0.62  0.72  0.75  0.76  0.76  0.75  0.75  0.74  0.74  0.71  0.71  % 1500
0.1 0.62  0.72  0.75  0.76  0.76  0.75  0.75  0.74  0.74  0.71  0.71  % 2200
0.1 0.70  0.79  0.83  0.84  0.84  0.84  0.84  0.83  0.83  0.82  0.71  % 3000
0.1 0.71  0.82  0.86  0.85  0.84  0.80  0.84  0.83  0.83  0.82  0.71  % 4500
0.1 0.74  0.84  0.84  0.74  0.84  0.80  0.84  0.83  0.83  0.82  0.71  % 6000
0.1 0.76  0.83  0.83  0.74  0.84  0.80  0.84  0.83  0.83  0.82  0.71  % 7500
0.1 0.76  0.83  0.83  0.74  0.84  0.80  0.84  0.83  0.83  0.82  0.71]; % 9000

% Motor speed vector corresponding to rows of efficiency table
mg_rpm=[0 1500 2200 3000 4500 6000 7500 9000];
```

Figure 7.30 MATLAB program listing for Example 7.4.1

```
% Maximum torque and corresponding speeds
trq_c=ones(1,24)*124;   % Constant torque part
for i=1: 67, trq_v(i)=124*2200/90/(i+24); end % Constant power part
max_trq=[ trq_c, trq_v];
mg_spd=0: 100: 9000;

figure
plot(mg_spd, max_trq)
xlabel('Motor Speed (rpm)')
ylabel('Motor/Generator Torque (Nm)')
hold on

% Produce contours of Iso-efficiency for motor
[C,h]=contour(mg_rpm, mg_trq(2:12), motor_eff(:,2:12)',[0.5 0.6 0.7 0.8 0.85]);
clabel(C)

% Generator and inverter efficiency
for i=1: 12
   for j=1:8
   gen_eff(j,i)= 2 -1/motor_eff(j,i); % Equation 7.44
   end
end
plot(mg_spd, -max_trq)
% Produce contours of Iso-efficiency for generator
[C,h]=contour(mg_rpm, -mg_trq(2:12), gen_eff(:,2:12)',[0.4 0.5 0.6 0.7 0.8 0.85]);
clabel(C)
grid
```

Figure 7.30   (*Continued*)
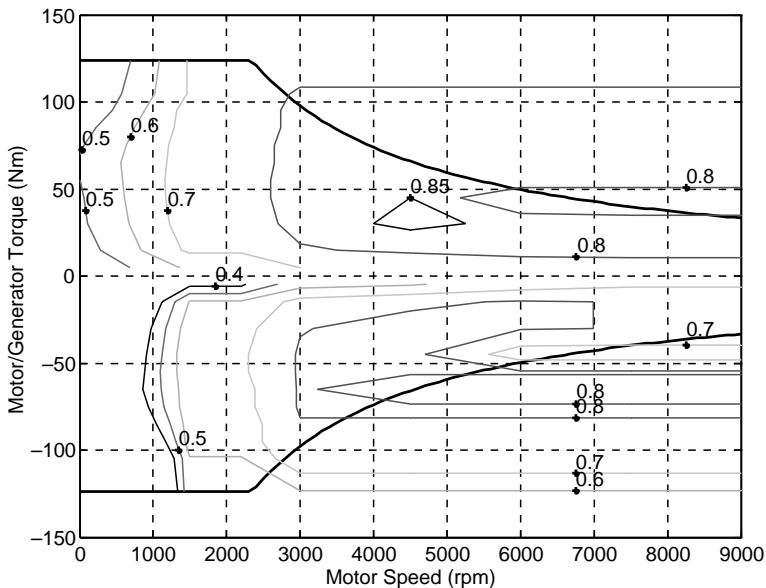
Figure 7.31   Efficiency maps of Example 7.4.1

7.4.3   The Battery

The battery is a critical component central to the success of electric and hybrid vehicles. Large power demands from the vehicle battery and high life expectations make it a very complicated system that requires instantaneous monitoring and management. The battery pack of an HEV is constructed by wiring battery cells typically in series to generate a high voltage for electric motor drive, but to develop higher currents the cells are sometimes also wired in parallel. The battery pack also comprises a number of sub-components including sensors for voltages, current, and temperature; a thermal conditioning system; a battery management system and power electronics to isolate the battery pack.

The two most important characteristics of a battery are its energy capacity and efficiency. The energy capacity of a battery is essential when long distance electric driving is concerned. Of course it is always possible to use larger battery packs but obviously this will at the same time increase the weight and cost. Therefore, the 'energy density' of a battery, defined as the ratio of its energy capacity to its weight, is a very important factor.

The battery capacity Q can be defined as the amount of free charge generated inside the battery and is measured in amp-hour (Ah). It represents the capability of the battery to generate electric current within a time span (e.g. an hour). Such electric current is called the discharge rate of the battery. The capacity may also be given in Watt-hour (Wh) which is the battery's Ah multiplied by its voltage.

7.4.3.1   State of Charge

The battery cell is a delicate system that can be permanently damaged if mistreated. Over-charging or over-discharging a battery cell may cause damage and result in reduced life. In order to avoid damage to the battery, therefore, it is necessary to estimate its present charge condition to assess how much it could be charged or discharged.

The state of charge (SOC) of a battery is a measure of the present charge capacity of the battery. It is the amount of capacity that is left after starting to discharge from a fully charged condition. What is meant by SOC is an indication of the fraction of charge remaining in each cell, and is measured in percentage (%) of the cell's full capacity. With an accurate measure of SOC, cell damage can be avoided by controlling the current. There is no sensor available to measure SOC directly and thus it must be estimated. In mathematical form, the instantaneous SOC can be expressed as:

$$SOC(t) = 1 - \frac{1}{Q_0} \int_0^t I(t)dt \qquad (7.45)$$

in which Q_0 is the fully charged capacity and $I(t)$ is the instantaneous discharge current of the battery. $I(t)$ is positive during discharging and negative during charging.

7.4.3.2   Battery Efficiency

A battery, like every physical system, loses some energy during power flow. The battery power loss is modelled by an ohmic power consumed by an internal resistance R_i shown in Figure 7.32. For a battery current I the loss is:

$$P_L = R_i I^2 \qquad (7.46)$$

The open-circuit voltage of the battery V_O is related to the close-circuit discharging voltage V_d by writing KVL for the discharging circuit of Figure 7.32:

$$V_d = V_O - R_i I \qquad (7.47)$$
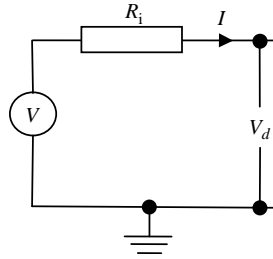
Figure 7.32   The internal resistance of a battery

Multiplying both sides by the current I and noting that the $V_d I$ term is the output power, results in:

$$P_o = P_i - P_L \tag{7.48}$$

The efficiency of discharging can be defined as the ratio of output power to input power, or:

$$\eta_{Bd} = \frac{R_d}{R_i + R_d} \tag{7.49}$$

in which R_d is load resistance during discharging:

$$R_d = \frac{V_d}{I} \tag{7.50}$$

R_d can be obtained by measuring the terminal voltage and current values.

In the charging phase, the direction of the current in Figure 7.32 reverses and the charging voltage V_c is higher than the open-circuit voltage. Following a similar procedure, for the efficiency of battery during charging, one can find:

$$\eta_{Bc} = 1 - \frac{R_i}{R_c} \tag{7.51}$$

with R_c defined similarly as:

$$R_c = \frac{V_c}{I} \tag{7.52}$$

The internal resistance R_i of a battery is not a constant value and is different during charge and discharge phases. It also depends on the amount of capacity of charge (SOC) of the battery. A typical variation of a battery's internal resistance with SOC for charging and discharging phases is shown in Figure 7.33.

Example 7.4.2

The variation of battery internal resistance with SOC during charging and discharging phases is given (in Ohm) as:

$$R_{ic} = 0.456 \times SOC^2 - 0.539 \times SOC + 0.933$$

$$R_{id} = -SOC^3 + 2.705 \times SOC^2 - 1.965 \times SOC + 1.498$$

Plot the efficiency maps of the battery in a power-SOC diagram by assuming a constant terminal voltage of 280 V.
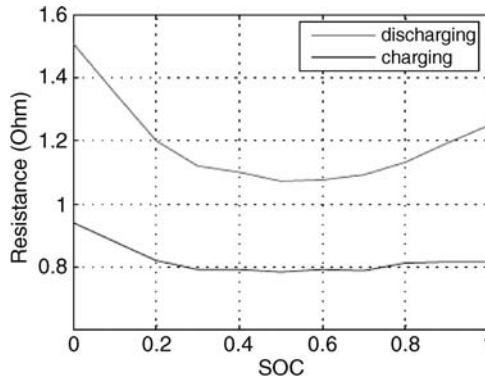
Figure 7.33 Typical variation of battery internal resistance

Solution

At a given power P the current and load resistance simply are:

$$I = \frac{P}{V} \text{ and } R = \frac{V}{I}$$

For both cases of discharging and charging the two parameters have identical values at specified terminal voltage and power.

A MATLAB program with listing given in Figure 7.34 is provided for the solution of this example. The values of the above parameters are evaluated at 150 points for each charging/

```
% Example 7.4.2
% Battery efficiency map

clc, close all, clear all

Vt=280;                % Battery terminal voltage
% Battery internal resistance polynomials
Pol_Ri_c=[0.456 -0.539 0.933];     % Charging
Ppl_Ri_d=[-1 2.705 -1.965 1.498];  % Discharging

% Generate 150 values for 'power', 'current' and 'circuit resistance'
for i=1: 150 ,   p(i)=i*100;    I(i)=p(i)/Vt;   Rcd(i)=Vt/I(i); end

for j=1: 11
   SOC(j)=(j-1)/10;    % 10 SOC values 10% apart
for i=1: 150
   % For discharging phase:
   Bat_eff_d(i, j)=Rcd(i)/(Rcd(i)+polyval(Pol_Ri_d, SOC(j)));
   % For charging phase:
   Bat_eff_c(i, j)=1-polyval(Pol_Ri_c, SOC(j))/Rcd(i);
end
end
```

Figure 7.34 The MATLAB listing of Example 7.4.2

```
[Cd,hd]=contour(SOC*100,  p/1000 ,Bat_eff_d,[0.82 0.86 0.9 0.94 0.98]);
clabel(Cd, hd)
hold on

[Cc,hc]=contour(SOC*100, -p/1000 ,Bat_eff_c,[0.86 0.9 0.94 0.98]);
clabel(Cc, hc)
xlabel('SOC (%)')
ylabel('Battery Output Power (kW)')
grid
```

Figure 7.34   (*Continued*)

discharging phase for power values of 0 to 15 kW. At 10 SOC values of from 0 to 100% the efficiency of battery is evaluated using Equation 7.49 (or 7.51). Making use of MATLAB 'contour', the contours of battery efficiency are drawn and the resulting plot is shown in Figure 7.35.
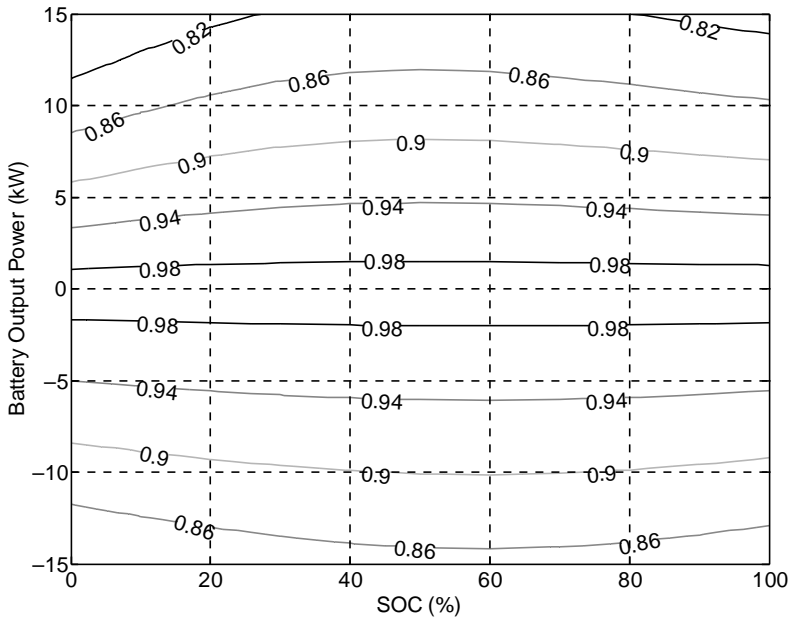
Figure 7.35   Battery efficiency map of Example 7.4.2

Example 7.4.3

A series hybrid vehicle of 1000 kg mass uses a battery pack of 150 V. The vehicle with a fully charged battery starts a driving cycle as shown in Figure 7.36.

A motor with the efficiency curve given in Figure 7.31 is driving the car via a single reduction gear. The vehicle speed is related to the motor speed by a factor of 0.03. The resistive forces acting on the vehicle can be obtained from $F_R = 200 + 0.4v^2$ (v is the speed of the vehicle in m/s).
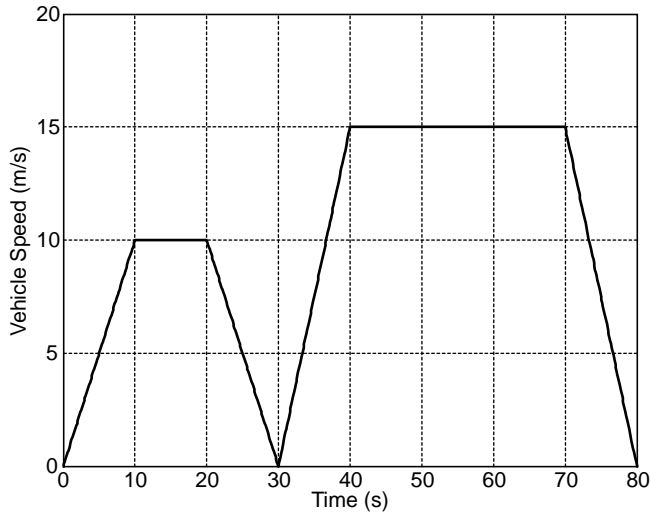
Figure 7.36   Driving cycle of Example 7.4.3

If the battery initially has a charge value of $Q_0 = 50$ Amp-h, max recharge current is 20 A and the efficiency of charging/discharging is 0.9 (constant):

(a) Derive equations for the motor speed, motor torque, motor power, battery current and battery SOC versus time.
(b) When the vehicle follows the driving cycle, plot the variations of parameters in (a) for different parts of the cycle.

Solution

(a) At a given vehicle speed v the motor speed is given by $\omega_M = \frac{v}{0.03}$ (rad/s).
   The motor torque is related to the traction force of the wheels by $T_M = 0.03 \times F_T$. The traction force equals the resistive force plus acceleration force: $F_T = 200 + 0.4v^2 + ma$.
   The motor output power is simply its torque multiplied by its speed.
   The input power to the motor (electric power) is its output power plus the lost power:

$$P_E = P_M + P_L$$

   The latter is found from the motor efficiency map, knowing the motor speed and torque. The battery current is obtained from electrical power demand of the motor divided by the battery voltage. The battery SOC can be obtained using Equation 7.45 and by integrating the battery current.

(b) A MATLAB program with listing given in Figure 7.37 is suitable for this example. The values of the above parameters are evaluated at several points for each 0.1 second of driving cycle. The program of Example 7.4.1 is also utilized for the generation of motor efficiency values.
   For the deceleration parts of the driving cycle, it is assumed that the motor goes into generator mode and recharges the battery with a maximum of 20 Amps.

```
% Example 7.4.3
clc, close all, clear all

m=1000;        % Vehicle mass
Q=10*3600;     % Battery Capacity
Vb=150;        % Battery Voltage
Bat_eff=0.9;   % Battery efficiency

Example_741    % Run Example 7.4.1 to generate motor/generator data

t=0: 0.1:80;   % Driving Cycle Time
% Define the driving cycle, Vehicle Speed (m/s)
v=t.*(t<=10)+10*(t>10 & t<=20)+(30-t).*(t>20 &t<=30)+1.5*(t-30).*(t>30 &t<=40)+...
    15*(t>40 &t<=70)+(120-1.5*t).*(t>70 &t<=80);
Dv=[diff(v)./diff(t) 0];                   %Vehicle acceleration (m/s^2)
Ft=200+0.4*v.^2+m*Dv;     %Traction Force (N)

% Requested Motor Torque and Power
Wm=(v/0.03);        % Motor speed (rad/s)
Tm=Ft*0.03;         % Motor torque (Nm)
Pm=Tm.*Wm;       % Motor output power (Watt)
mg_spd=mg_rpm*pi/30;     % Motor/Generator speed in rad/s
mg_trq=[-fliplr(mg_trq(2:12)) mg_trq(1) mg_trq(2:12)];     % M/G full torque range

% compute motor/generator losses
[T1,w1]=meshgrid(mg_trq(12:23),mg_spd(2:8));
mg_out_pwr1=T1.*w1;
m_loss_pwr=(1./motor_eff(2:8, 1:12)-1).*mg_out_pwr1;
g_loss_pwr=(1./gen_eff(2:8, 1:12)-1).*mg_out_pwr1;

% Losses at zero torque are taken same as adjacent points
mg_loss_pwr=[fliplr(g_loss_pwr(:,2:12)) m_loss_pwr(:,2)
m_loss_pwr(:,2:12)];

% Losses at zero speeds are taken same as adjacent points
mg_loss_pwr=[mg_loss_pwr(1,:);mg_loss_pwr];

% compute input power
[T,w]=meshgrid(mg_trq, mg_spd);
mg_out_pwrg=T.*w;
mg_in_pwrg=mg_out_pwrg+mg_loss_pwr;

Pin=interp2(mg_trq, mg_spd, mg_in_pwrg, Tm, Wm);        % Interpolate input powers

Ib=Pin/Vb/Bat_eff    % Battery current
Ib(Ib<-20)=-20;         % Charge current must not exceed -20 A
I=zeros(length(t),1);SOC=zeros(length(t),1);
for i=1:length(t)
   I(i)=quad(@(x)interp1(t,Ib,x),eps,t(i)); % Integration of Battery Current
   SOC(i)=1-I(i)/Q;  % State of Charge
end
% Now plot the figures
```

Figure 7.37   MATLAB listing of Example 7.4.3
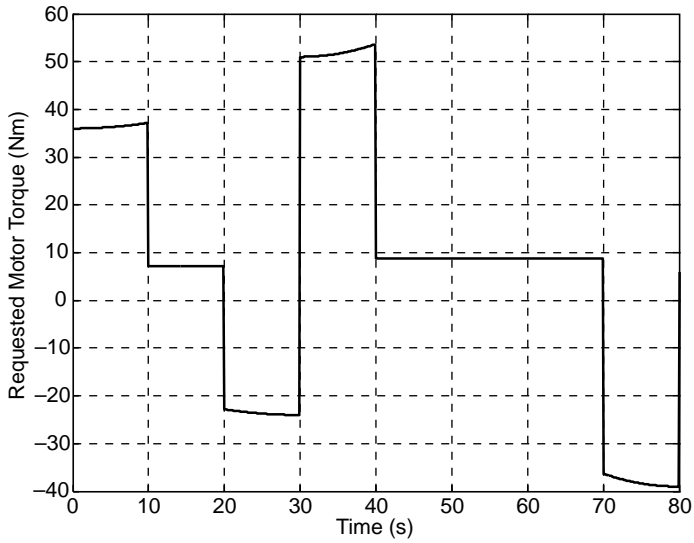
Figure 7.38 Motor output torque of Example 7.4.3 during one cycle

The resulting plots for the variations of different parameters in a single driving cycle are shown in Figures 7.38–7.41.
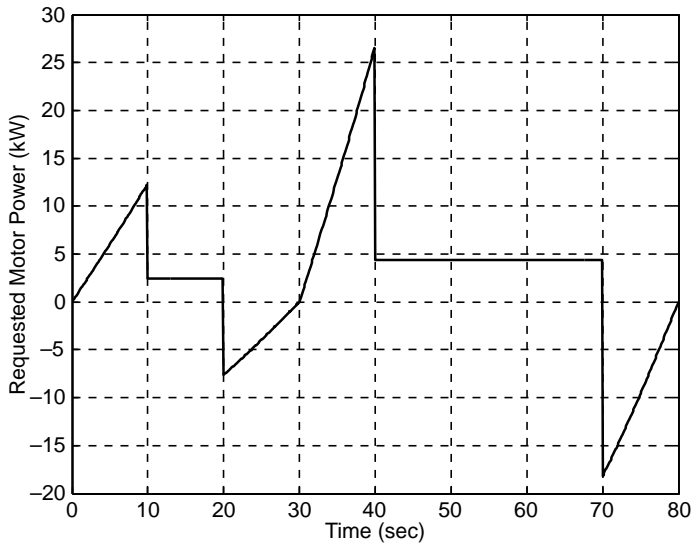
Figure 7.39 Motor output power of Example 7.4.3 during one cycle
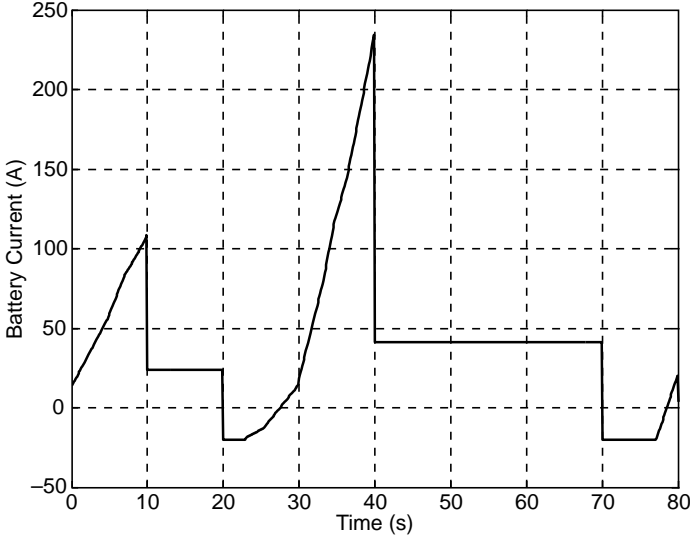
Figure 7.40   Battery current of Example 7.4.3 during one cycle
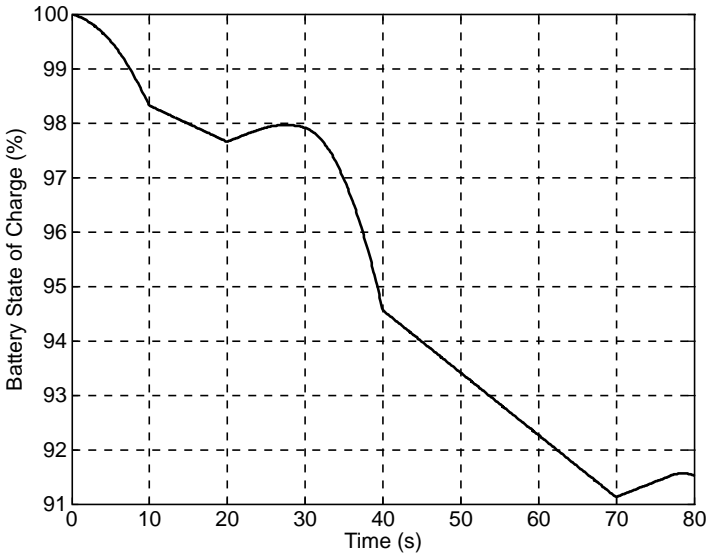
Figure 7.41   Battery SOC of Example 7.4.3 during one cycle

7.4.3.3   Battery Management System

The battery pack is an expensive component of the hybrid vehicles and it is important to prolong its life by implementing proper management schemes. There are several factors affecting battery performance and life. The discharge strategy of a battery is of particular importance as the performance of the batteries is

reduced if they are deeply discharged regularly. The battery performance is highly dependent on temperature and different battery types work best within specified ranges of temperatures.

A battery pack consists of several battery cells stacked in series. The number of the battery cells in a pack increases the total voltage of the overall pack. To develop a voltage of 400 V using 4.2 V cells, a stack of 96 cells is necessary. When batteries are used in series, the state of health of every single cell will be important because the malfunctioning of any of the cells will lead to the failure of the entire battery pack. Moreover, if one cell in a pack has slightly less capacity than the other cells, then its state of charge will gradually deviate from the rest of the cells over multiple charge/discharge cycles. This will eventually cause deep discharge of that particular cell and thus permanent damage. To prevent this from happening, each cell's voltage must be monitored to determine its state of charge. If the SOC of a cell is found to be out of balance, it should be individually charged (or discharged) to balance its state of charge with other cells.

An automotive battery management system (BMS) has to work in real time in a rapidly varying environment involving continuous charging and discharging. Battery lifetimes for automotive applications exceed 10 years and the BMS must carefully control and monitor the batteries. Hybrid vehicle batteries require both high power charge capabilities for regenerative braking and high power discharge capabilities for the launch assist or boost. For this reason, their batteries must be maintained at a SOC that can discharge the required power but still have enough headroom to accept the necessary regenerative power without risking overcharging the cells.

The BMS has two major tasks: (1) protecting the cells; and (2) keeping the individual cells in optimum SOC. One of the prime functions of the BMS is to provide the necessary monitoring and control to protect the cells from going into out of tolerance operating conditions. Battery overheating is one example of these for which the cooling fans can be turned on and if the overheating becomes excessive, then the battery must be disconnected. Since over-charging and under-discharging are two of the prime causes of battery failure, determining the SOC of each individual cell in the battery pack is necessary to check for uniform charge in all of the cells in order to verify that individual cells do not become overstressed.

If the HEV battery is fully charged, the capability for charging during regenerative braking will be reduced and hence braking efficiency will be diminished. On the other hand, deep discharging damages the battery and must be prevented. Therefore, two upper and lower limits for the battery SOC are defined. The lower limit is set to prevent over-discharge which shortens the life of the battery and the upper limit is set to leave some room for absorbing the kinetic energy of the vehicle during braking. Typical values for the battery operating ranges shown in Figure 7.42 are different for EVs, HEVs and PHEVs due to their different usage in the vehicle. For EVs and PHEVs, the working range is typically as low as 20% and as high as 95%. For HEVs, the minimum working SOC ranges from 40% up to 60% and the maximum working SOC ranges from 60% up to 80%. For SOC values below the working range, no discharging is allowed and the vehicle is unable to work in electric mode. If the SOC value is higher than the high working value, the battery is never charged by the engine but it may be charged through the regenerative braking.

7.5   HEV Performance Analysis

Typical driving conditions of a vehicle are very diverse and cannot therefore be fully anticipated. In particular, normal driving of a vehicle includes extensive use of part load conditions that are not easy to model. Special full load maximum performance cases, however, are simpler to model.
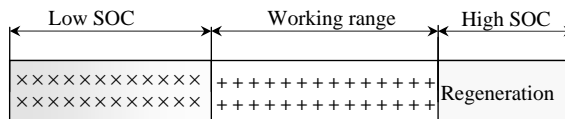
Figure 7.42   Battery operating ranges

The performance and operation of hybrid electric vehicles, on the other hand, greatly depend on the type of hybridization. The performance of a series hybrid vehicle is basically dependent on the characteristics of its electric motor. The operation of a parallel HEV at the three major modes of pure engine, pure electric and hybrid, however, is influenced by the way power is controlled and managed.

7.5.1   Series HEV

The driving performance of a series hybrid vehicle is governed by its electric motor characteristics. The traction force produced at the driving wheels is the result of the motor torque T_m amplified by the reduction gear ratio n:

$$F_T = \frac{n\eta_d T_m}{r_W} \tag{7.53}$$

in which η_d is the efficiency of driveline from motor to the wheels and r_W is the effective radius of the driving wheels. The typical full load performance of a motor was shown in Figure 7.27 in which two regimes of constant torque and constant power were present. Propelling the vehicle in its full performance is achieved when the motor follows its full load curve. The whole performance of the vehicle can be divided into two separate regions of constant torque and constant power. The governing equations will be different at each phase.

7.5.1.1   Constant Torque Phase

With reference to Section 3.6, the speed of the vehicle starting from rest during the constant torque phase can be described by:

$$v(t) = \beta \tanh \frac{\beta c}{m} t, \quad \beta > 0 \tag{7.54}$$

where:

$$\beta = \sqrt{\frac{F_T - F_0}{c}} \tag{7.55}$$

The maximum speed at the end of constant torque phase is where the motor is at its base speed ω_b:

$$v_b = \frac{r_w}{n} \omega_b \tag{7.56}$$

The time to reach this speed can be obtained from following relation:

$$t_b = \frac{m}{\beta c} \tanh^{-1} \frac{v_b}{\beta} \tag{7.57}$$

The distance travelled during this constant torque period is:

$$s_b = \frac{m}{c} \left(\ln \sqrt{\frac{\beta^2}{\beta^2 - v_b^2}} \right) \tag{7.58}$$

It is obvious that at time t_b the maximum power of motor is utilized and after this point the power remains a constant value $P_{\max}$:

$$P_{max} = T_{max}\omega_b = \frac{F_T v_b}{\eta_d} \tag{7.59}$$

that is, proportional to the base speed ω_b of motor or the base velocity v_b of the vehicle. In other words, for higher base velocities, the motor power must be larger. On the other hand, a higher base velocity means a longer base time t_b which means the high acceleration of the vehicle lasts longer. In terms of vehicle performance, this is a good factor but it can only be achieved at the expense of larger motor powers.

7.5.1.2   Constant Power Phase

The governing equations for the constant power phase of the vehicle motion can be obtained by making use of the results of Sections 3.5.4 and 3.5.8. The maximum vehicle speed can be determined by using:

$$v_{max} = e + h \tag{7.60}$$

in which:

$$e = (a+d)^{\frac{1}{3}}, h = \text{sgn}(a-d)|a-d|^{\frac{1}{3}} \tag{7.61}$$

$$a = \frac{P_{max}}{2c}, \ b = \frac{F_0}{3c}, \ d = (a^2 + b^3)^{0.5} \tag{7.62}$$

The time to reach a desired speed v can be obtained from the equation below:

$$t = k_1 \ln \frac{v_{max} - v}{\sqrt{v^2 + vv_{max} + k}} + k_2 \, Arc \tan \frac{2v + v_{max}}{\sqrt{4k - v_{max}^2}} + C \tag{7.63}$$

in which C is the constant of integration and must be determined from an initial condition. The coefficients k, k_1 and k_2 are found from:

$$k = \frac{P_{max}}{cv_{max}} \tag{7.64}$$

$$k_1 = -\frac{m}{c} \cdot \frac{v_{max}}{2v_{max}^2 + k} \tag{7.65}$$

$$k_2 = \frac{k_1}{v_{max}} \cdot \frac{2k + v_{max}^2}{\sqrt{4k - v_{max}^2}} \tag{7.66}$$

Theoretically, the time to reach the maximum speed is infinity. A reasonable time can, however, be obtained for the time to reach very close to the final velocity (e.g. 98% of it) by first obtaining the constant C for the initial condition of v_b at t_b (i.e. end of constant torque phase), and then substituting a desired value for v (e.g. 0.98 of v_{max}) into Equation 7.63.

Example 7.5.1

An electric motor used in an EV has a maximum torque of 124 Nm up to the base speed of 2200 rpm. The vehicle information is given in Table 7.9:

(a) Plot the motor torque-speed diagram.
(b) Determine the base velocity and maximum velocity of the vehicle. Also specify the motor speed at the maximum speed.

(c) Verify the answer of (b) by plotting the tractive and resistive forces in a single diagram.

(d) Determine the base velocity time and the times to reach 98%, 99% and 99.5% of the maximum vehicle speed.

Table 7.9   Vehicle information for Example 7.5.1

Parameter	Description	Value	Unit
m	Vehicle mass	1200	kg
f_R	Coefficient of rolling resistance	0.02	–
c	Overall aerodynamic coefficient	0.4	–
r_W	Wheel effective radius	0.3	m
n_f	Final drive (reduction gear) ratio	5.0	–
η_d	Efficiency of driveline	0.95	–

Solution

Direct use of the available equations can lead to the required information. Due to the complex formulae, however, a MATLAB program will be useful. This program is listed in Figure 7.43.

(a) The motor torque-speed plot consists of two constant torque and constant power parts. The first part can be constructed simply by the information given for the maximum torque and base speed. The constant power in the second part is obtained by multiplying the maximum torque by the base speed. The torque at any given speed then is the value of the constant power divided by the speed (in rad/s). The result is shown in Figure 7.44.

```
% Example 7.5.1

clc, close all, clear all
m=1200;    % Vehicle mass (kg)
fR=0.02;    % Rolling resistance coefficient
Ca=0.4;    % Overall aerodynamic coefficient
rW=0.3;    % Wheel effective radius (m)
nf=5.0;    % The ratio of reduction gear
Tm=124;    % Constant motor torque (Nm)
wb=2200;    % Motor base speed (rpm)
eta=0.95;   % Driveline efficiency

F0=m*9.81*fR; Pmax=Tm*wb*pi/30;

% Part (a)- Torque-speed diagram
m_spd=0: 100: 9000;
m_spd=m_spd*pi/30;
nt=round(91*wb/9000);
trq_c=ones(1,nt)*Tm;   % Constant torque part
for j=nt+1: 91, trq_v(j)=Pmax/m_spd(j); end % Constant power part
m_trq=[trq_c, trq_v(nt+1:91)];
figure, plot(m_spd*30/pi, m_trq), hold on, grid
xlabel('Motor Speed (rpm)'), ylabel('Motor/Generator Torque (Nm)')
```

Figure 7.43   The MATLAB listing of Example 7.5.1

```
% Part (b)- Base and Maximum velocities
beta=sqrt((nf*eta*Tm/rW-F0)/Ca);
vb=min(wb*pi*rW/nf/30, beta);
Pmax=eta*Pmax;
a=Pmax/2/Ca;
b=F0/3/Ca;
d=sqrt(a^2+b^3);
e=(a+d)^(1/3);
h=sign(a-d)*abs(a-d)^(1/3);
vmax=e+h;

% Part (c)- Plot FT-FR curve
FT=nf*eta*m_trq/rW;
v=rW*m_spd/nf;
FR=F0+Ca*v.*v;
figure, plot(v, FT, v, FR, '--'), grid
xlabel('Velocity (m/s)'), ylabel('Traction/Resistive force (N)')

% Part(c)- Maximum travel time
tb=m*atanh(vb/beta)/beta/Ca;
v98=0.98*vmax;
k=Pmax/Ca/vmax;
k1=-m*vmax*Ca/(2*vmax^2+k);
k4=sqrt(4*k-vmax^2);
k2=k1*(2*k+vmax^2)/vmax/k4;
k3=sqrt(vb^2+vb*vmax+k);
C=tb-k1*log((vmax-vb)/k3)-k2*atan((2*vb+vmax)/k4);
k3=sqrt(v98^2+v98*vmax+k);
t=C+k1*log((vmax-v98)/k3)+k2*atan((2*v98+vmax)/k4)
```

Figure 7.43 (*Continued*)
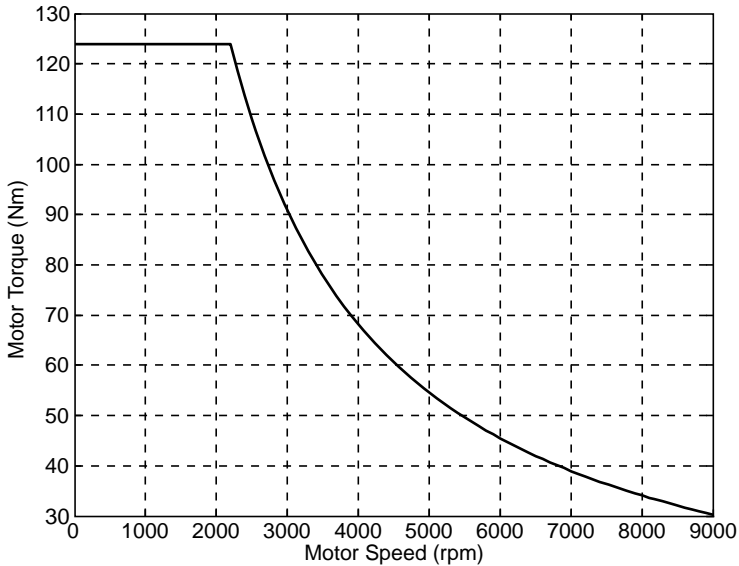
Figure 7.44 The torque-speed diagram of the motor
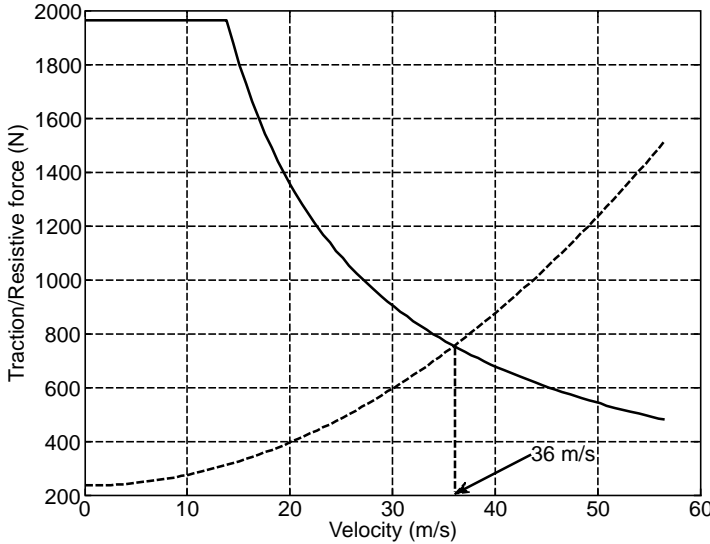
Figure 7.45 Maximum speed at intersection point of tractive and resistive forces

(b) The value of base speed obtained from Equation 7.56 is 13.8 m/s. The final velocity is determined by using Equation 7.60 and the result is 36 m/s. The motor speed at the maximum vehicle speed will be 600 rad/s (5730 rpm).

(c) The intersecting point of the force diagram of Figure 7.45 verifies the result of part (b).

(d) From Equation 7.57 the time of base speed is 9.8 s. Equations 7.63–7.66 are used to estimate the time to reach the maximum speed by evaluating the speed at 0.98, 0.99 and 0.995 of the maximum speed. The results are 88, 104.7 and 121.4 s.

7.5.2 Parallel HEV

The performance of a parallel HEV depends primarily on its mode of operation. In the electric-only mode, the performance is similar to that of a series HEV discussed in Section 7.5.1. In the engine-only mode, the performance is similar to that of a conventional vehicle discussed in detail in Chapters 3 and 4.

In the hybrid mode, the performance can be analyzed depending on the control strategy that specifies the power distribution of the two sources of energy. The maximum performance of a parallel hybrid vehicle is obtained when both the ICE and motor simultaneously produce their maximum torques to propel the vehicle. The resulting traction force depends on the gear ratios of both the engine and the motor:

$$F_T = \frac{n_e \eta_{de} T_e}{r_W} + \frac{n_m \eta_{dm} T_m}{r_W} \tag{7.67}$$

where n is the gear ratio from the prime mover to the driving wheel (subscripts e and m stand for engine and motor respectively). In the following example the performance of a parallel HEV will be examined.

Example 7.5.2

A parallel HEV with the information given in Table 7.10 uses a motor with specifications given in Example 7.5.1. The engine WOT curve is of the form:

$$T_e = -4.45 \times 10^{-6}\omega_e^2 + 0.0317\omega_e + 55.24, \ 1000 < \omega_e < 6000 \text{ rpm}$$

The motor output is directly connected to the final drive whereas the output of ICE is connected through a five-speed transmission with gear ratios 4.0, 2.8, 1.85, 1.25 and 0.85.

For a maximum driving performance of the vehicle:

(a) Plot the ICE and motor torque-speed diagrams in a single figure.
(b) Plot the total tractive force diagram of the vehicle against the forward speed. Also include the resistive force curve and find the maximum vehicle speed.
(c) Find the final speed of the vehicle for electric-only mode by using the method described in Example 7.5.1.
(d) Obtain the final speed of the vehicle at engine-only mode by plotting the tractive-resistive force diagrams. Also include a diagram for electric-only mode.

Table 7.10   Vehicle information for Example 7.5.2

Parameter	Description	Value	Unit
m	Vehicle mass	1500	kg
f_R	Coefficient of rolling resistance	0.02	–
c	Overall aerodynamic coefficient	0.4	–
r_W	Wheel effective radius	0.3	m
n_f	Final drive ratio	4.0	–
η_t	Efficiency of transmission	0.95	–
η_f	Efficiency of final drive	0.95	–

Solution

A MATLAB program with the listing of Figure 7.46 is prepared for this example.

(a) The motor torque-speed variations are similar to that of the previous example with the exception that its speed is taken up to 6000 rpm. The engine torque-speed variation is calculated from the given formula. The result is shown in Figure 7.47.

(b) The tractive force resulting from the engine torque will be different at each gear. The speed of the vehicle at each gear varies according to the revolution speed of the prime movers. The total tractive force at each gear is obtained simply by summing the engine and motor parts. The result is plotted in Figure 7.48. The intersecting point of the tractive force diagram with the resistive force curve in gear 5 indicates the final speed of 198.5 km/h. Note that at gear 1 it is assumed that the traction force at zero speed corresponds to the engine torque at a speed of 1000 rpm.

(c) This part is exactly similar to the previous example and thus has been excluded from the program listing. The result is 34.8 m/s (125.4 km/h) for the maximum speed in electric-only mode.

```
% Example 7.5.2              Parallel HEV performance

% Vehicle data: refer to Table 7.9
n_g=[4.0 2.8 1.8 1.2 0.8];   % Transmission ratios 1-4
n=n_g*nf;                    % Total gear ratios
F0=m*9.81*fR;
Pmmax=Tm*wb*pi/30;           % Maximum motor torque

% Part (a)- Torque-speed diagram
e_spd=1000: 60: 6000;   % Engine speed range (rpm)
m_spd=0: 50: 6000;      % Motor speed range
m_spd=m_spd*pi/30;
trq_c=ones(1,45)*Tm;    % Constant torque part
for j=46: 121, trq_v(j)=Pmmax/m_spd(j); end % Constant power part
m_trq=[trq_c, trq_v(46:121)];          % Motor torque
e_trq=-4.45e-6*e_spd.*e_spd+0.0317*e_spd+55.24; % Engine torque

figure, hold on, grid
plot(m_spd*30/pi, m_trq, '--', e_spd, e_trq)
xlabel(Speed (rpm)'), ylabel(Torque (Nm)')

% Part (b)- Tractive force diagram
Figure, hold on, grid
FTm=nf*eta_f*m_trq/rW;  % Motor traction force
nn=0;  % Only for gear 1
for j=1: 5
   max_vn=max(e_spd)*pi*rW/n(j)/30; % Maximum speed for gear j
   v=0: max_vn/120: max_vn;    % Speed range for gear j
   e_spd=1000: 5000/(120-nn): 6000;   % Engine speed range (rpm)
   e_trq=-4.45e-6*e_spd.*e_spd+0.0317*e_spd+55.24; % Engine torque

   FTs_en=[zeros(1, nn), eta_t*eta_f*e_trq*n(j)/rW];          % Traction due to engine

   FT(:, j)=FTs_en+FTm;               % Total traction force
   plot(v*3.6, FT(:, j))
   nn=20;  % For gears other than 1
end
   FR=F0+Ca*v.*v;
   plot(v*3.6, FR, '--')
xlabel('Vehicle Speed (km/h)'), ylabel('Total traction force (N)')

% Part (d)- Engine-only maximum speed
figure, grid, hold on
   FTe=eta_t*eta_f*e_trq*n(5)/rW; % Traction due to engine
   max_vn=max(e_spd)*pi*rW/n(5)/30;
   min_vn=min(e_spd)*pi*rW/n(5)/30;
   v=min_vn: (max_vn-min_vn)/100: max_vn;        % Speed range of gear 5

   plot(v*3.6, FTe)
% Include the plot for Electric-only maximum speed
FTm=nf*eta_f*m_trq/rW; % Traction due to motor
v=rW*m_spd/nf;
FR=F0+Ca*v.*v;              % Resistive force
plot(v*3.6, FTm, v*3.6, FR, '--'), xlabel('Velocity (m/s)')
ylabel('Traction/Resistive force (N)')
```

Figure 7.46   The MATLAB listing of Example 7.5.2
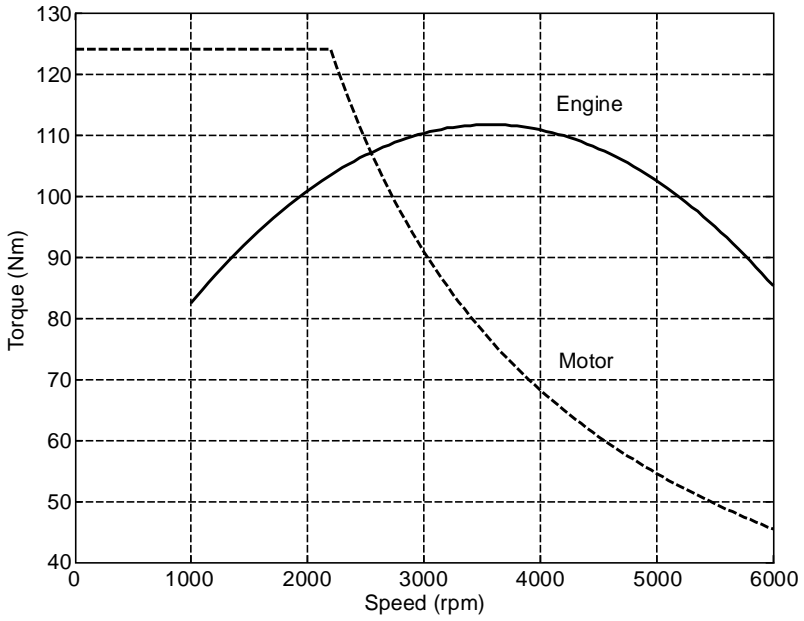
Figure 7.47   The ICE and motor torque-speed diagrams
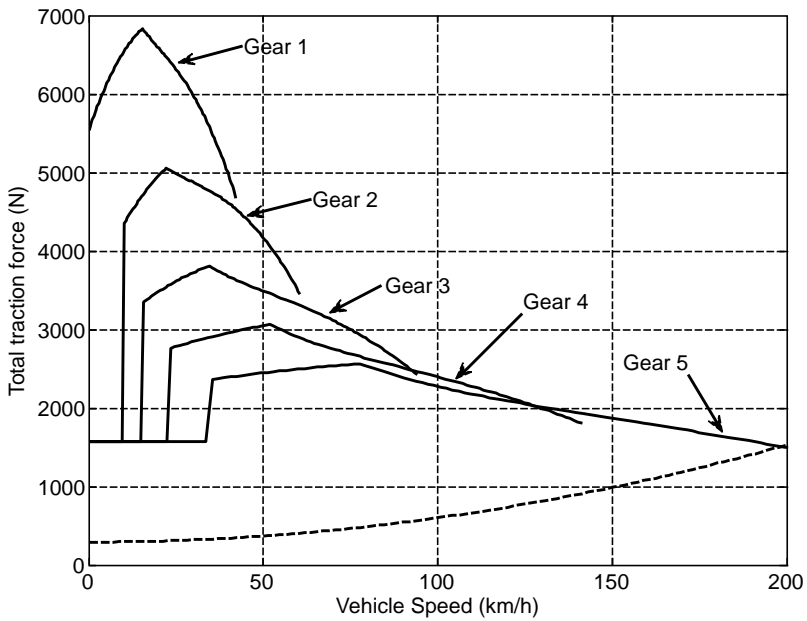
Figure 7.48   Total tractive force at different transmission gears

(d) A force diagram for the engine-only mode is shown in Figure 7.49 at gear 5. The maximum vehicle speed is 156 km/h. In the same plot the motor traction diagram is also included. The result of case (c) is verified.
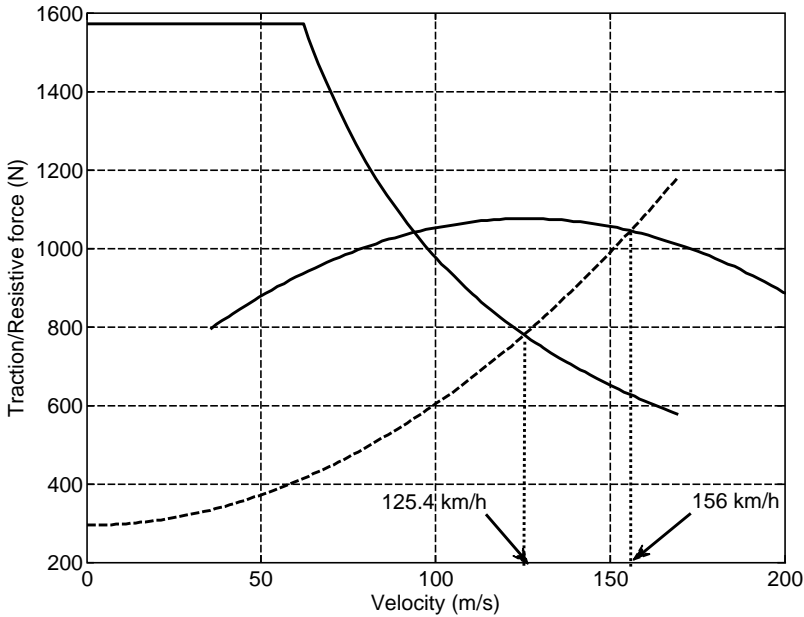
Figure 7.49   Maximum vehicle speeds in engine-only and electric-only modes

7.6   HEV Component Sizing

One of the critical choices in the hybrid vehicle designs is the relative size of the IC engine and the electric motor. Using a large electric motor will require more electric power and thus requiring a larger, heavier, and more expensive battery. The size of components, on the other hand, depends on the performance requirements; for example, if a long electric range is needed, using a large battery is inevitable, or to obtain high acceleration during the electric-only mode, a large electric motor must be chosen.

Another decisive factor in the selection of components for an HEV is the overall cost and the fuel economy of the vehicle. Therefore, a good design is the one with the required performance at lower cost and fuel consumption.

7.6.1   General Considerations

The design of an HEV is a complicated task that requires a multidisciplinary knowledge of several relevant sciences. In this section, we intend to discuss the general design issues briefly. In order to get a general understanding of the differences between the conventional and hybrid powertrains, let us take an example of converting a conventional vehicle to a hybrid electric vehicle. The major changes include adding at least one electric motor and related mechanical devices together with a large battery pack to the base vehicle. Several problems in such conversion include:

- insufficient space for the motor, the battery and control boxes;
- conflict between the existing controllers (e.g. ECU) and the new controllers;
- extra sensors and on-board displays are necessary;
- existing alternator cannot charge the new battery;
- extra mass is added to the vehicle.

In addition, there are some existing components that are not compatible with the new system such as the existing battery, starter motor and alternator. Also when electric-only mode of operation is selected, other unexpected difficulties will be faced, such as problems in braking due to loss of engine vacuum and booster function, loss of power assist in steering and loss of the air conditioning compressor.

This example indicates that the structure and configuration of an HEV are basically different from a conventional vehicle and thus it must be designed independently based on its own specifications and requirements. The critical design issues are discussed in the following section.

7.6.1.1   Downsized Engine

It is obvious that the desired performance for a vehicle requires a specific amount of power to be installed in the vehicle. When the electric motor takes a share of the installed power, then the engine can be downsized relative to its original size in a conventional vehicle. This will allow a smaller engine on an HEV with a lower size and weight to be used.

On the other hand, an IC engine has low efficiencies at low loads and high revolutions (see Chapter 5) and its optimum operation is restricted to certain regions. In an HEV, the use of the electric motor allows the engine to operate close to its most efficient points for a range of vehicle speeds and loads and in turn to improve the overall fuel economy and emissions. Obviously the engine alone cannot produce a performance similar to that of a conventional vehicle, but with the assistance from the electric motor both the performance and fuel economy could be improved.

7.6.1.2   Electric Accessory Drive

When the vehicle is powered in electric mode, the accessories typically driven by the engine must now be driven by other means. Typical accessories include alternator, steering pump, AC compressor and water pump. Apart from the water pump and alternator that must work when the engine is on, the others must be available on demand even when the engine is off. Therefore, in an HEV it is necessary to drive the accessories by electrical power.

7.6.1.3   Sizing

The sizing of HEV components can be approached from different viewpoints. Overall vehicle performance is one of the important measures for the design of components and thus the motor size must be suitable for this purpose. On the other hand, a vehicle with acceptable performance must at the same time have low energy consumption and emissions. In addition, the cost of a vehicle and its components have to be as low as possible. These factors are usually contradictory and thus the sizing of components involves some compromise decisions.

7.6.2   Sizing for Performance

The performance of vehicle is a key factor in its selection by the owner. One of the basic steps in sizing the components is to determine the minimum sizes to achieve the required vehicle performance. Four of the major performance requirements for the vehicle can be considered as:

- achieving a desired maximum speed v_{max} on the level road;
- achieving a desired maximum speed v'_{max} on a specified slope θ;
- accelerating up to a desired speed v_d during a desired time t_d;
- negotiation of a desired slope at low speeds.

The first three requirements are related to the installed power, whereas the fourth requirement is related to the available torque. More details on the sizing of major HEV components are discussed in following sections.

7.6.2.1 Series HEV

For the series HEVs, the electric motor is the only traction source and must be capable of producing all the performance characteristics such as the maximum required acceleration and speed. Based on such requirements the overall characteristics of the motor can be specified.

Size of the Motor
The desired performance characteristics for the vehicle were defined as four requirements for the vehicle speed, acceleration time and grading. The first criteria can be considered as having a desired steady speed v_{max} over a flat or sloping road. The motor must be able to achieve this performance by generating the necessary torque and power. The tractive or resistive power requirement P_{rfs} for the required steady speed simply is:

$$P_{rfs} = F_R v_{max} \tag{7.68}$$

where F_R is the total resistive force comprising the rolling resistance, gravitational and aerodynamic forces (see Section 3.4):

$$F_R = F_{RR} + F_g + F_A = mg(f_R \cos \theta + \sin \theta) + cv_{max}^2 \tag{7.69}$$

In which θ is the slope angle. Therefore, the motor output power is:

$$P_{mfs} = \frac{v_{max}}{\eta_d} \left[mg(f_R \cos \theta + \sin \theta) + cv_{max}^2 \right] \tag{7.70}$$

in which η_d is the driveline efficiency.
    Alternatively, the desired performance of the vehicle can be regarded as achieving a desired speed v_d when accelerating from a standstill during a specified time t_d. Again it is the motor's responsibility to produce sufficient power P_{ma} to accelerate the vehicle. Consider the torque-speed diagram of a typical electric motor shown in Figure 7.50. This desired time is the summation of two terms:

$$t_d = t_{CT} + t_{CP} \tag{7.71}$$

in which t_{CT} is the time elapsed in the constant torque phase and t_{CP} is the time vehicle accelerated in the constant power phase (Figure 7.50). The two portions can be determined by using Equations 7.57 and 7.63 written as follows:

$$t_{CT} = \frac{m}{\beta c} \tanh^{-1} \frac{v_b}{\beta} \tag{7.72}$$

$$t_{CP} = k_1 \ln \frac{v_{max} - v_d}{\sqrt{v_d^2 + v_d v_{max} + k}} + k_2 Arc \tan \frac{2v_d + v_{max}}{\sqrt{4k - v_{max}^2}} + C \tag{7.73}$$
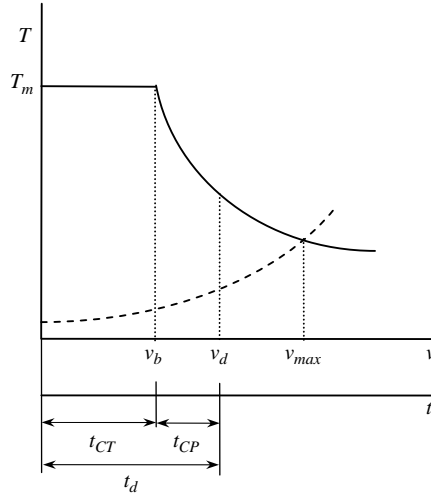
Figure 7.50 Required performance from a motor

where:

$$C = -k_1 \ln \frac{v_{\max} - v_b}{\sqrt{v_b^2 + v_b v_{\max} + k}} - k_2 Arc \tan \frac{2v_b + v_{\max}}{\sqrt{4k - v_{\max}^2}} \qquad (7.74)$$

Coefficients k, k_1 and k_2 in Equation 7.73 are all dependent only on the P_{ma} of the motor, whereas β in Equation 7.72 is dependent on the $T_{\max}$ of the motor. At the end of the constant-torque phase (i.e. at $t = t_{CT}$) we have:
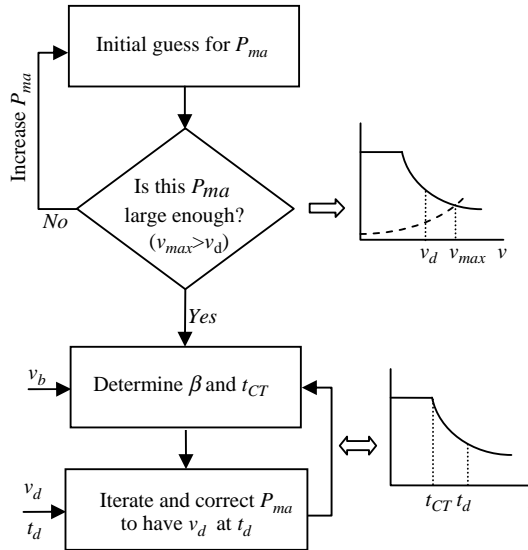
Figure 7.51 Process to determine motor power for a given v_b

$$\eta_d P_{ma} = F_T v_b \tag{7.75}$$

Thus β can be expressed in terms of P_{ma} and v_b:

$$\beta = \sqrt{\frac{1}{c}\left(\frac{\eta_d P_{ma}}{v_b} - F_0\right)} \tag{7.76}$$

Therefore if only v_b is specified, for any required time t_d the motor power P_{ma} can be determined in an iterative process using Equation 7.71 as the constraint. This is illustrated in Figure 7.51 starting with an initial estimate for the motor power and refining it by an iteration process using Equation 7.71 as the constraint.

Example 7.6.1

A series HEV is designed to perform its 0–100 km/h acceleration in 20 seconds. For the vehicle with the properties given in Table 7.11, plot the variations of P_{ma}, the wheel torque T_W, and the times t_{CT} and t_{CP} as v_b varies from 5 to 25 m/s.

Table 7.11   Vehicle information for Example 7.6.1

Parameter	Description	Value	Unit
m	Vehicle mass	1200	kg
f_R	Coefficient of rolling resistance	0.02	–
c	Overall aerodynamic coefficient	0.4	–
r_W	Wheel effective radius	0.3	m
η_d	Efficiency of driveline	0.95	–

Solution

A MATLAB program as listed in Figures 7.52 and 7.53 is prepared based on the process of Figure 7.51 and Equations 7.72 to 7.76. The main part of the program is the iteration process that is carried out in a separate function called 'delta_t' and invoked from the main program. This function returns with the final value of P_{ma} that satisfies the constraint Equation 7.73 while the required speed v_d occurs at the desired time t_d. The condition of motor maximum speed at vehicle maximum speed is used to determine the ratio of the reduction gear.

The results of the program are those plotted in Figures 7.54 and 7.55. It can be seen that for the specified vehicle the motor power rating increases with the increase in the base velocity. On the other hand, the minimum power rating is obtained for the minimum base velocity (even zero). The wheel torque, however, is decreasing with the base velocity but it has a minimum at a certain point. The motor torque can be determined once the gear ratio of the reduction gear is selected.

Figure 7.55, on the other hand, shows the constraint implying the desired velocity occurs at 20 seconds.

```
% Example 7.6.1

clc, close all, clear all

global eta vb Ca F0 m vd td   % share data with function 'delta_t'

m=1200;     % Vehicle mass (kg)
fR=0.02;    % Rolling resistance coefficient
Ca=0.4;     % Overall aerodynamic coefficient
rW=0.3;     % Wheel effective radius (m)
eta=0.95;   % Driveline efficiency
vd=100;     % Desired speed (km/h)
td=20;      % Desired time (sec)

F0=m*9.81*fR;
vd=vd/3.6;

Pmax =(F0*vd+Ca*vd^3)/eta; % Minimum power for having 'vmax = vd'

for i=1: 81
    vb=5+(i-1)/4;
    vbi(i)=vb;
% Iteration process is done in a separate function 'delta_t'
    Pmax=fsolve(@delta_t, Pmax, optimset('Display','off'))
    Pma(i)=Pmax;
% Pmax is at hand, determine the motor properties
    Tw(i)= eta*Pmax*rW/vb;          % Wheel torque
FT= Tw(i)/rW;
beta=sqrt((FT-F0)/Ca);
if vb >= vd    % This means the desired speed takes place during constant torque phase
        tct(i)=m*atanh(vd/beta)/beta/Ca;   % This will be the desired time
        tcp(i)=0;
else
        tct(i)=m*atanh(vb/beta)/beta/Ca;

a=eta*Pmax/2/Ca; b=F0/3/Ca; d=sqrt(a^2+b^3); e=(a+d)^(1/3);
h=sign(a-d)*abs(a-d)^(1/3); vmax=e+h;
k=eta*Pmax/Ca/vmax;
k1=-m*vmax*Ca/(2*vmax^2+k);
k4=sqrt(4*k-vmax^2);
k2=k1*(2*k+vmax^2)/vmax/k4;
k3=sqrt(vb^2+vb*vmax+k);
C= -k1*log((vmax-vb)/k3)-k2*atan((2*vb+vmax)/k4);
k3=sqrt(vd^2+vd*vmax+k);
tcp(i)=C+k1*log((vmax-vd)/k3)+k2*atan((2*vd+vmax)/k4);
end
end

% Plot the results
```

Figure 7.52   The main program listing of Example 7.6.1

```
function dt=delta_t(Pmax)      % function called from the main program

global eta vb Ca F0 m vd td

beta=sqrt((eta*Pmax/vb-F0)/Ca);
if vb >= vd      % This means the desired speed takes place during constant torque phase
        tct=m*atanh(vd/beta)/beta/Ca;    % This will be the desired time
        tcp=0;
else
        tct=m*atanh(vb/beta)/beta/Ca;

a=eta*Pmax/2/Ca; b=F0/3/Ca; d=sqrt(a^2+b^3); e=(a+d)^(1/3);
h=sign(a-d)*abs(a-d)^(1/3); vmax=e+h;
k=eta*Pmax/Ca/vmax;
k1=-m*vmax/Ca/(2*vmax^2+k);
k4=sqrt(4*k-vmax^2);
k2=k1*(2*k+vmax^2)/vmax/k4;
k3=sqrt(vb^2+vb*vmax+k);
C= -k1*log((vmax-vb)/k3)-k2*atan((2*vb+vmax)/k4);
k3=sqrt(vd^2+vd*vmax+k);
tcp=C+k1*log((vmax-vd)/k3)+k2*atan((2*vd+vmax)/k4);
end

dt= tct+tcp-td; % function returns when dt=0
```

Figure 7.53   The function of Example 7.6.1
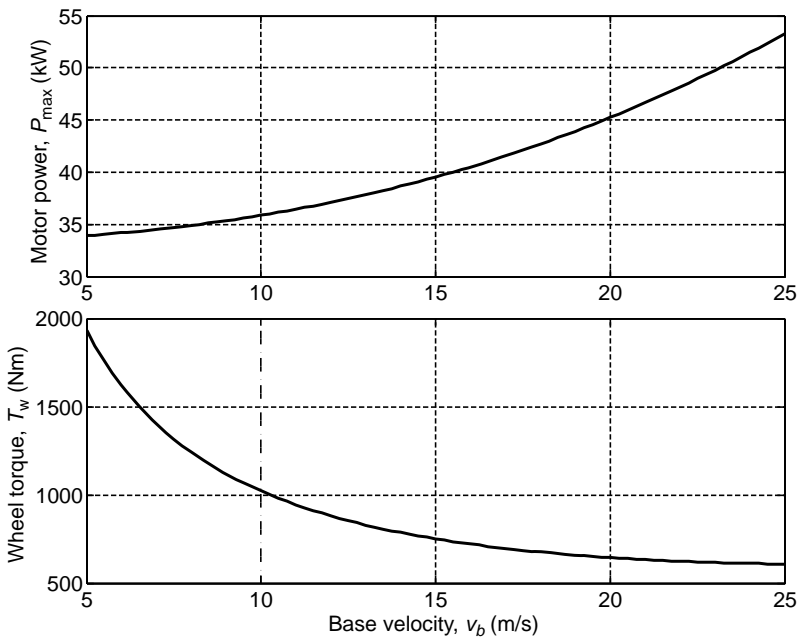
Figure 7.54   The variation of motor power and wheel torque with base velocity v_b
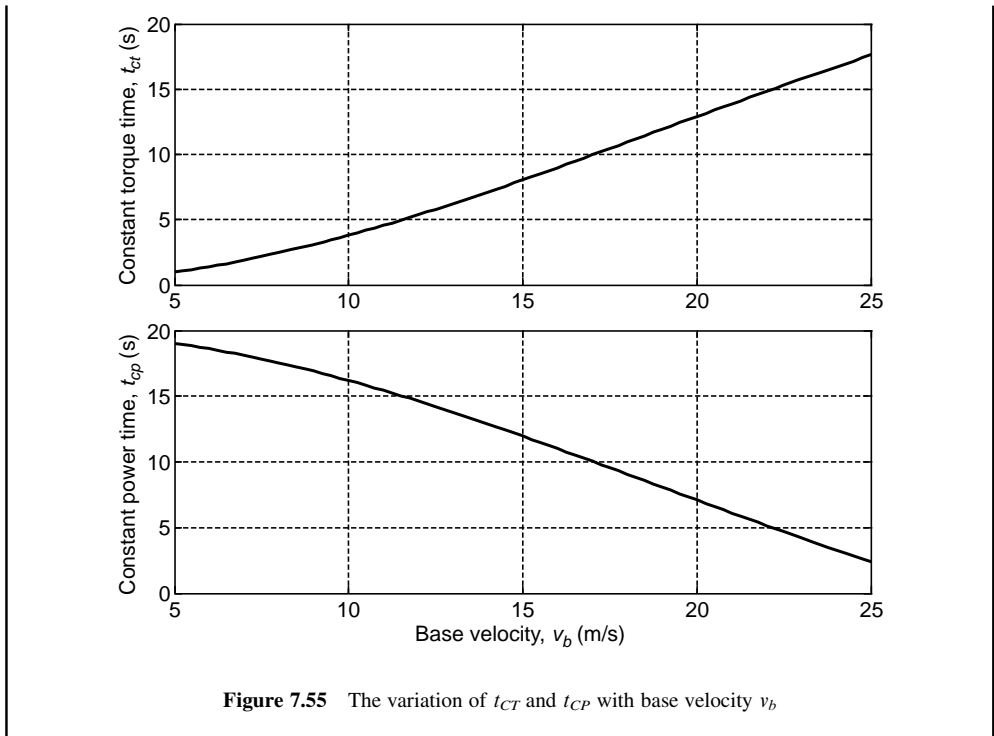
Figure 7.55   The variation of t_{CT} and t_{CP} with base velocity v_b

The foregoing example showed that the motor properties can be determined if the base velocity is specified. In a real problem, however, even v_b is an unknown quantity depending on the motor characteristics and cannot be specified before the motor is selected.

An alternative approach is to only consider a desired velocity v_d for the vehicle performance and generate useful plots for the design parameters. In this method, for selected motor powers, any other parameter such as v_b or t_{CT} is varied and the other design parameters are determined. For the vehicle of Example 7.6.1 and for the same desired velocity of 100 km/h, the output results of this approach are depicted in Figures 7.56–7.59 for $n_g = 5.0$. Figure 7.56 shows that for lower times, greater motor powers are required. From Figure 7.56, for a 20-second desired time of Example 7.6.1, all power ratings (33 kW and higher) seem to be selectable. The other important factor in selecting the motor, however, is its torque capacity and Figure 7.57 can be used for this purpose. For instance, if the motor torque is limited to 200 Nm, a motor with the minimum power of 33 kW cannot achieve less than around 22 seconds. The 43 kW motor for this torque limit of 200 Nm has a t_d of about 17 seconds. An interpolation between the two results gives a power rating of around 37 kW that can produce a desired time of 20 s. The base velocity for this motor is around 11 m/s and this result can also be verified using the results on Example 7.6.1 (Figure 7.54).

If the motor torque has lower limiting values, it is clear that low required time values cannot be achieved. To resolve this problem, larger reduction gears must be used.

Two alternative approaches were discussed to determine the motor power according to the maximum speed or acceleration performance requirements. Obviously the two criteria for final speed and acceleration performance do not necessarily lead to equal power requirements and the greater of the two power values must be selected. Once the motor power P_m is obtained, the other required properties of the motor can be determined. The maximum speed requirements lead to definite power values (Equation 7.73), whereas the acceleration performance produces implicit results and needs a further selection process.
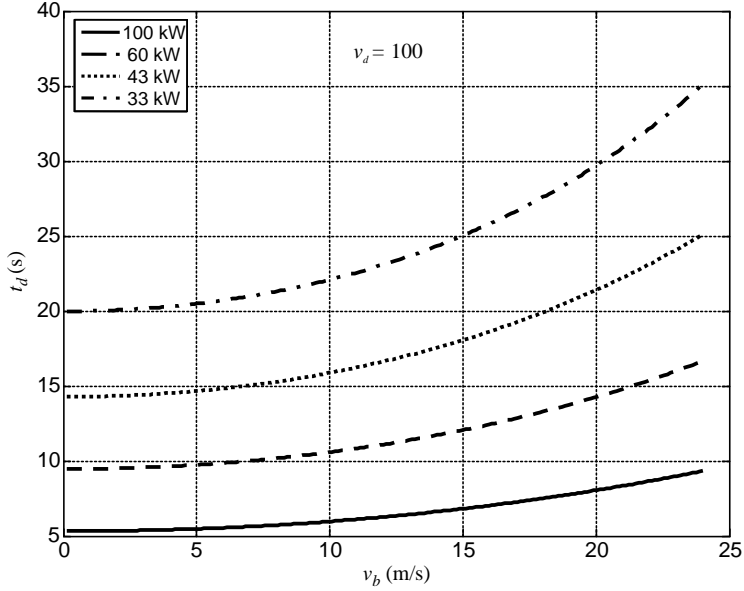
Figure 7.56   The plot of desired time vs v_b at different power ratings
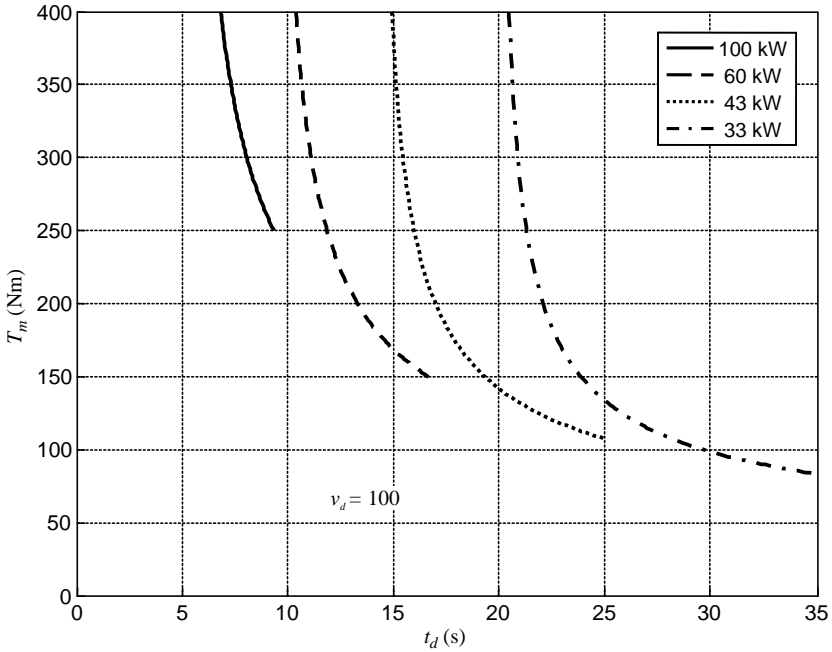
Figure 7.57   The plot of motor torque T_m vs desired time at different power ratings
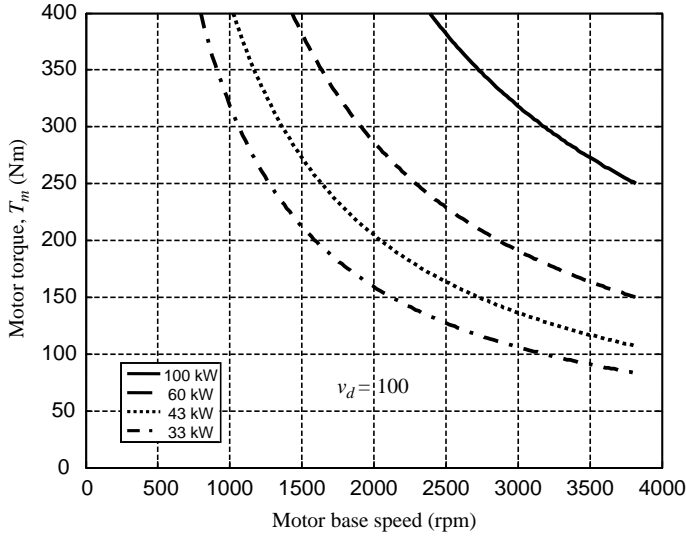
Figure 7.58 The plot of motor torque vs its base speed at different power ratings

There are two means of having $P_{mfs} > P_{ma}$ or $P_{mfs} < P_{ma}$. In the former case when the acceleration performance for different base velocities (e.g. Figure 7.54) is constructed, in the upper curve a horizontal line with the value of P_{mfs} will intersect the curve and the base velocity and wheel torque (from the lower curve) can be obtained. The motor torque based on the power P_{mfs}, denoted by T_{mP}, can be calculated from:

$$T_{mP} = \frac{P_{mfs}r_W}{n_g v_b} \tag{7.77}$$
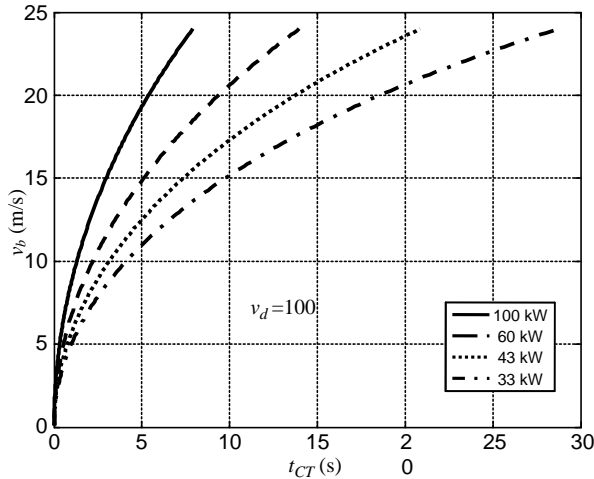
Figure 7.59 The plot of base velocity vs t_{CT} at different power ratings

provided that the reduction gear ratio n_g is available. The motor speed usually has a limiting value and this may be used to determine the value of n_g:

$$n_g = \frac{\omega_{\max} r_W}{v_{\max}} \tag{7.78}$$

where $\omega_{\max}$ is the limiting speed of the motor and $v_{\max}$ is the maximum vehicle speed. The value of n_g will have an influence not only on the motor speed but also on its torque. A low value of n_g results in a small motor speed but a large motor torque.

The motor torque must additionally fulfil the requirement of a desired grading at low speeds, that is:

$$T_{mG} \geq \frac{F_G r_W}{\eta_d n_g} \tag{7.79}$$

in which F_G is the grading force at steady low speeds:

$$F_G = mg(f_R \cos \theta + \sin \theta) \tag{7.80}$$

The value of the motor torque obtained from Equation 7.79 will not necessarily be consistent with the result of Equation 7.77. If T_{mP} larger than T_{mG} is obtained, then the base velocity already determined is correct and ω_b is calculated from:

$$\omega_b = \frac{v_b n_g}{r_W} \tag{7.81}$$

Otherwise, v_b must be recalculated from:

$$v_b = \frac{\eta_d P_{mfs}}{F_G} \tag{7.82}$$

and the motor properties will be P_{mfs}, T_{mG} and ω_b calculated from Equations 7.81 and 7.82. It should be noted that in this case the acceleration performance is better than initially specified. In other words, the time for the desired speed v_d will be lower than the desired time t_d. The whole process is shown in Figure 7.60a.
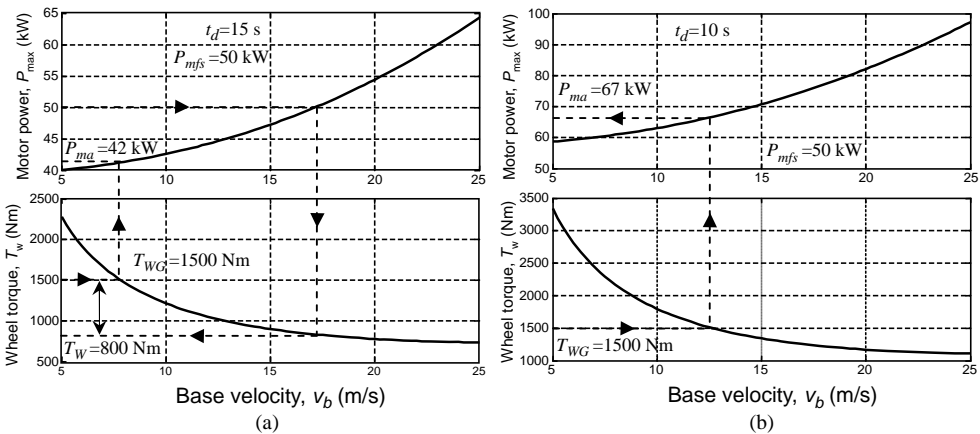
Figure 7.60 The two cases of (a) $P_{mfs} > P_{ma}$ and (b) $P_{mfs} < P_{ma}$

Now if $P_{mfs} < P_{ma}$ is the case, this means that when the performance curves for acceleration are plotted (see Figure 7.60b), the power values in the upper curve are all greater than P_{mfs}. In order to choose the proper power for the motor in this case, again the gradeability should be considered. In the lower curve with the value of T_{mG} the base speed is found and in the upper curve, the power P_{ma} is obtained. Hence for this case, the motor properties are P_{ma}, T_{mG} and ω_b calculated from Equation 7.81. It is also worth noting that in this case the maximum speed of the vehicle will be greater than that initially specified.

For quick reference, the sequence for determining the motor properties is summarized below:

(a) Determine the motor power(s) to achieve the desired speed(s) on level and sloping roads and take the larger value as the candidate for the motor power P_m.
  - Generate the acceleration results similar to Figure 7.59.
  - Calculate the n_g from Equation 7.78.
  - If the value of motor power obtained in (a) lies in the upper curve of acceleration performance (Figure 7.60a), (it means the power for the maximum speed of vehicle is greater than the power for acceleration), then the motor power is P_{mfs} and:
    - o Calculate the motor torque from both Equations 7.75 and 7.77 (T_{mP} and T_{mG}).
    - o If $T_{mP} > T_{mG}$, then the motor properties are T_{mP} and its related v_b value.
    - o If $T_{mP} < T_{mG}$, then the motor properties are T_{mG} and v_b obtained from Equation 7.82.
(b) If the motor power value obtained in (a) does not lie in the upper curve of acceleration performance (Figure 7.60b), (it means the power for the maximum speed of vehicle is lower than the power for acceleration), then the motor power is P_{ma} and:
  - Calculate the motor torque from Equation 7.79 (T_{mG}).
  - In the lower curve of the acceleration performance, at the T_{mG} value obtain the base velocity and in the upper curve, the motor power P_{ma}.

Size of the Engine

In a series HEV, the engine must be able to produce enough energy necessary for the sustainable motion of the vehicle without utilizing the battery energy. At a cruising speed of v_c, the required motor output power to overcome the resistive forces can be determined using Equation 7.73. The engine power must also include the power loss in the driveline, therefore the total engine power for cruising, P_{ec} is:

$$P_{ec} = \frac{v_c}{\eta_G \eta_{Ec} \eta_M \eta_d} \left[mg(f_R \cos\theta + \sin\theta) + cv_c^2 \right] \tag{7.83}$$

where η_G, η_{Ec}, η_M and η_d are the efficiencies of generator, electric converter, motor and driveline respectively.

In a general driving situation that also involves acceleration a_G of the vehicle, the term ma_G should also be included inside the brackets. Since large accelerations occur at low vehicle speeds v_L, the aerodynamic term can be ignored and for such cases the engine power for accelerating, P_{ea} is:

$$P_{ea} = \frac{mv_L}{\eta_G \eta_{Ec} \eta_M \eta_d} \left[a_G + g(f_R \cos\theta + \sin\theta) \right] \tag{7.84}$$

In order to compare these two types of engine power requirements, let us define an overall aerodynamic coefficient per mass of vehicle c_{pm}:

$$c_{pm} = \frac{\rho_A C_d A_F}{2m} \tag{7.85}$$

Then, it is possible to calculate a specific engine power (power per mass) for different speeds and accelerations. Figure 7.61 is generated for a c_{pm} of equal to 2.25×10^{-4}, rolling resistance coefficient of
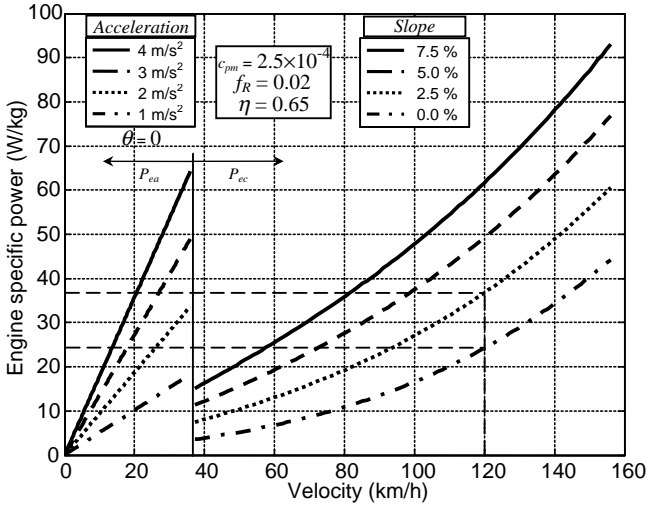
Figure 7.61   The engine specific power rating

0.02 and an overall efficiency of 0.65, for both low speed and high speed ranges. In the low speed range, a flat road is considered and for the vehicle accelerations of 1, 2, 3, and 4 m/s^2, the engine power requirements at different speeds up to 20 m/s are calculated. In the high speed range, for slopes of 0, 2.5, 5.0 and 7.5%, the variations of engine specific power at different vehicle speeds are determined.

To supply power for a cruising speed of 120 km/h on a level road, the specific power is 24 W/kg, whereas for the same speed on a 2.5% slope it will be 37 W/kg (for a 1200 kg vehicle the engine power values are 28.8 and 44.4 kW respectively). The first choice will also provide the necessary power for cruising at 93, 72 and 58 km/h speeds on roads with 2.5, 5.0 and 7.5% slopes respectively. This power from the engine may only partly support the necessary power for the steady acceleration of the vehicle (accelerations of 4, 3, 2 and 1 m/s^2 up to 12, 18, 25 and 45 km/h speeds).

As the high accelerations of the vehicle occur within the constant torque phase of the traction motor, the acceleration is almost constant in this phase. For a high acceleration performance from the standstill up to base speed v_b (km/h), the variation of acceleration during the constant torque phase will be something like that shown in Figure 7.62. For a base speed of 50 km/h in 5 seconds, an acceleration of around 3 m/s^2 is needed. This requires a motor power of around 60 kW (see Figure 7.59) and an engine power of about 90 kW. For this vehicle the 0–100 km/h time is around 12 seconds (see Figure 7.56). Thus even the second choice for the engine (44.4 kW) can only produce half of the required power for such acceleration. Increasing the engine size will increase the weight and cost and therefore it is better to have the remaining power supplied by the battery if such high accelerations are required.

Size of the Battery

The battery must produce enough power to achieve the required performance over a multitude of driving conditions. In the previous section we discussed a design case in which the instantaneous power requested by the motor was greater than the supplied engine power. The deficit must be produced by the battery. In mathematical form, the battery output power is:

$$P_B \geq \frac{P_M}{\eta_M} - P_e \tag{7.86}$$

in which the first term is P_{in} the input power to the motor. The capacity of a battery is usually given in kW-hour (kWh). Determining the size of battery for the vehicle requires additional information including
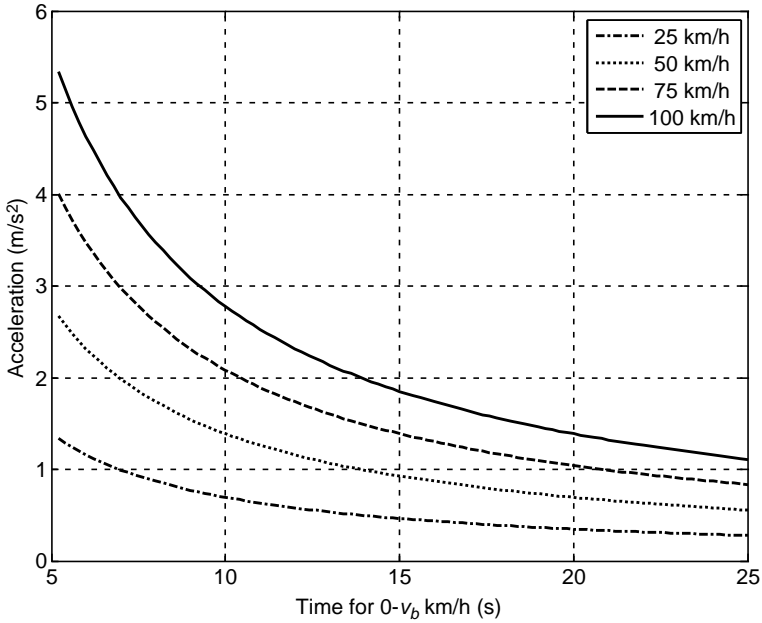
Figure 7.62   Constant torque accelerations at different $0\text{-}v_b$ (km/h) times

the 'all-electric' range of the vehicle and charging/discharging patterns. If the vehicle is designed to operate over large electric ranges (e.g. 60 km), obviously it will need larger capacities.

The charging/discharging pattern also has an important effect on the battery size. Let us rewrite Equation 7.45 in the form (assuming a constant working voltage):

$$SOC(t) = 1 - \frac{1}{E_0} \int_0^t P(t)dt \tag{7.87}$$

in which E_0 is the battery capacity in Wh. At time t_1 SOC is:

$$SOC(t_1) = 1 - \frac{1}{E_0} \int_0^{t_1} P(t)dt \tag{7.88}$$

Thus $\Delta SOC = SOC(t_2) - SOC(t_1)$ is:

$$\Delta SOC = -\frac{1}{E_0} \int_{t_1}^{t_2} P(t)dt \tag{7.89}$$

The integral term is the net energy ΔE, taken from or given to the battery in the time span t_1 to t_2. For a zero ΔE the SOC will remain unchanged, whereas for negative and positive ΔE values, the SOC will increase or decrease respectively. If both the ΔSOC and ΔE can be estimated in a reasonable working interval, then the battery capacity E_0 simply is:

$$E_0 = \frac{\Delta E}{\Delta SOC} \tag{7.90}$$

The working range for SOC discussed earlier (see Section 7.4.3.3) is a good value for ΔSOC and ΔE is best determined over a wide range of battery operation in which the value of ΔSOC occurs. The vehicle starts with the battery's upper working limit SOC_H and it must finish at the same SOC level at the end of driving cycle. Energy is supplied to the battery to keep its SOC unchanged between the start and the end of the cycle. The net energy consumption during such cycles simply is the average power consumption (efficiency of the battery included) times the cycle time Δt. Therefore the battery capacity can be determined from the following equation:

$$E_0 = \frac{P_{av}\Delta t}{SOC_H - SOC_L} \tag{7.91}$$

Example 7.6.2

Determine the component sizes of a series HEV with the vehicle properties of Table 7.11, in order to achieve the following performance:

(a) maximum speed of 160 km/h on a flat road;
(b) gradeability of 5% at 120 km/h;
(c) 0–100 km/h acceleration time of 15 seconds;
(d) gradeability of 45% at low speeds;
(e) all-electric range of 20 km at speed of 60 km/h.

The maximum allowable motor speed is 6000 rpm. The maximum and minimum SOC values are 0.8 and 0.2 respectively.

The overall efficiencies $\eta_G, \eta_{Ec}, \eta_M$ and η_d are 0.85, 0.95, 0.85 and 0.95. The battery efficiency is 0.9.

Solution

Motor Properties
The sequence introduced for the motor sizing will be used. To obtain the first requirement of 160 km/h final speed, the motor output power simply is (Equation 7.70)

$$P_{mfs} = \frac{v_{max}}{\eta_d}(mf_R g + cv_{max}^2). \text{ The numerical result is 48 kW.}$$

The second requirement similarly is: $P_m = \frac{v}{\eta_d}[cv^2 + mg(f_R \cos\theta + \sin\theta)]$. The numerical result of 44.5 kW for this case is lower than that for the maximum speed. Thus $P_m = 48$ kW must be selected.

For (c) the MATLAB program of Example 7.6.1 can be used for $t_d = 15$ s, and the result is shown in Figure 7.63. The ratio of reduction gear is obtained from the motor speed limitation (Equation 7.78): $n_g = \frac{\omega_{max}}{v_{max}} r_w = 4.24$.

For the motor power of 48 kW, the base speed and wheel torque are 13.4 m/s and 1020 Nm. The corresponding motor torque then simply is $T_{mP} = 1020/4.24 = 240$ Nm.

For (d) the tractive force must be larger than the resistive force at low speed and from Equation 7.79: $T_{mG} = 376$ Nm.
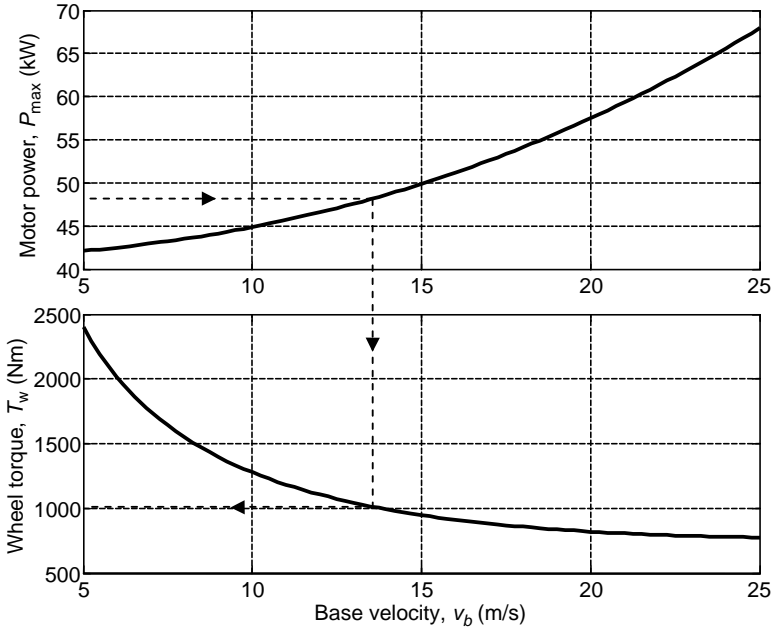
Figure 7.63   Acceleration performance results for Example 7.6.2

Since $T_{mP} < T_{mG}$, then the motor torque must be taken T_{mG} and v_b from Equation 7.80 is: $v_b = 9.03$ m/s and $\omega_b = 1220$ rpm. The motor properties are shown in Figure 7.64. With these values, the performances of the vehicle are shown in Figure 7.65. It is clear that the final speed and gradeability requirements are exactly met, while the final speed at 5% slope is improved (125 km/h instead of 120 km/h). Also the required time t_d is reduced to 13.5 second from initial 15 seconds (not shown in Figure 7.65).

Engine Power

From Equation 7.83 the engine power at the cruising speed of 120 km/h on a level road and with overall efficiency of 0.6521 is 34.9 kW. For the same speed on a 5% grade the power is a much larger value of 65.0 kW. The former is also suitable for an average acceleration of 0.75 m/s^2 at average speed of 20 m/s.

Battery Size

For a motor overall efficiency of 0.85, the minimum battery output power from Equation 7.86 is 21.7 kW.

To determine the battery capacity, the average power and its duration can be obtained from:

$$P_{av} = \frac{v_{av}}{\eta_G \eta_{Ec} \eta_b}(mf_R \, g + cv_{av}^2) = 7.95 \text{ kW and } \Delta t = \frac{20}{60} = 0.33\text{h}.$$

The battery capacity from Equation 7.91, therefore, is: $E_0 = 4.4$ kWh.
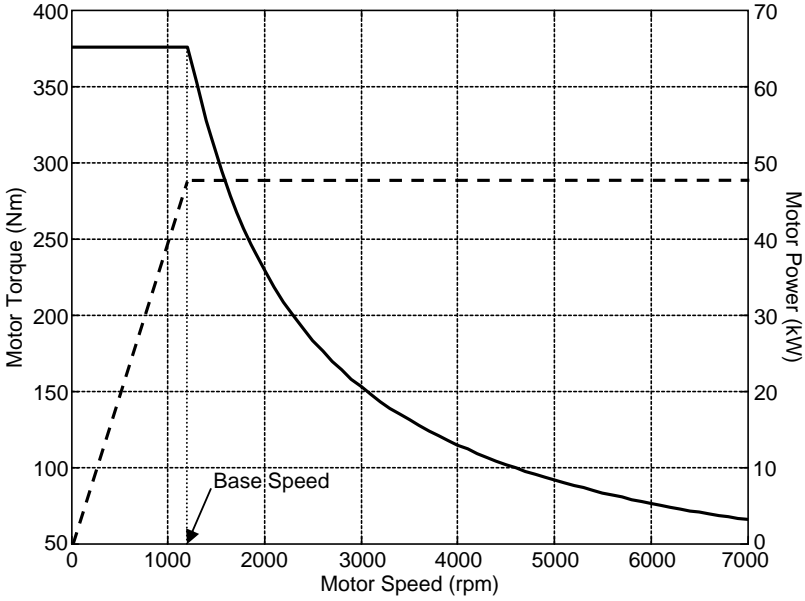
Figure 7.64   The motor properties for Example 7.6.2
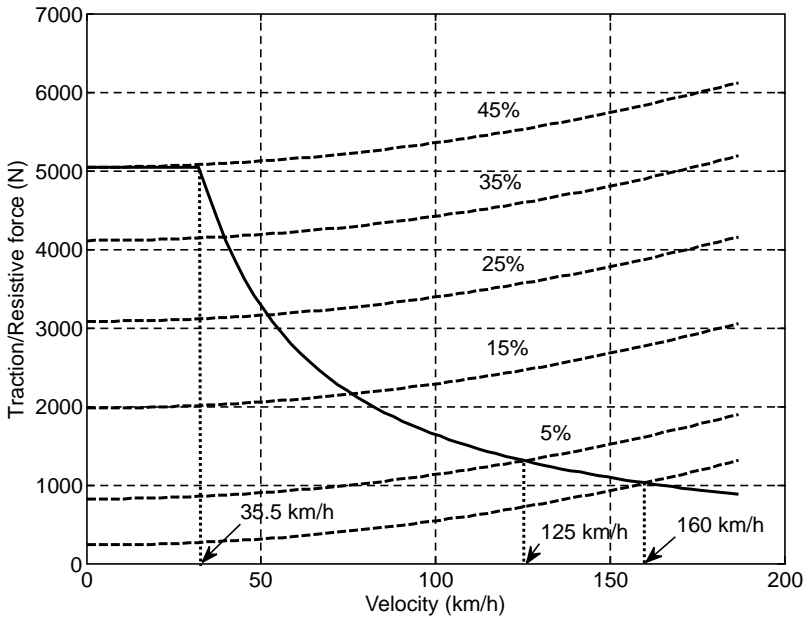
Figure 7.65   The final performances of the vehicle in Example 7.6.2

7.6.2.2 Parallel HEV

The electric-only mode of operation of a parallel HEV depends only on its electric motor specifications, however, only a limited performance is usually expected in electric-only mode. For the desired performance of the vehicle in this mode, the electric motor can be designed based on the methods discussed earlier in previous section. In practice, the design of the electric motor, however, must be performed in relation to the design of the engine, as the two traction sources produce the motive force for the motion of the vehicle.

Engine Power
The engine in a parallel HEV is designed to propel the vehicle at high steady speeds without any help from the electric source. At a desired high speed v_H the tractive power balances the resistive power and the motive power must also overcome the driveline losses. The necessary engine power, therefore, is:

$$P_e = \frac{v_H}{\eta_d} \left[mg(f_R \cos\theta + \sin\theta) + c v_H^2 \right] \tag{7.92}$$

The design could be analyzed for a flat road ($\theta = 0$) or a mild slope at a desired speed v_H. It should be noted that the high steady speed of the vehicle is not determined by the engine power, but is governed by the engine torque and the overall gear ratio (see Chapter 3). Therefore, the power rating obtained from this analysis is only an initial estimation of the engine maximum power and should be finalized when the torque-speed characteristics are also available.

Electric Motor Power
Here we consider a parallel hybrid with only one electric motor that is connected to the driving wheels through a single reduction gear. The electric motor is designed to supply assisting power for the high acceleration part of the motion as well as the low speed stop-start portions of the driving cycles. As the driving conditions are extremely varied, an exact estimation of the motor properties is impossible.

As an attempt to estimate the motor power, it is reasonable to consider the high acceleration motion of the vehicle in which a desired speed v_d is expected during a specified time t_d when the vehicle starts from the rest. Such vehicle performance must be achieved by simultaneous supply of power from both the engine and electric motor. For a total power of P_{tot} supplied by both the engine and motor, the governing equation is (see Section 7.5.1.2):

$$t_d = k_1 \ln \frac{v_{max} - v_d}{\sqrt{v_d^2 + v_d v_{max} + k}} + k_2 Arc \tan \frac{2v_d + v_{max}}{\sqrt{4k - v_{max}^2}} + C \tag{7.93}$$

in which:

$$C = -k_1 \ln \frac{v_{max}}{\sqrt{k}} - k_2 Arc \tan \frac{v_{max}}{\sqrt{4k - v_{max}^2}} \tag{7.94}$$

$$k = \frac{P_{tot}}{c v_{max}} \tag{7.95}$$

$$k_1 = -\frac{m}{c} \cdot \frac{v_{max}}{2v_{max}^2 + k} \tag{7.96}$$

$$k_2 = \frac{k_1}{v_{max}} \cdot \frac{2k + v_{max}^2}{\sqrt{4k - v_{max}^2}} \tag{7.97}$$

$$v_{max} = e + h \tag{7.98}$$

$$e = (a+d)^{\frac{1}{3}}, \ h = \text{sgn}(a-d)|a-d|^{\frac{1}{3}} \tag{7.99}$$

$$a = \frac{P_{tot}}{2c}, \ b = \frac{F_0}{3c}, \ d = (a^2 + b^3)^{0.5} \tag{7.100}$$

For a given desired speed v_d and time t_d, the total power can be determined by the application of Equation 7.93. Then, the motor power for high acceleration can be regarded as the difference between the total power and the engine power:

$$P_{ma} = P_{tot} - P_e \qquad (7.101)$$

It is important to note that the acceleration performance is actually based on the availability of the total tractive force and not the power. Hence the assumption of a total maximum power delivery by motor and engine does not necessarily lead to an actual tractive effort with a desired acceleration performance.

The other requirement from the motor is to produce sufficient tractive power for low speed stop-start circumstances. This includes a variety of driving conditions with different power requirements. An estimate for this power can be obtained from well-known standard driving cycles. At low speed stop-start motions the required power for the motor is (see Equation 7.84):

$$P_{msg} = \frac{mv}{\eta_d} a_G + \frac{mv}{\eta_d} g(f_R \cos\theta + \sin\theta) \qquad (7.102)$$

The first term is the power requirement for the acceleration and depends only on the driving pattern. The second term is the power requirement due to the resistive forces and depends mainly on the slope of the road. In order to evaluate the magnitudes of each part in Equation 7.102, we shall examine a standard urban driving cycle in the following example.

In a design process for the electric motor, different driving cycles and grading requirements can be considered at low speed stop-start motions so that the tractive force is only produced by the motor. The maximum value of motor power obtained in this process is P_{msg} of Equation 7.102. It should be noted that P_{msg} should not become unnecessarily large by assuming larger grades, because in such circumstances the engine torque can also assist the motor.

In any case, after the two power values P_{ma} and P_{msg} were determined from Equations 7.101 and 7.102, the larger of the two should be taken as the motor power. The other motor specifications such as the torque and base speed values must be determined by using additional information.

Example 7.6.3

The speed-time information in the first 200 second segment of ECE15 driving cycle (see Section 5.3) is given in Table 7.12. (In the actual driving cycle this segment repeats four times.)

Table 7.12   Cycle information for Example 7.6.3

Time (s)	Speed (km/h)	Time (s)	Speed (km/h)	Time (s)	Speed (km/h)
0	0	56	15	135	35
6	0	61	32	143	50
11	0	85	32	155	50
15	15	93	10	163	35
23	15	96	0	176	35
25	10	112	0	178	32
28	0	117	0	185	10
44	0	122	15	188	0
49	0	124	15	195	0
54	15	133	35	200	0

(a) Plot the driving cycle.
(b) Determine and plot the acceleration of the cycle.

(c) Determine and plot the power requirement to accelerate a unit mass of the vehicle.

(d) Determine and plot the power requirement per unit mass of vehicle to overcome resistive forces. Consider a rolling resistance coefficient of 0.02 and grades of 0, 10, 20 and 30%.

(e) For a vehicle of 1200 kg mass and driveline efficiency of 0.95, determine the motor power requirement for this cycle.

Solution

(a) The first 200-second segment of ECE15 cycle is plotted in Figure 7.66.

(b) The cycle acceleration can be obtained by following MATLAB commands:

```
t = 0: 0.1: max(t0); v = interp1(t0,v0,t);
a = [diff(v)./diff(t) 0]; %Vehicle acceleration (m/s^2)
```

Where t0 and v0 are two row vectors containing the time and speed values. The plot of acceleration is given in Figure 7.67.

(c) The power requirement to accelerate 1 kg of the vehicle is speed times the acceleration ($v.a_G$) and can be determined by a simple command 'va=a.*v'. The result is plotted in Figure 7.68.

(d) The resistive forces include the rolling resistance, gravity and aerodynamic forces. Since the cycle is low speed, the aerodynamic force is small and is ignored (Equation 7.102). The power per unit mass is simply $F_R.v/m$. The following MATLAB loop simply obtains the results for the four grades of 0, 10, 20 and 30%:
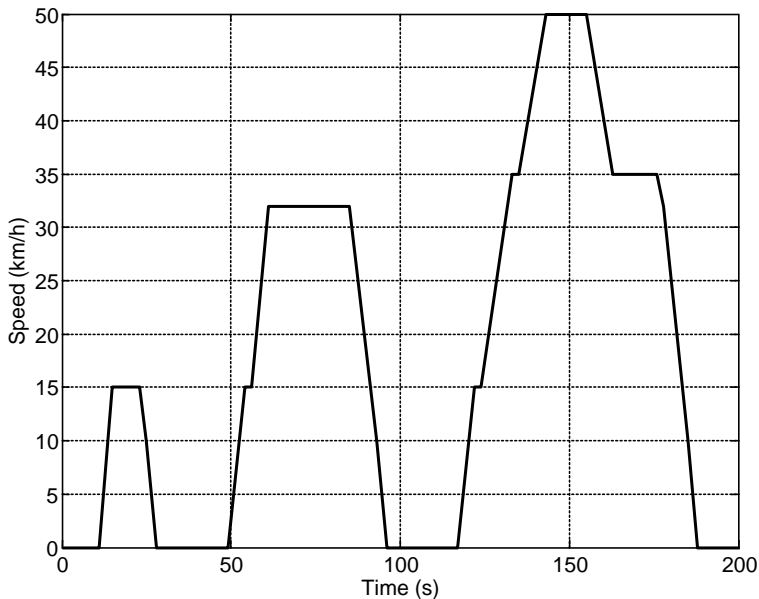
Figure 7.66   First segment of the ECE15 driving cycle
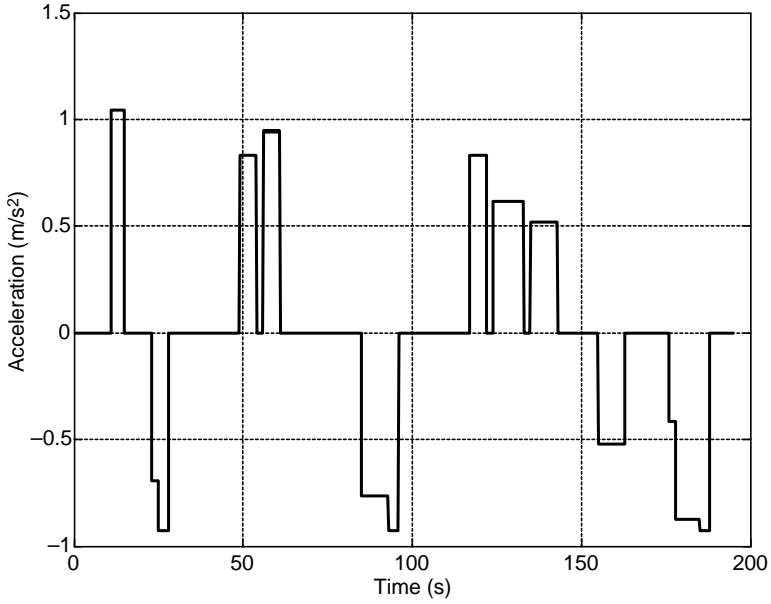
Figure 7.67   Acceleration profile for the driving cycle of Figure 7.66
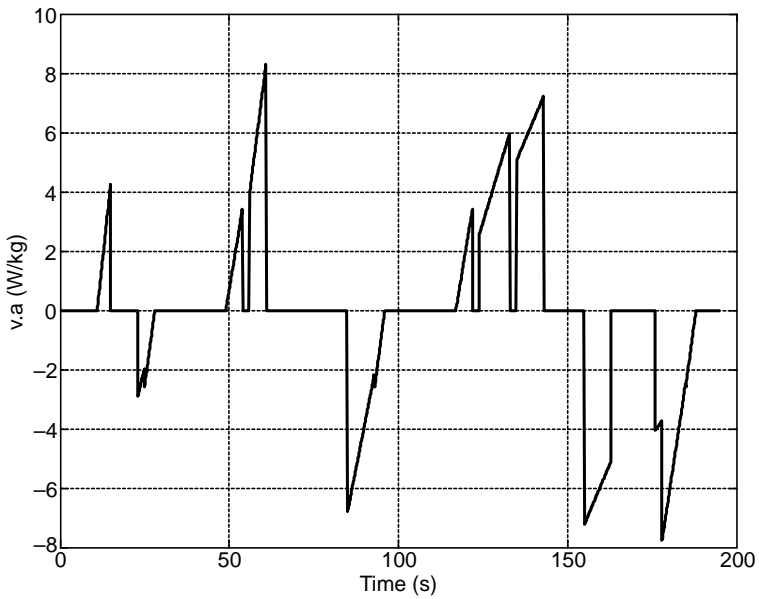
Figure 7.68   Specific power due to acceleration for the driving cycle of Figure 7.66

for i=1: 4, vfr(i, :)=v*9.81*(0.02*cos(atan((i-1)/10))+sin(atan((i-1)/10))); end

Figure 7.69 illustrates the variation of the power requirement for the unit mass of the vehicle.

(e) For the given vehicle, the maximum power requirement for acceleration on this cycle according to Figure 7.68 is 8.2×1200/0.95 or 10.4 kW. The power requirements to overcome the resistive forces according to Figure 7.69 are around 3.0, 20, 36.5 or 53 kW on a flat, 10%, 20% or 30% grade respectively. The total motor power is the summation of the two parts (Equation 7.102).
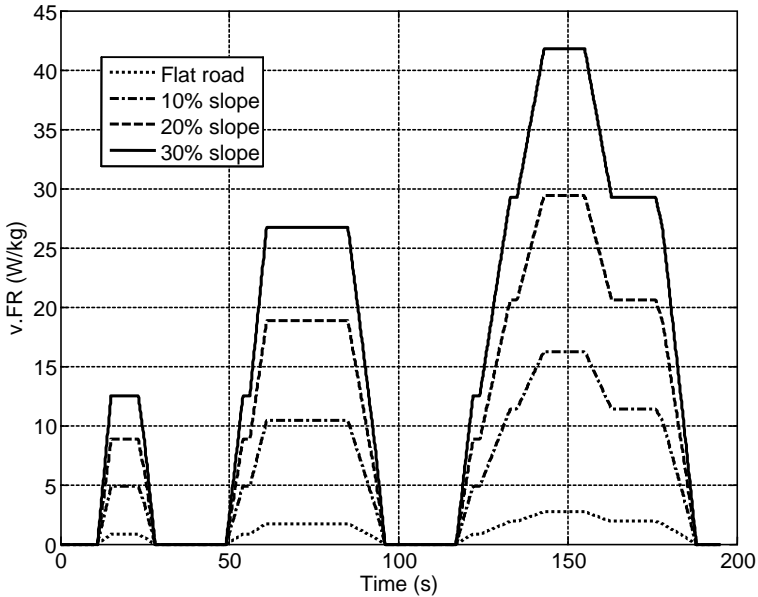
Figure 7.69   Specific power due to resistive forces for the driving cycle of Figure 7.66

Size of the Battery

The battery must be capable of producing instantaneous power to achieve performance requirements as well as containing enough energy for the continuous operation of the system. The electric power of the battery in a parallel hybrid vehicle should be larger than the demand of the electric motor, or:

$$P_B \geq \frac{P_M}{\eta_M} \tag{7.103}$$

The battery capacity is designed in order that the motor energy requirements are met either during a pure electric acceleration phase or during motion on an urban driving cycle. Equations 7.90 and 7.91 are still applicable for this purpose.

Example 7.6.4

Determine the component sizes of a parallel HEV with the same properties of Example 7.6.2 and the same performances except:

- Consider a 0–100 km/h time of 10 seconds.
- The motor must be capable of propelling the vehicle on a 5% slope ECE15 driving cycle.
- Consider an all-electric range of 10 km on an ECE15 flat cycle with no regeneration.
- The minimum and maximum SOC values are 0.4 and 0.8 respectively.
- The overall motor and battery efficiencies are 0.85 and 0.9.

Solution

The design steps are straightforward, nevertheless to follow the solution more easily a MATLAB program is also provided in Figure 7.70 and its accompanying function in Figure 7.71.

Engine Power

As the requirement is the same as for the Example 7.6.2, the engine power rating in this case is again 48 kW.

```
% Example 7.6.4

clc, close all, clear all

global eta Ca F0 m vd td

% Vehicle data
m=1200;    % Vehicle mass (kg)
fR=0.02;   % Rolling resistance coefficient
Ca=0.4;    % Overall aerodynamic coefficient
rW=0.3;    % Wheel effective radius (m)
eta=0.95;  % Driveline efficiency
theta_1=5;  % Gradeability at high speed (%)
theta_2=45;  % Gradeability at low speed (%)
vmax=160;   % Maximum vehicle speed (km/h)
v2=120;     % Grading high speed (km/h)
SOC_H=0.8;
SOC_L=0.4;
vd=100;     % Desired speed (km/h)
td=10;      % Desired time (s)

F0=m*9.81*fR;
vmax=vmax/3.6;
v2=v2/3.6;
theta_1=atan(theta_1/100);
theta_2=atan(theta_2/100);
vd=vd/3.6;
```

Figure 7.70   The main MATLAB program for Example 7.6.4

```
% Determine the engine power to achieve the desired max speed
Pmax_e1=(Ca*vmax^3+F0*vmax)/eta;
% Determine the engine power to achieve the desired gradeability
Pmax_e2=(Ca*v2^3+m*9.81*(fR*cos(theta_1)+sin(theta_1))*v2)/eta;
Pe=max(Pmax_e1, Pmax_e2); % The engine power is the maximum of the two

% Determine the total power generated by engine + motor to achieve 'vd' at 'td'
Pt=fsolve(@Ptot, Pe, optimset('Display','off'))        % call function 'Ptot'
Pma=Pt-Pe;    % Equation 7.101

% Determine the motor power for ECE15 driving cycle
vaG=8.3;        % From Figure 7.68
vFR=8.0;        % From Figure 7.69 at 5% grade
Pmsg=(vaG+vFR)*m/eta;    % Equation 7.102
Pm=max(Pma, Pmsg); % The motor power is the maximum of the two

% Determine the battery power
% use 'va' and 'vfr' from Example 7.6.3
pcycle=m*(va/3.6^2+vfr(1, :)/3.6);   % The power demand in a cycle (flat)

% pcyclep is the positive part of pcycle
pcm=mean(pcyclep)/etam/etab;% Average of positive power divided by efficiencies

nc=10000/x;   % Number of segments in 10 km ('x' is distance per cycle)
tc=nc*200/3600;        % Total travel time in hours
Ec=pcm*tc/1000;              % Total energy consumption during 10 km travel (kWh)
Eb=Ec/(SOC_H-SOC_L);          % Battery capacity (kWh)
```

Figure 7.70   (*Continued*)

```
function dt=Ptot(Pmax)          % function called from the main program

global eta Ca F0 m vd td

a=eta*Pmax/2/Ca;
b=F0/3/Ca;
d=sqrt(a^2+b^3);
e=(a+d)^(1/3);
h=sign(a-d)*abs(a-d)^(1/3);
vmax=e+h;

k=eta*Pmax/Ca/vmax;
k1=-m*vmax/Ca/(2*vmax^2+k);
k4=sqrt(4*k-vmax^2);
k2=k1*(2*k+vmax^2)/vmax/k4;
k3=sqrt(k);
C=-k1*log(vmax/k3)-k2*atan(vmax/k4);
k3=sqrt(vd^2+vd*vmax+k);
tcp=C+k1*log((vmax-vd)/k3)+k2*atan((2*vd+vmax)/k4);

dt=tcp-td;       % function returns when dt=0
```

Figure 7.71   The MATLAB function for Example 7.6.4

Motor Power

To obtain the motor power from Equation 7.101, an iteration process is involved. This has been performed in the function 'Ptot'. Upon the return from the 'fsolve' statement the total power to obtain 0–100 speed within 10 seconds is 57.3 kW and P_{ma} is $57.3 - 48 = 9.3$ kW. However, by making use of Figures 7.68 and 7.69 (interpolate for 5% slope), Equation 7.102 results in $P_{msg} = 20.6$ kW. Thus the motor power is selected as 21 kW.

Battery

From Equation 7.103 the power of the battery should be larger than 24.2 and, for instance, 25 kW could be selected.

For the battery capacity the requirement is 10 km of travel on an ECE15 driving cycle. The total power consumption during the cycle with no regeneration can be obtained by adding up the results of Figure 7.68 and the lower part of Figure 7.69 multiplied by the vehicle mass. The result for the positive part is illustrated in Figure 7.72. The average value of this power divided by the efficiencies of the motor and the battery is 2.4 kW. The total energy consumption during the 10 km travel as the value of average power times the total travel time is 1.32 kWh. The battery capacity from Equation 7.91 is 3.3 kWh.
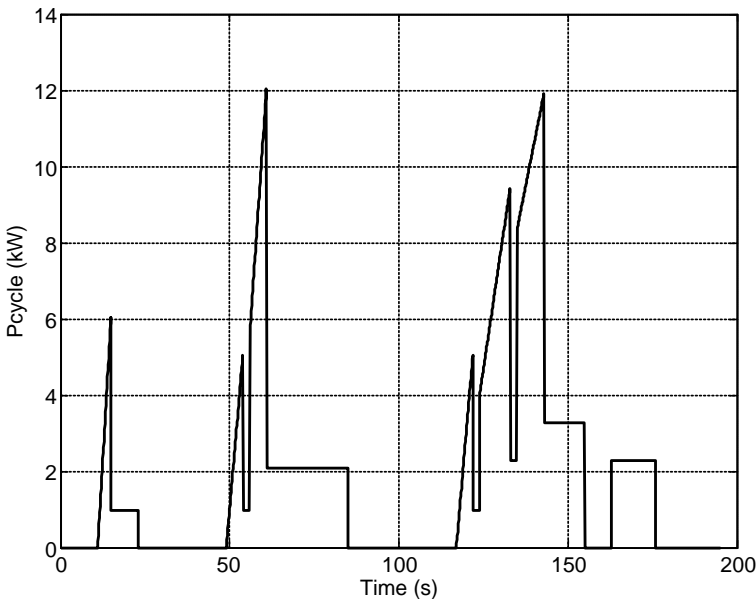
Figure 7.72 The positive power demand in a single segment of the driving cycle

7.6.3 Optimum Sizing

Hybrid electric vehicles are designed around minimizing the fuel consumption, exhaust emissions and manufacturing costs without compromising HEV performance such as vehicle maximum speed, expected acceleration and gradeability. Sizing the HEV components for performance, discussed in the foregoing
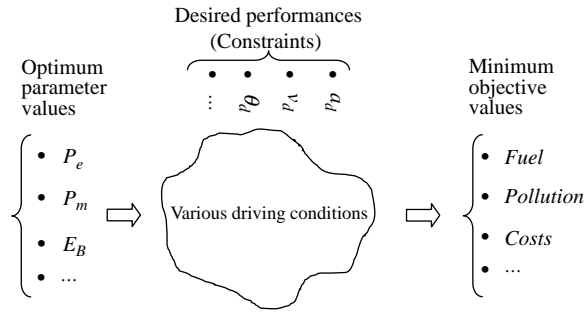
Figure 7.73 Component optimization concept

section, does not necessarily lead to the above objectives. A more successful HEV design requires optimal sizing of its key mechanical and electrical components in order not only to maintain or enhance driving performance but also to minimize the objective parameters such as the fuel consumption, emissions, costs and wear under various driving conditions that have to be taken into account.

The optimization concept illustrated in Figure 7.73 implies that there is a set of optimum parameter values for the vehicle (e.g. engine power P_e, motor power P_m, battery size E_b, etc.) such that if the vehicle is used in various driving conditions with desired performance qualities, the energy consumption and emissions of the vehicle as well as several other objective measures would be minimized.

In mathematical terms, this is an optimization problem of the following general form:Find a solution

$$x = [x_1, x_2, x_3, \ldots, x_n] \tag{7.104}$$

that minimizes the objective function:

$$J(x) = w_1 f_1(x) + w_2 f_2(x) + \cdots + w_m f_m(x) \tag{7.105}$$

subject to the following constraints:

$$g_i(x) \geq 0, i = 1, 2, \ldots, p \tag{7.106}$$

in which:

x_i (i = 1, 2, ..., n) are the n optimum values of HEV parameters,
f_i (i = 1, 2, ..., m) are the m objective values that should be minimized,
w_i (i = 1, 2, ..., m) are the weighting factors for balancing among the objective values and
g_i (i = 1, 2, ..., p) are the p constraint equations that must additionally be met.

Examples for x_i are engine and motor powers P_e and P_m. Examples for f_i are fuel consumption FC and cost C. Examples for g_i are 0–100 km/h time of 10 seconds (i.e. $g_1 = 10 - t_{100}$) and the maximum speed of 180 km/h (i.e. $g_2 = v_{max} - 180$).

In theory, the optimization result must be independent of the vehicle driving patterns. In other words, in any driving conditions, the HEV components should be optimum. The optimization processes, however, are unable to solve the problem independently of driving patterns and instead consider various driving cycles in order to broaden their usefulness. Therefore, the design of an HEV that considers only a few driving cycles is likely to be only partially optimal.

The efficiency of an HEV, in addition, depends on the management of its different energy elements. A successful component optimization process of an HEV, therefore, should also include power control parameters. This means prior to component sizing, the control strategies for the power management of the

HEV system should also be developed. There are several approaches to the solution of this problem (e.g. see [3]) but they are all beyond the scope of this book.

7.7 Power Management

The energy expenditure of a hybrid vehicle is crucial to the goal of achieving improved fuel efficiency compared with conventional vehicles. This needs more efficient use of energy sources such as chemical (fuel) or electric (battery) energies. The instantaneous flow of energy therefore must be monitored and controlled in a hybrid vehicle in order that the total energy expenditure is kept as low as possible. This requires a *power management* strategy as the rate of energy consumption is the power. Thus a control system is necessary for the hybrid vehicle in order to manage all the engine, motor-generator, battery and transmission elements at their best operating points. Each element also requires a control system to regulate its outputs according to the desired values at different conditions. For example, an engine management system (EMS) is responsible for monitoring and controlling the engine operation in diverse working conditions (see Section 2.7). When an input is specified (throttle), then the EMS will control the injection and ignition systems in order to optimize the engine performance.

A *supervisory* control system with the structure shown in Figure 7.74 takes the overall control of the hybrid vehicle and determines the best operating point of each component according to the driver's demands and information received from the vehicle, environment and component outputs. The commands issued by this controller are fed to the local controllers of all components as their inputs and these low level controllers are responsible for regulating the required outputs of each individual component.
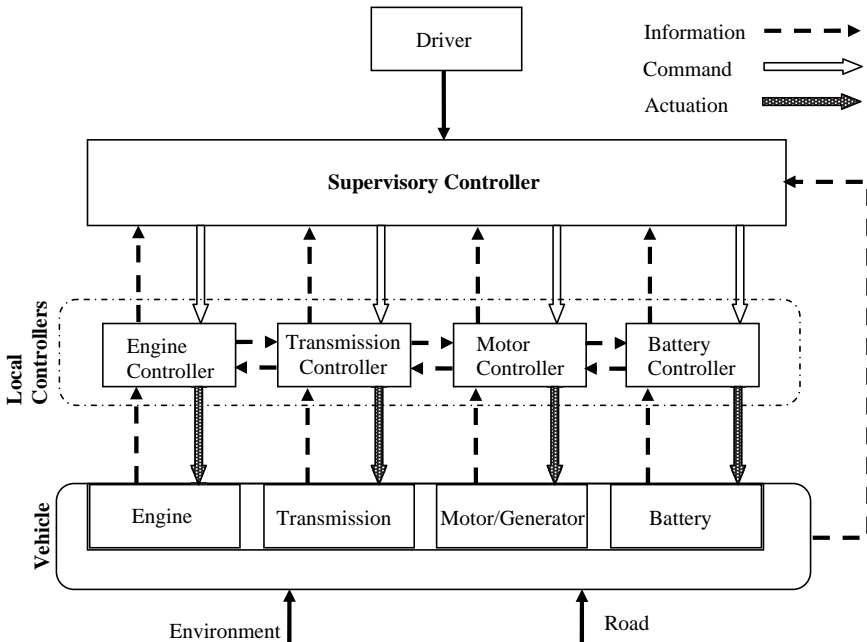
Figure 7.74 HEV control hierarchy

7.7.1   Control Potential

The potential for the energy efficient motion of the hybrid vehicles stems from the availability of two energy sources with the possibility of using them under more efficient working conditions than would be possible if only one source is used. The combination of the two sources allows each source to be used one at a time or both together according to load requirements and hence provides opportunities for energy optimization.

7.7.1.1   Engine Shutdown

Engine idling is one of the everyday occurrences in driving situations such as warming up the engine, waiting for someone, stopping in queues and in traffic. There have been debates on the necessity of turning the engine off at idling as the fuel is wasted and the air is polluted unnecessarily. Engine shutdown at vehicle stops, therefore, is useful in reducing pollution, heat, noise and fuel consumption. On the other hand, when a conventional ICE vehicle is at rest, the engine still provides power for some of accessories such as A/C and alternator (if the battery needs charging). Moreover a vehicle with a stopped engine cannot drive off immediately. In addition, starting the engine needs energy and frequent engine start/stops have damaging effects on the starter and the battery. Therefore a question remains of how frequently the engine can be stopped and restarted but relative to the extra costs and energy used. The answer is not simple due to the diversity of vehicles, engines and working conditions, but nonetheless, figures as low as '10 seconds' have been proposed for the minimum vehicle stop time that the engine shut down is beneficial.

However, hybrid designs allow the possibility of shutting down the engine with no concerns. In other words, when vehicle stops for a period of time, the engine can be turned off but the A/C will still work and vehicle can drive off immediately on electric power.

7.7.1.2   Economic Regions for ICE

The engine fuel efficiency was discussed in Chapter 5 and it was pointed out that the fuel consumption will be lower if the engine works in low BSFC regions of engine torque-speed map. In HEVs it is possible to arrange for engine to work in its more efficient map areas (Figure 7.75) by changing its load at a specified working condition.

7.7.1.3   Regeneration

The vehicle attains kinetic energy when it accelerates to a certain speed. This energy is wasted (transformed into heat) in normal vehicles as the vehicle comes to a stop. In hybrid vehicles there is the possibility of regaining a part of the kinetic energy (regeneration) by using the generator to develop braking torque. There are other influencing factors that can affect the efficiency of regenerative braking, as discussed next.

The Generator
The function of the generator is to apply resistive torque on the wheel that in turn causes the tyre to produce the braking force (see Section 3.10). The torque of a generator is dependent on its rotating speed and power as shown in Figure 7.27 (for a motor). It is evident that only at low speeds can the generator apply high torques and when the speed is high the torque is low (i.e. low braking force). In other words, the generator is unable to produce high braking forces at high speeds.

The Battery
The battery SOC or its charging current impose constraints on the regenerating energy. When the SOC is high, charging the battery might not be possible. The charging current of the battery will always be a major
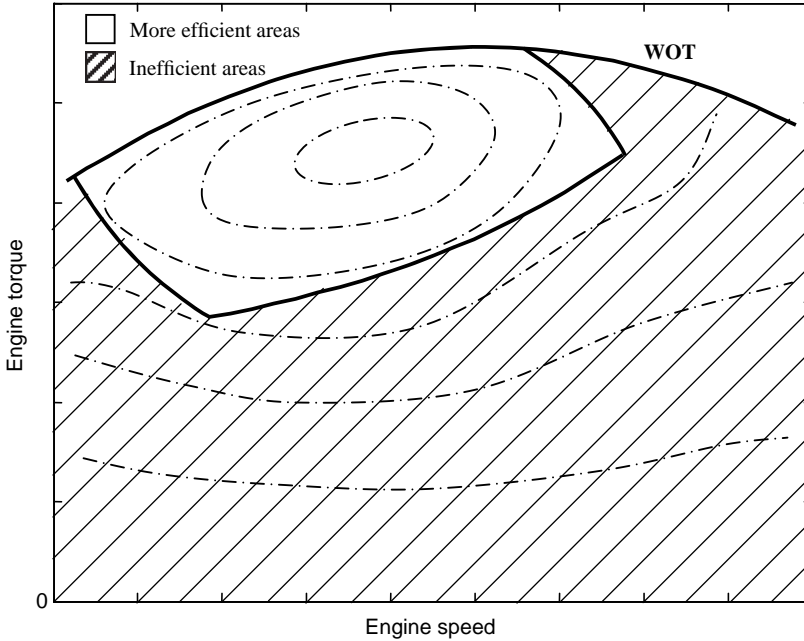
Figure 7.75   More efficient areas in engine torque-speed map

limiting factor in absorbing the energy during regenerative braking. In addition, the efficiency of the generator and the battery also reduces the effectiveness of the regenerative braking. The mechanical power P_m available at generator input during braking is:

$$P_m(t) = ma(t)v(t) - P_R(t) \tag{7.107}$$

in which $a(t)$ is the instantaneous deceleration (a positive value) and P_R is the power loss due to resistive forces (i.e. rolling resistance and aerodynamic forces). The available power for the absorption by the battery during the regenerative braking is:

$$P_{ba}(t) = \eta_{gb}P_m(t) \tag{7.108}$$

where η_{gb} is the overall efficiency of the generator-battery system during charging. Assuming a constant voltage V with a maximum current I for the battery during regenerative charging, the maximum absorbable power by the battery is:

$$P_{bm} = VI \tag{7.109}$$

If the rate of input mechanical energy is larger than P_{bm}/η_{gb}, the battery only absorbs P_{bm} otherwise the value in Equation 7.108 will be absorbed. The efficiency of regenerative braking at each instant is defined as the ratio of absorbed power P_b to the potentially available mechanical power at the generator input:

$$\eta_r(t) = \frac{P_b(t)}{P_m(t)} \tag{7.110}$$

The overall efficiency of the regenerative braking during the braking phase is the ratio of relevant energies:

$$\eta_r = \frac{E_b}{E_m} = \frac{\int_{t_0}^{t_1} P_b(t)dt}{\int_{t_0}^{t_1} P_m(t)dt} \tag{7.111}$$

At low speeds so that $P_m < P_{bm}/\eta_{gb}$ Equation 7.110 simply reduces to $\eta_r = \eta_{gb}$, so is Equation 7.111 for constant values of the overall efficiency of the generator-battery system.

Example 7.7.1

A hybrid vehicle with 1000 kg mass is to stop within 100 m distance with an initial speed of 100 km/h. If the battery with a voltage of 200 V can be charged at a maximum current of 100 A, what percentage of vehicle kinetic energy will be absorbed by the battery? The overall efficiency of the generator-battery combination is 0.85. Ignore the power loss due to resistive forces.

Solution

The total energy of vehicle simply is $0.5\,mv^2 = 385.8\,\text{kJ}$ (the energy of rotating masses is ignored). The deceleration and time of stop are (the resistive forces other than the brake force are ignored):

$$a = \frac{v^2}{2x} = 3.858\,\text{m/s}^2 \quad \text{and} \quad t_b = \frac{v}{a} = 7.2\,\text{s}.$$

P_{bm} from Equation 7.109 is 20 kW. According to Equation 7.107, before time $t^* = t_b - \frac{P_{bm}}{\eta m a^2} = 5.619\,\text{s}$ the input mechanical power is larger than the maximum absorbable power. The total absorbed energy by the battery therefore is:

$$E_b = P_{bm}t^* + \int_{t^*}^{t_b} \eta_{gb}P_m(t) = 128.2\,\text{kJ}$$

That is only 33.2% of the total energy.

The Driving Pattern

The driving pattern affects the value of energy that is lost during braking. For example, driving in city traffic entails a cycle of low speed accelerations followed by decelerations. Highway driving, on the other hand, involves higher speeds producing higher energies that are also lost with braking. Nonetheless, the energy recovery ratio in a hybrid vehicle under urban driving conditions can be higher for frequent low speed acceleration/deceleration cycles. The reason is that the high energy rates involved in highway speeds cannot efficiently be recovered by the electric system.

Example 7.7.2

The vehicle of Example 7.7.1 with the same battery travels the NEDC cycle. Compare the maximum recoverable energies during the urban and highway parts of the cycle shown in Figure 7.76 by obtaining the regenerative efficiencies. Ignore the power loss of resistive forces.
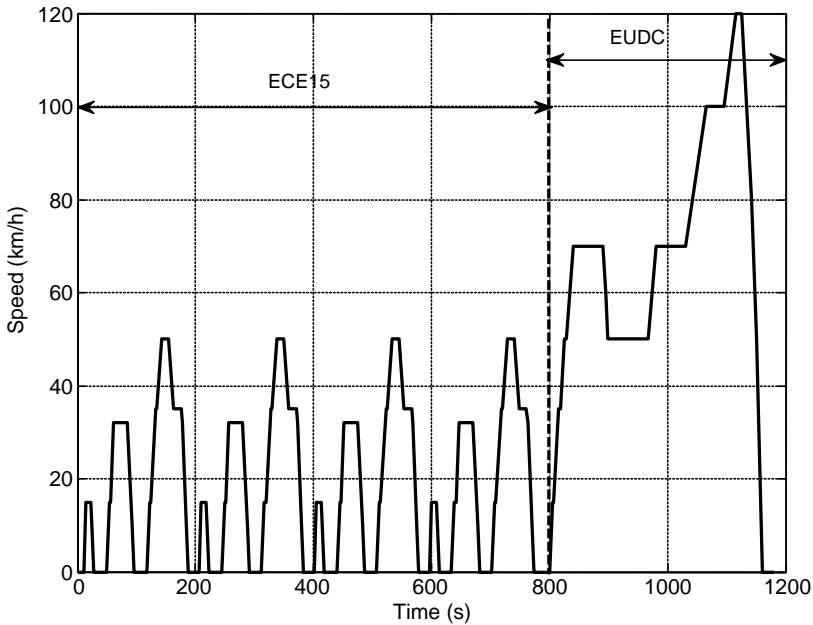
Figure 7.76   NEDC cycle of Example 7.7.2

Solution

The ECE part of the cycle is four times repetition of a three-part cycle. In the first part braking takes place in 5 seconds from an initial speed of 15 km/h. Maximum braking power during this period is $mav_0 = 3.47\,\text{kW} < 20/0.85 = 23.53\,\text{kW}$. Thus the recovered energy is

$$E_{b11} = \int_0^5 \eta mav(t) = 7.38\,\text{kJ}.$$

In the second part, braking is done from 32 km/h in 11 s. The maximum braking power is 7.18 kW < 23.53 kW and the recovered energy in this part is $E_{b12} = 33.58\,\text{kJ}$. In part three, initially braking reduces the speed from 55 km/h to 35 km/h within 8 s and then to a complete stop in 12s. In both phases the available power is less than the maximum absorbable value and thus the absorbed energy is $E_{b13} = 99.2\,\text{kJ}$. The total recovered energy during the ECE cycle therefore is $E_{bECE} = 4 \times E_{b1} = 560.64\,\text{kJ}$.

For EUDC cycle braking first takes place at 70 km/h and during 8 s speed is reduced to 50. In this part the braking power is still lower than 23.53 kW and E_{b21}=78.7 kJ. The second braking phase starts at 120 km/h and within 34 seconds the vehicle comes to a complete stop. The maximum mechanical power reaches 32.68 kW > 23.53. Similar to Example 7.7.1, the time at which the braking power reduces to 23.53 kW is 9.52 s (at a speed of 86.4 km/h). The recovered energy is obtained as $E_{b22} = 435.2$ kJ. The total regenerative power in this phase is $E_{bEUDC} = 513.9$ kJ.

The available energy values for ECE and EUDC are $E_{ECE} = 659.6$ kJ and $E_{EUDC} = 648.2$ kJ. Therefore the efficiencies of regenerative braking are:

$$\eta_r(\text{ECE}) = 85\% \quad \text{and} \quad \eta_r(\text{EUDC}) = 79.3\%.$$

It is worth noting that a higher efficiency in the second phase of EUDC cycle compared to the value obtained in Example 7.7.1 is due to a lower deceleration in EUDC.

The Driving Axle

In normal braking, the braking forces are applied on both front and rear axles, however, the generator (usually M/G) is typically only attached to the driving wheels on a single axle. Therefore the maximum possible energy absorption will depend on the braking capacity of that axle (either front or rear). On the other hand, the required braking torques in vehicles are larger than those that a generator can produce and thus electric braking alone is not sufficient and conventional mechanical brakes are also therefore required on an HEV.

Braking Stability

The best braking performance is obtained if the braking force on a vehicle is distributed according to the ideal braking curve shown in Figure 7.77 that prevents the rear wheels from locking up before the front wheels. However, the brake forces in the vehicles are usually applied on a linear basis (brake force line) that satisfies the rear wheel lock-up criterion up to large decelerations. Therefore the regenerative braking
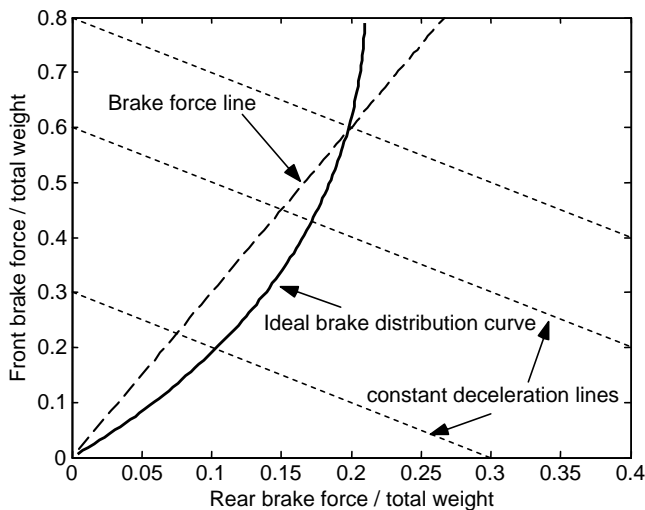
Figure 7.77   Brake force distribution

should also follow the same rules and take a balanced share of the total braking force. More details on the braking performance and regenerative braking can be found in [5 and 6].

7.7.2   Control

In order to improve the fuel economy and reduce emissions, the power management controller has to decide which operating mode of the hybrid vehicle to be used, and to determine the optimal split between the two power sources while meeting the driver demands and sustaining the battery state of charge. This is usually performed according to different methodologies and strategies.

7.7.2.1   Methodology

Power management methodologies can be classified into two categories, namely *rule-based* and *mathematical model-based* techniques. The first type employs control algorithms such as simple or Fuzzy logic rules for decision-making. These control types classify the operating conditions into several cases and use *if-then* rules to choose the best operating point among the possible cases. Rule-based algorithms do not use formal mathematical approaches and instead rely on the expert knowledge of the system behaviour and thus their performance depends on how they are tuned.

The mathematical model-based methodologies use optimization techniques based on the mathematical models of the system components and determine the best instantaneous split of power between the two sources in order to achieve the best performance with minimum fuel consumption and emission. These methodologies include *static* and *dynamic* methods. The former technique uses the steady-state component efficiency maps whereas the latter takes into account the dynamic nature of the system when performing the optimization and as a result under the transient conditions the dynamic approach leads to more accurate results albeit at the expense of more intense computations.

7.7.2.2   Strategy

The overall strategy of power management control is effectively the set of rules that must be employed in order that the objectives of the control system are met. In the rule-based methodologies, the rules are directly applied in every instant and control outputs are determined. In other methodologies in which an optimization process is involved, an objective function is typically introduced and its magnitude is minimized while additional constraints are fulfilled (similar to the method discussed in Section 7.6.3).

The basic rules for the rule-based methodologies are based on the vehicle torque and power demands (see Figure 7.78):

- When the torque demand is higher than the engine torque, the motor should assist if battery SOC allows.
- At low speeds if power demand is low, only the electric motor is used since the engine is inefficient in such cases.
- At greater power demands below the motor maximum power curve, the motor alone can work if the SOC is large enough, otherwise the engine alone can deliver the power. A hybrid mode with both the motor and engine power split can also be used based on the efficiency of the system.

The basic strategy used in practice is *charge sustaining* which is beneficial in utilizing the maximum potential of electric propulsion. This means that whenever possible, the electric motor is used to propel the vehicle either in electric-only or in electric assist modes. This strategy is especially useful under stop-start driving conditions in city traffic in which the motor must launch the vehicle frequently. Obviously if the amount of charge of the battery or the SOC is to remain unchanged, the input and output energies to the battery must be balanced. The *engine on/off* technique is employed in order to supply energy to the
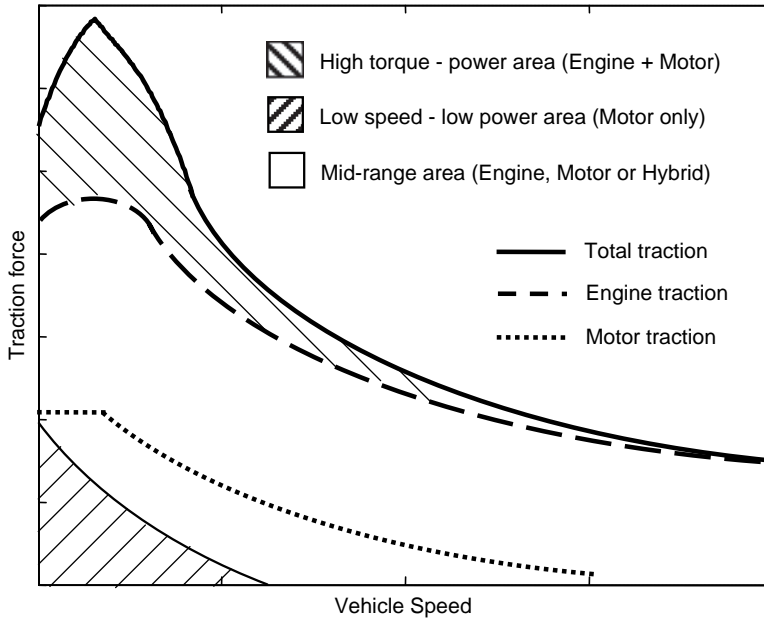
Figure 7.78 Tractive force-speed diagram with high torque and low power areas

battery when its SOC drops to a permissible low level. When no input power from the engine to the battery is needed (the SOC reaches its high level) and the vehicle propulsion is independent of engine, it can be turned off.

7.8 Conclusion

This chapter dealt with the fundamentals of hybrid electric vehicle concepts as well as design issues. The classification and operating modes of HEVs were discussed starting from the basic series and parallel types up to the more sophisticated power split versions. The characteristics of major HEV components and their modelling issues were explained. Then the performance analysis of the hybrid vehicles was considered and mathematical models were provided. Component sizing as an important issue in HEV design was considered and details of sizing based on vehicle performance were discussed. The HEV power management was briefly introduced and some overall design guidelines were discussed.

It is important to note that the crucial concept of hybrid vehicles is their energy efficiency compared to conventional vehicles. This is achieved by very careful design and use of the vehicle components at their most efficient points. Success depends on how the vehicle energy consumption is managed and how vehicle energy is regained through regenerative braking. The design of hybrid systems as well as their accurate performance evaluation requires specialist software as well as the availability of detailed component behaviours, in particular, their operating efficiencies.

7.9 Review Questions

7.1 What are the main reasons for the development of hybrid vehicles?
7.2 What is the basic classification for the hybrid electric vehicles?
7.3 In your view, is a series HEV more efficient than a conventional vehicle? Why?

7.4 Name and explain the operation modes of an HEV.

7.5 What are the benefits of the parallel HEV over the series-parallel HEV?

7.6 What is the main difference between the series-parallel HEVs and power-split HEVs?

7.7 Explain the degree of hybridization and the classification of hybrids based on it.

7.8 What are the power split devices?

7.9 Describe the power circulation? Is it useful?

7.10 What is the SOC and why is important?

7.11 Explain the BMS and its important tasks.

7.12 Describe the methods of sizing the HEV components.

7.13 Explain how the optimum sizing of an HEV component is related to the driving patterns.

7.14 What is the supervisory control in HEVs? What are the low level controllers?

7.15 Explain the potential areas available for an HEV controller in order to enhance the fuel economy and reduce the emissions.

7.16 What is regeneration? Explain the influencing factors in regeneration.

7.17 Explain the methodologies and strategies of HEV control systems.

7.10   Problems

Problem 7.1

Consider the simple PSD of Section 7.3.1 under a transient (dynamic) working condition and derive equations to replace Equations 7.4, 7.5 and 7.7.

Problem 7.2

Repeat Example 7.3.4 considering global component efficiencies of 0.8, 0.8, 0.95 and 0.98 for MG1, MG2, PSD and the reduction gear respectively. For MGs use identical efficiencies for motor or generator modes (Hint: Derive necessary relations for power losses and circulating power).

Problem 7.3

The vehicle of Example 7.3.4 starts the motion in 'electric-only' mode up to speed of 30 km/h, then the engine is started and the vehicle is propelled in 'engine-only' mode with full throttle. Plot the vehicle performance curves up to 20 seconds after motion starts. The motor has a base speed of 1200 rpm.

Problem 7.4

Work Example 7.3.4 for the EM-PSD with $k_p = 1.5$

Problem 7.5

The overall efficiency of a battery can be regarded as:

$$\eta_b = \frac{E_d}{E_c}$$

in which E_d and E_c are the discharged and charged energies of the battery. A simple experiment is designed in which a battery cell is discharged and charged again in a controlled manner. Energy is given to a consumer from a battery at a constant current I during time t_f. At this time period, the voltage of battery remains a constant V. Then the battery is charged at the same voltage V, current I and time t_f:

(a) Derive an equation for the overall efficiency of the battery.

(b) For a battery with open terminal voltage of 11.2 V and internal resistance of 0.05 ohm, plot the efficiency of battery for different currents.

Problem 7.6

In Example 7.4.3 if the battery must be charged when the SOC is below 60%, determine the time at which the engine must be started to recharge the battery and also calculate the distance travelled by then.

Problem 7.7

Consider the vehicle and driving cycle of Example 7.4.3 and determine:

(a) Total tractive energy consumption in a cycle;
(b) Total regenerative energy and its ratio to the tractive energy.

Problem 7.8

Rework Example 7.5.1 by including the torque-speed characteristics of the motor that has a base speed of 1000 rpm but with the same maximum power.

Problem 7.9

Repeat Example 7.7.1 for maximum battery charging currents of 20, 50 and 70 A. Also plot the variation of regenerating efficiency with maximum charging current.

Results: 7.3%, 78.6% and 31.6%.

Problem 7.10

Repeat Example 7.7.2 for maximum battery charging currents of 20, 50 and 70 A. (Hint: write a MATLAB program.)

Result for $I = 20$ A: 78.6% and 31.6%.

Problem 7.11

Repeat Example 7.7.1 with a rolling resistance coefficient of 0.015 and overall drag factor of 0.3.

Problem 7.12

Repeat Example 7.7.2 with a rolling resistance coefficient of 0.015 and overall drag factor of 0.3.

Problem 7.13

The generator of Example 7.7.1 has a maximum torque of 200 Nm up to a base speed of 1200 rpm, and a reduction gear ratio of 5.0. The rolling radius of the wheel is 30 cm. Calculate the regenerative braking efficiency (The braking force is produced only by the generator).

Problem 7.14

Use the generator of Problem 7.13 with a maximum torque of 150 Nm to rework Example 7.7.2.

Further Reading

Alongside the upsurge of interest in hybrid vehicles since 2000, several textbooks have appeared on the subject dealing with electric vehicles (EVs), hybrid electric vehicles (HEVs) and fuel cell vehicles (FCVs).

An excellent introduction to EVs is provided by Larminie and Lowry [6]. The book is mainly descriptive and focuses on the design of EVs, with chapters specializing in their components – batteries and motors, for example. There is also some basic material describing fuel cells and the use of hydrogen as a vehicle power source. The book has been extensively used by undergraduate students and the Appendices include some simple, but useful examples using MATLAB code. The definitive reference on EVs is by Chan and Chau [7]. Professor Chan is a pioneer of EV technology in academic circles and has built up a world-recognized centre of excellence at Hong Kong University. The book concentrates on a comprehensive analysis of the design of EVs, but also includes discussion of more general issues relating to energy and the environment. Also, a substantial chapter is devoted to the problems of infrastructure and charging.

There are two good textbooks on HEVs. The textbook by Ehsani et al. [5] covers the fundamentals, theory and design of EVs, HEVs and FCVs. As well as providing the background theory and equations, design examples with simulation results are provided. The book stems from the research and teaching carried out at Texas A & M University and so it provides an excellent introduction to the subject area. The authors spend a considerable time describing the behaviour of internal combustion engines (ICEs) which of course, are just as important as the electrical components in a hybrid powertrain – and the ICE power map characteristics for hybrid applications are usually different from those designed for conventional vehicles. Miller's book [8] also provides an excellent reference book for EVs and HEVs. In particular, the benefits of different HEV architectures are critically compared; then in Chapters 3 and 4, Miller goes into admirable depth on the design specifications of hybrid powerplants followed by a detailed study of sizing the drive system. The entire book, therefore, has a strong practical design theme running through it.

Finally, for those readers who require further background information on fuel cells, there is another excellent introductory text by Larminie and Dicks [9] which provides a thorough overview of their design and performance.

References

[1] Ren, Q., Crolla, D.A. and Wheatley, A. (2007) Power Split Transmissions for Hybrid Electric Vehicles, in *Proc EAEC 2007 Congress*, Budapest.

[2] Mashadi, B. and Emadi, M. (2010) Dual Mode Power Split Transmission for Hybrid Electric Vehicles, *IEEE Transactions on Vehicular Technology*, 59(7).

[3] Guzzella, L. and Sciarretta, A. (2005) *Vehicle Propulsion Systems: Introduction to Modelling and Optimisation*. Springer, ISBN 978-3-549-25195.

[4] Wong, J.Y. (2001) *Theory of Ground Vehicles*, 3rd edn, John Wiley & Sons, Inc., ISBN 0-470-17038-7.

[5] Ehsani, M., Gao, Y., Gay, S.E. and Emadi, A. (2005) *Modern Electric, Hybrid Electric and Fuel Cell Vehicles: Fundamentals*, Theory and Design. CRC Press, ISBN 0-8493-3154-4.

[6] Larminie, J. and Lowry, J. (2003) *Electric Vehicle Technology Explained*. John Wiley & Sons, Ltd, ISBN 0-470-85163-5.

[7] Chan, C.C. and Chau, K.T. (2001) *Modern Electric Vehicle Technology*. Oxford University Press, ISBN 0-19-850416-0.

[8] Miller, J.M. (2004) *Propulsion Systems for Hybrid Vehicles*. Institution of Electrical Engineers, ISBN 0-86341-336-6.

[9] Larminie, J. and Dicks, A. (2003) *Fuel Cell Systems Explained*, 2nd edn. John Wiley & Sons, Ltd, ISBN 978-0-470-84857-9.

Appendix

An Introduction to Bond Graph Modelling

A.1 Basic Concept

The basic concept in bond graph analysis is to specify the flow of energy in a system. The energy flow in any system is always governed by simultaneous intervention of two independent parameters. In the bond graph method these two parameters are defined by the general terms of Effort e and Flow f. The power of the instantaneous energy flow is product of these two factors:

$$P(t) = e(t) \cdot f(t) \tag{A.1}$$

Momentum (p) and *Displacement* (q) are defined as:

$$p = \int e(t) dt \tag{A.2}$$

$$q = \int f(t) dt \tag{A.3}$$

Therefore *Energy* (E) from Equation A.1 is

$$E = \int e.f \, dt = \int f(t) \, dp = \int e(t) \, dq \tag{A.4}$$

An energy port in a bond graph is the gateway for energy exchange. Should an element exchange energy in a single way (e.g. heat) that element is called a one-port (or single-port) element. A multi-port element, therefore, is an element that exchanges energy in different ways (e.g. heat, electrical, mechanical, etc.).

A.2 Standard Elements

The elements in a bond graph are models of components in real systems. As far as energy is concerned, an element of a system is either a source of energy or consumes energy. Consuming energy may result in the

dissipation of energy (usually as heat), transient storage or transforming it to another useful form. With this brief explanation, the bond graph elements can be categorized as *Sources* (or Active elements), *Passive* elements, *Converters*, and *Junctions*.

A.2.1 Sources

Energy sources are devices that contain one sort of energy and, when connected to a system, the flow of energy is established. As stated earlier, any sort of energy has both flow and effort components. Sources in a bond graph are distinguished by their dictating component; in other words, an energy source can only dictate either flow or effort factors and cannot control the other factor.

A *flow source* S_f, therefore, is an energy source that has a specific flow level f^* and, when connected to a system, energy will be passed to the system with a flow value of f^*. The value of effort of the flow source will depend on the energy demand of the connected system. For an ideal source of flow, the flow level f^* is independent of energy demand and always remains unchanged. An example of a flow source in mechanical systems is a large moving body with a constant speed (e.g. the Earth, a train, etc.) and in electrical systems the current source in electrical circuits is an example.

An *Effort source* S_e, is an energy source that has a specific effort level e^* and, when connected to a system, energy will be passed to the system with effort value of e^*. Again, the value of flow to the system depends on the energy demand of that system and cannot be controlled by the source. For ideal effort sources, the value e^* will not be altered by the energy drain from the source. Examples of effort sources in mechanical and electrical systems are a force and a battery respectively. In bond graphs, simple arrows are used to indicate the direction of energy flow. The bond graph graphical symbols for the effort and flow sources are shown in Figure A.1.

Energy sources are single-port elements since they transmit only one sort of energy to the systems.

A.2.2 Passive Elements

There are three types of passive elements in the bond graphs, namely *Resistive*, *Capacitive* and *Inertia* elements. These are all single port elements that receive energy from the system and either dissipate it or increase their energy level.

A *Resistive* element (*R* element) is any element that has a static relation between its *effort* and *flow* of the form:

$$e = \Phi_1(f) \tag{A.5a}$$

The function Φ_1 in general is non-linear but for the sake of simplicity a linear function will be assumed hereinafter. Thus Equation A.5a can be simplified to:

$$e = Rf \tag{A.5b}$$

in which R is the constant slope of e versus f for the linear assumption. According to Equation A.1, power flow from this element is:

$$P = Rf^2 \tag{A.6}$$

$$S_f \xrightarrow[\;f^*\;]{\;e\;} \text{System} \qquad\qquad S_e \xrightarrow[\;f\;]{\;e^*\;} \text{System}$$

(a) (b)
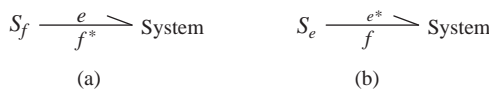
Figure A.1 Bond graph graphical symbols for (a) flow source and (b) effort source

$$\text{System} \xrightarrow[f]{e} R$$
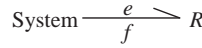
Figure A.2   Graphical symbol for Resistive or R element

Table A.1   Examples for R elements

Element	System	Standard symbol	Bond graph symbol	Mathematical relations
Resistor	Electrical	i ⟶ R ⟵ i / V	$\dfrac{e\,(V)}{f(i)} \!\!\searrow\!\! R$	$V = R\,i, \quad P = Ri^2$
Damper	Mechanical	F ⟶ B ⟵ F / v	$\dfrac{e\,(F)}{f\,(v)} \!\!\searrow\!\! R$	$F = B\,v, \quad P = Bv^2$

The graphical symbol for the R element is depicted in Figure A.2 and examples of the resistive elements in mechanical and electrical systems are summarized in Table A.1.

A *Capacitive* element (C element) is any element that has a static relation between its *effort* and *displacement*, i.e.:

$$e = \Phi_2(q) \tag{A.7}$$

Again a linear function Φ_2 will be assumed here and as a result we will have:

$$e = kq \tag{A.8}$$

in which k is the constant slope of e versus q in the linear case. The graphical symbol for the C element is depicted in Figure A.3 and examples of the capacitive elements in electrical and mechanical systems are summarized in Table A.2.

An *Inertia* element (I element) is any element that has a static relation between its *momentum* and *flow*, or:

$$p = \Phi_3(f) \tag{A.9}$$

$$\text{System} \xrightarrow[f]{e} C$$
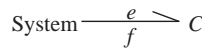
Figure A.3   Graphical symbol for Capacitive or C element

Table A.2   Examples for C elements

Element	System	Standard symbol	Bond graph symbol	Mathematical relations
Capacitor	Electrical	i ⟶ C ⟵ i / V	$\dfrac{e\,(V)}{f\,(i)} \!\!\searrow\!\! C$	$V = k\,q = \dfrac{1}{C}\displaystyle\int i\,dt$
Spring	Mechanical	F ⟶ k ⟵ F / v	$\dfrac{e\,(F)}{f\,(v)} \!\!\searrow\!\! C$ $(1/k)$	$F = k\,x = k\displaystyle\int v\,dt$

$$\text{System} \xrightarrow{\quad \dfrac{e}{f} \quad} I$$
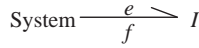
Figure A.4 Graphical symbol for Inertia or I element

Table A.3 Examples for I elements

Element	System	Standard symbol	Bond graph symbol	Mathematical relations
Inductance	Electrical	$i \xrightarrow{\quad L \quad} i$ $\quad V \quad$	$\dfrac{e\,(V)}{f\,(i)} \rightarrow I\,(L)$	$p_L = Li = \displaystyle\int V_L dt$
Mass	Mechanical	$F \rightarrow \boxed{m} \xrightarrow{\quad v}$	$\dfrac{e\,(F)}{f\,(v)} \rightarrow I$	$p = mv = \displaystyle\int F dt$

Assuming a linear function Φ_3 for our case:

$$p = If \tag{A.10}$$

in which I is the constant slope of p versus f for the linear relationship. The graphical symbol for the I element is shown in Figure A.4 and examples of the inertia elements in electrical and mechanical systems are summarized in Table A.3.

A.2.3 Two Port Elements

Two port elements are basically *converters* of energy and receive the energy in one port, convert it and transfer it to the output port. Ideal two-port elements do not use or waste energy. The general bond graph representation of a two-port element is shown in Figure A.5.

For an ideal 2-port element the energy balance means:

$$e_1 f_1 = e_2 f_2 \tag{A.11}$$

There are two types of two-port elements, namely, transformers and gyrators that will be described below.

A.2.3.1 Transformer

A transformer *TF* is a two-port element in which the input and output efforts are proportional:

$$e_2 = me_1 \tag{A.12}$$

in which m is proportionally constant and is called the transformer module. In bond graphs m is placed above the transformer as shown in Figure A.6.

$$\xrightarrow{\quad \dfrac{e_1}{f_1} \quad} \text{TP} \xrightarrow{\quad \dfrac{e_2}{f_2} \quad}$$
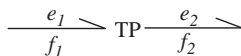
Figure A.5 Bond graph symbol for a general two-port element

$$\underrightarrow{\quad\dfrac{e_1}{f_1}\quad}\overset{m}{\text{TF}}\underrightarrow{\quad\dfrac{e_2}{f_2}\quad}$$
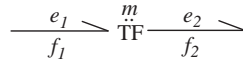
Figure A.6   Bond graph representation of transformer element

According to Equation A.11, for a transformer element, the relation between flows is:

$$f_1 = mf_2 \tag{A.13}$$

In electrical systems a transformer uses two or more windings wrapped around an iron core and transforms energy from the input winding to the output winding(s). The magnetic field produced by an alternating current in the input coil induces an alternating current in the output coil(s). If the output voltage is greater than the input voltage the transformer is a step-up type, or conversely it can be a step-down transformer. Examples of transformer elements in mechanical systems are a lever, a belt drive and a gear set.

A.2.3.2   Gyrator

A gyrator GY is a two-port element in which the input effort and its output flow are proportional:

$$f_2 = re_1 \tag{A.14}$$

in which r is the proportionally constant and is called the gyrator ratio. In bond graphs similar to transformer case, r is placed above the gyrator. According to Equation A.11, for a gyrator element the relation between input flow and output effort is:

$$f_1 = re_2 \tag{A.15}$$

A rotating mass in a mechanical system has a gyroscopic property. Figure A.7 shows a simple gyroscope consisting of a spinning rotor with a fixed axis inside a light frame. Applying a torque T_x about the x axis will not turn the frame around the x axis, but it will instead turn it around the y axis due to the gyroscopic effect. The governing relation is:

$$T_x = J\Omega\omega_y \tag{A.16}$$

in which J is the mass moment of inertia of the rotor and Ω is the spin speed. Similarly for input torque T_y the rotation is around the x axis (-x strictly speaking)

$$T_y = J\Omega\omega_x \tag{A.17}$$
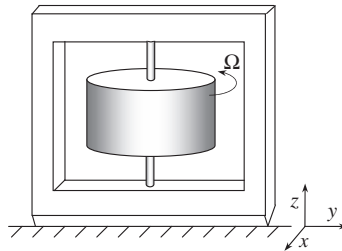
Figure A.7   A simple gyroscopic
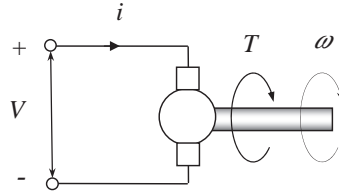
Figure A.8   A DC motor

The two axes x and y can be regarded as input and output axes and since torque and speed are effort and flow, Equations A.16 and A.17 are of the forms of Equations A.14 and A.15 respectively with r being the inverse of $J\Omega$.

In an electrical system, a DC motor has its output torque proportional to the input current and at the same time its output speed is proportional to the input voltage. With reference to Figure A.8, one can write:

$$T = k_m\, i, \quad (e_2 = k_m f_1) \tag{A.18}$$

$$V = k_m\, \omega, \quad (e_1 = k_m f_2) \tag{A.19}$$

that is, equivalent to a gyrator with its r inverse of the proportionality constant k_m.

A.2.4   Junctions

Junctions are elements in bond graphs that are responsible for the implementation of the law of conservation of energy. There are two types of junctions: common-effort and common-flow.

A *common effort* junction also known as 0-node, is a meeting point for several energy bonds with equal efforts. Consider a general case of three bonds meeting at a 0-node shown in Figure A.9.

With the condition of common efforts, it can be written:

$$e_1 = e_2 = e_3 \tag{A.20}$$

The application of the law of conservation of energy will result in:

$$f_1 + f_2 + f_3 = 0 \tag{A.21}$$

Similarly a *common flow* junction, also called 1-node, is a meeting point for several energy bonds with equal flows. Three bonds meeting at a 1-node are illustrated in Figure A.10 and with the condition of common flow, the equations are:

$$f_1 = f_2 = f_3 \tag{A.22}$$

$$e_1 + e_2 + e_3 = 0 \tag{A.23}$$
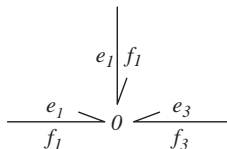
Figure A.9   A common effort junction (0-node)
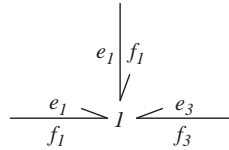
Figure A.10   A common flow junction (1-node)

A.3   Constructing Bond Graphs

Constructing the bond graph for a physical system is a simple task of putting together the bond graph symbols of individual elements in the system. The best way to learn the construction of bond graphs is to work through several examples as follows.

Example A.3.1

Construct the bond graph for the basic mechanical system of Figure A.11.
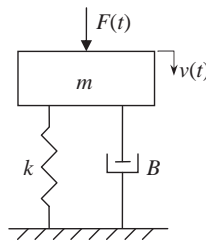
Figure A.11   Basic mechanical system of Example A.3.1

Solution

In Figure A.11 one distinguishes four different elements: forcing function $F(t)$, mass element m, spring element k and damper element B. The forcing function is a source of energy and since the dictating component for the source is its effort (force), thus it is a source of effort S_e. The three remaining elements are all passive elements or consumers and bond graph symbols for all three were given earlier.

In order to construct the bond graph, one important point is to see how the elements are connected. Note that the system elements can only connect with one another through junctions and two-port elements. Here there is no two-port element so one should look for junctions only. A 0-junction is where elements with equal efforts (forces) are connected and a 1-junction is where elements of equal flow (speed) are connected. It is easy to note that the spring and damper elements have bottom ends fixed and have equal speeds at upper ends. So these two elements have equal speeds and should be connected through a 1-junction.

The mass element is a one-end element and when compared with two-end elements of spring and damper in a mechanical system, it may cause confusion. In order to resolve any confusion of this kind, the mass element can always be replaced with a two-end element that has its second end connected to the ground. Application of this rule to the system of Figure A.11 will result in Figure A.12, from which it can be seen that the mass element is also in the same situation as the two other elements. Since the force also has similar velocity, therefore, all four elements are joined by a common-flow junction as shown in Figure A.13.
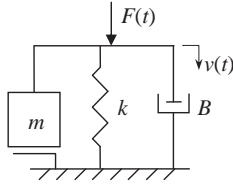
Figure A.12 Equivalent sketch for system of Figure A.11
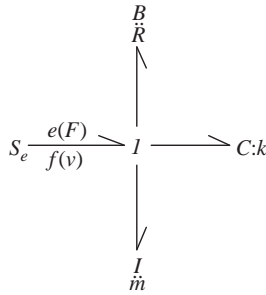
Figure A.13 Bond graph of Example A.3.1

Example A.3.2

Construct the bond graphs of the electrical systems shown in Figure A.14.

(a) Series   (b) Parallel
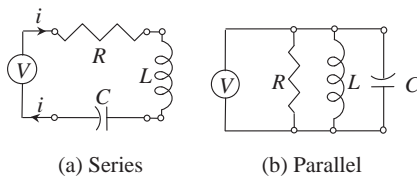
Figure A.14 Electrical circuits of Example A.3.2

Solution

In circuit (a) three passive elements are in series, so that an equal current i will pass through them all and also through the voltage source. Thus all four elements are connected through a common flow junction. The result is the bond graph of Figure A.15a. The same elements are in parallel in the circuit of Figure A.14b. All three passive elements are connected to both ends of the voltage source, so that a common effort junction should connect them all in a bond graph. The result is shown in Figure A.15b.

(a)   (b)
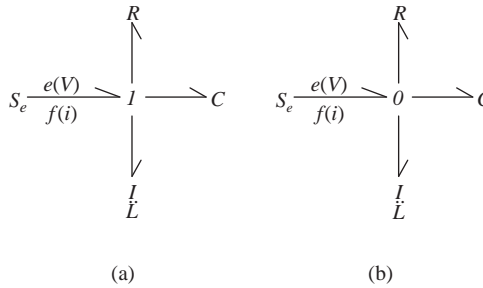
Figure A.15   Bond graphs of Example A.2.2

Example A.3.3

Construct the bond graph of the electromechanical system of Figure A.16.
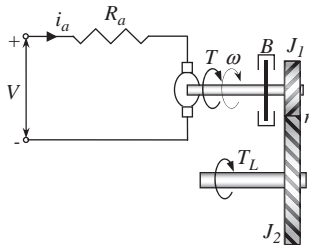
Figure A.16   System of Example A.3.3

Solution

The system consists of a DC motor with its output shaft attached to a gear set. A viscous friction element is also present to model the bearing frictions. The load torque T_L is acting on the output shaft.

The main source of energy is electrical voltage source that provides the motor armature current i_a. This current also flows through the resistor R_a and the armature produces a shaft torque

proportional to the current. In bond graph terms the input source is connected to a 1-node together with the resistor and the armature. The armature is a gyrator that receives electrical energy and produces mechanical torque proportional to its input current. The armature torque drives the damper as well as the small gear with a common speed (these two elements are in a common flow junction). The remaining torque is amplified by the gear set (i.e. a transformer) and drives the larger gear with inertia J_2. The load torque acts like a source of effort at the output shaft. The bond graph representation of the system according to the description is shown in Figure A.17.
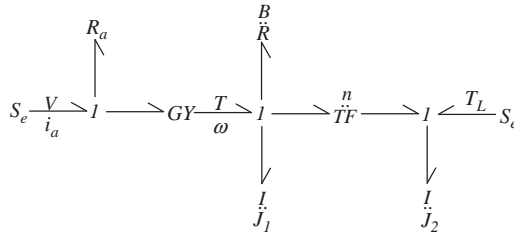
Figure A.17 Bond graph of system of Example A.3.3

A.4 Equations of Motion

Modelling tools eventually lead to the derivation of governing equations of motion of the systems. For bond graphs, this process starts by specifying the state variables. For this reason, bond graphs use a technique in which Causality Strokes are inserted.

A.4.1 Causality

For I and C elements the relationship between their efforts and flows is governed by integrals. Let us consider the I element, for instance, for which the flow is obtained from integration of its effort (see Equations A.2 and A.10):

$$f(t) = \frac{1}{I} \int e(t) dt \tag{A.24}$$

Equation A.24 means that in an I element the effort is the cause of energy transfer. In other words, when effort is received by the element, the flow is generated after a delay. An example is the mass in mechanical systems. Applying a force to a mass produces speed. In fact, at time zero there is a force but speed is zero. After some time elapses, speed will result. Thus in I elements the flow always lags the effort. It is said the effort in these elements is the *cause* and flow is the *effect*.

In C elements the opposite is true, since the effort and flow change places in Equation A.24:

$$e(t) = \frac{1}{C} \int f(t) dt \tag{A.25}$$

Therefore in a C element, flow is the *cause* and the effort is the *effect*. Causality plays an important role in determining the system state variables and for this reason the causality must be specified in a bond graph. To this end, a *Stroke* '|' is used to specify the causality of each element in the bond graph. Table A.4 summarizes the causality strokes of different bond graph elements.

Table A.4 Causality strokes for bond graph elements

Element	Basic symbol	Stroked symbol	Alternative
I	$\longrightarrow I$	$\longrightarrow\vert I$	Avoid
C	$\longrightarrow C$	$\vert\longrightarrow C$	Avoid
R	$\longrightarrow R$	$\vert\longrightarrow R$	$\longrightarrow\vert R$
S_e	$S_e\longrightarrow$	$S_e\longrightarrow\vert$	None
S_f	$S_f\longrightarrow$	$S_f\vert\longrightarrow$	None
TF	$\longrightarrow TF\longrightarrow$	$\vert\longrightarrow TF\vert\longrightarrow$	$\longrightarrow\vert TF\longrightarrow\vert$
GY	$\longrightarrow GY\longrightarrow$	$\vert\longrightarrow GY\longrightarrow\vert$	$\longrightarrow\vert GY\vert\longrightarrow$

The last column in Table A.4 indicates that there are alternative causality assignments for the bond graph elements. For I and C elements the alternative strokes are at the other ends. In fact, the strokes given to I and C elements shown in Table A.4 are called integral causality since the relation between the flow and effort of these elements is of the integral type. However, in a physical system it is possible that I and C elements can receive alternative causality (called differential causality). It is recommended to avoid this type of causality if possible. For R elements the causality is not important and both forms can be assigned. For the sources, no alternatives for causality assignment is permitted.

Junctions are very important when causality strokes are assigned. The reason is that in every junction there is only one band which controls the property of that junction (i.e. flow or effort) and it is called the *Strong* band. This means, for instance, in a 1-node, all connected elements that have equal flows, the flow is dictated by only one of the elements. An example is a source of flow connected to a 1-node, obviously all elements will have the flow of the source. Conventionally the strong bond in a common-flow junction receives the causal stroke outside of the junction and the other bonds receive their strokes inside the junction. For a common-effort junction the opposite applies (i.e. the strong bond receives the stroke inside of the junction). Figure A.18 illustrates the causality strokes of both common-flow and common-effort junctions. It is clear that in a 0-junction only one stroke appears inside the junction and in a 1-junction only one stroke appears outside of the junction. The existence of more than one strong bond in a junction indicates a violation of the law of conservation of energy and thus the result is invalid.

A.4.2 Assignment Procedure

Causality assignment procedure in a bond graph is not unique and everyone may use a different way of inserting the strokes. However, there are a few points that are useful to consider before assigning the causal strokes.

- Sources are good starting points since their strokes are definite.
- Try to assign integral causalities for all I and C elements.
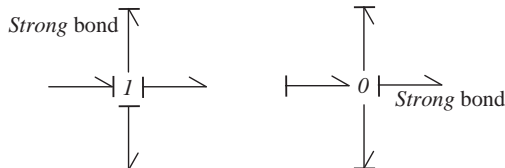
Figure A.18 Causal strokes of typical 1-junctions and 0-junctions

- Assign them one by one to avoid mistakes.
- Check the strokes of all junctions and make sure there is only one strong bond in each joint.

Example A.4.1

Assign the causal strokes in the bond graph of Example A.3.3.

Solution

The result is given in Figure A.19. Starting with sources in this case only specifies their own strokes and no further information is obtained. In the second step the *I* element in the middle 1-junction is given an integral stroke. This specifies the strong bond of the junction and other strokes are inserted inside the junction. The gyrator to the left of the junction and the transformer to the right both receive their appropriate strokes (see Table A.4). The two remaining elements are R_a and *I* in the first and last 1-junctions and they receive their strokes according to the status of strokes in the junctions where they belong. It is observed that for the *I* element of the last junction, a differential stroke is assigned. This is acceptable since between the two gears of Figure A.16 no elastic element exists and the speeds of each gear are directly related.
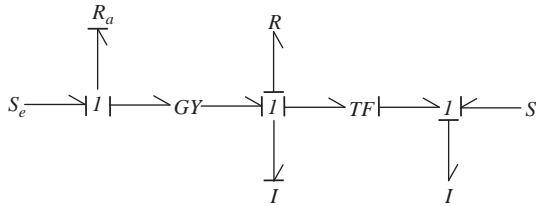
Figure A.19   Causal strokes for the bond graph of system of Example A.4.1

A.4.3 *Bond Graph Numbering*

Numbering bond graphs is optional but useful since it assigns a number to each element in the bond graph and makes easy to describe a system. The numbering method is also optional and a bond graph can be numbered in different ways. Nevertheless, it is better to number the graph sequentially starting from 0 or 1. A recommended procedure is as follows:

1. Assign number 0 to the source.
2. If there is more than one source, assign 0 to the main source and to the others 00, etc.
3. Assign numbers 1, 2,3, etc. to the integrally stroked *I* and *C* elements.
4. Next number the differentially stroked *I* and *C* elements.
5. Then number the R elements.
6. Continue numbering the other remaining bonds.

Example A.4.2

Number the bond graph of Example A.3.4.

Solution

The main source is assigned 0 and the other 00. There is only one integrally stroked I element, which receives number 1, and the second I element gets number 2. The two R elements are assigned 3 and 4 and the rest of bonds are numbered from 5 to 8. The result is given in Figure A.20.
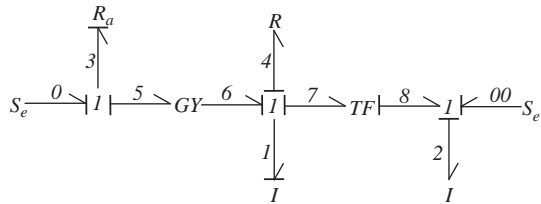
Figure A.20   Bond graph numbering for system of Example A.4.2

A.4.4   Component Equations

The governing equations of a system are usually obtained by putting together the equations of individual elements of the system. Useful forms of equations for several elements in the bond graph are summarized in Table A.5.

A.4.5   Bond Graph Simplifications

Sometimes the nodes and elements in a bond graph are arranged so that some parts of the graph can be simplified. Examples of bond graph modifications will be described below.

Table A.5   Useful equations for bond graph elements

Element	Name	Equation	Reference
S_e	Source of effort	$e = S_e$	–
S_f	Source of flow	$f = S_f$	–
I	Inertia element	$f = \frac{p}{I}$	Eq. A.10
C	Capacitance element	$e = k\,q$	Eq. A.8
R	Resistance element	$e = Rf$	Eq. A.6
TF	Transformer	$e_o = me_i$	Eq. A.12
GY	Gyrator	$f_o = re_i$	Eq. A.14
0	0-junction	$\sum f_i = 0$	Eq. A.21
1	1-junction	$\sum e_i = 0$	Eq. A.23
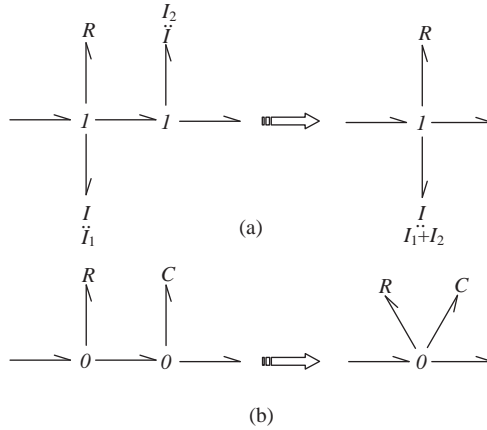
Figure A.21   Adjacent node simplifications: (a) *1* junctions and (b) *0* junctions

- Adjacent *1* or *0* junctions of same type: two adjacent *1* or *0* junctions can be merged to obtain only one node. Figure A.21 illustrates examples of this kind.
- Equivalent *I* or *R*: Sometimes at both ends of a transformer there are *1* junctions with *I* or *R* elements. This combination can be simplified by taking the elements to either end of the transformer by substituting an equivalent value. Figure A.22 shows the original system and its two alternatives for *I* elements. The equivalent inertias I' and I'' are obtained from following equations. For the *R* elements, the results are exactly similar.

$$I' = I_1 + \frac{1}{m^2} I_2 \tag{A.26}$$

$$I'' = I_2 + m^2 I_1 \tag{A.27}$$

It should be noted that by using the equivalent inertias, the occurrence of derivative causality for *I* elements is also prevented.

A.4.6   Derivation of Equations of Motion

Once the bond graph is constructed and causal strokes are assigned, the process for the derivation of equations of motion can be easily followed. The first step in this process is to find the state variables of the
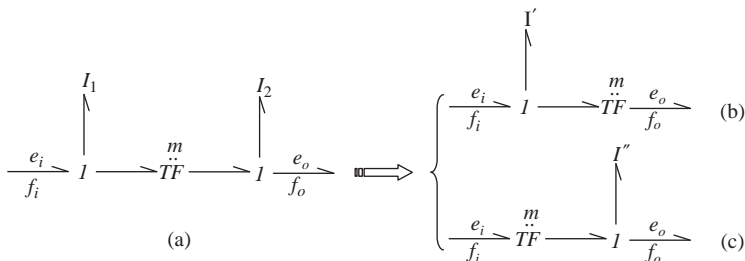
Figure A.22   Equivalent inertias in a transformer

system that are the momentum and displacements of those I and C elements of the bond graph with integral causality. This is why care should be taken to assign integral strokes to as many I and C elements as possible in the bond graph, since an inadequate number of state variables cannot explain the system behaviour. In fact, according to the definition, the state variables are the minimum number of variables that fully describe the state of a system at any instant.

Upon identification of the state variables, there will be one differential equation of motion for each state variable. Since the state variables belong to either the I-elements or the C-elements, the differential equations of motion are of the following basic forms:

$$\frac{dp_i(t)}{dt} = e_i(t) \tag{A.28}$$

$$\frac{dq_j(t)}{dt} = f_j(t) \tag{A.29}$$

In which e_i (i = 1, 2, ...) are the efforts of the I elements with integral causality, and p_i are their momentums (that are system state variables). Similarly f_j (j = 1, 2, ...) are the flows of the C elements with integral causality and q_j are their displacements. The task of obtaining the governing equations of motion, therefore, reduces to writing the efforts and flows of the specified I and C elements in terms of state variables (i.e. in terms of p and q). This can be done by making use of equations given in Table A.5. Equations A.28 and A.29 show that the equations of motion of the system are obtained as a set of first order differential equations. This is the advantage of the bond graph method, since the solution of such equations is straightforward by using available software such as MATLAB.

Example A.4.3

For the torsional vibrating system shown in Figure A.23 derive the equations of motion.
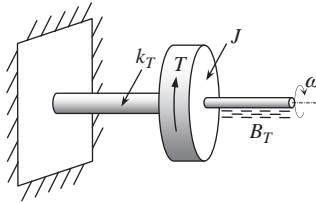
Figure A.23   A torsional vibrating system

Solution

This system is a torsional equivalent of the mass-spring-damper system discussed in Example A.2.1. External torque T, inertia J, torsional spring k_T and torsional damper B_T replace F, m, k and B of the linear system. The bond graph of the system, therefore, is exactly similar to that depicted in Figure A.13. The result after applying numbering and assigning causality strokes is

shown in Figure A.24. As is clear, both I and C elements have received integral strokes and thus the system has two state variables p_1 and q_2.
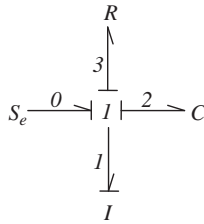
Figure A.24 Bond graph of Example A.4.3

The equations of motion of the system are $\frac{dp_1}{dt} = e_1$ and $\frac{dq_2}{dt} = f_2$. In order to find the final forms of the equations, parameters e_1 and f_2 must be written in terms of state variables p_1 and q_2. From Table A.5, the available equations for the elements are:

$$f_1 = \frac{p_1}{I_1}$$

$$e_2 = k_2 q_2$$

$$e_3 = R_3 f_3$$

$$e_0 = S_e$$

These equations do not provide direct solution for the two unknowns. For junction 1 we have:

$$f_2 = f_3 = f_1 = \frac{p_1}{I_1}$$

which is the solution to the second differential equation. To find e_1 we have to write the effort summation for the junction $(e_0 - e_1 - e_2 - e_3 = 0)$ from which we have:

$$e_1 = e_0 - e_2 - e_3 = S_e - k_2 q_2 - R_3 \frac{p_1}{I_1}$$

that is, only in terms of state variables (and known quantities). Thus the final forms of the equations of motion are:

$$\frac{dp_1}{dt} = S_e - k_2 q_2 - R_3 \frac{p_1}{I_1}$$

$$\frac{dq_2}{dt} = \frac{p_1}{I_1}$$

It might raise a question of how this result is related to a traditional solution of standard mass-spring-damper system of the form $m\ddot{x} + B\dot{x} + kx = F$ (or for our case $J\ddot{\theta} + B_T\dot{\theta} + k_T\theta = T$), that is a second order differential equation. To answer this question it should be recalled the *order reduction* process in which a second order differential equation can be broken into two first order

equations by change of variable. For instance, by defining $x_1 = J\theta$ and $x_2 = J\dot{\theta}$, the second order equation $J\ddot{\theta} + B_T\dot{\theta} + k_T\theta = T$ can be reduced to two following first order equations:

$$\frac{dx_2}{dt} = T - \frac{k_T}{J}x_1 - \frac{B_T}{J}x_2$$

$$\frac{dx_1}{dt} = x_2$$

Substituting $p_1 = J\dot{\theta}$ (momentum of rotating inertia) and $q_2 = \theta$ (displacement of torsional spring) and making use of $S_e = T, I_1 = J, k_2 = k_T$ and $R_3 = B_T$, the bond graph equations of motion will be exactly identical to the two above equations. Hence, the bond graph equations of motions are already in reduced form.

Example A.4.4

Derive the equations of motion for the system of Example A.3.3.

Solution

The numbered and stroked bond graph of the system was given in Figure A.20. Since only one integrally stroked element exists in the system, there would be only 1 state variable p_1. Thus the equation of system reads:

$$\frac{dp_1}{dt} = e_1 = e_6 - e_4 - e_7$$

e_6 can be found from the gyrator relation:

$$e_6 = rf_5(f_3) = r\frac{e_3}{R_3}$$

The value in the parenthesis is equal to the adjacent parameter (e.g. $f_5 = f_3$) and e_3 is obtained from effort balance of the first node:

$$e_3 = e_0 - e_5 = S_e - \frac{f_6(f_1)}{r} = S_e - \frac{p_1}{rI_1}$$

e_4 simply is

$$e_4 = R_4f_4(f_1) = R_4\frac{P_1}{I_1}.$$

In order to determine e_7, from the transformer and the effort balance of the last node, we have:

$$e_7 = \frac{e_6}{m} = \frac{1}{m}(e_2 + e_{00})$$

e_{00} is the effort source at the right (S'_e), but e_2 cannot be obtained in usual manner since I_2 is differentially stroked. For such cases, a differentiation is necessary.

For I_2 we write:

$$\int e_2 dt = I_2 f_2(f_8) = I_2 \frac{f_7(f_1)}{m} = \frac{I_2}{mI_1} p_1$$

Thus:

$$e_2 = \frac{I_2}{mI_1} \frac{dp_1}{dt}$$

After substituting e_6, e_4 and e_7 into the first equation and rearranging, the final result is:

$$\frac{dp_1}{dt} = \frac{m^2 I_1}{I_2 + m^2 I_1} \left(\frac{r}{R_3} (S_e - \frac{p_1}{rI_1}) - R_4 \frac{p_1}{I_1} - \frac{S'_e}{m} \right)$$

Index